

General Disclaimer

One or more of the Following Statements may affect this Document

- This document has been reproduced from the best copy furnished by the organizational source. It is being released in the interest of making available as much information as possible.
- This document may contain data, which exceeds the sheet parameters. It was furnished in this condition by the organizational source and is the best copy available.
- This document may contain tone-on-tone or color graphs, charts and/or pictures, which have been reproduced in black and white.
- This document is paginated as submitted by the original source.
- Portions of this document are not fully legible due to the historical nature of some of the material. However, it is the best reproduction available from the original submission.

NASA LEWIS FINAL TECHNICAL REPORT

NAG 3-67 (6/2/80-7/31/81)

(NASA-CR-169533) PREDICTION OF SOUND
RADIATION FROM DIFFERENT PRACTICAL JET
ENGINE INLETS Final Technical Report, 2
Jun. 1980 - 31 Jul. 1982 (Georgia Inst. of
Tech.) 365 p HC A16/MF A01

N83-13936

Unclas
01139

CSSL 20A G3/71

**PREDICTION OF SOUND RADIATION FROM
DIFFERENT PRACTICAL JET ENGINE INLETS**

By

**William L. Meyer
Ben T. Zinn**



GEORGIA INSTITUTE OF TECHNOLOGY

**A UNIT OF THE UNIVERSITY SYSTEM OF GEORGIA
SCHOOL OF AEROSPACE ENGINEERING
ATLANTA, GEORGIA 30332**

1982



NASA LEWIS FINAL TECHNICAL REPORT

NAG 3-67 (6/2/80 - 7/31/82)

**PREDICTION OF SOUND RADIATION FROM
DIFFERENT PRACTICAL JET ENGINE INLETS**

BY

William L. Meyer

Ben T. Zinn

**SCHOOL OF AEROSPACE ENGINEERING
GEORGIA INSTITUTE OF TECHNOLOGY
ATLANTA, GA. 30332**

ABSTRACT

This report summarizes the work performed under NASA Lewis Grant Number NAG 3-67 entitled, "Prediction of Sound Radiation from Different Practical Jet Engine Inlets" during the two year period from June 2, 1980 to July 31, 1982. The objectives of this study included the following: (1) upgrade existing computer codes which were based upon a special integral representation of the external solutions of the Helmholtz equation, so that they would yield accurate results for the acoustic radiation patterns in the field surrounding an axisymmetric body for non-dimensional wave numbers, based on duct radius, of up to twenty; (2) check the accuracy of these computer programs by the use of the point source method for the generation of "exact" solutions and then by comparison with the results of other experimental and theoretical studies; and, (3) use these computer codes in a parametric study of the dependence of the radiated sound field on input modal distribution, wave number, and inlet lip shape. The results of this study show that: (1) as the wave number (i.e., cut-off ratio) is increased for a given input modal distribution that the acoustic radiation peak moves towards the inlet centerline and becomes more compact (i.e., narrows); (2) as the input mode number is increased for a given cut-off ratio the acoustic radiation peak moves away from the inlet centerline and becomes more compact; and, (3) as the inlet lip becomes thicker the acoustic radiation peak moves towards the centerline of the inlet and becomes more compact.

TABLE OF CONTENTS

	Page
I. Introduction	1
II. The Langley Bellmouth Inlet	5
III. The Thin Lipped Elliptical Inlet	8
IV. The Thick Lipped Elliptical Inlet	10
V. The Effect of Inlet Curvature on Acoustic Radiation Patterns	12
VI. References	14
VII. Tables	16
VIII. Figures	19

I. INTRODUCTION

This report summarizes the work performed under NASA Lewis Contract Number NAG 3-67 during the period June 2, 1980 to July 31, 1982. This research program was concerned with the determination of the radiation patterns around different practical jet engine inlet configurations when subjected to different excitation conditions. This was accomplished in two phases, with the first phase completed during the first year of this contract and the second phase the following year.

During the first year of this project the computer codes required for this investigation were developed. The initial task of this first phase was the upgrading of existing computer codes for the calculation of both the surface and field distributions of the acoustic quantities of interest (i.e., the acoustic potential and acoustic velocity normal to the wall). The theoretical basis for these programs is presented in Refs. 1-3. These references track the development of a unique integral formulation of the acoustic radiation problem and its application in the calculation of two dimensional, three dimensional and cylindrically symmetric radiation patterns. The cylindrically symmetric formulation of Ref. 3 (See Appendix A of Ref. 4.) was used in this investigation as all of the inlet geometries investigated were axisymmetric. The details of the upgrading of the computer codes is presented in Ref. 4. This initial computer code development work was accomplished using the NASA Lewis QCSEE inlet configuration of Ref. 5 and was checked against "exact" solutions generated by the point source method as described in Ref. 3.

The second task completed during the first year was the consolidation of the two main computer programs, along with the many smaller computer programs developed to do such things as calculate the cut-off wave numbers for various modes, the generation of input modal distributions and the geometrical shapes of the bodies of interest, and the data plotting routines into a coherent package of programs. This program package was then used to investigate the acoustic behavior of five different inlet configurations; namely: the NASA Langley Bellmouth^{6,7}; the NASA Lewis JT15D-1 Ground Test Nacelle^{8,9}; and three hyperbolic inlets of 50, 70 and 90 degree divergence angles, similar to those investigated by Y. C. Cho^{10,11}. Although the main objective of this study was to compare the radiation patterns generated by the integral technique¹⁻³ with those calculated/measured in other theoretical/experimental studies, reflection coefficients were also calculated at the duct exit plane for certain specific inlet configurations where these results were available. The results of these studies are presented in Ref. 12.

During the first half of the second contract year a series of 35 computer runs were performed for the NASA Langley Bellmouth inlet configuration^{6,7}. These 35 computer runs provide a parametric study of the dependence of the sound radiated from this inlet geometry upon the specified input modal distributions and the cut-off ratios given in Table I. For each of these runs, both the distribution of the reflection coefficient at the duct exit plane and the distribution of the SPL (Sound Pressure Level) in the field were calculated. These results were cross plotted holding the input

modal distribution or the cut-off ratio constant and can be found in Ref. 13.

During the final half year of this two year contract the computer programs were updated to run on the new computer systems here at Georgia Tech as the old CDC Cyber 70/74 system was replaced by two new CDC Cyber computers; a 730 and a 760. Also, with the new campus network in operation, printouts could be obtained on site rather than only at the computer center which greatly reduced printing costs. This network also allowed the down loading of data files from the CDC computers to the Hewlett-Packard 2100 series mini-computer in the School of Aerospace Engineering for plotting. Having accomplished this, the computer program which uses the calculated surface distributions on the body to calculate the radiated sound field outside the body was modified at the sponsor's request to: (1) calculate the acoustic radiation pattern all around the body from 0 to 180 degrees from the inlet centerline at one degree increments instead of from 0 to 90 degrees in two degree increments; and, (2) to calculate the radial distributions of the reflection coefficients across the inlet at five axial stations from the straight duct exit plane to the inlet exit plane. This updated field code was then re-run for the 35 cases done previously for the NASA Langley Bellmouth inlet configuration. The field data was then plotted and cross plotted as before (See Ref. 13.) holding either the input modal distribution or the cut-off ratio constant. The distributions of the reflection coefficients at the five axial stations were also plotted for the five cases run for each of the two input modal distributions (i.e., $(M, N) = (4,1)$ and $(4,3)$).

Two elliptical inlet geometries were supplied by the sponsor for study and they will be designated here as the "thin" and "thick" lipped elliptical inlets. Thirty five computer runs were done for each of these inlet configurations at the same input conditions as was done for the NASA Langley Bellmouth inlet configuration (See Table I.). The same plots and cross plots were obtained for each of these geometries and the results are presented herein. In addition, the radiation patterns generated by all 105 computer runs were cross plotted varying the inlet geometry while holding the input modal distributions and the cut-off ratios constant. These plots are also presented in this report.

II. THE LANGLEY BELLMOUTH INLET

Figures 1-3 represent the distributions of the calculational points on the surface of the theoretical model used to simulate the NASA Langley Bellmouth inlet for the various computer runs. The open circles are the points where the acoustic quantities are calculated while the locations denoted by the small crosses are those used in the integration procedure. The arrows represent the outward normals from the body at the various points on the body as these plots offer a visual check of the geometric input data for the computer programs. One should note that the driver plane also represents the duct exit plane as there is no straight duct section connected to the inlet lip. This was done to conserve computer space, which was limited in the old Cyber computers, and computing time, which goes up roughly as the square of the number of points used on the surface of the body, as the effect of a straight duct connected to the inlet lip was not investigated in this study. Finally, it should be noted that the theoretical geometry is terminated in all cases by a 2:1 ellipse as the Helmholtz equation is elliptic and is therefore only applicable to closed bodies.

Descriptions of the computer runs conducted for each of the three geometries investigated are presented in Table II. Since the required computer runs for this parametric study cover a wide range of input modes and cut-off ratios (i.e., wave numbers), the number of calculational points on the body was not the same for all of the runs. This is due to the fact that as the wave number (cut-off ratio) is increased more points must be used on the body in the longitudinal direction to adequately describe the distributions of

the acoustic quantities on the surface of the body. Also, as the input mode number is increased, the number of points in the tangential direction must be increased for the same reason.

In Figs. 4 and 5 the modulus and phase of the radial distributions of the reflection coefficients are presented at five axial locations along the inlet starting at the duct exit plane, (i.e., the driver plane), station 1, and ending at the inlet exit plane, station 5. These stations are separated by equal axial distances so that station 3 is located at the middle of the inlet lip. The non-dimensional axial distances of these stations from the driver plane are given in Table III where the reference distance is the radius at the driver plane. Figures 4 and 5 present the results for the input modes of $(M,N) = (4,1)$ and $(M,N) = (4,3)$, respectively. These plots show that as the acoustic wave moves out of the inlet the modulus of the reflection coefficient steadily decreases as does the phase. Also, as the wave number (cut-off ratio) goes up the modulus of the reflection coefficient decreases while its phase increases.

The radiation patterns for the 35 cases run for the Langley Bellmouth are presented in Ref. 13 (See Figs. 4-38.) and therefore will not be repeated here. When these data are displayed on separate plots the results are not easy to compare and therefore trends are not obvious. To alleviate this problem, these data are compared in plots of the relative SPL (Sound Pressure Level) in decibels and the phase in degrees versus the angular location in Figs. 6-10. Each of these plots describes SPL levels referenced to the point in the field where the maximum SPL occurs for each case. Each figure contains the SPL in dB plotted in two different ways so that trends

can easily be detected. For example, the same data are plotted in Figs. 6a & c and 6b & d where in Figs. 6a & b the curve are all referenced to the same SPL level (i.e., zero) in Figs. 6c & d each curve is referenced to a different SPL level. The actual data was calculated at one degree increments on a circle centered at the inlet exit plane with a radius of 20.33 driver radii. Each figure contains all of the results for the various cases run for each input mode (i.e., Fig. 6 contains the results for an input mode of $(M,N) = (1,1)$, etc.). One should note that there is a change of scale in Figs. 6a & b and in Figs. 7a & b and that some of the cases are repeated for clarity as is done in Figs. 6c & d, 6e & f, 7c & d, and 7e & f. One should also note that since the theoretical geometry outside and behind the inlet lip does not model the true geometry of the actual inlet, the results in the field past 90 degrees from the centerline are suspect and at best only provide the qualitative trends of the sound distribution in these locations.

In Figs. 11-16 the relative SPL and phase distributions of the sound fields associated with the Langley Bellmouth are presented. Specifically, these figures describe cases where the cut-off ratio is held constant and the input modal distribution is varied. As in the previous set of figures, the relative SPL is plotted in two different ways in each figure for clarity.

III. THE THIN LIPPED ELLIPTICAL INLET

The model geometries used for the 35 cases run for the thin lipped elliptical inlet are given in Figs. 17-19. As with the Langley Bellmouth inlet, three different numerical approximations were employed for various input conditions. The runs for which each approximation was used are presented in Table II. One should note that the nominal point spacings on this inlet are half of those used on the Langley Bellmouth thereby making the calculations more accurate. This was done for the following reasons: (1) with the new computers more points could be taken on the surface of the body as more computational space was available; and, (2) since the inlet lip is considerably smaller, a closer point spacing was necessary to adequately describe the relatively faster changing curves. This inlet lip consists of a 2:1 ellipse whose semi-major axis is 0.2 of the non-dimensional driver radius, a . It is capped with a semi-circle of radius $0.025a$ and has a 2:1 ellipse as its outer wall and is terminated by yet another 2:1 ellipse.

In Figs. 20-24 the SPL in dB are plotted and tabulated from 0 to 90 degrees in two degree increments. Each figure contains all of the plots for the cases run for each modal input (e.g., Fig. 20 consists of the 9 plots, one for each cut-off ratio, for an input mode of $(M,N) = (1,1)$, etc.). These data represent actual values generated in each case and not just the relative values. Also, when comparing these plots, care must be exercised as all of the plots do not use the same limits.

The modulus and phase of the radial distributions of the reflection coefficients are presented in Figs. 25 and 26 for input modal distributions of

$(M,N) = (4,1)$ and $(4,3)$, respectively. The results for this inlet configuration show that the reflection coefficients don't follow the same trends over the entire spectrum of investigated wave numbers for both input modal distributions. For example, the modulus of the reflection coefficient decreases as the wave moves down the inlet in Figs. 25a,c,e and g, while it increases in Figs. 25 i and k.

In Figs. 27-31 the relative SPL in dB and phase in degrees are plotted. Each figure represents all of the cases run for the thin lipped elliptical inlet for a given input modal distribution. As before, the relative SPL is plotted in two ways in each figure for the sake of clarity. Also, as before, some of the curves are replotted for certain cases (e.g., see Fig. 27a & b) for ease of comparison and because the scales change between these plots. It is of interest to note that although the lobe which contains the maximum SPL changes for the Langley Bellmouth inlet (See Fig. 10a & b.) when the $(M,N) = (4,4)$ mode is cut-on (See Table I.), this does not happen for the thin lipped elliptical inlet. While in the Langley Bellmouth inlet the maximum SPL moves from the first lobe (closest to the centerline) to the third lobe as the wave number increases, the maximum SPL always remains in the third lobe for the thin lipped elliptical inlet.

The radiation patterns are re-plotted in Figs. 32-37 holding the cut-off ratio constant and varying the input mode. Again, the relative SPL is plotted in two different ways in each figure so that trends are more easily discernable.

IV. THE THICK LIPPED ELLIPTICAL INLET

Figures 38-40 contain the model of representations used for the thick lipped elliptical inlet geometry. As with the other two inlet geometries, these three different numerical descriptions of the model of the geometry are used for certain of the 35 computer runs done for this geometry (See Table II.). The inlet lip is simply twice as large as the thin lipped inlet geometry so that it too is described by a 2:1 ellipse whose semi-major axis is $0.4a$ instead of $0.2a$. It is also capped with a semi-circle (of radius $0.05a$) and terminated by a 2:1 ellipse.

The SPL in dB is both plotted and tabulated for the 35 cases run for this geometry (See Table I.) in Figs. 41-45. As before, each figure contains the plots for all of the cases run for a particular input mode. One should note again that these plots are of the actual SPL values calculated in the programs and that the scales on all of the plots are not the same.

In Figs. 46 and 47 the modulus and phase of the radial distributions of the reflection coefficients at five stations down the inlet are presented. Each figure contains the plots of all of the cases run for a particular mode. As with the thin lipped elliptical inlets results, these distributions do not follow consistent trends as the wave number is increased or as the waves move down the inlet. The axial locations of the different stations are given in Table III.

The relative SPL in dB and phase in degrees of the acoustic radiation patterns outside the inlet are plotted in Figs. 48-52. As before, each figure

represents all of the cases run for a given mode for the thick lipped elliptical inlet. Also, the relative SPL is plotted in two ways in each figure and in Figs. 48 and 49 some of the curves are duplicated in separate plots for ease of comparison.

In Figs. 53-58 the radiation patterns are re-plotted holding the cut-off ratio constant in each case rather than the input mode. Each figure consists of three plots; two of the relative SPL in dB and one of the phase in degrees. The data for these plots were generated at one degree increments and the plots were obtained by having the computer draw straight lines between these data points. This accounts for the sharp corners observed on some of the curves (See Fig. 58a.) and the gaps in the curves when they cross 180 degrees (See Fig. 58c.).

V. THE EFFECT OF INLET LIP CURVATURE ON ACOUSTIC RADIATION PATTERNS

The principle goal of this parametric study was to show the effect of inlet lip curvature on the acoustic radiation patterns generated by the same acoustic excitation. In the course of this study 35 computer runs were made for each of the three inlet geometries; the Langley Bellmouth, the thin lipped elliptical inlet, and the thick lipped elliptical inlet; for the same input model distributions (See Table I.). Since the duct exit/driver plane was non-dimensionalized to one for each geometry the acoustic excitation applied in the computer program was the same for each geometry. This does not mean, however, that the same acoustic power was supplied in each case as this is an elliptic problem and conditions at the driver plane depend upon the properties on the remaining boundaries. In these studies the acoustic potential (which is directly related to the acoustic pressure) was specified as the boundary condition at the driver plane while a zero normal acoustic velocity (i.e., a hard wall) was specified on the rest of the body. This means that in each case the normal acoustic velocity was calculated on the driver plane which, in turn, resulted in a different acoustic power out of the driver (and therefore the inlet) for each case.

Two options for normalization of the radiation patterns were therefore available: (1) normalize with respect to the peak radiated acoustic pressure; or, (2) normalize the curves with respect to the total radiated power (which for a hard walled geometry is equivalent to the power out of the driver). Since this study was more interested in the shape of the

acoustic radiation patterns, than in the total power radiated, the first normalization scheme was used. The second normalization scheme would entail the calculation of the PWL (Sound Power Level) in the field rather than the SPL (Sound Pressure Level) and then an integration under the curve for the normalization factor. It had previously been found by the authors of this report that in general the PWL and SPL curves are very similar⁴ and almost interchangeable in the field surrounding the inlet. This being the case, the effect of the second type of normalization on the curves can easily be determined by inspection; that is, by doing a rough estimate of the area under the curves. One must be careful however as the area of the sphere must be taken into account so that the middle must be more heavily weighted than the ends.

The results of the 105 computer runs are presented in Figs. 59-63. Each figure contains all of the plots for each input mode, one plot for each cut-off ratio (wave number). An examination of these figures reveals two trends; which are: (1) as the inlet lip gets larger the maximum radiation peak moves further towards the centerline (in front of the inlet); and (2) as the inlet lip thickens, the maximum radiation peak becomes narrower and better defined. Both of these trends are consistent with the expectation that a larger inlet lip will better focus the radiated acoustic energy.

IV. REFERENCES

1. Bell, W. A., Meyer, W. L., and Zinn, B. T., "Predicting the Acoustics of Arbitrarily Shaped Bodies Using an Integral Approach," AIAA Journal, Vol. 15, No. 6, pp. 813-820, June 1977.
2. Meyer, W. L., Bell, W. A., Stallybrass, M. P., and Zinn, B. T., "Boundary Integral Solutions of Three Dimensional Acoustic Radiation Problems," Journal of Sound and Vibration, Vol. 59, No. 2, pp. 245-262, July 1978.
3. Meyer, W. L., Bell, W. A., Stallybrass, M. P., Zinn, B. T., "Prediction of the Sound Field Radiated from Axisymmetric Surfaces," Journal of the Acoustical Society of America, Vol. 63, No. 2, pp. 631-638, March 1979.
4. Zinn, B. T. and Meyer, W. L., "Prediction of Sound Radiation from Different Practical Jet Engine Inlets," NASA Lewis Semi-Annual Status Report, Contract No. NAG 3-67, (6/2/80-11/30/80).
5. Miller, B. A., Dastoli, B. J. and Wesoky, H. L., "Effect of Entry-Lip Design on Aerodynamics and Acoustics of High-Throat-Mach-Number Inlets for the Quiet, Clean, Short-Haul Experimental Engine," NASA TM X-3222, Lewis Research Center, Cleveland, Ohio, May 1975.
6. Ville, J. M. and Silcox, R. J., "Inlet Contour and Flow Effects on Radiation," AIAA Paper Number 80-0966, June 1980.

7. Ville, J. M. and Silcox, R. J., "Experimental Investigation of the Radiation of Sound from an Unflanged Duct and a Bellmouth Including the Flow Effect," NASA Technical Paper 1697, August 1980.
8. Heidmann, M. F., Saule, A. V. and McArdle, J. G., "Analysis of Radiation Patterns of Interaction Tones Generated by Inlet Rods in the JT15D Engine," AIAA Paper Number 79-0581, March 1979.
9. Heidmann, M. F., Saule, A. V. and McArdle, J. G., "Analysis of Radiation Patterns of Interaction Tones Generated by Inlet Rods in the JT15D Engine," NASA TM-79074, March 1979.
10. Cho, Y. C., "Sound Radiation from Hyperboloidal Inlet Ducts," AIAA Paper Number 79-0677, March 1979.
11. Cho, Y. C., "Rigorous Solutions for Sound Radiation from Circular Ducts with Hyperbolic Horns or Infinite Plane Baffle," Journal of Sound and Vibration, Vol. 69, No. 3, pp. 405-425, 1980.
12. Zinn, B. T. and Meyer, W. L., "Prediction of Sound Radiation from Different Practical Jet Engine Inlets," NASA Lewis Semi-Annual Status Report, Contract No. NAG 3-67, (12/1/80-5/30/81).
13. Zinn, B. T. and Meyer, W. L., "Prediction of Sound Radiation from Different Practical Jet Engine Inlets," NASA Lewis Semi-Annual Status Report, NASA-CR-165120, Contract No. NAG 3-67, (6/1/81-12/1/81).

ORIGINAL PAGE IS
OF POOR QUALITY

TABLE I

Non-Dimensional wave Numbers Used in Computer Runs

Cut-Off Ratios	(Tangential, Radial) Modes				
	(1,1)	(2,1)	(4,1)	(6,1)	(4,3)
-----	-----	-----	-----	-----	-----
1.005	1.850	3.009	5.345	9.695	12.74
1.015	1.869	3.100	5.398	9.792	12.87
1.064	1.959	3.249	5.658	10.26	13.49
1.155	2.127	3.527	6.142	11.14	14.65
1.305	2.403	3.985	6.940	12.59	16.55+
1.556	2.865	4.752	8.275	15.01*	19.73+‡
1.740		5.314			
2.040	3.756				
2.150		6.566			
2.500	4.603				
2.870	5.284				

* (8,2) Mode cut-on

+ (4,4) Mode cut-on

‡ (4,5) Mode cut-on

TABLE II

Number of Points Used in the Surface Integrations

Number of Points on the Body	Nominal Point Spacing on the Body	Range of Non-Dimensional Wave Numbers (ka)
---------------------------------	--------------------------------------	---

LANGLEY BELLMOUTH INLET

102	0.04	0 --> 5
155	0.025	5 --> 12
189	0.02	12 --> 20

THIN LIPPED ELLIPTICAL INLET

97	0.02	0 --> 5
146	0.0125	5 --> 12
179	0.01	12 --> 20

THICK LIPPED ELLIPTICAL INLET

116	0.02	0 --> 5
176	0.0125	5 --> 12
216	0.01	12 --> 20

Number of Points in Tangential Integration	Range of Tangential Mode Numbers (M)
---	---

32	0 --> 3
64	4 --> 7
96	8 --> 11

ORIGINAL PAGE IS
OF POOR QUALITY

TABLE III

Axial Distances for the Calculation of the Radial
Distributions of the Reflection Coefficients in the Inlets

Station Number	Langley Bellmouth Inlet	Thin Lipped Elliptical Inlet	Thick Lipped Elliptical Inlet
1	0.0	0.0	0.0
2	0.267	0.05	0.1
3	0.535	0.1	0.2
4	0.802	0.15	0.3
5	1.069	0.2	0.4

ORIGINAL PAGE 18
OF POOR QUALITY

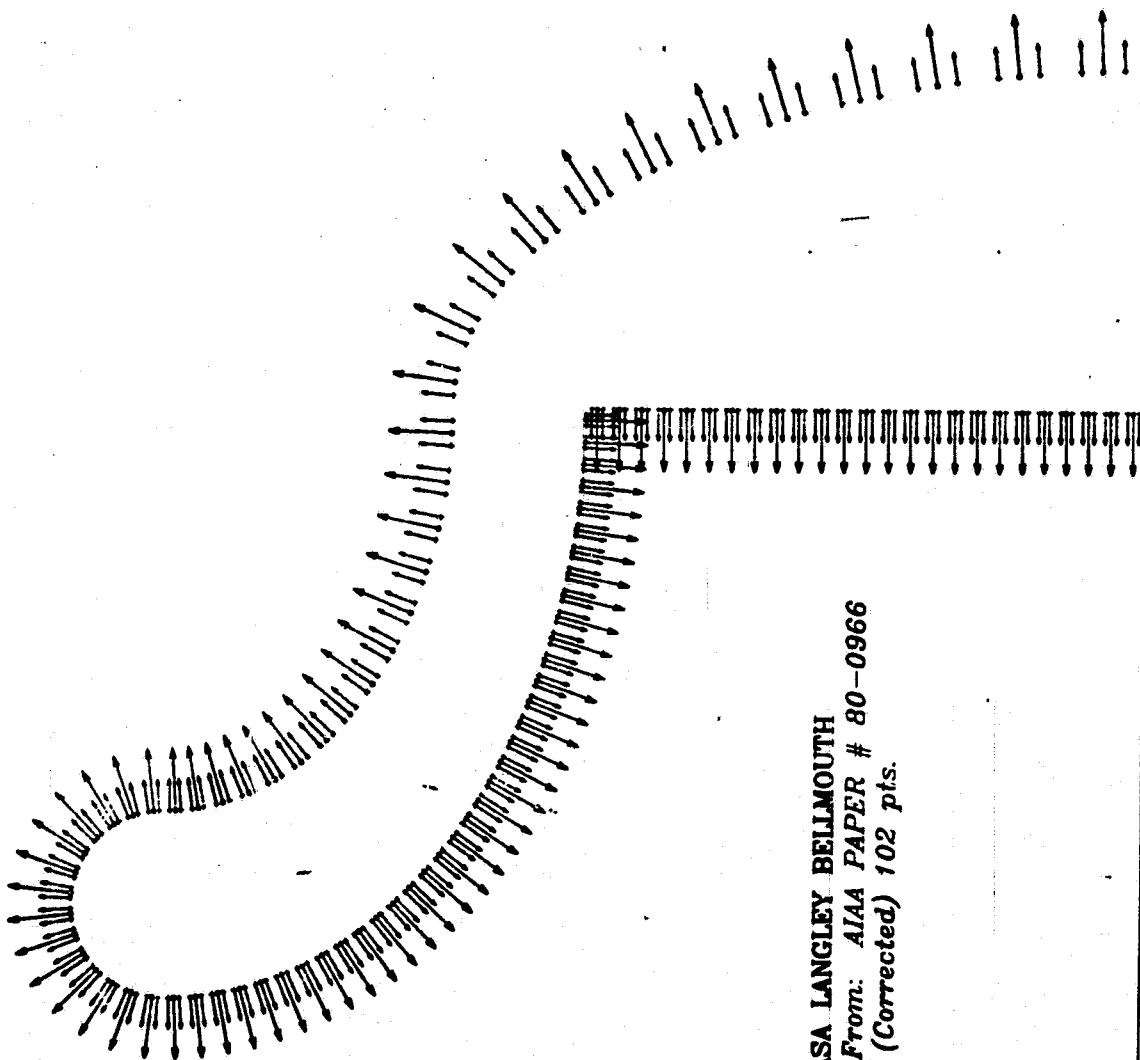
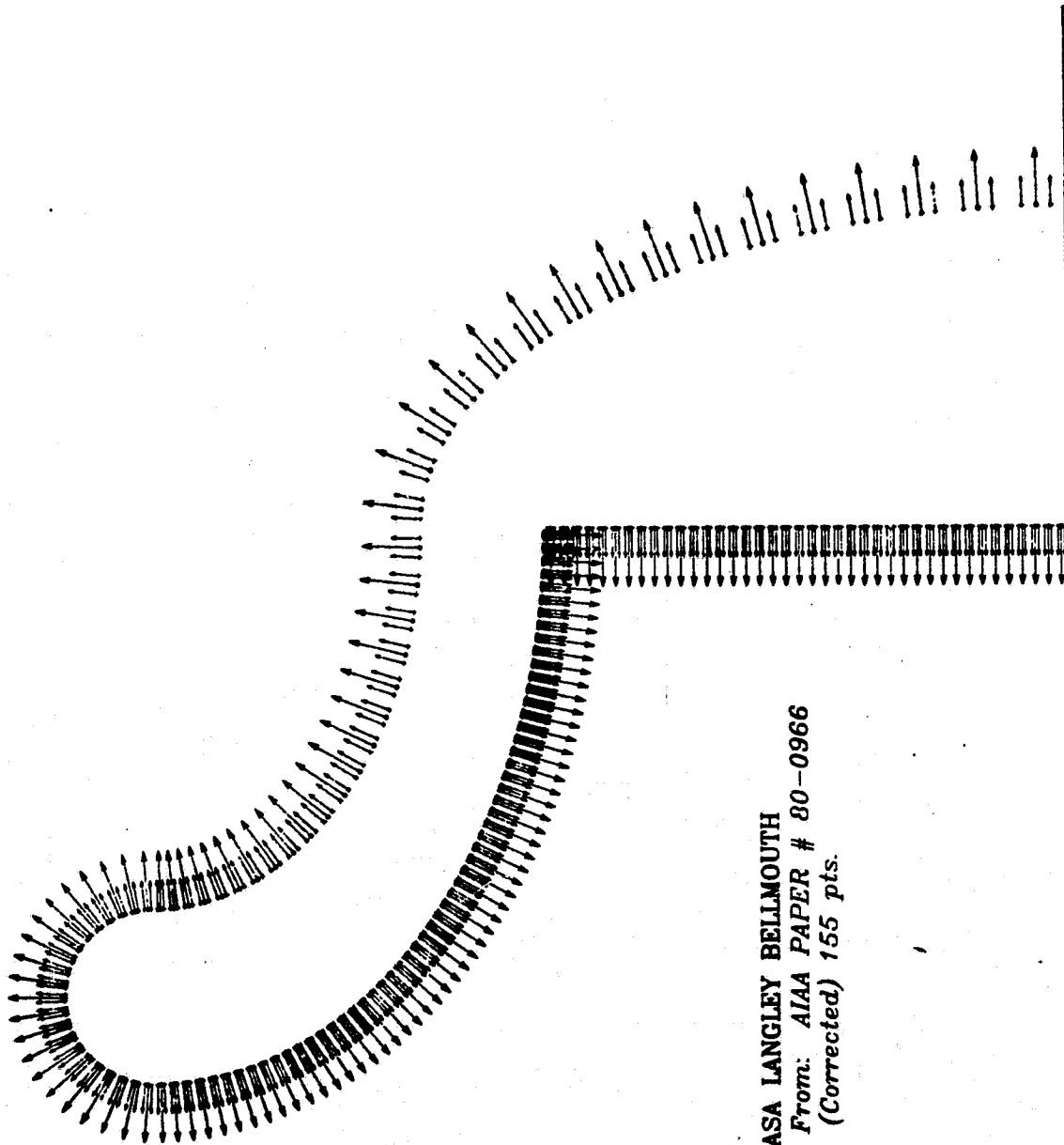


Fig. 1

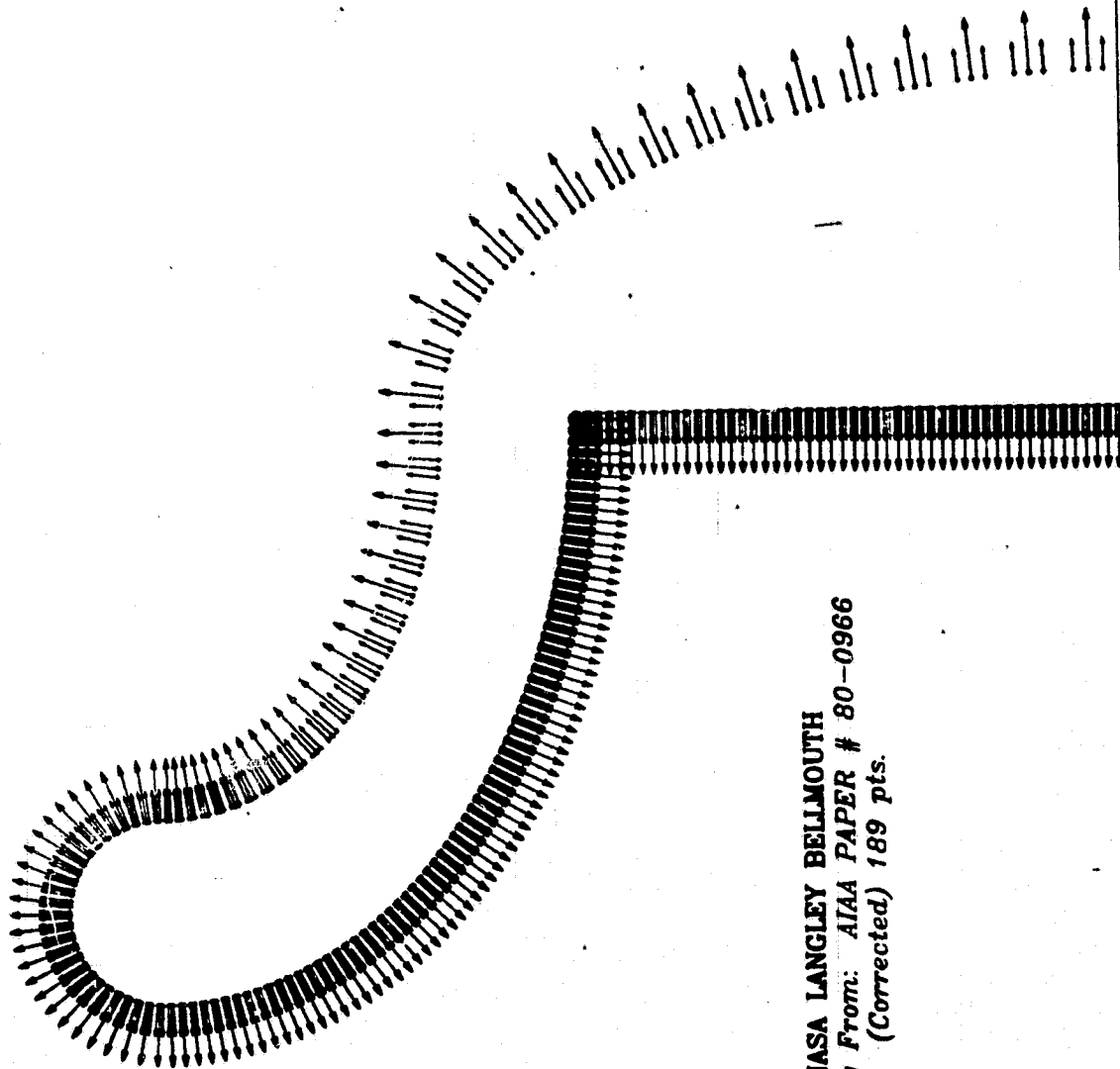
ORIGINAL PAGE IS
OF POOR QUALITY



NASA LANGLEY BELLMOUTH
Geometry From: AIAA PAPER # 80-0966
(Corrected) 155 pts.

Fig. 2

ORIGINAL PAGE IS
OF POOR QUALITY



NASA LANGLEY BELLMOUTH
Geometry From: AIAA PAPER # 80-0966
(Corrected) 189 pts.

Fig. 3

ORIGINAL PAGE IS
OF POOR QUALITY

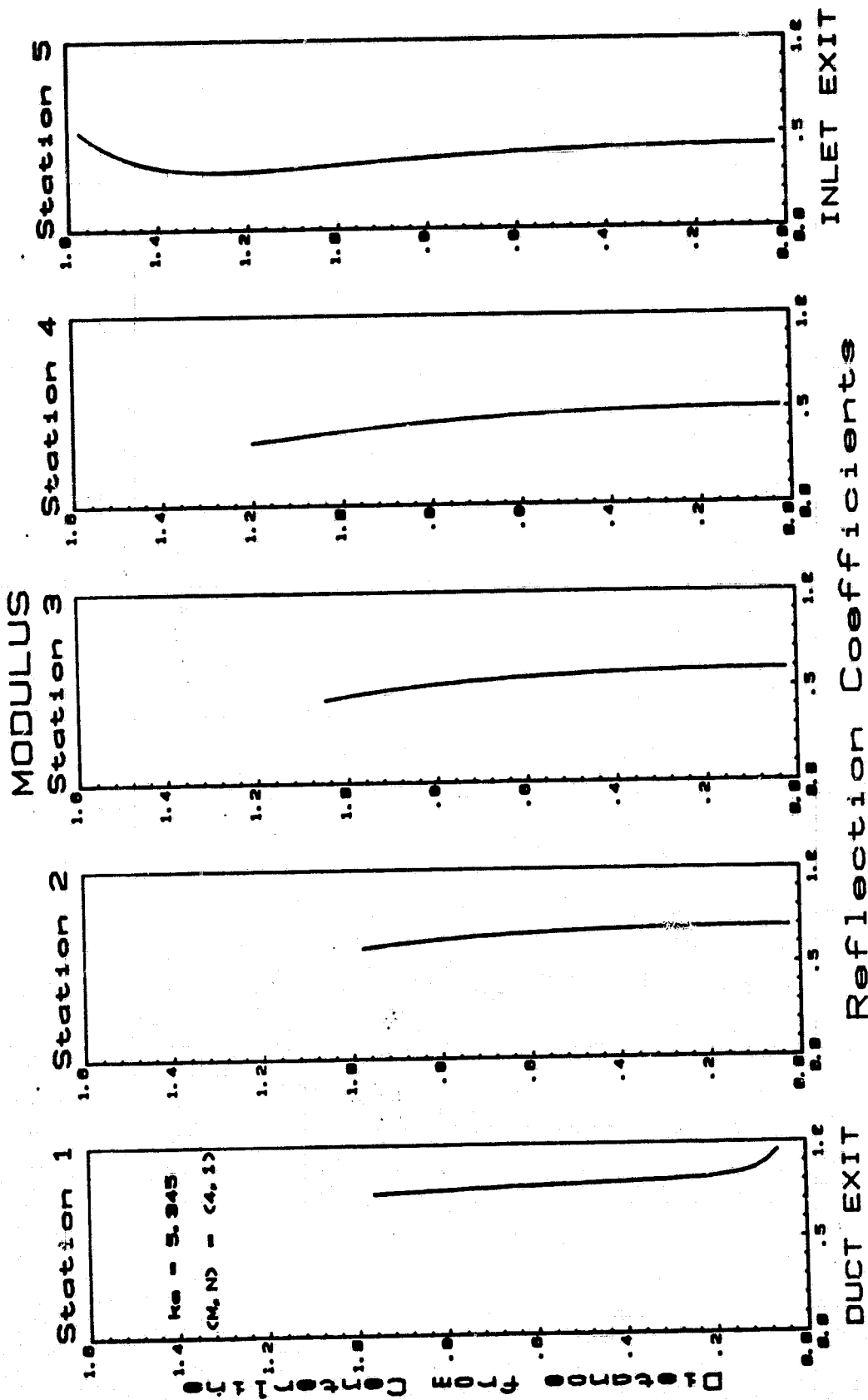


Fig. 4a

LANGLEY BELLMOUTH

ORIGINAL PAGE IS
OF POOR QUALITY

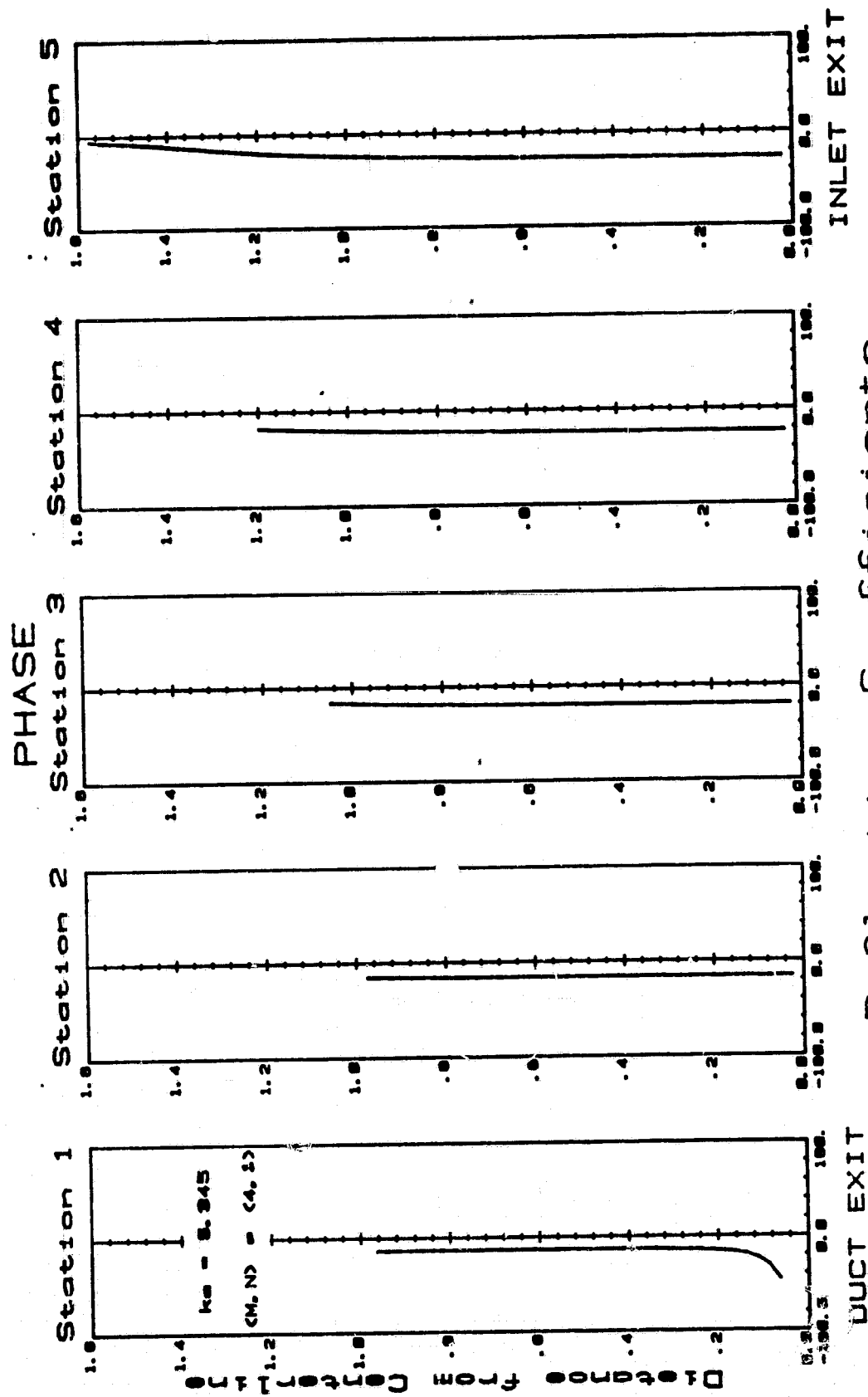


Fig. 4b

ORIGINAL PAGE IS
OF POOR QUALITY

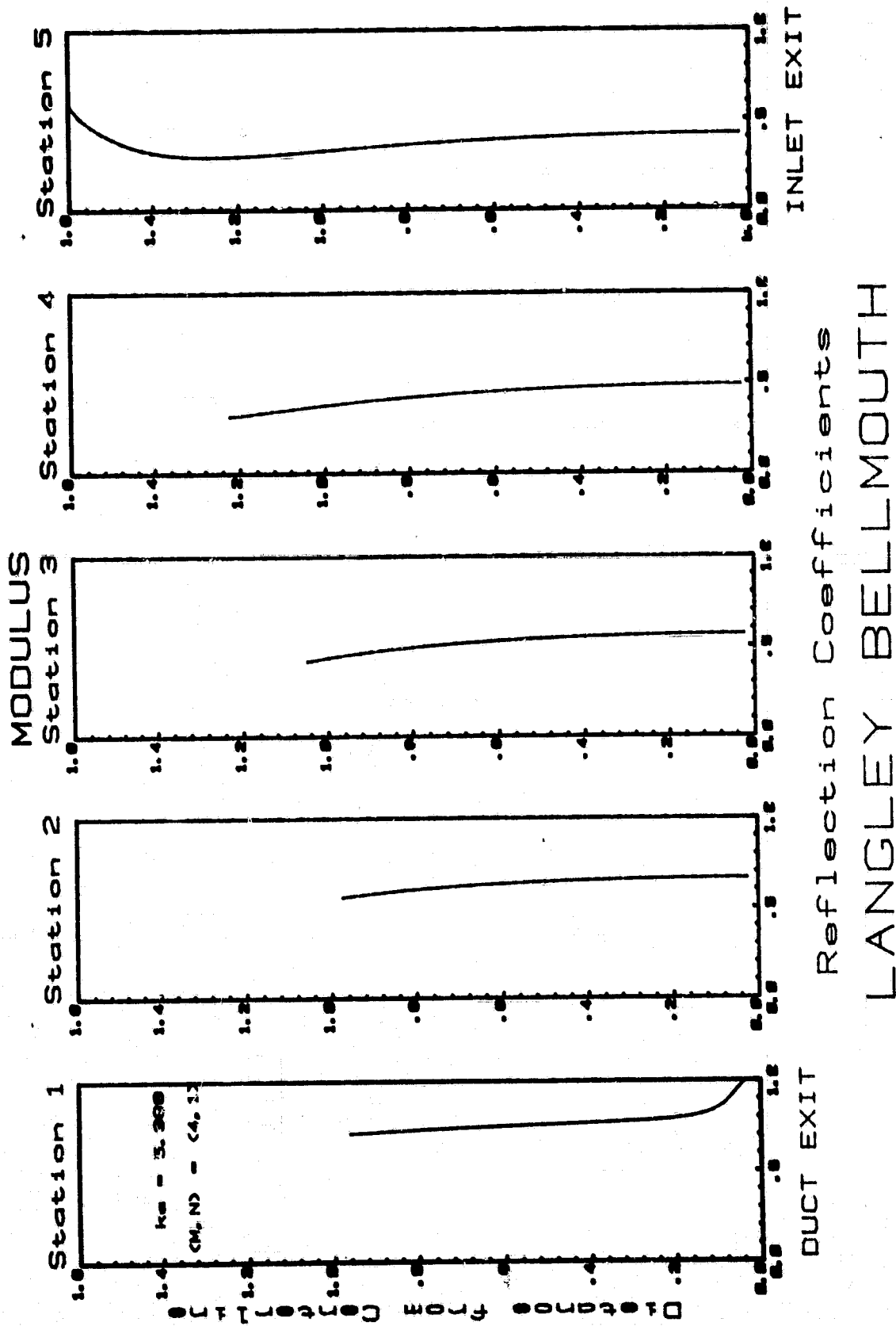


Fig. 4c

ORIGINAL PAGE IS
OF POOR QUALITY

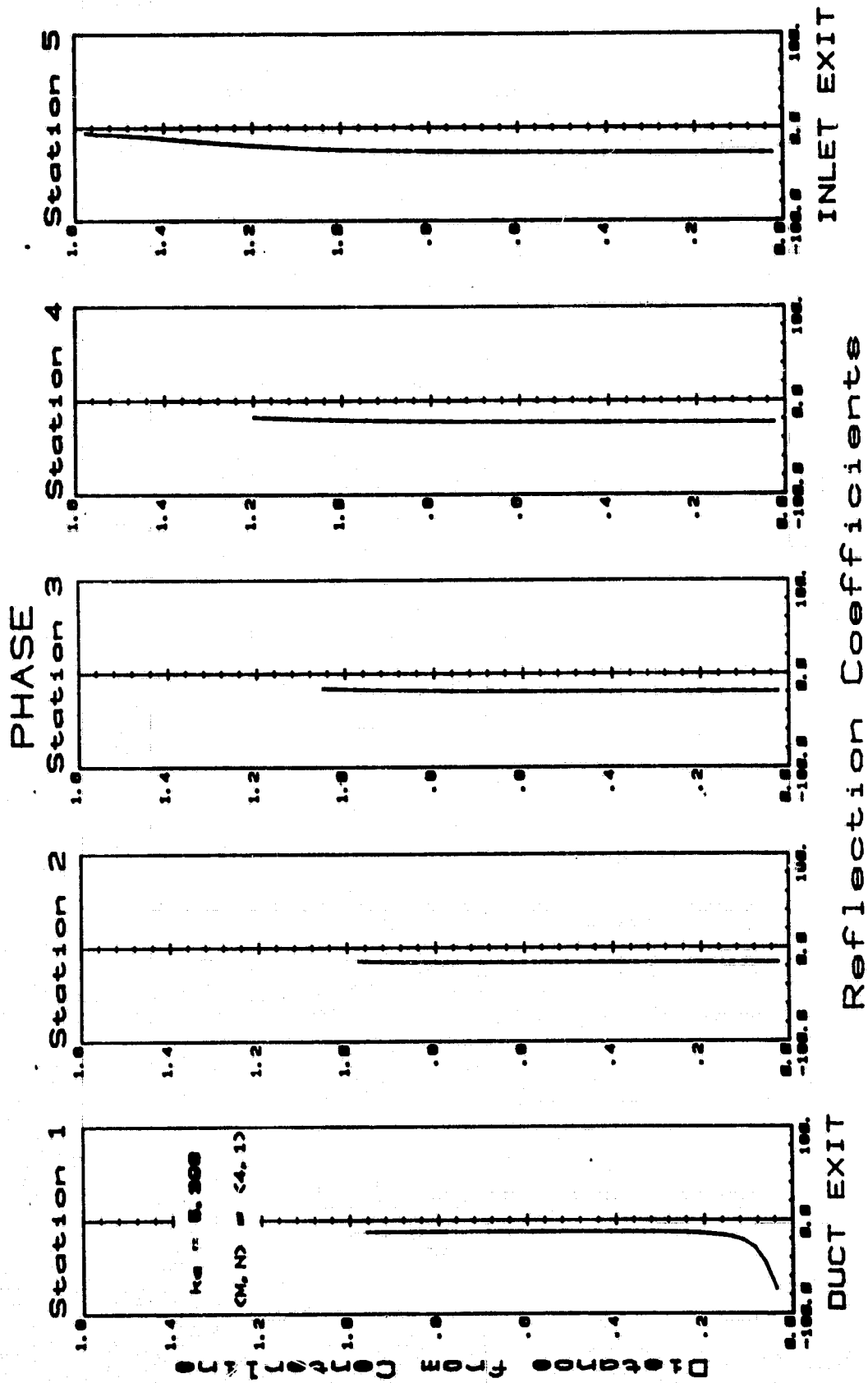


Fig. 4d

LANGLEY BELLMOUTH

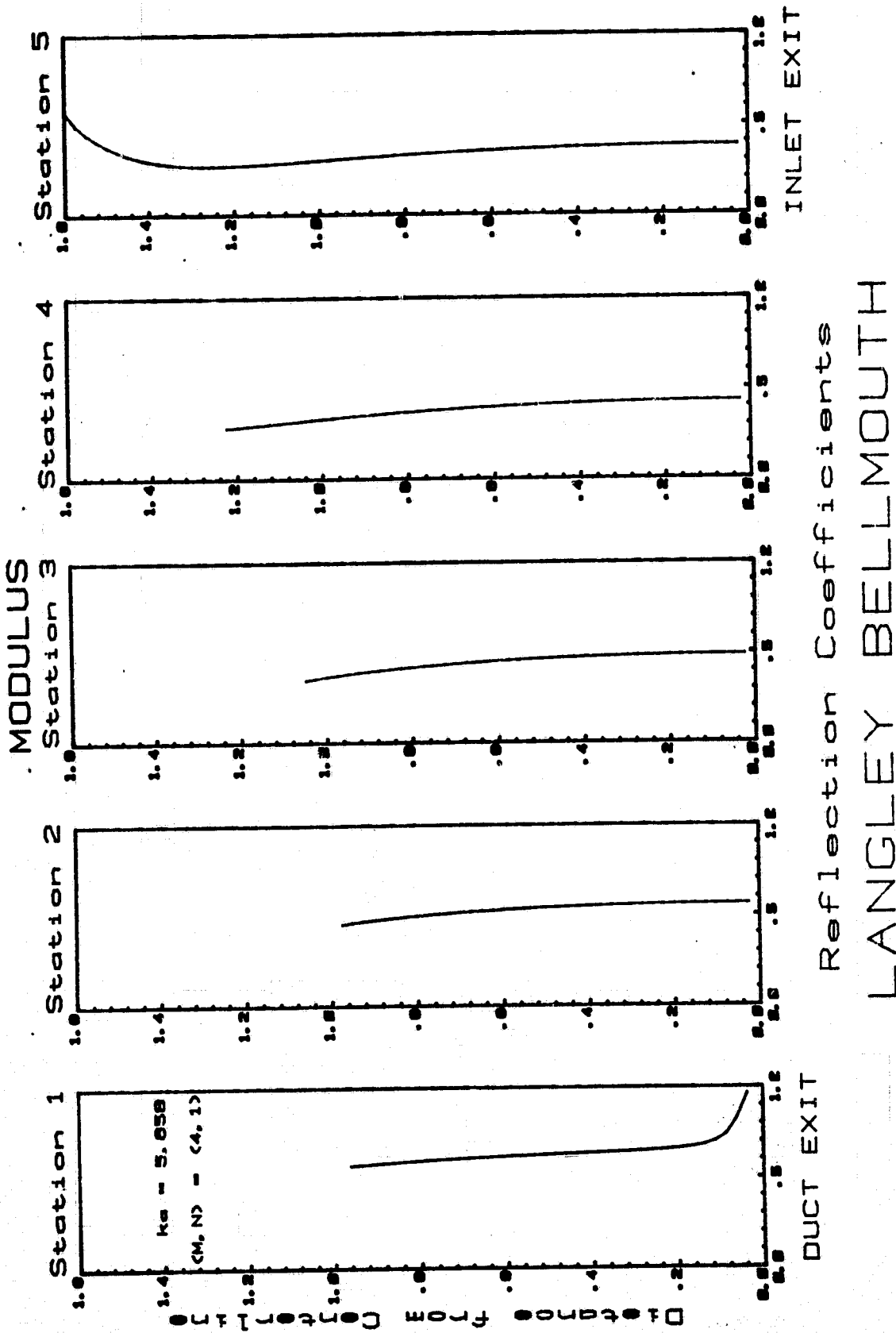
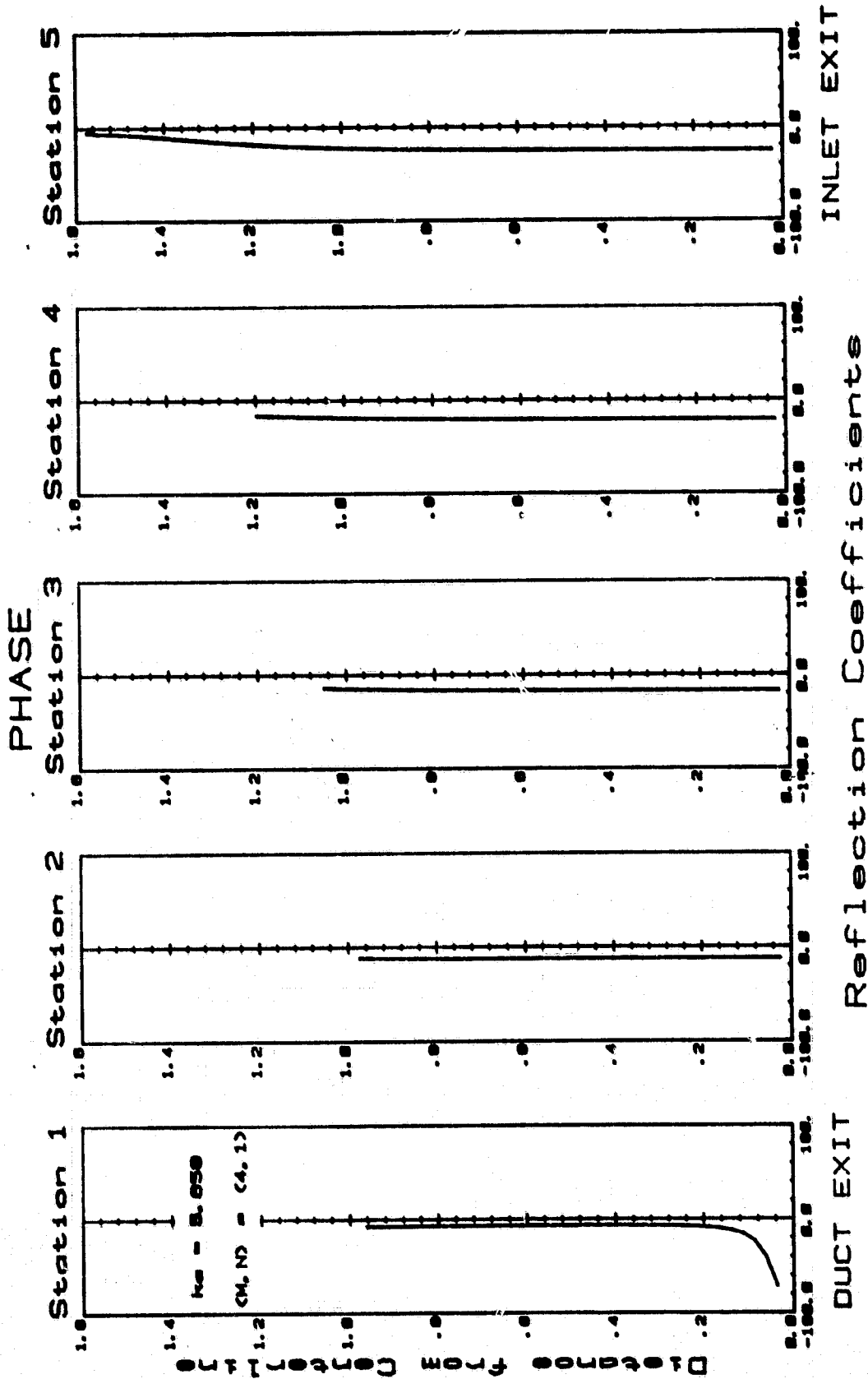


Fig. 4e

ORIGINAL PAGE IS
OF POOR QUALITY



LANGLEY BELLMOUTH

Fig. 4f

ORIGINAL PAGE IS
OF POOR QUALITY

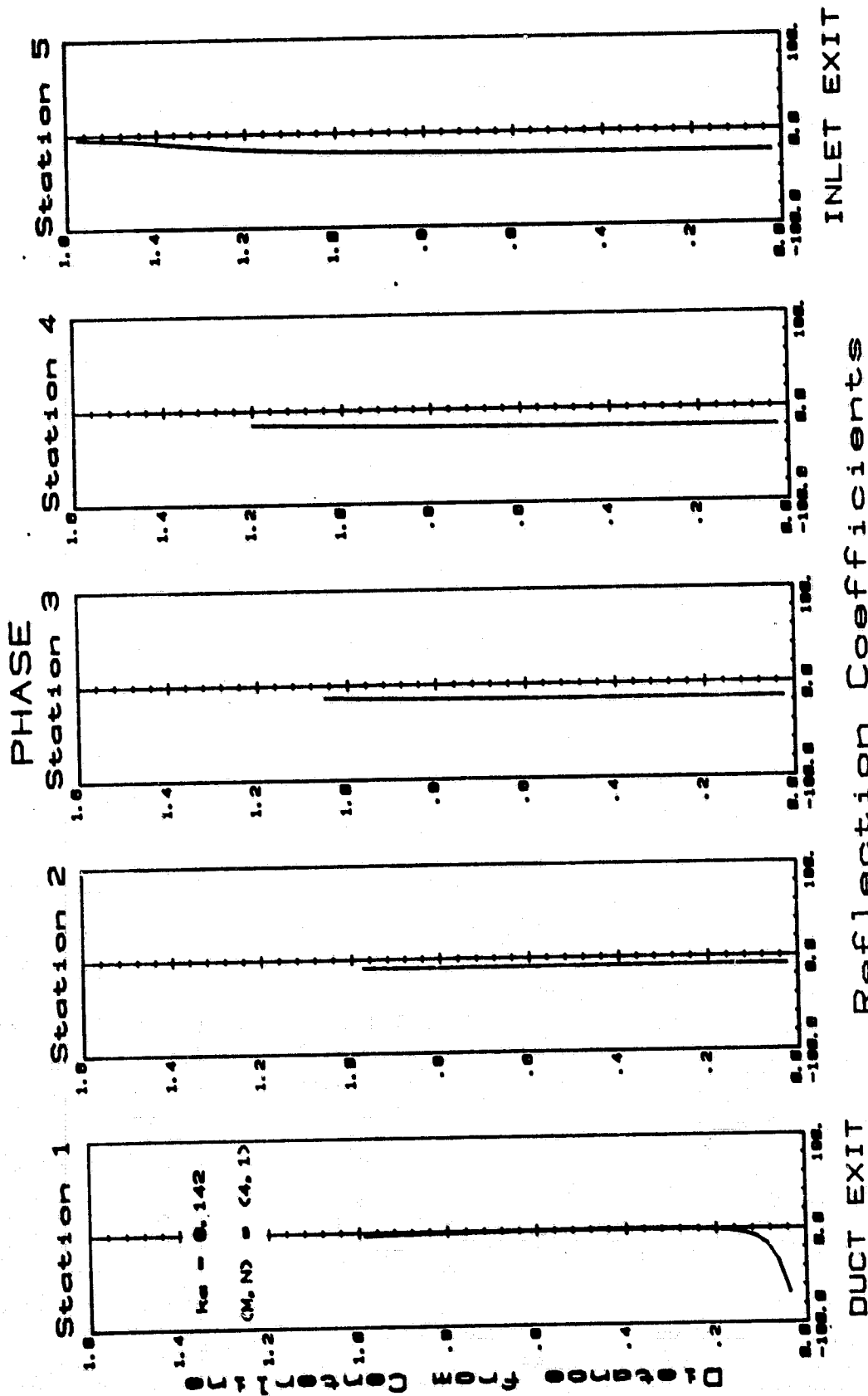


Fig. 48

ORIGINAL PAGE IS
OF POOR QUALITY

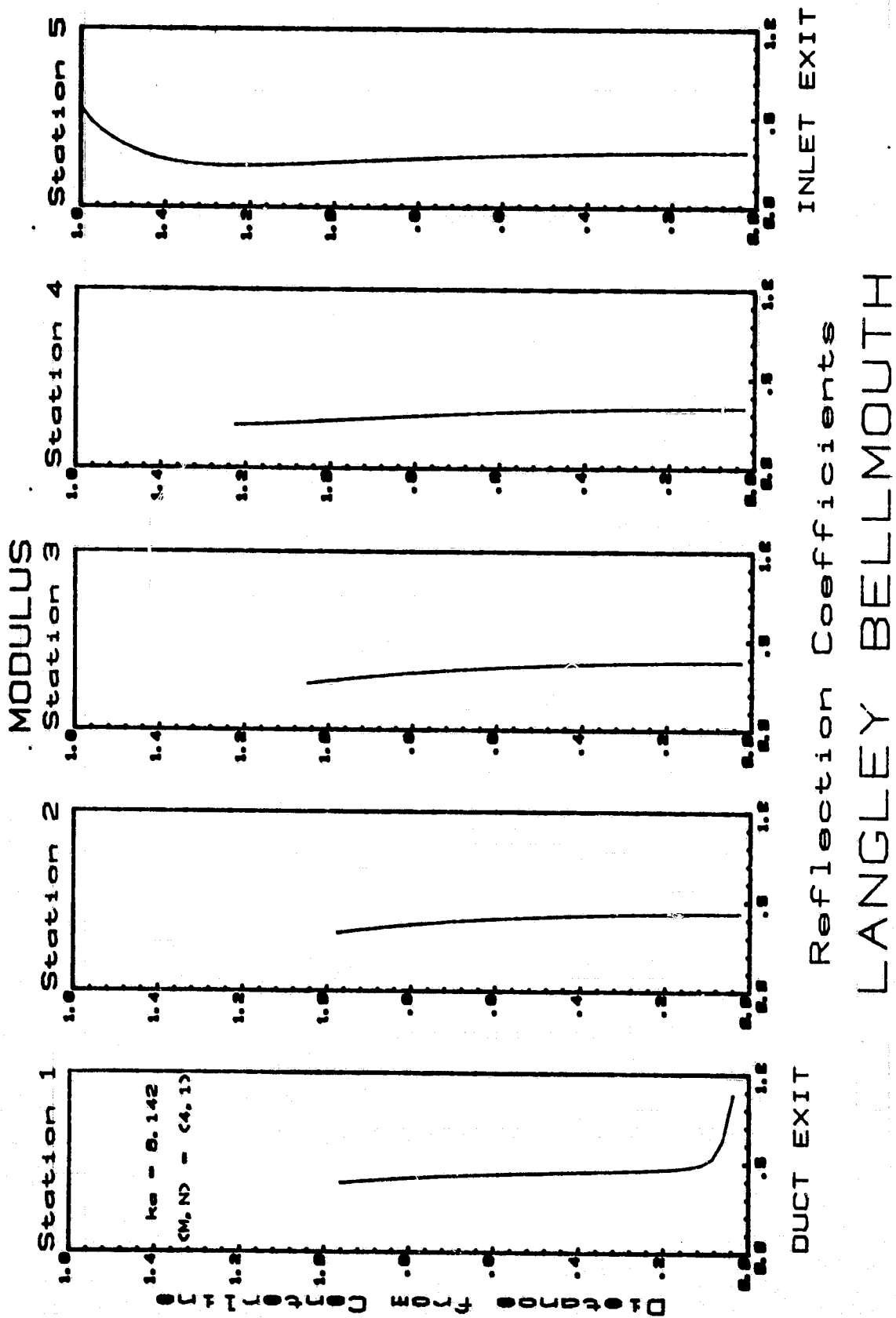


Fig. 4h

ORIGINAL PAGE IS
OF POOR QUALITY

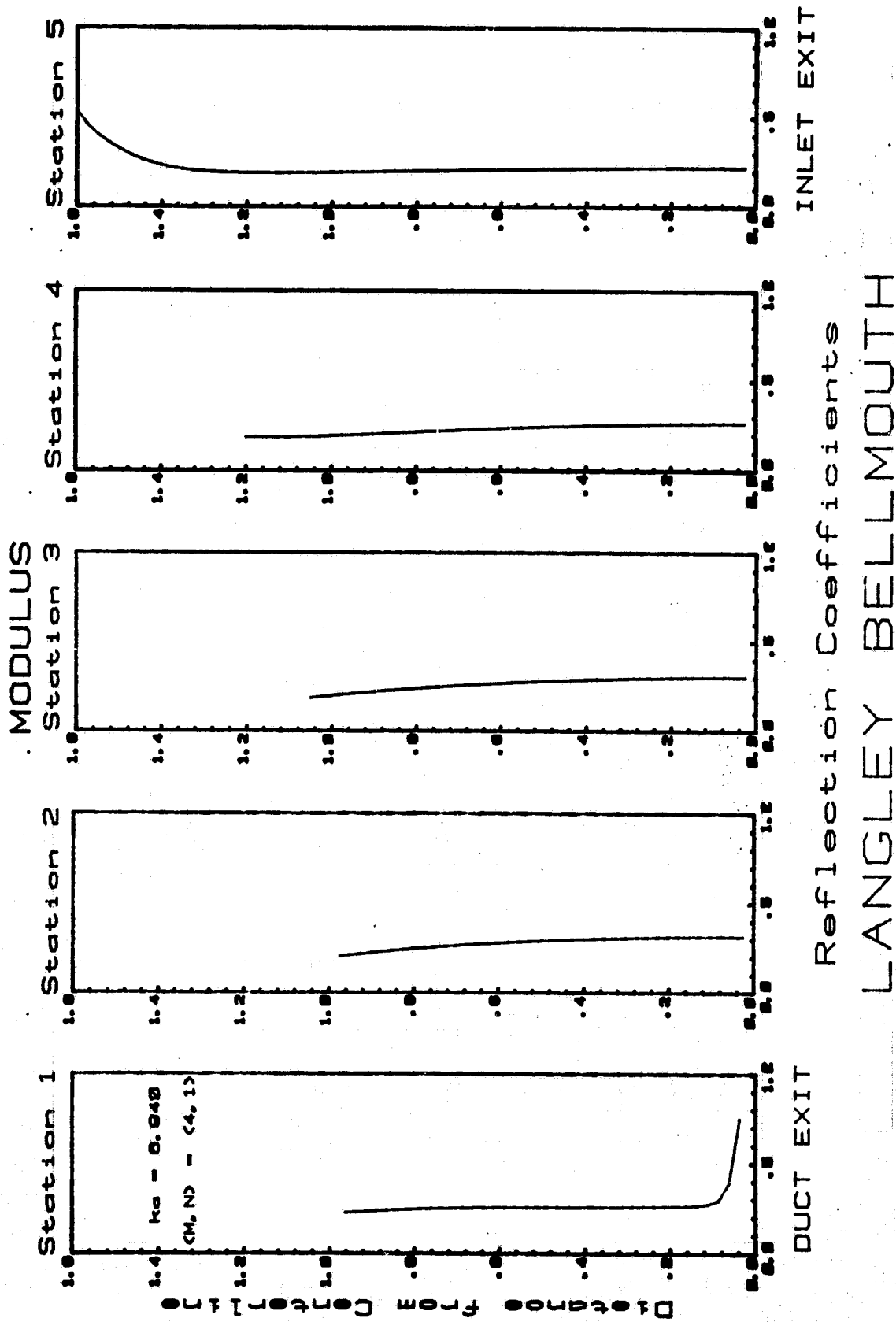
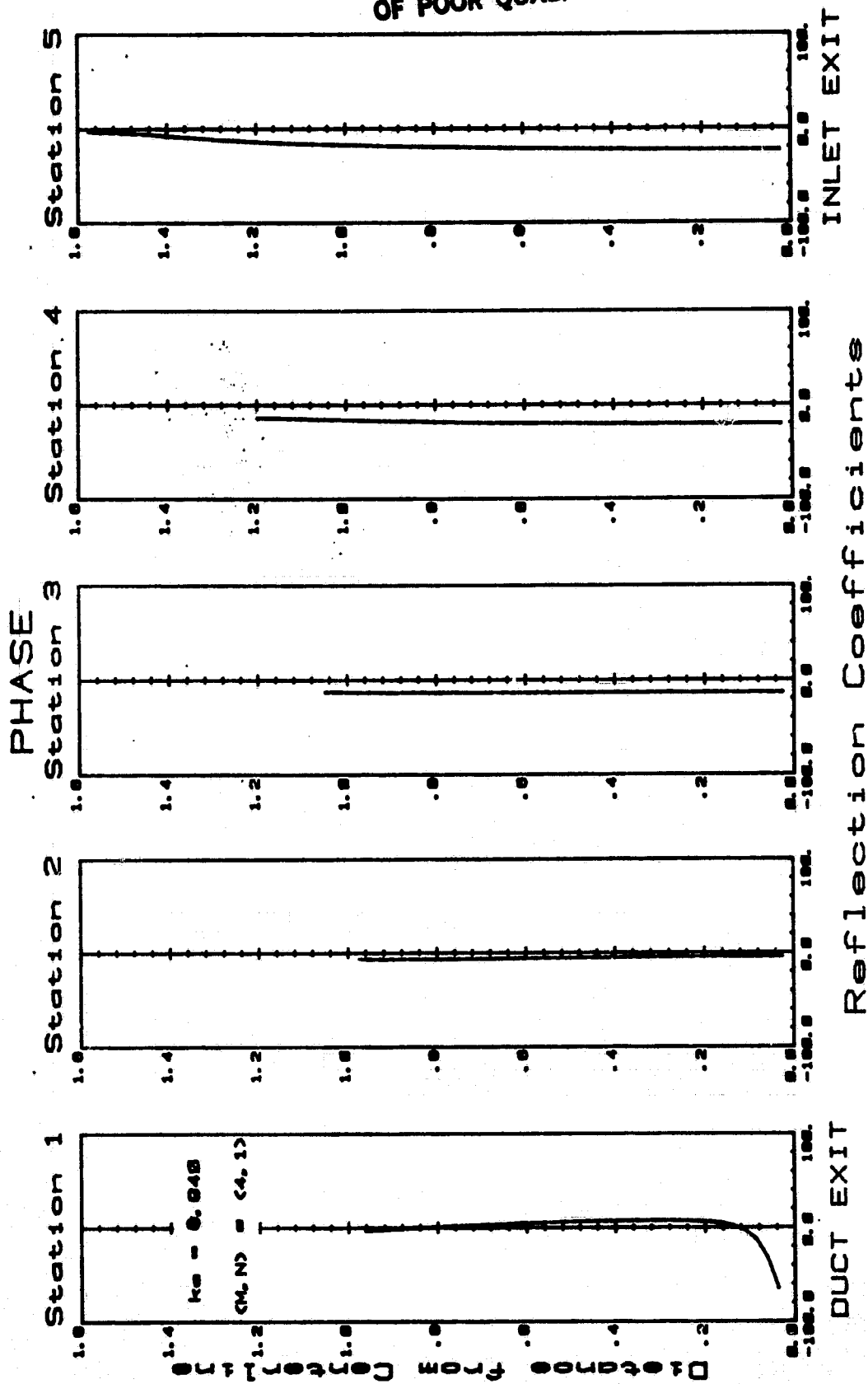


Fig. 41

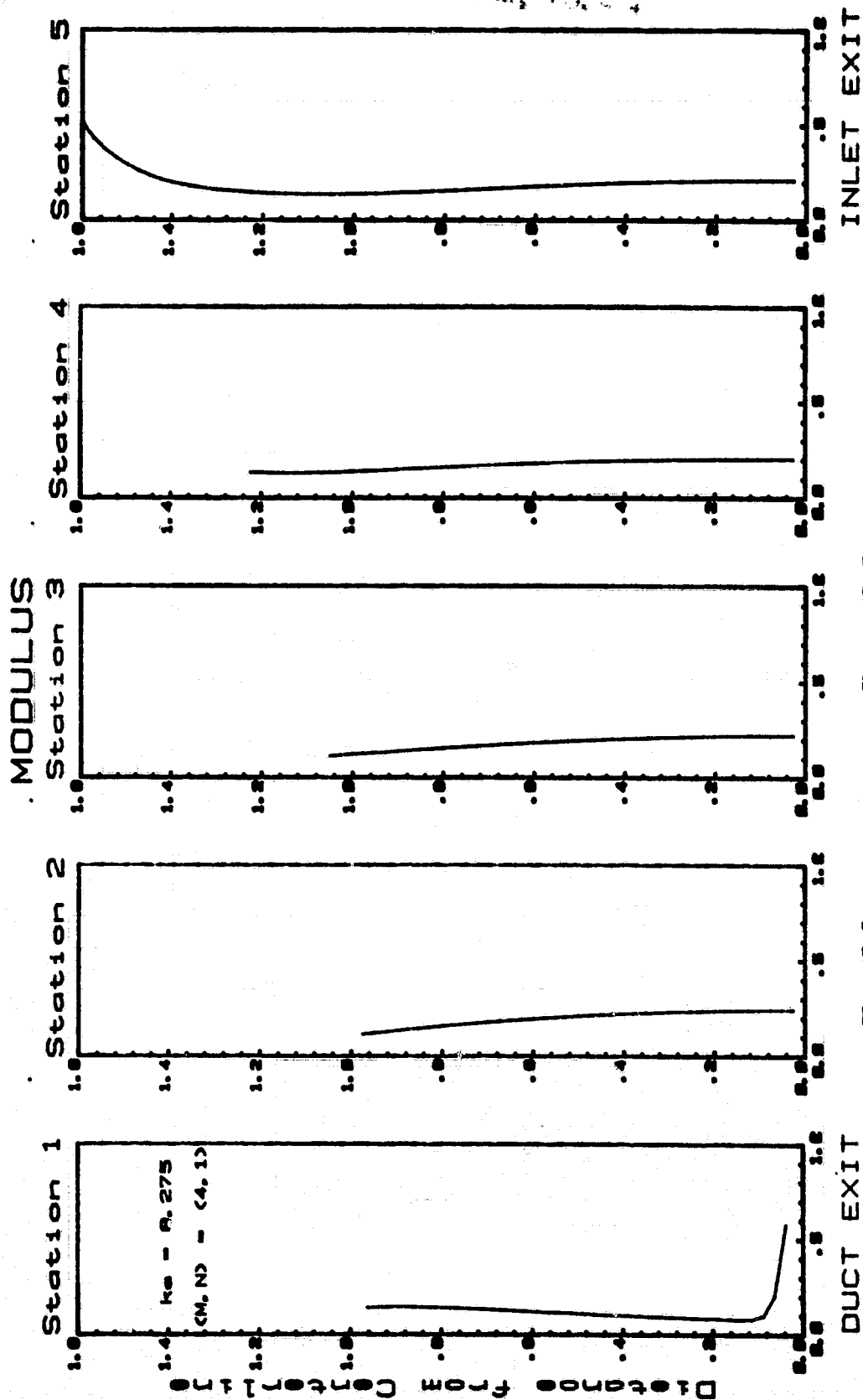
2 2000 1000000
 71140 2000 1000000
 ORIGINAL PAGE IS
 OF POOR QUALITY



LANGLEY BELLMOUTH

Fig. 4j

ORIGINAL PAGE IS
OF POOR QUALITY



ORIGINAL PAGE IS
OF POOR QUALITY

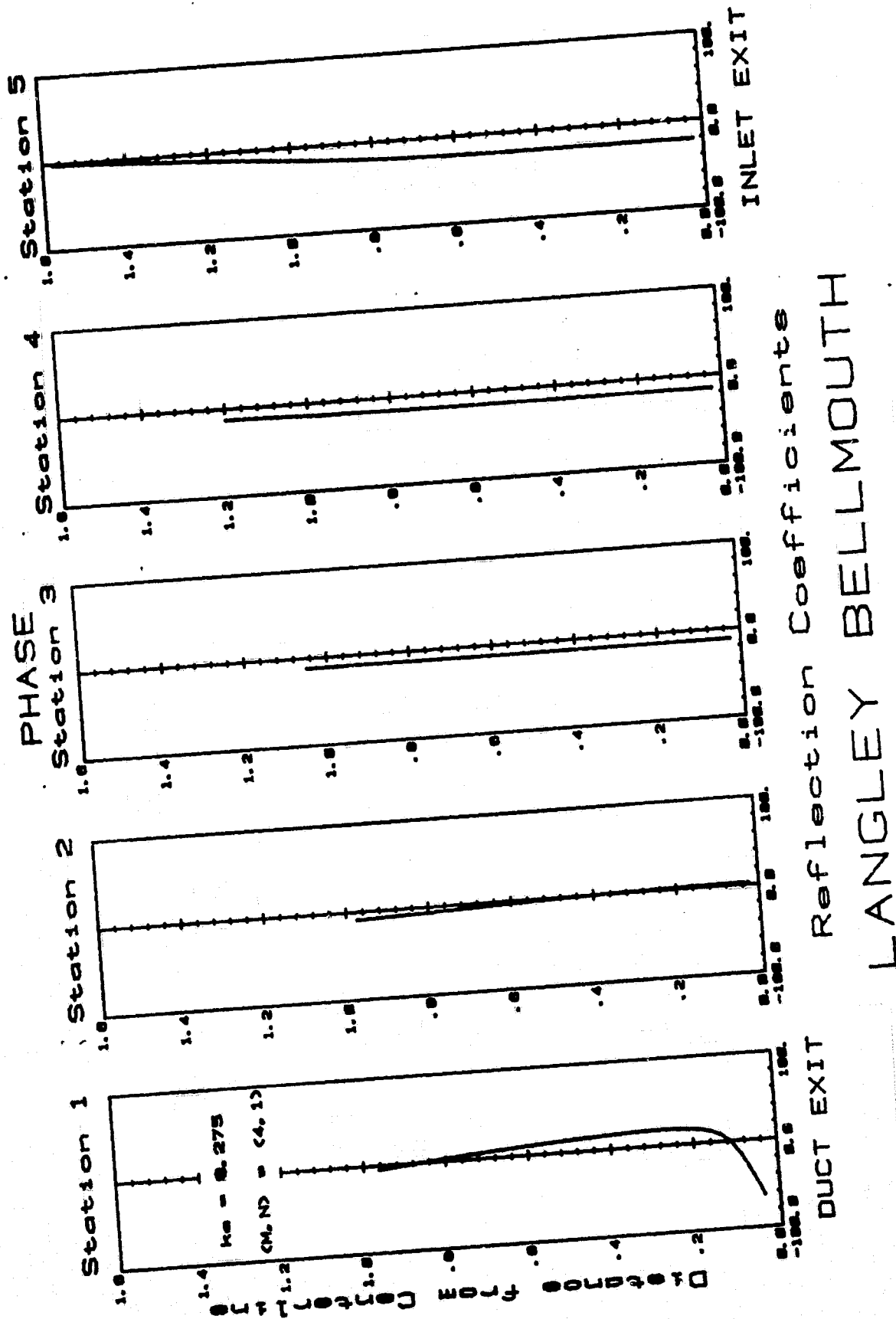


Fig. 41

ORIGINAL PAGE IS
OF POOR QUALITY

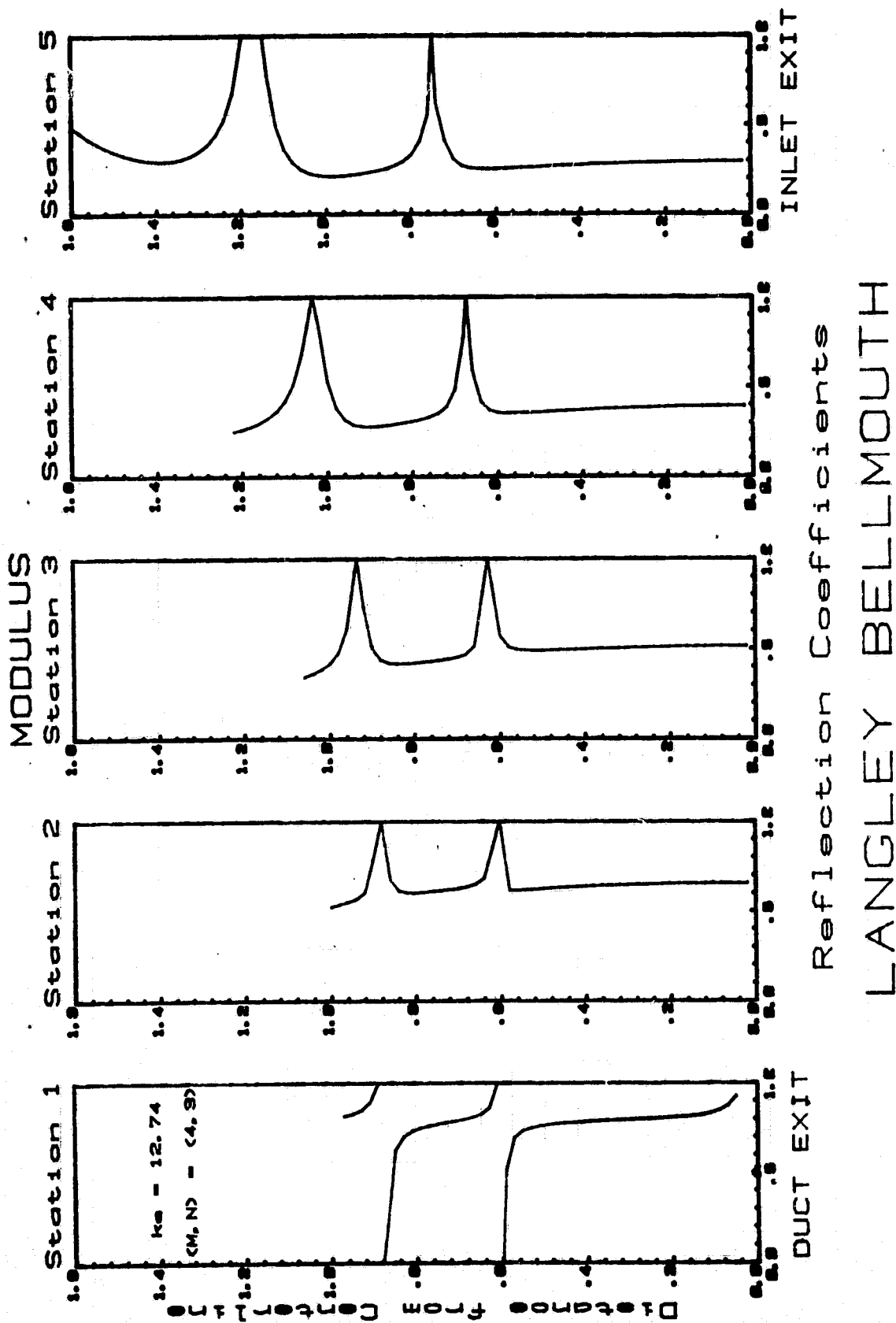
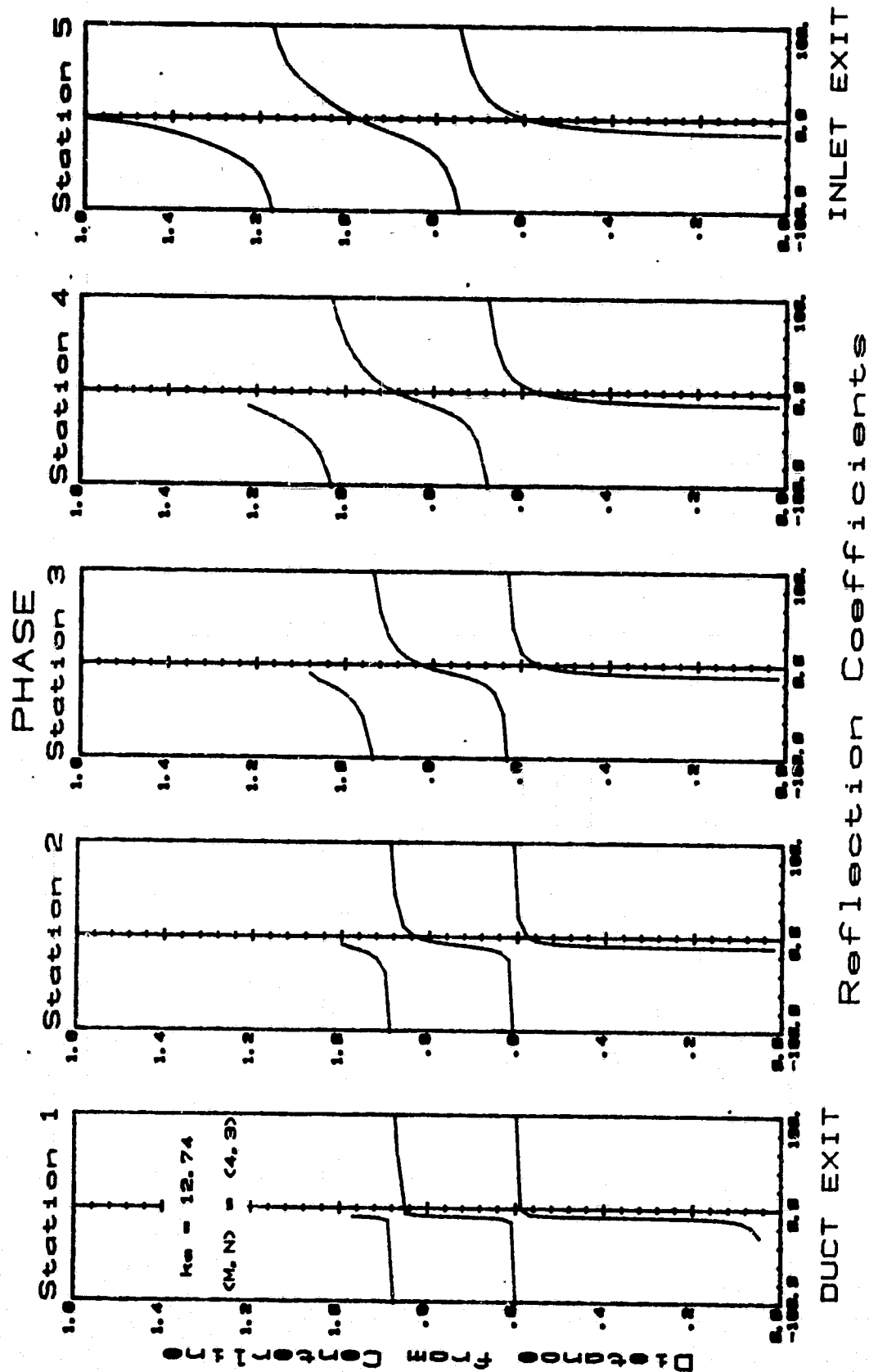


Fig. 5a

ORIGINAL PAGE IS
OF POOR QUALITY



LANGLEY BELLMOUTH

Fig. 5b

ORIGINAL PAGE IS
OF POOR QUALITY

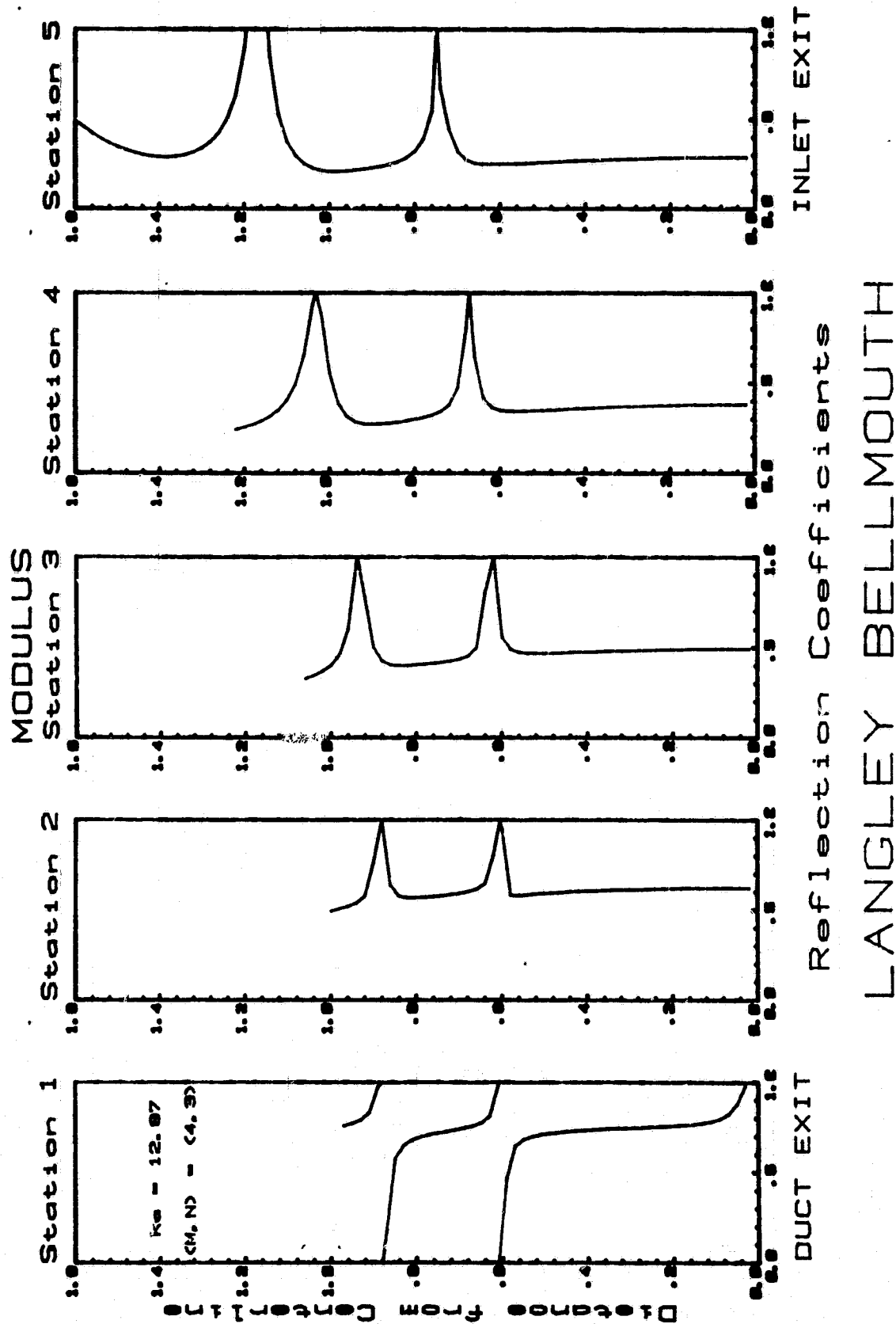


Fig. 5c

ORIGINAL PAGE IS
OF POOR QUALITY

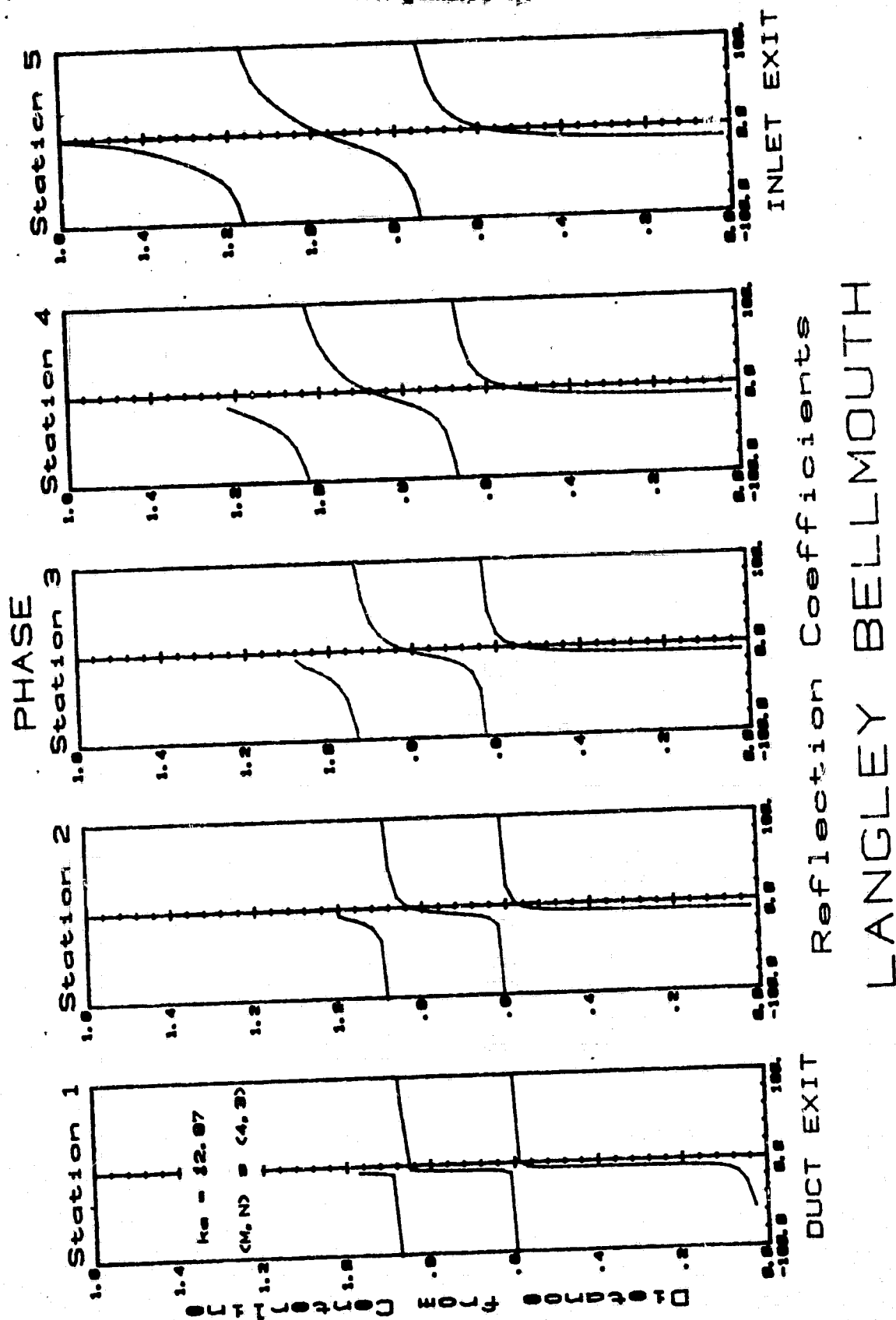
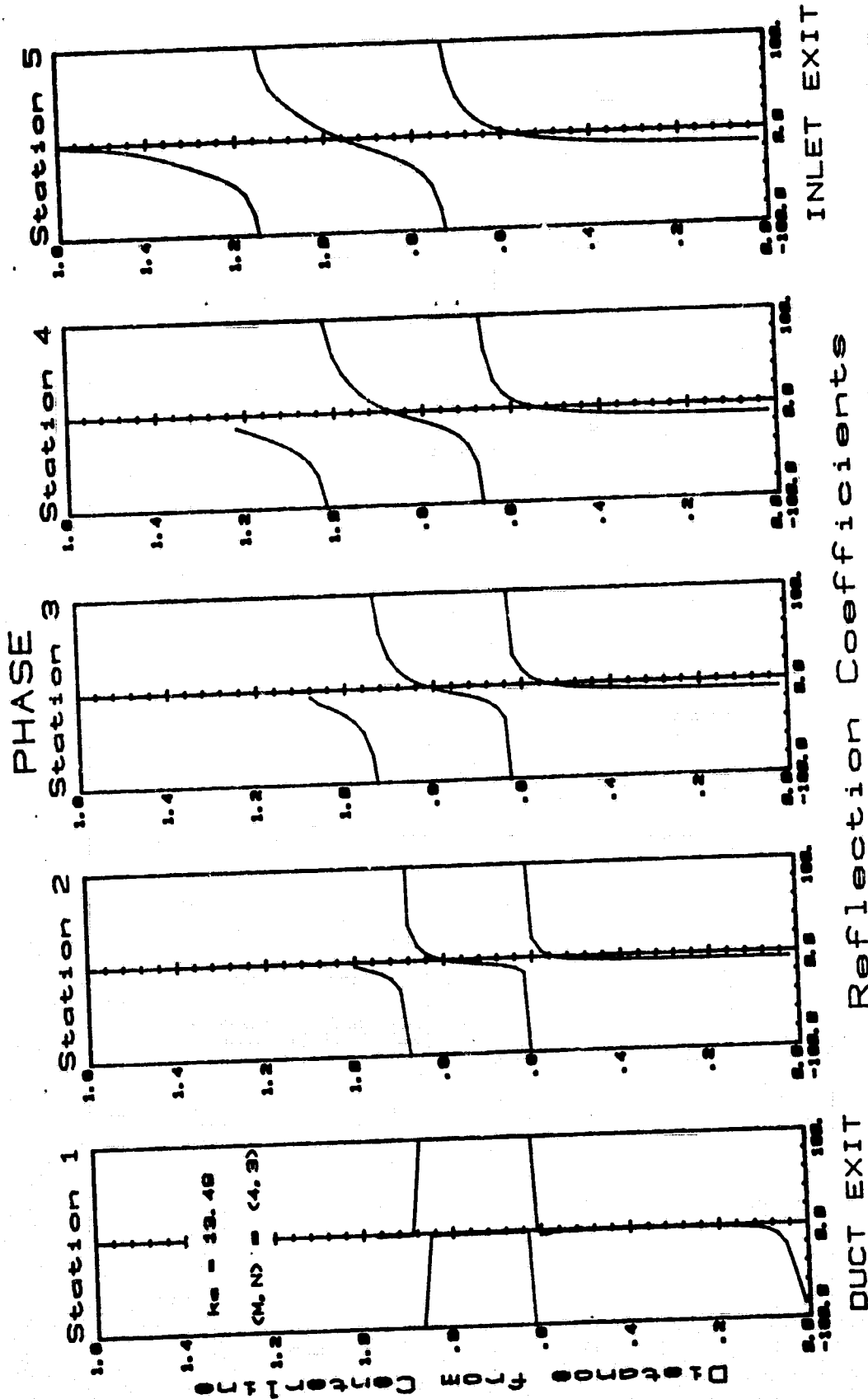


Fig. 5d

LANGLEY BELLMOUTH

Fig. 5c

ORIGINAL PAGE IS
OF POOR QUALITY



LANGLEY BELLMOUTH

Fig. 5f

ORIGINAL PAGE IS
OF POOR QUALITY

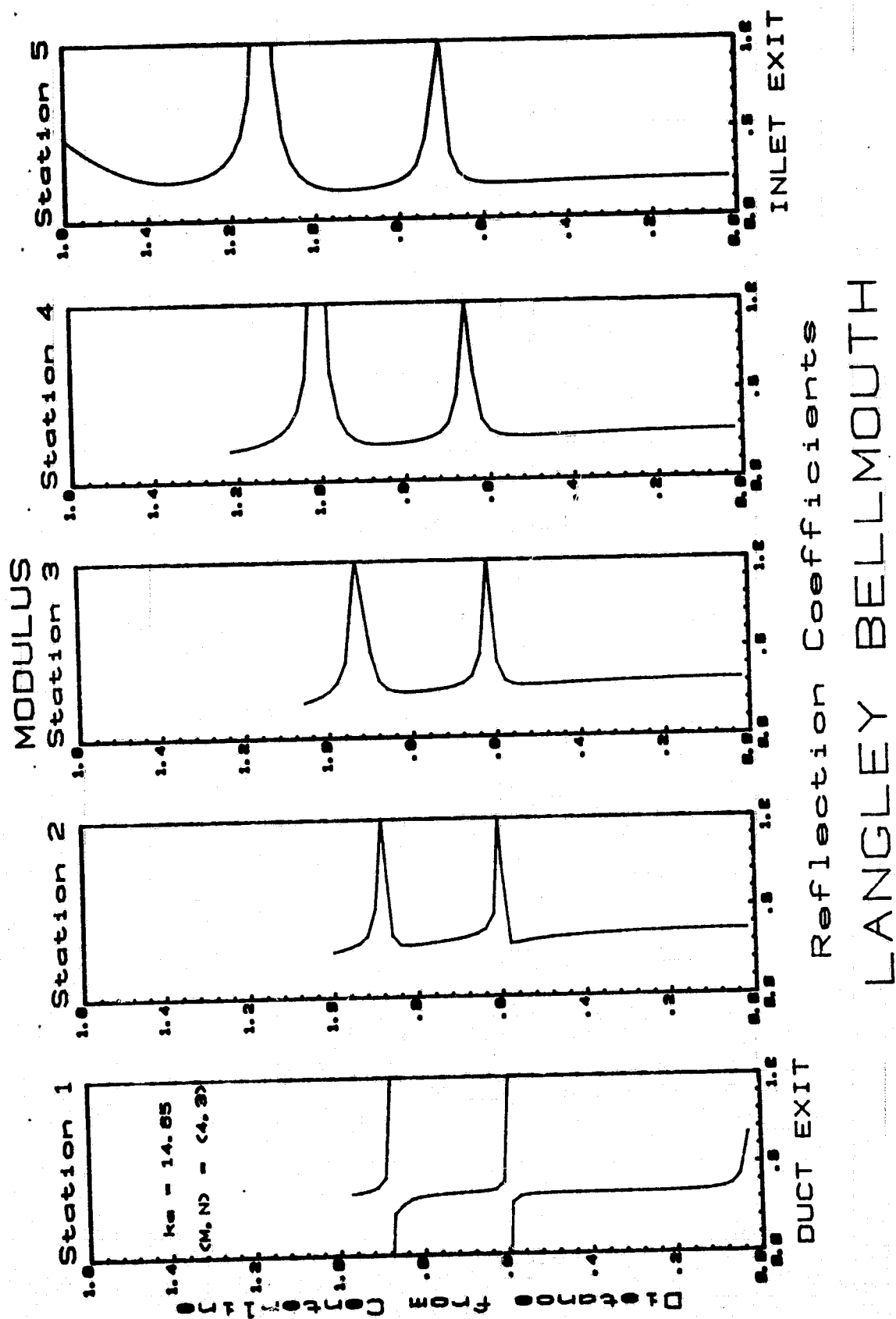


Fig. 5g

ORIGINAL PAGE IS
OF POOR QUALITY

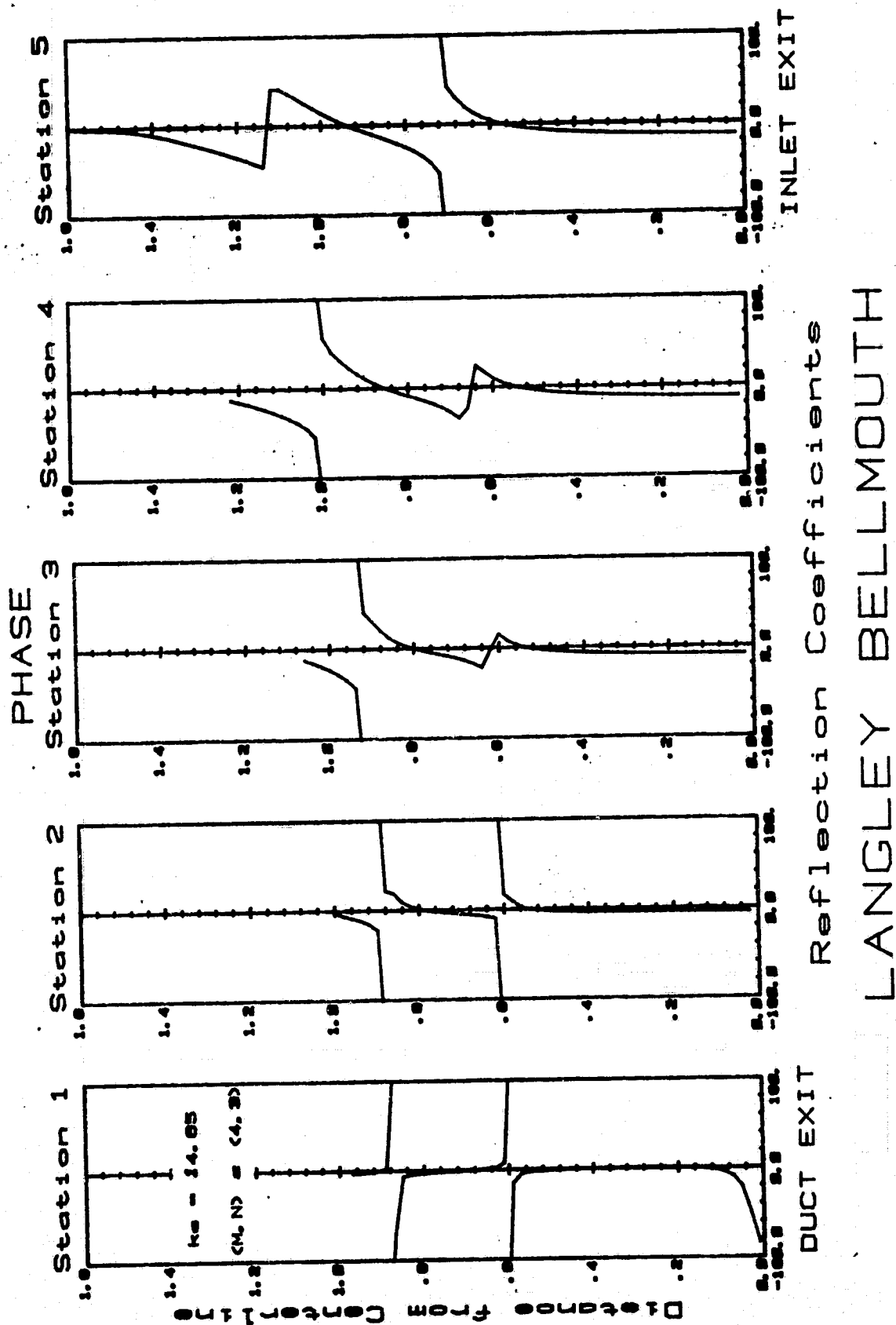


Fig. 5h

ORIGINAL PAGE IS
OF POOR QUALITY

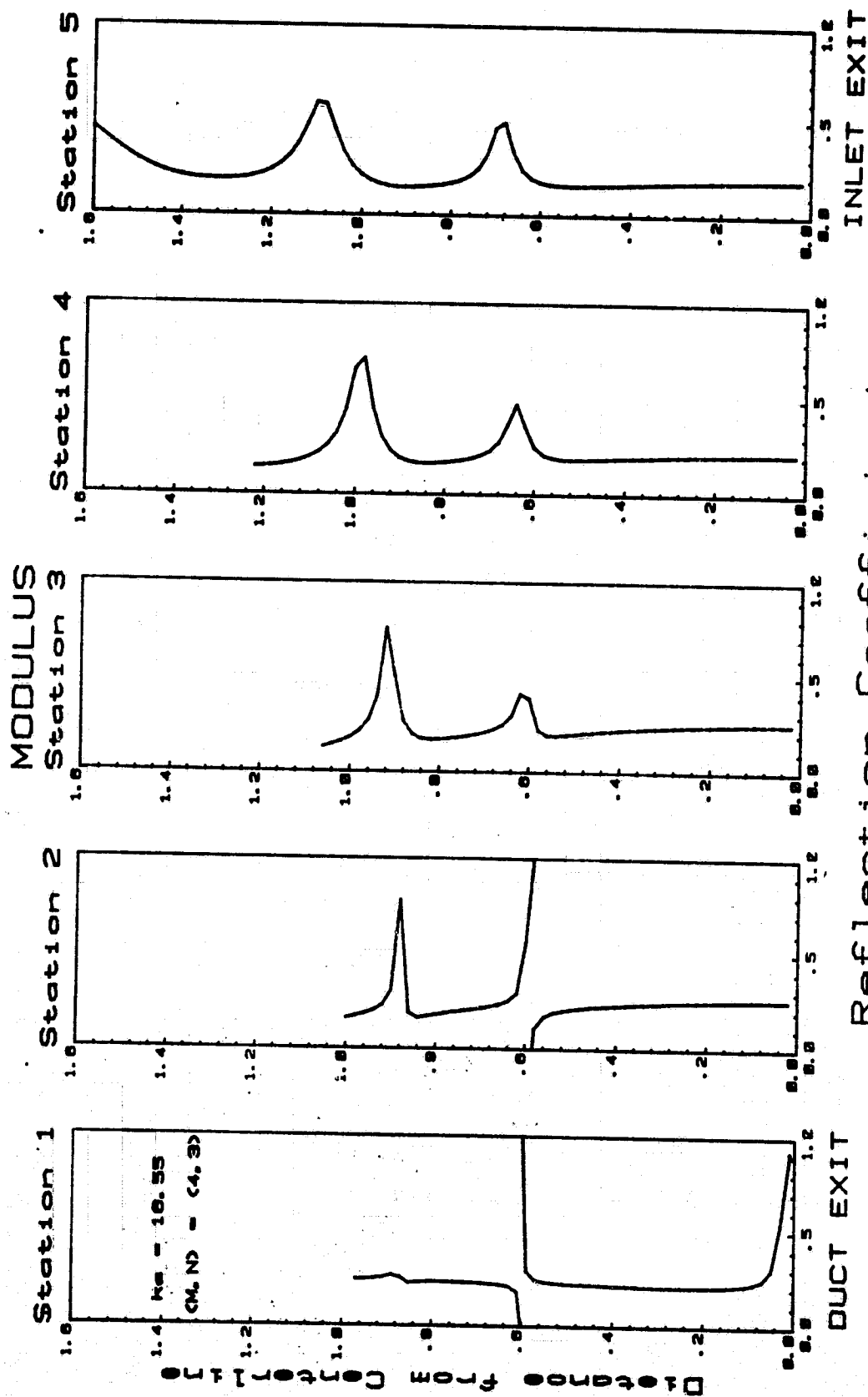


Fig. 51

ORIGINAL PAGE 13
OF POOR QUALITY

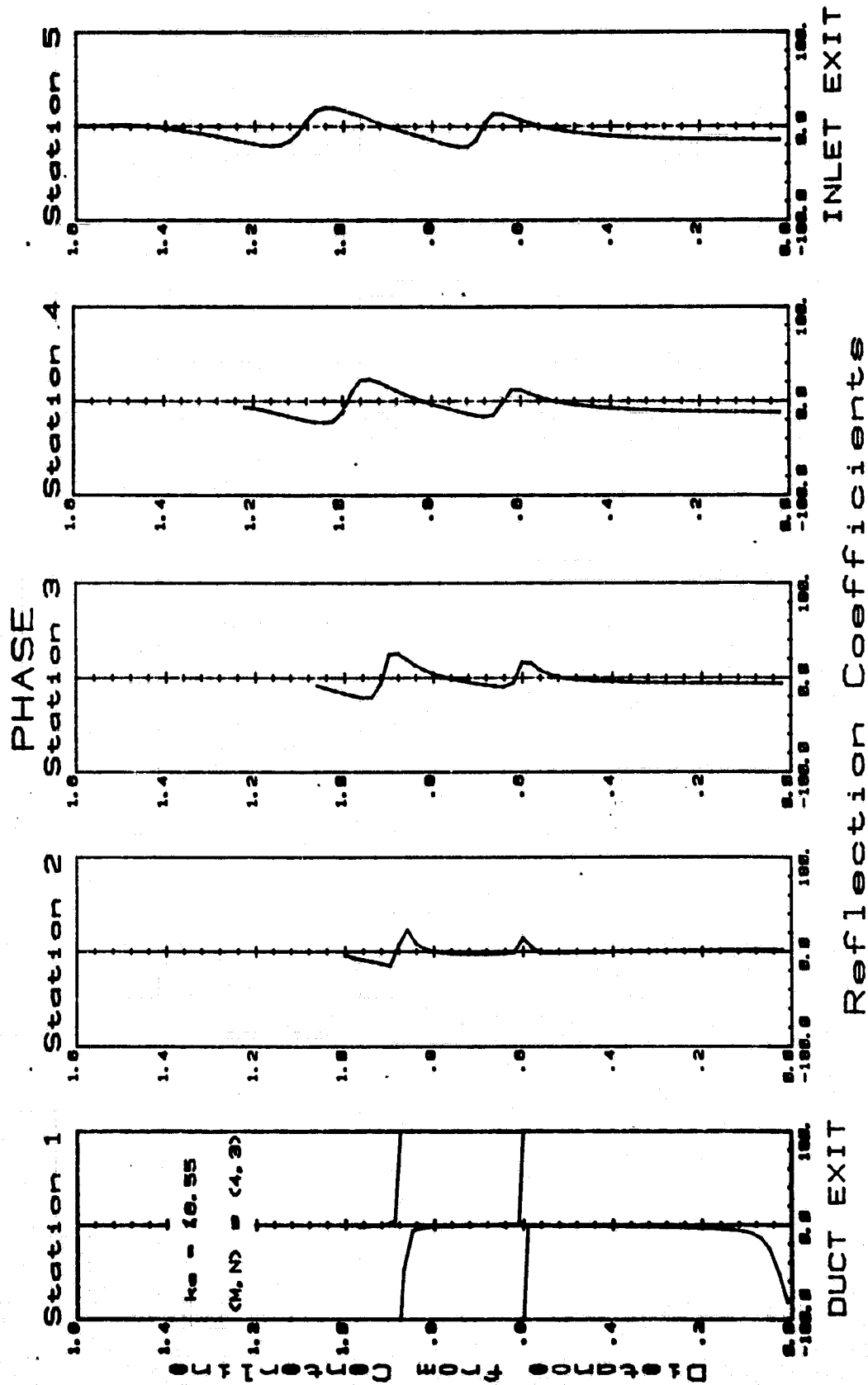


Fig. 5j

LANGLEY BELLMOUTH

ORIGINAL PAGE IS
OF POOR QUALITY

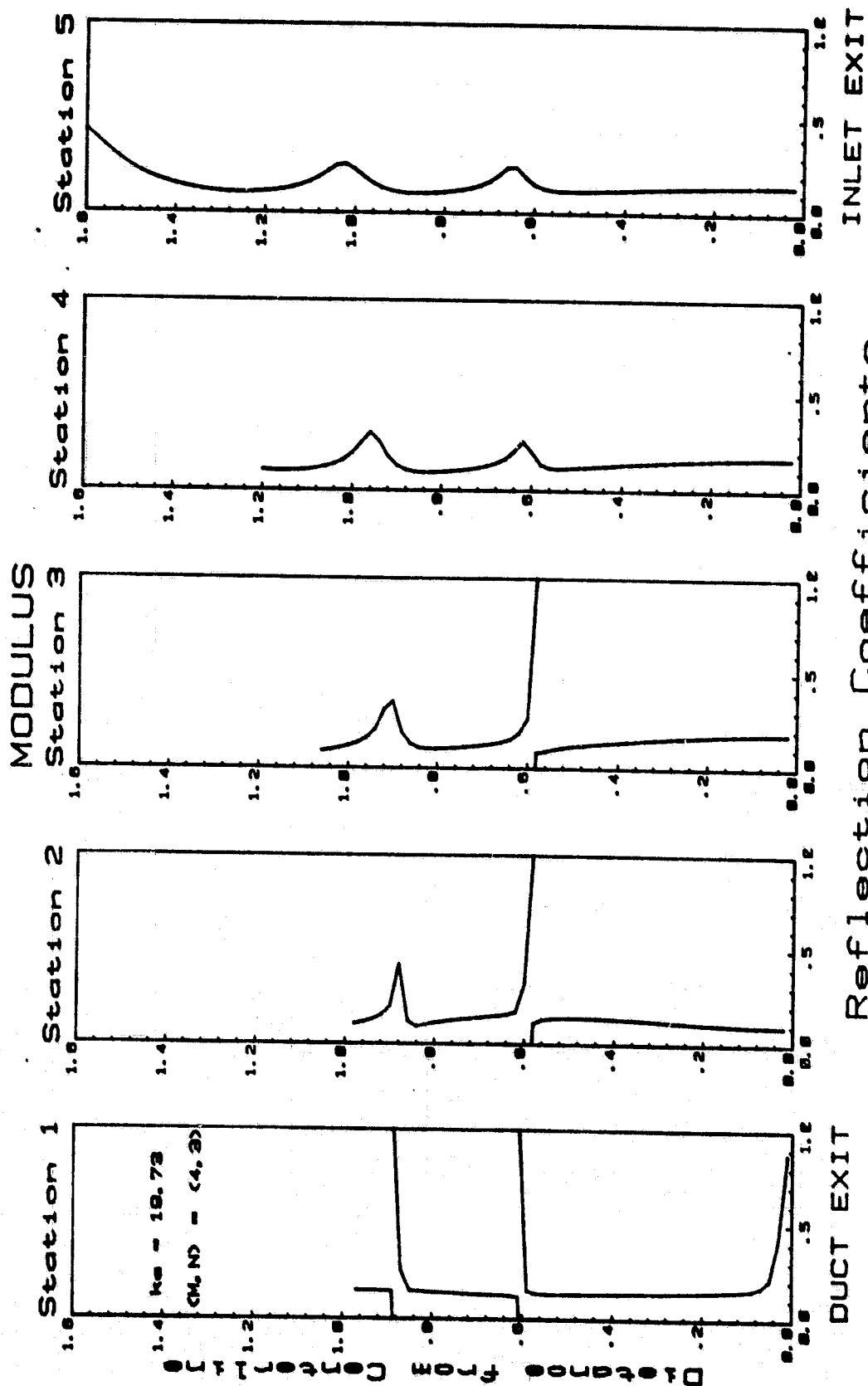


Fig. 5k

LANGLEY BELLMOUTH

ORIGINAL PAGE IS
OF POOR QUALITY

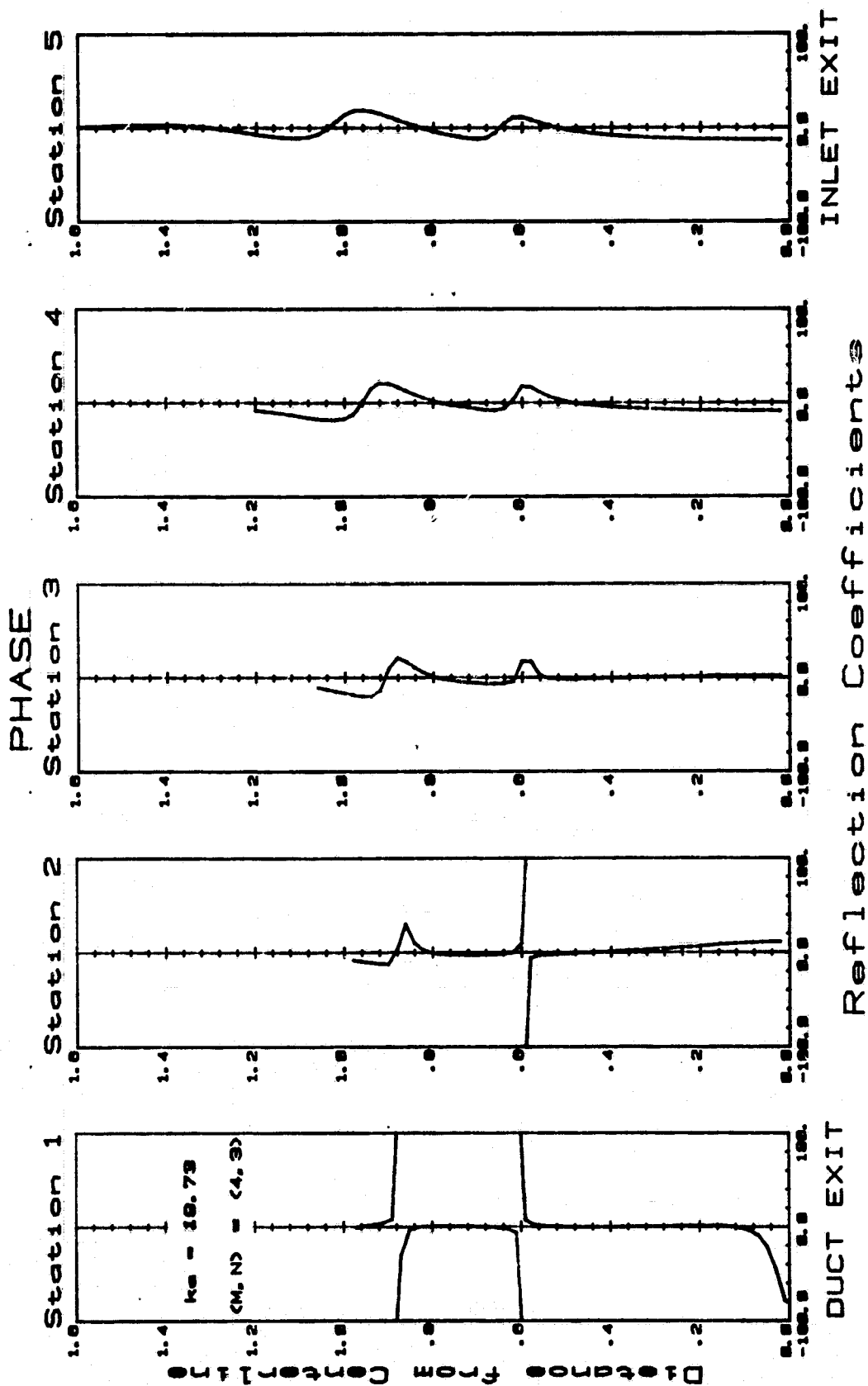
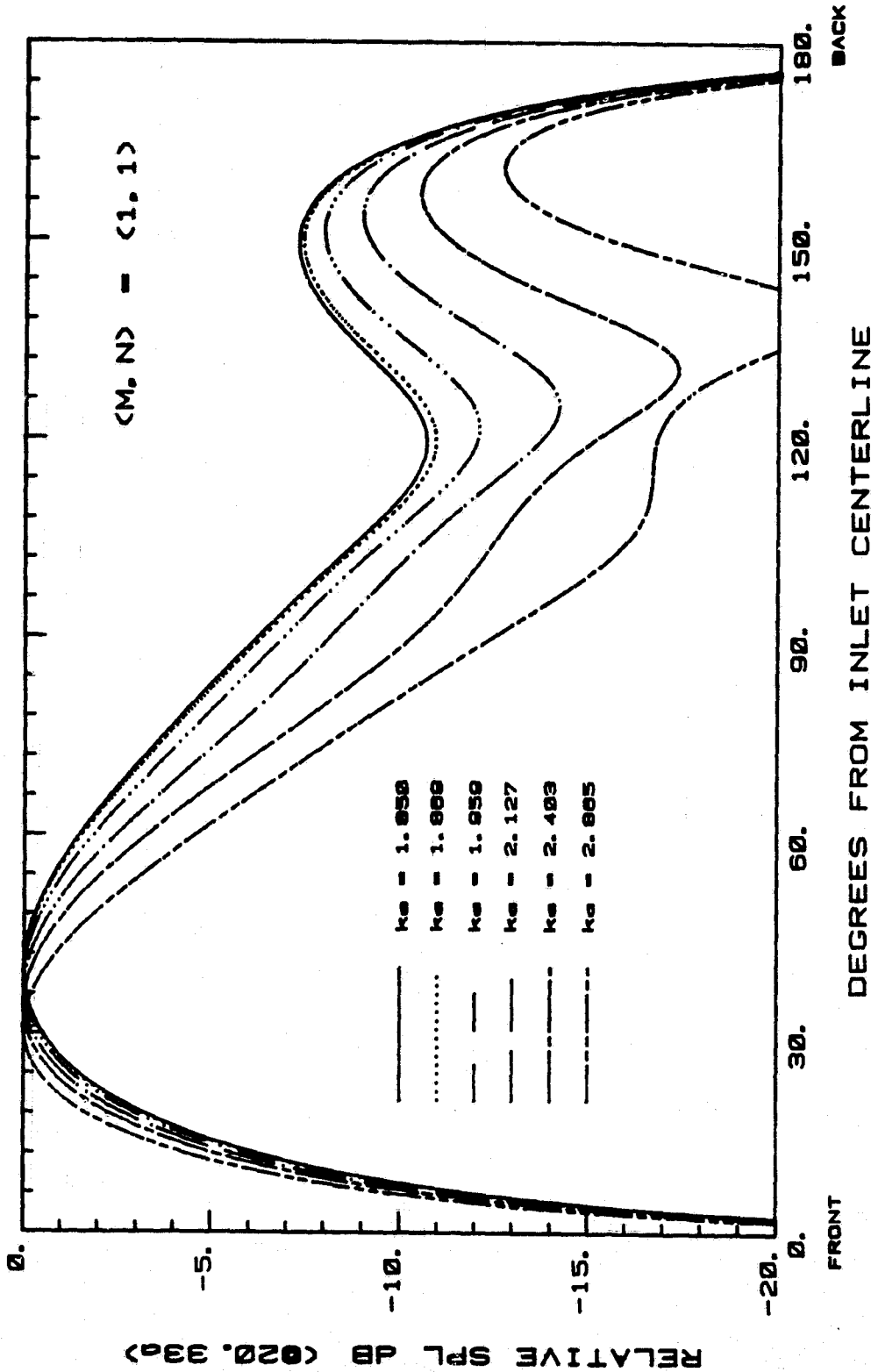


Fig. 51

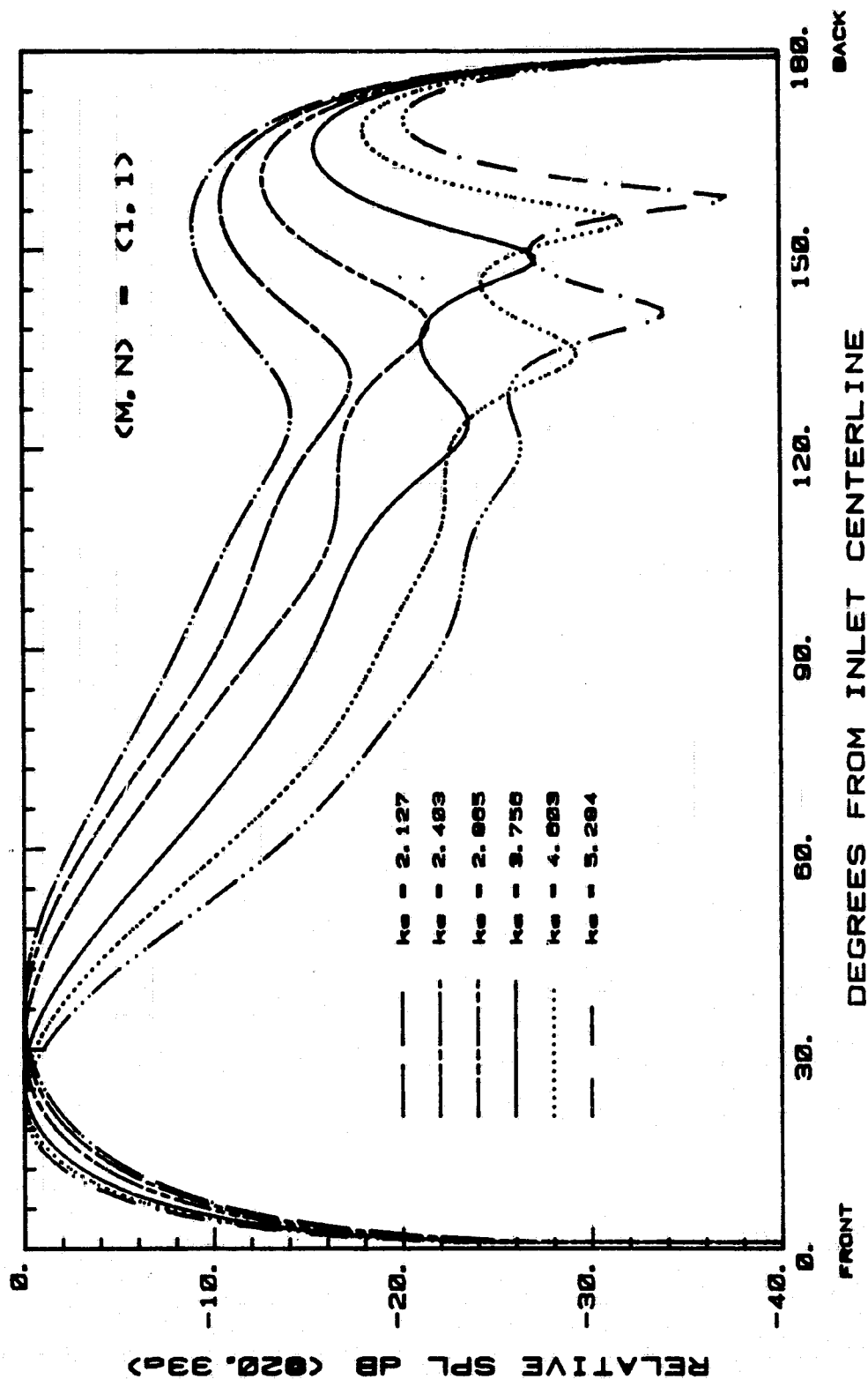
LANGLEY BELLMOUTH



LANGLEY BELLMOUTH

Fig. 6a

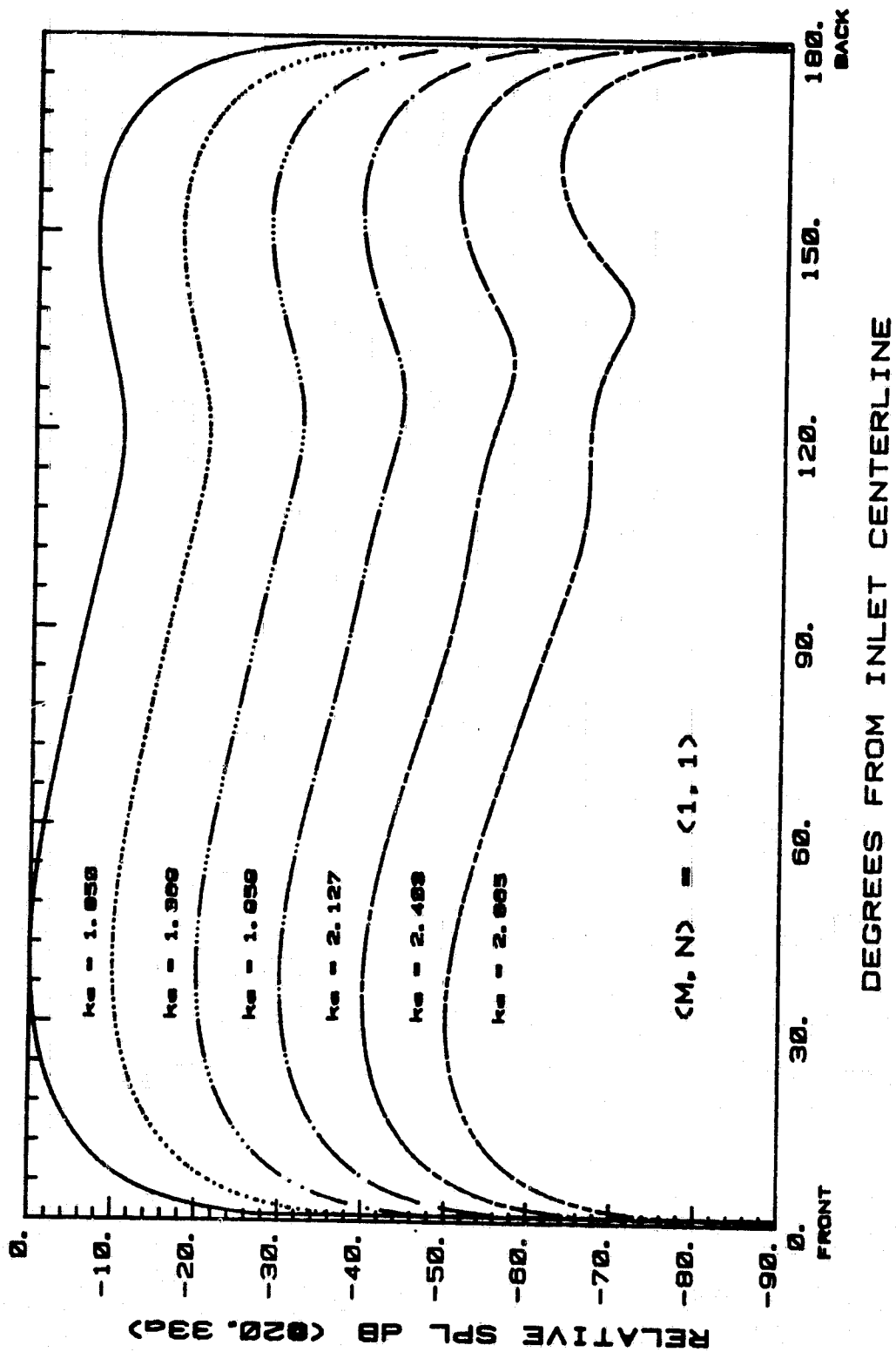
ORIGINAL PAGE IS
OF POOR QUALITY



LANGLEY BELLMOUTH

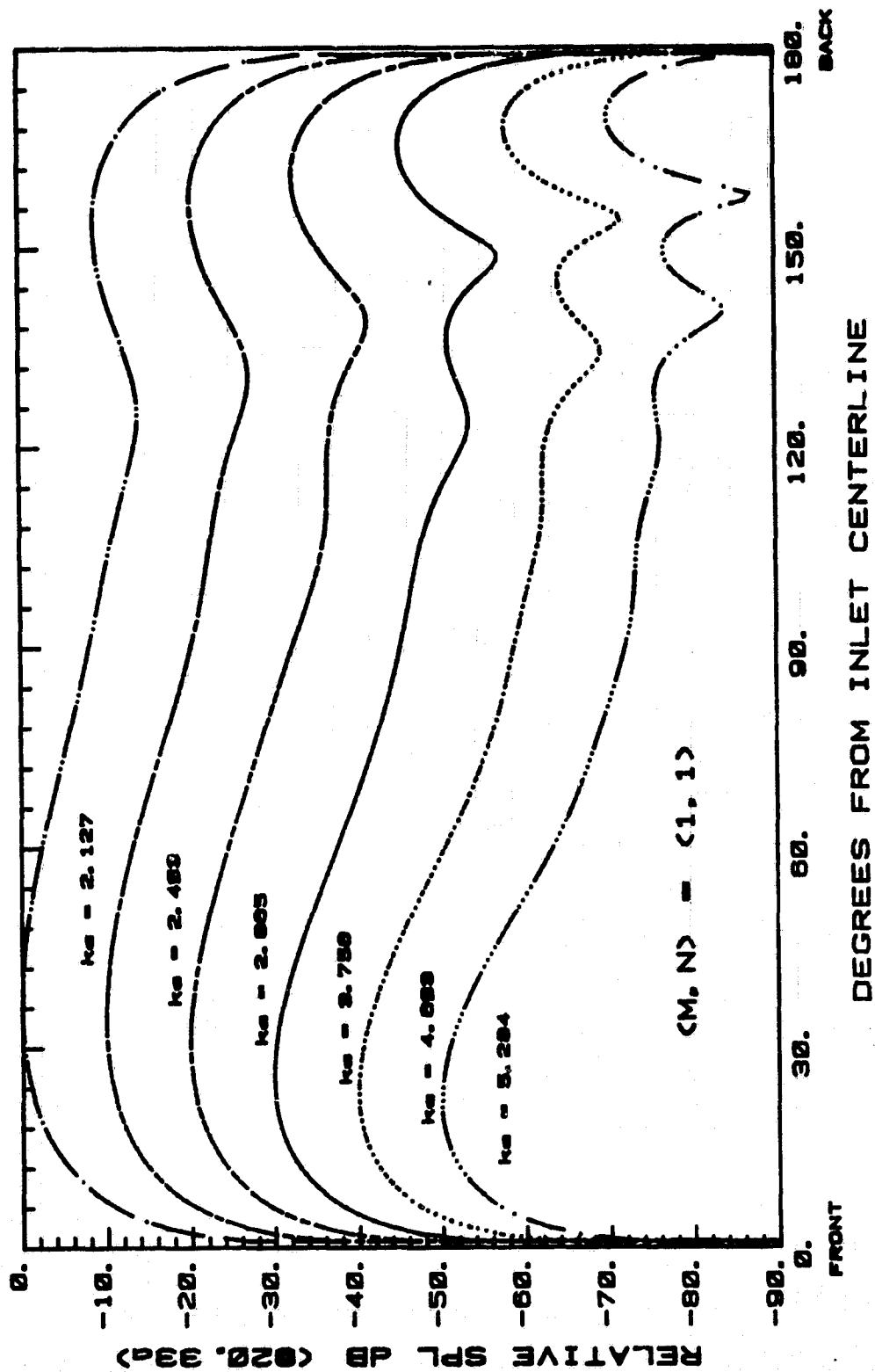
Fig. 6b

ORIGINAL PAGE IS
OF POOR QUALITY



LANGLEY BELLMOUTH

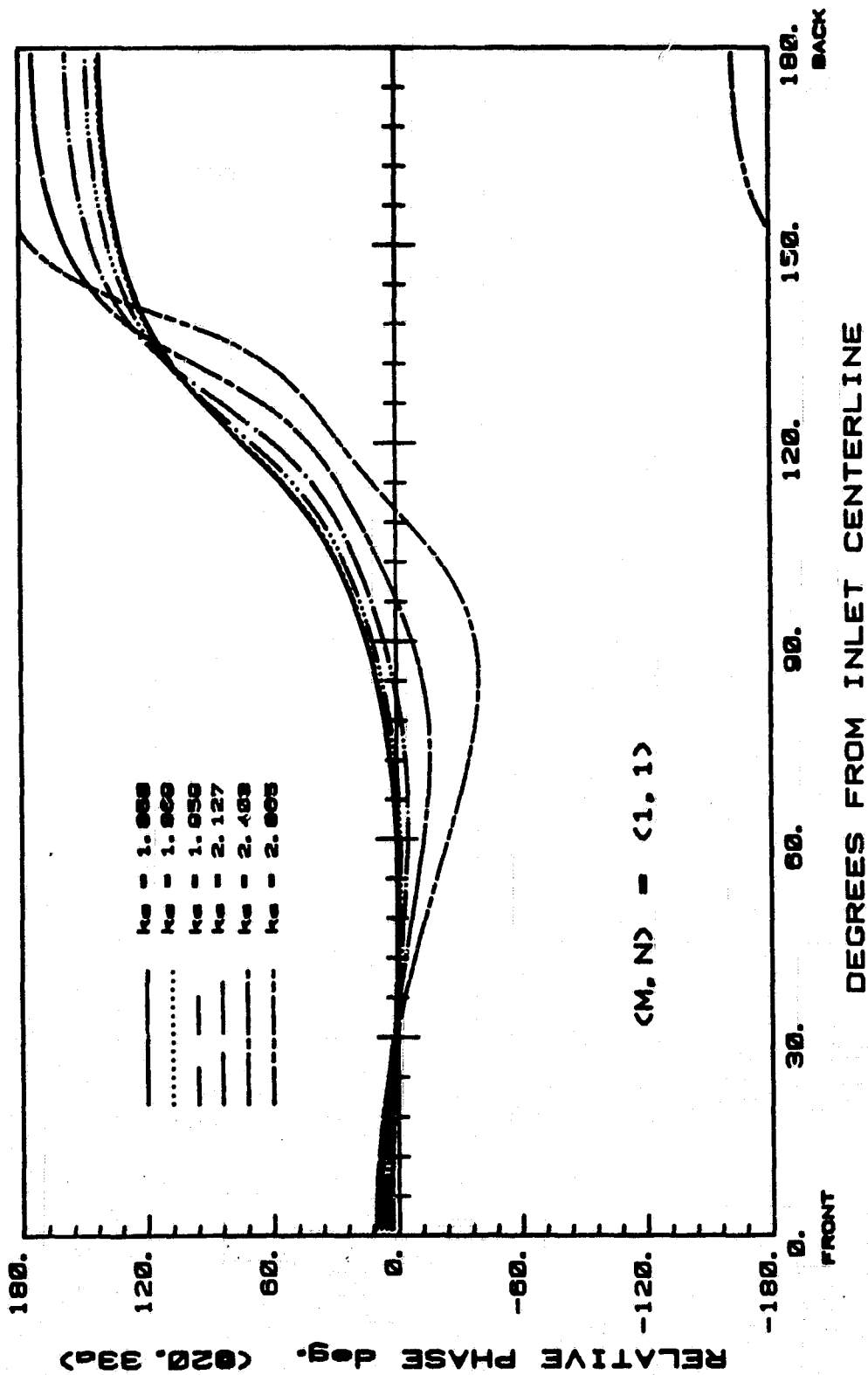
Fig. 6c



LANGLEY BELLMOUTH

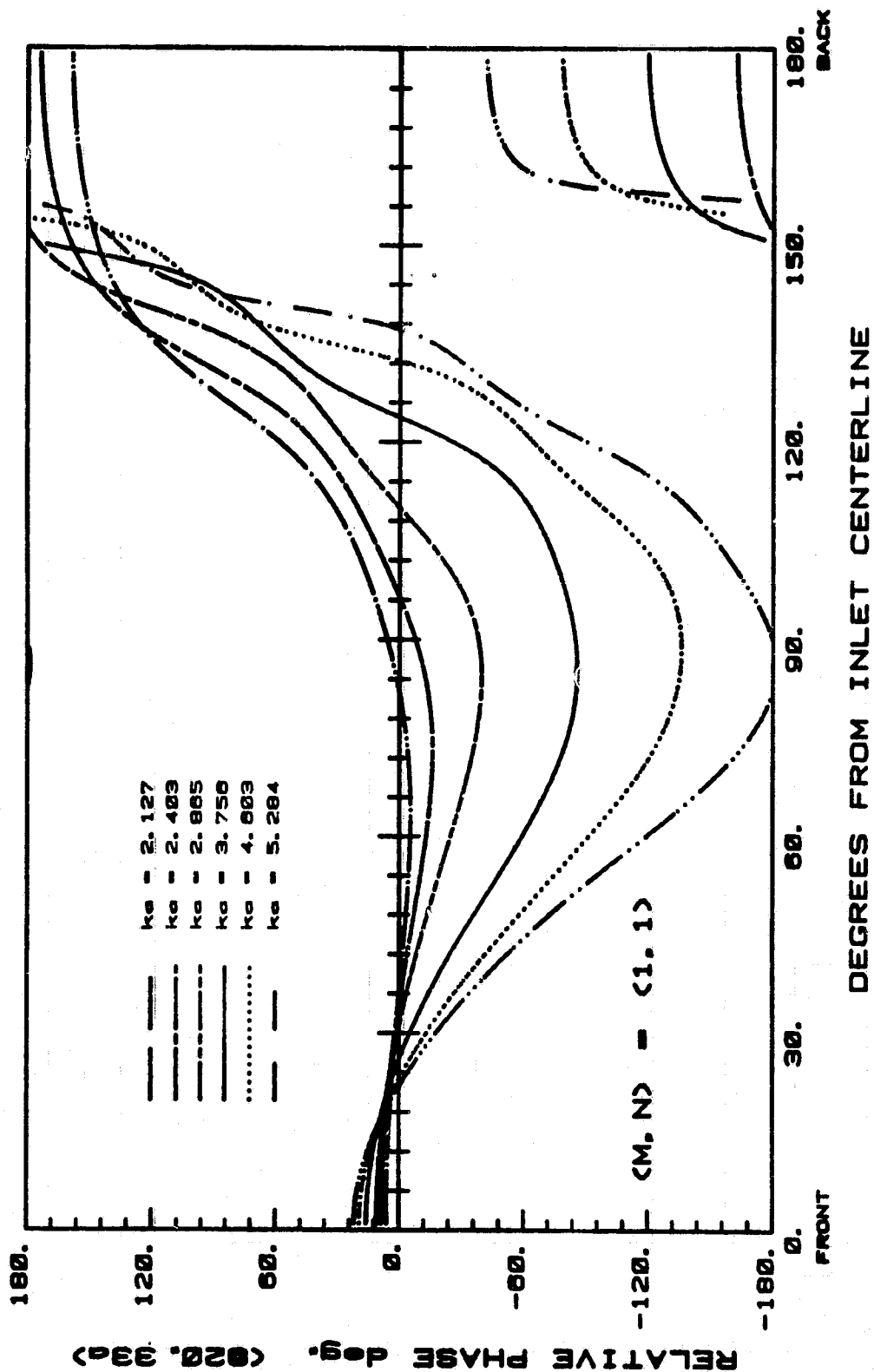
Fig. 6d

ORIGINAL PAGE IS
OF POOR QUALITY



LANGLEY BELLMOUTH

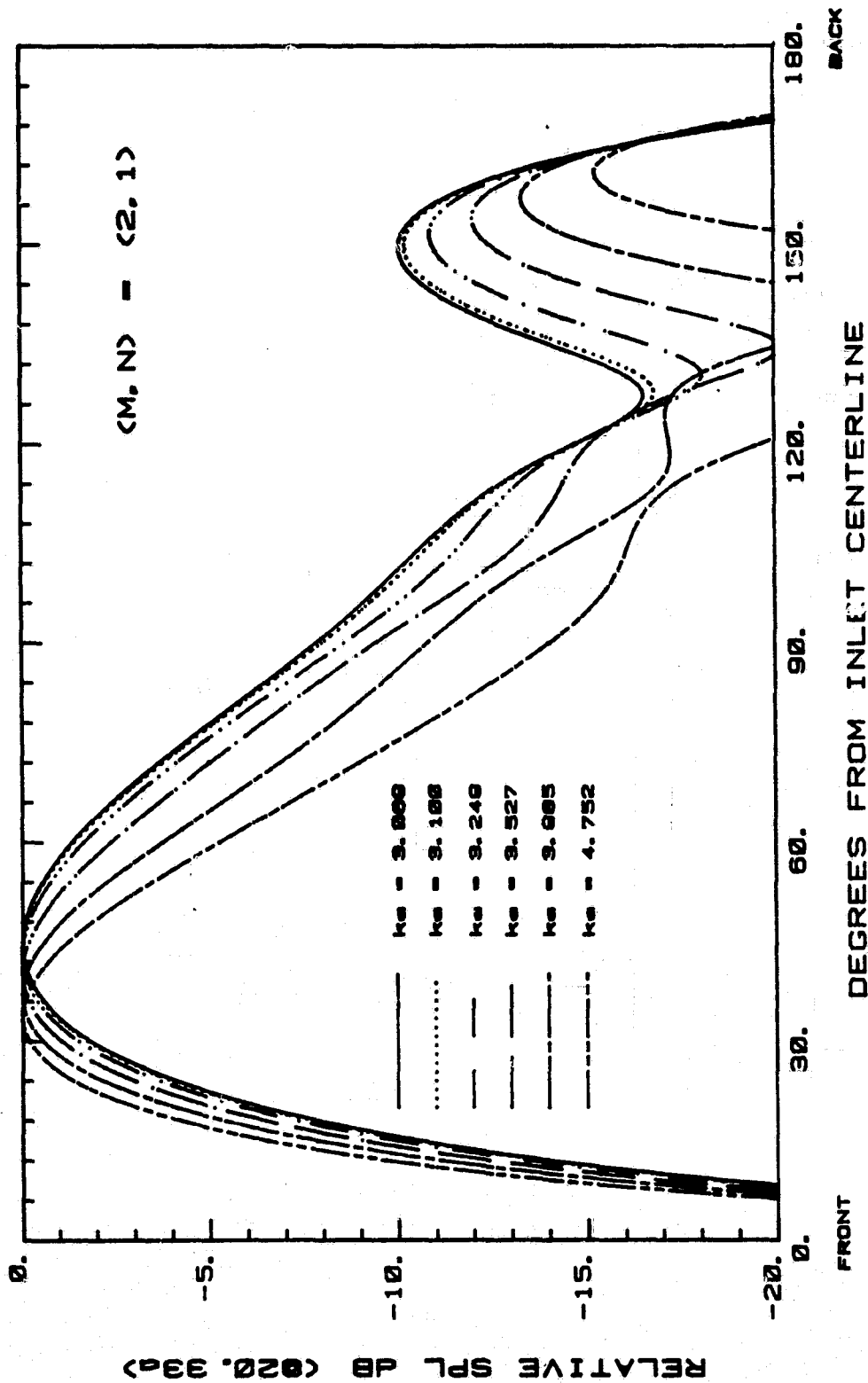
Fig. 6e



LANGLEY BELLMOUTH

Fig. 6f

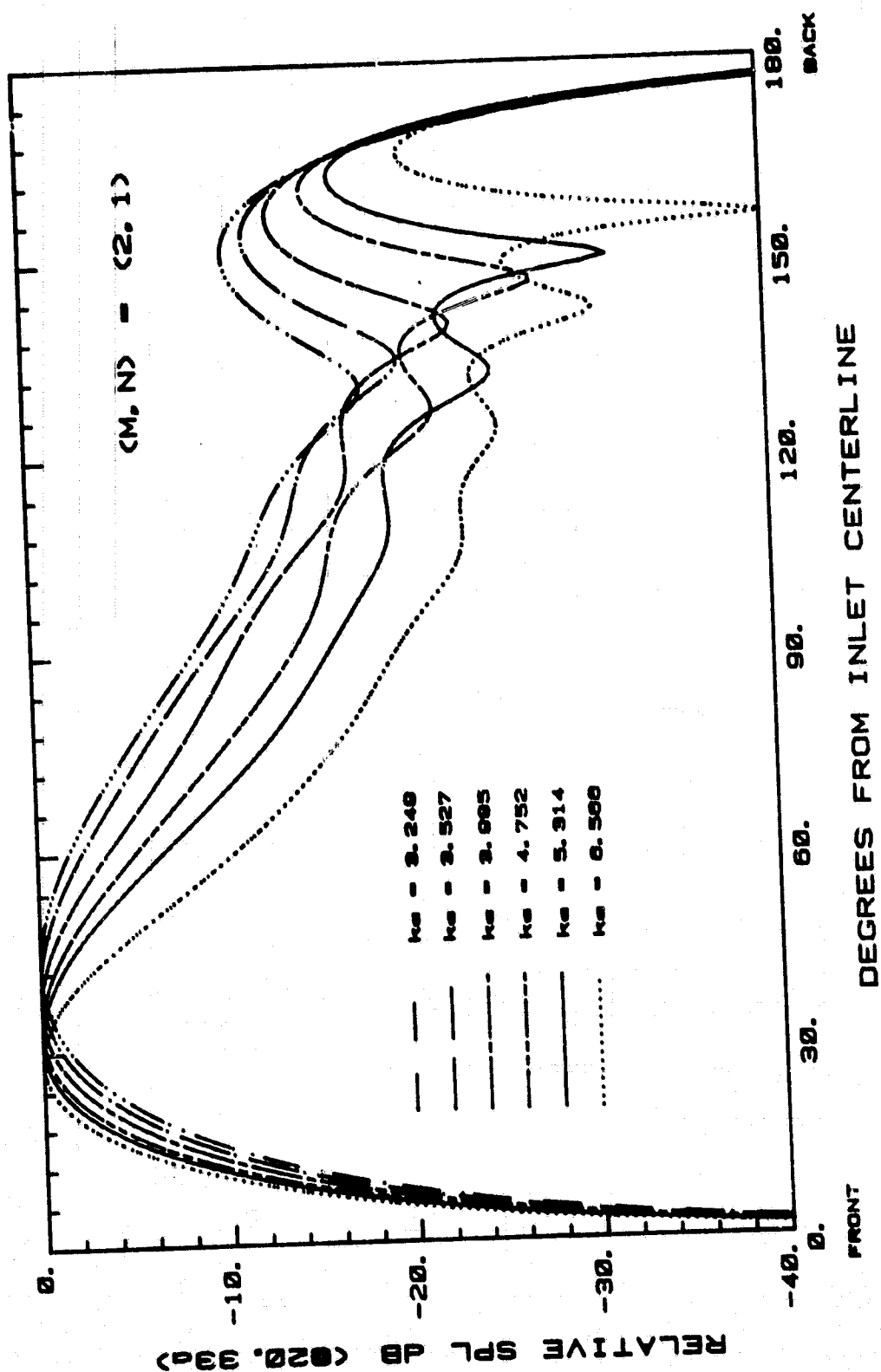
ORIGINAL PAGE IS
OF POOR QUALITY



LANGLEY BELLMOUTH

Fig. 7a

ORIGINAL PAGE IS
OF POOR QUALITY



LANGLEY BELLMOUTH

Fig. 7b

ORIGINAL PAGE IS
OF POOR QUALITY

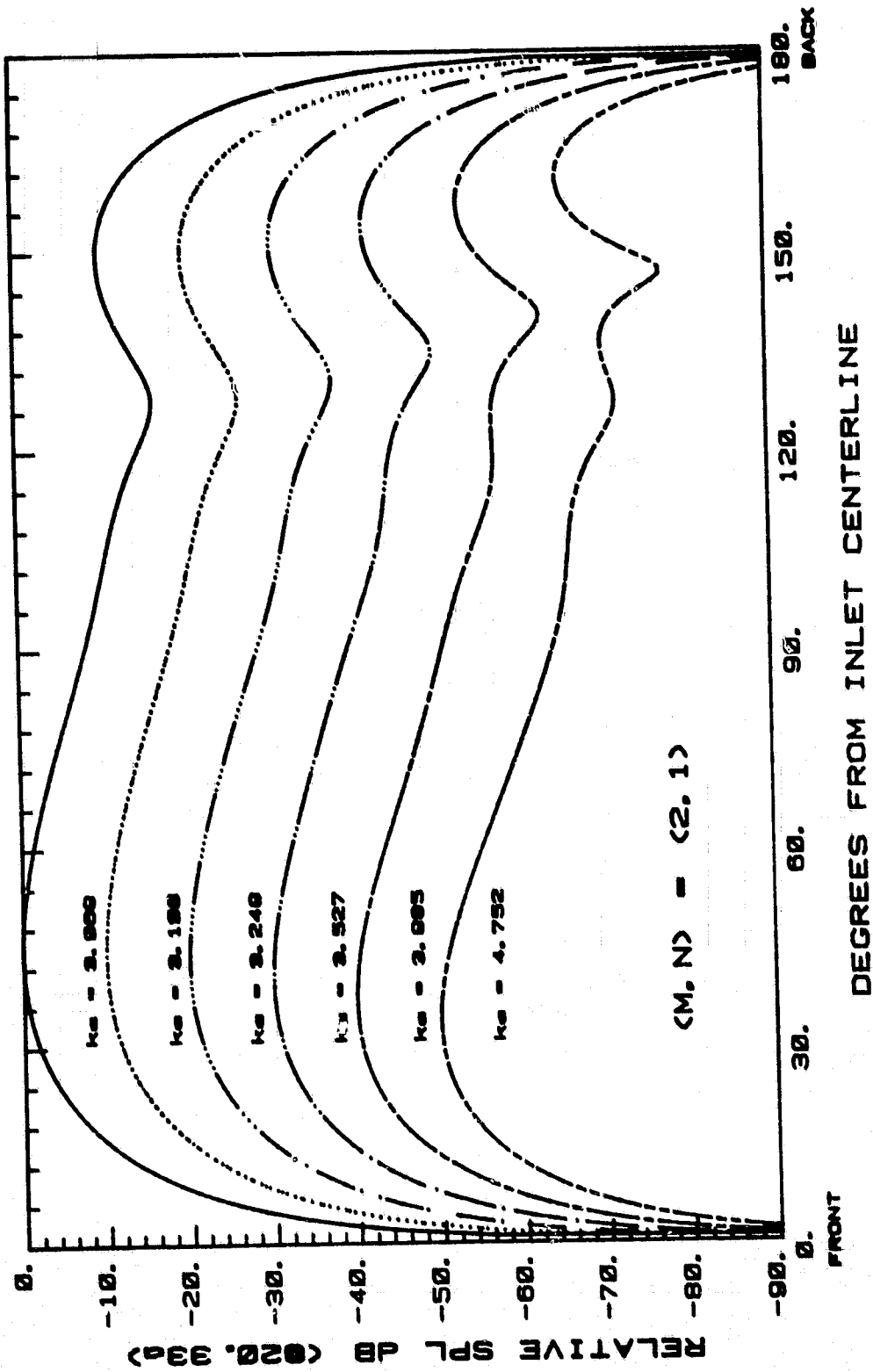
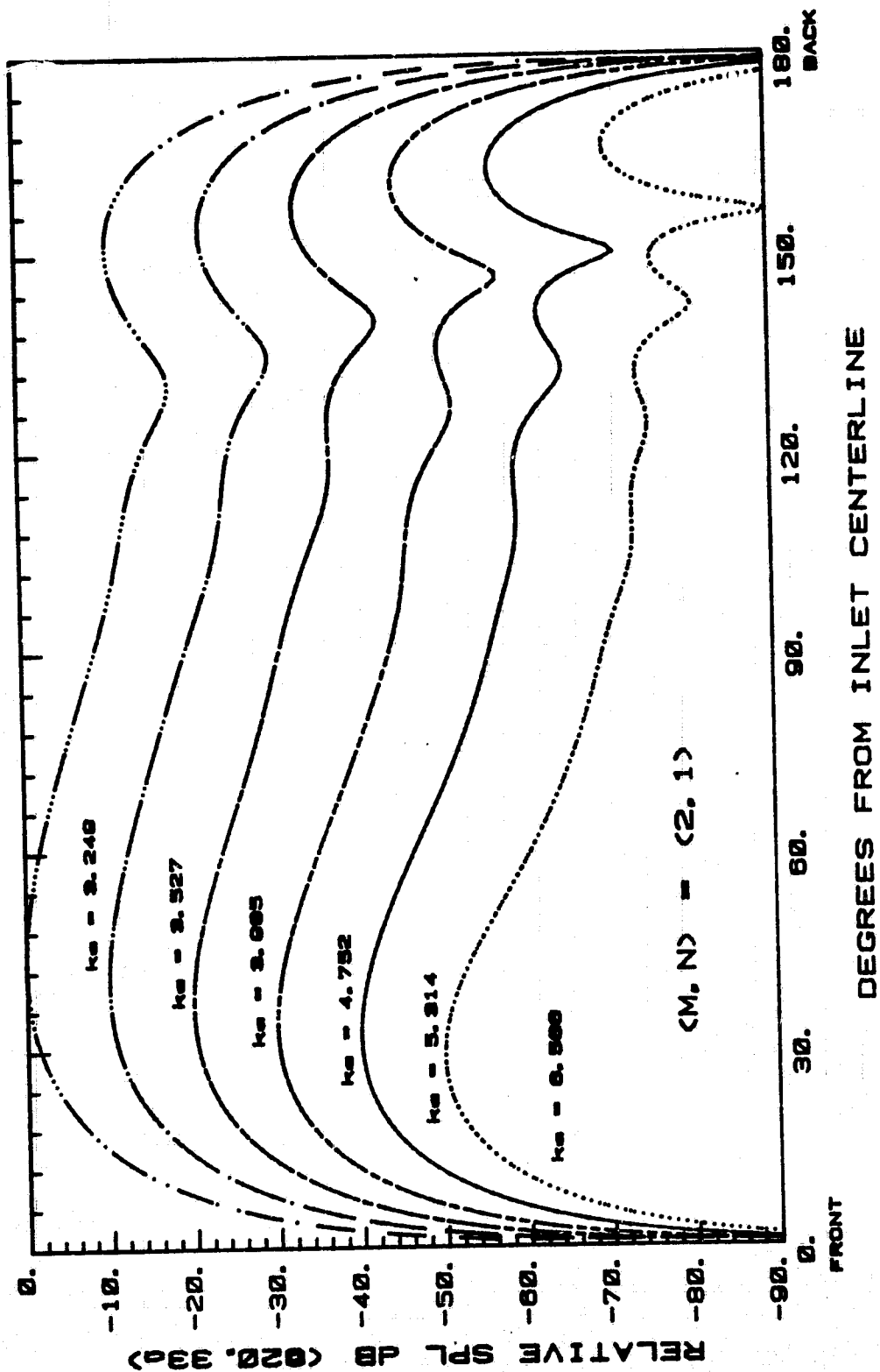


Fig. 7c

LANGLEY BELLMOUTH

ORIGINAL PAGE 13
OF POOR QUALITY



LANGLEY BELLMOUTH

Fig. 7d

ORIGINAL PAGE IS
OF POOR QUALITY

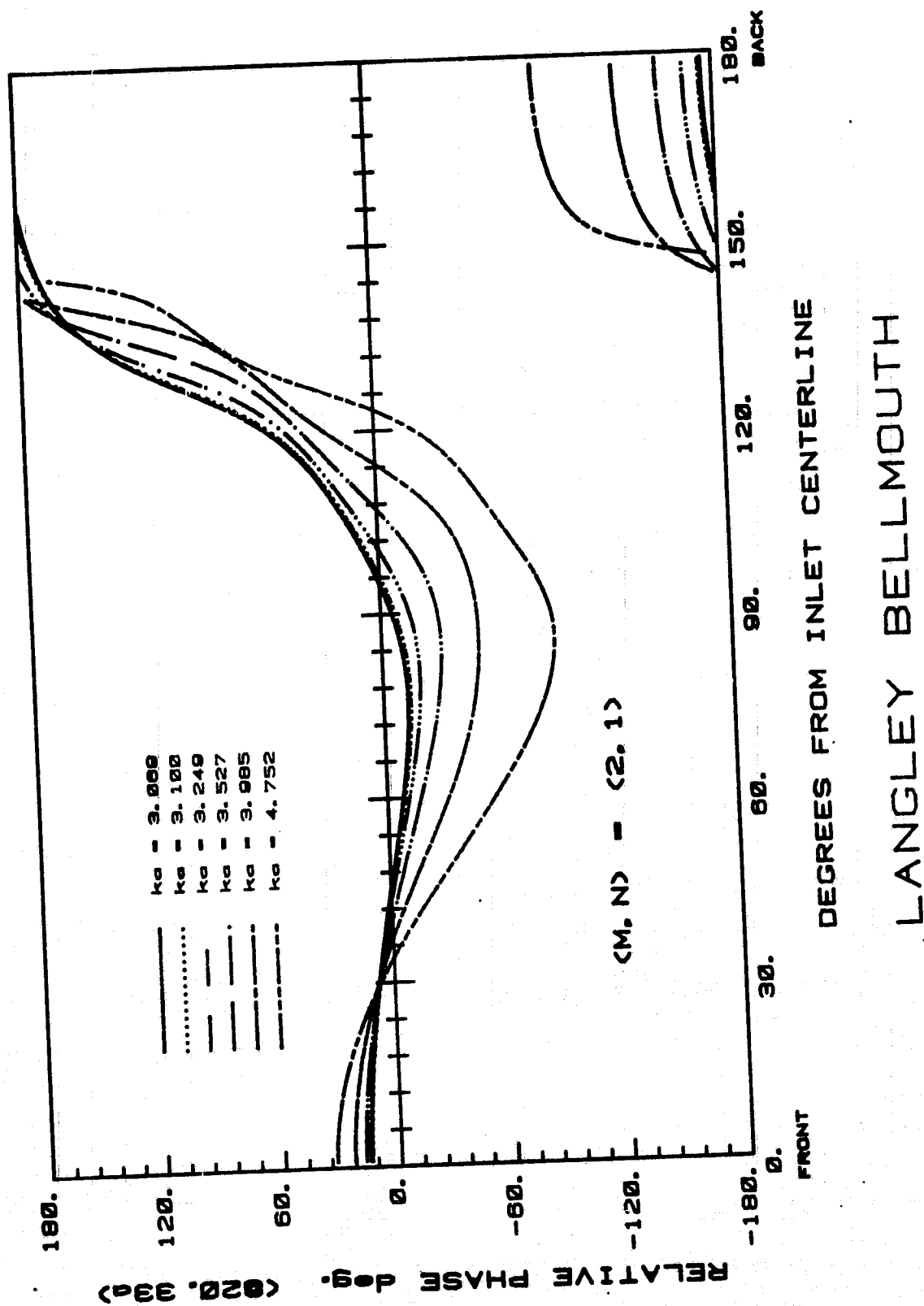
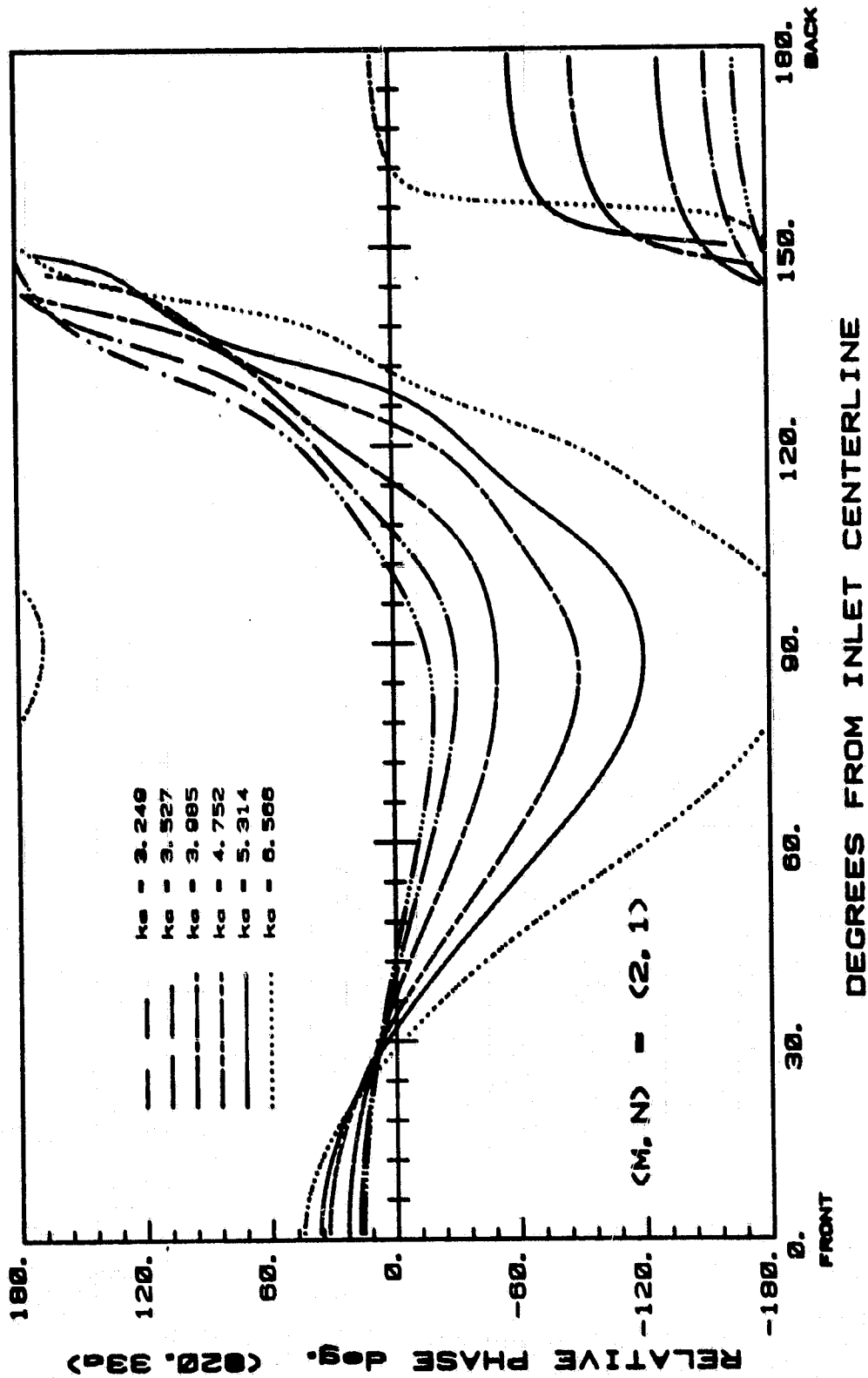


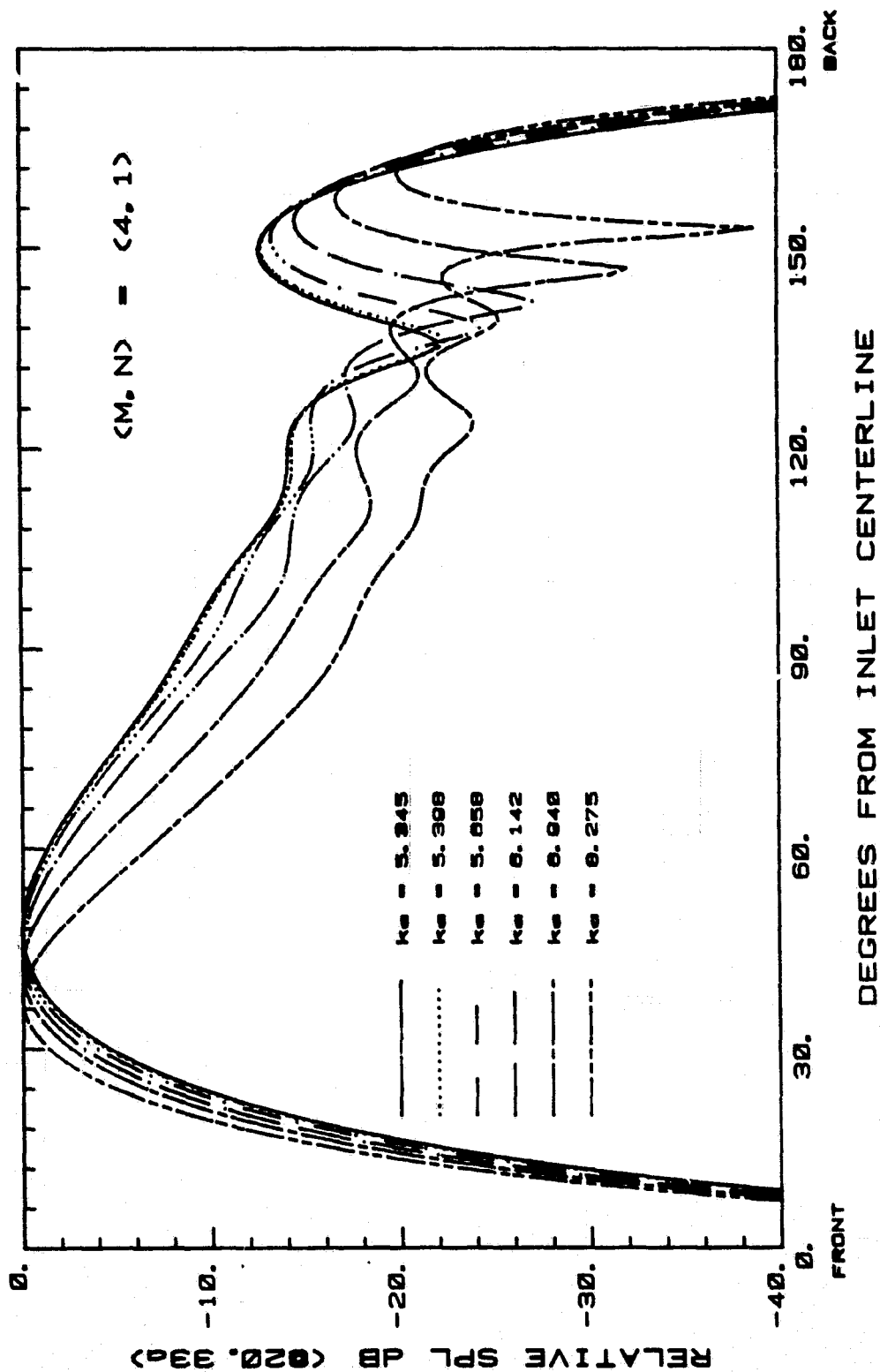
Fig. 7e

ORIGINAL PAGE IS
OF POOR QUALITY



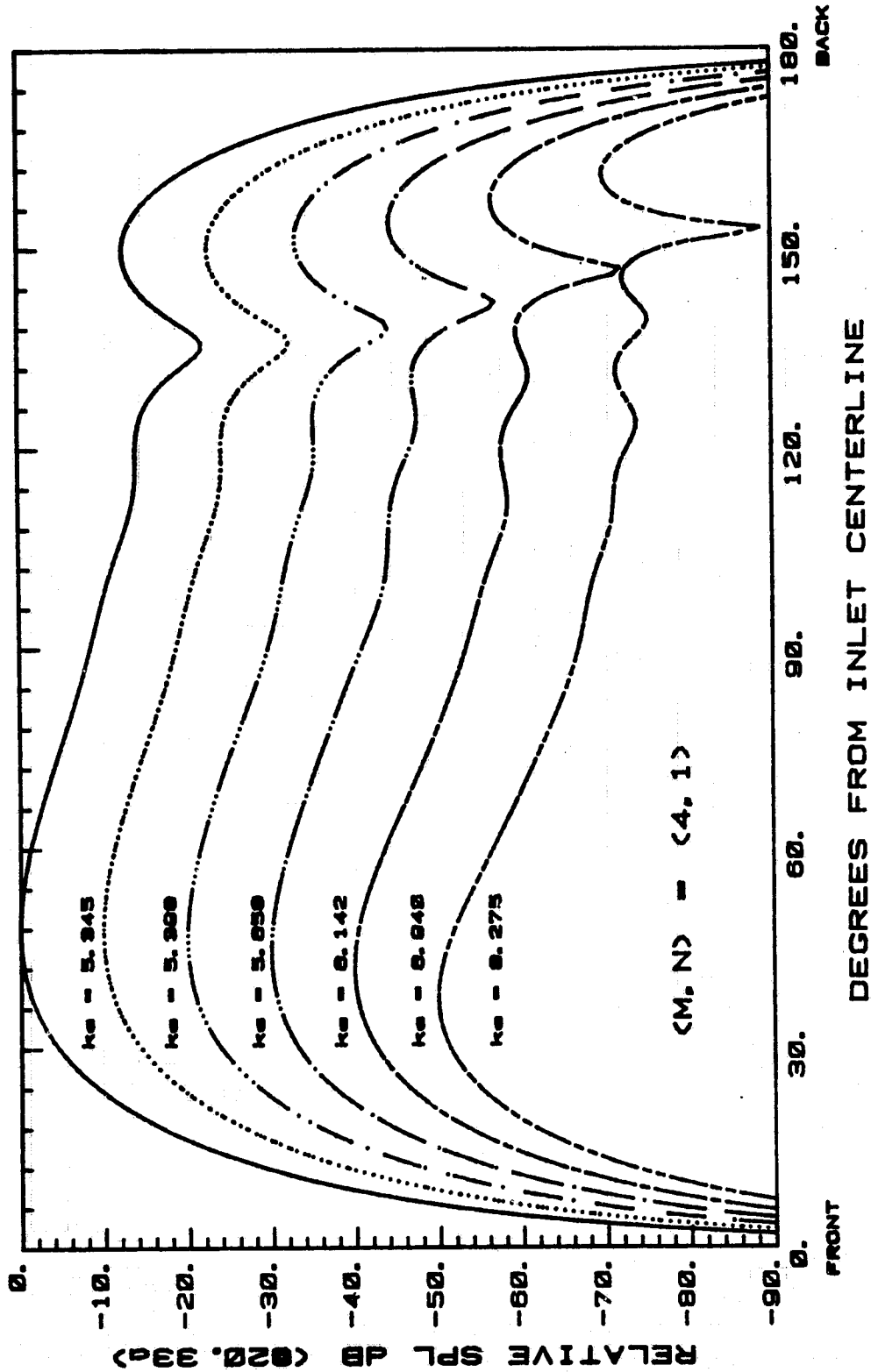
LANGLEY BELLMOUTH

Fig. 7f



LANGLEY BELLMOUTH

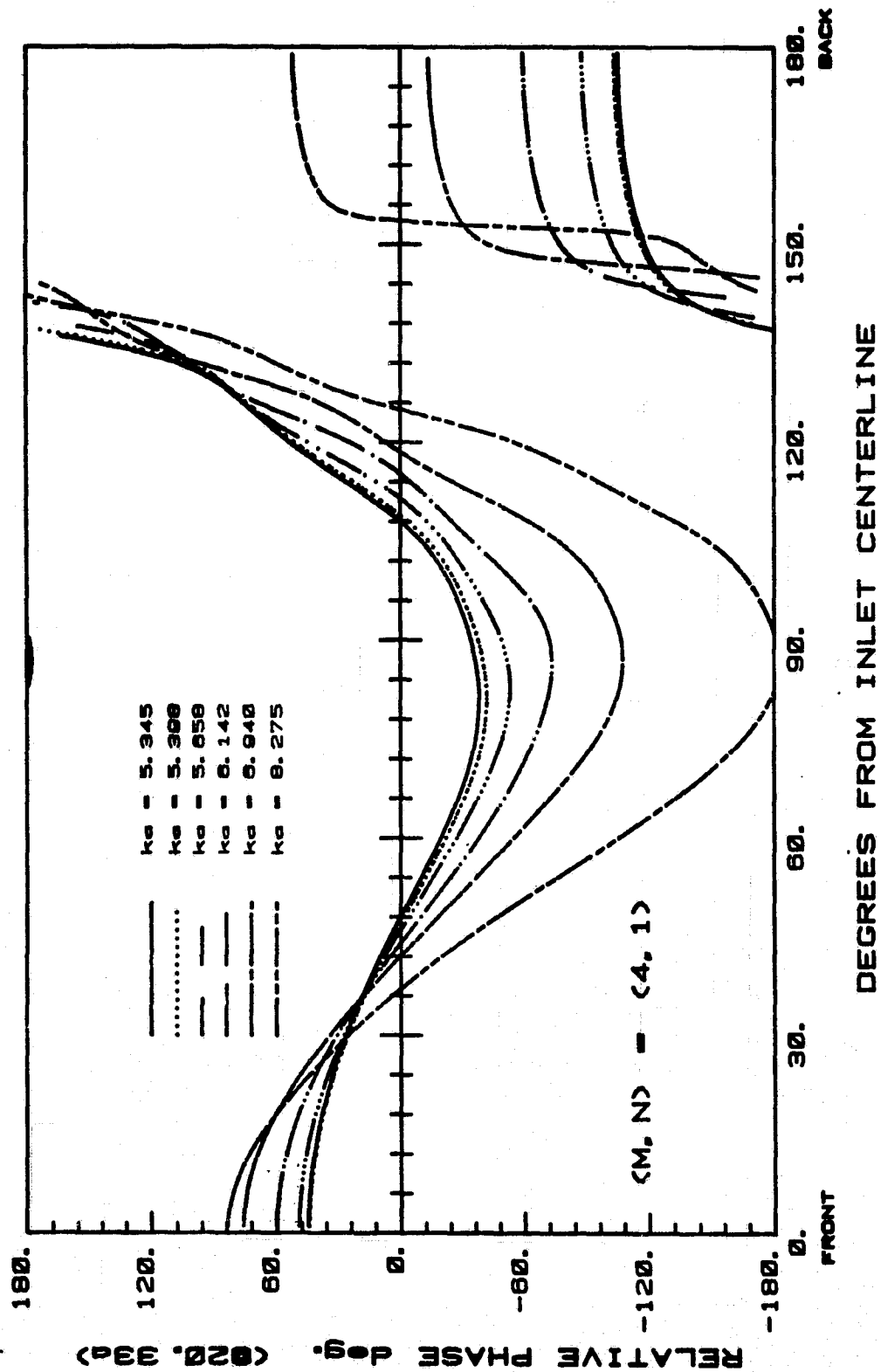
Fig. 8a



LANGLEY BELLMOUTH

Fig. 8b

ORIGINAL PAGE IS
OF POOR QUALITY



LANGLEY BELLMOUTH

Fig. 8c

ORIGINAL PAGE IS
OF POOR QUALITY

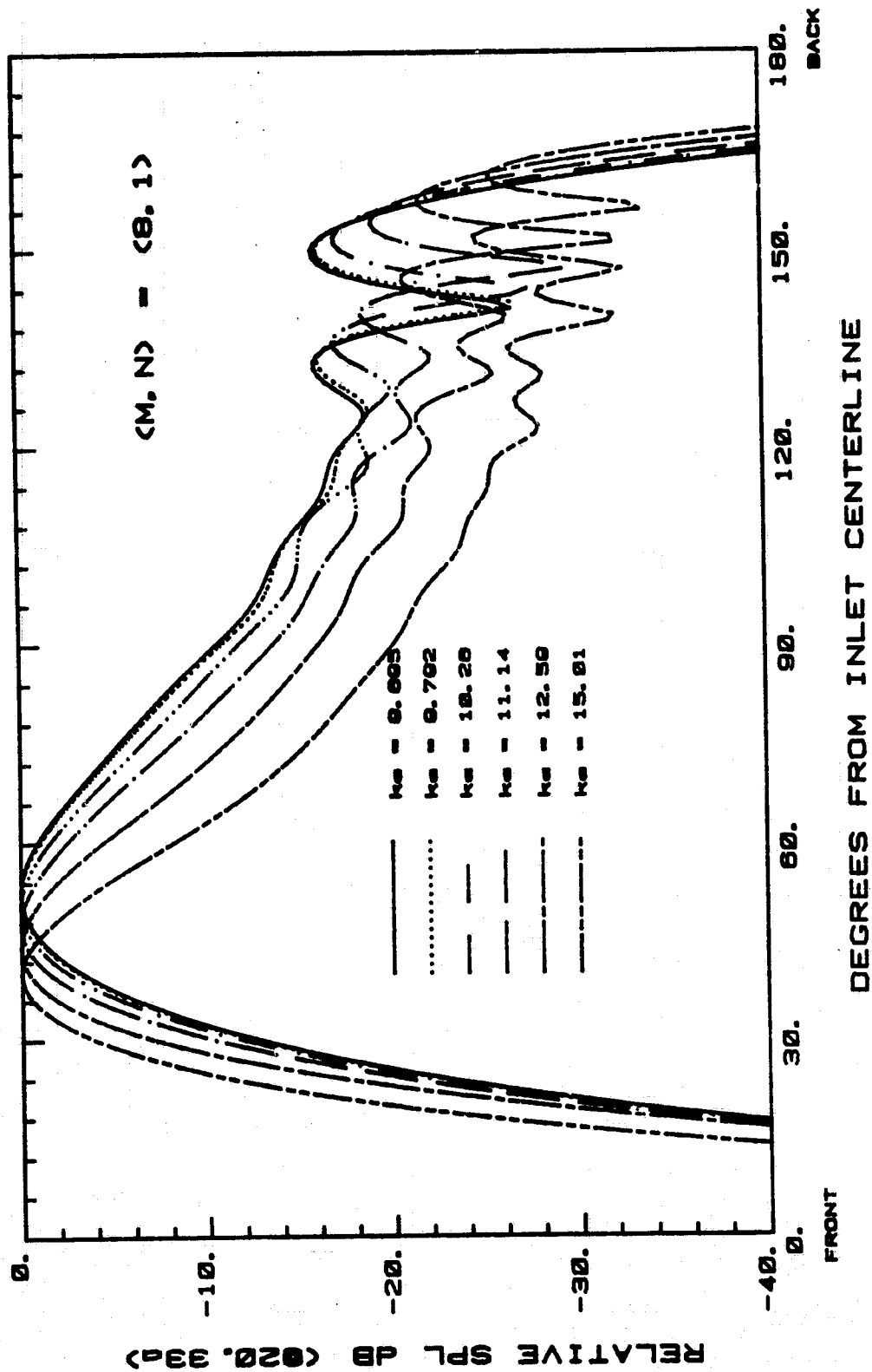
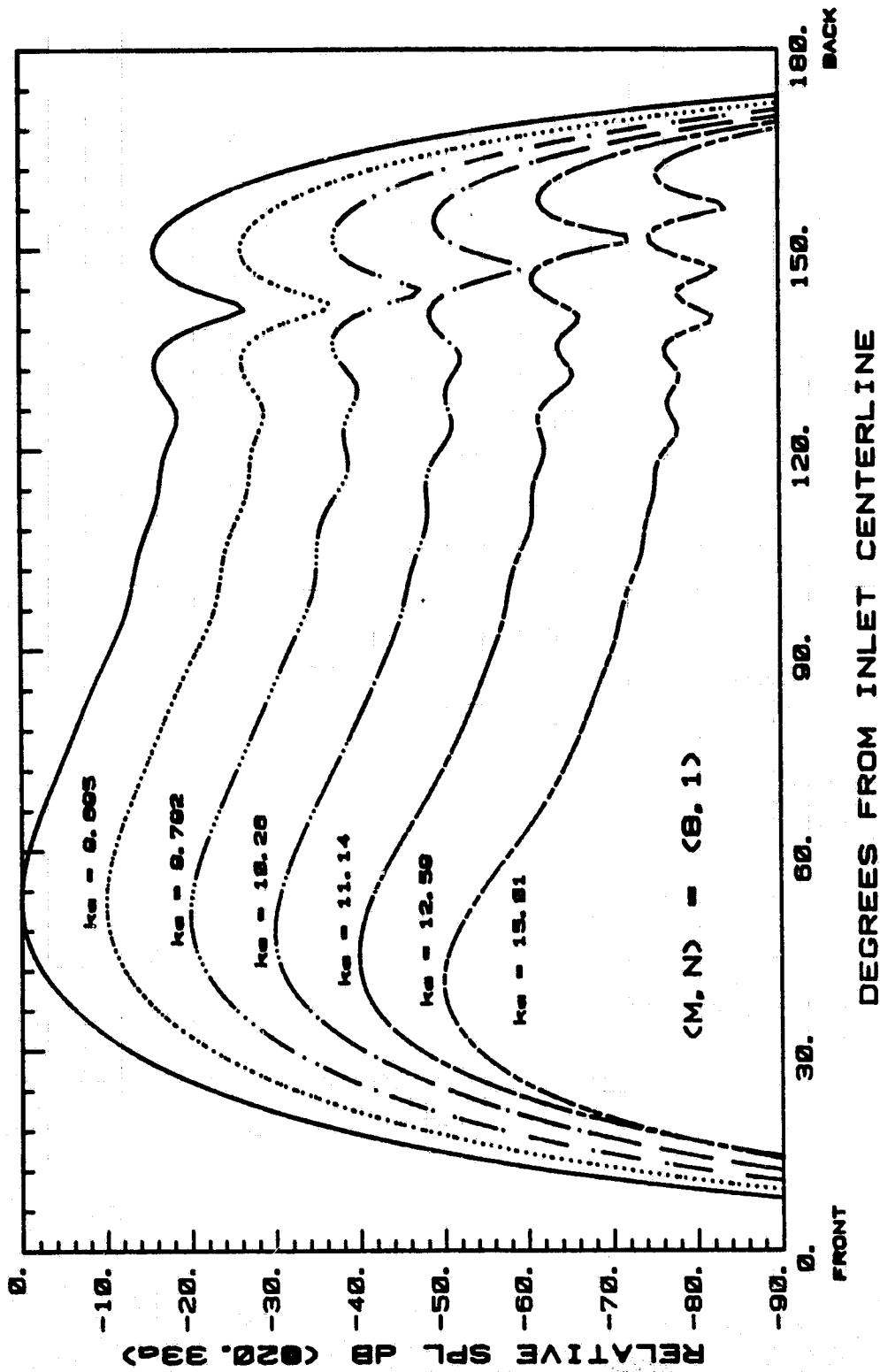


Fig. 9a



LANGLEY BELLMOUTH

Fig. 9b

ORIGINAL PAGE IS
OF POOR QUALITY

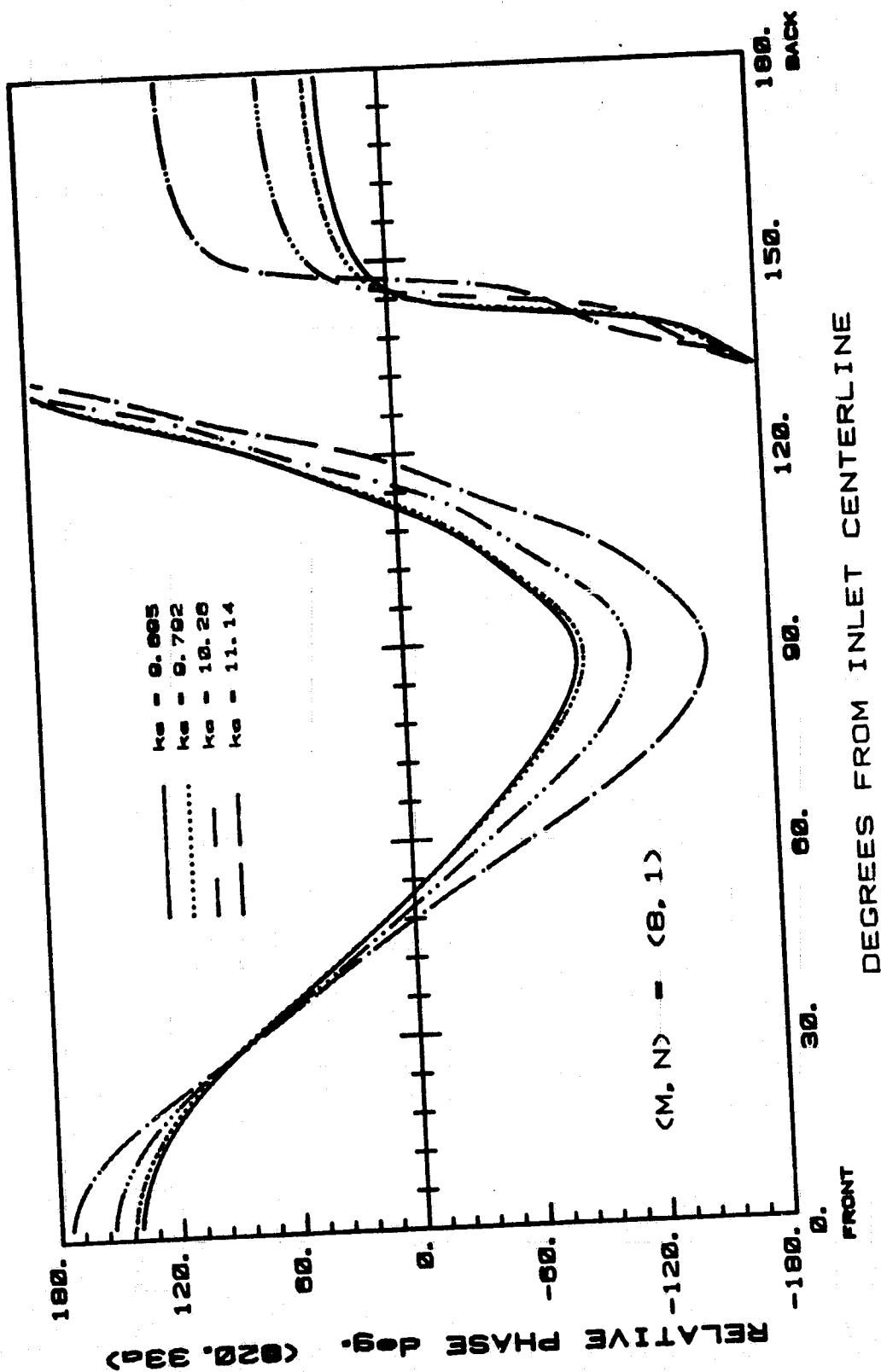


Fig. 9c

LANGLEY BELLMOUTH

ORIGINAL PAGE IS
OF POOR QUALITY

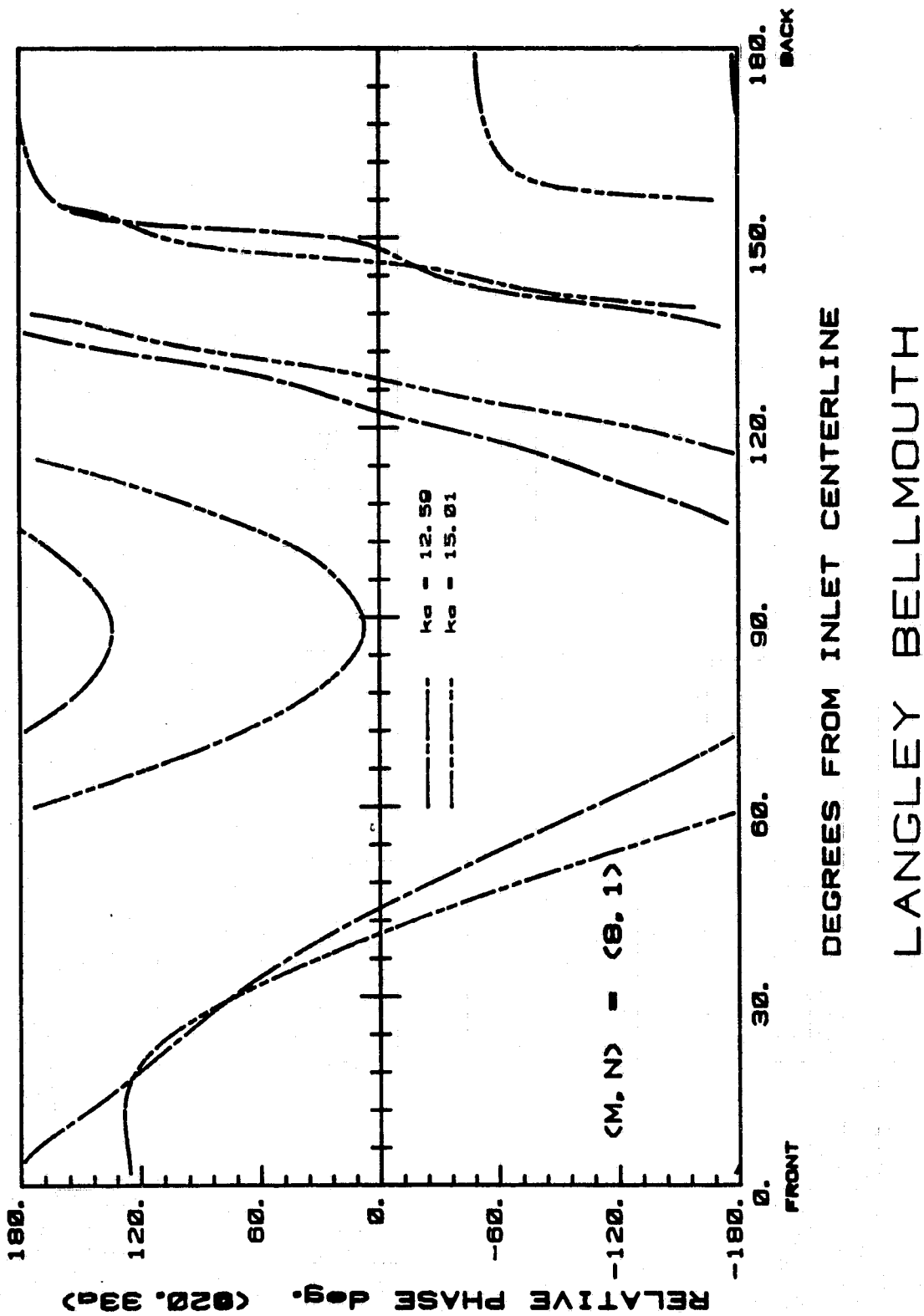
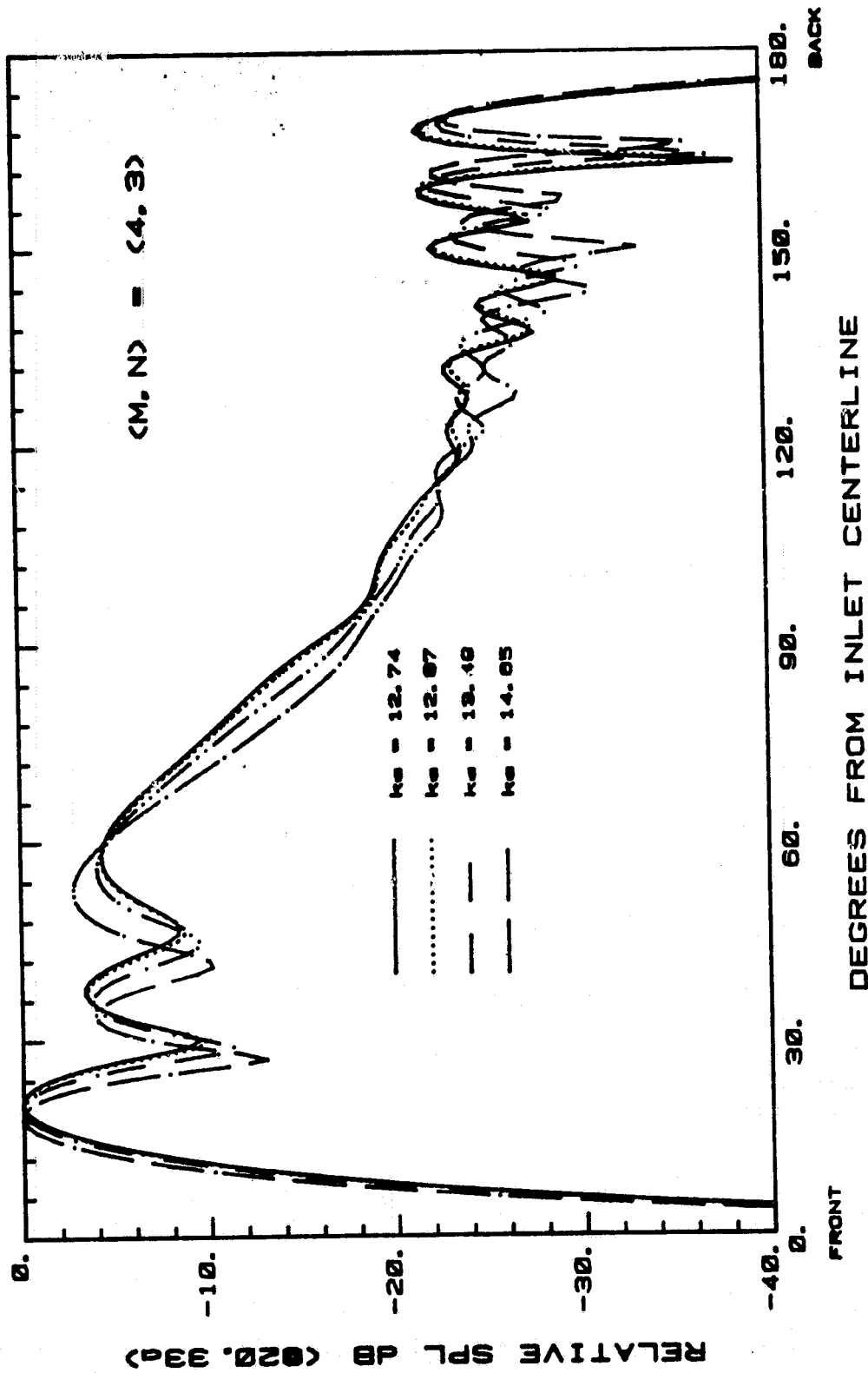


Fig. 9d

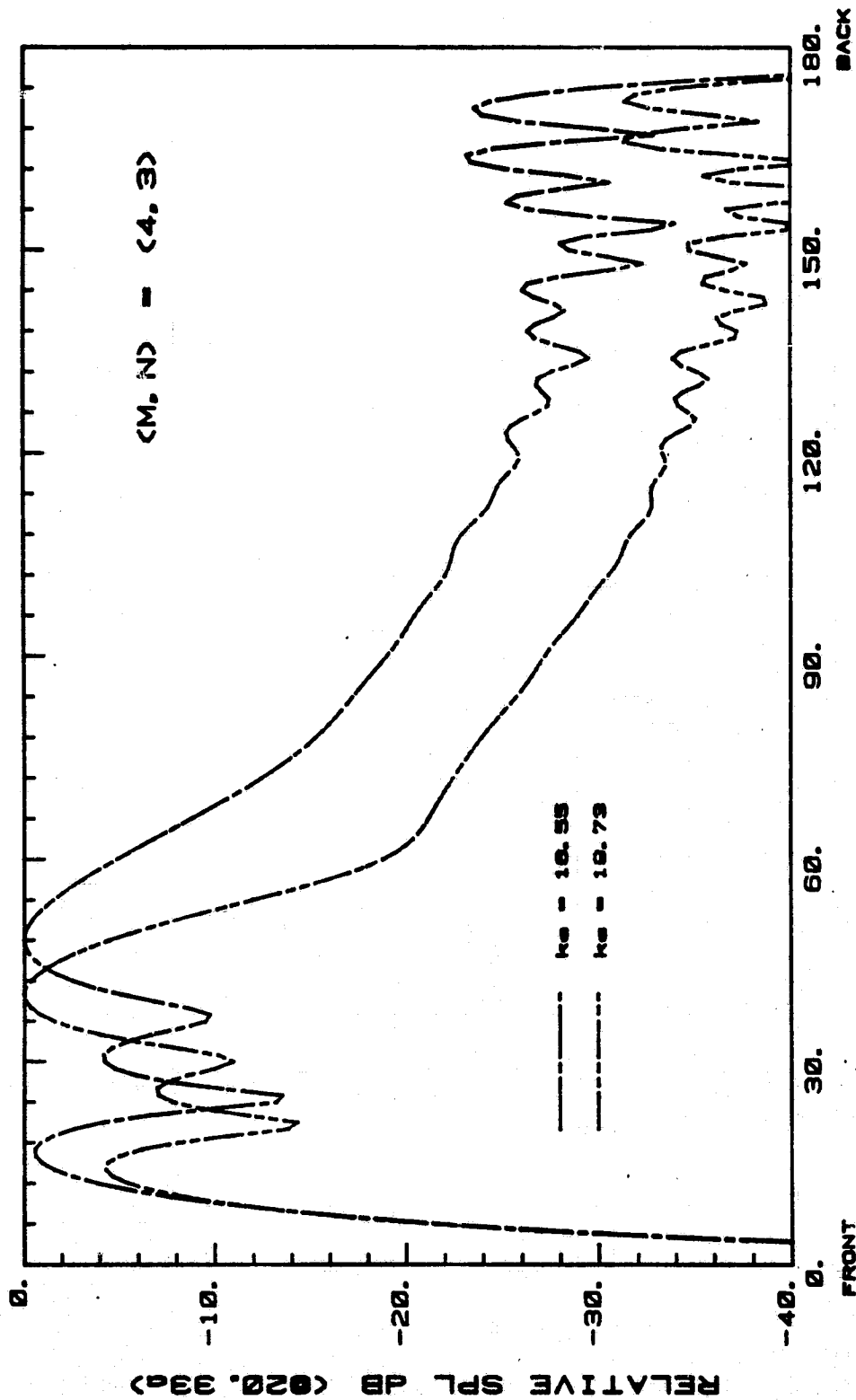
ORIGINAL PAGE 13
OF POOR QUALITY



LANGLEY BELLMOUTH

Fig. 10a

ORIGINAL PAGE IS
OF POOR QUALITY



LANGLEY BELLMOUTH

Fig. 10b

ORIGINAL PAGE IS
OF POOR QUALITY

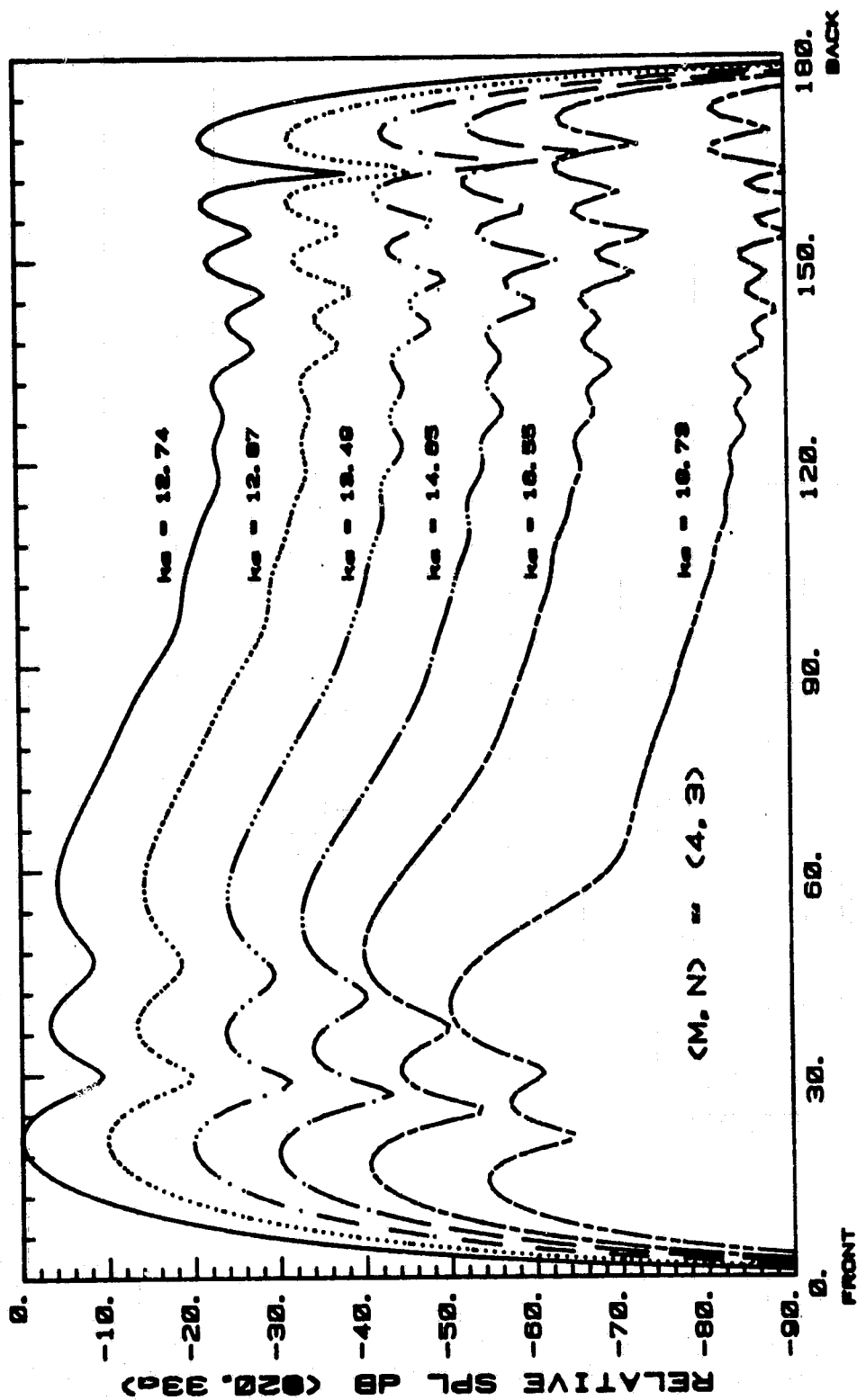
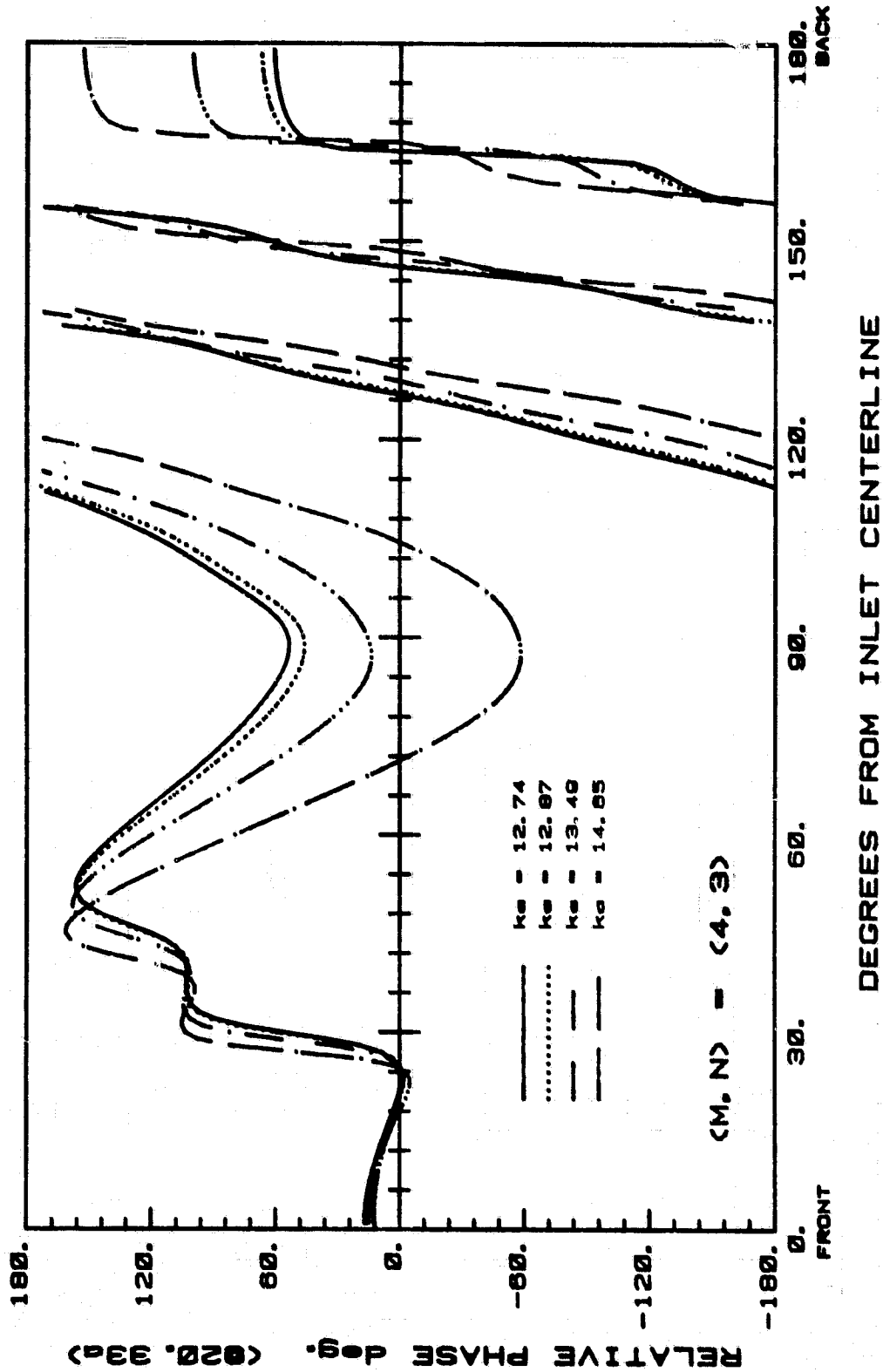


Fig. 10c

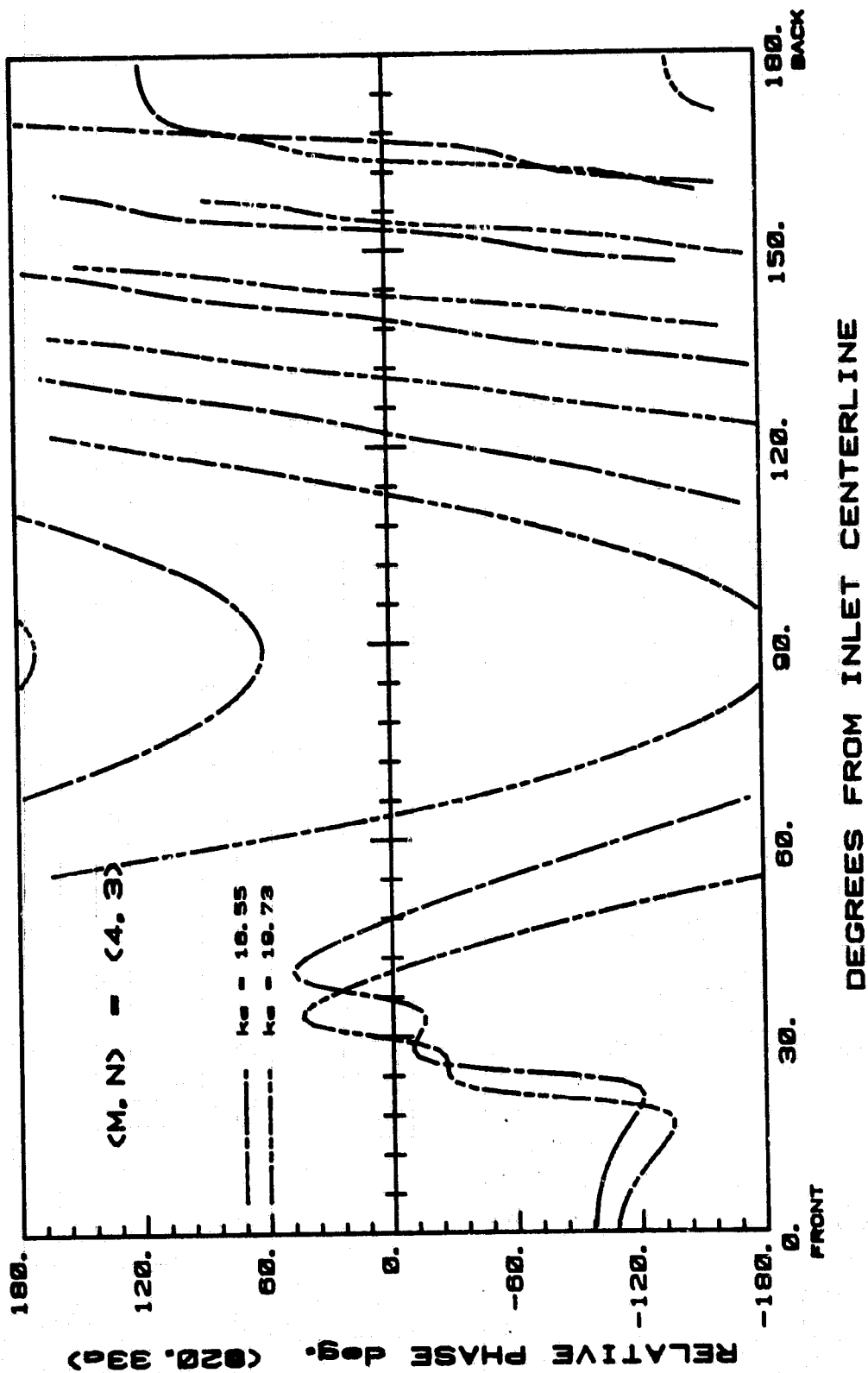
ORIGINAL PAGE IS
OF POOR QUALITY



LANGLEY BELLMOUTH

Fig. 10d

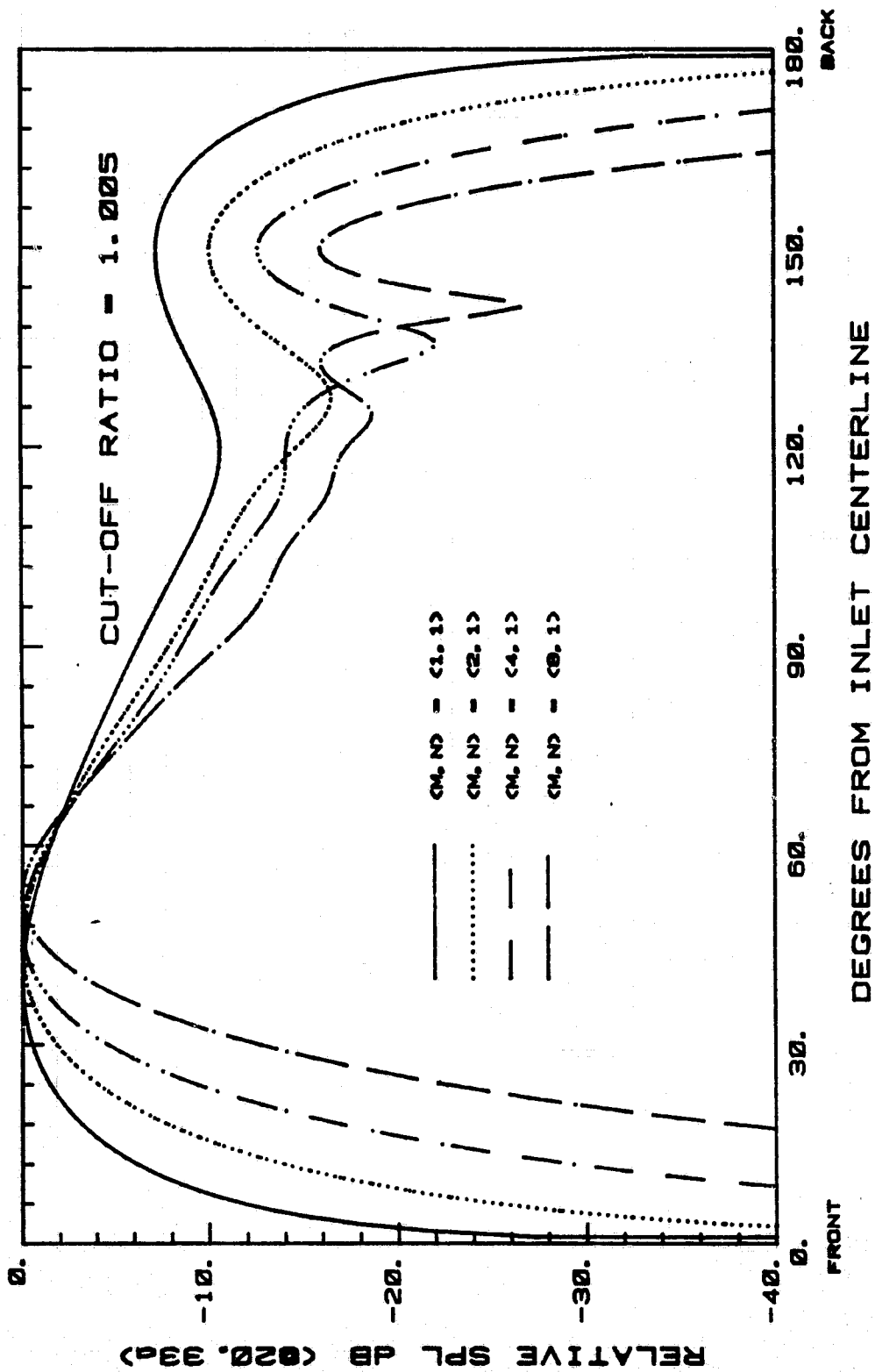
ORIGINAL PAGE IS
OF POOR QUALITY



LANGLEY BELLMOUTH

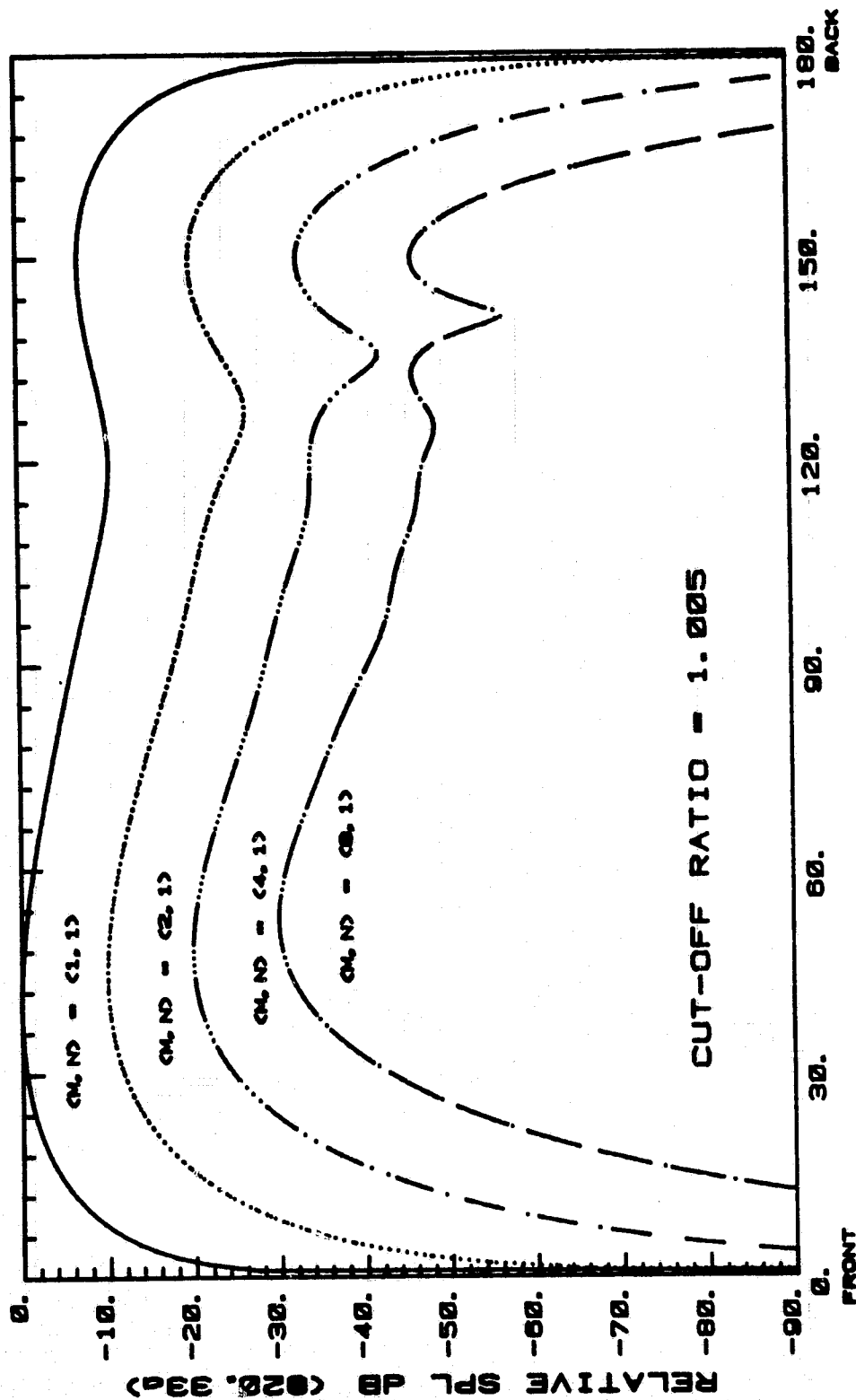
Fig. 10e

ORIGINAL PAGE IS
OF POOR QUALITY



LANGLEY BELLMOUTH

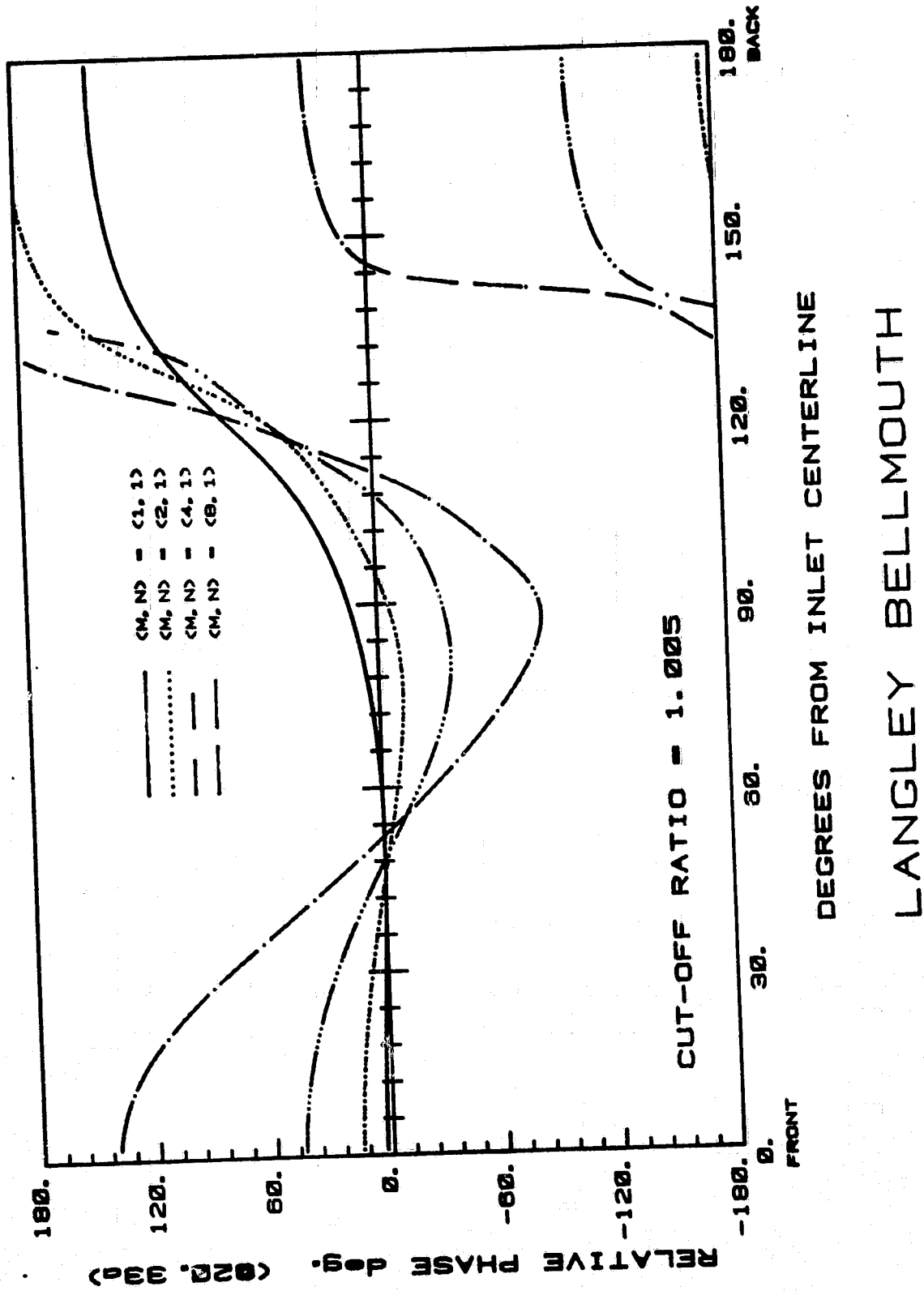
Fig. 11a



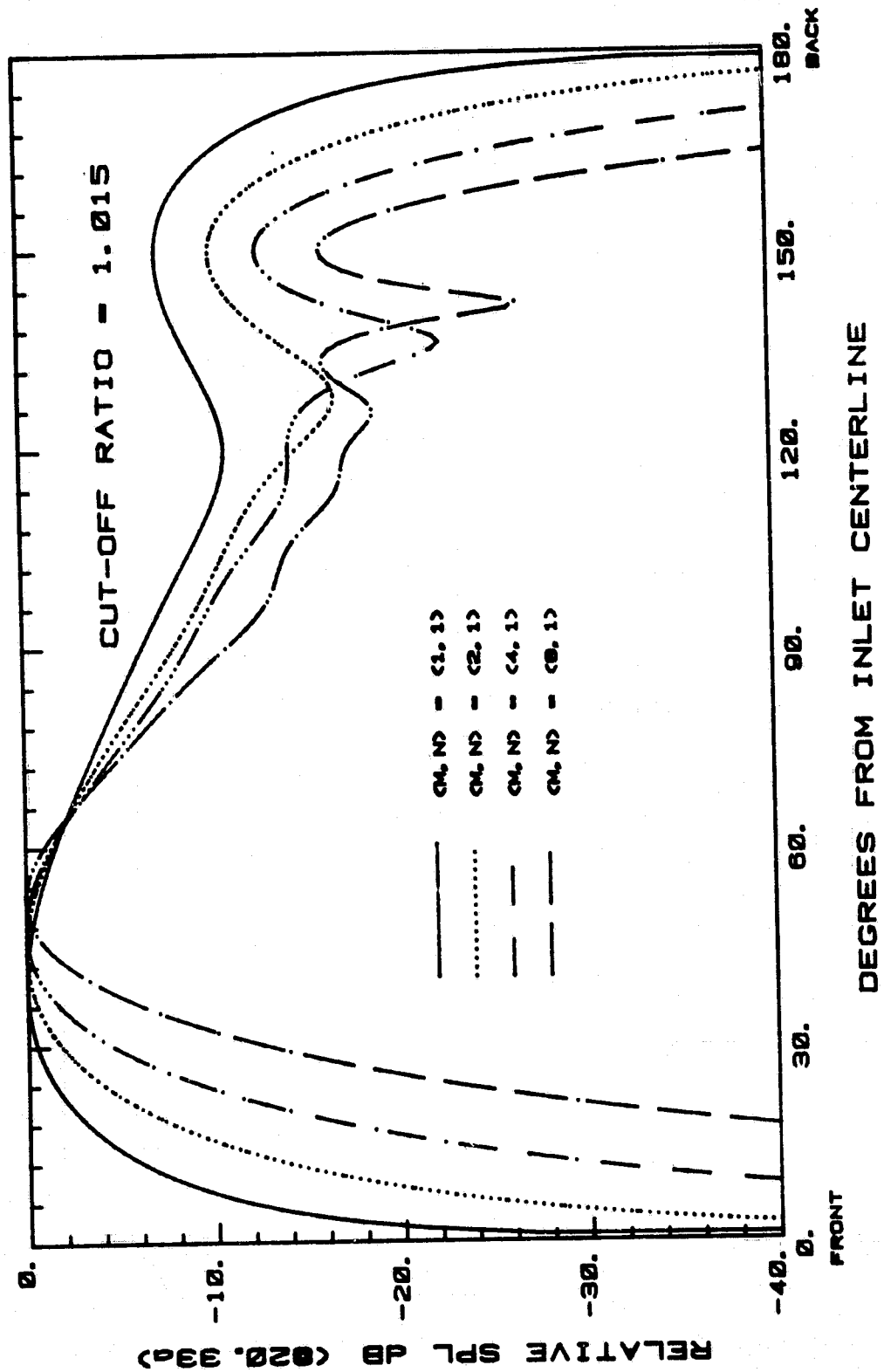
DEGREES FROM INLET CENTERLINE

LANGLEY BELLMOUTH

Fig. 11b



ORIGINAL PAGE IS
OF POOR QUALITY



LANGLEY BELLMOUTH

Fig. 12a

ORIGINAL PAGE IS
OF POOR QUALITY

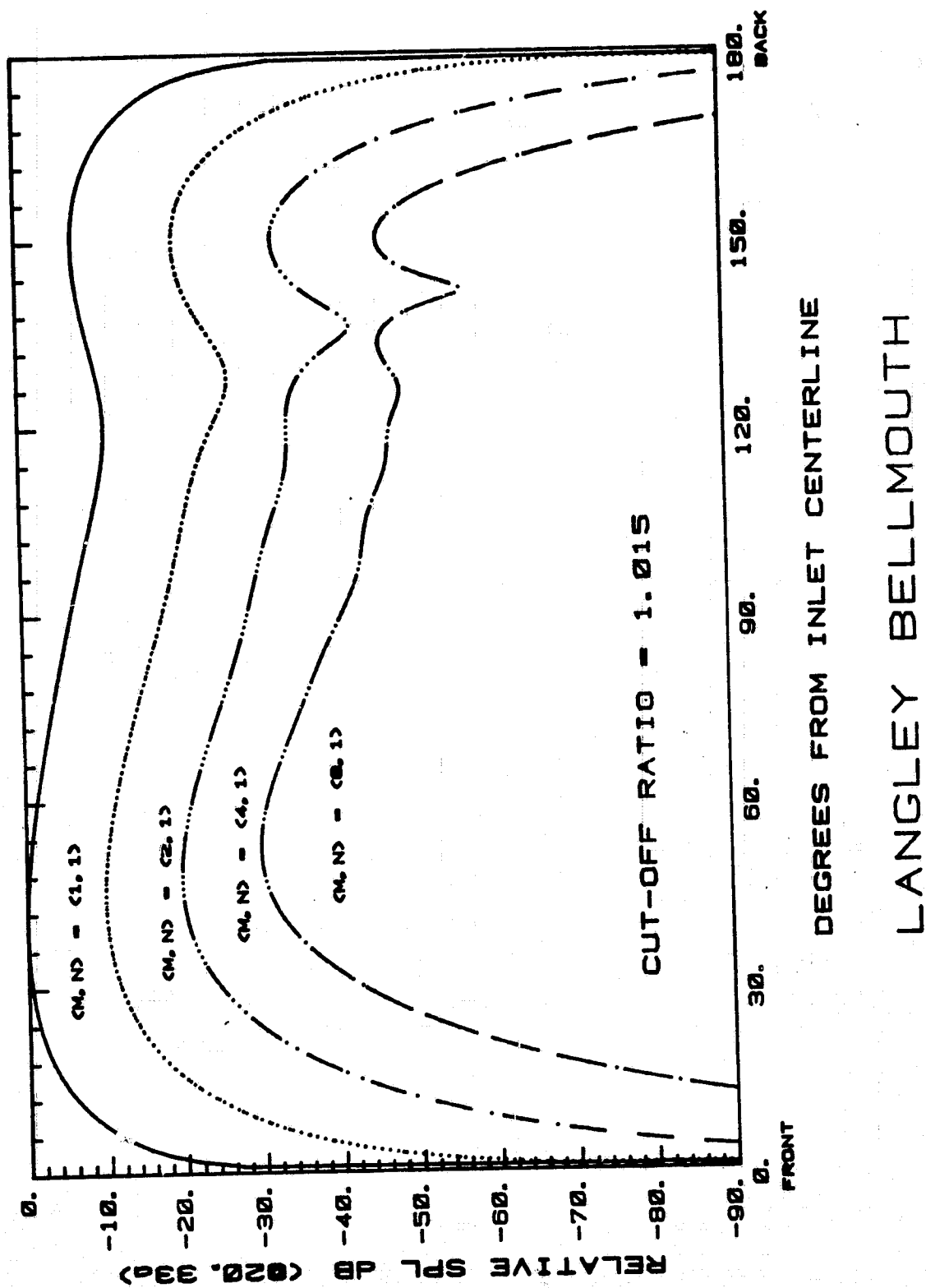
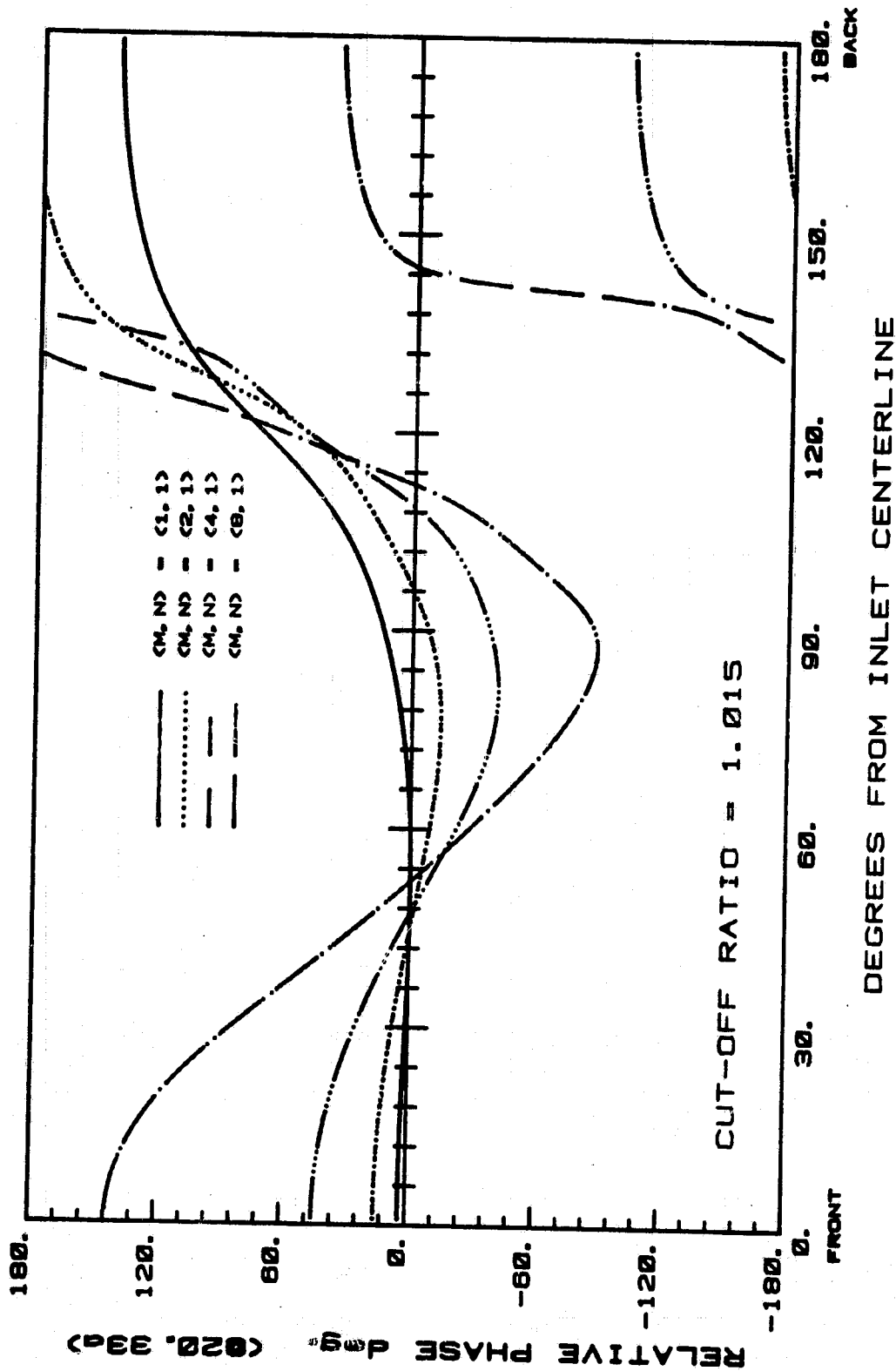


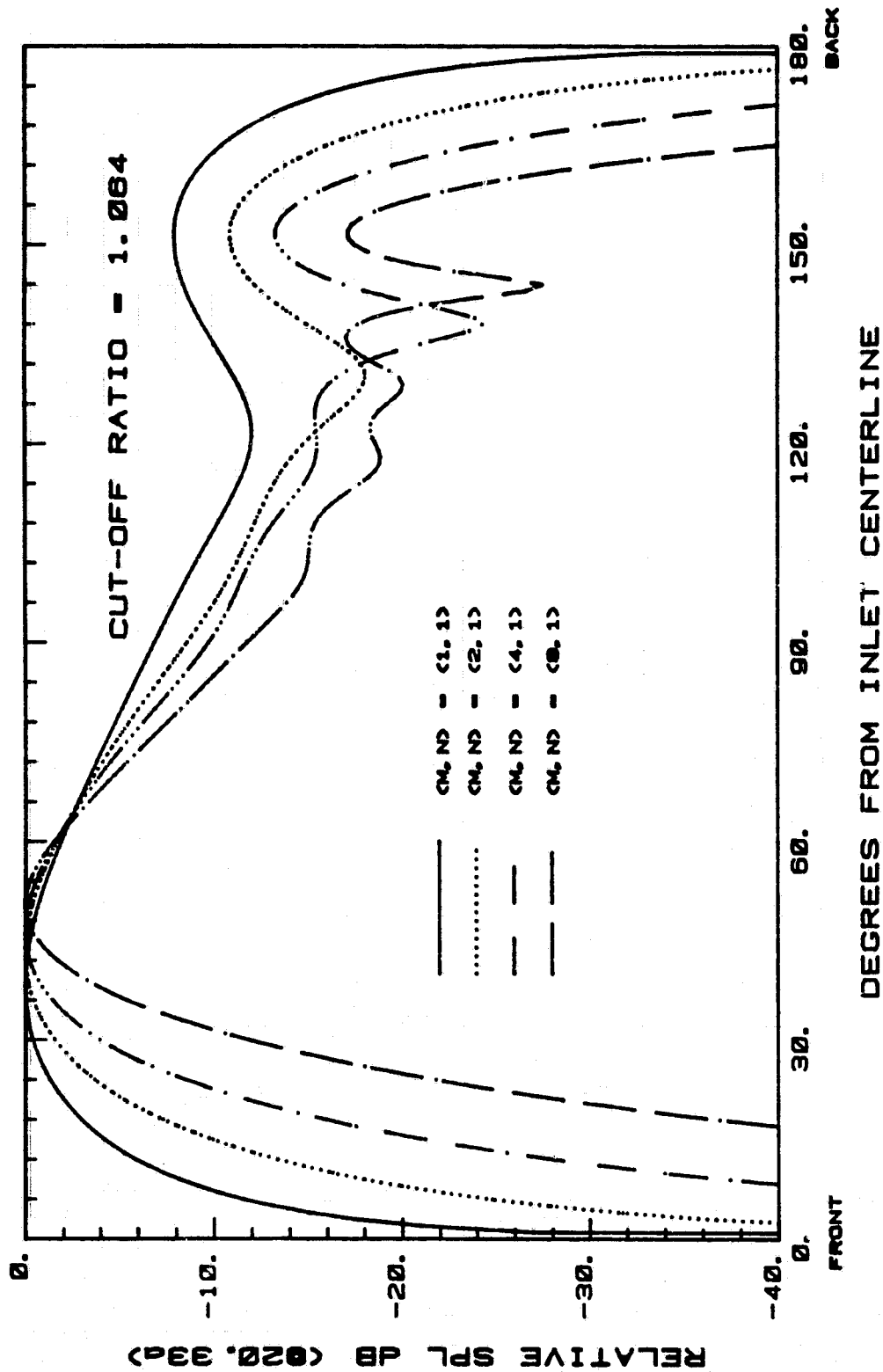
Fig. 12b



LANGLEY BELLMOUTH

Fig. 12c

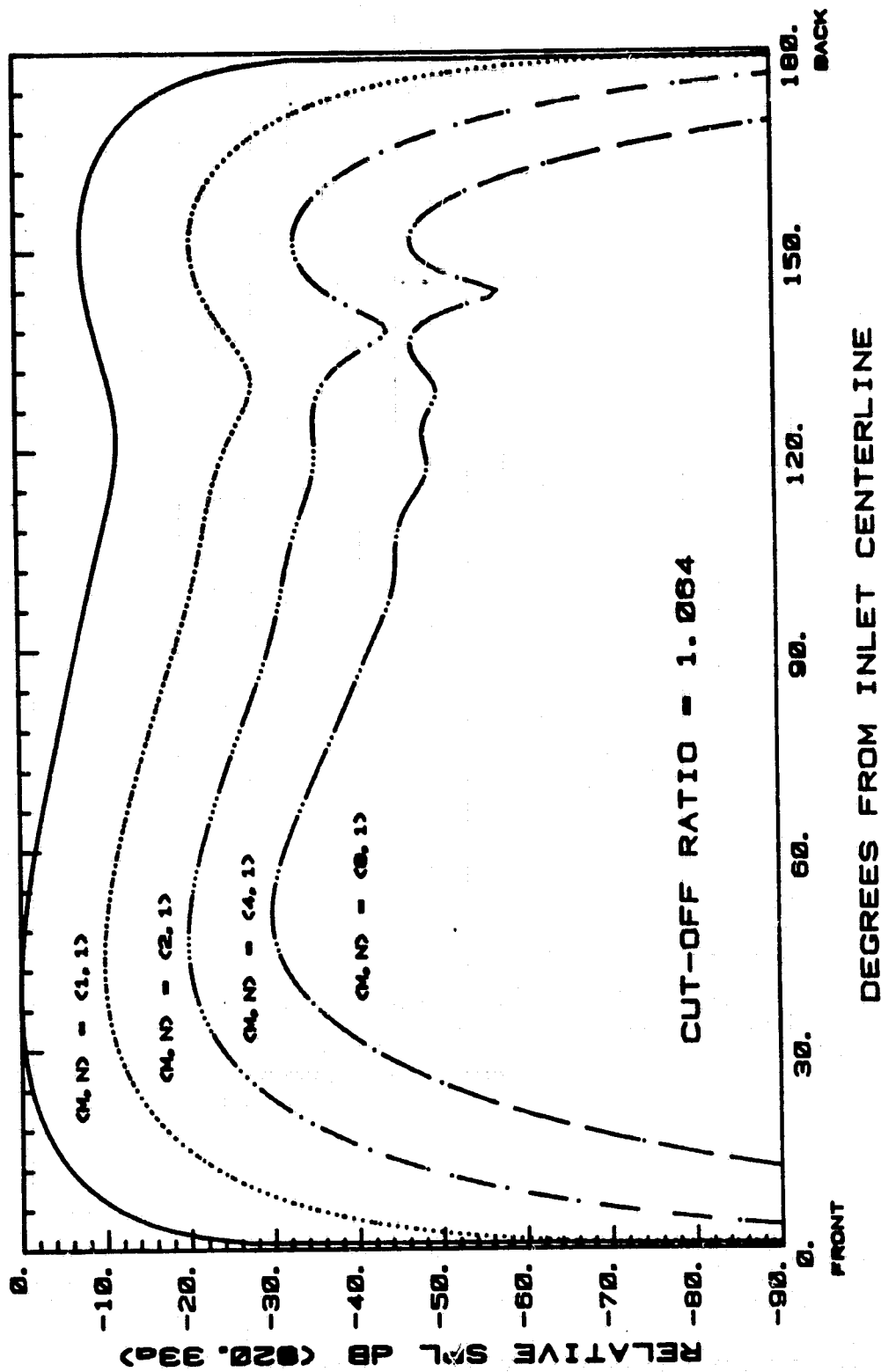
ORIGINAL PAGE IS
OF POOR QUALITY



LANGLEY BELLMOUTH

Fig. 13a

ORIGINAL PAGE IS
OF POOR QUALITY



LANGLEY BELLMOUTH

Fig. 13b

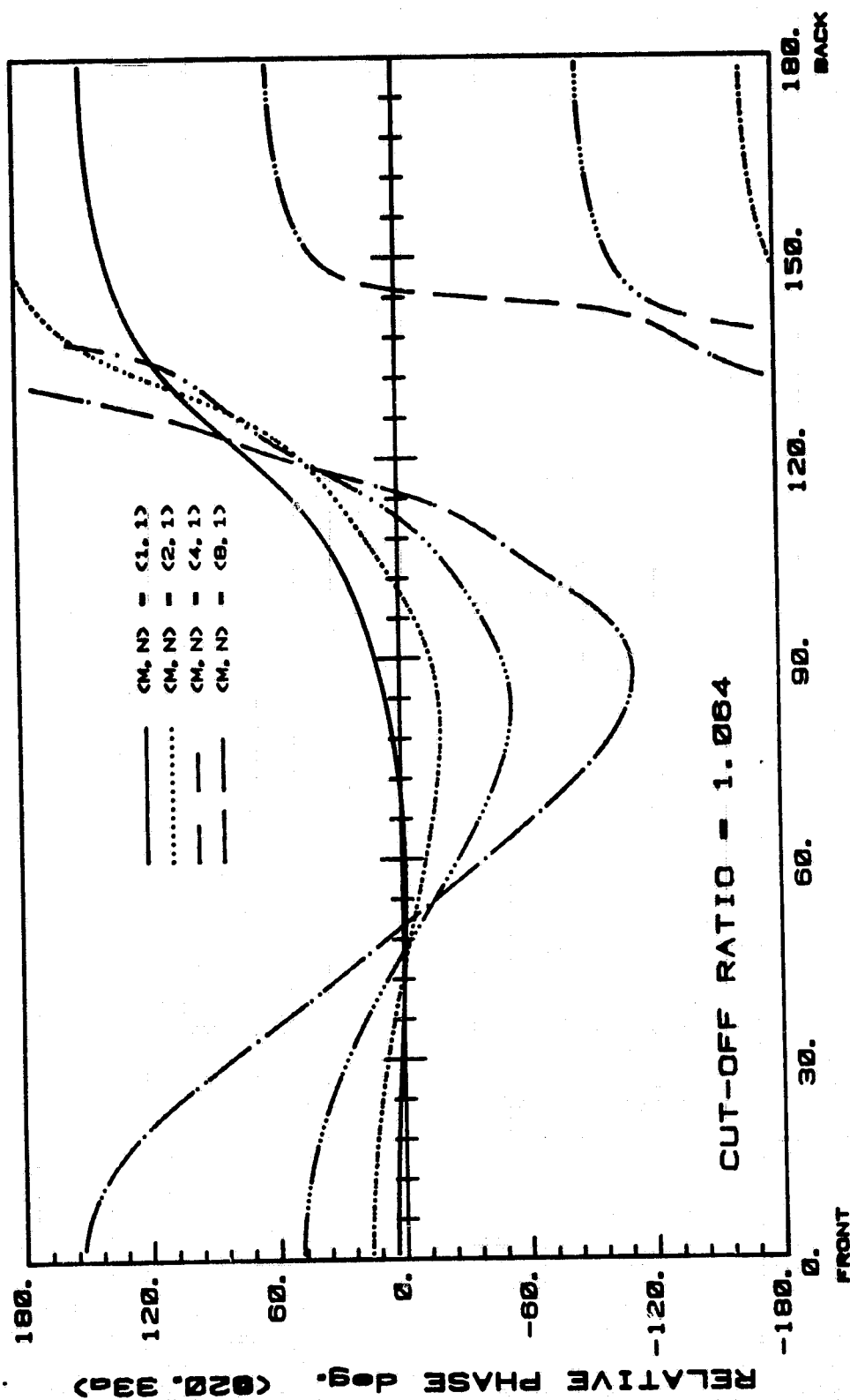
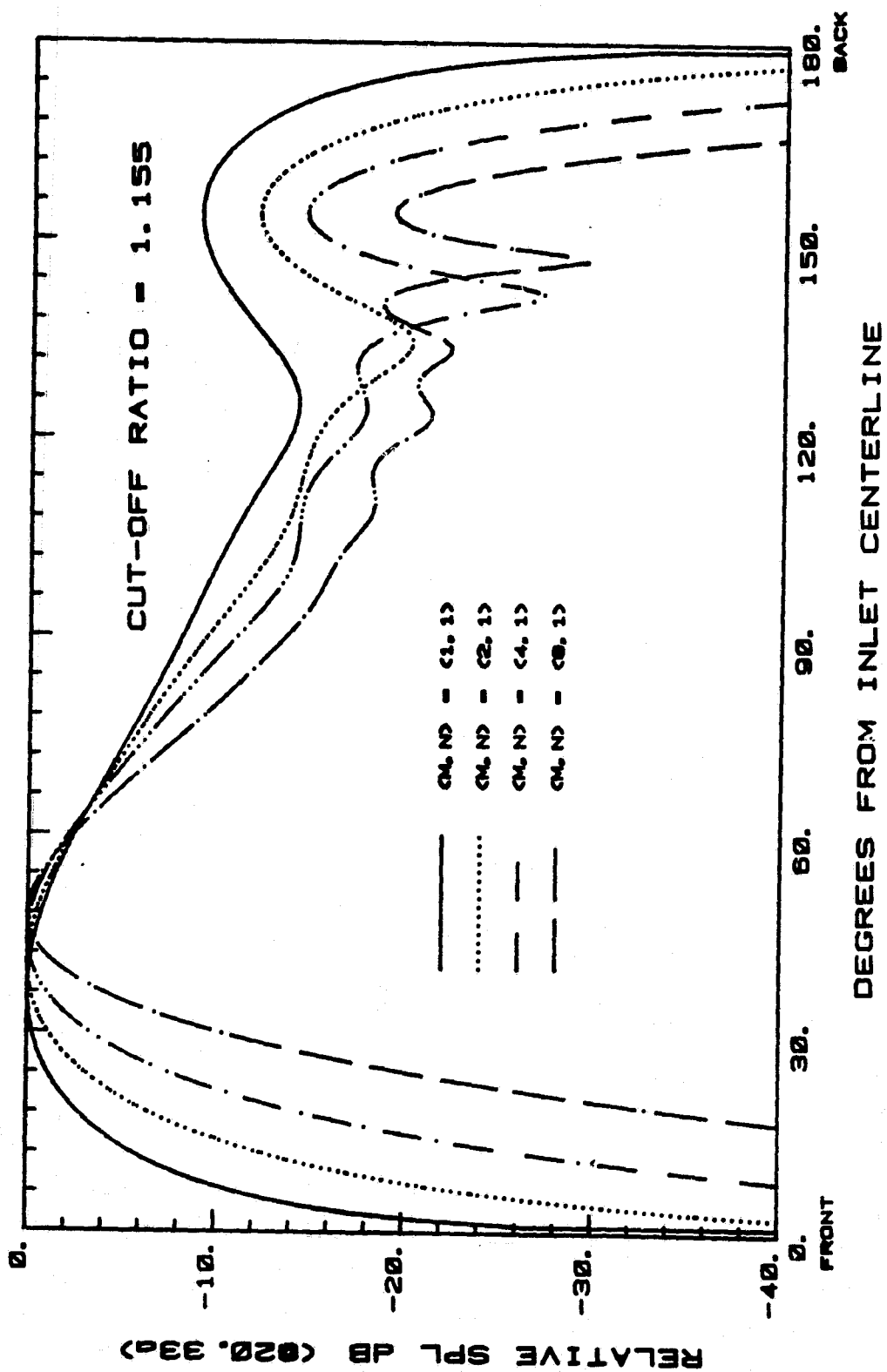


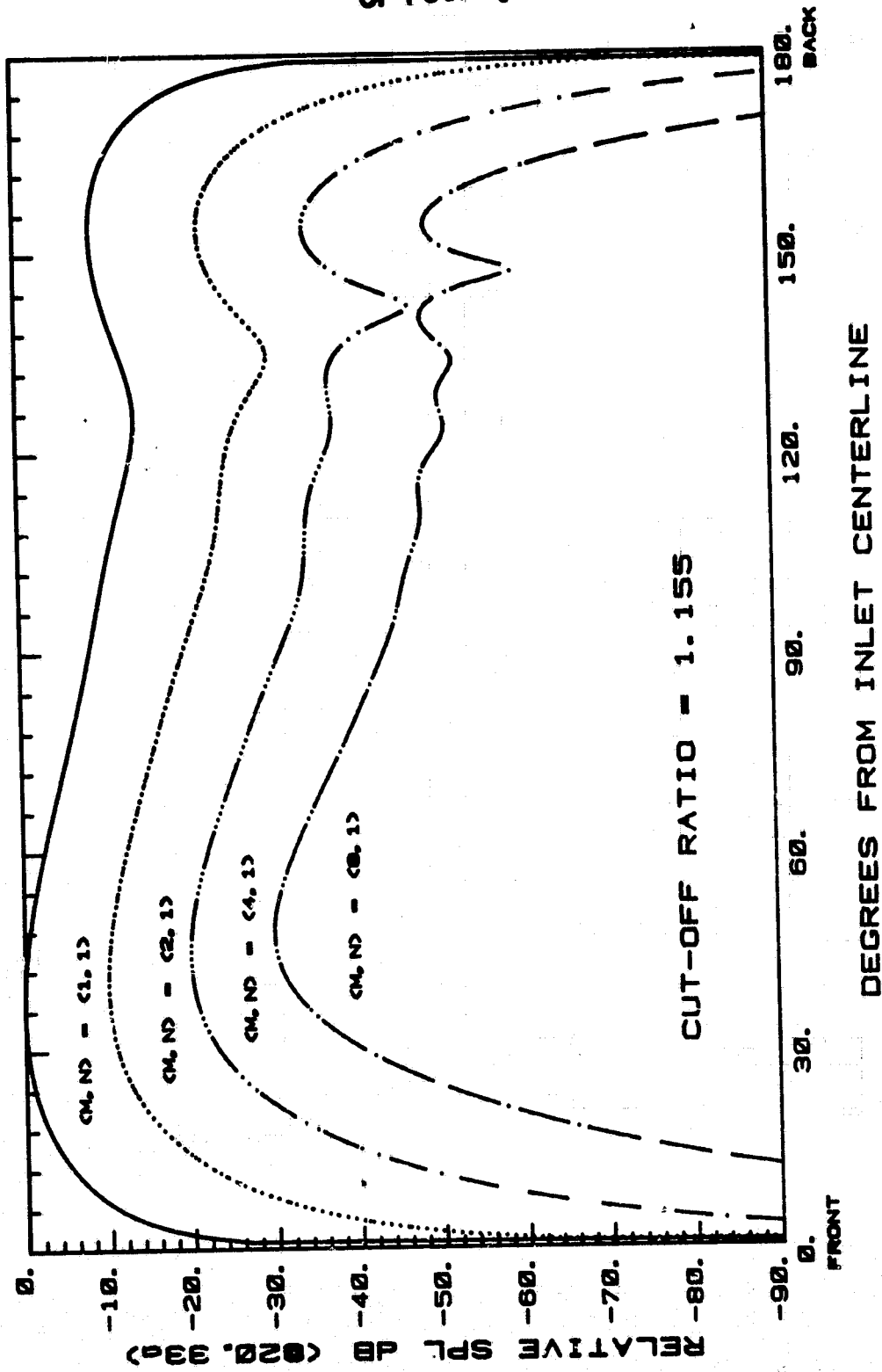
Fig. 13c



LANGLEY BELLMOUTH

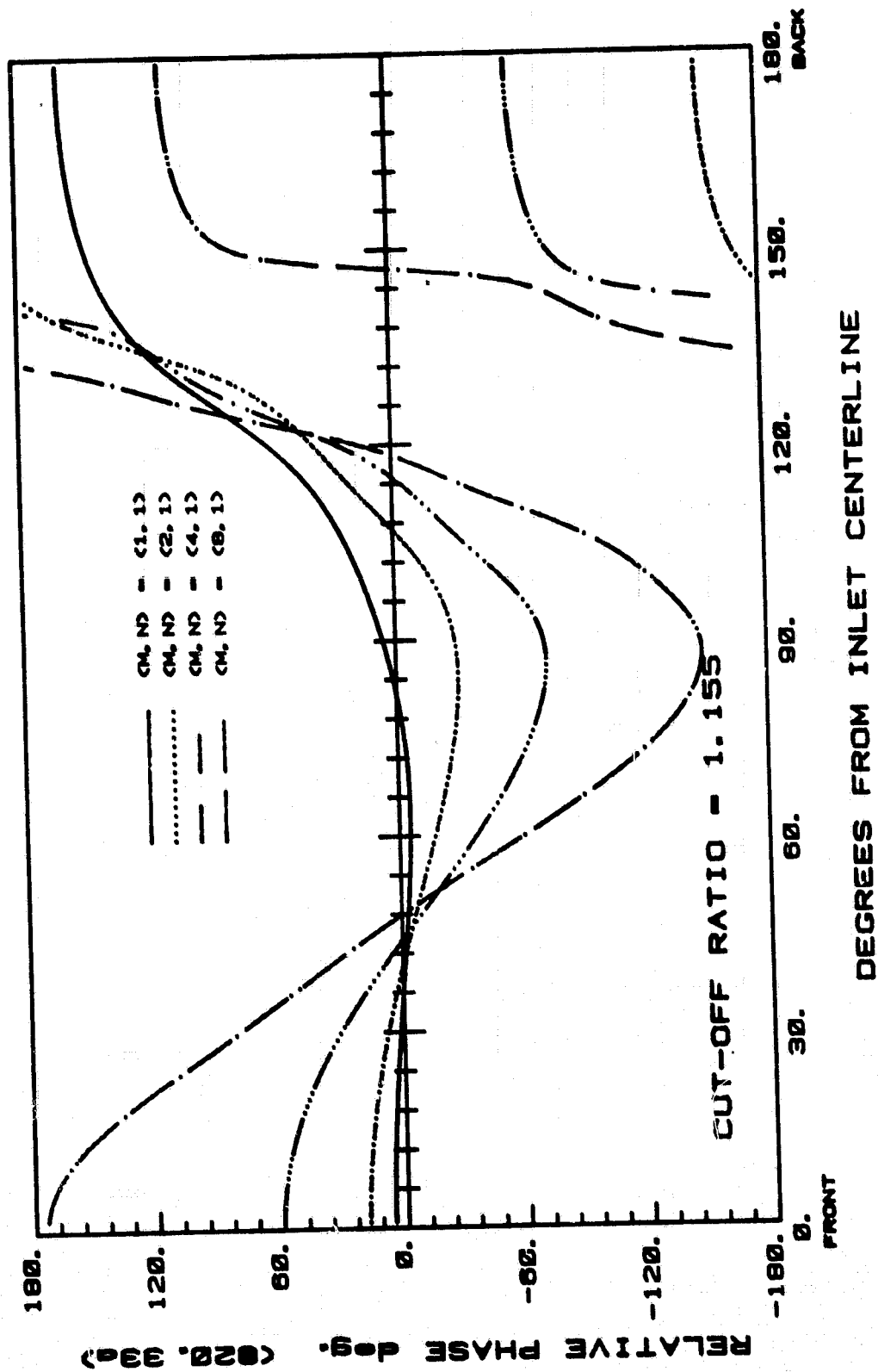
Fig. 14a

ORIGINAL PAGE IS
OF POOR QUALITY



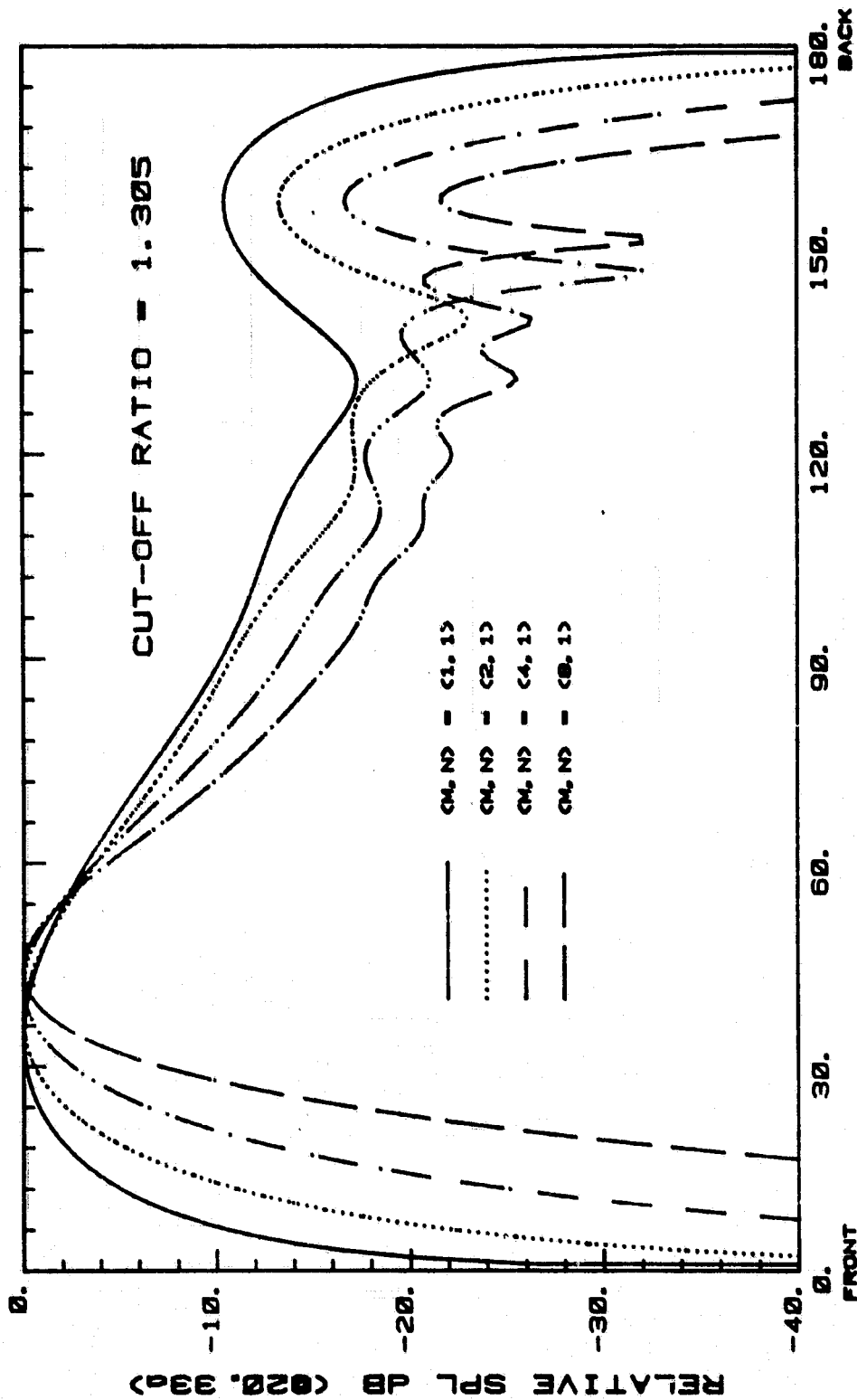
LANGLEY BELLMOUTH

Fig. 14b



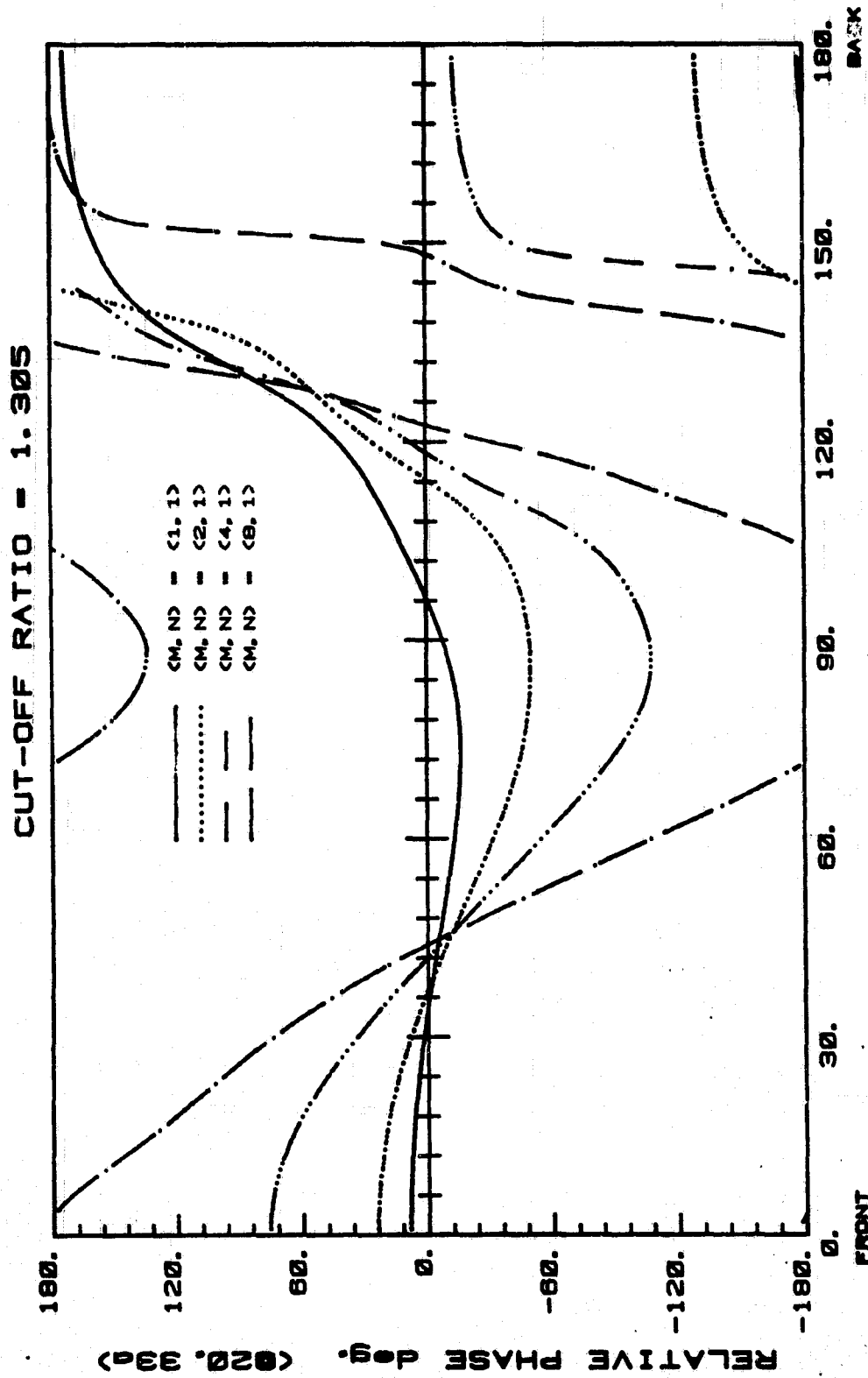
LANGLEY BELLMOUTH

Fig. 14c

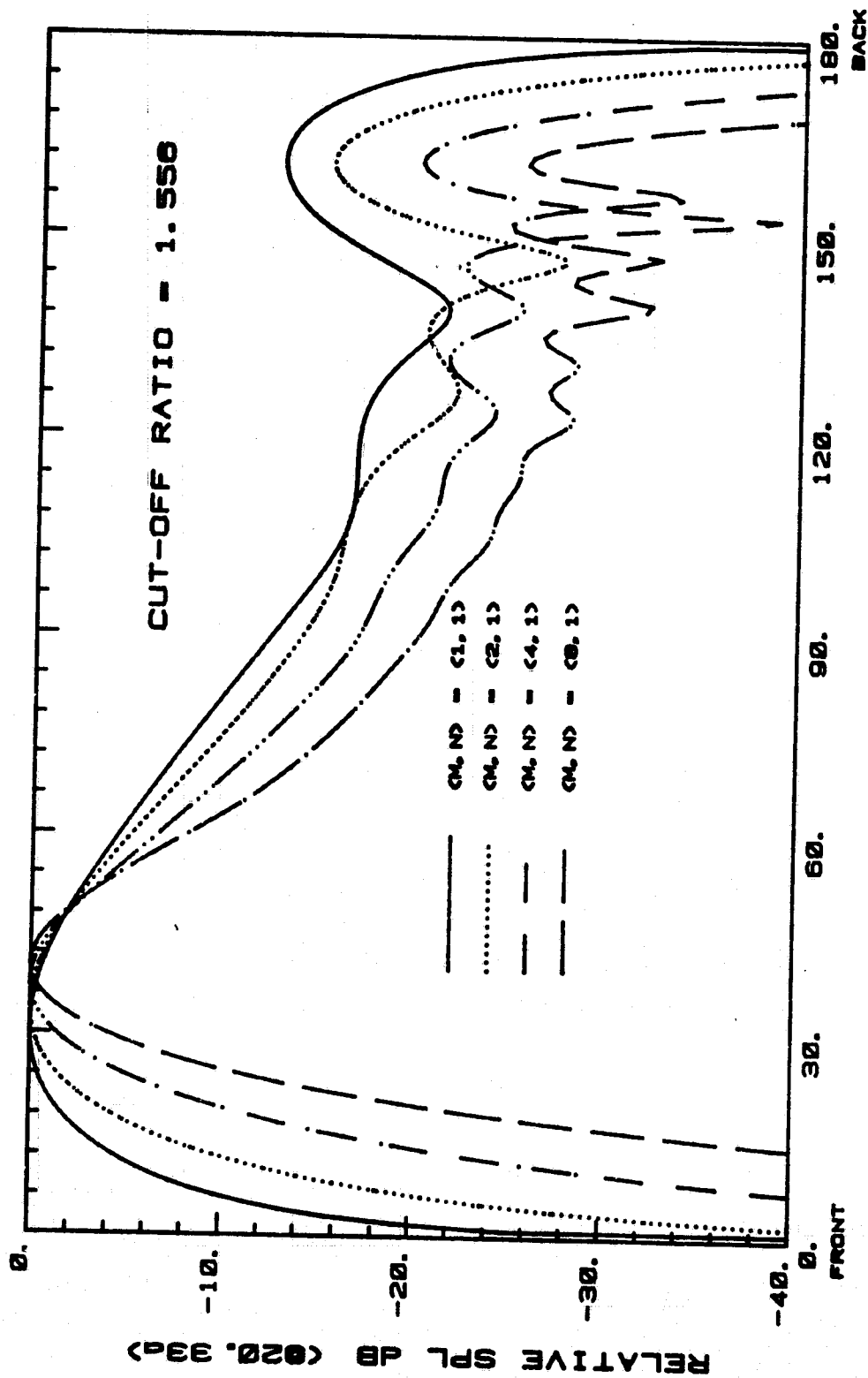


LANGLEY BELLMOUTH

Fig. 15a



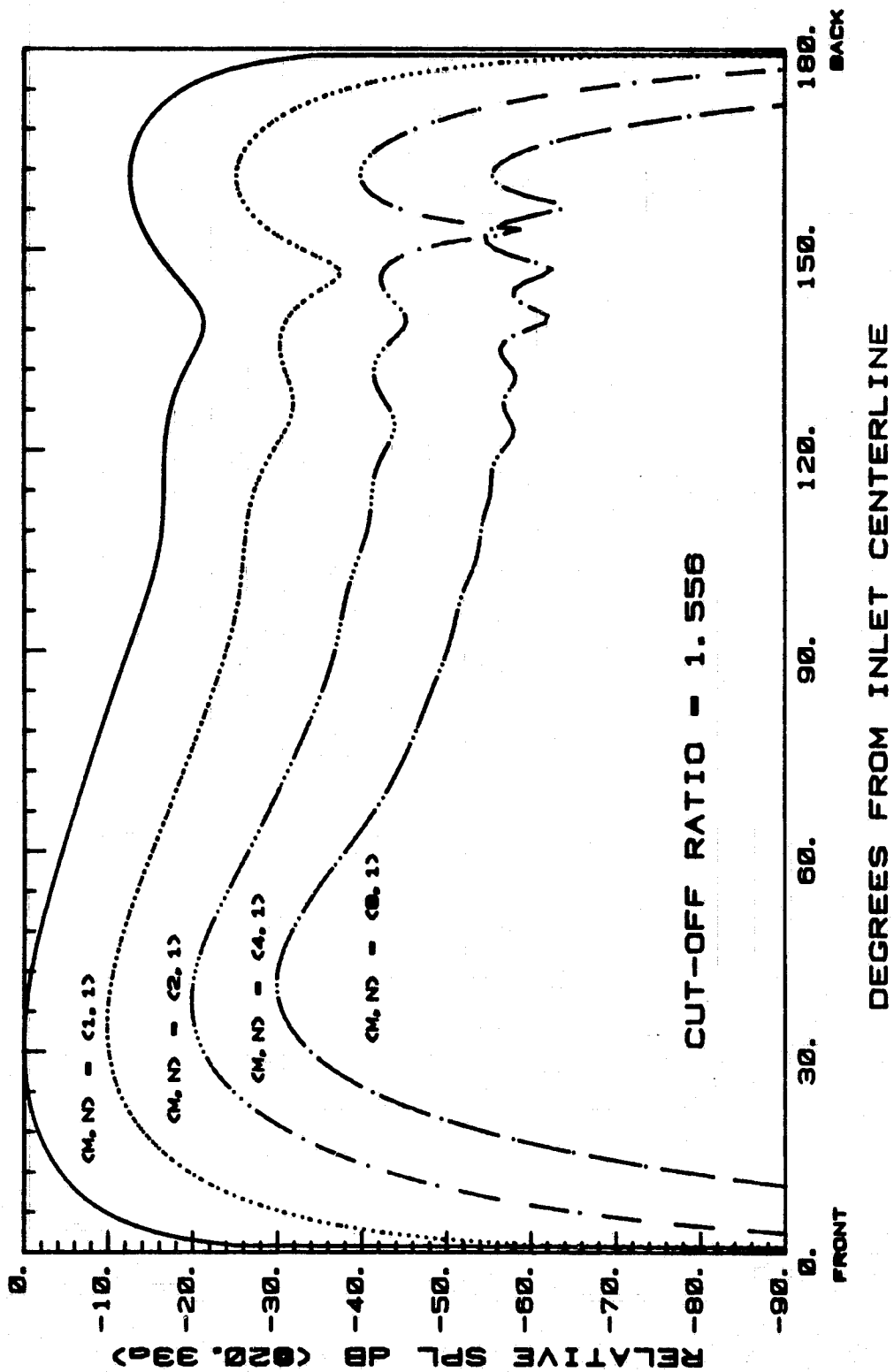
ORIGINAL PAGE 13
OF POOR QUALITY



LANGLEY BELLMOUTH

Fig. 16a

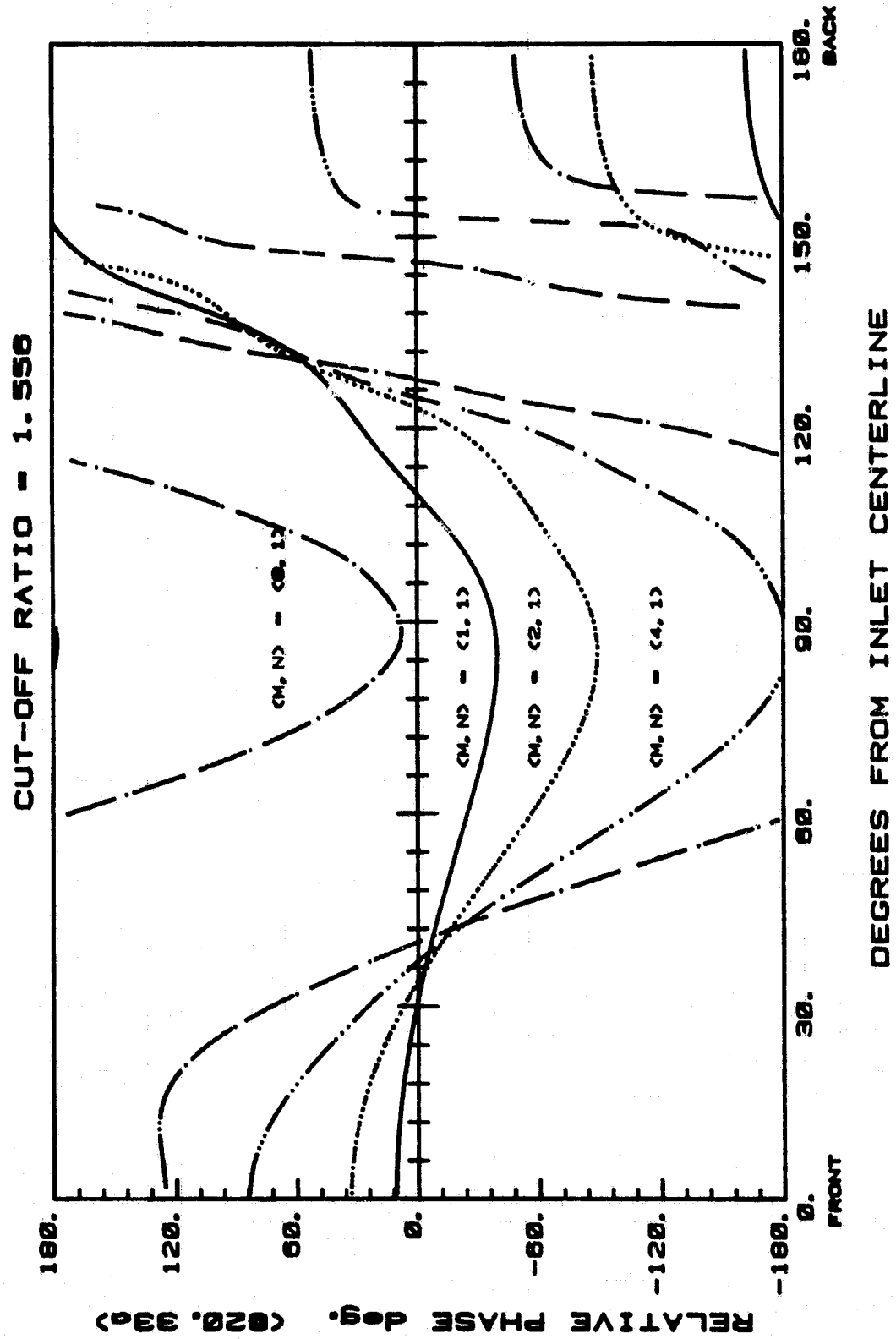
ORIGINAL PAGE IS
OF POOR QUALITY



LANGLEY BELLMOUTH

Fig. 16b

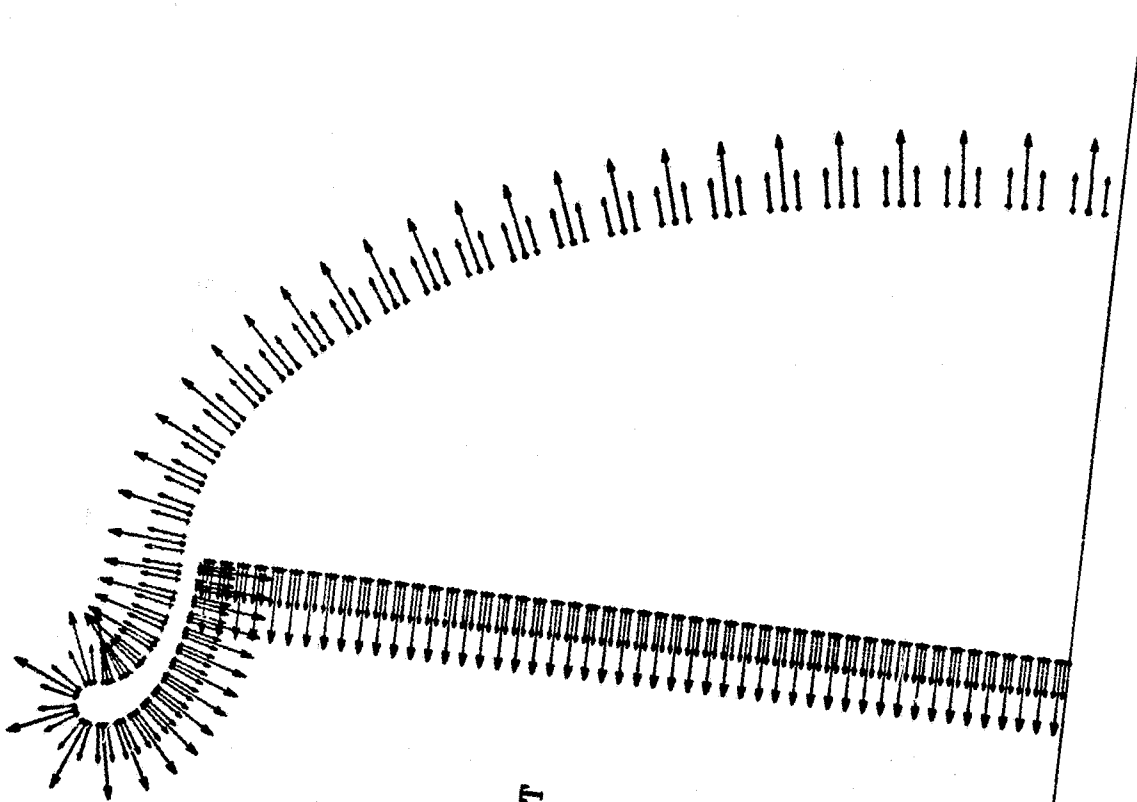
ORIGINAL PAGE IS
OF POOR QUALITY



LANGLEY BELLMOUTH

Fig. 16c

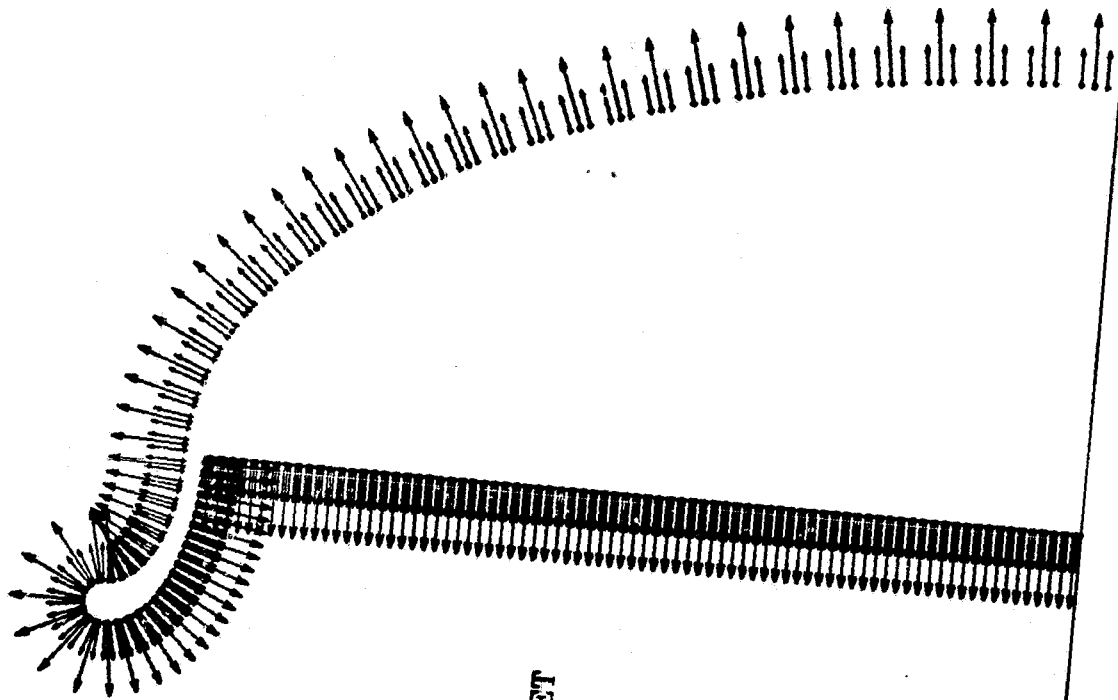
ORIGINAL PAGE IS
OF POOR QUALITY



THIN LIPPED ELLIPTICAL INLET
97 pts.

Fig. 17

ORIGINAL PAGE IS
OF POOR QUALITY

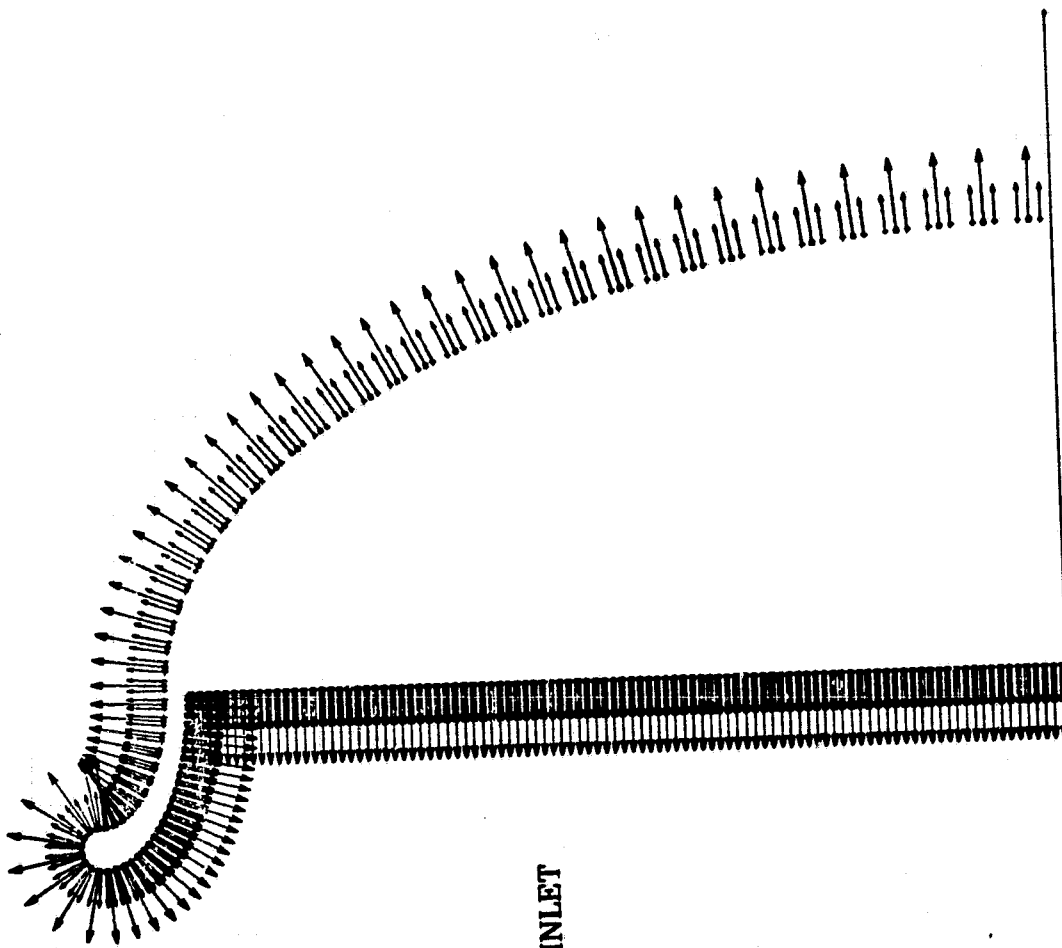


THIN LIPPED ELLIPTICAL INLET

146 pts.

Fig. 18

ORIGINAL PAGE IS
OF POOR QUALITY



THIN LIPPED ELLIPTICAL INLET

179 pts.

Fig. 19

THIN LIPPED ELLIPTICAL INLET

Deg	SPL	Deg	SPL
0	104	45	104
2	104	46	104
4	104	48	104
6	104	50	104
8	104	52	104
10	104	54	104
12	104	56	104
14	104	58	104
16	104	60	104
18	104	62	104
20	104	64	104
22	104	66	104
24	104	68	104
26	104	70	104
28	104	72	104
30	104	74	104
32	104	76	104
34	104	78	104
36	104	80	104
38	104	82	104
40	104	84	104
42	104	86	104
44	104	88	104
		90	104

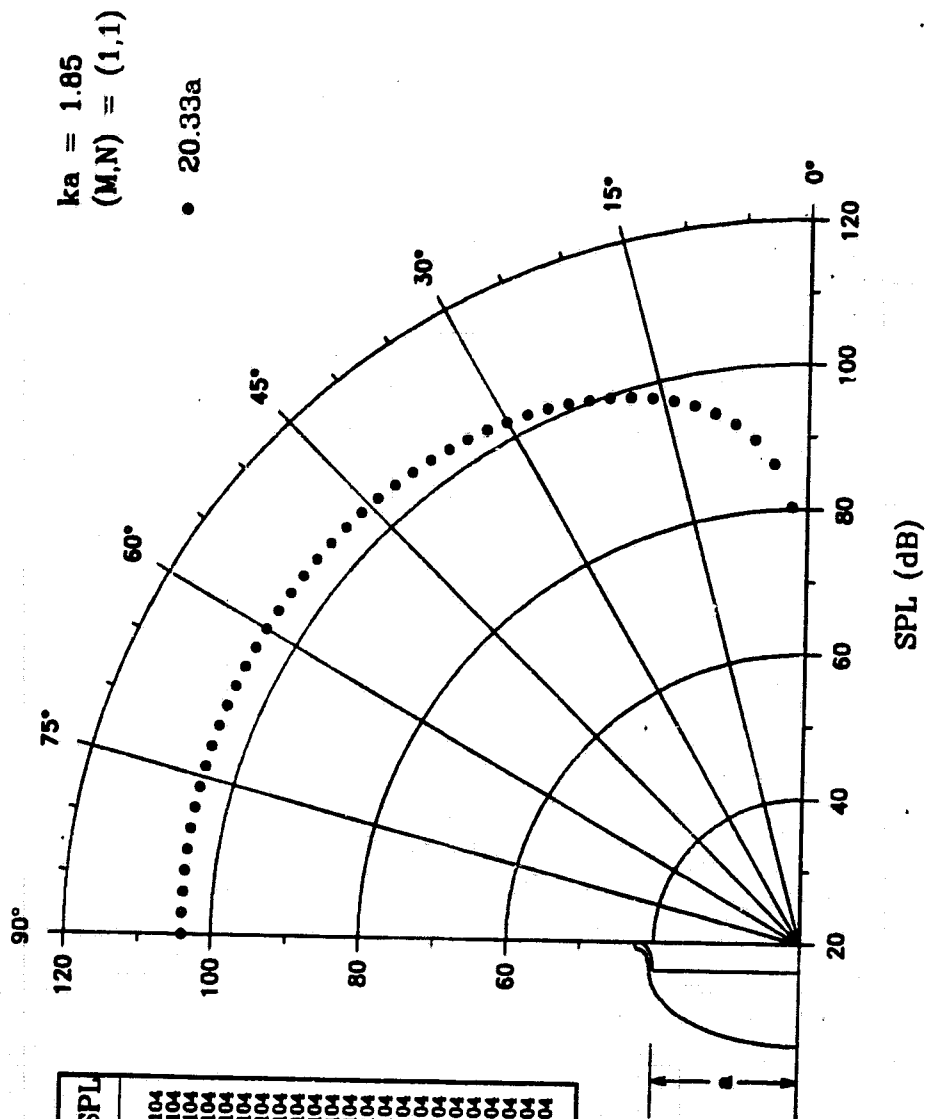


Fig. 20a

ORIGINAL PAGE IS
OF POOR QUALITY

THIN LIPPED ELLIPTICAL INLET

$ka = 1.87$
 $(M,N) = (1,1)$

• 20.33a

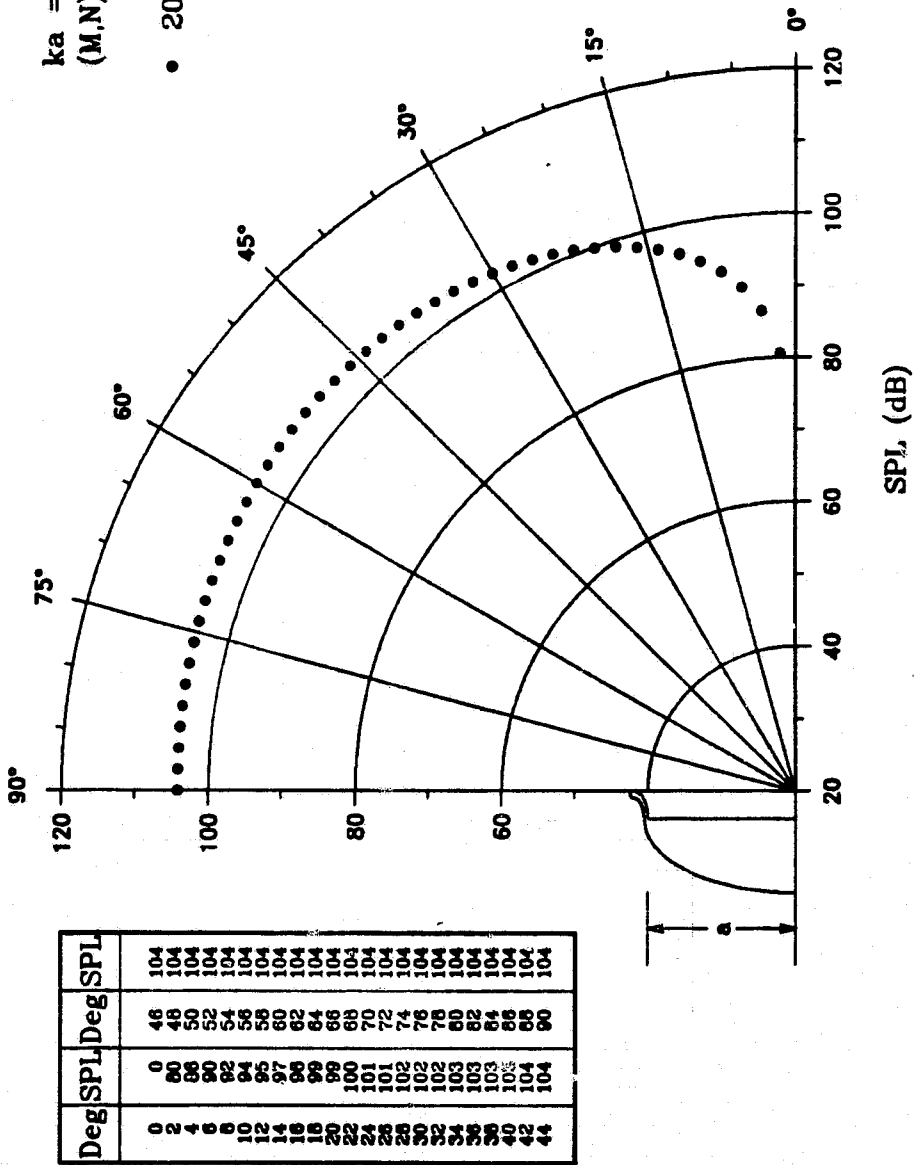


Fig. 20b

ORIGINAL PAGE IS
 OF POOR QUALITY

THIN LIPPED ELLIPTICAL INLET

$ka = 1.96$
 $(M,N) = (1,1)$

• 20.33a

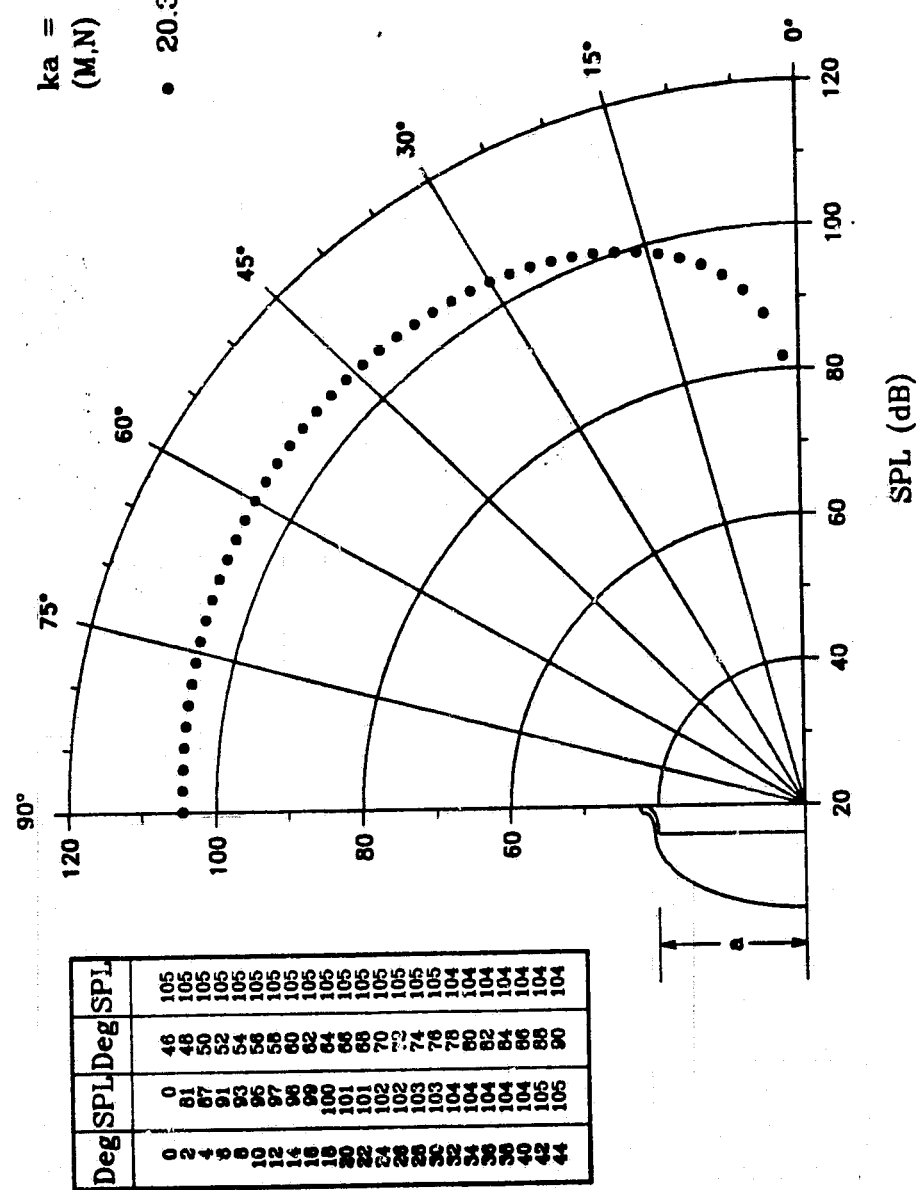


Fig. 20c

ORIGINAL PAGE 19
 OF POOR QUALITY

THIN LIPPED ELLIPTICAL INLET

ORIGINAL PAGE IS
OF POOR QUALITY

$ka = 2.13$
 $(M,N) = (1,1)$

• 20.33a

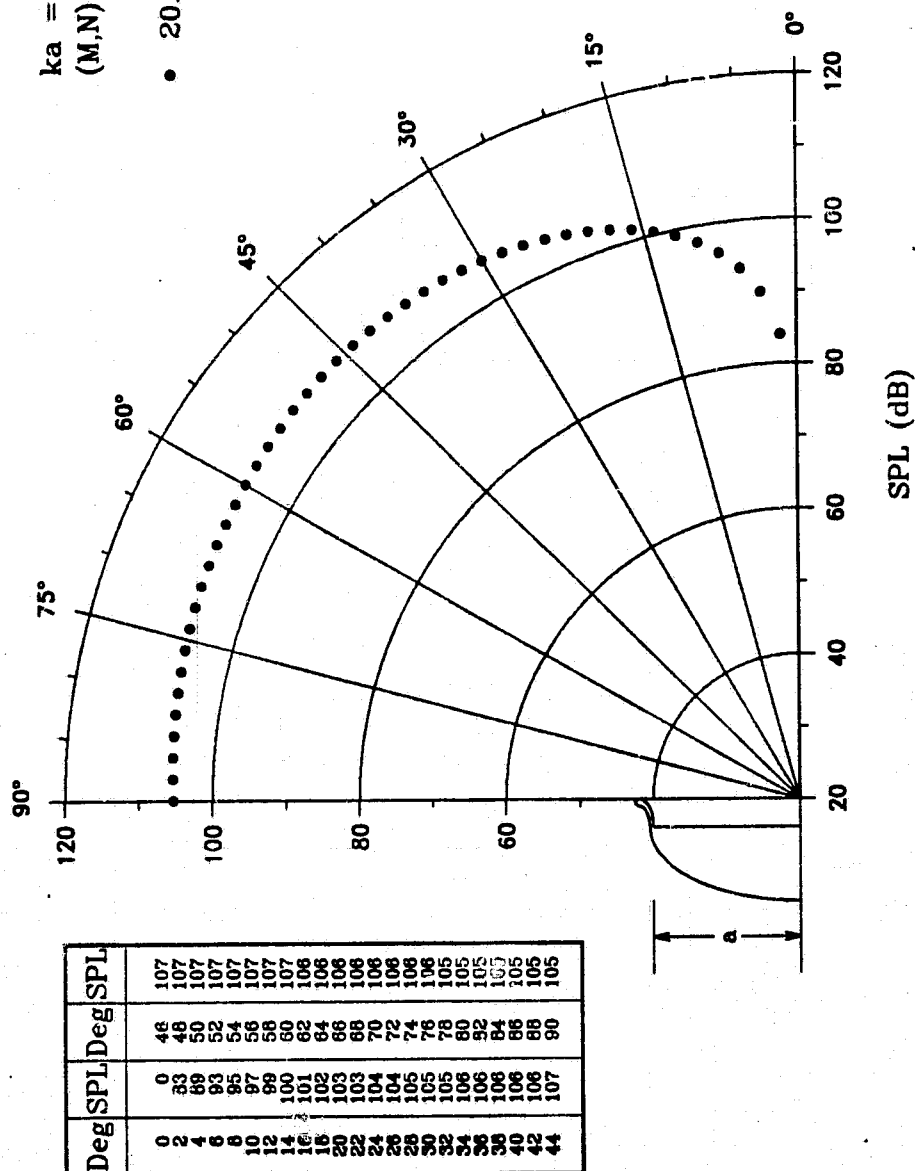
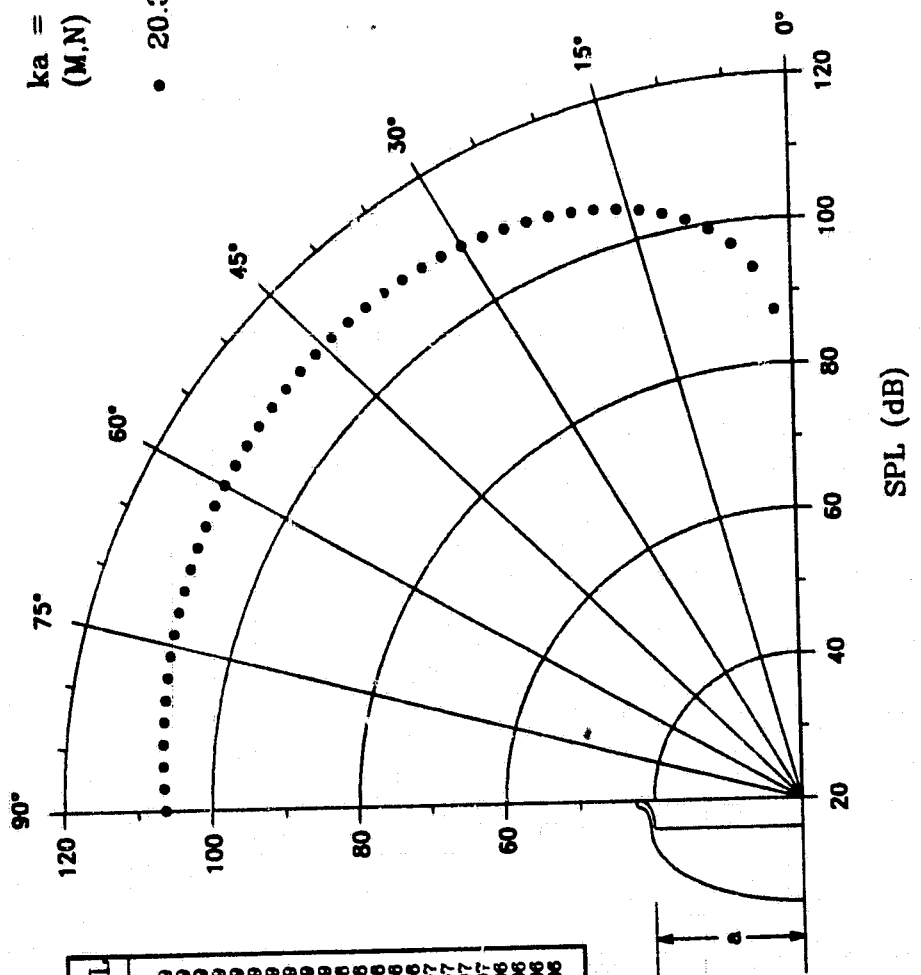


Fig. 20d

THIN LIPPED ELLIPTICAL INLET

$ka = 2.40$
 $(M,N) = (1,1)$
 \bullet 20.33a



Deg	SPL	Deg	SPL
0	87	46	109
2	93	48	109
4	96	50	109
6	99	52	109
8	101	54	109
10	102	56	109
12	103	58	109
14	104	60	109
16	105	62	109
18	106	64	109
20	107	66	109
22	107	68	108
24	108	70	108
26	108	72	108
28	108	74	108
30	109	76	107
32	109	78	107
34	109	80	107
36	109	82	106
38	109	84	106
40	109	86	106
42	109	88	106
44	109	90	106

Fig. 20e

ORIGINAL PAGE IS
 OF POOR QUALITY

THIN LIPPED ELLIPTICAL INLET

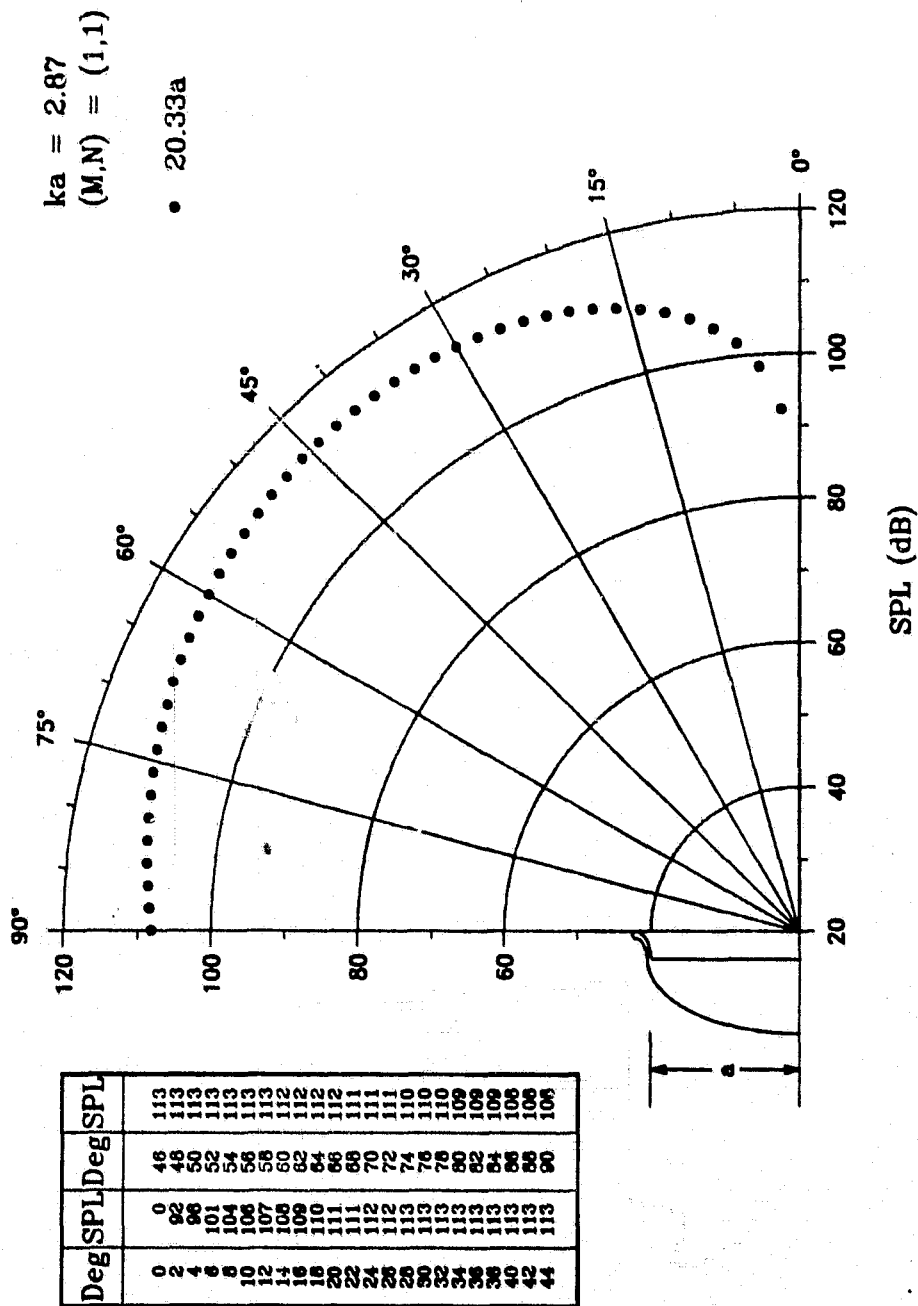


Fig. 20f

ORIGINAL PAGE IS
OF POOR QUALITY

THIN LIPPED ELLIPTICAL INLET

$ka = 3.76$
 $(M,N) = (1,1)$

• 20.33a

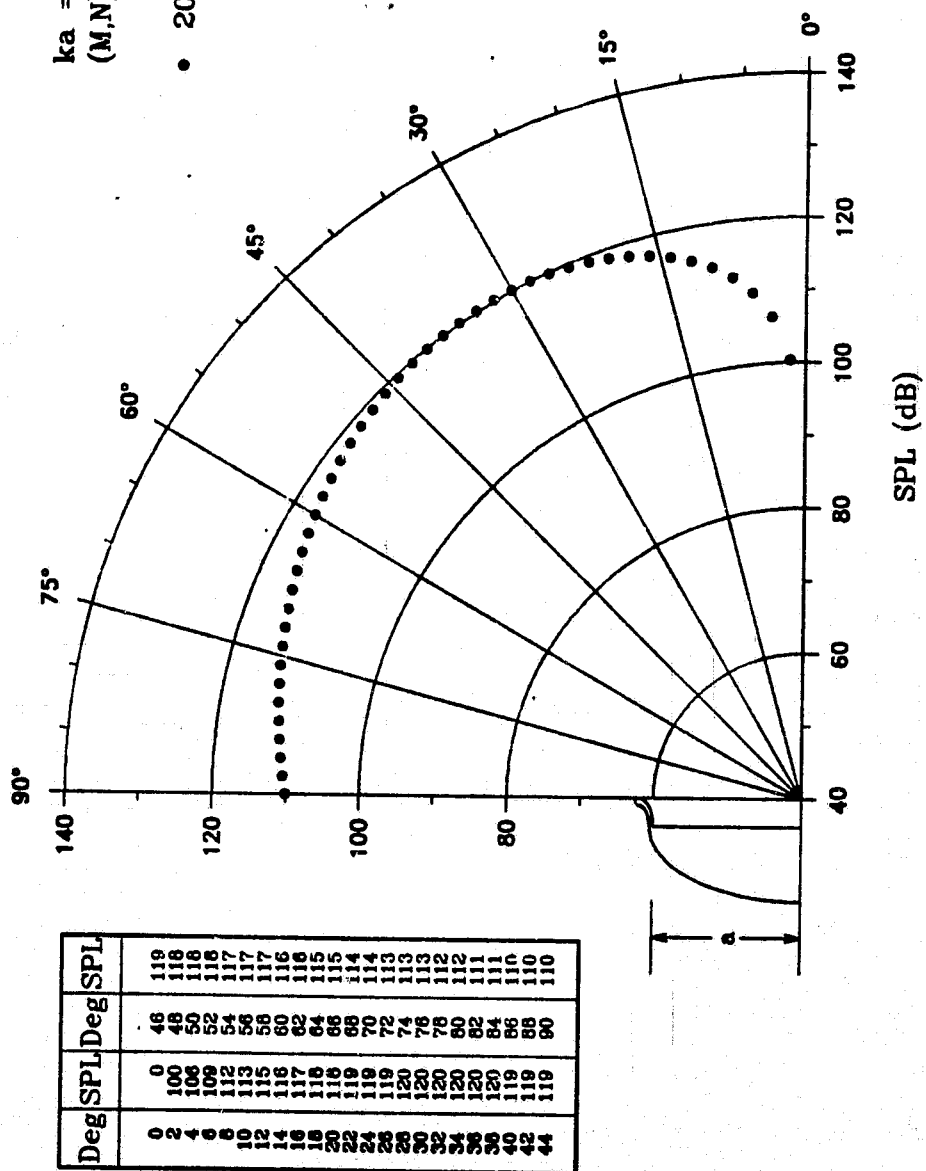


Fig. 20g

ORIGINAL PAGE 13
 OF POOR QUALITY

THIN LIPPED ELLIPTICAL INLET

ORIGINAL PAGE IS
OF POOR QUALITY

$ka = 4.60$
(M,N) = (1,1)

• 20.33a

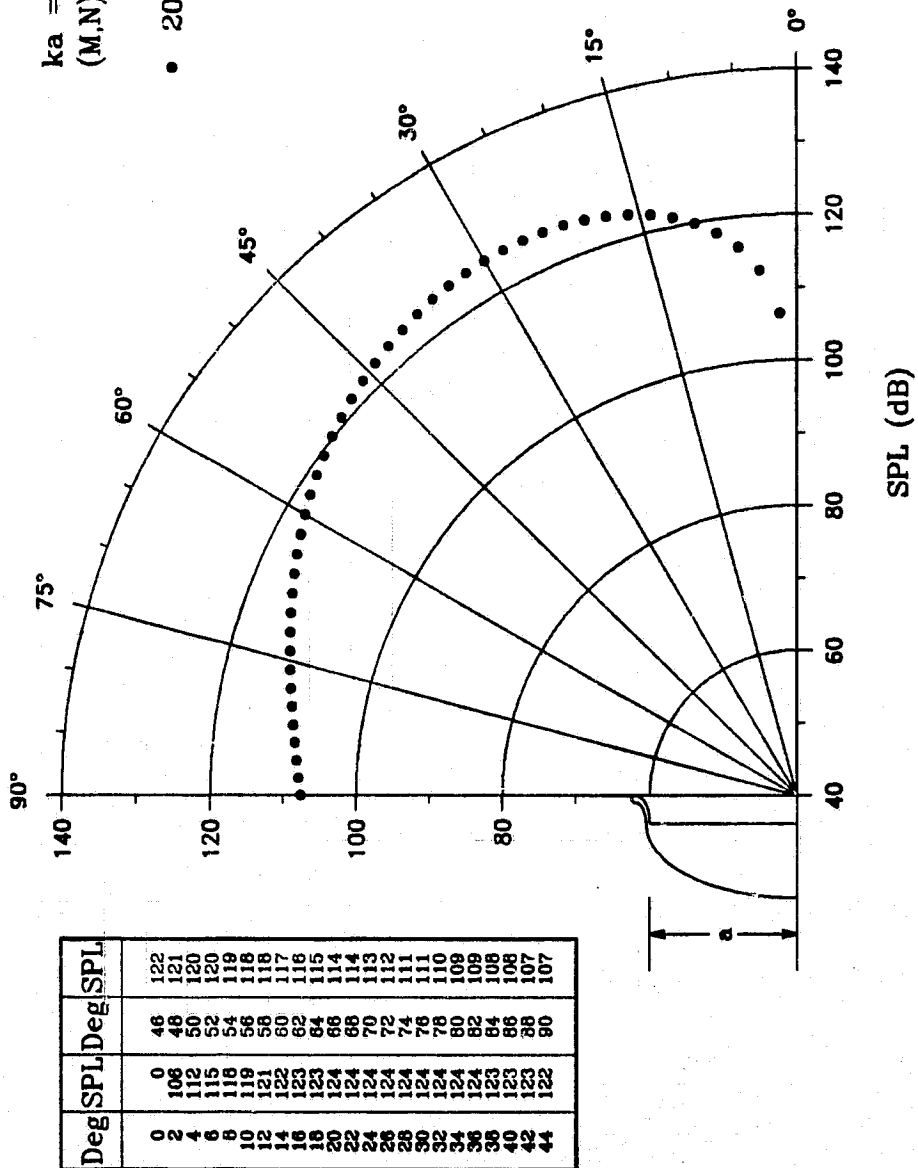


Fig. 20h

THIN LIPPED ELLIPTICAL INLET

$ka = 5.28$
 $(M,N) = (1,1)$
 $\bullet 20.33a$

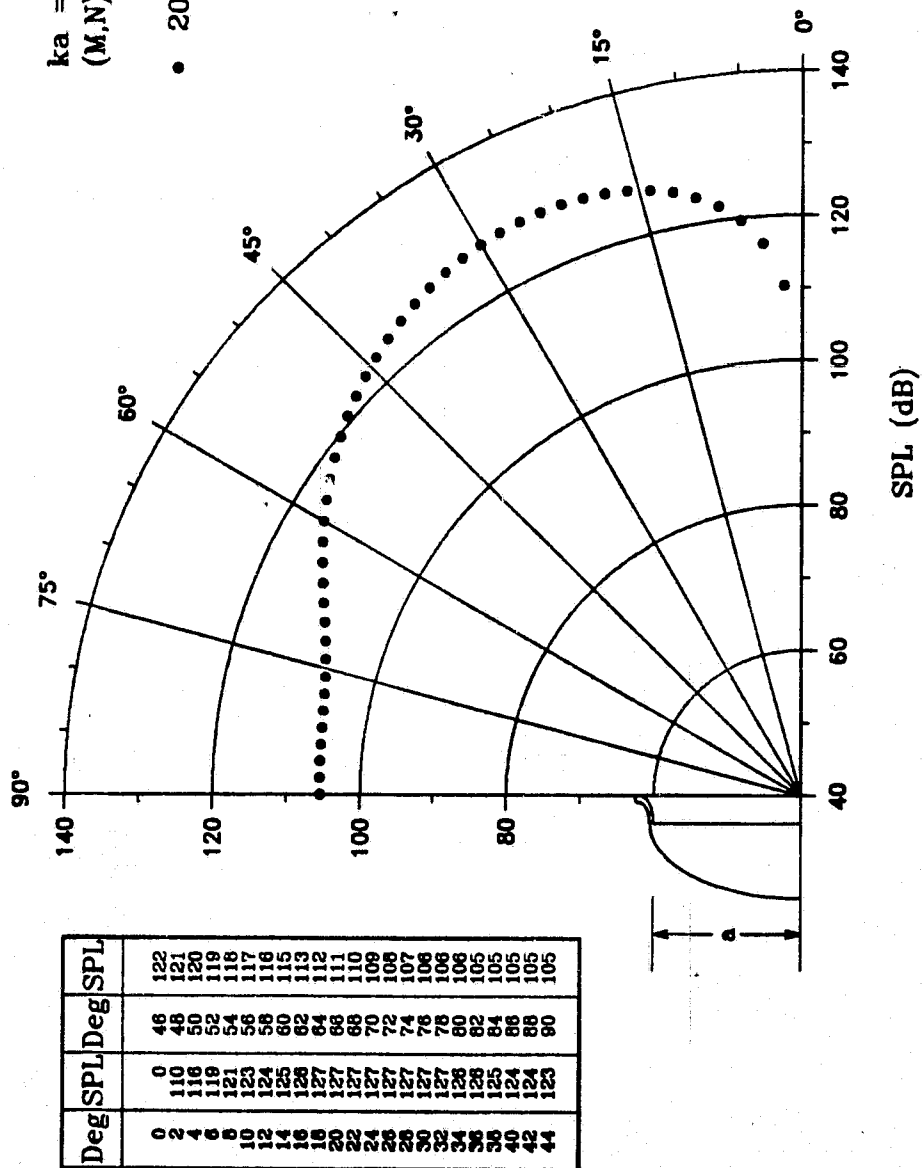


Fig. 201

THIN LIPPED ELLIPTICAL INLET

$ka = 3.07$
 $(M,N) = (2,1)$

• 20.33a

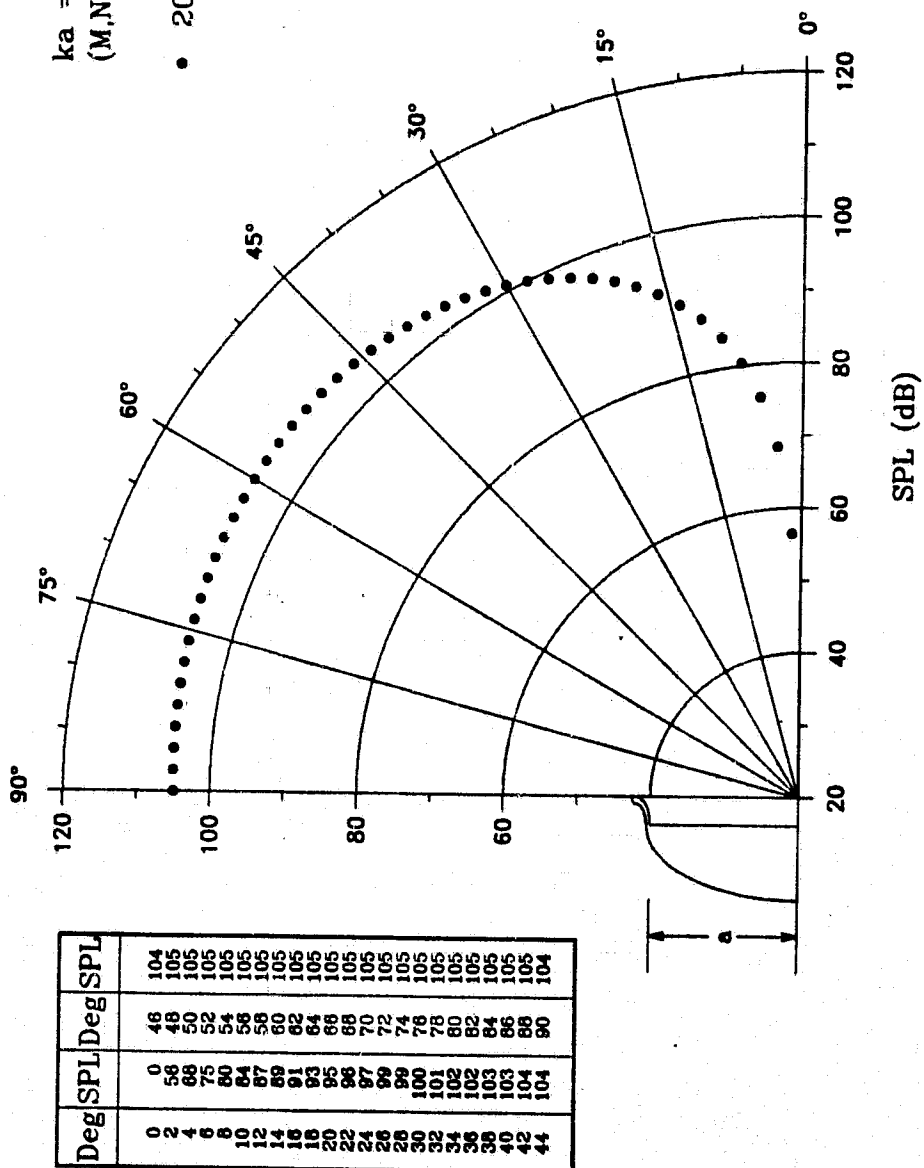


Fig. 21a

ORIGINAL PAGE IS
 OF POOR QUALITY

THIN LIPPED ELLIPTICAL INLET

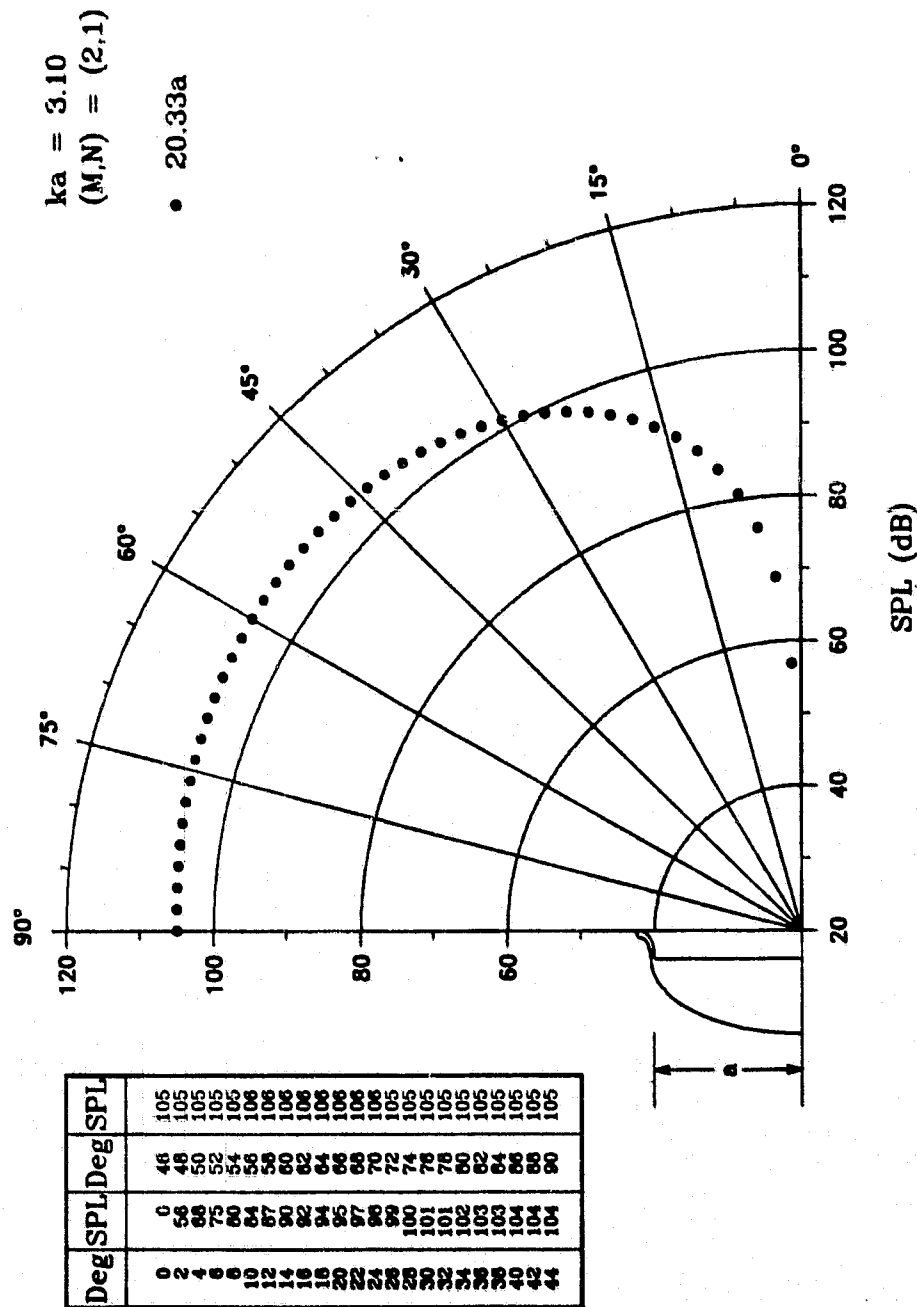


Fig. 21b

ORIGINAL PAGE IS
OF POOR QUALITY.

THIN LIPPED ELLIPTICAL INLET

$ka = 3.25$
 $(M,N) = (2,1)$

• 20.33a

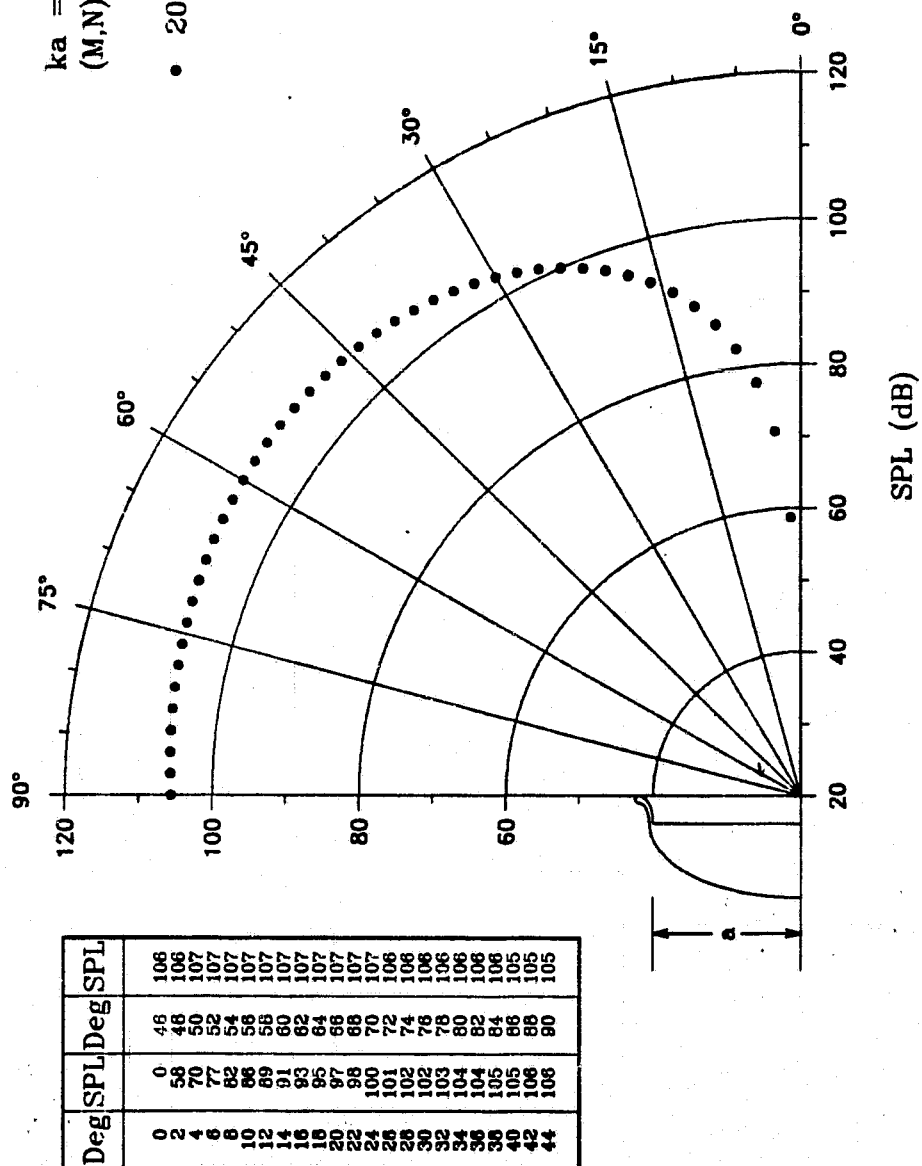


Fig. 21c

ORIGINAL PAGE 13
 OF POOR QUALITY

THIN LIPPED ELLIPTICAL INLET

$ka = 3.53$
 $(M,N) = (2,1)$

• 20.33a

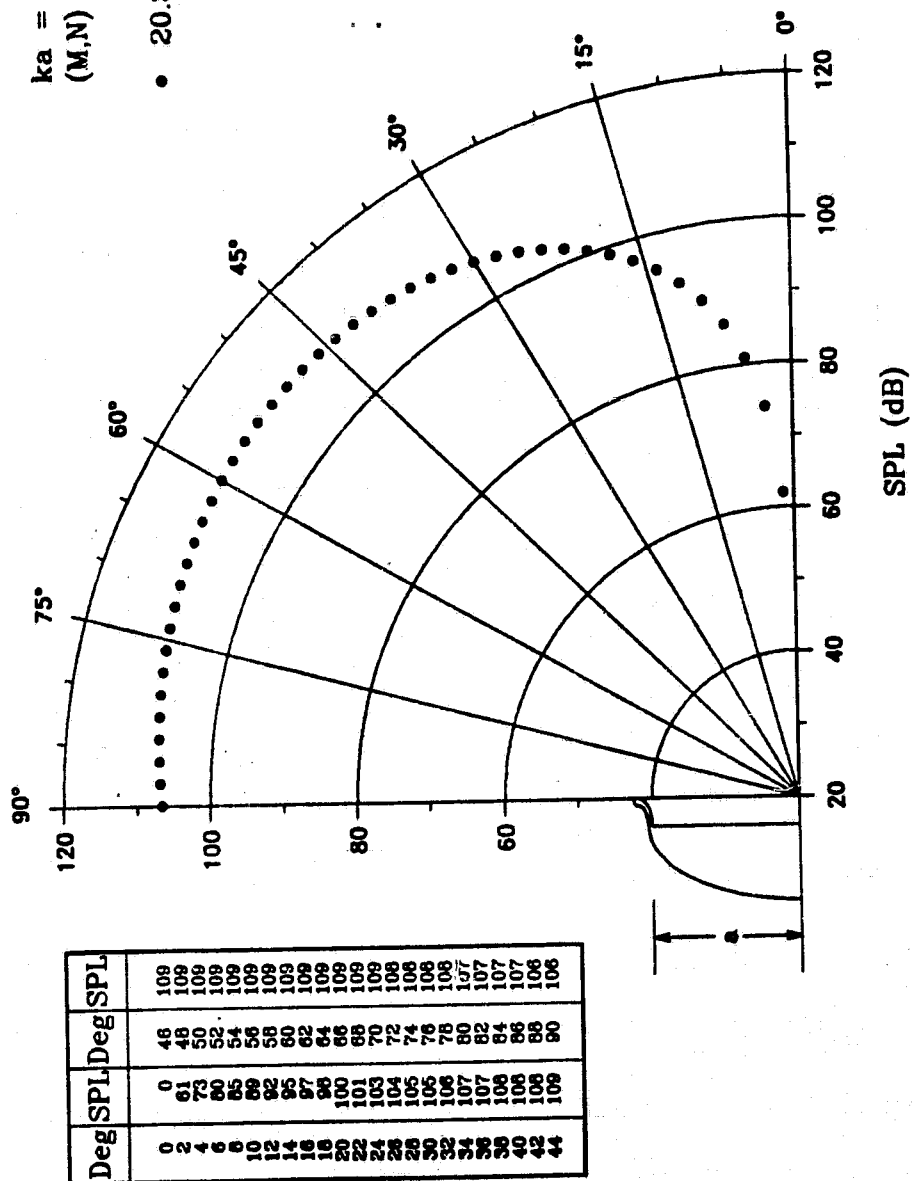


Fig. 21d

THIN LIPPED ELLIPTICAL INLET

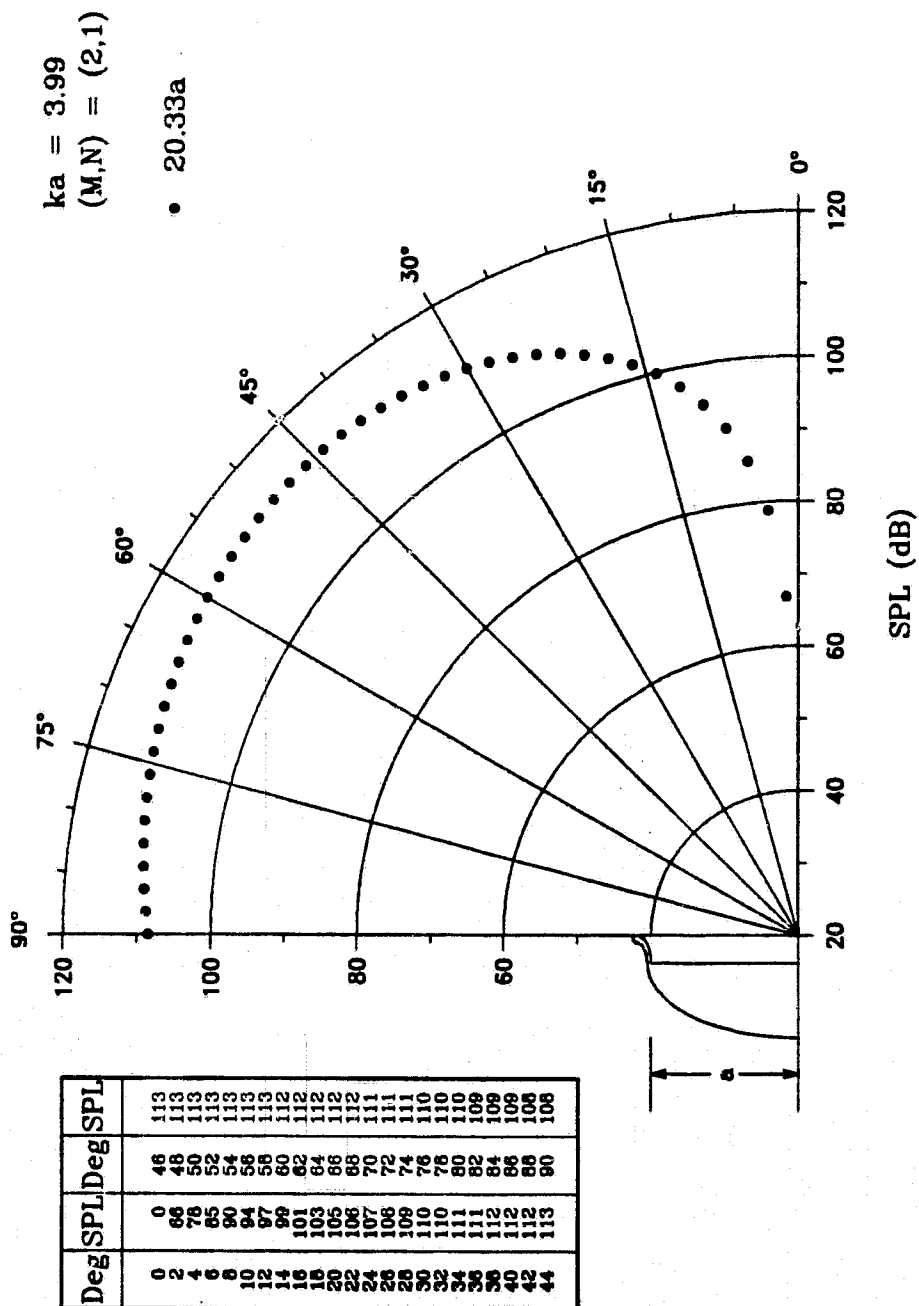


Fig. 21e

ORIGINAL PAGE IS
OF POOR QUALITY

THIN LIPPED ELLIPTICAL INLET

ORIGINAL PAGE 13
OF POOR QUALITY

$ka = 4.75$
(M,N) = (2,1)

• 20.33a

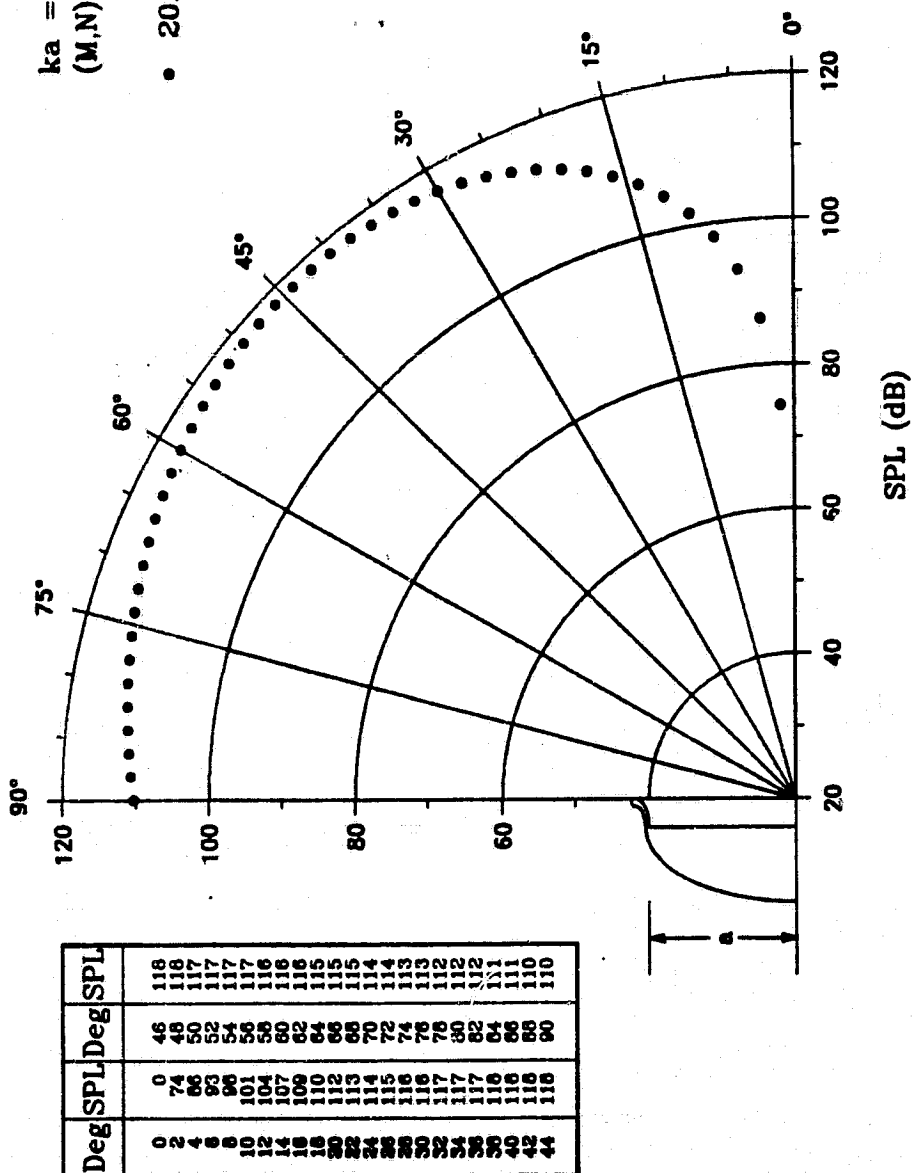


Fig. 21f

THIN LIPPED ELLIPTICAL INLET

ORIGINAL PAGE IS
OF POOR QUALITY

$ka = 5.31$
 $(M,N) = (2,1)$

• 20.33a

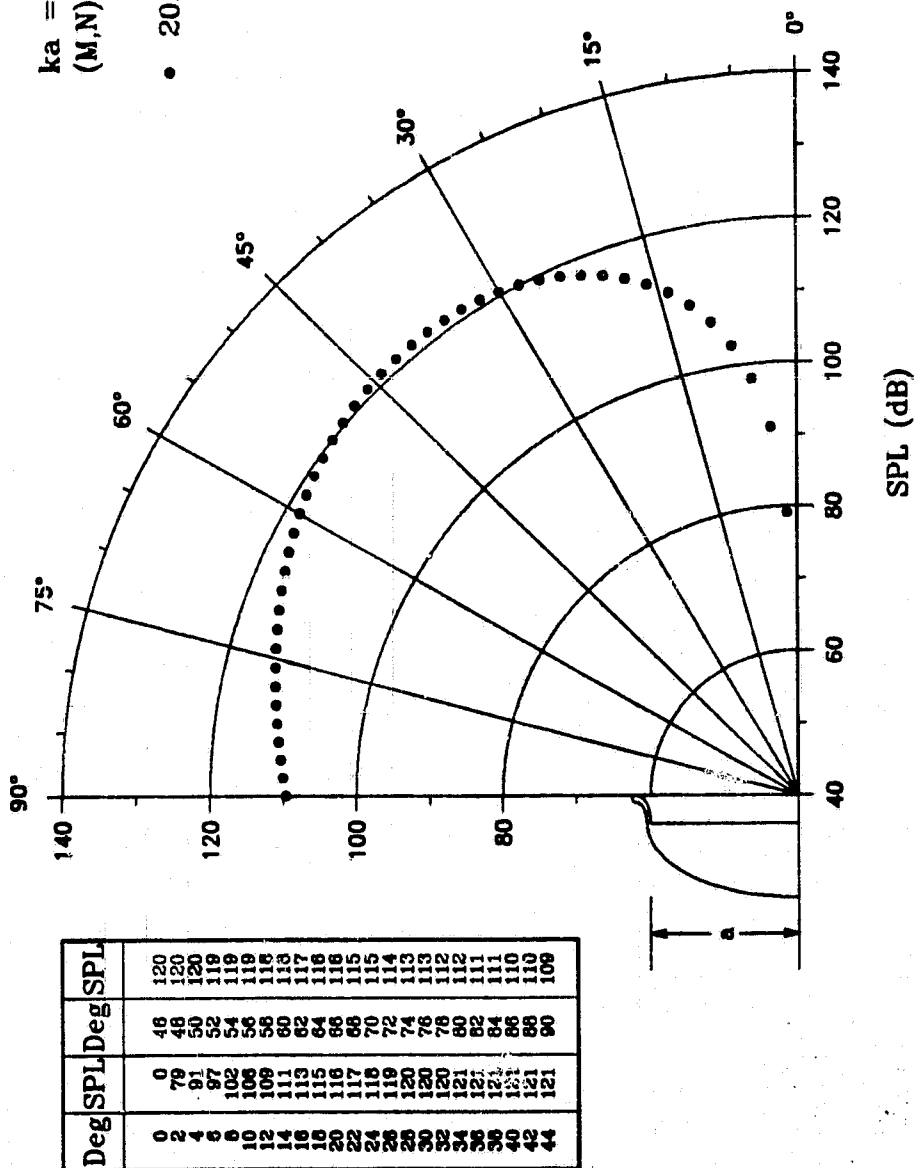


Fig. 218

THIN LIPPED ELLIPTICAL INLET

$ka = 6.57$
 $(M,N) = (2,1)$
 $\bullet 20.33a$

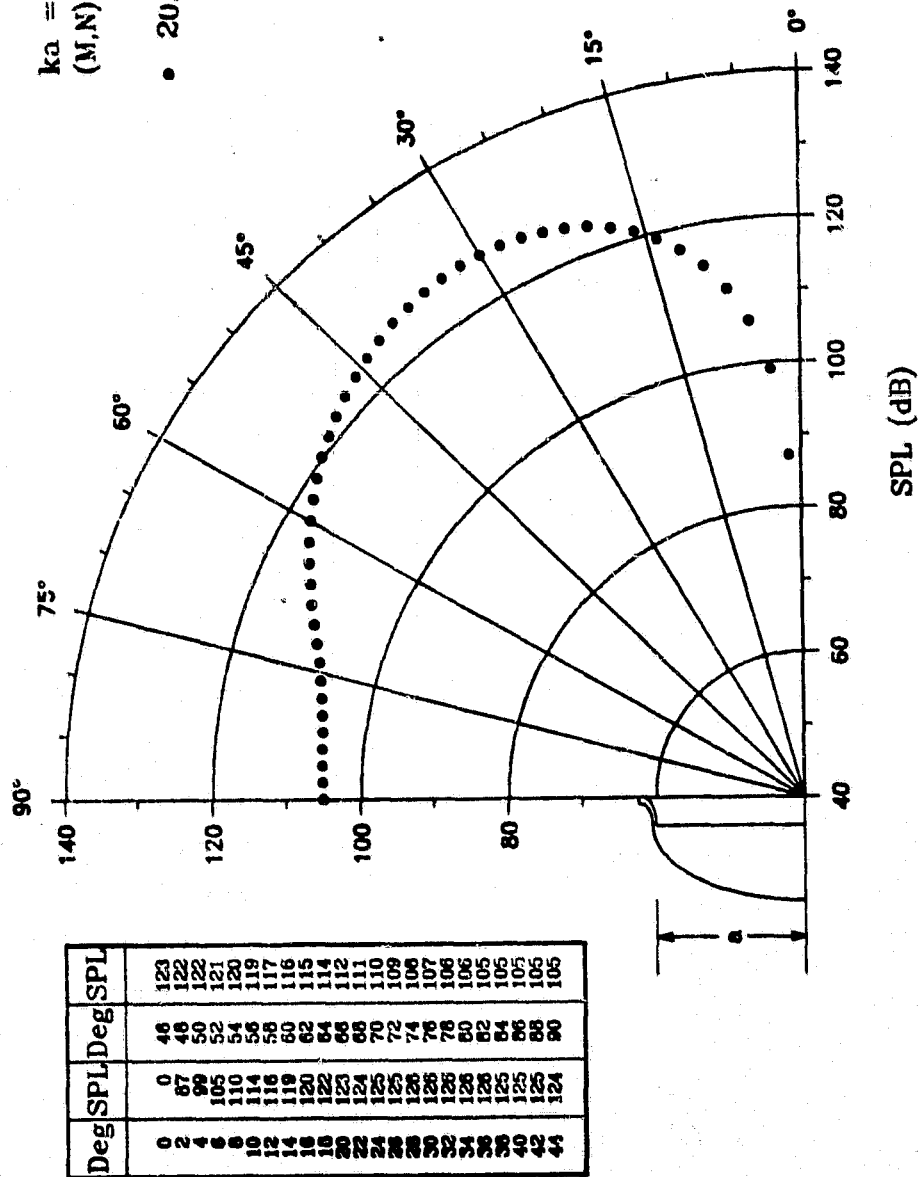


Fig. 21h

ORIGINAL PAGE IS
OF POOR QUALITY

THIN LIPPED ELLIPTICAL INLET

$ka = 5.35$
 $(M,N) = (4,1)$

• 20.33a

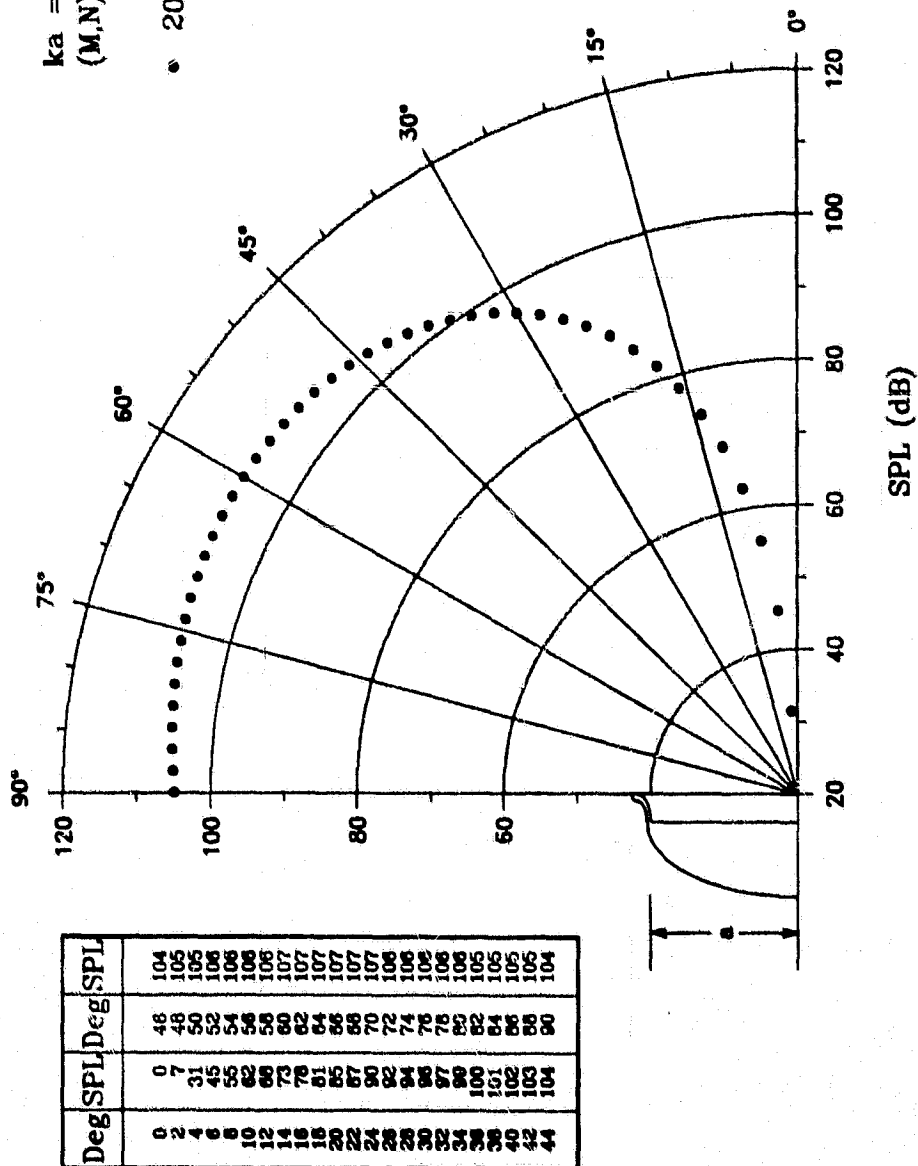
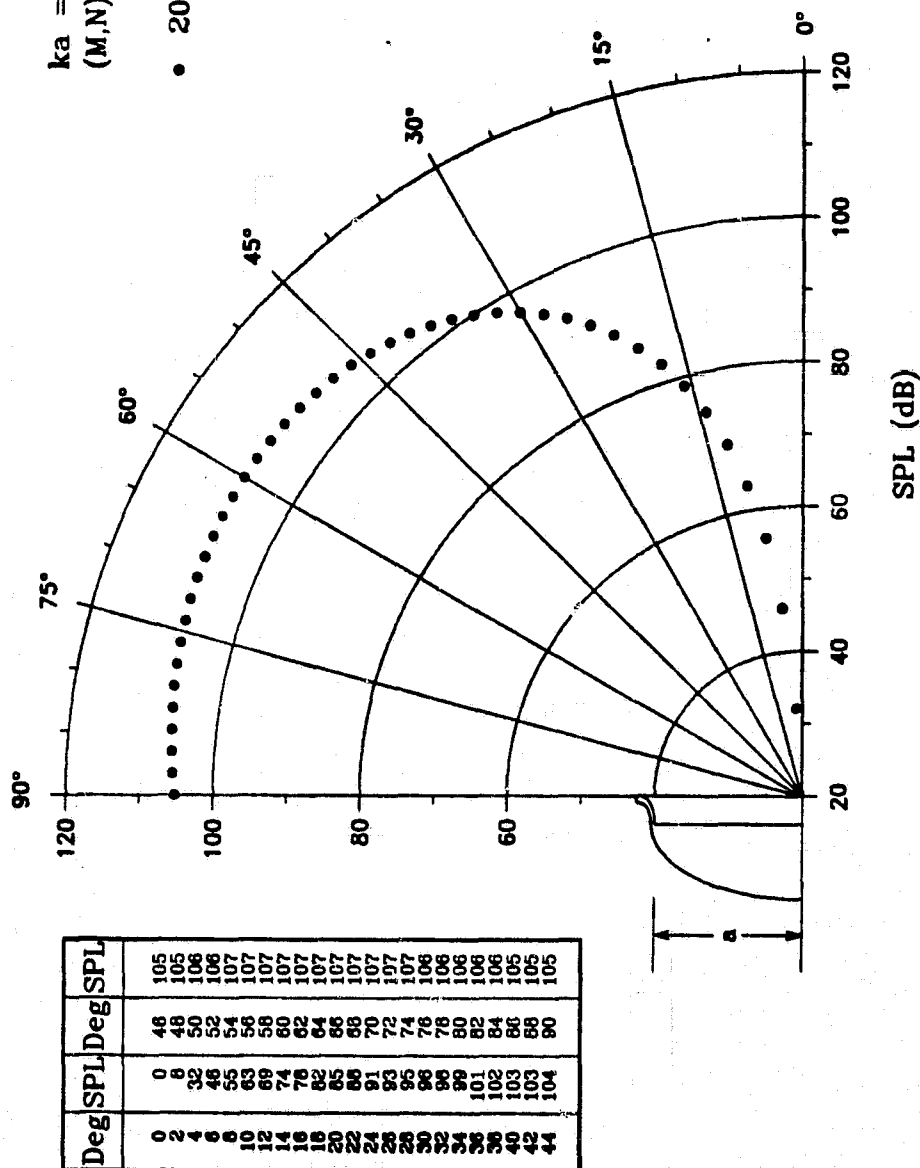


Fig. 22a

ORIGINAL PAGE IS
 OF POOR QUALITY

THIN LIPPED ELLIPTICAL INLET

$ka = 5.40$
 $(M,N) = (4,1)$
 • 20.33a



ORIGINAL PAGE IS
OF POOR QUALITY

Fig. 22b

THIN LIPPED ELLIPTICAL INLET

$ka = 5.66$
 $(M,N) = (4,1)$

• 20.33a

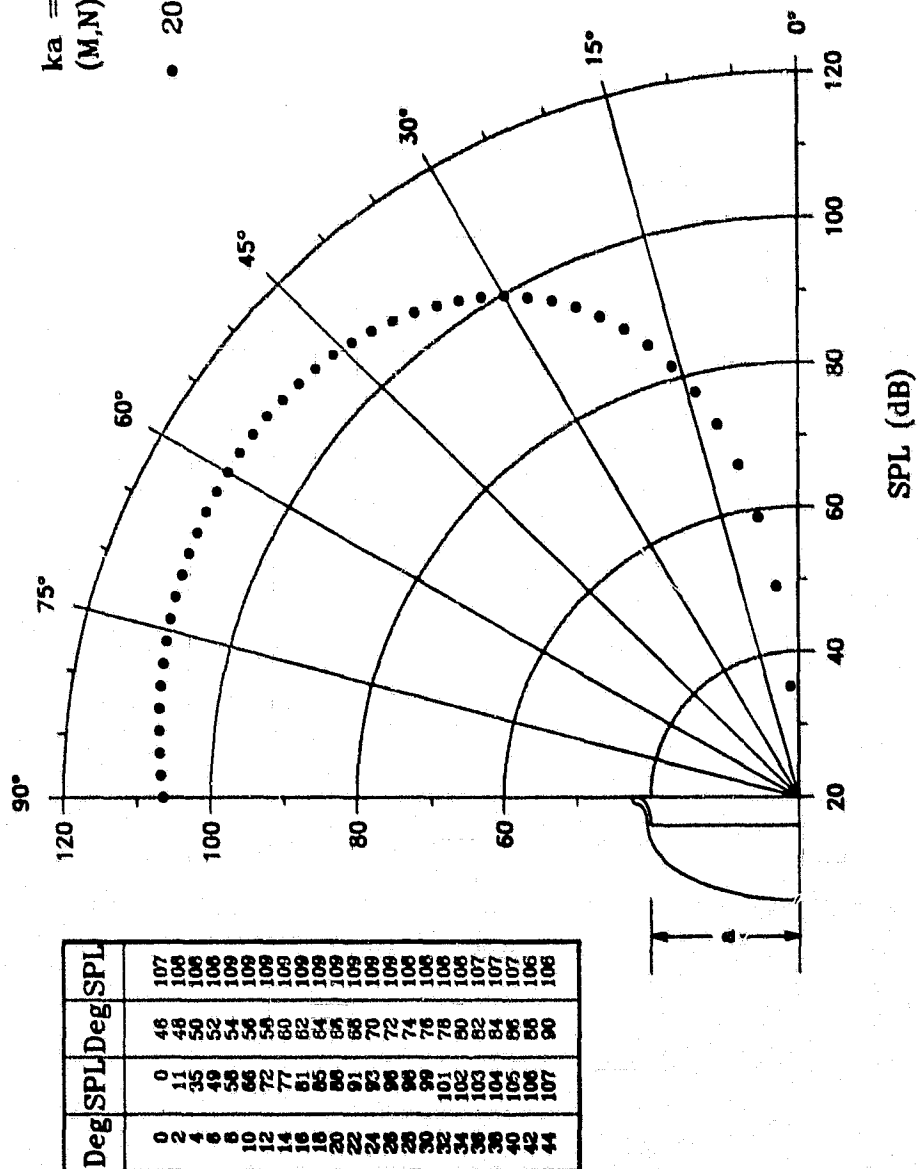


Fig. 22c

ORIGINAL PAGE IS
 OF POOR QUALITY

THIN LIPPED ELLIPTICAL INLET

$ka = 6.14$
 $(M,N) = (4,1)$

• 20.33a

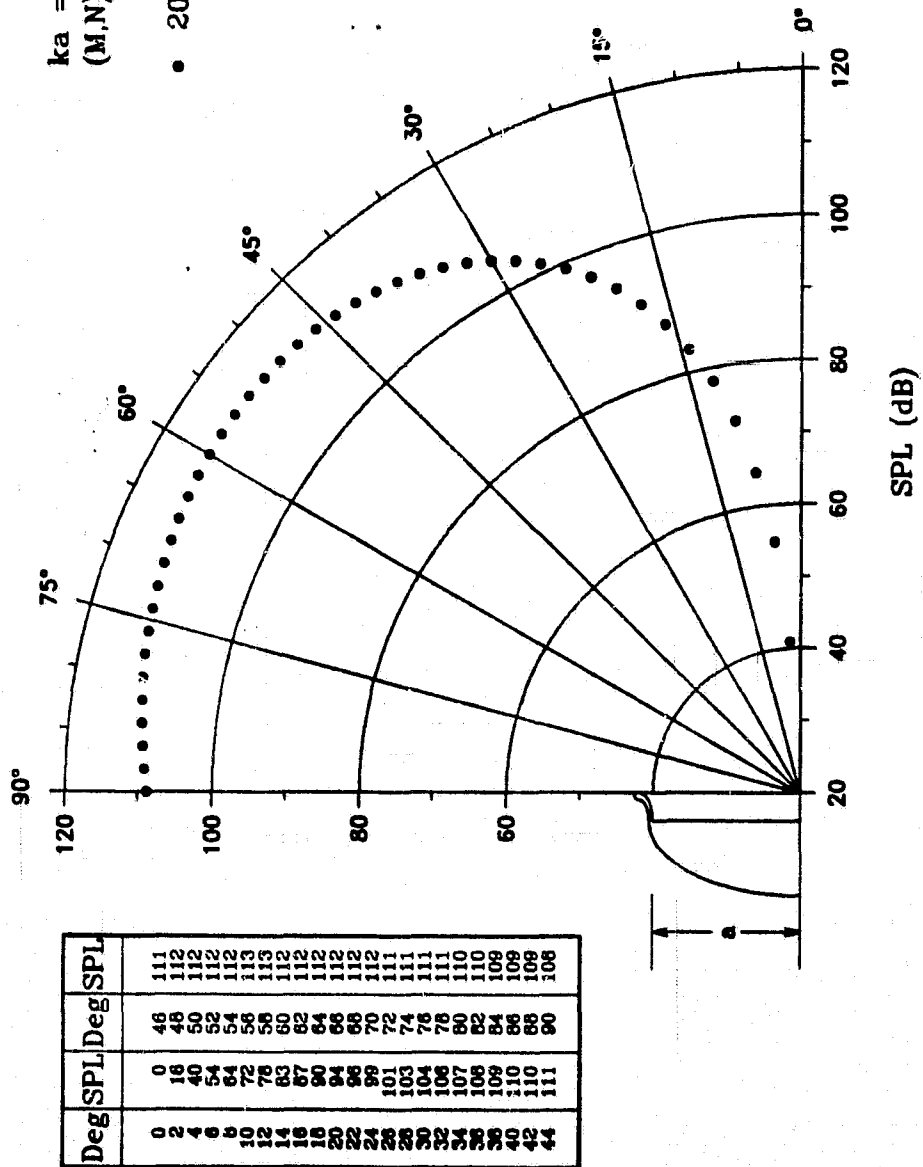


Fig. 22d

ORIGINAL PAGE 13
 OF POOR QUALITY

THIN LIPPED ELLIPTICAL INLET

$ka = 6.94$
 $(M,N) = (4,1)$

• 20.33a

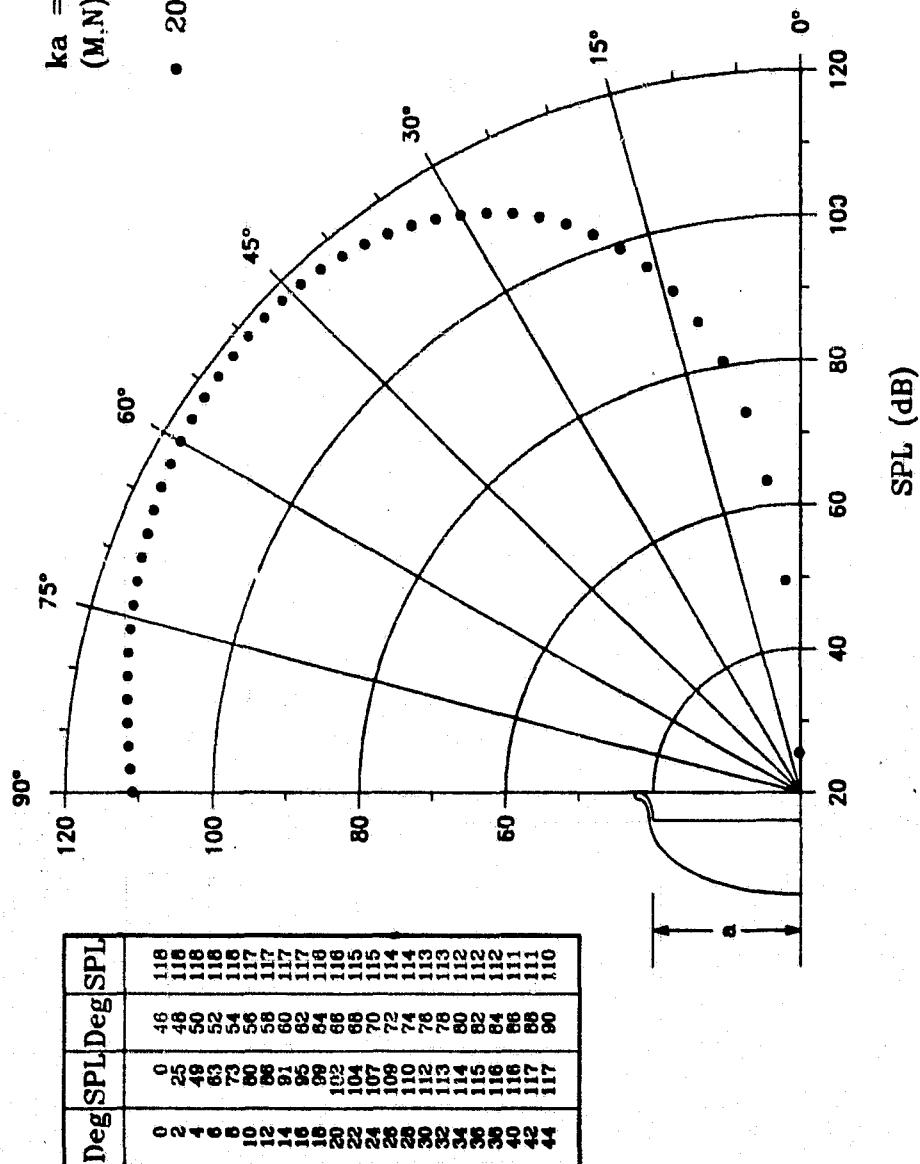


Fig. 22e

ORIGINAL PAGE 10
 OF POOR QUALITY

THIN LIPPED ELLIPTICAL INLET

$ka = 8.28$
 $(M,N) = (4,1)$

• 20.33a

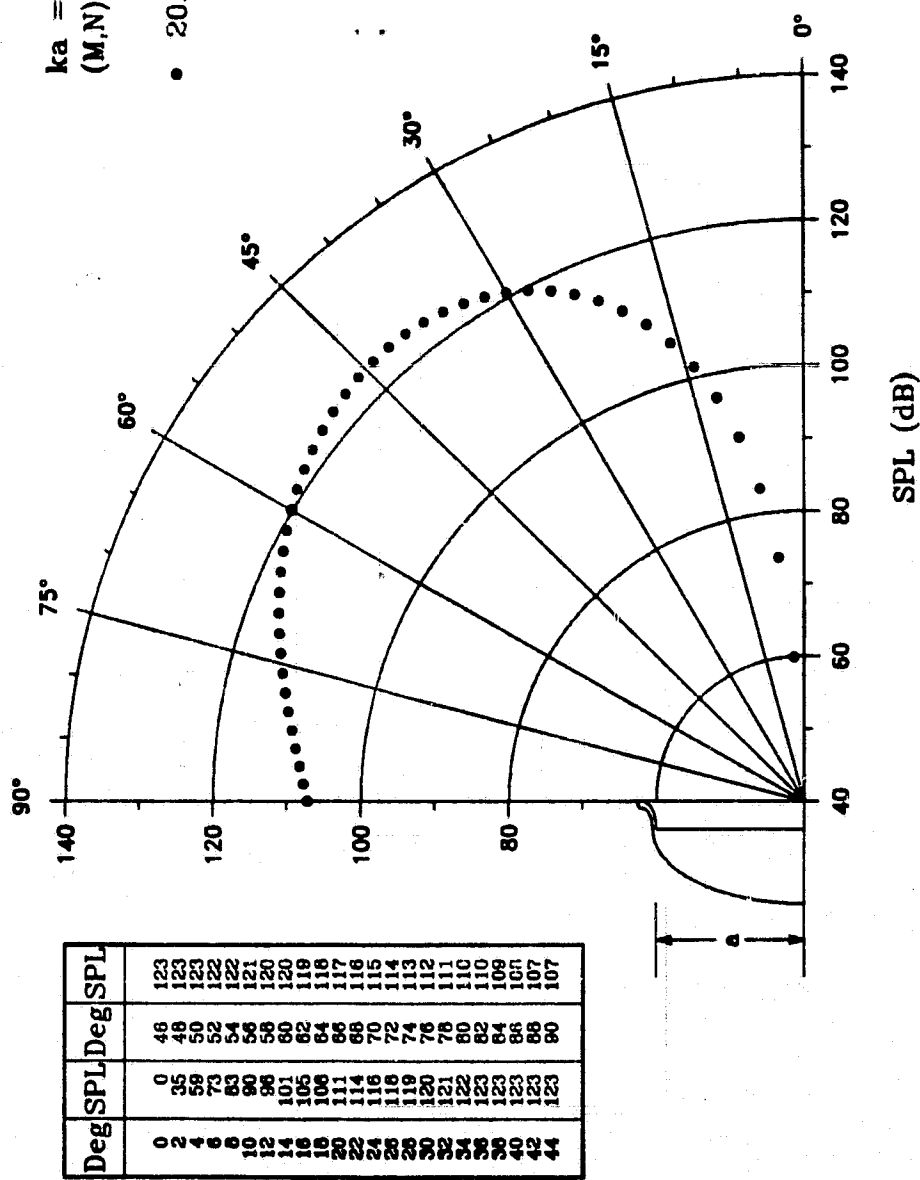


Fig. 22f

ORIGINAL PAGE IS
 OF POOR QUALITY

THIN LIPPED ELLIPTICAL INLET

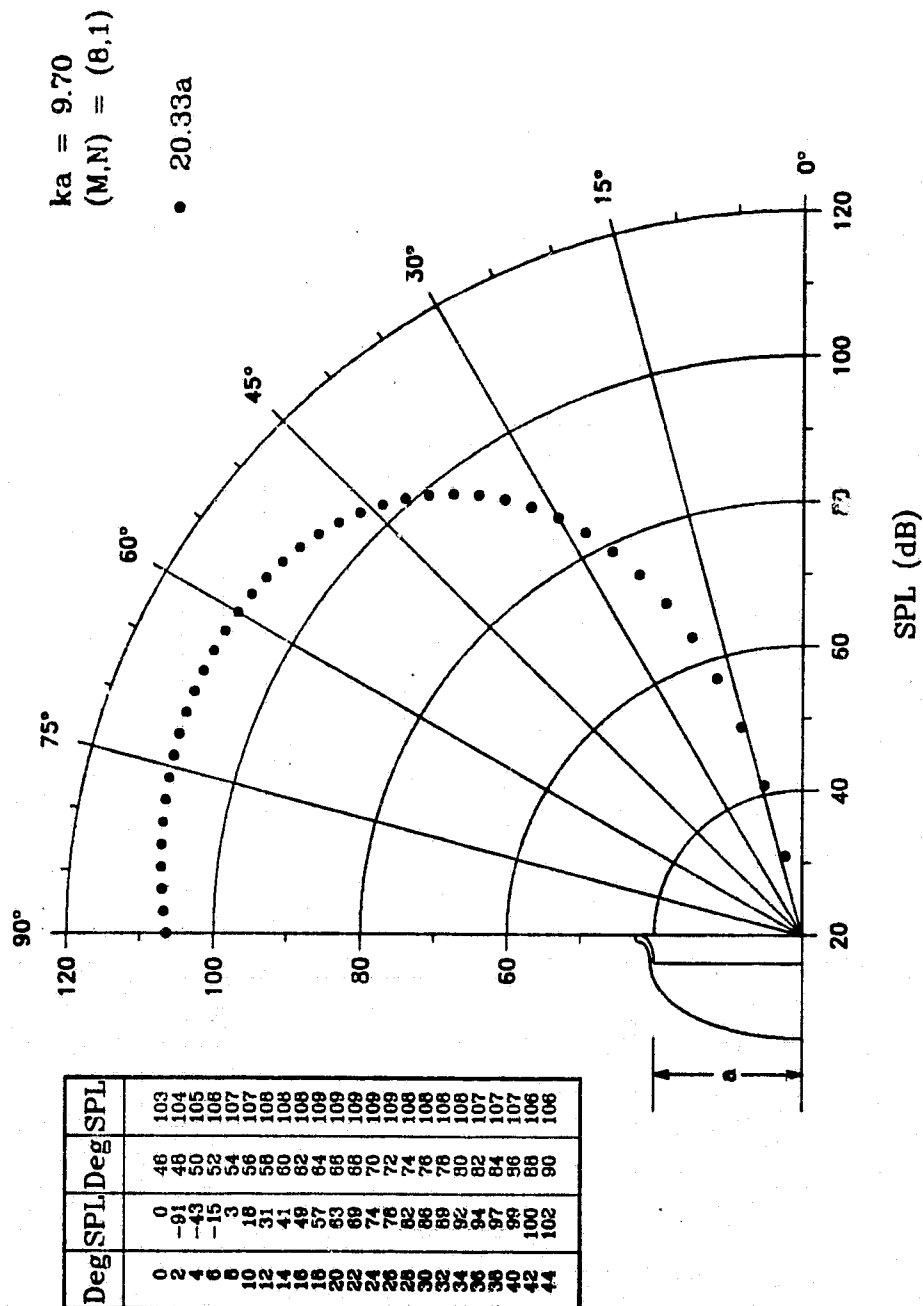


Fig. 23a

ORIGINAL PAGE IS
OF POOR QUALITY

THIN LIPPED ELLIPTICAL INLET

Deg	SPL	Deg	SPL
0	104	45	105
2	105	48	106
4	106	50	107
6	107	52	108
8	108	54	109
10	109	56	110
12	110	58	111
14	111	60	112
16	112	62	113
18	113	64	114
20	114	66	115
22	115	68	116
24	116	70	117
26	117	72	118
28	118	74	119
30	119	76	120
32	120	78	121
34	121	80	122
36	122	82	123
38	123	84	124
40	124	86	125
42	125	88	126
44	126	90	127

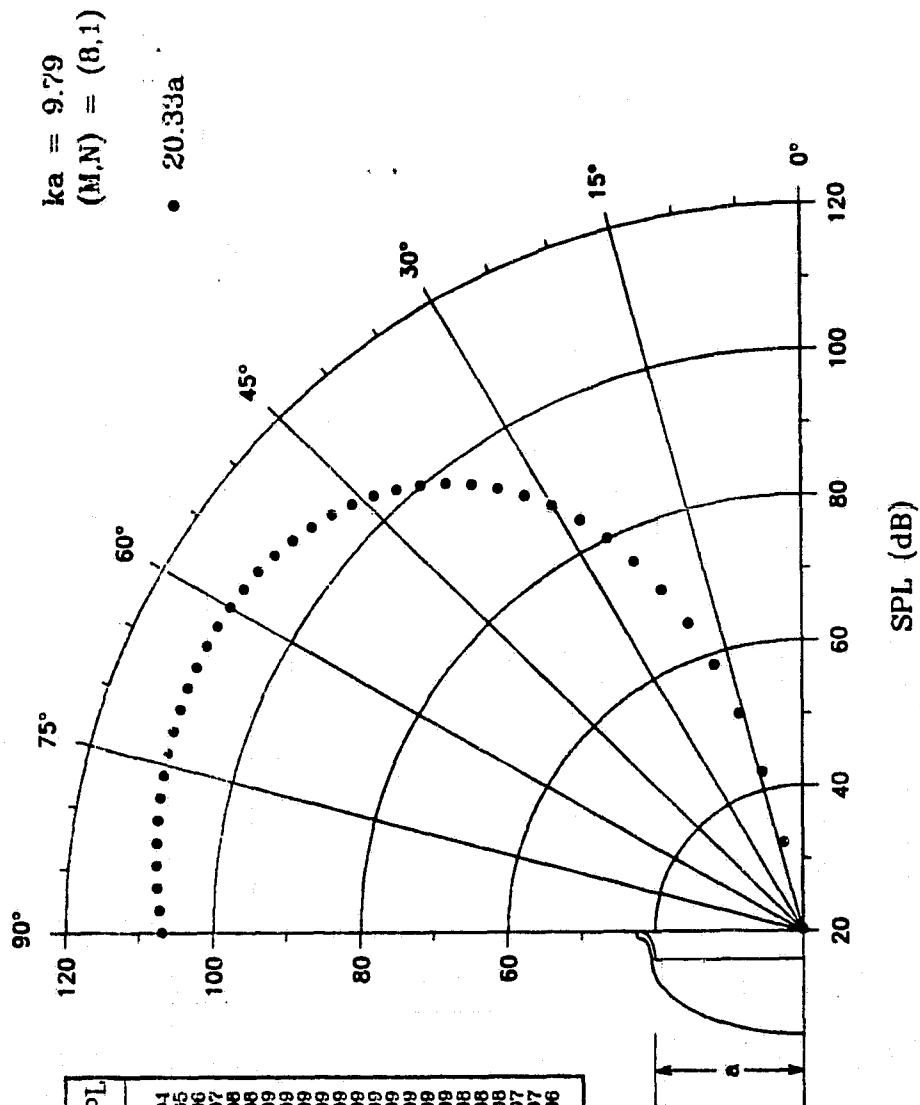


Fig. 23b

ORIGINAL PAGE IS
OF POOR QUALITY

THIN LIPPED ELLIPTICAL INLET

$ka = 10.26$
 $(M,N) = (8,1)$

• 20.33a

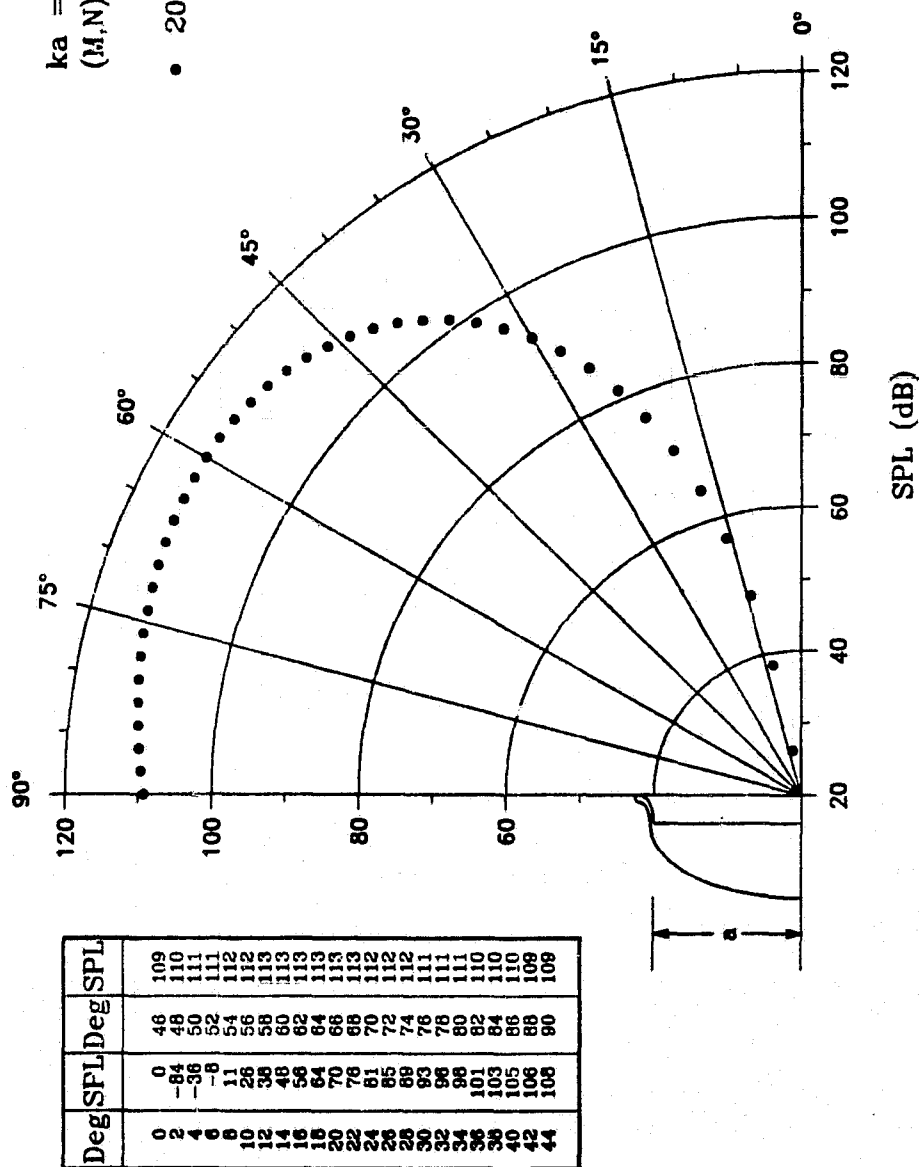


Fig. 23c

ORIGINAL PAGE IS
 OF POOR QUALITY

THIN LIPPED ELLIPTICAL INLET

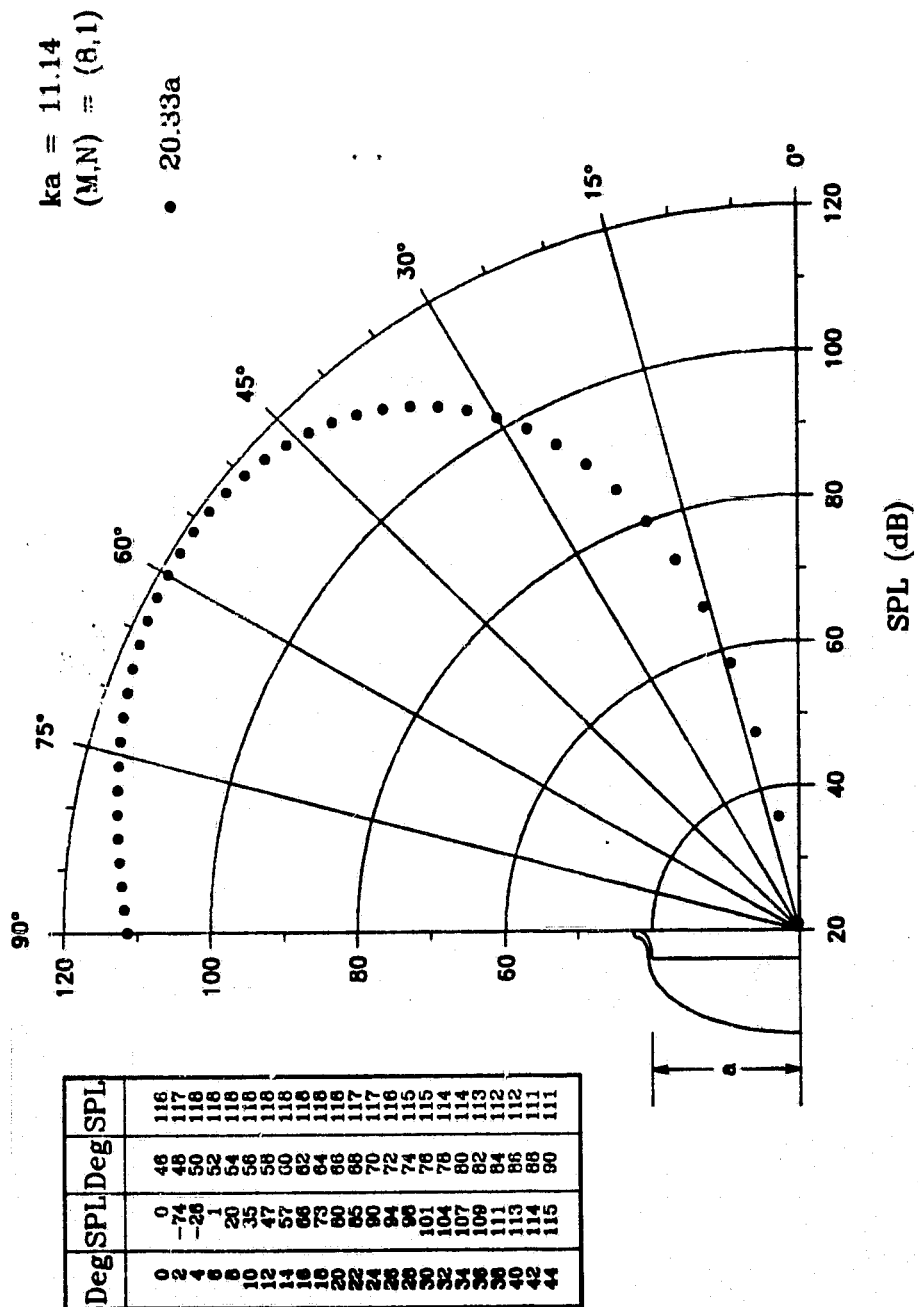


Fig. 23d

ORIGINAL PAGE 13
OF POOR QUALITY.

THIN LIPPED ELLIPTICAL INLET

$ka = 12.59$
 $(M,N) = (8,1)$

• 00.33a

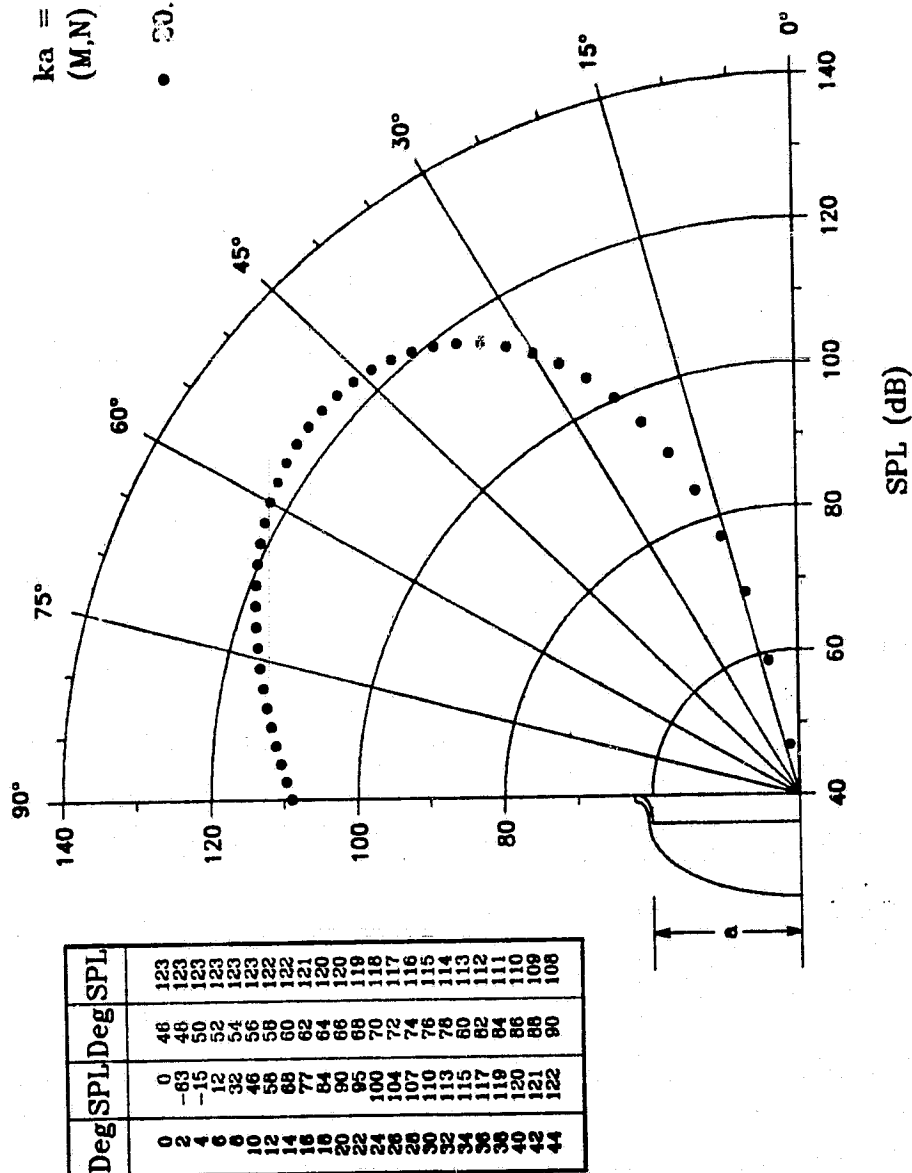


Fig. 23e

ORIGINAL PAGE IS
 OF POOR QUALITY

THIN LIPPED ELLIPTICAL INLET

$ka = 15.01$
 $(M,N) = (8,1)$

• 20.33a

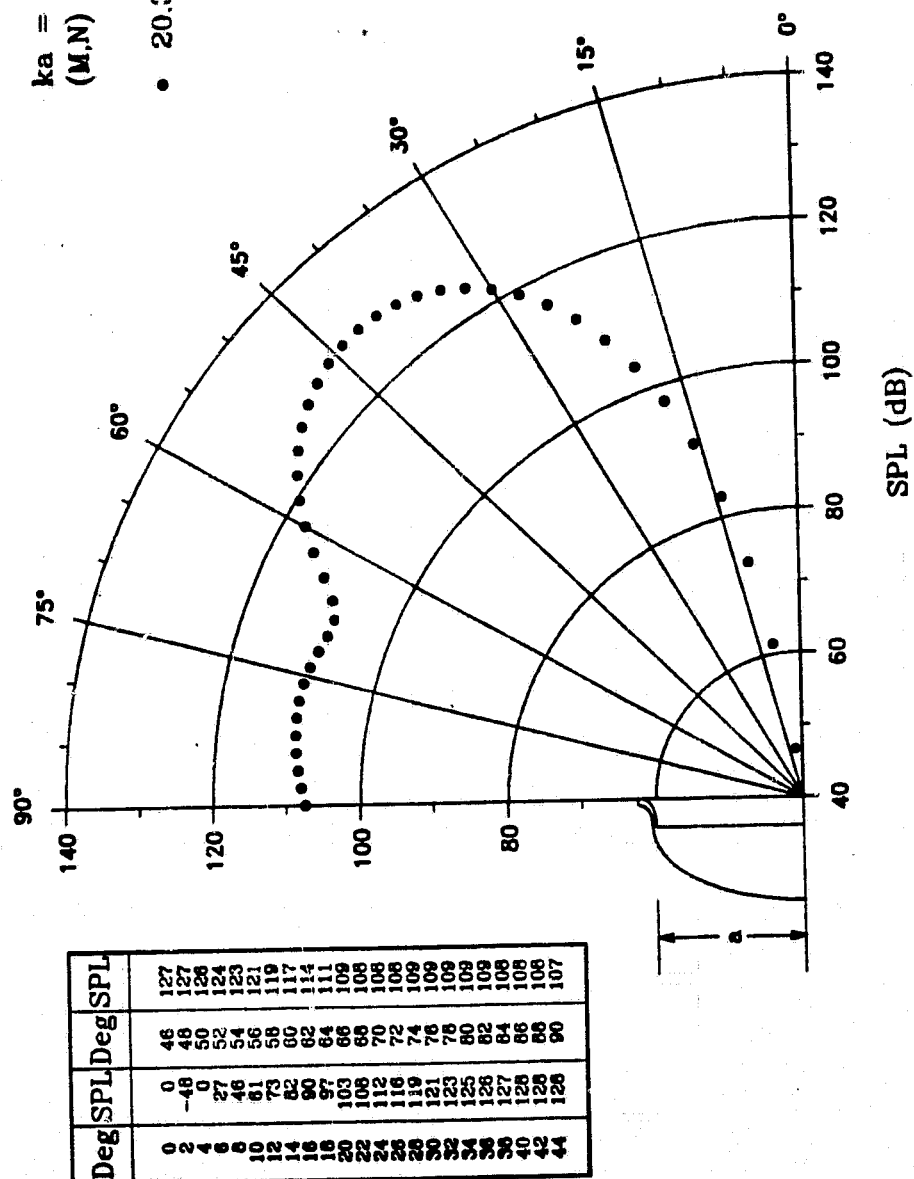


Fig. 23f

ORIGINAL PAGE IS
 OF POOR QUALITY

THIN LIPPED ELLIPTICAL INLET

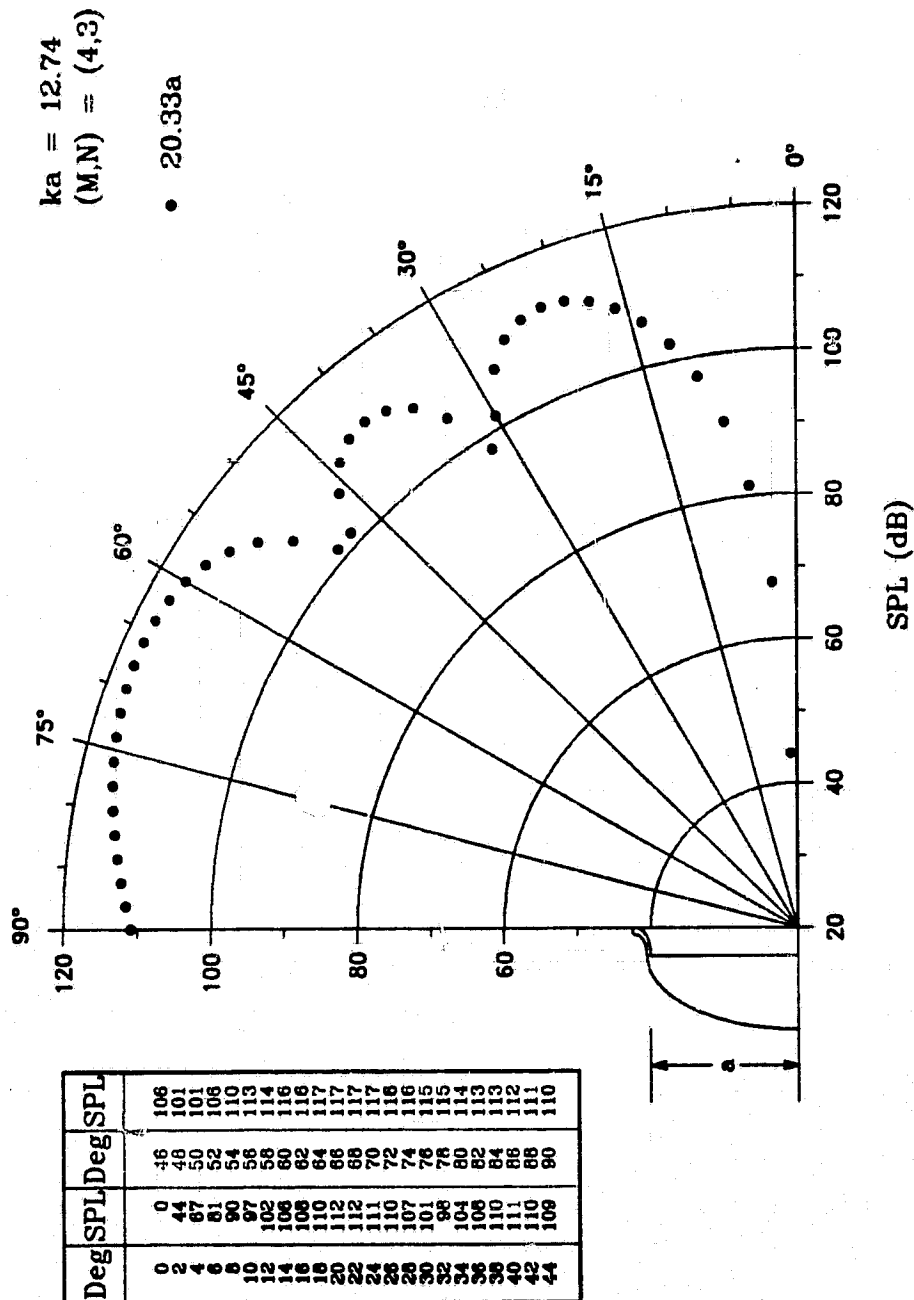


Fig. 24a

ORIGINAL PAGE 13
OF POOR QUALITY

THIN LIPPED ELLIPTICAL INLET

$ka = 12.87$
 $(M,N) = (4,3)$
 \bullet 20.33a

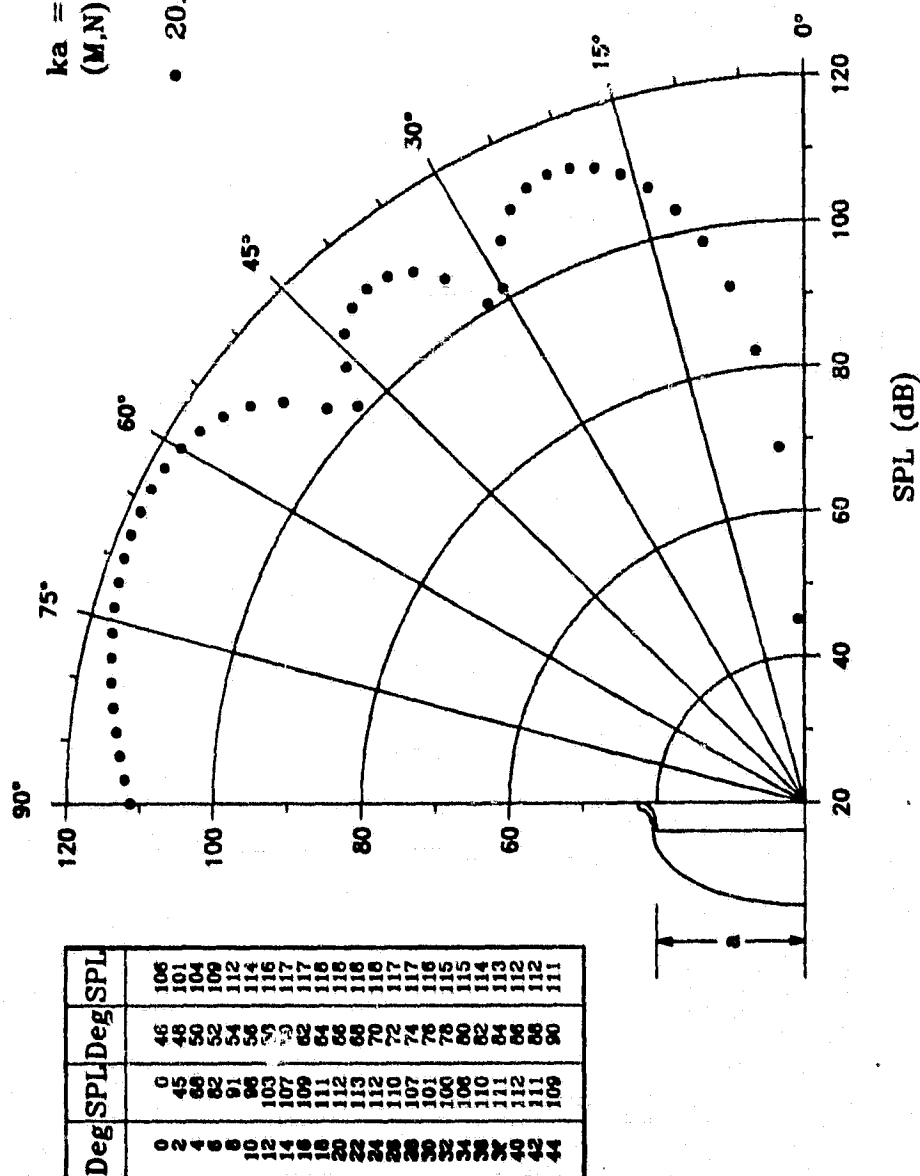


Fig. 24b

ORIGINAL PAGE IS
 OF POOR QUALITY

THIN LIPPED ELLIPTICAL INLET

$ka = 13.49$
 $(M,N) = (4,3)$

• 20.33a

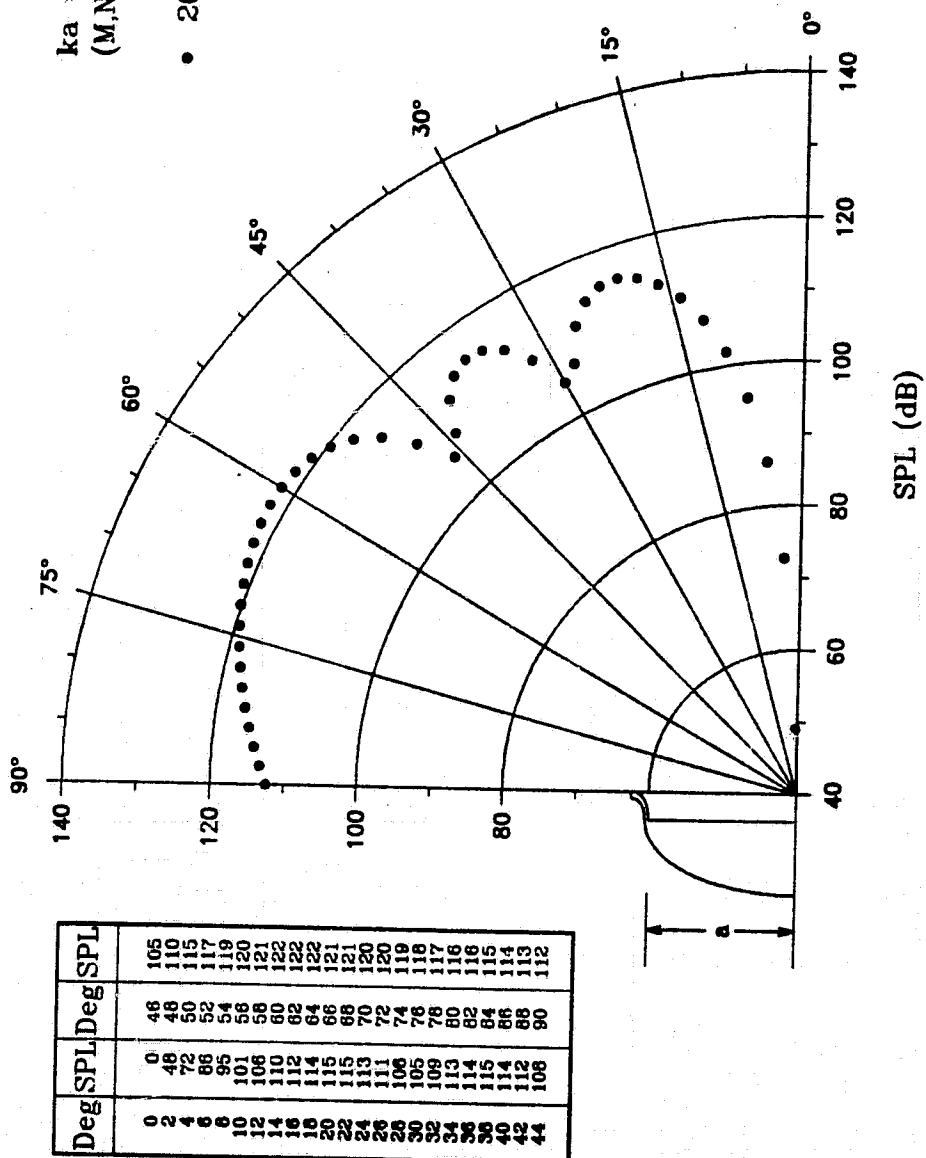


Fig. 24c

ORIGINAL PAGE 13
 OF POOR QUALITY

THIN LIPPED ELLIPTICAL INLET

$ka = 14.65$
 $(M,N) = (4,3)$
 $\bullet 20.33a$

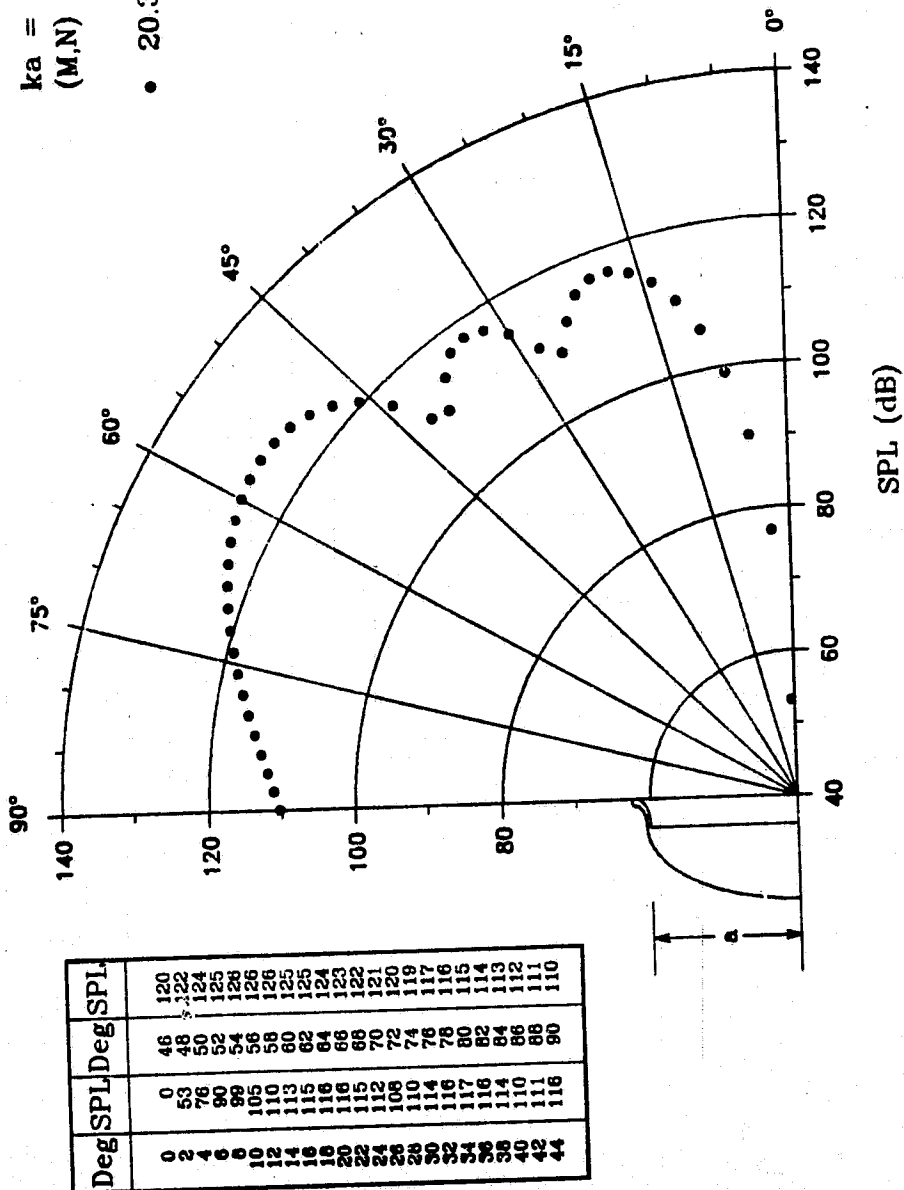


Fig. 24d

ORIGINAL PAGE IS
 OF POOR QUALITY

THIN LIPPED ELLIPTICAL INLET

ORIGINAL PAGE 13
OF POOR QUALITY

$ka = 16.55$
 $(M,N) = (4,3)$

• 20.33a

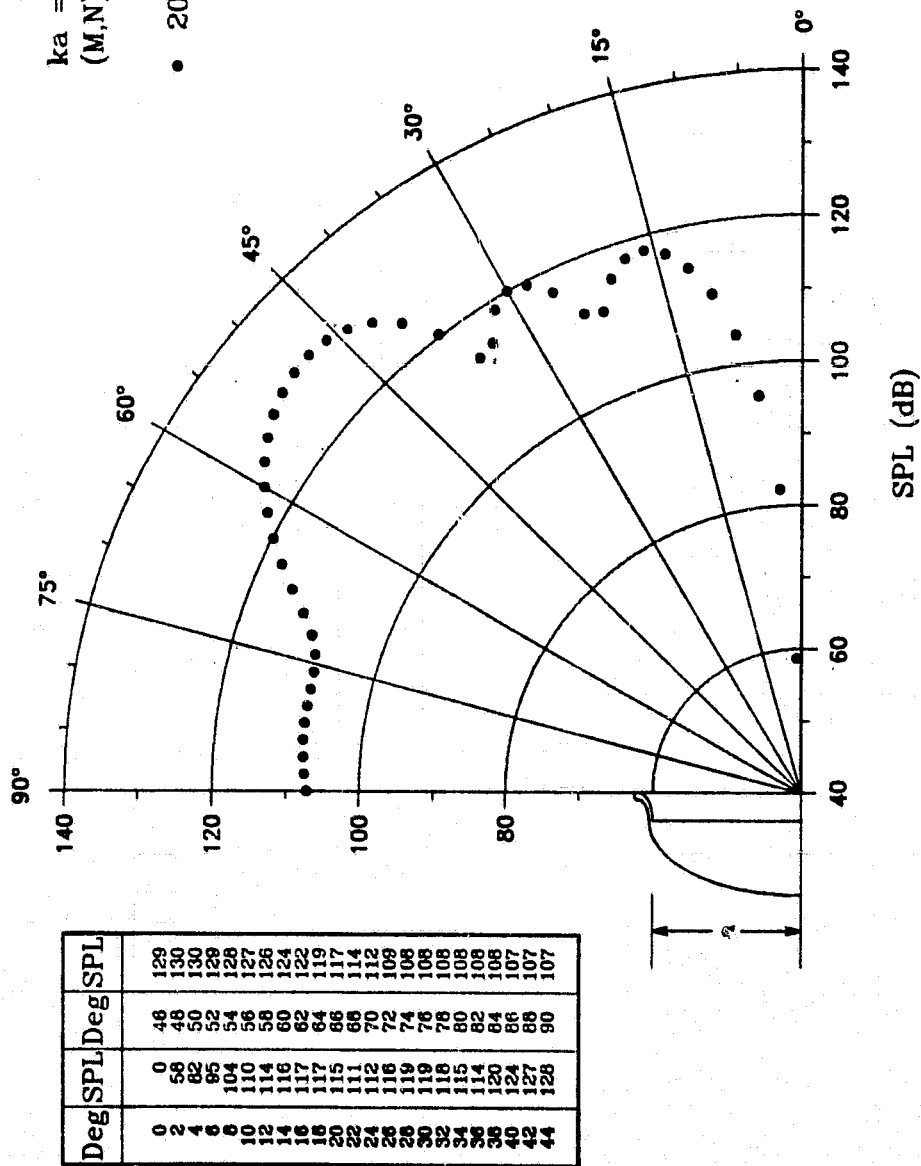


Fig. 24e

THIN LIPPED ELLIPTICAL INLET

$ka = 19.73$
 $(M,N) = (4,3)$

• 20.33a

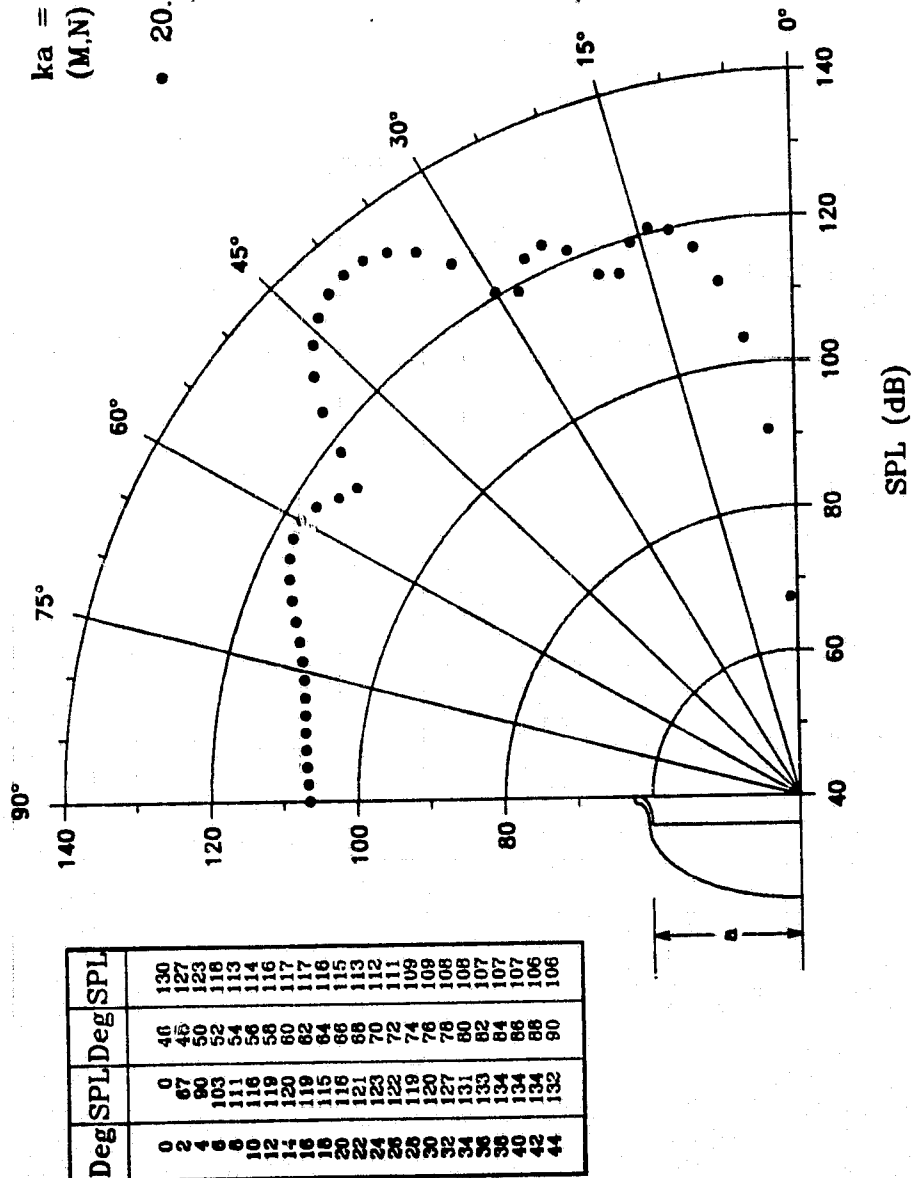


Fig. 24f

ORIGINAL PAGE 13
 OF POOR QUALITY

MODULUS

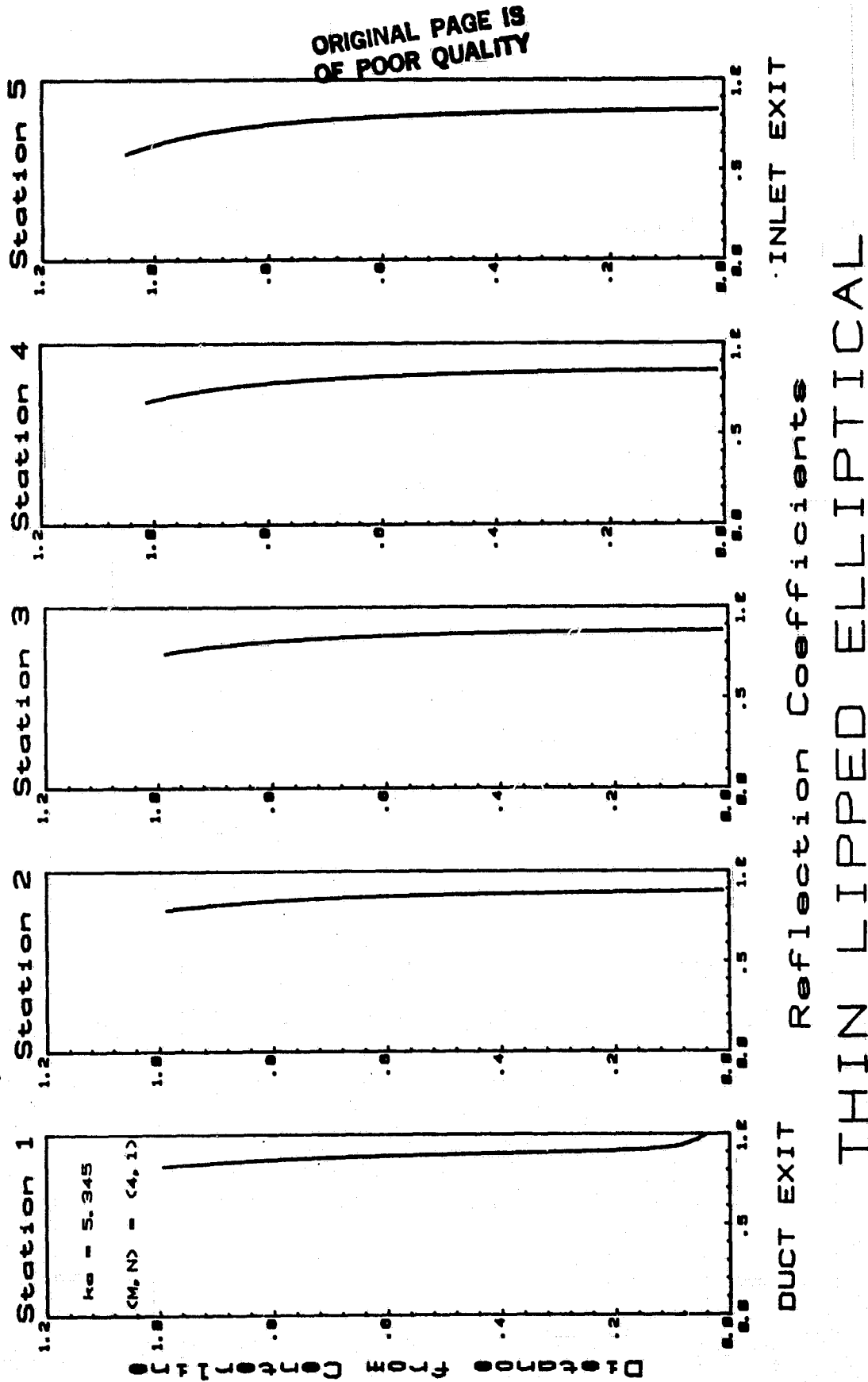


Fig. 25a

ORIGINAL PAGE IS
OF POOR QUALITY

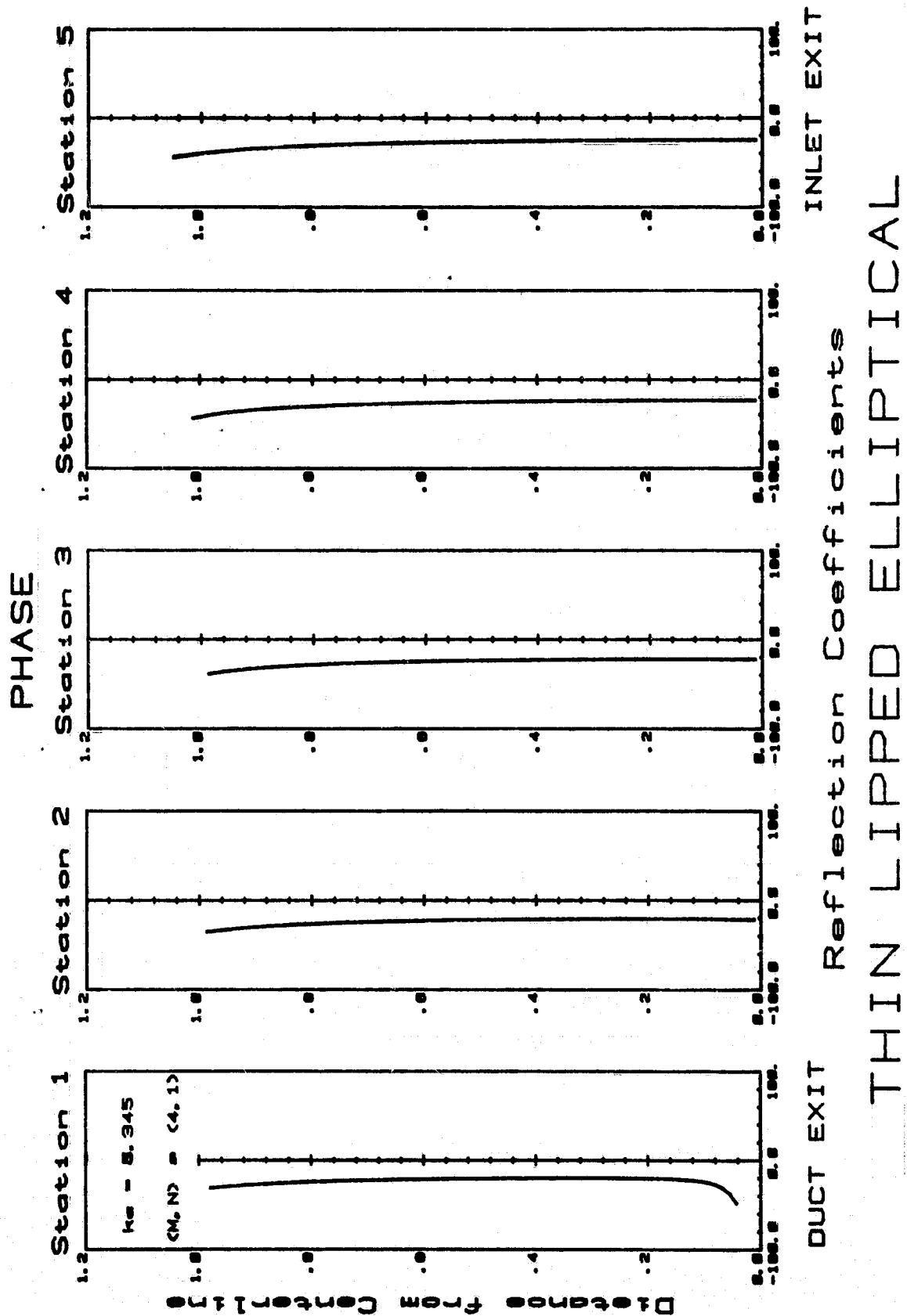


Fig. 25b

ORIGINAL PAGE IS
OF POOR QUALITY

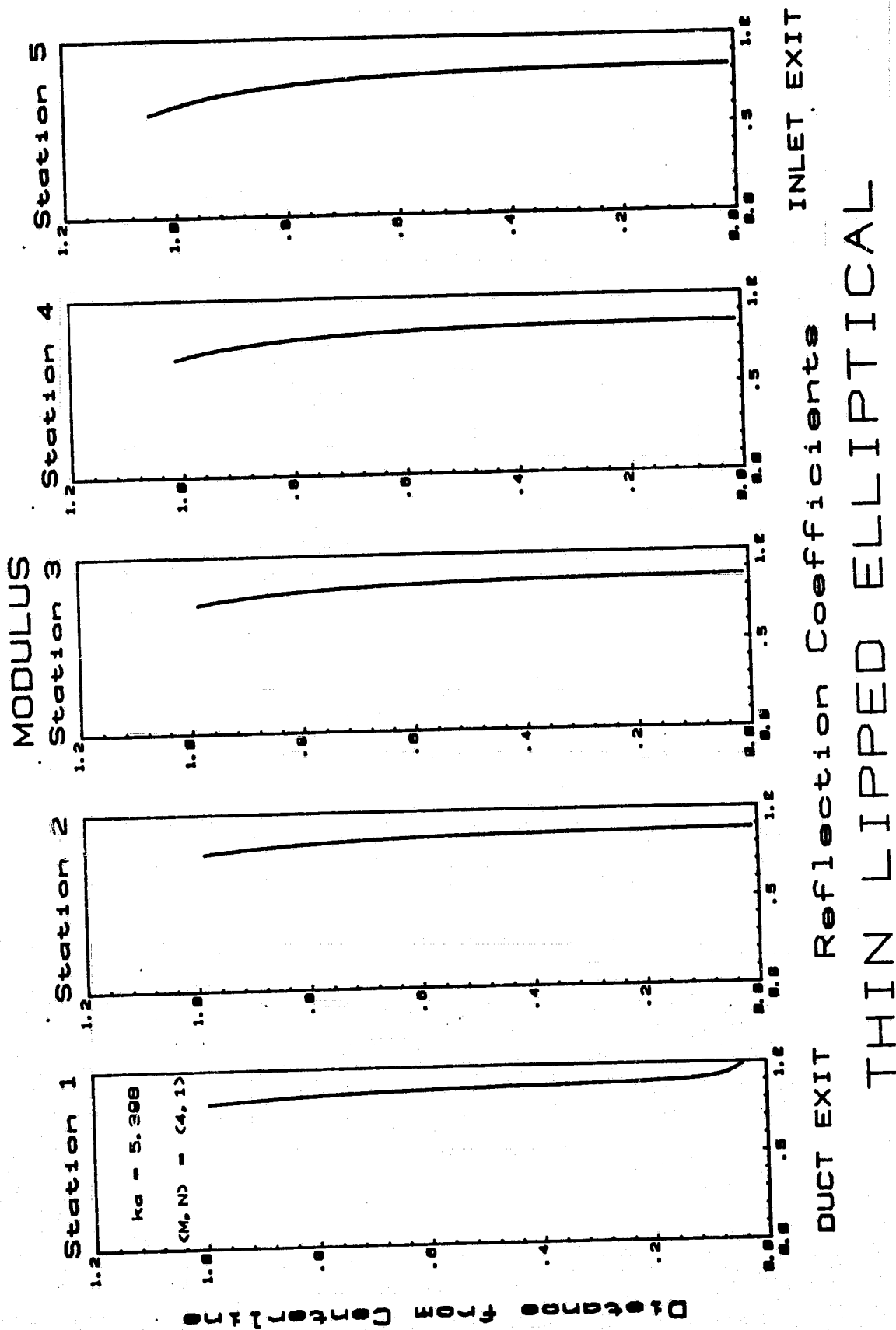


Fig. 25c

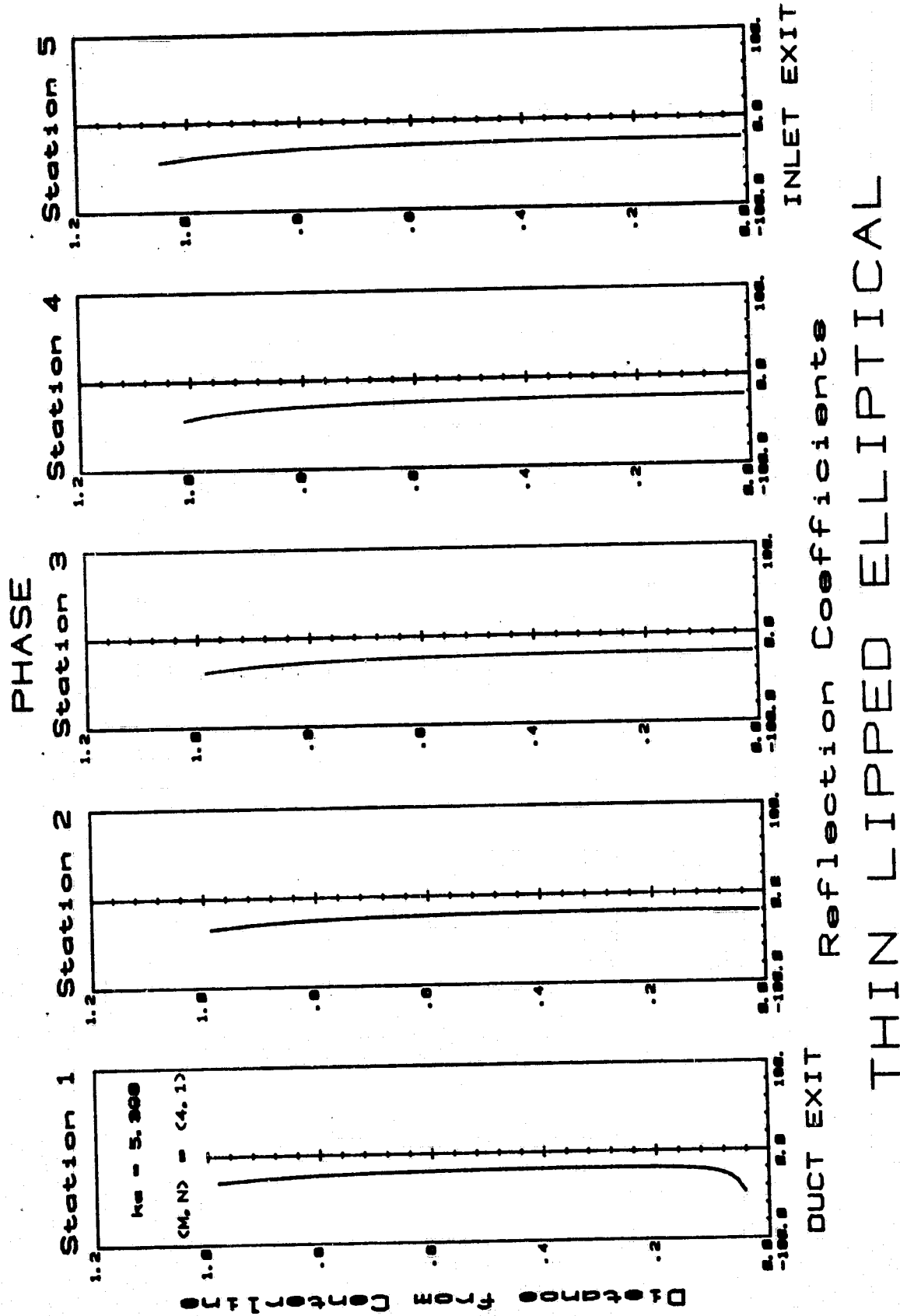


Fig. 25d

ORIGINAL PAGE IS
OF POOR QUALITY

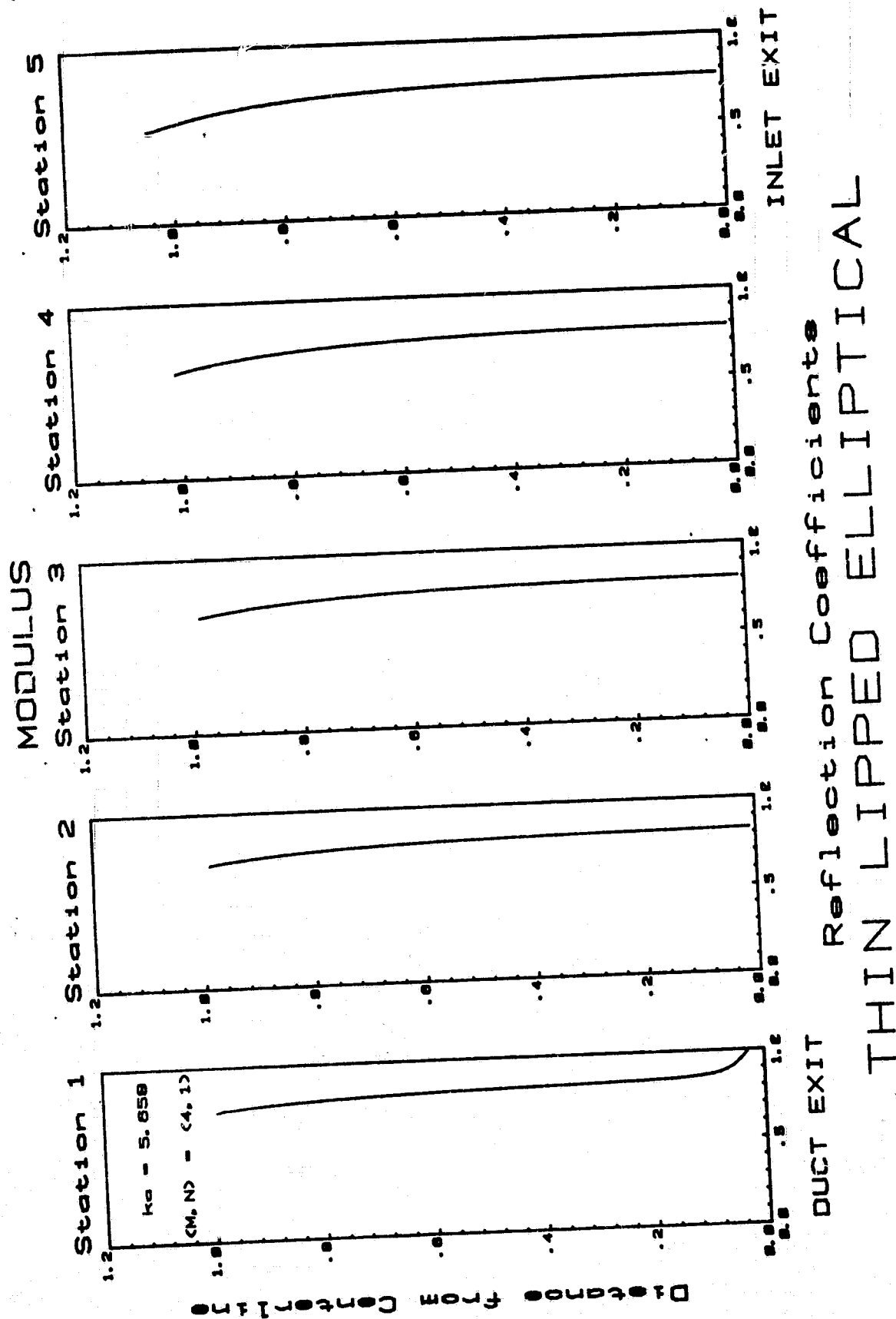


Fig. 25e

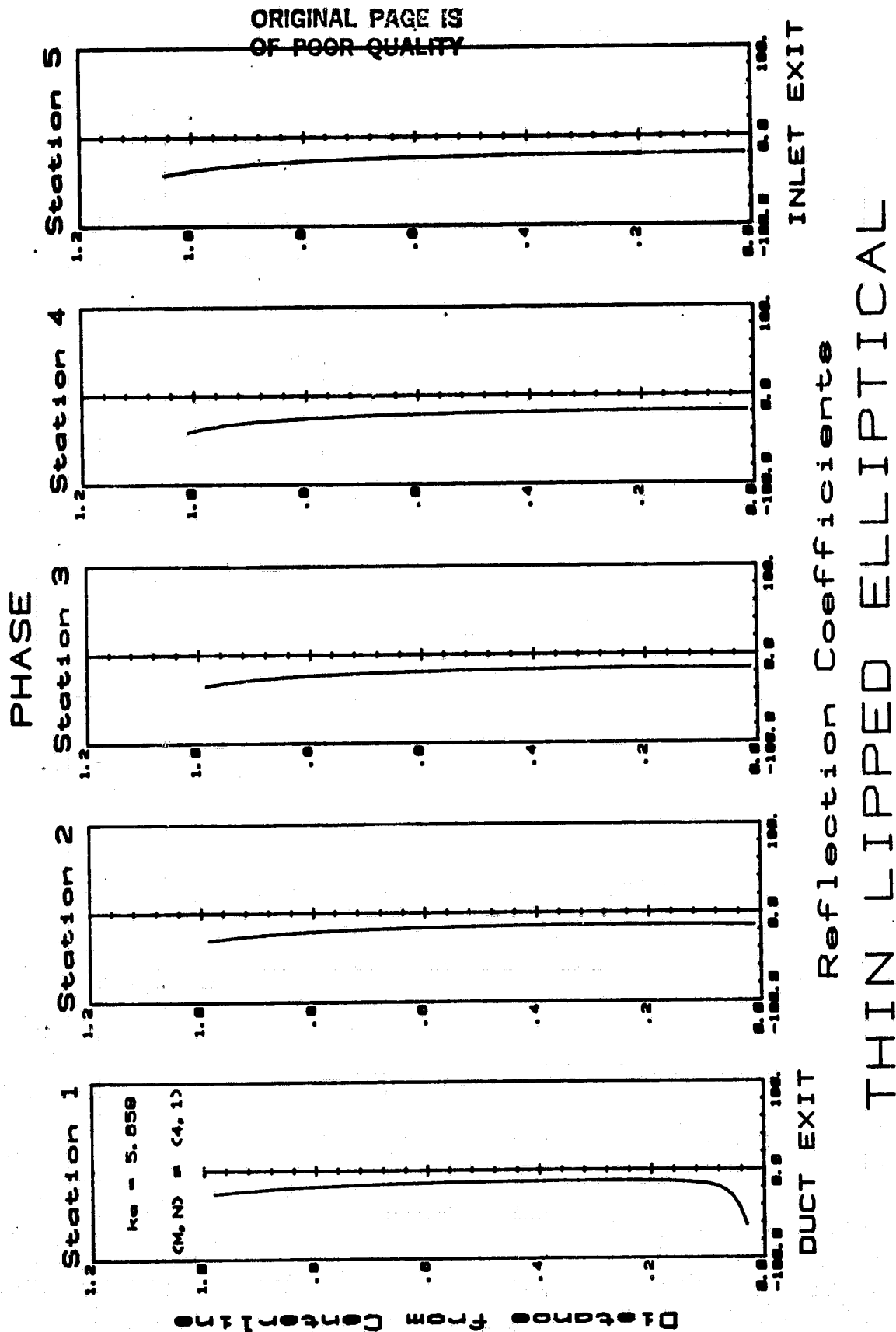


Fig. 25f

ORIGINAL PAGE IS
OF POOR QUALITY

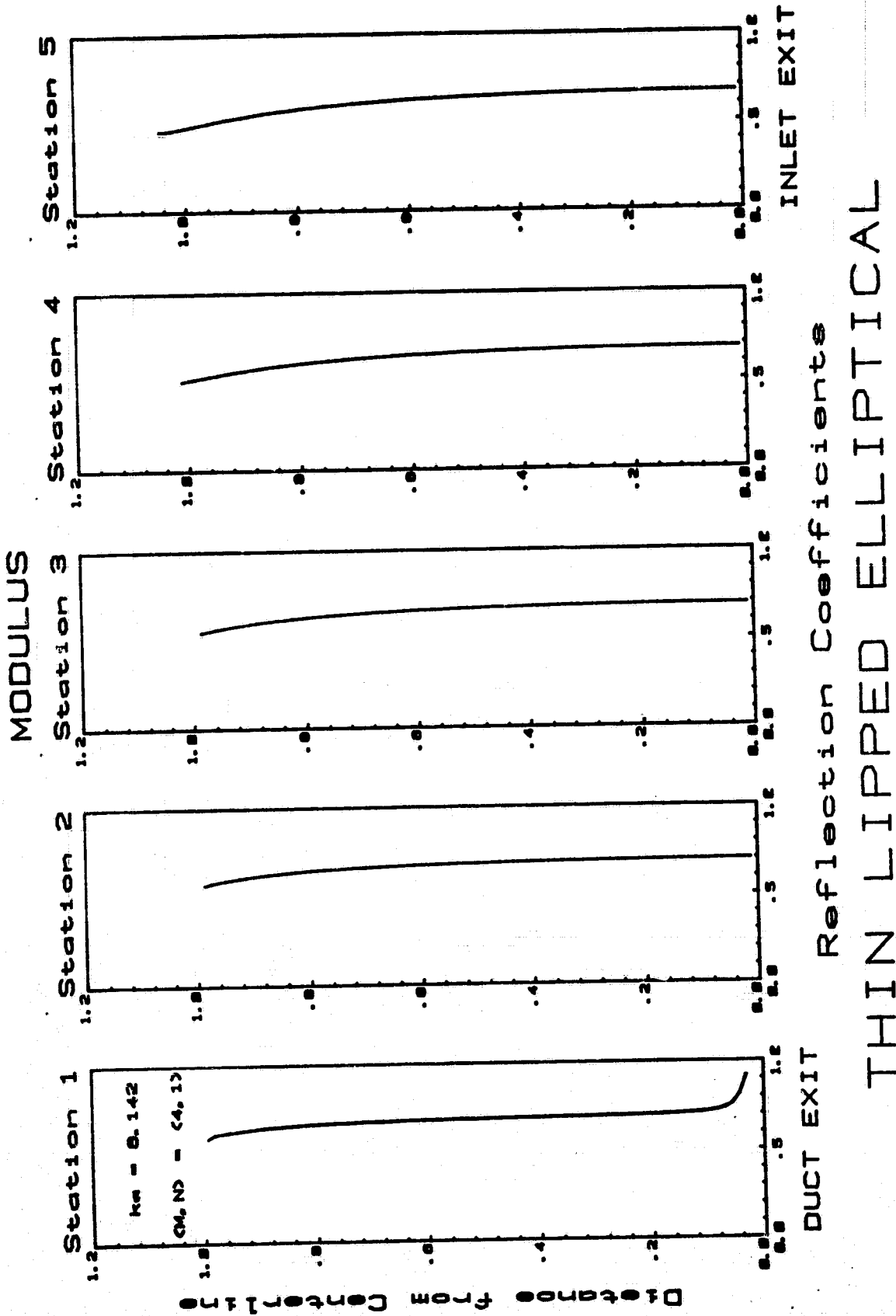
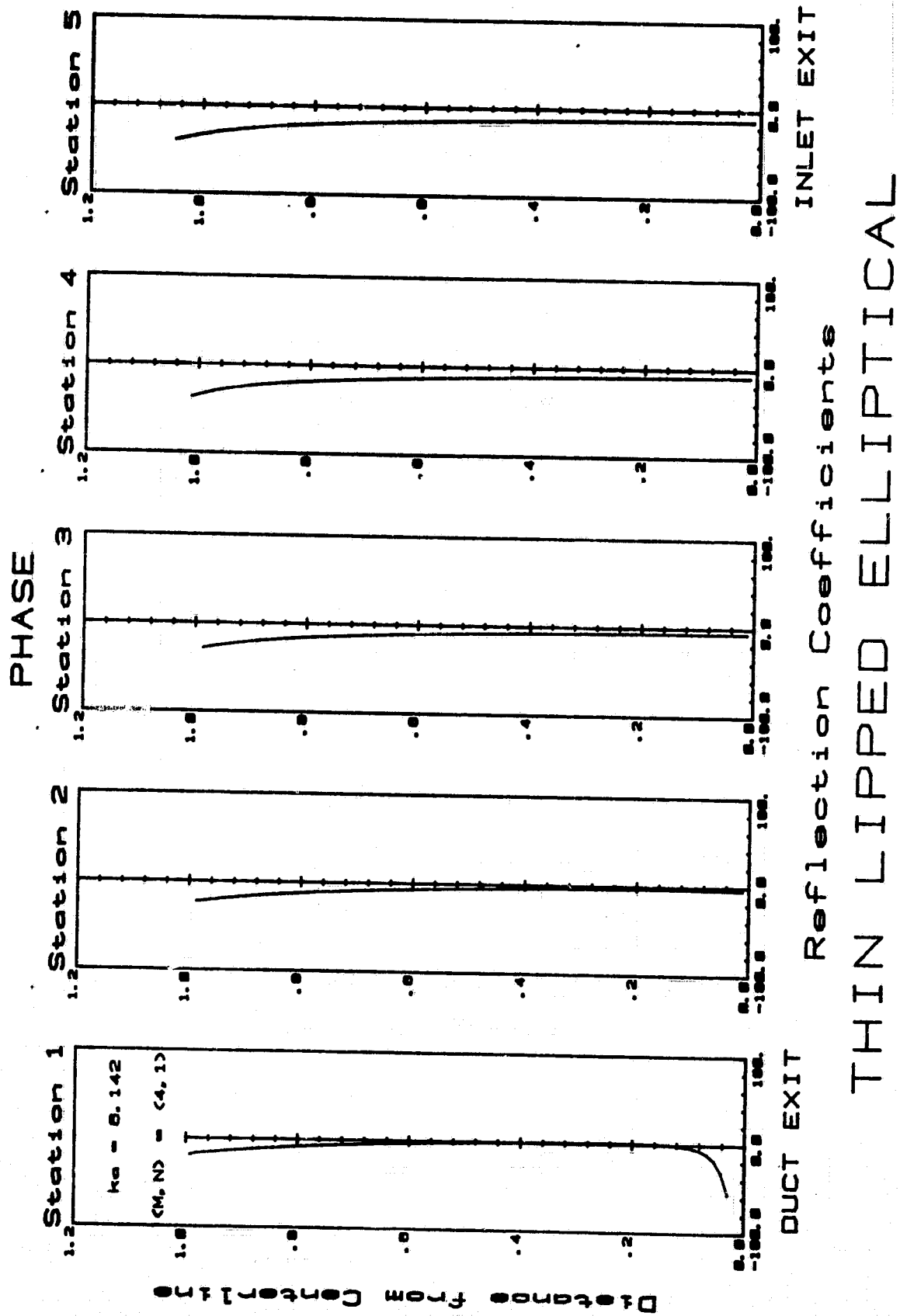
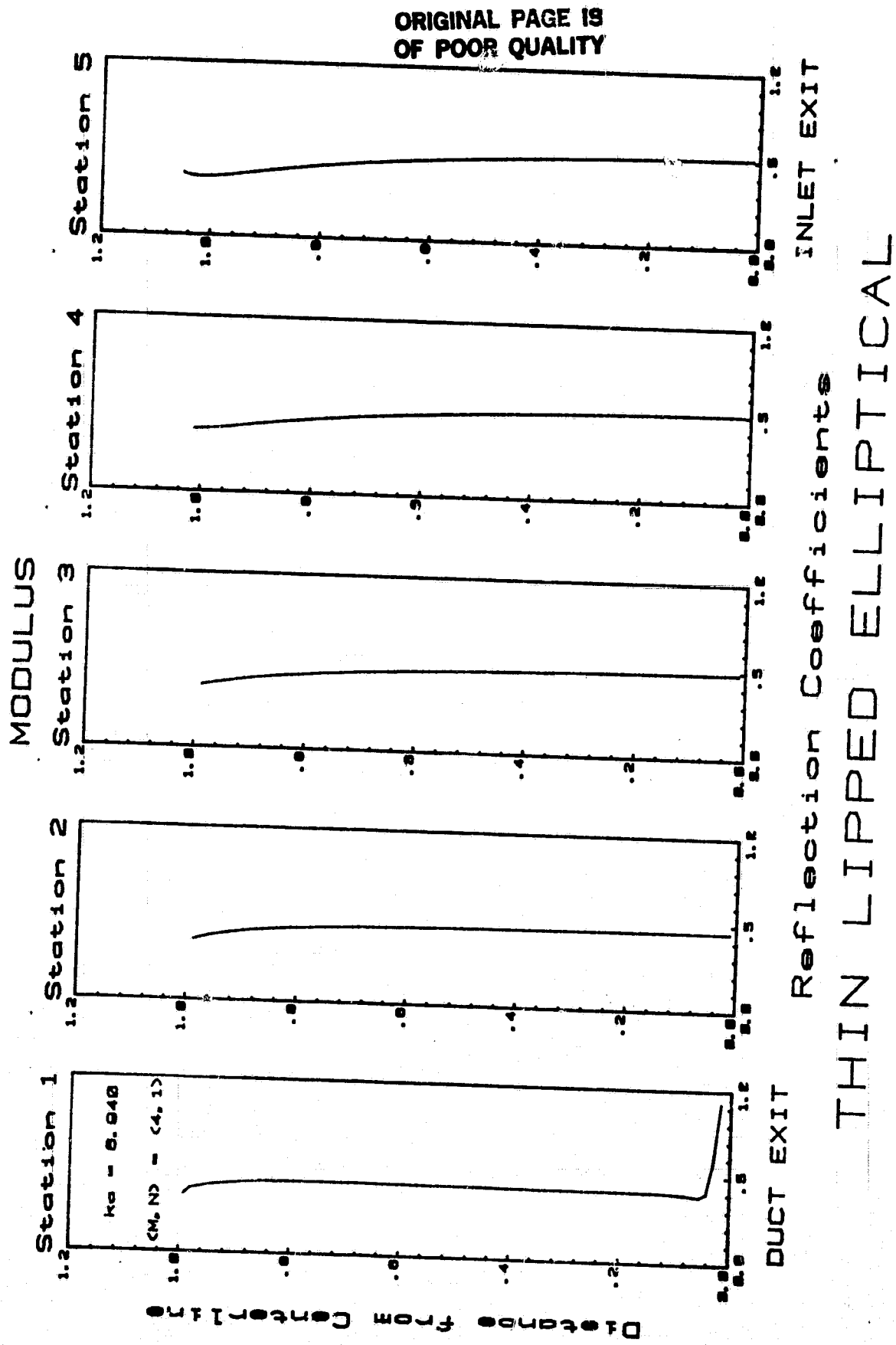


Fig. 25g

ORIGINAL PAGE IS
OF POOR QUALITY





Fig, 25i

ORIGINAL PAGE IS
OF POOR QUALITY

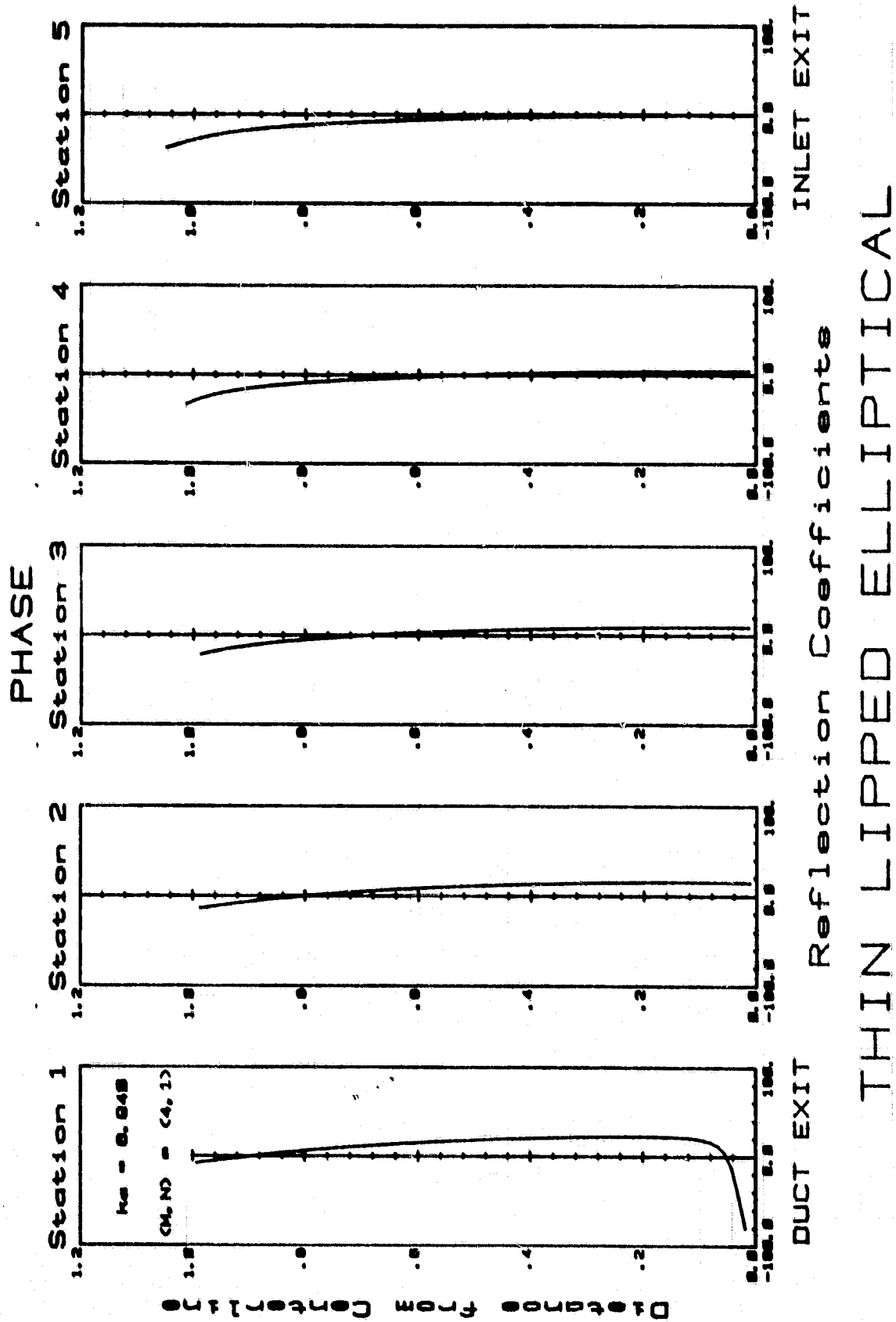


Fig. 25j

ORIGINAL PAGE IS
OF POOR QUALITY

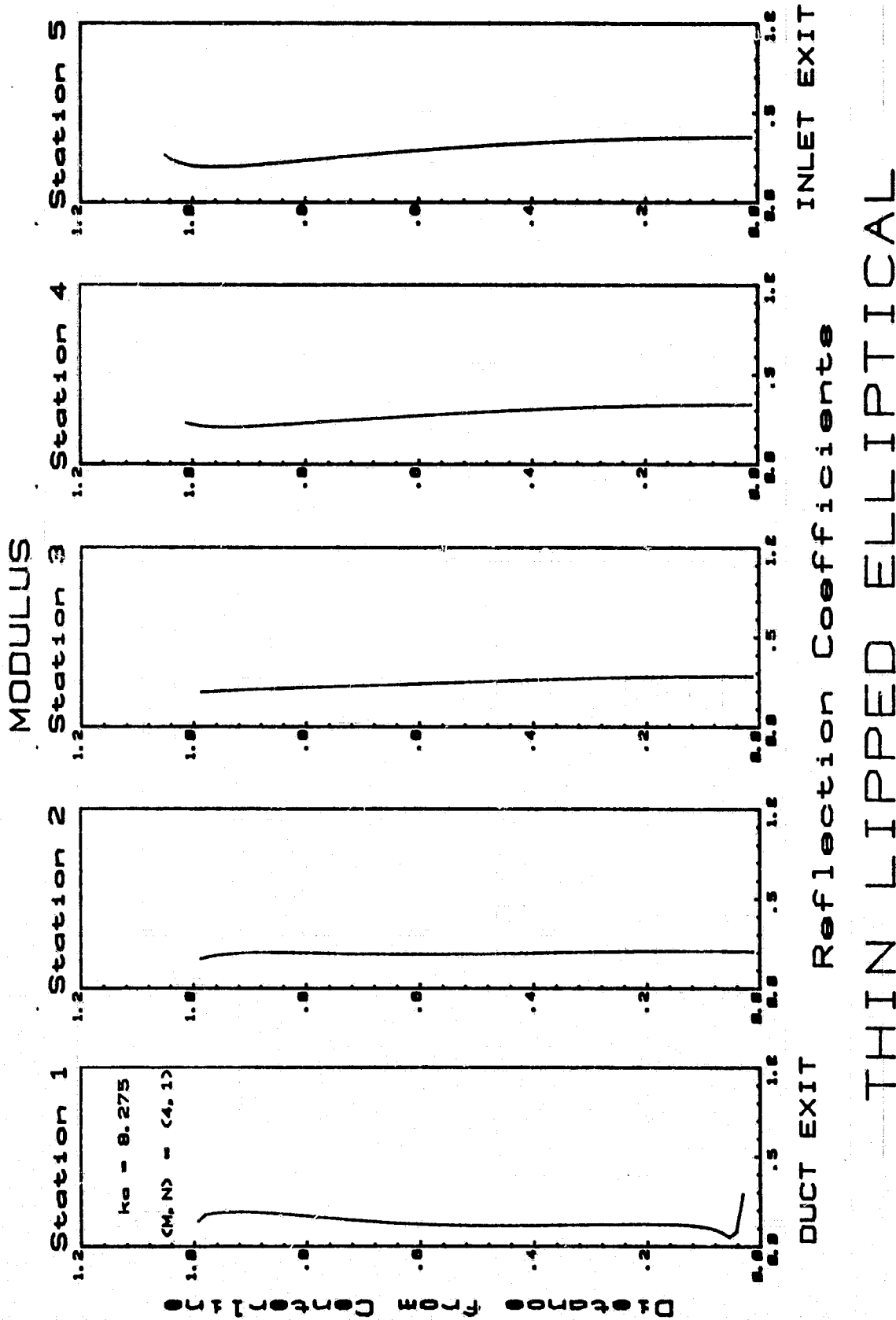


Fig. 25k

ORIGINAL PAGE IS
OF POOR QUALITY

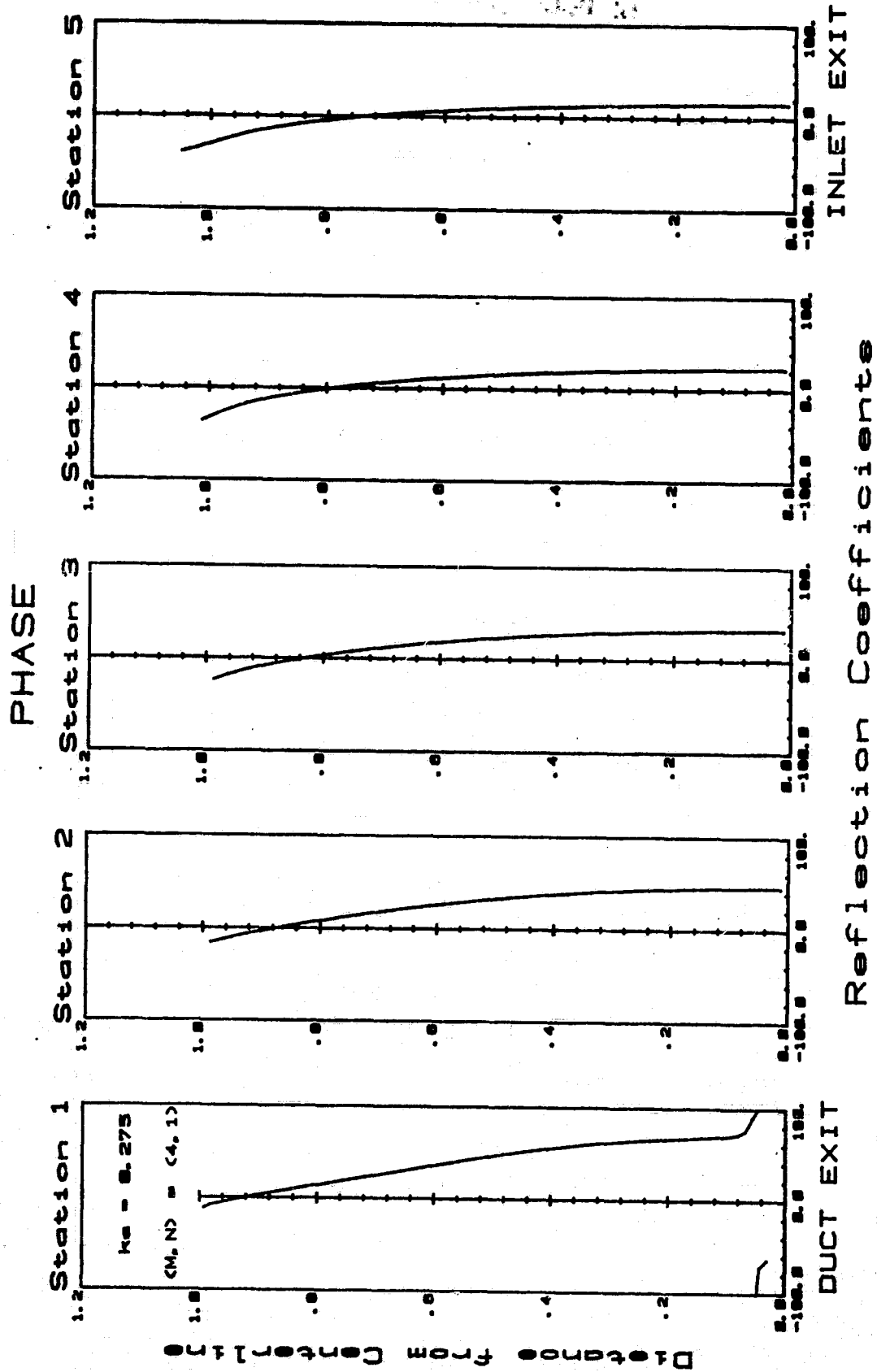
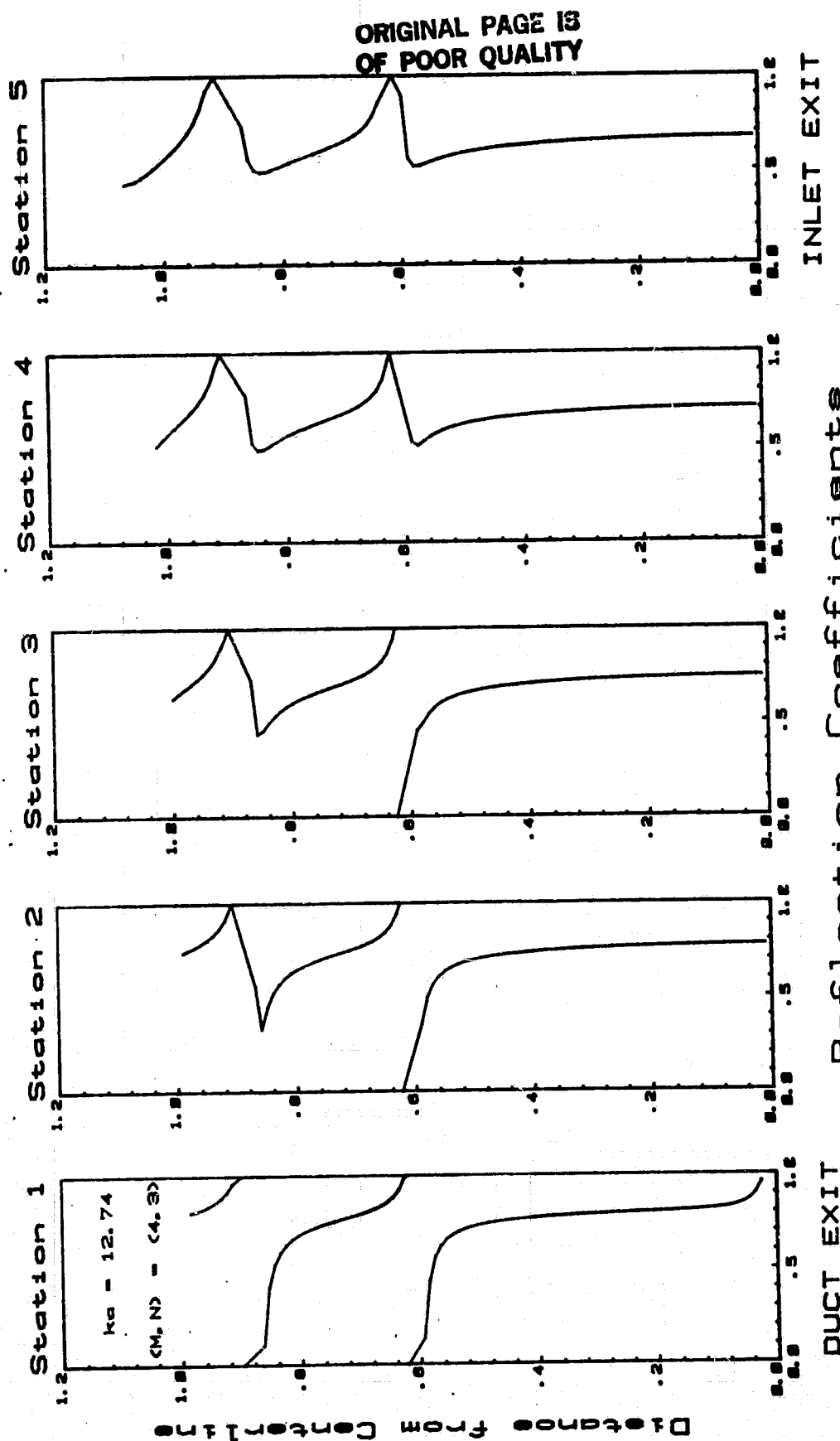


Fig. 251

THIN LIPPED ELLIPTICAL

MODULUS



THIN LIPPED ELLIPTICAL

Fig. 26a

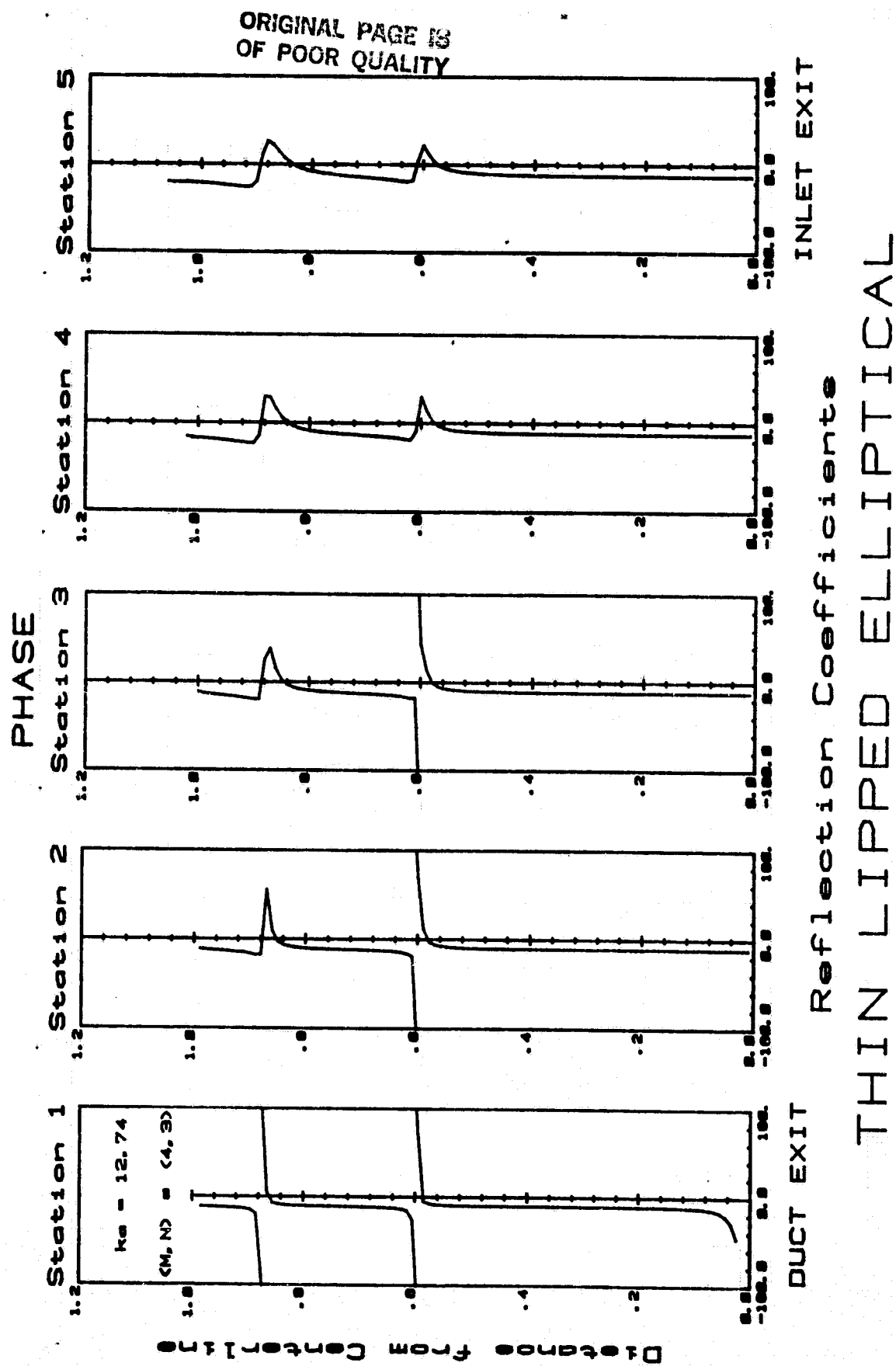
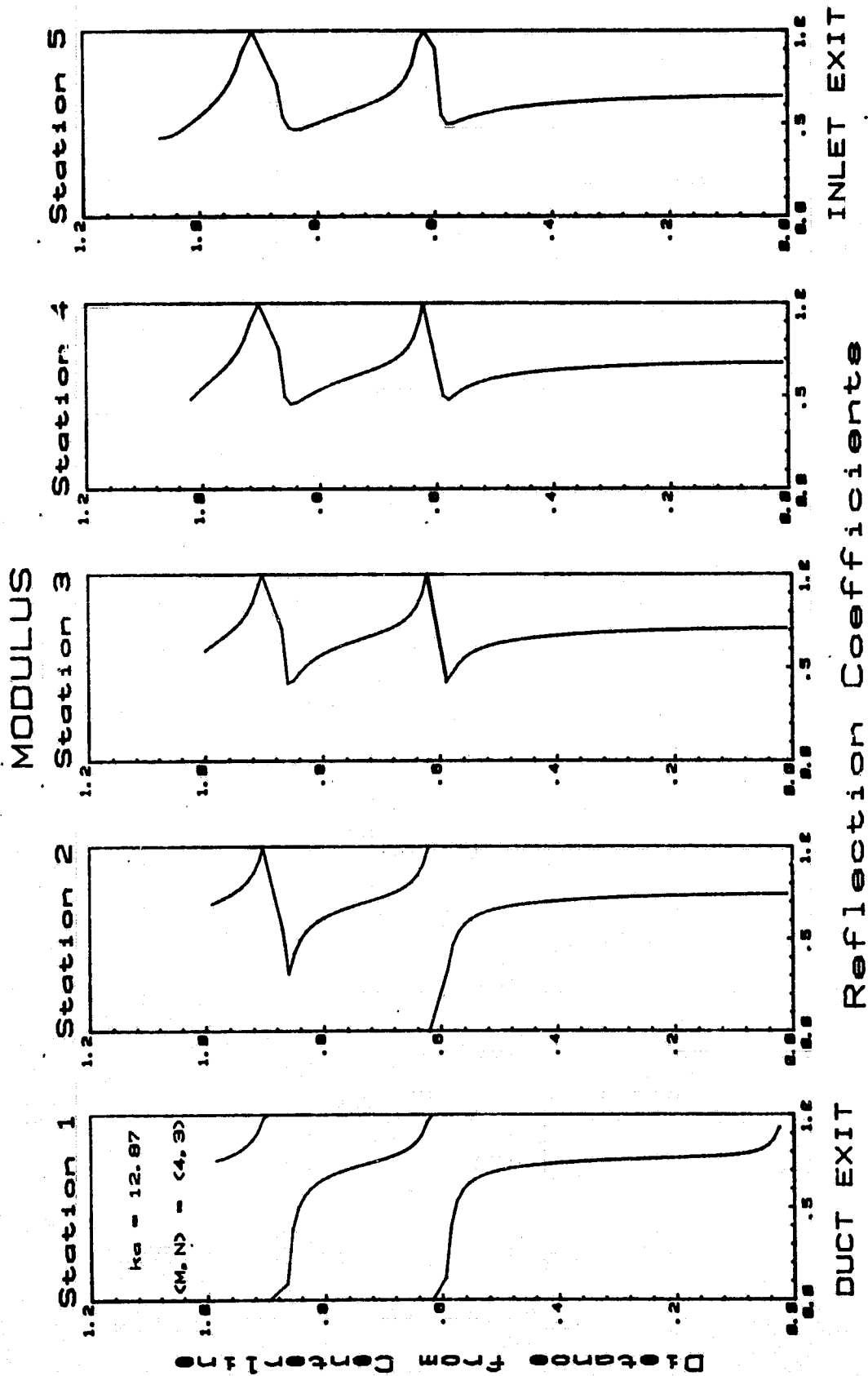


Fig. 26b

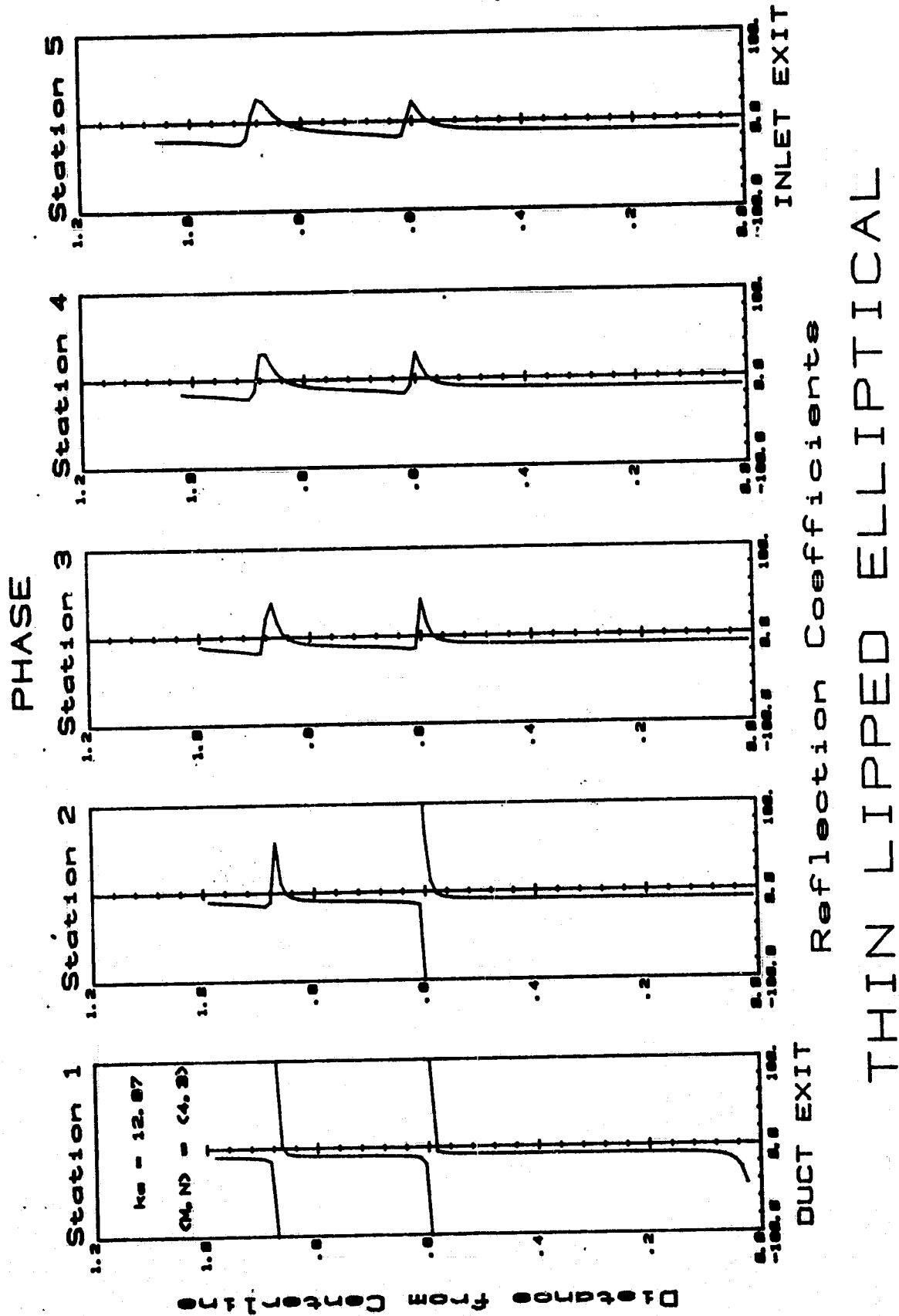
ORIGINAL PAGE IS
OF POOR QUALITY



THIN LIPPED ELLIPTICAL

Fig.26c

ORIGINAL PAGE IS
OF POOR QUALITY



ORIGINAL PAGE IS
OF POOR QUALITY

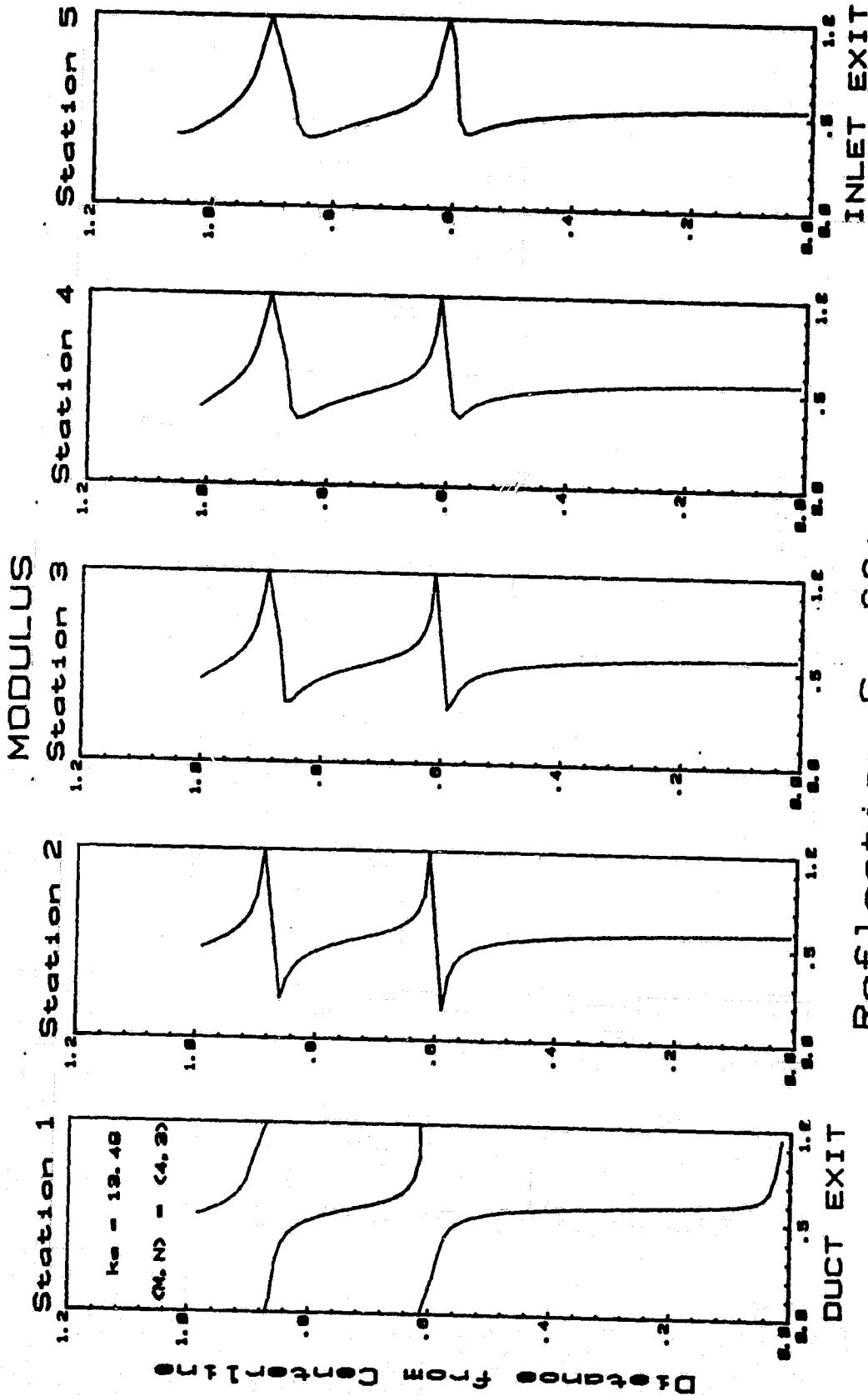


Fig. 26e

ORIGINAL PAGE IS
OF POOR QUALITY

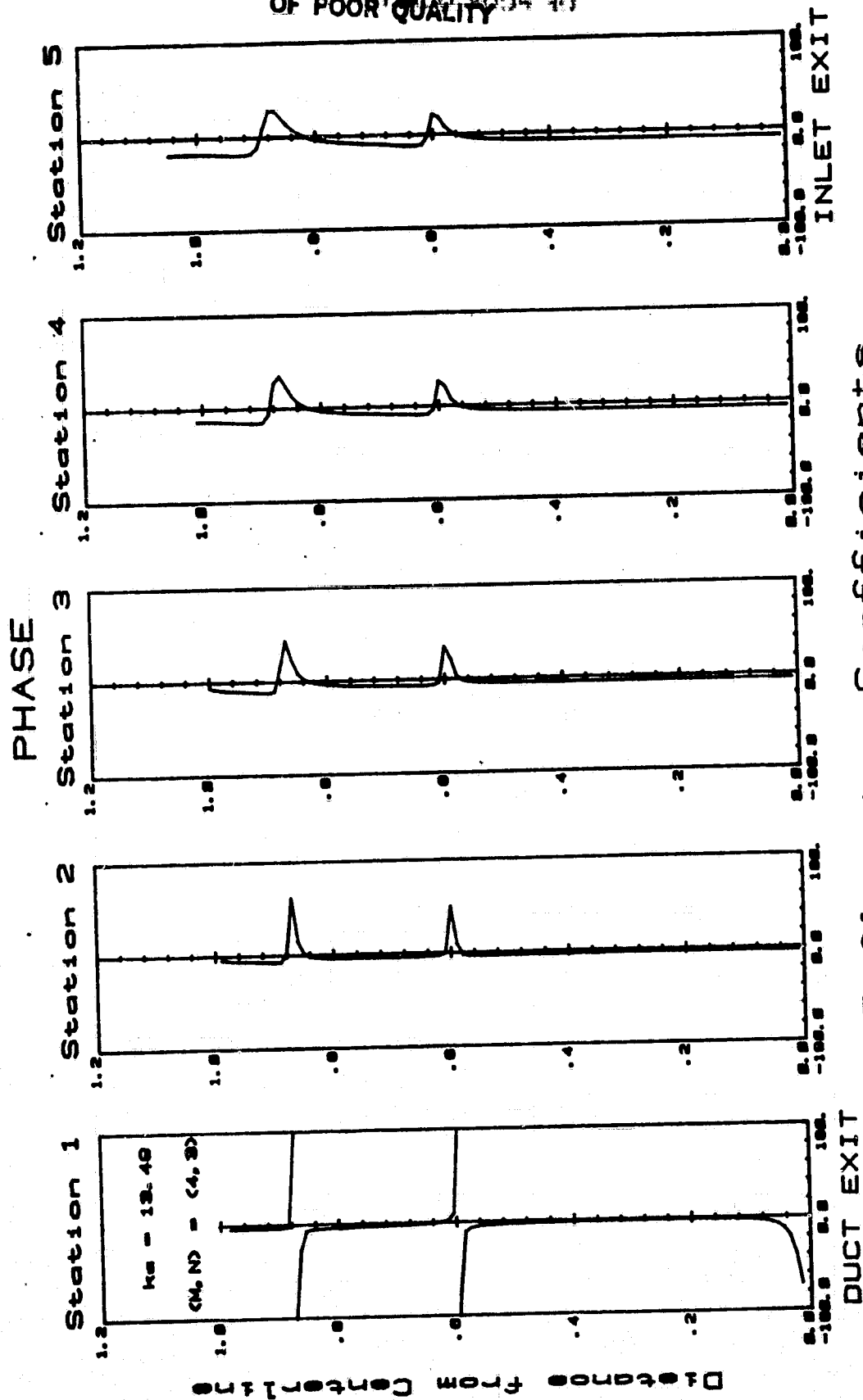


Fig. 26f

MODULUS

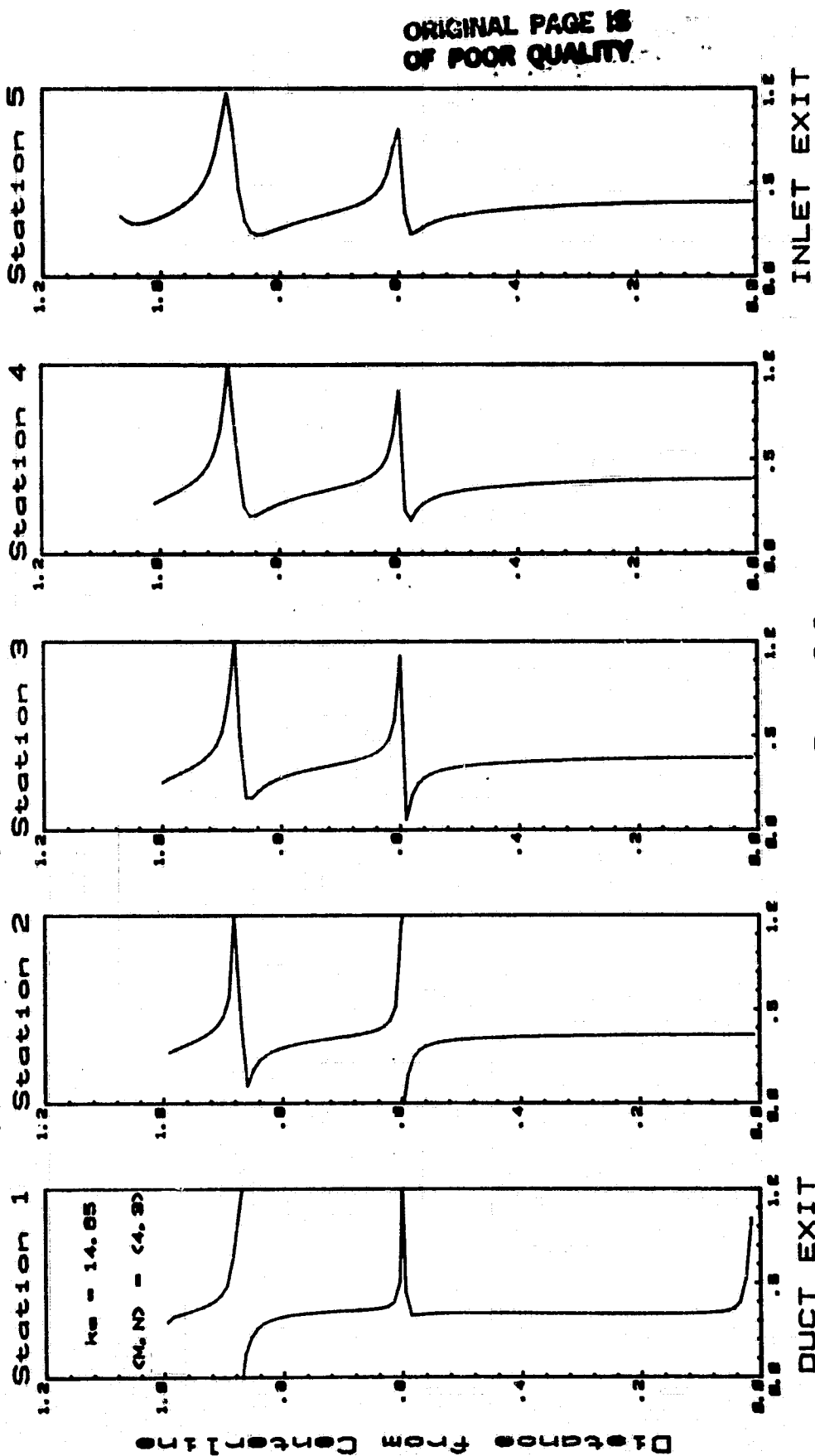


Fig. 26g

THIN LIPPED ELLIPTICAL

ORIGINAL PAGE IS
OF POOR QUALITY

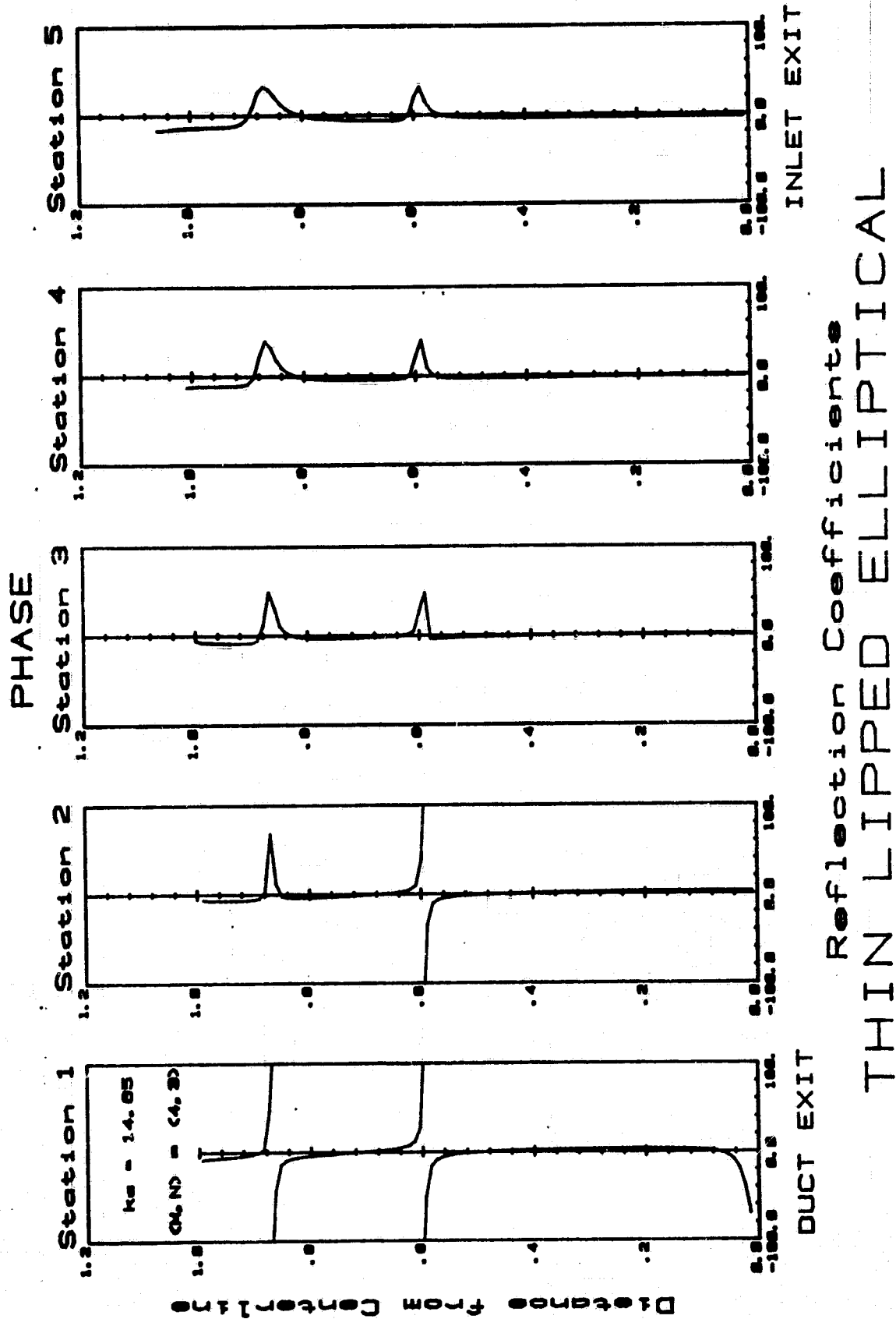


Fig. 26h

ORIGINAL PAGE IS
OF POOR QUALITY

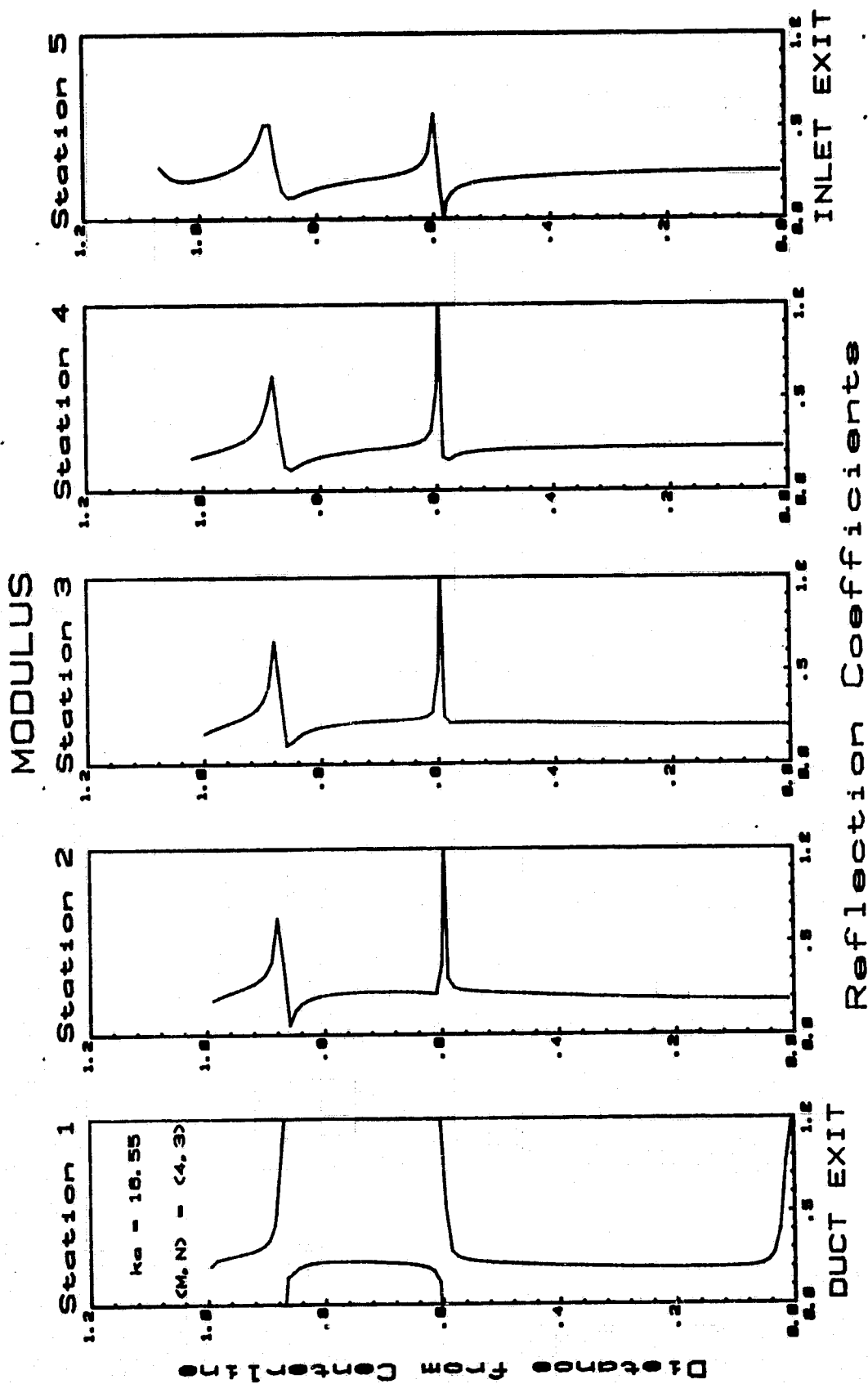


Fig. 26i

THIN LIPPED ELLIPTICAL

ORIGINAL PAGE IS
OF POOR QUALITY

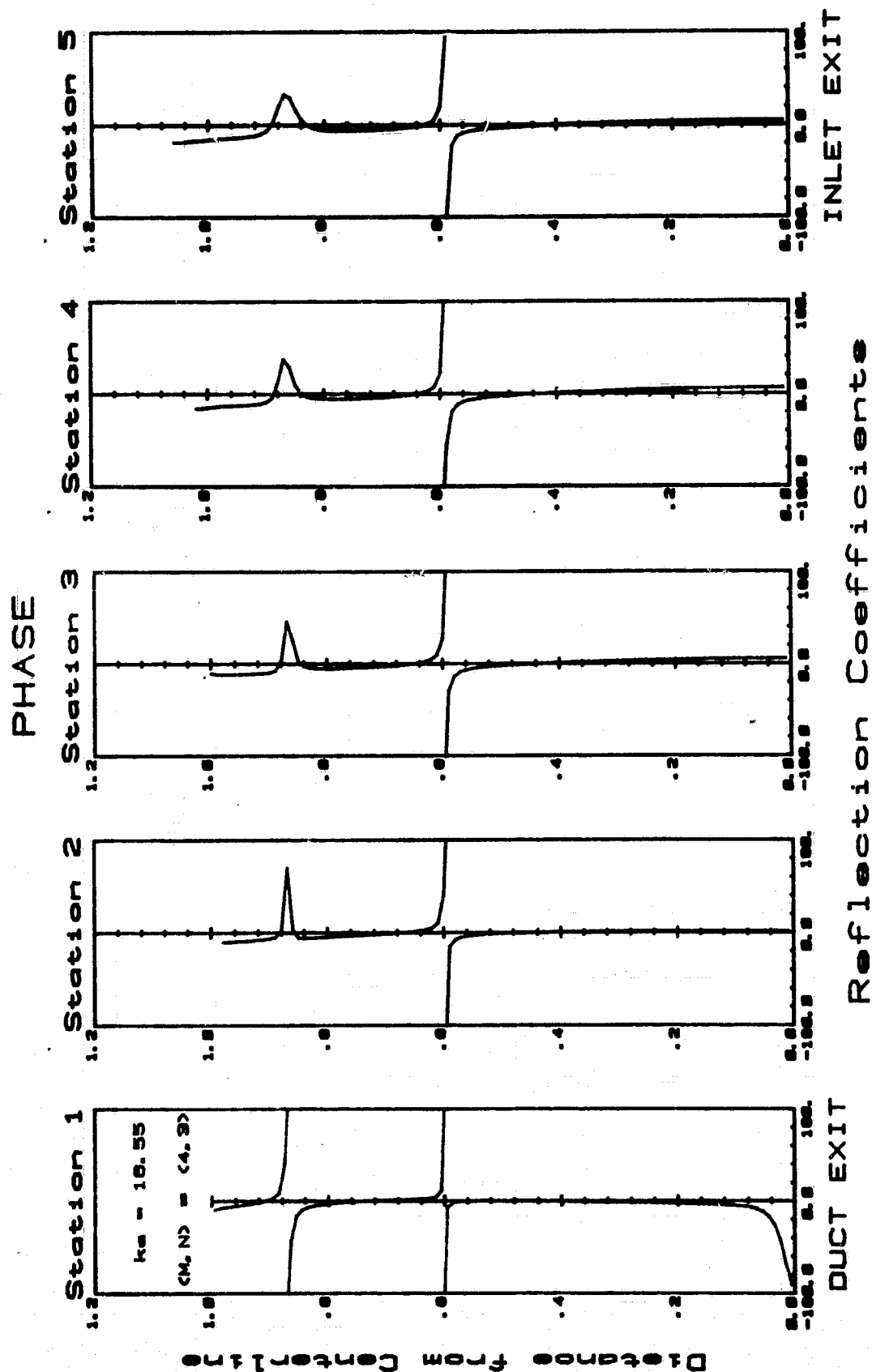


Fig. 26j

ORIGINAL PAGE IS
OF POOR QUALITY

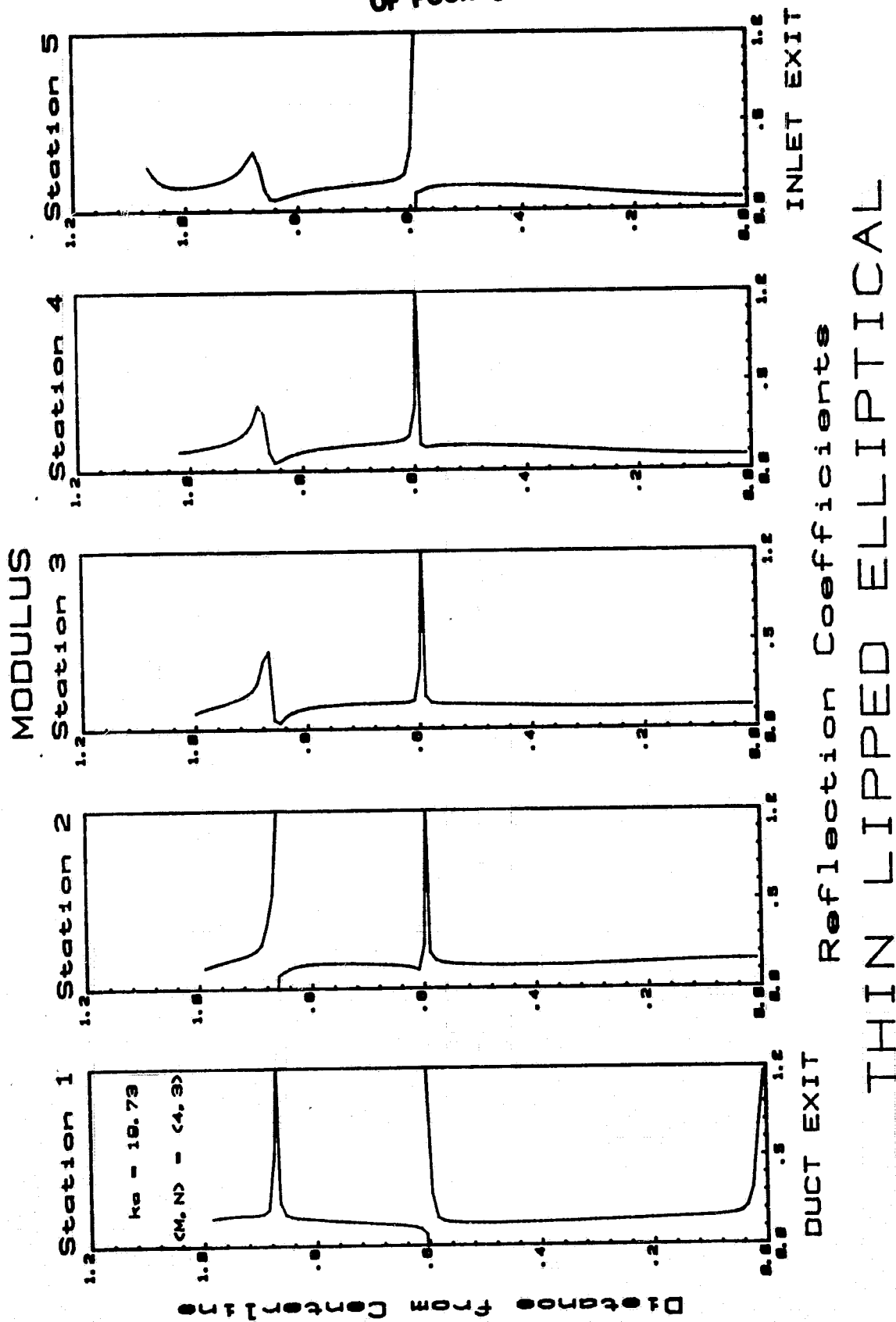


Fig. 26k

ORIGINAL PAGE IS
OF POOR QUALITY.

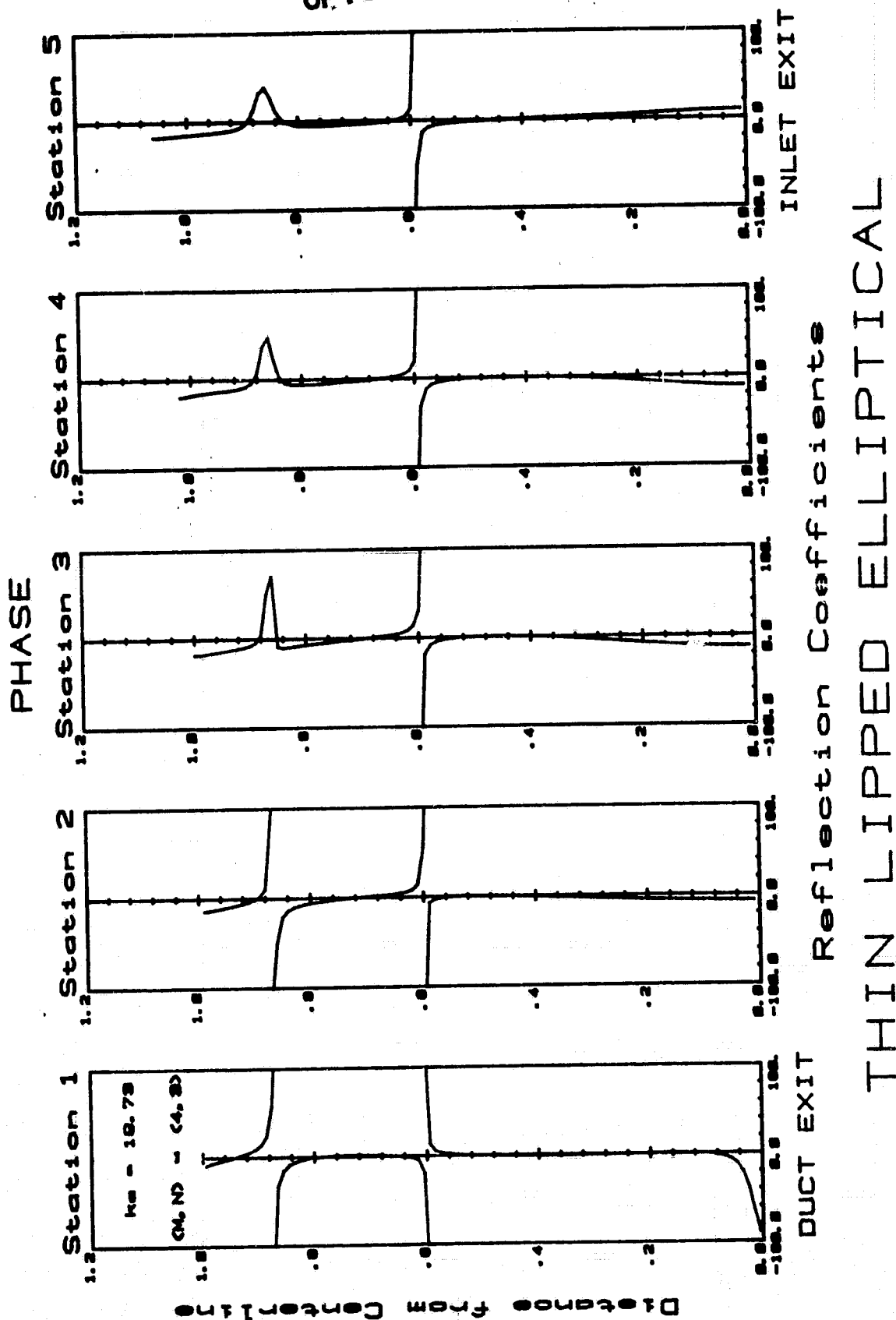


Fig. 261

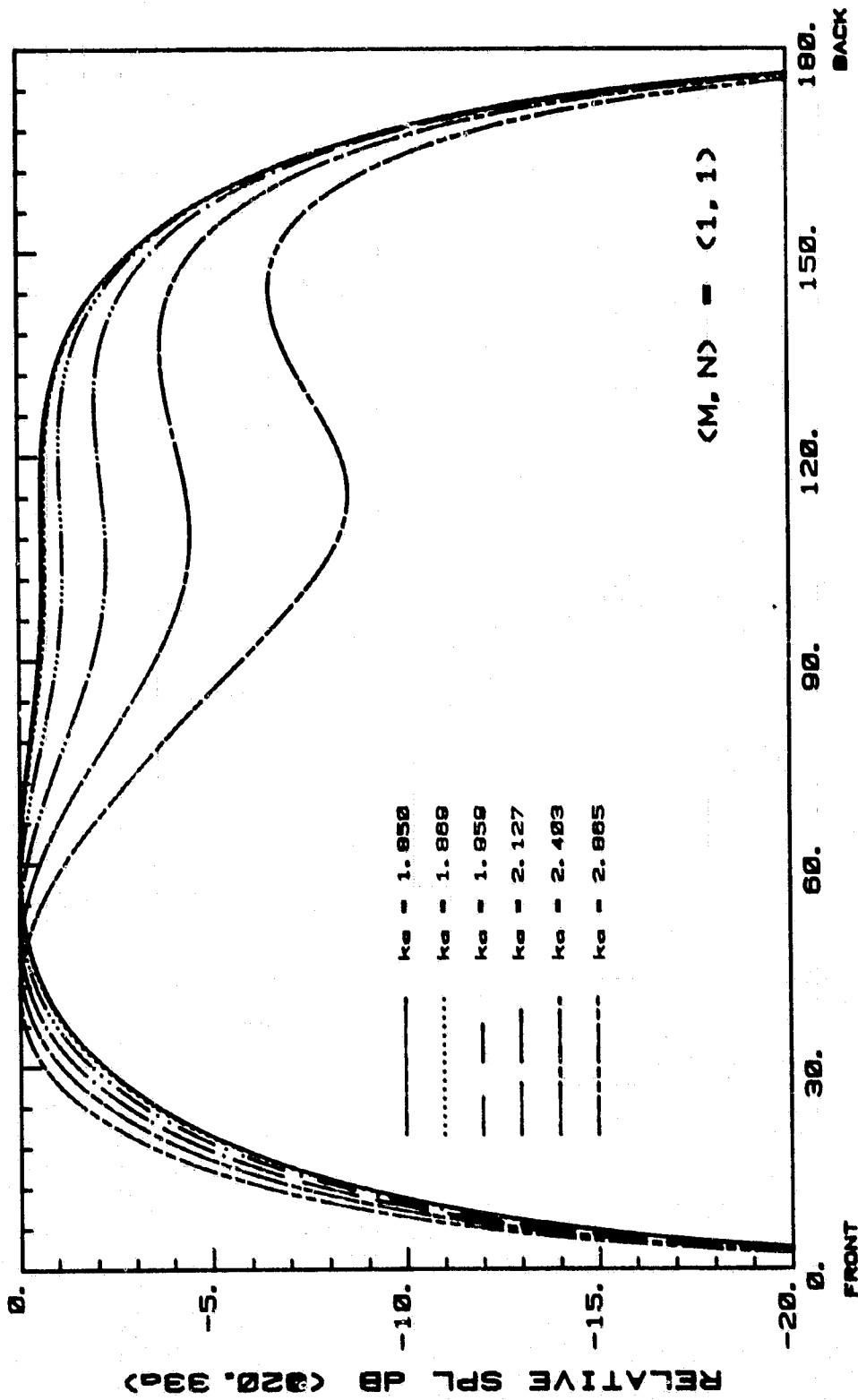
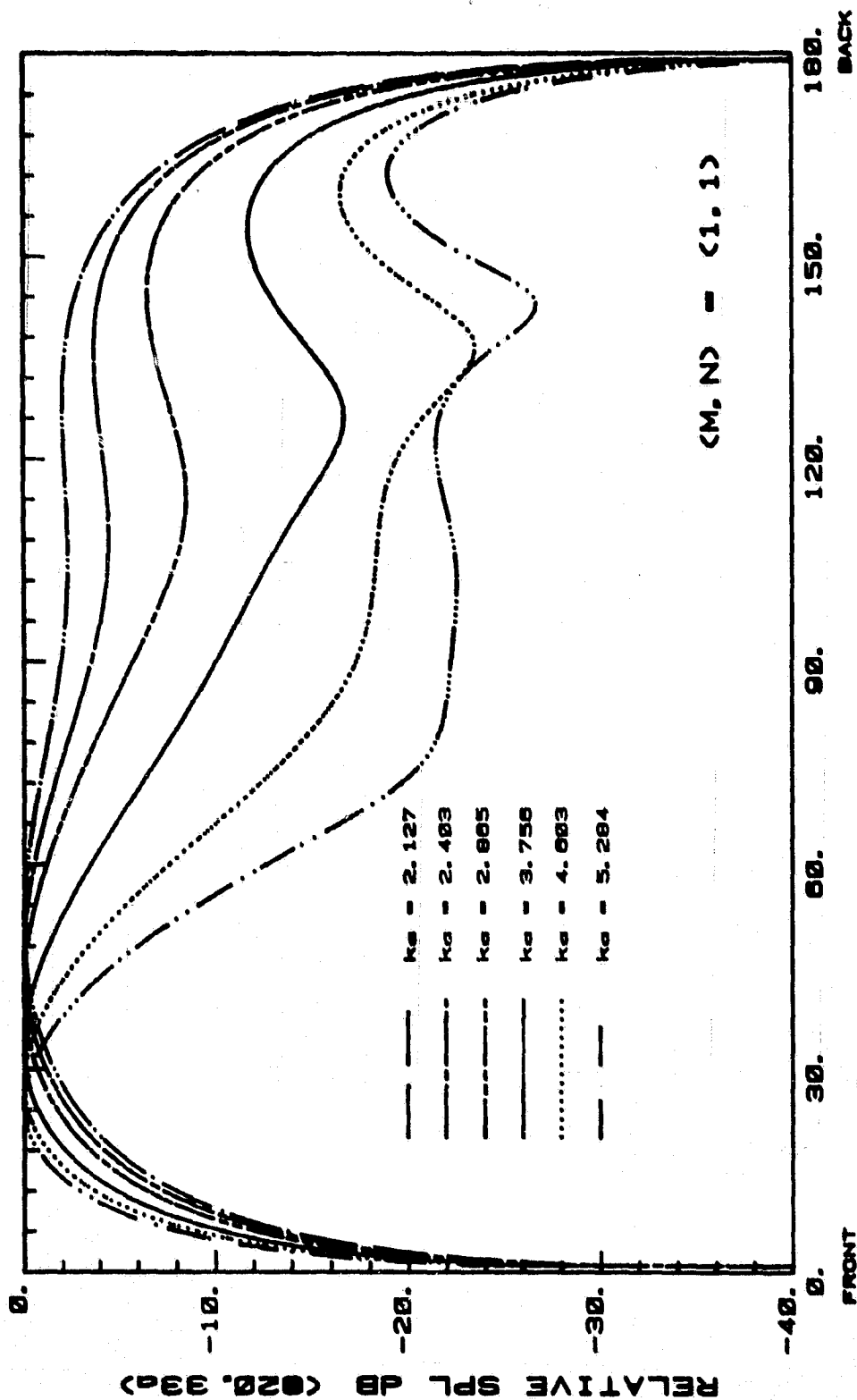


Fig. 27a

THIN LIPPED ELLIPTICAL INLET

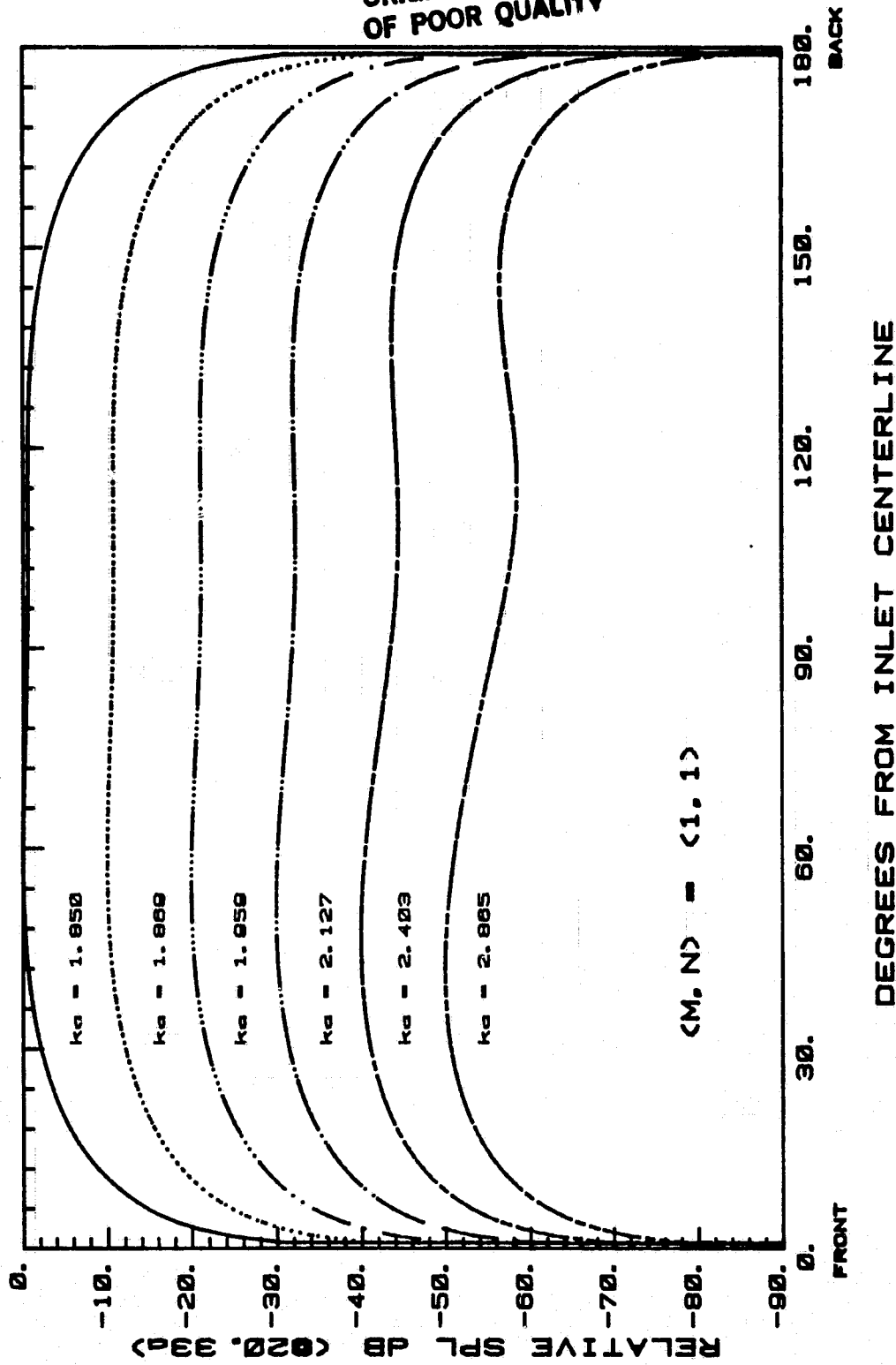
ORIGINAL PAGE IS
OF POOR QUALITY



THIN LIPPED ELLIPTICAL INLET

Fig. 27b

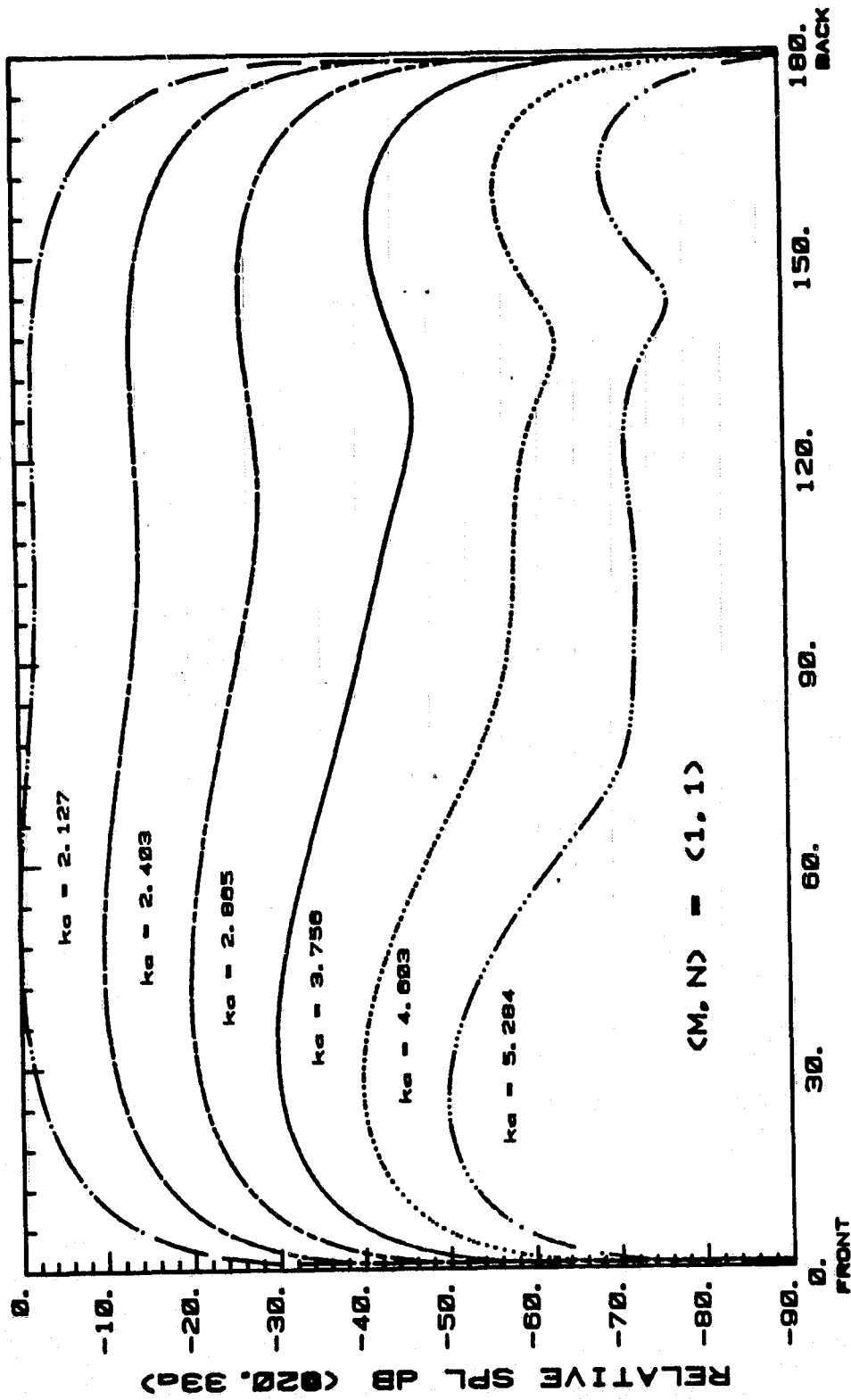
ORIGINAL PAGE IS
OF POOR QUALITY



THIN LIPPED ELLIPTICAL INLET

Fig. 27c

ORIGINAL PAGE IS
OF POOR QUALITY

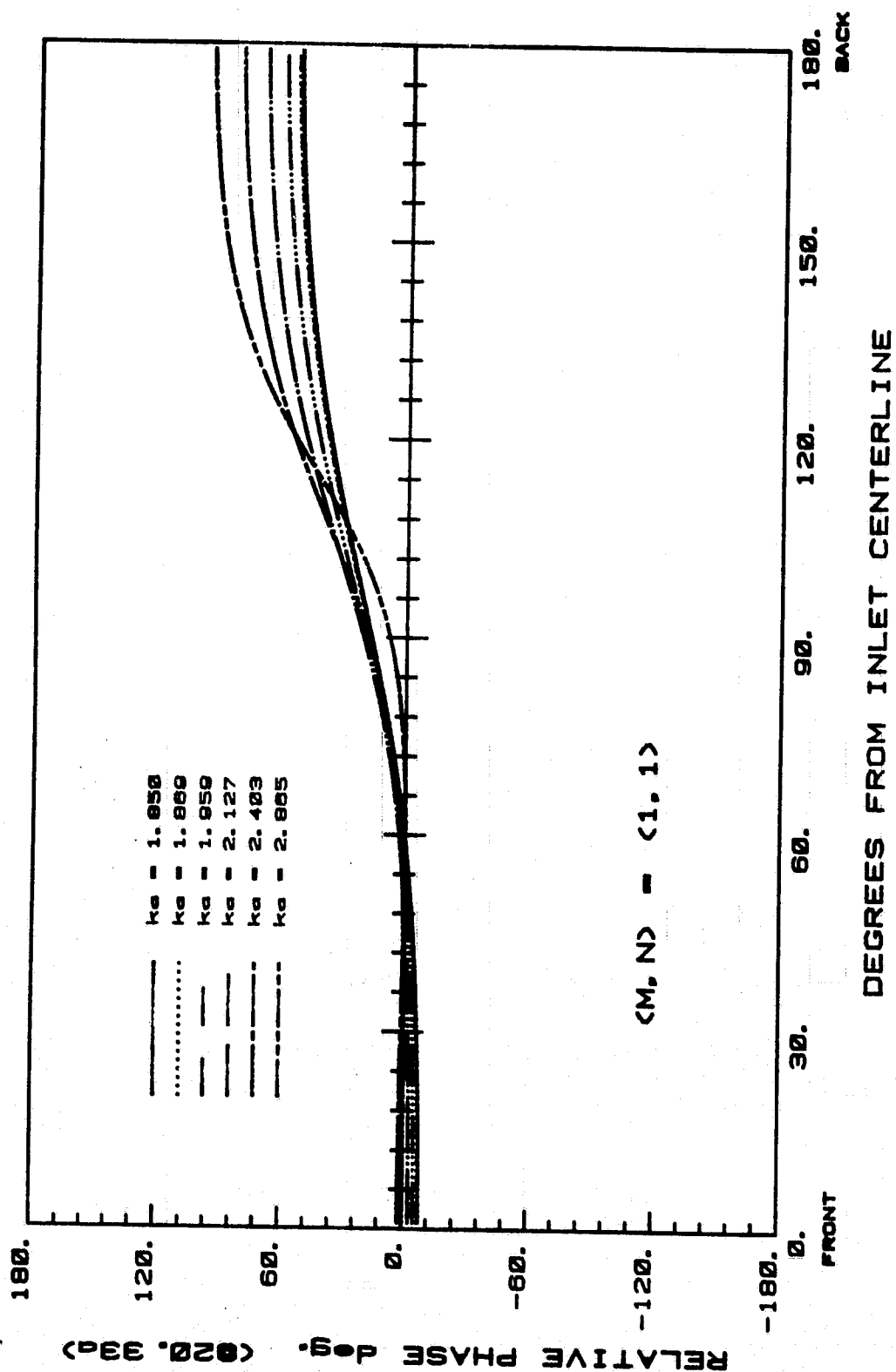


DEGREES FROM INLET CENTERLINE

THIN LIPPED ELLIPTICAL INLET

Fig. 27d

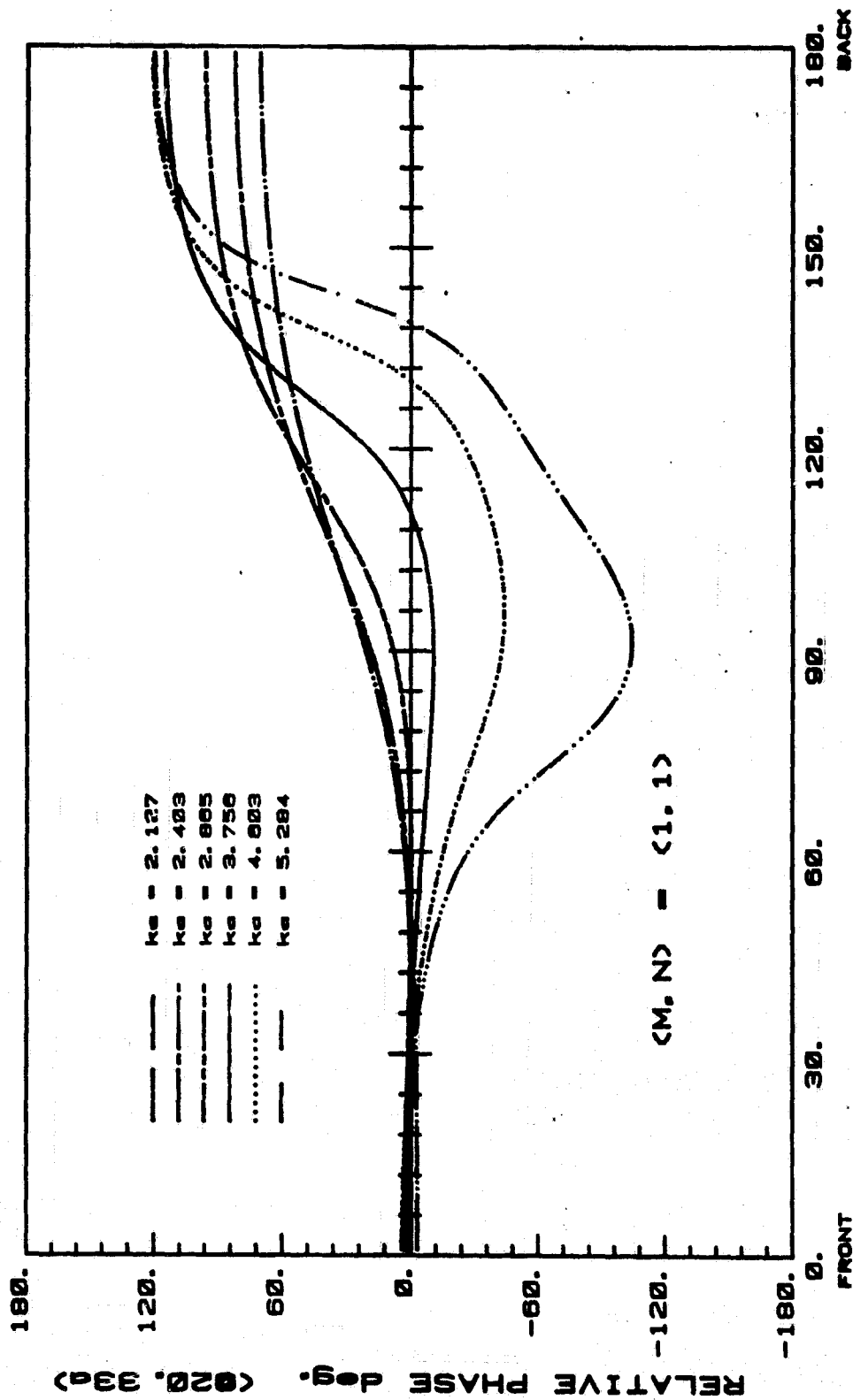
ORIGINAL PAGE IS
OF POOR QUALITY



THIN LIPPED ELLIPTICAL INLET

Fig. 27e

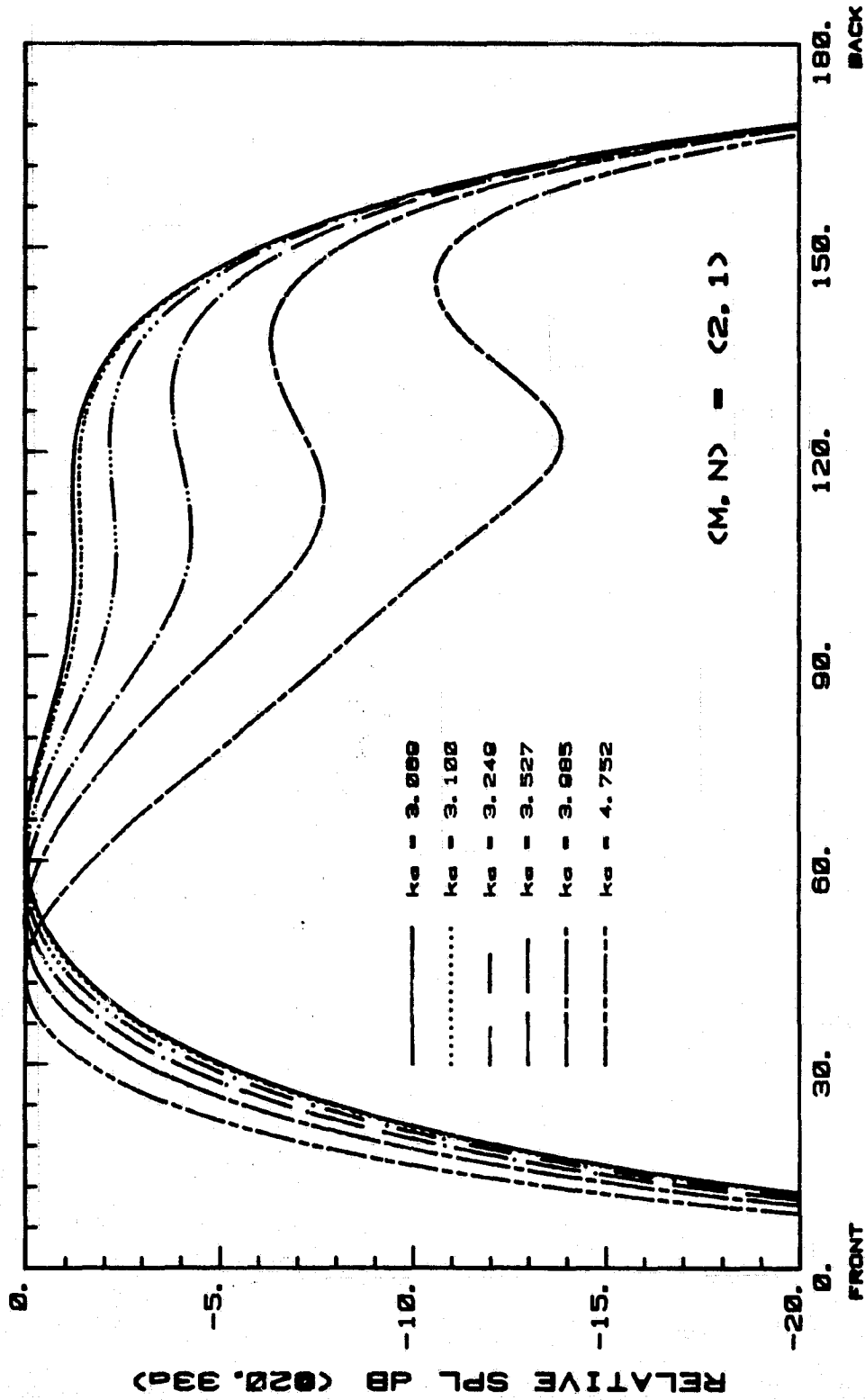
ORIGINAL PAGE IS
OF POOR QUALITY



THIN LIPPED ELLIPTICAL INLET

Fig. 27f

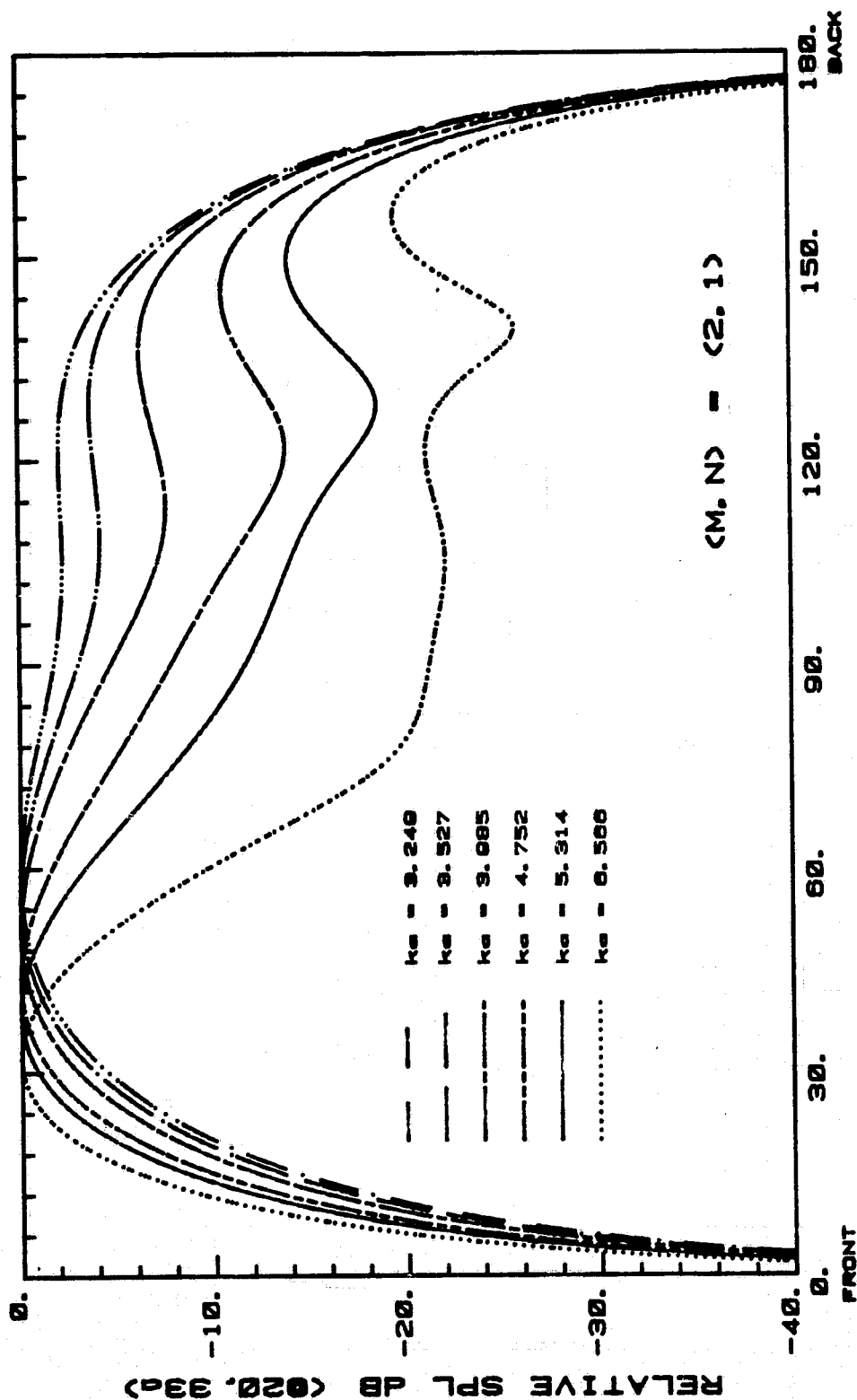
ORIGINAL PAGE IS
OF POOR QUALITY



THIN LIPPED ELLIPTICAL INLET

Fig. 28a

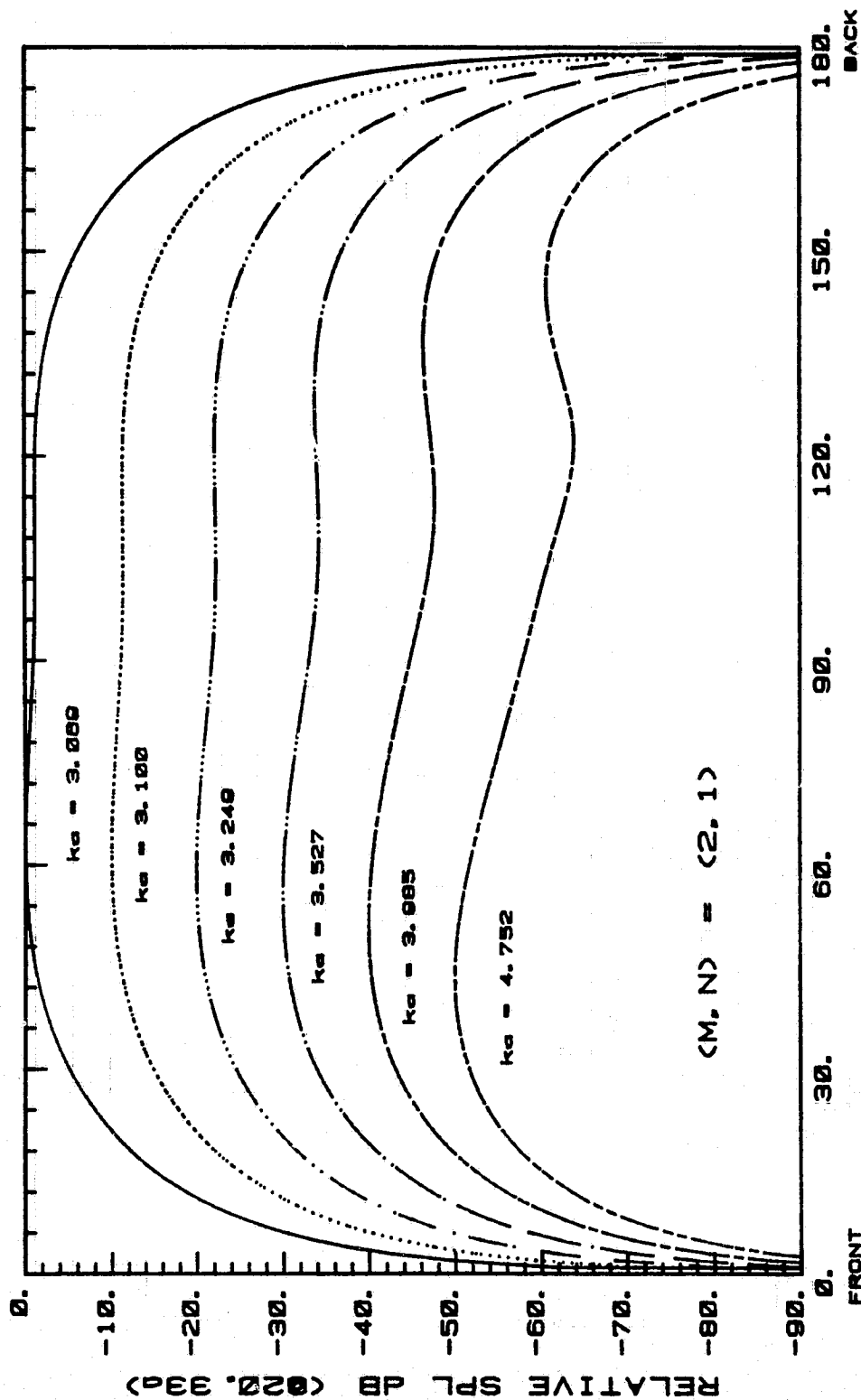
ORIGINAL PAGE IS
OF POOR QUALITY



THIN LIPPED ELLIPTICAL INLET

Fig. 28b

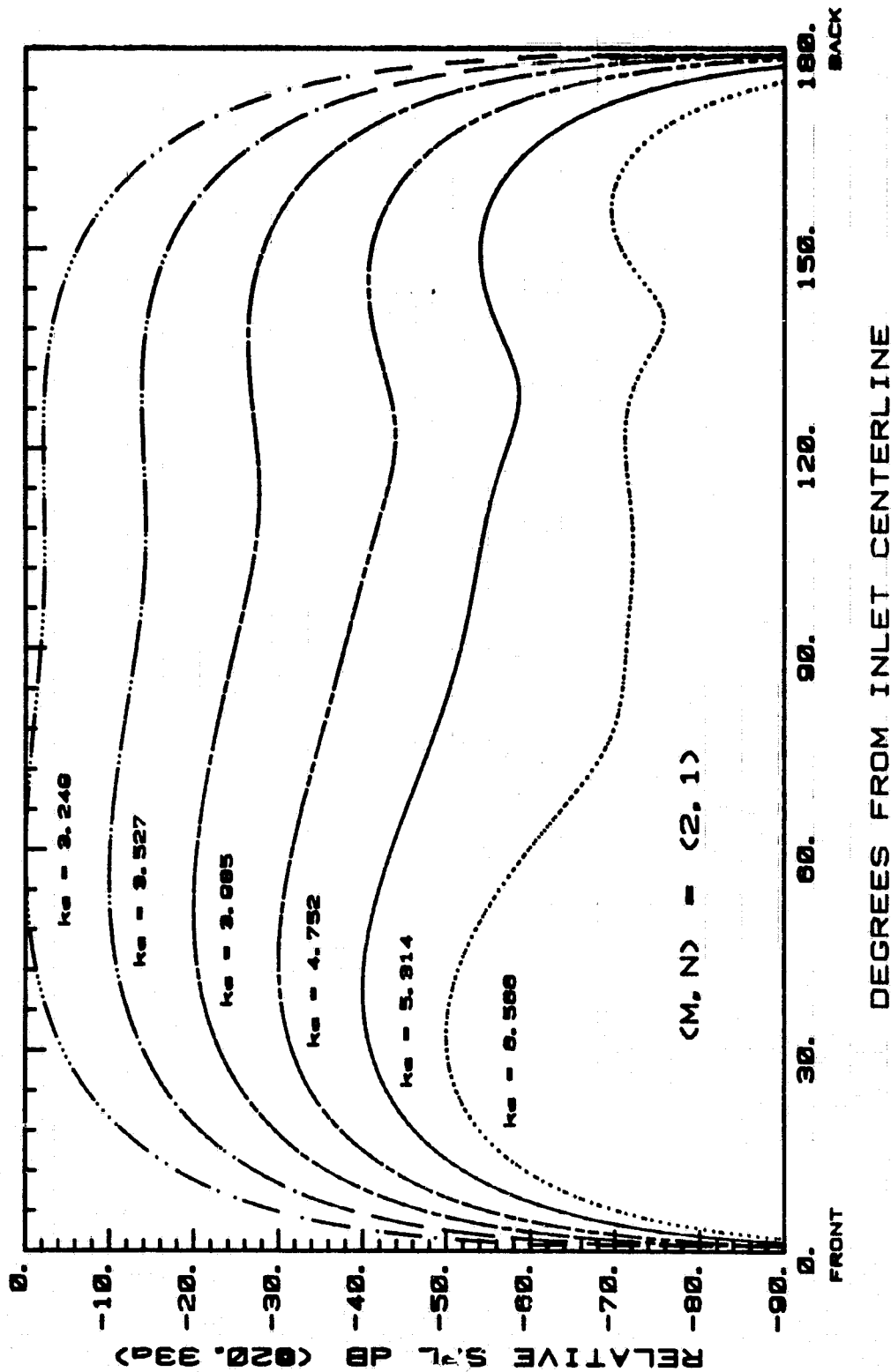
ORIGINAL PAGE IS
OF POOR QUALITY



THIN LIPPED ELLIPTICAL INLET

Fig. 28c

ORIGINAL PAGE IS
OF POOR QUALITY



THIN LIPPED ELLIPTICAL INLET

Fig. 28d

ORIGINAL PAGE IS
OF POOR QUALITY

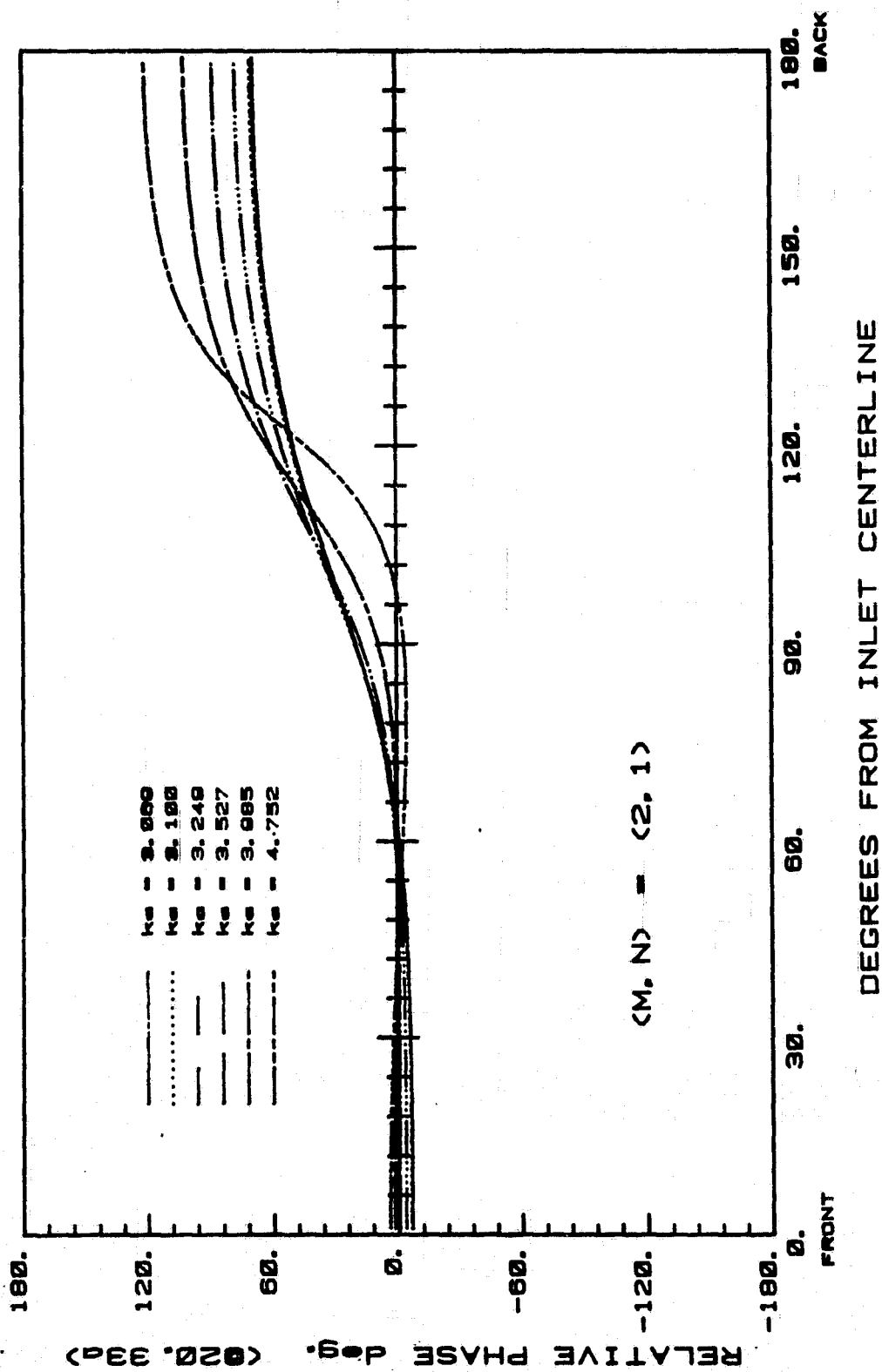
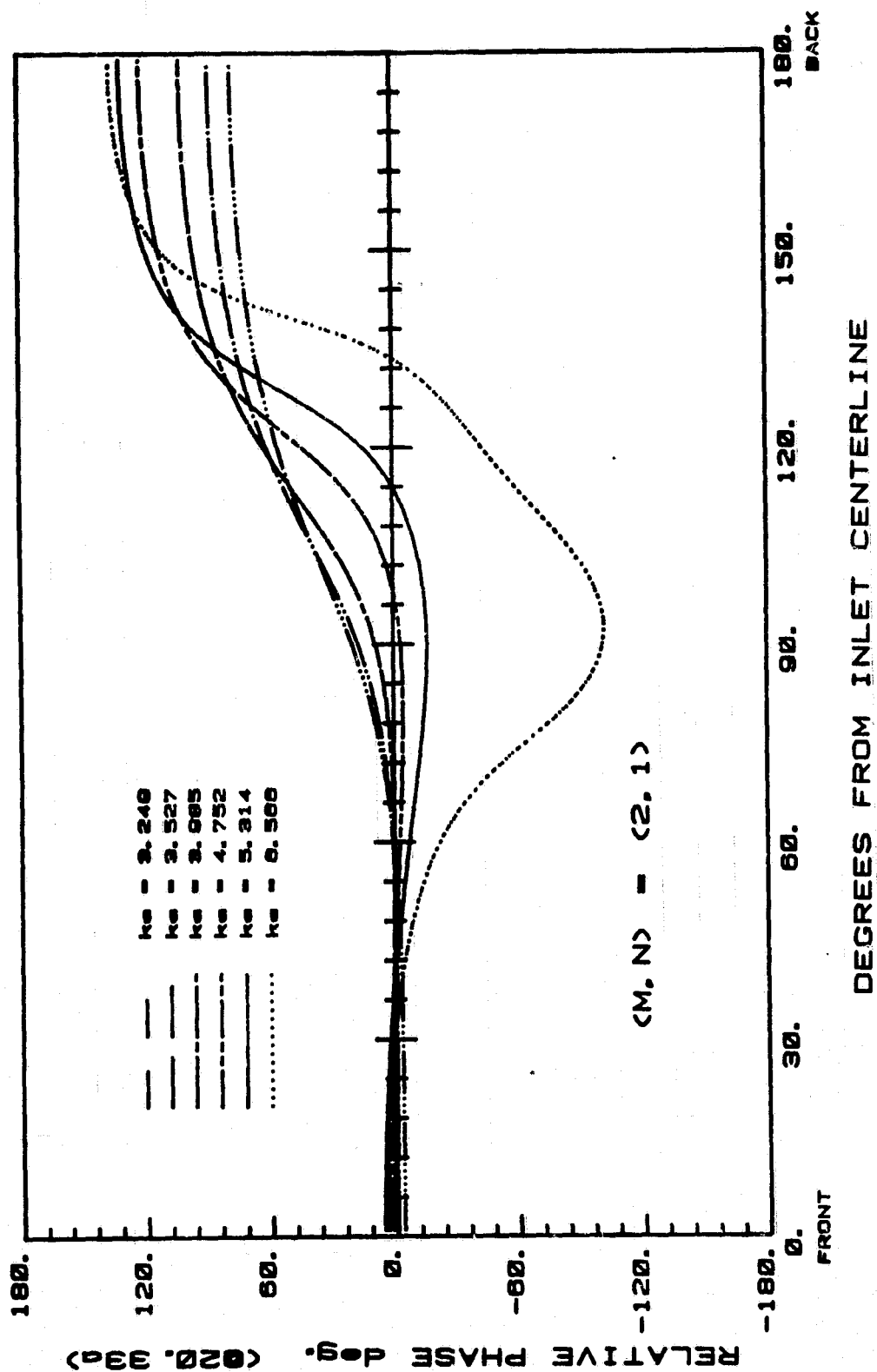


Fig. 28e

THIN LIPPED ELLIPTICAL INLET

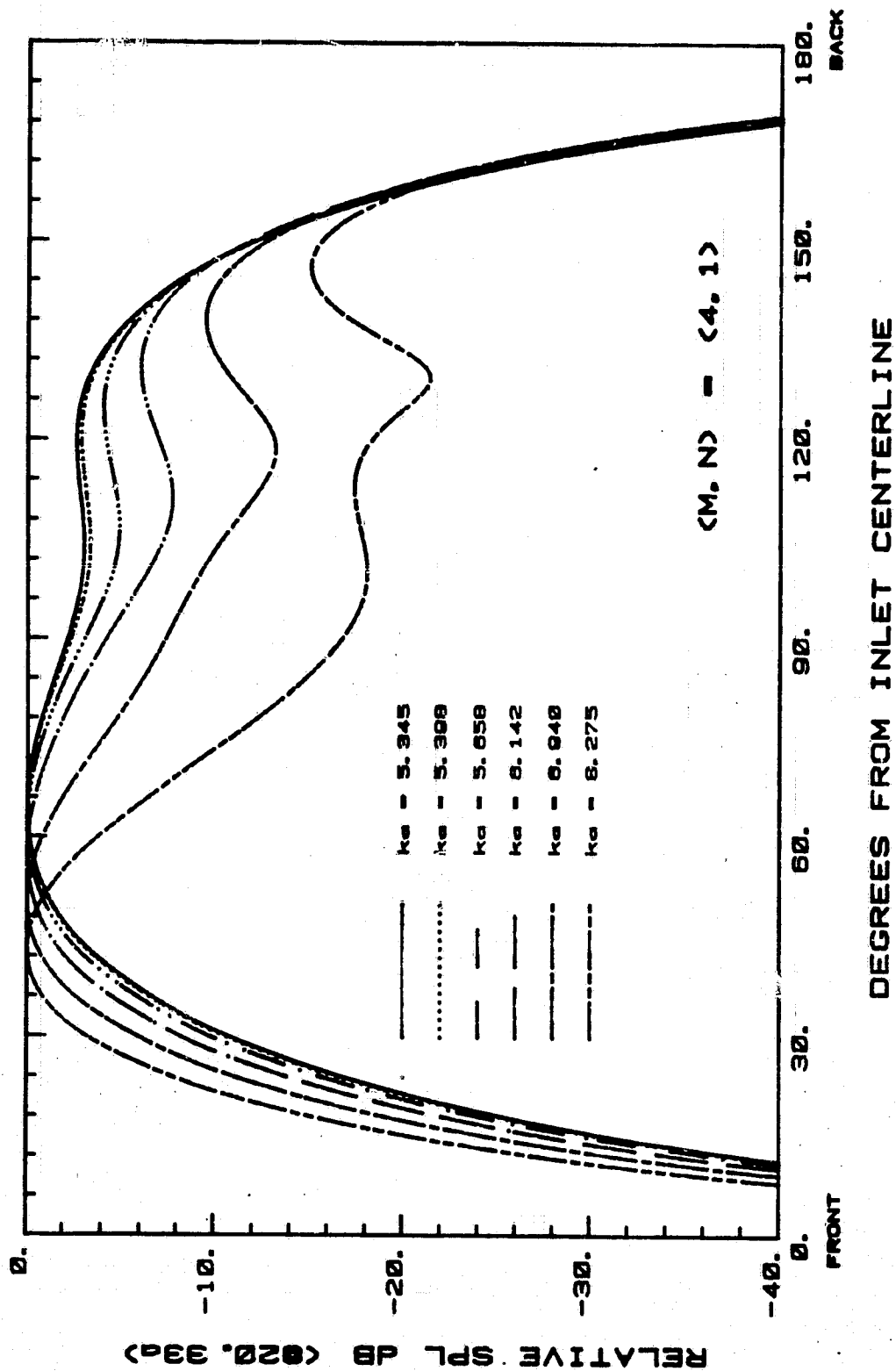
ORIGINAL PAGE IS
OF POOR QUALITY



THIN LIPPED ELLIPTICAL INLET

Fig. 28f

ORIGINAL PAGE IS
OF POOR QUALITY



THIN LIPPED ELLIPTICAL INLET

Fig. 23a

ORIGINAL PAGE IS
OF POOR QUALITY

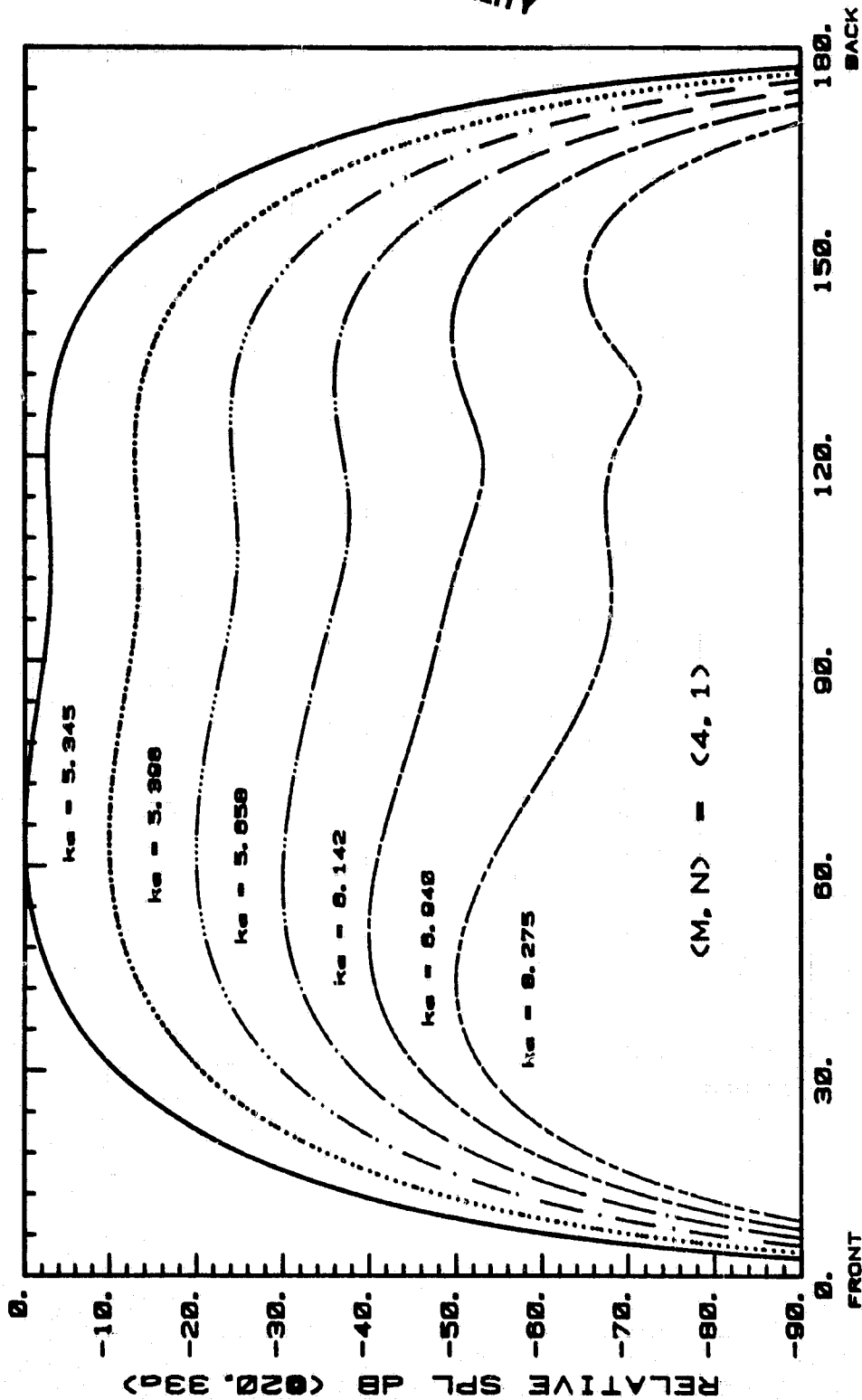
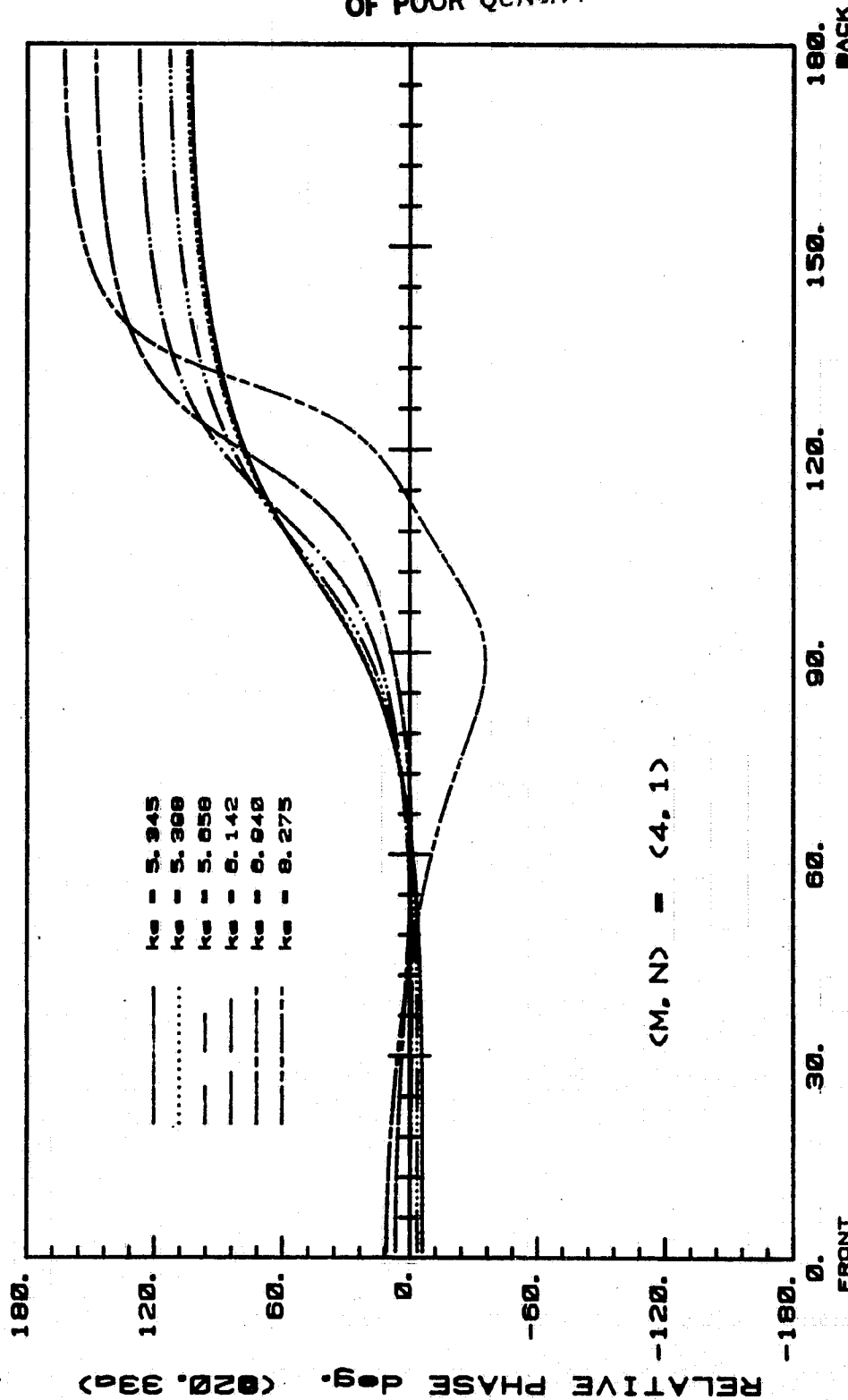


Fig. 29b

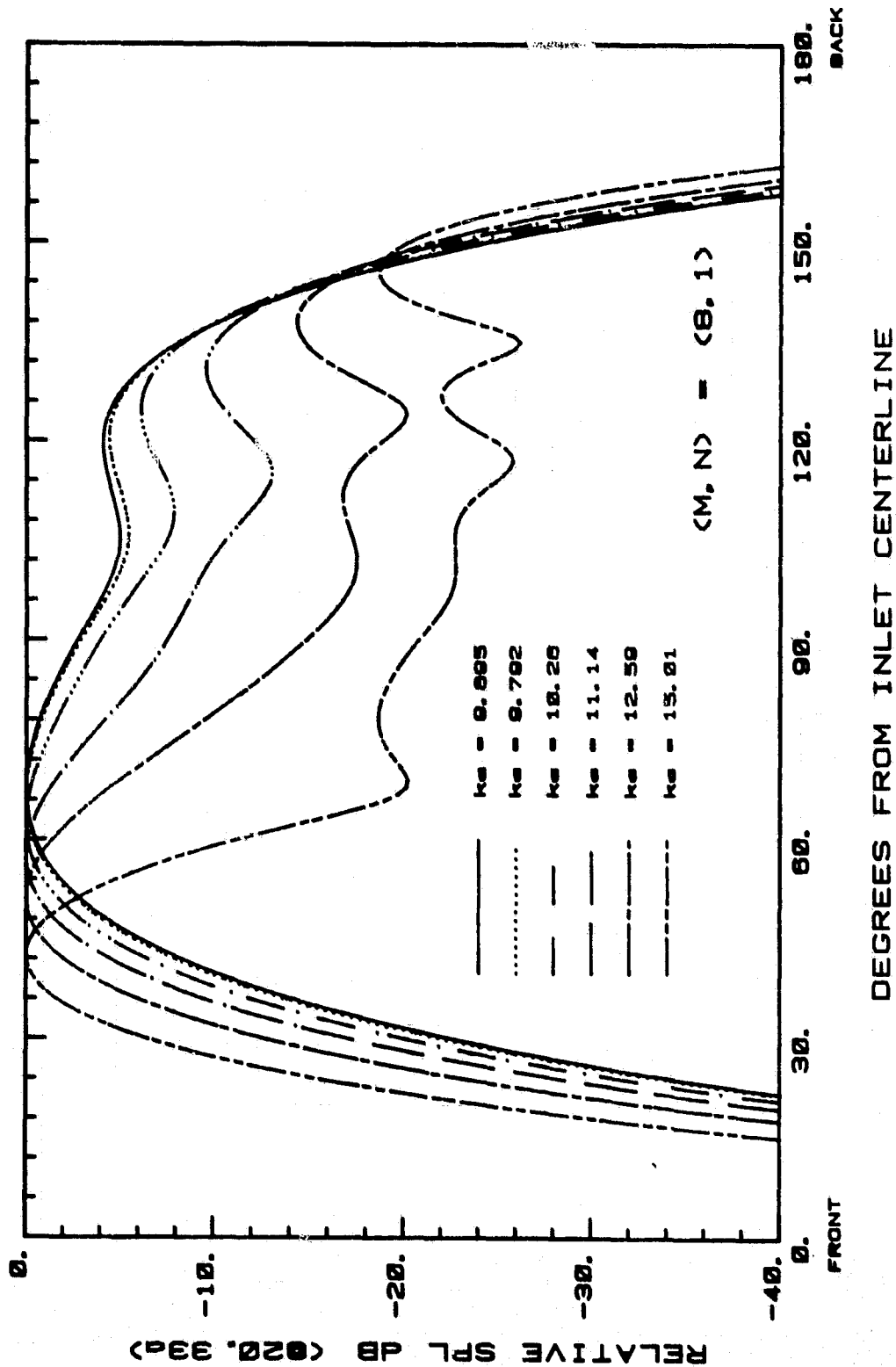
ORIGINAL PAGE IS
OF POOR QUALITY



THIN LIPPED ELLIPTICAL INLET

Fig. 29c

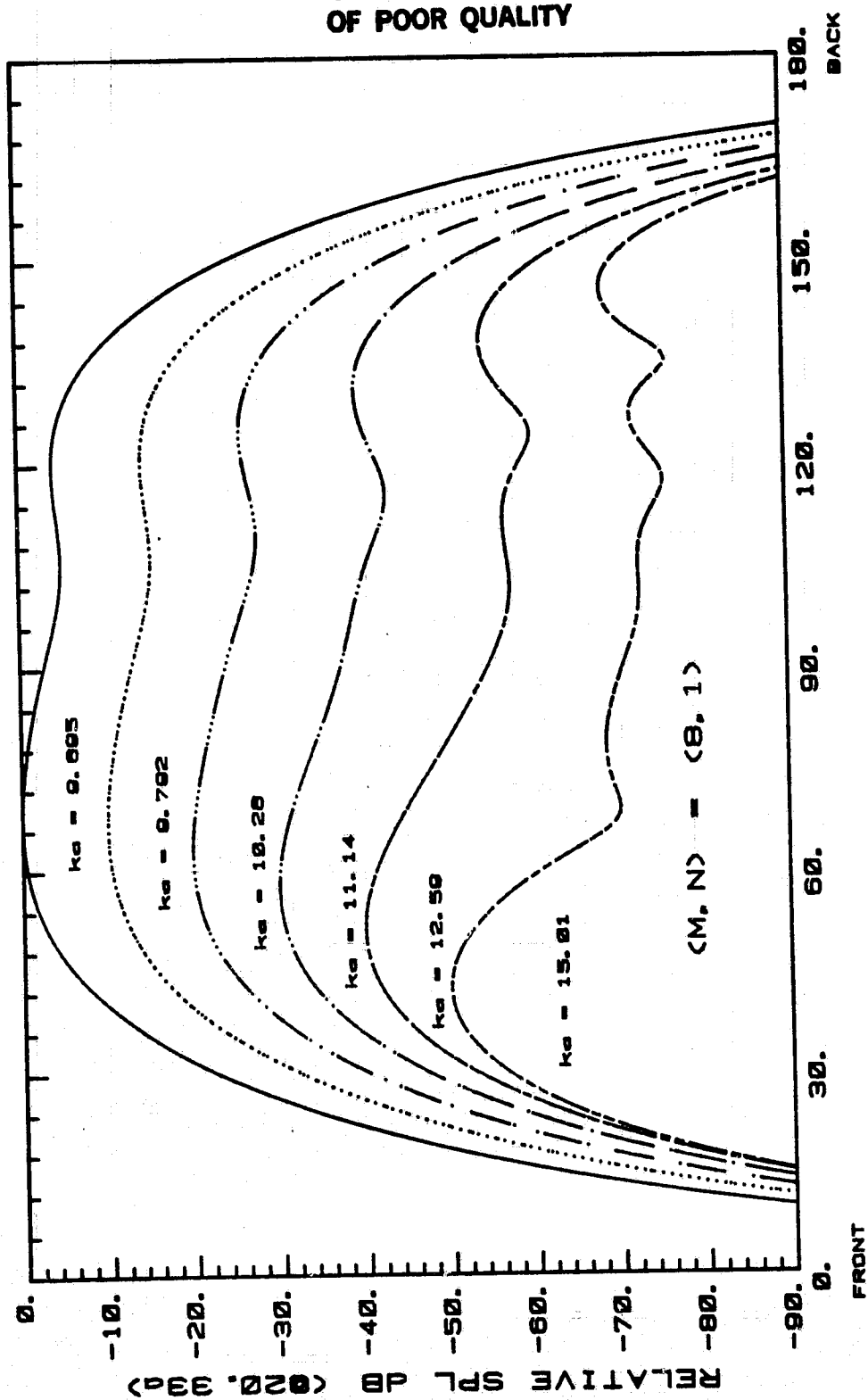
ORIGINAL PAGE IS
OF POOR QUALITY



THIN LIPPED ELLIPTICAL INLET

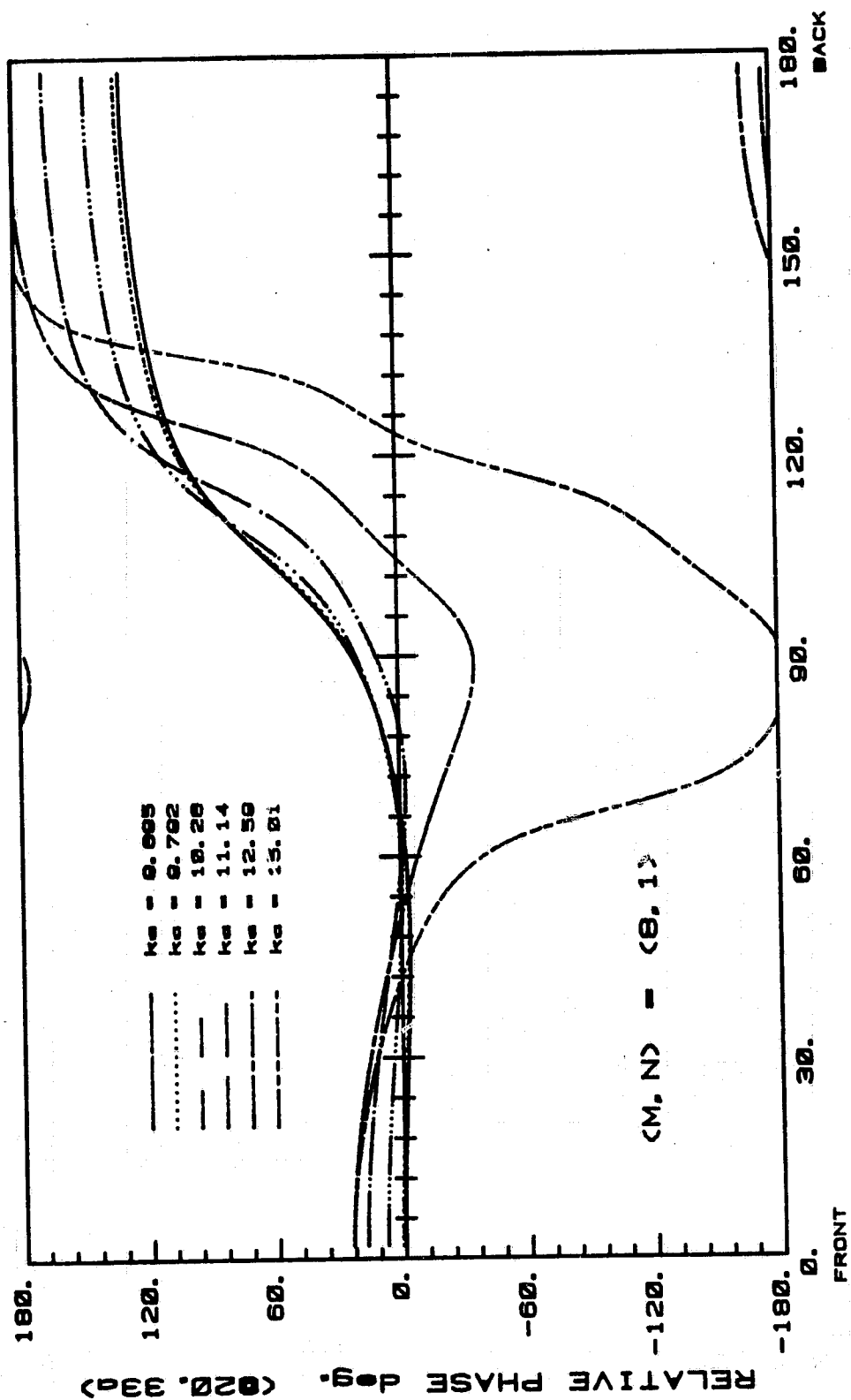
Fig. 30a

ORIGINAL PAGE IS
OF POOR QUALITY



THIN LIPPED ELLIPTICAL INLET

Fig. 30b



THIN LIPPED ELLIPTICAL INLET

Fig. 30c

ORIGINAL PAGE IS
OF POOR QUALITY.

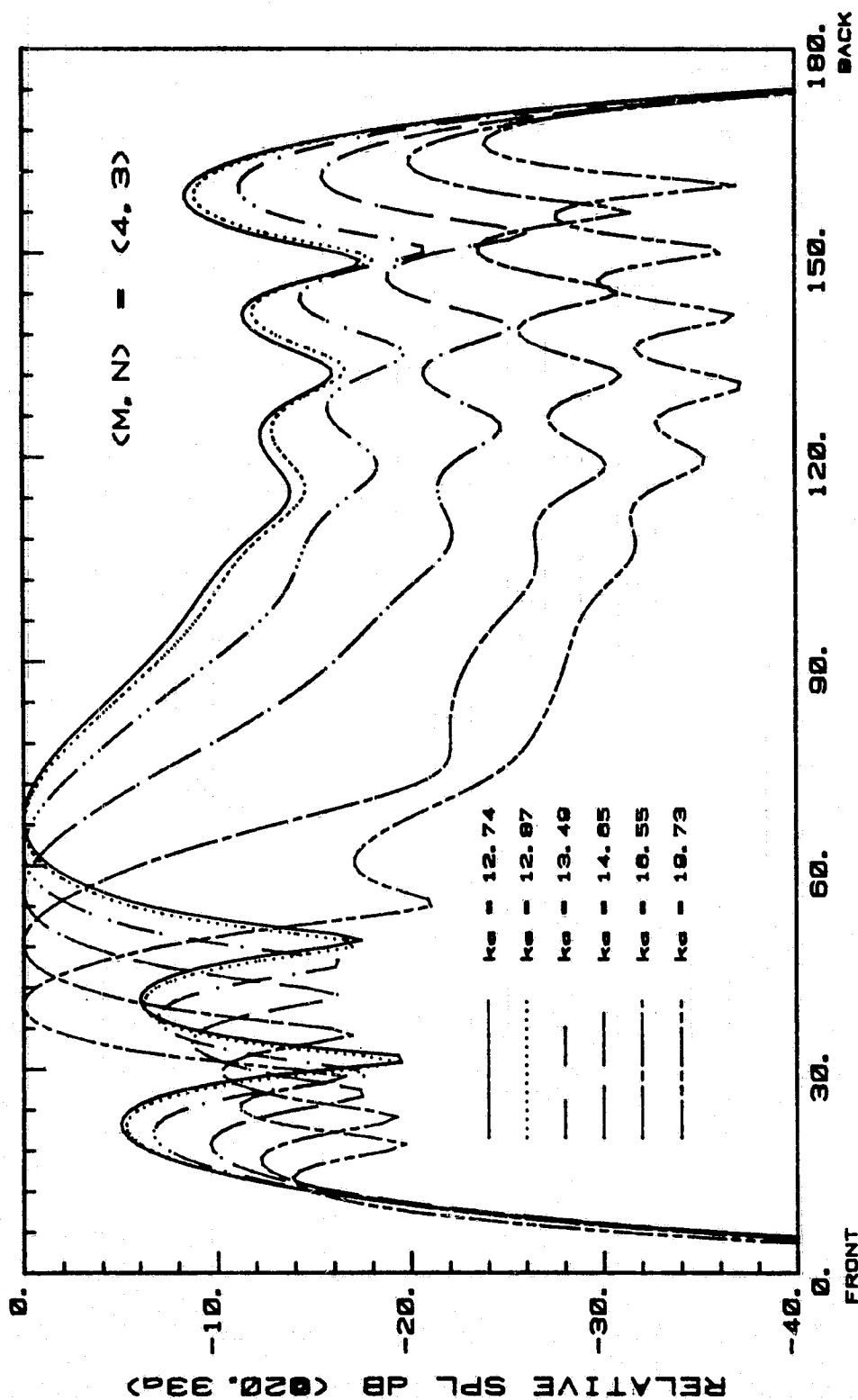
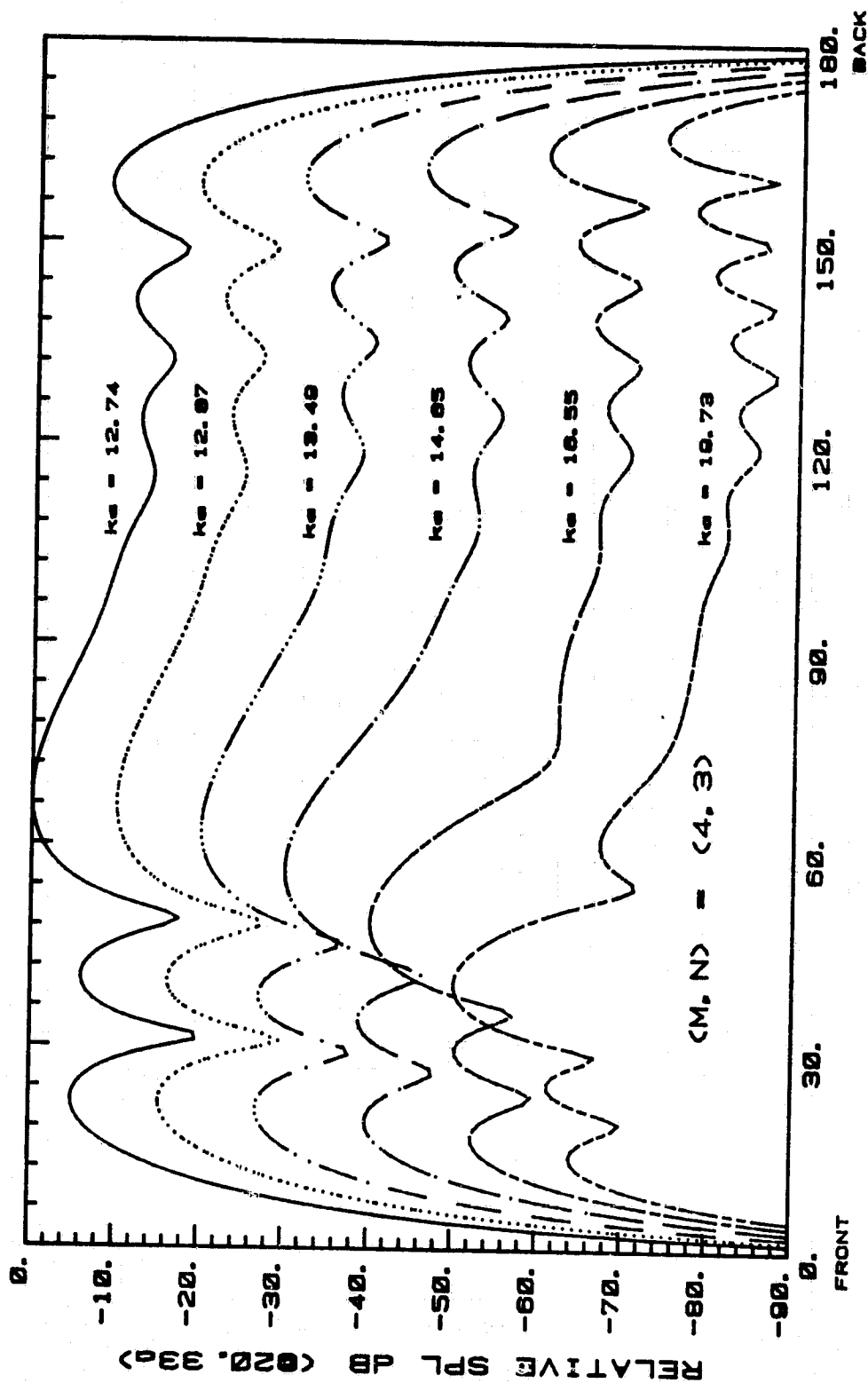


Fig. 31a

THIN LIPPED ELLIPTICAL INLET

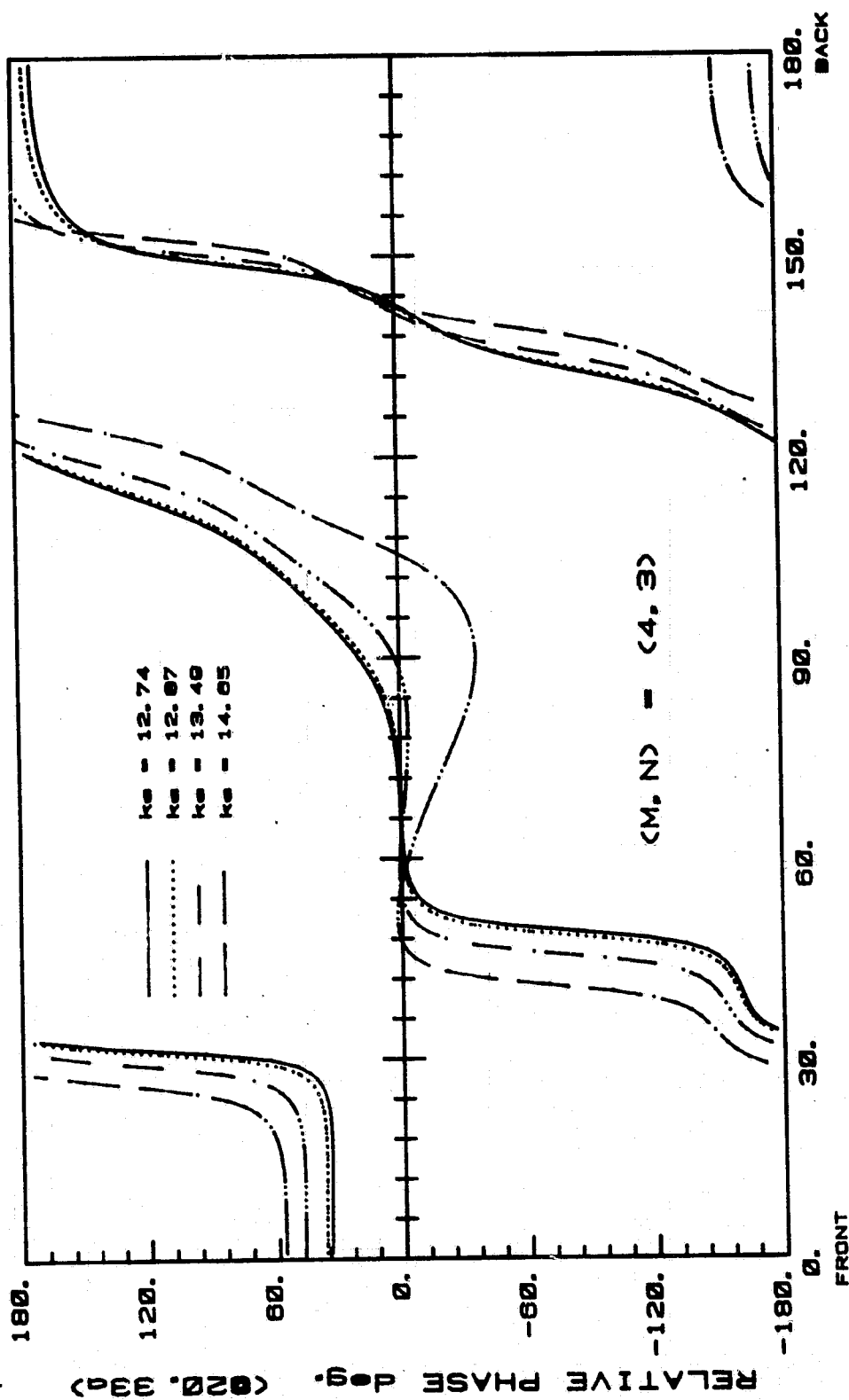
ORIGINAL PAGE IS
OF POOR QUALITY



DEGREES FROM INLET CENTERLINE

THIN LIPPED ELLIPTICAL INLET

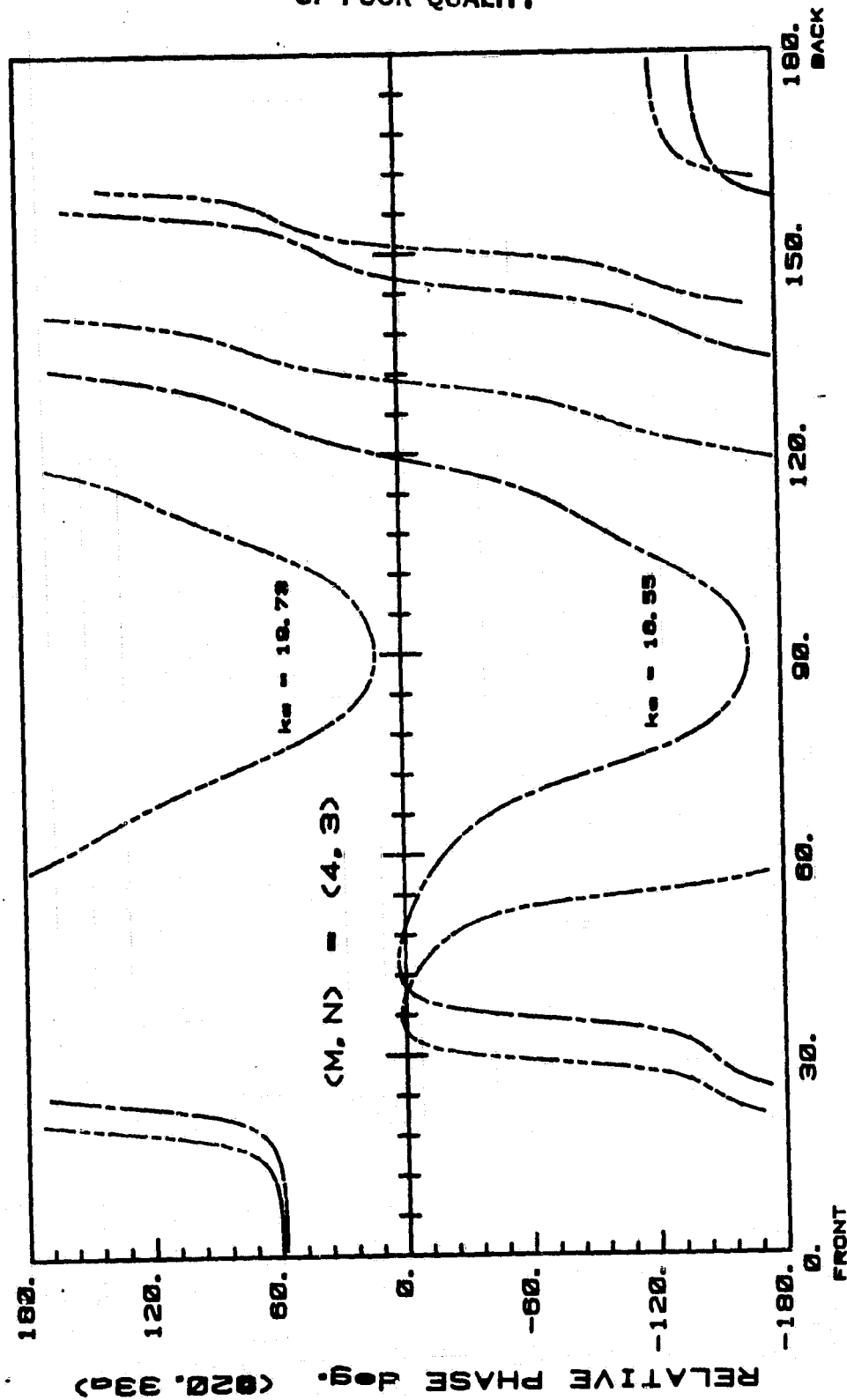
Fig. 31b



THIN LIPPED ELLIPTICAL INLET

Fig. 31c

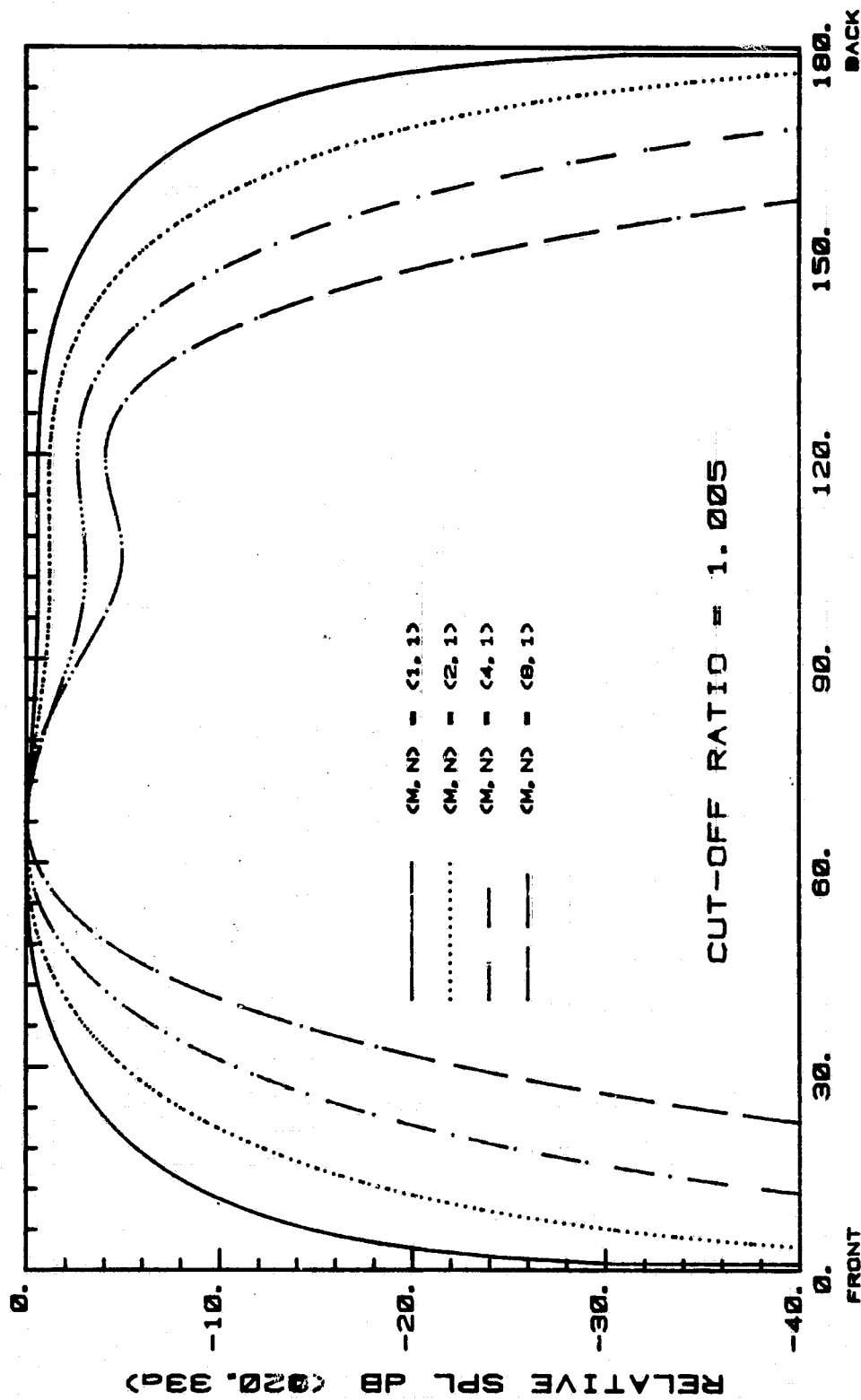
ORIGINAL PAGE 18
OF POOR QUALITY



THIN LIPPED ELLIPTICAL INLET

Fig. 31d

ORIGINAL PAGE 13
OF POOR QUALITY

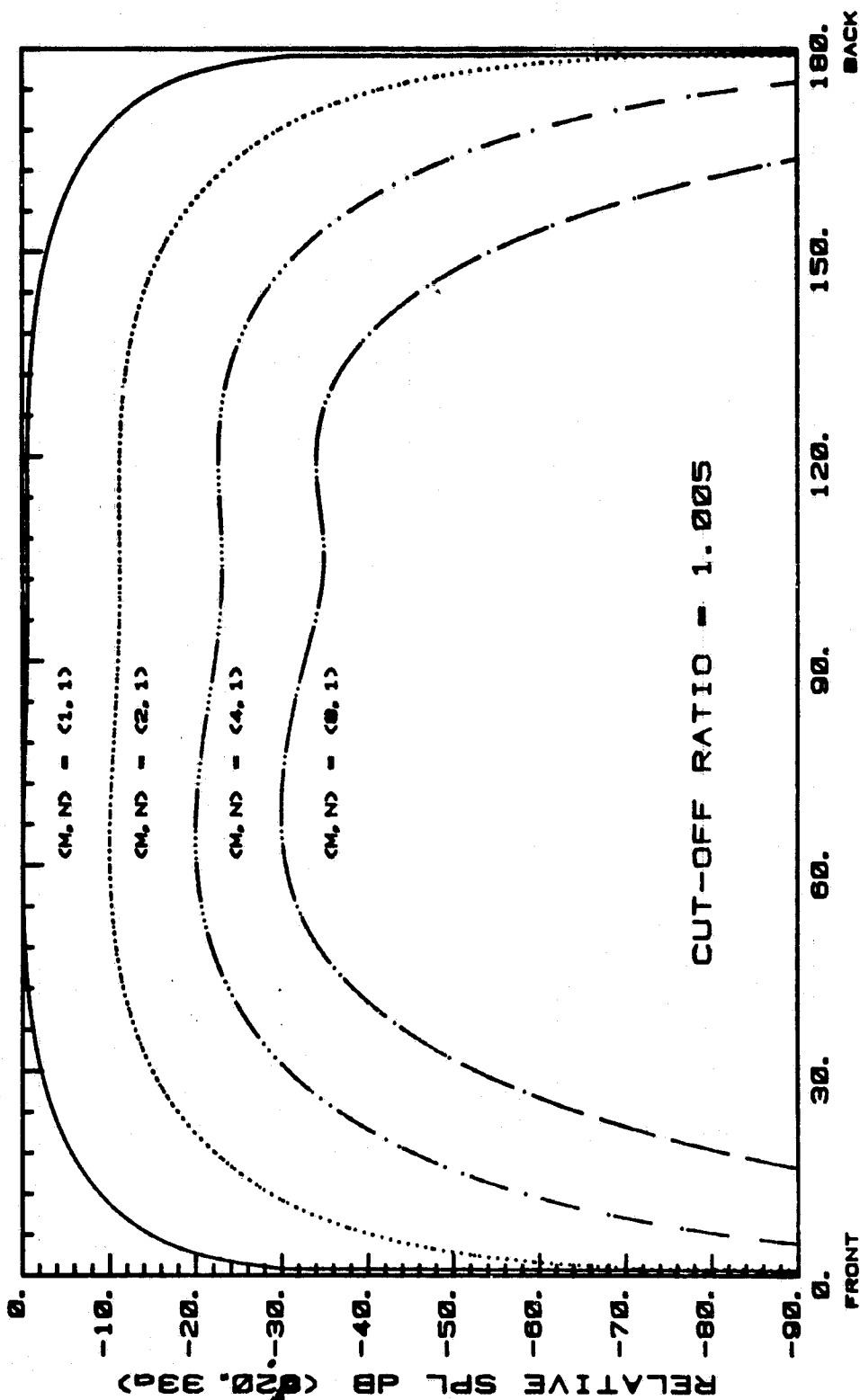


DEGREES FROM INLET CENTERLINE

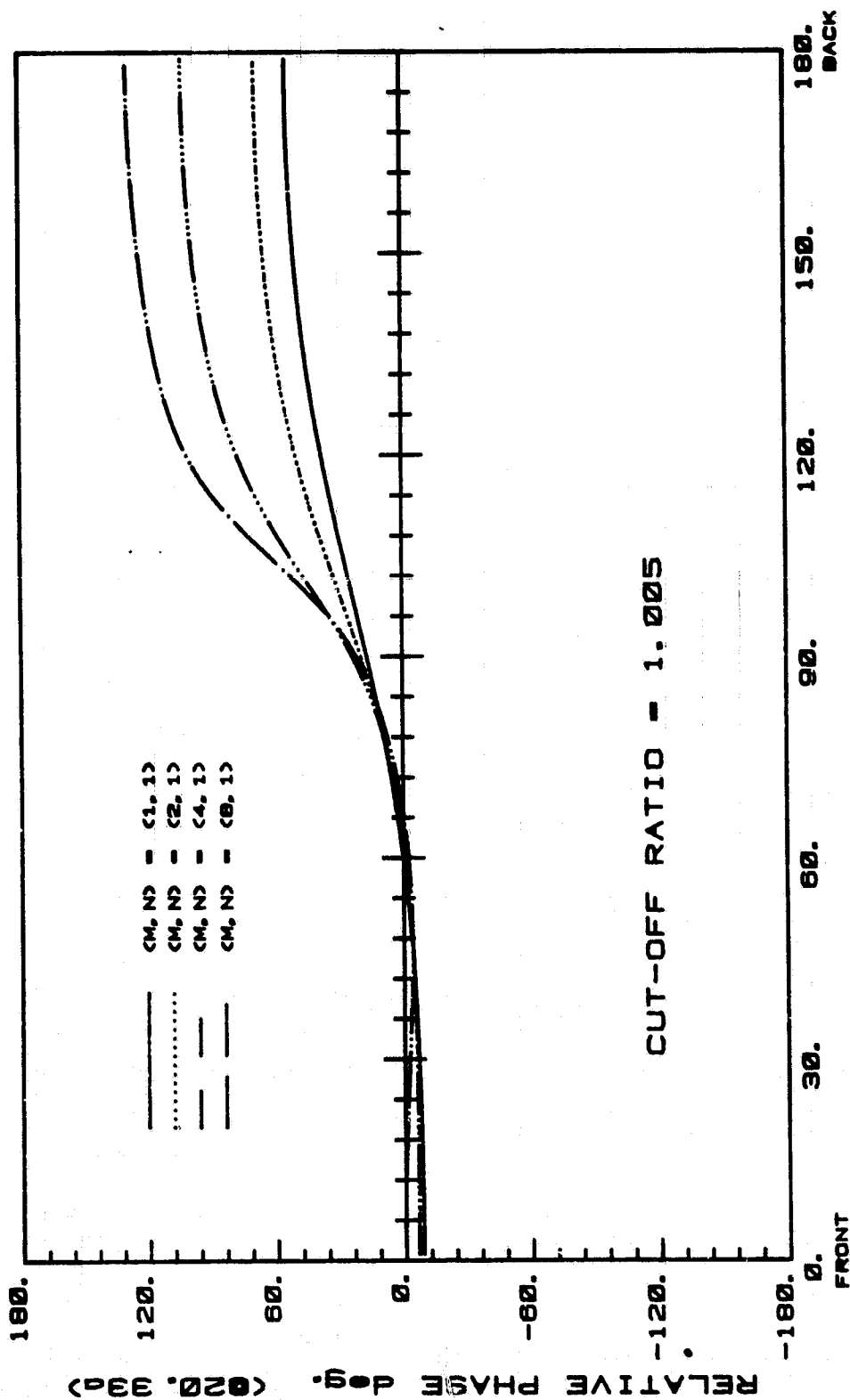
THIN LIPPED ELLIPTICAL INLET

Fig. 32a

ORIGINAL PAGE IS
OF POOR QUALITY



ORIGINAL PAGE IS
OF POOR QUALITY



THIN LIPPED ELLIPTICAL INLET

Fig. 32c

ORIGINAL PAGE IS
OF POOR QUALITY

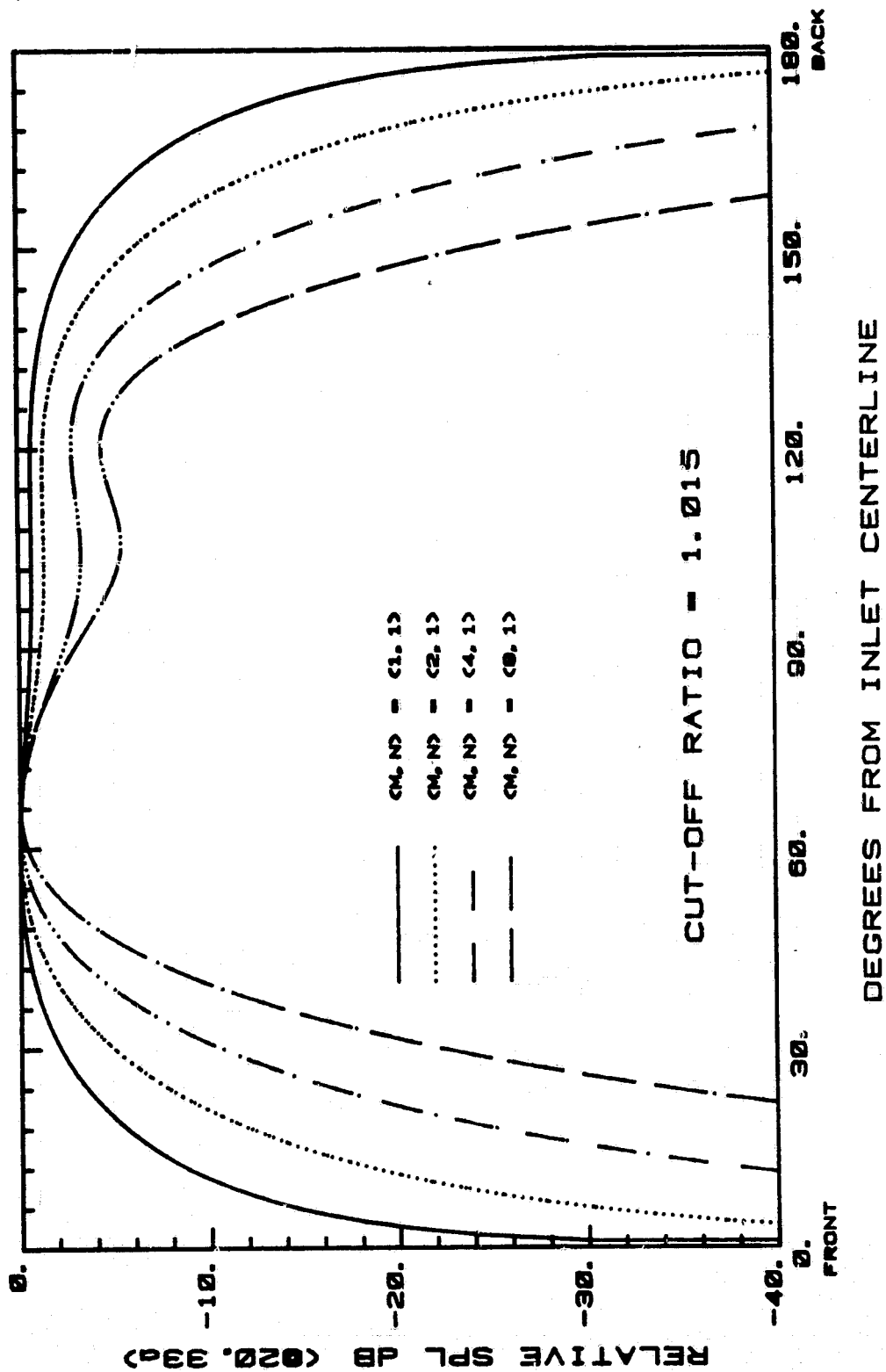
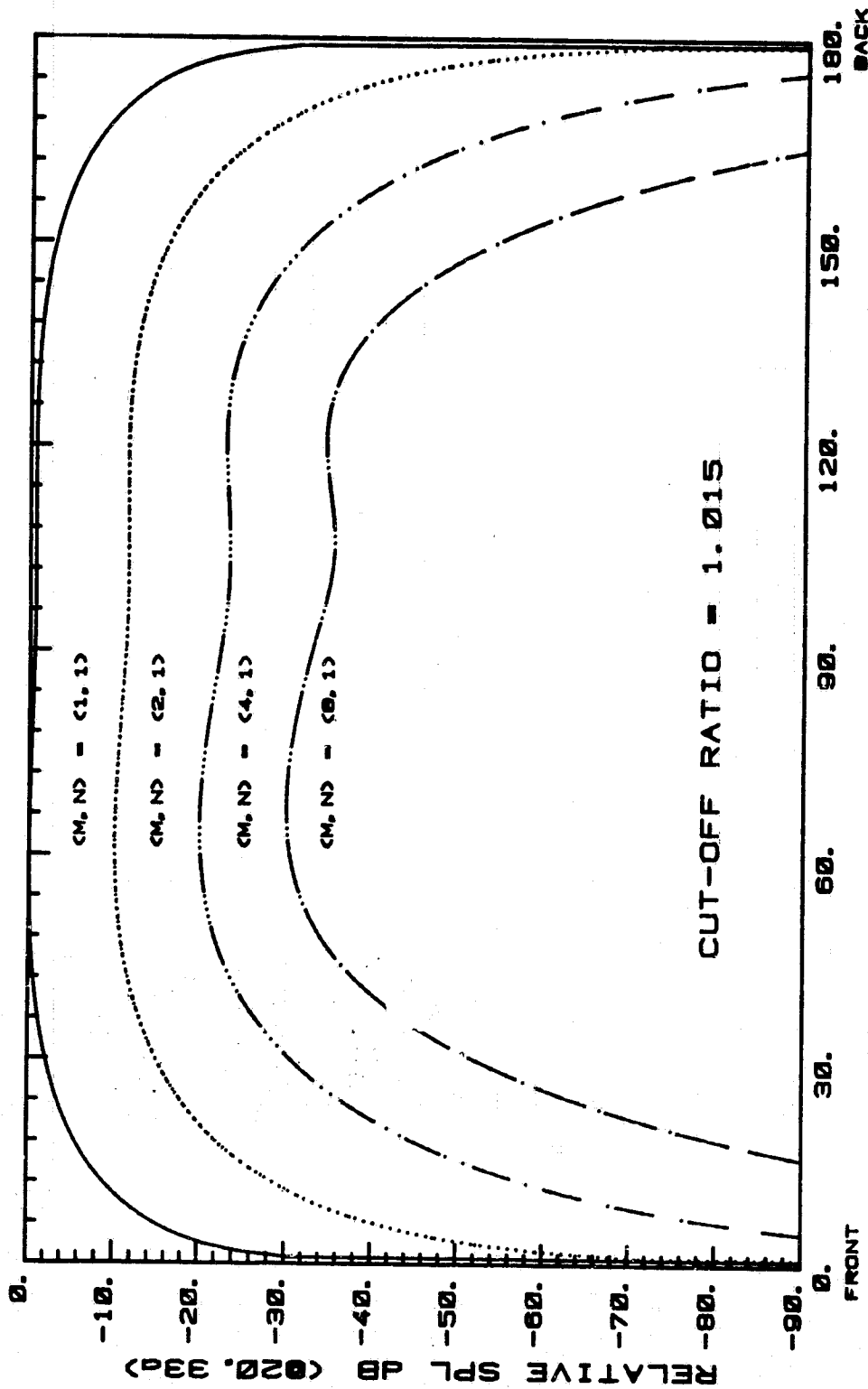


Fig. 33a

THIN LIPPED ELLIPTICAL INLET

ORIGINAL PAGE IS
OF POOR QUALITY .

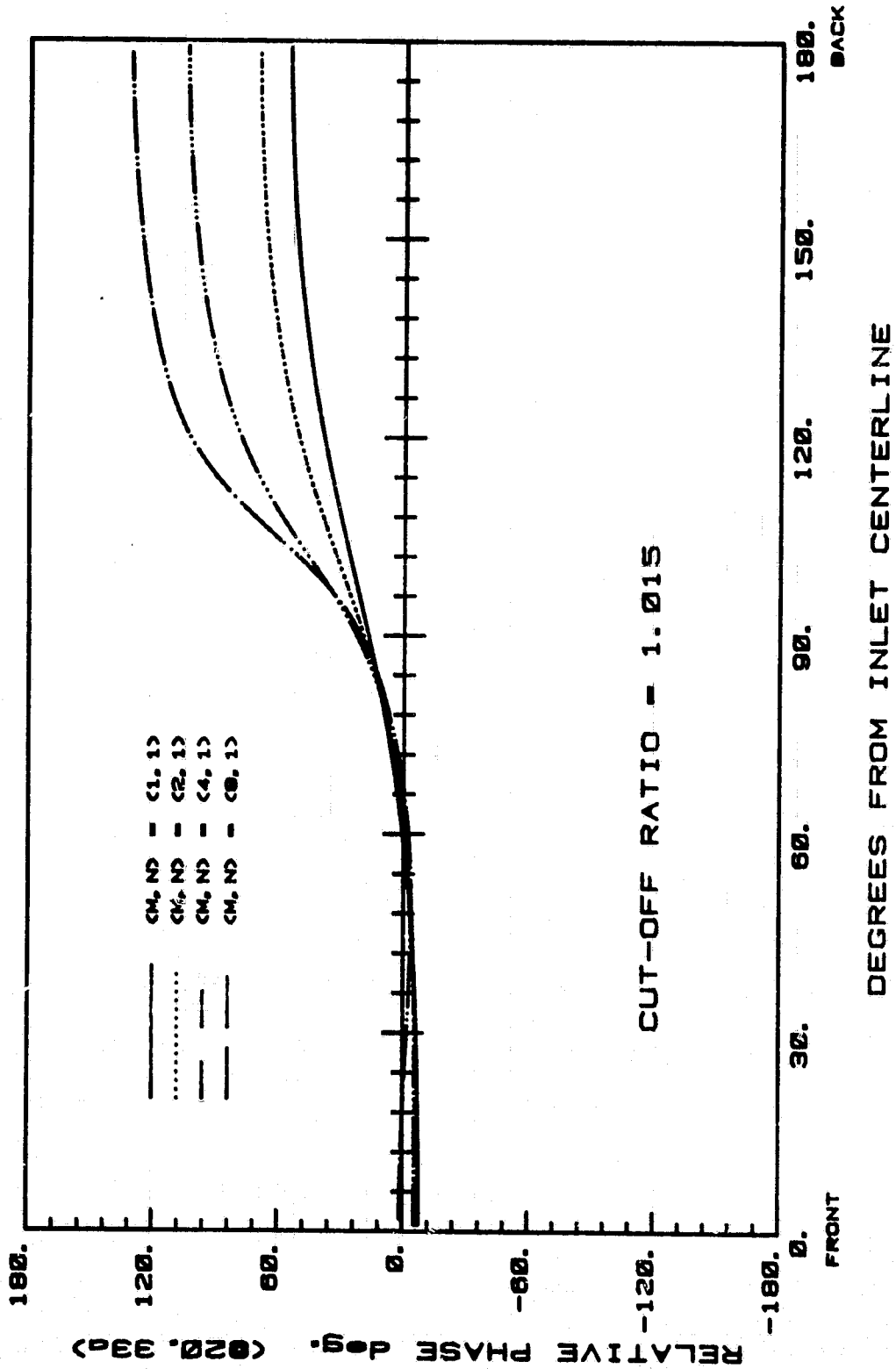


DEGREES FROM INLET CENTERLINE

THIN LIPPED ELLIPTICAL INLET

Fig. 33b

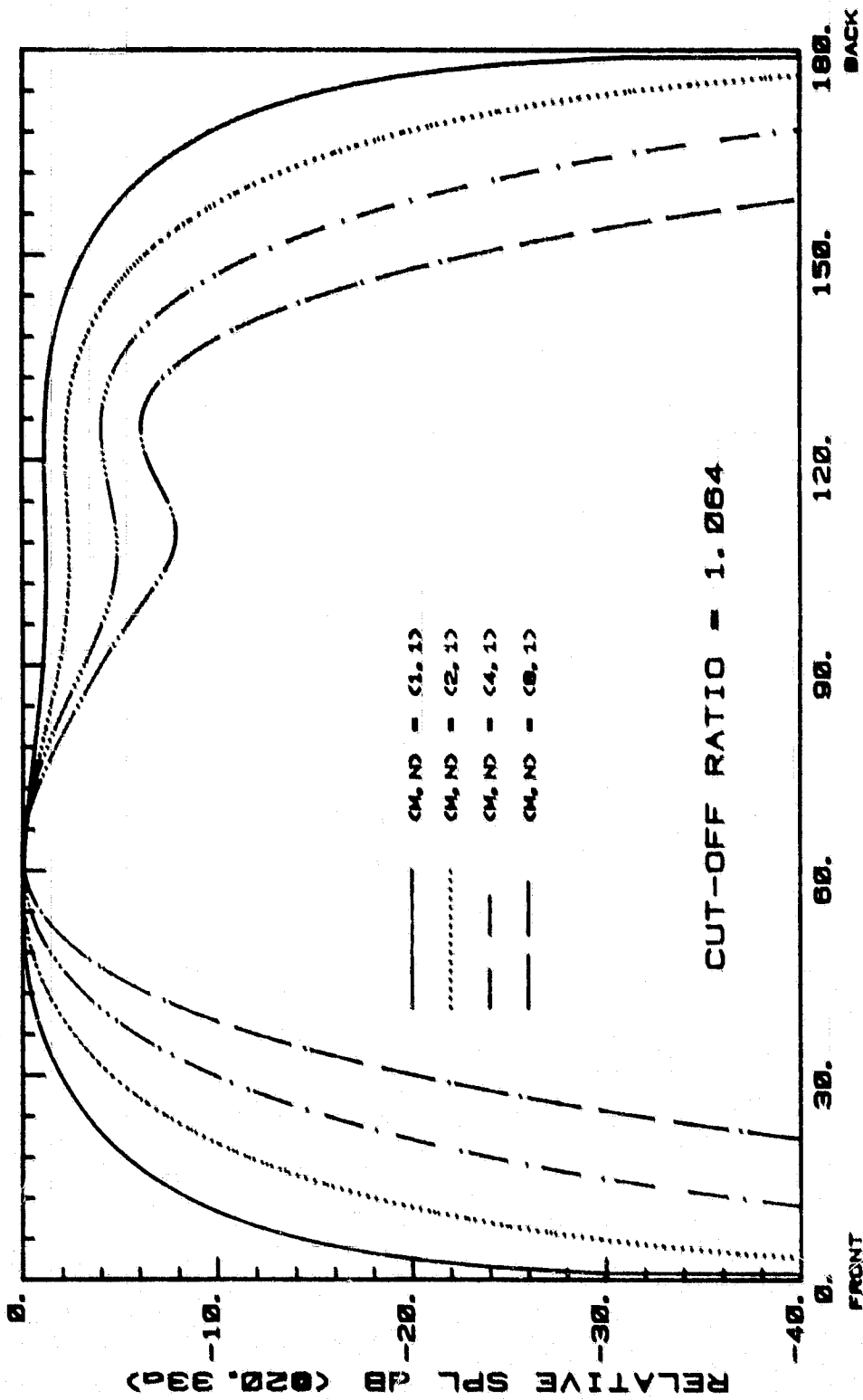
ORIGINAL PAGE IS
OF POOR QUALITY



THIN LIPPED ELLIPTICAL INLET

Fig. 33c

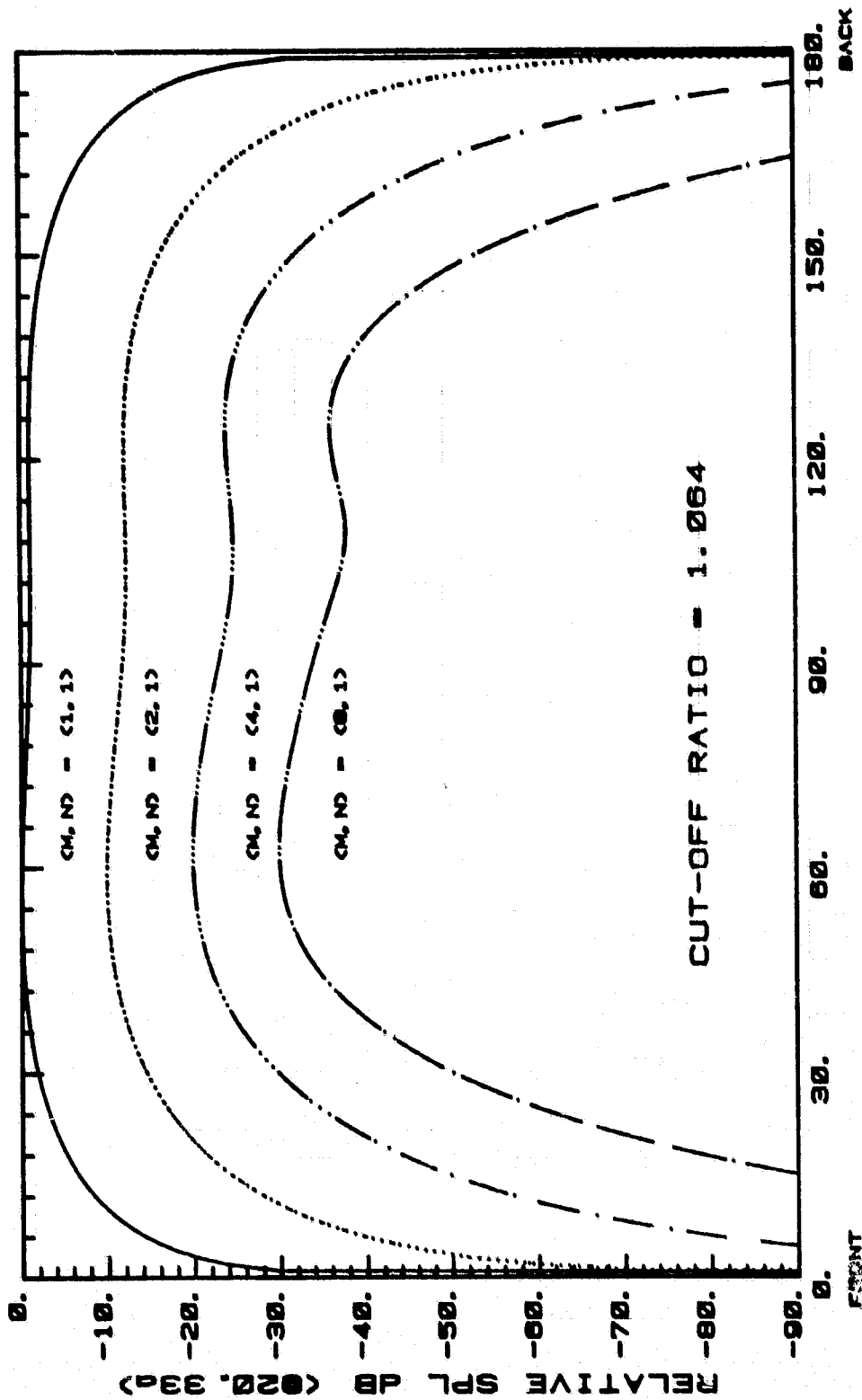
ORIGINAL PAGE IS
OF POOR QUALITY



DEGREE FROM INLET CENTERLINE

THIN LIPPED ELLIPTICAL INLET

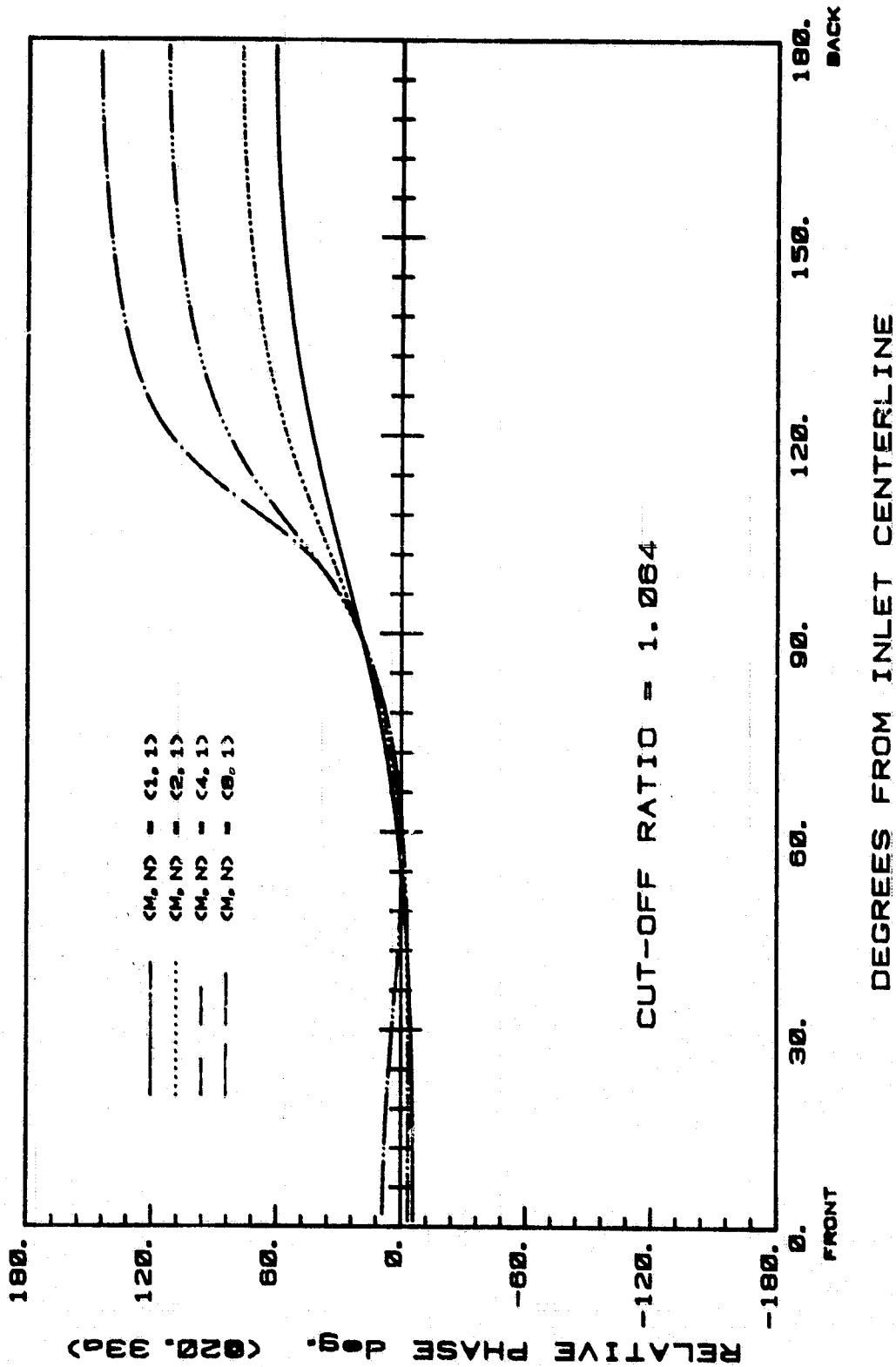
Fig. 34a



DEGREES FROM INLET CENTERLINE

THIN LIPPED ELLIPTICAL INLET

Fig. 34b



THIN LIPPED ELLIPTICAL INLET

Fig. 34c

ORIGINAL PAGE IS
OF POOR QUALITY

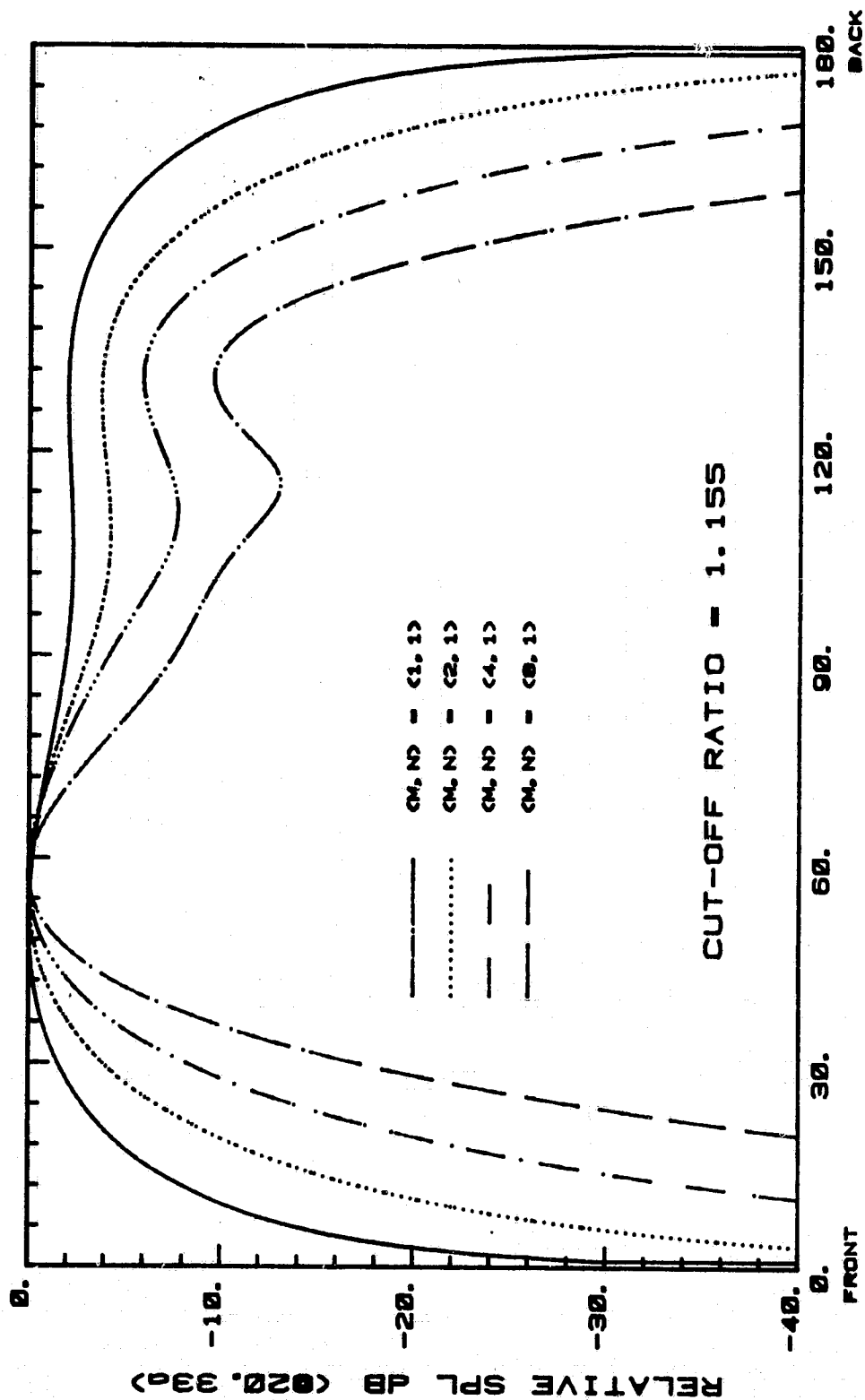
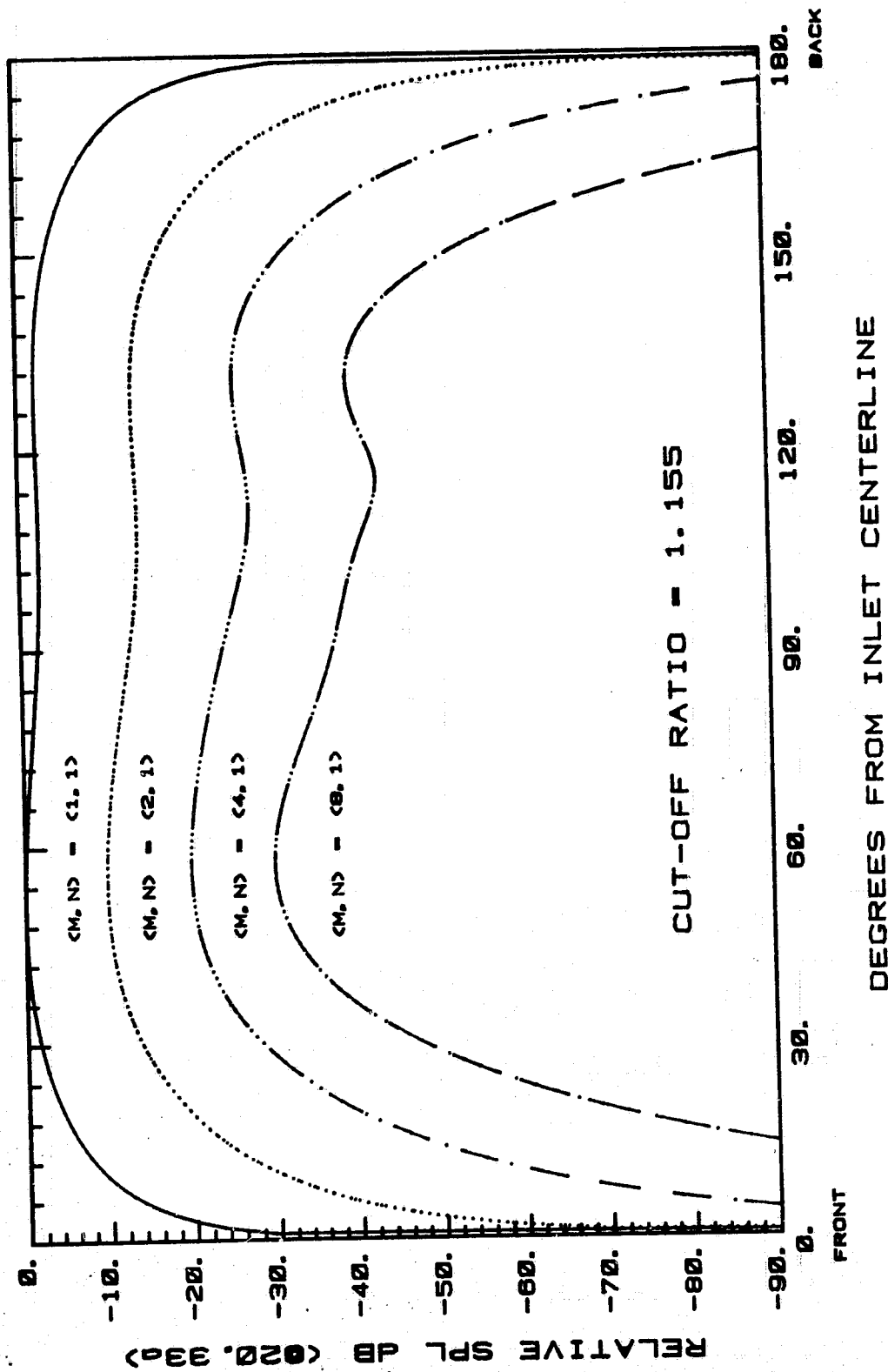


Fig. 35a

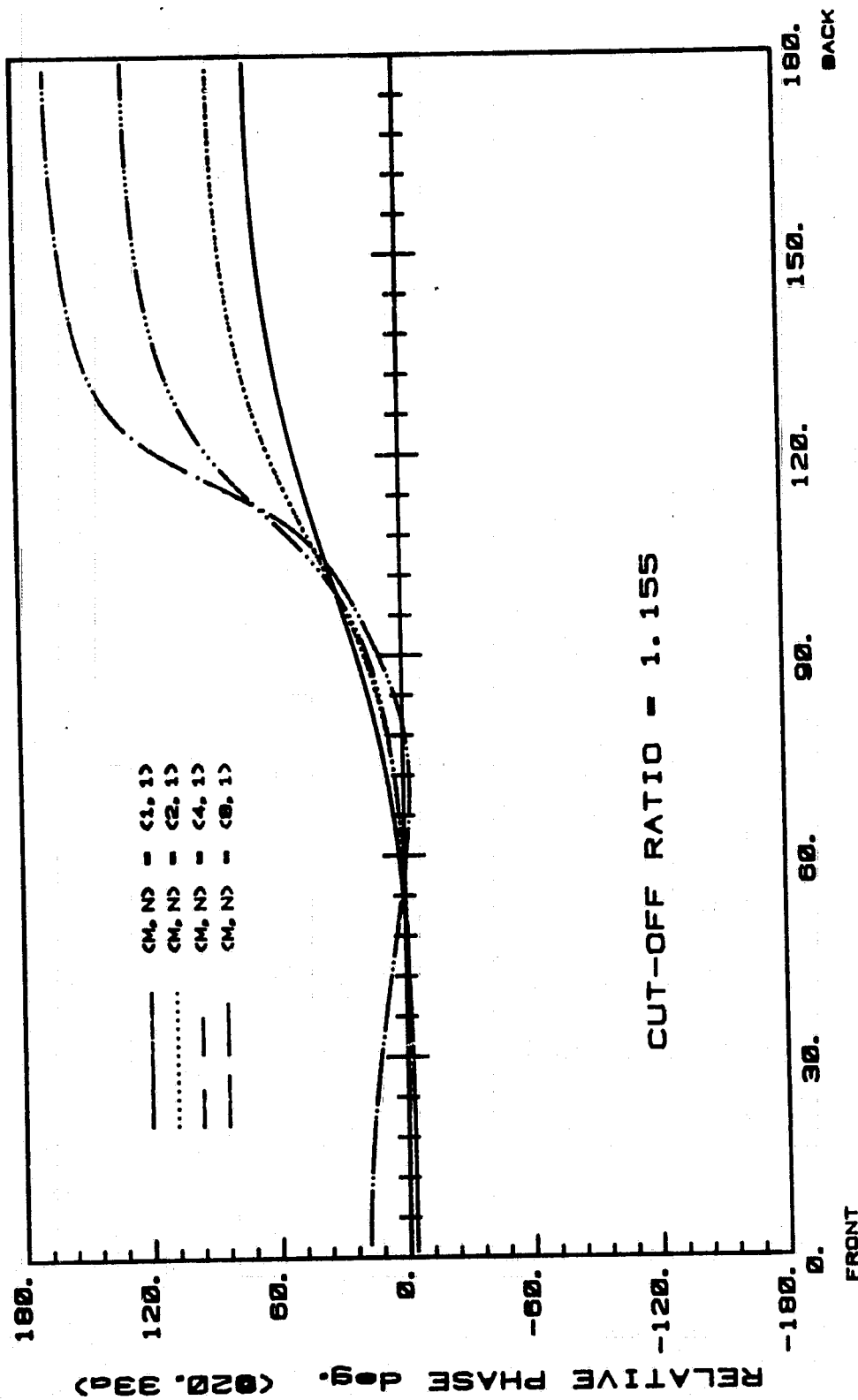
ORIGINAL PAGE IS
OF POOR QUALITY



THIN LIPPED ELLIPTICAL INLET

Fig. 35b

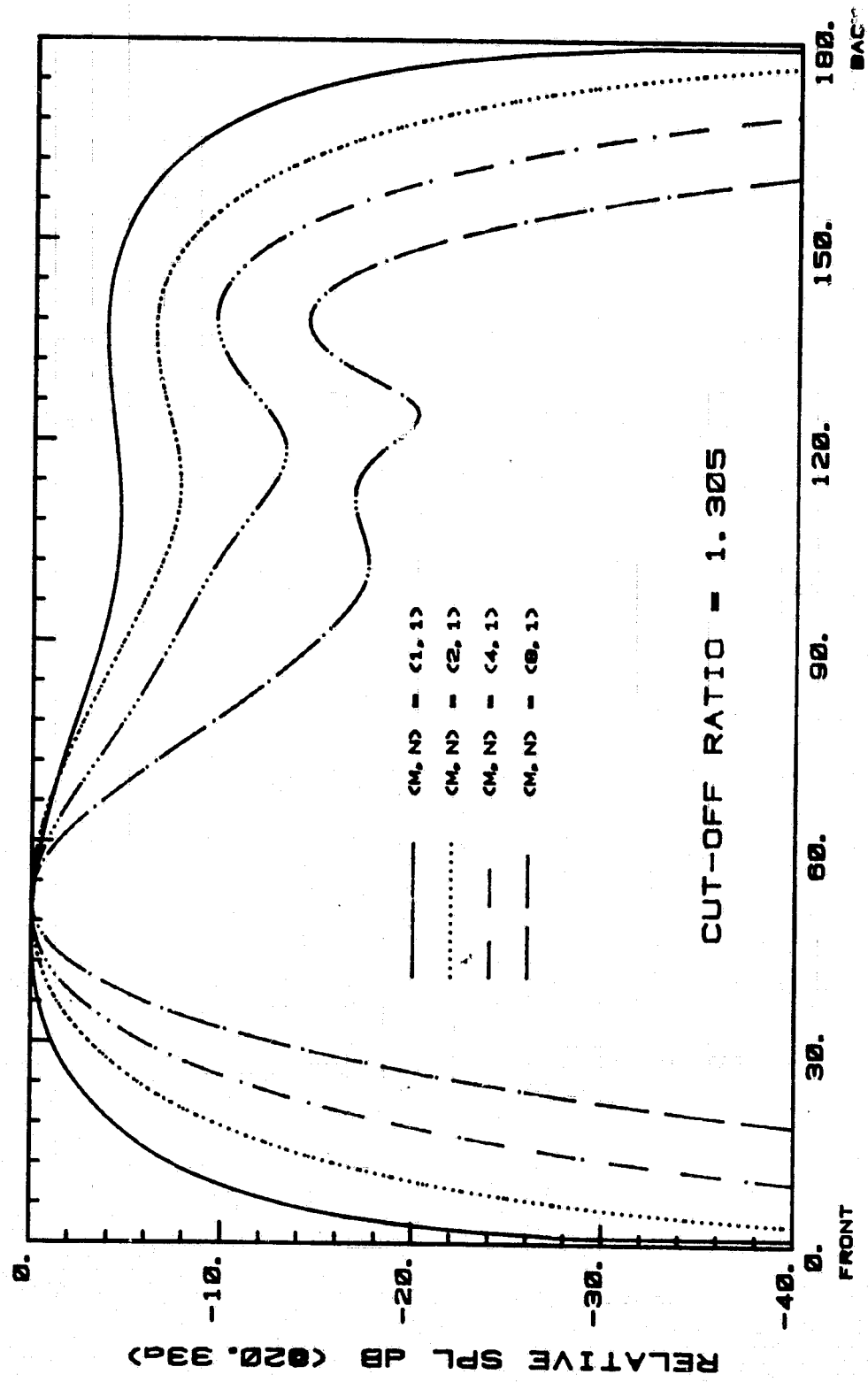
ORIGINAL PAGE IS
OF POOR QUALITY



THIN LIPPED ELLIPTICAL INLET

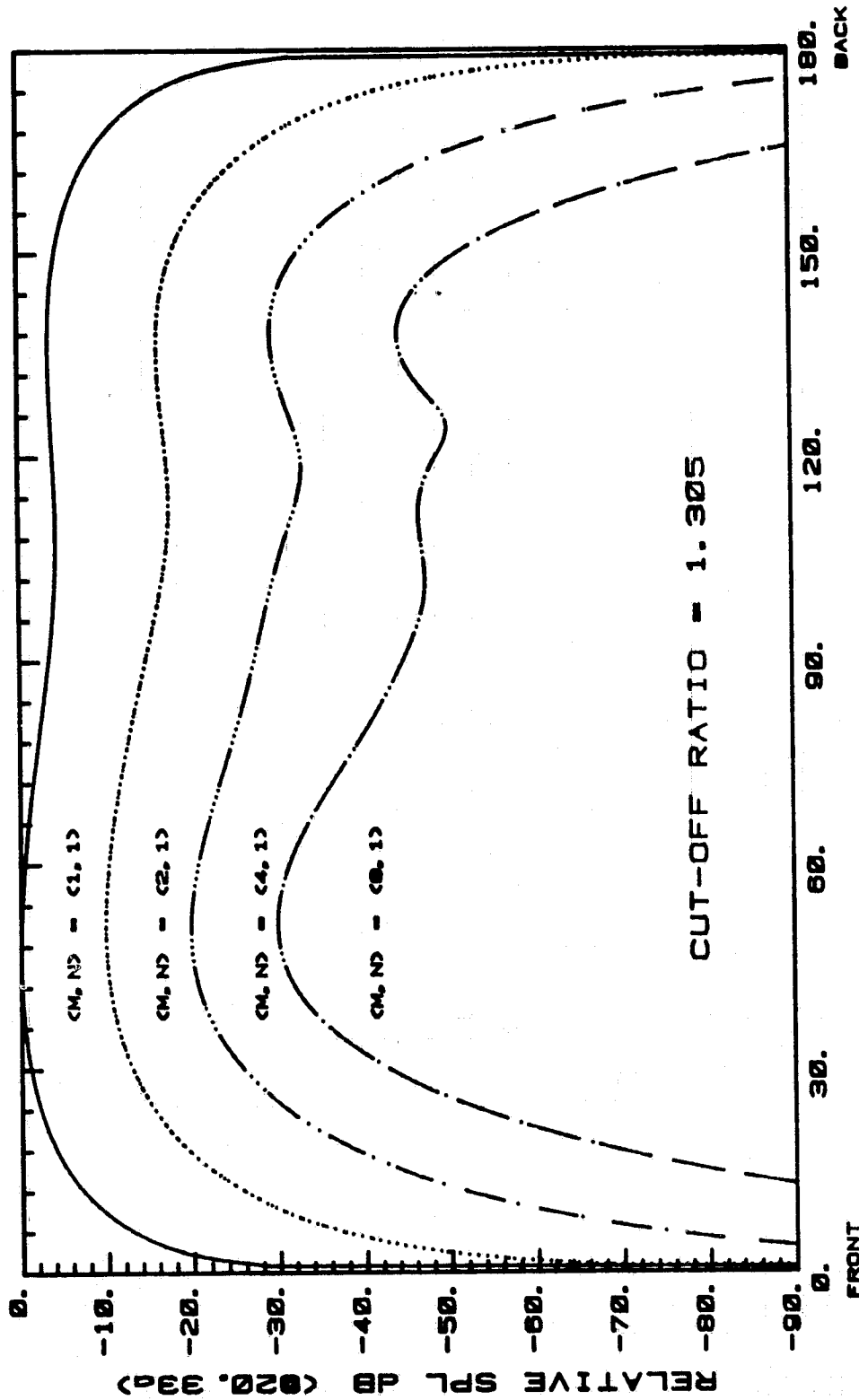
Fig. 35c

ORIGINAL PAGE IS
OF POOR QUALITY



THIN LIPPED ELLIPTICAL INLET

Fig. 36a



THIN LIPPED ELLIPTICAL INLET

Fig. 36b

ORIGINAL PAGE IS
OF POOR QUALITY

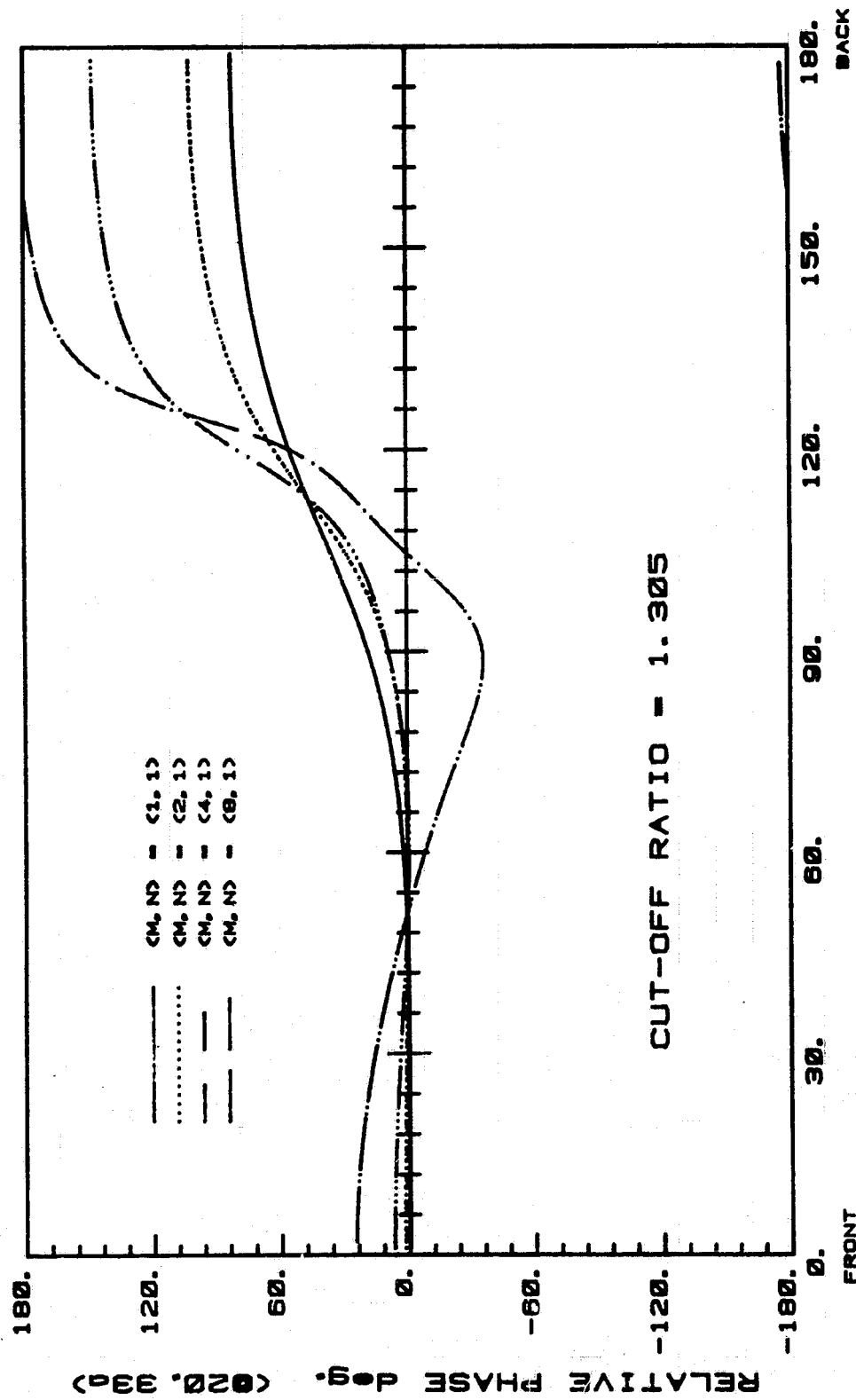
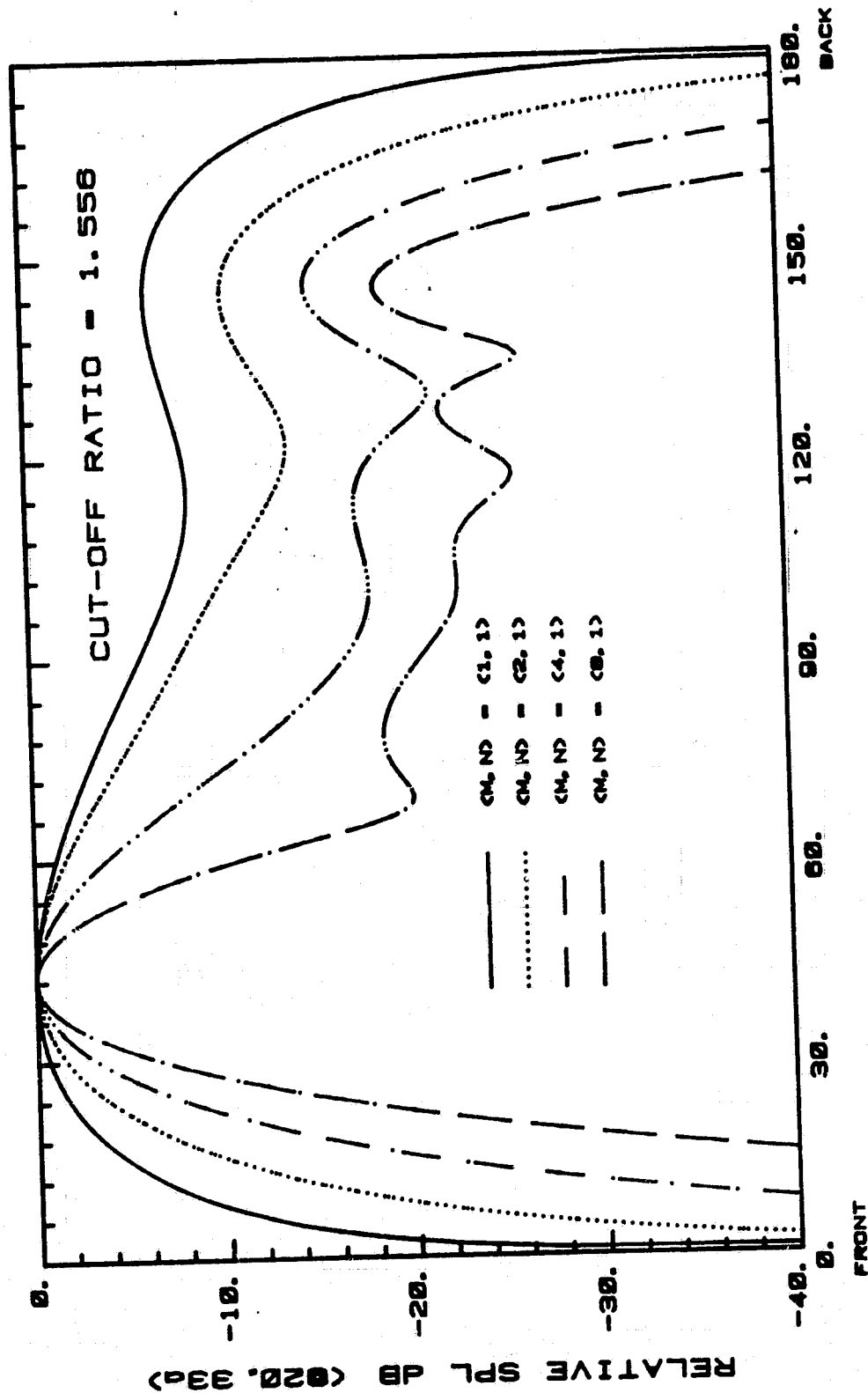


Fig. 36c

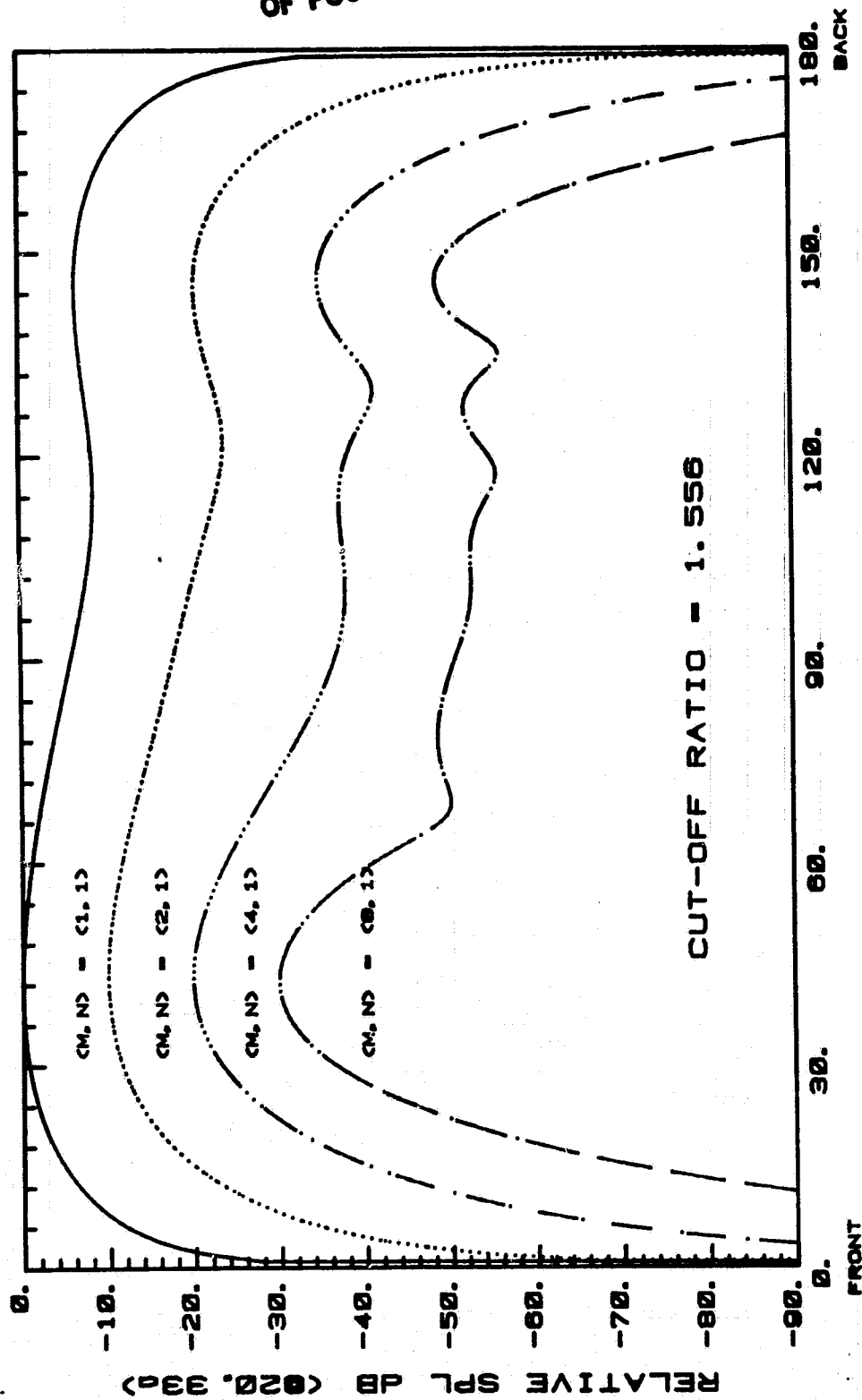
ORIGINAL PAGE 13
OF POOR QUALITY



THIN LIPPED ELLIPTICAL INLET

Fig. 37a

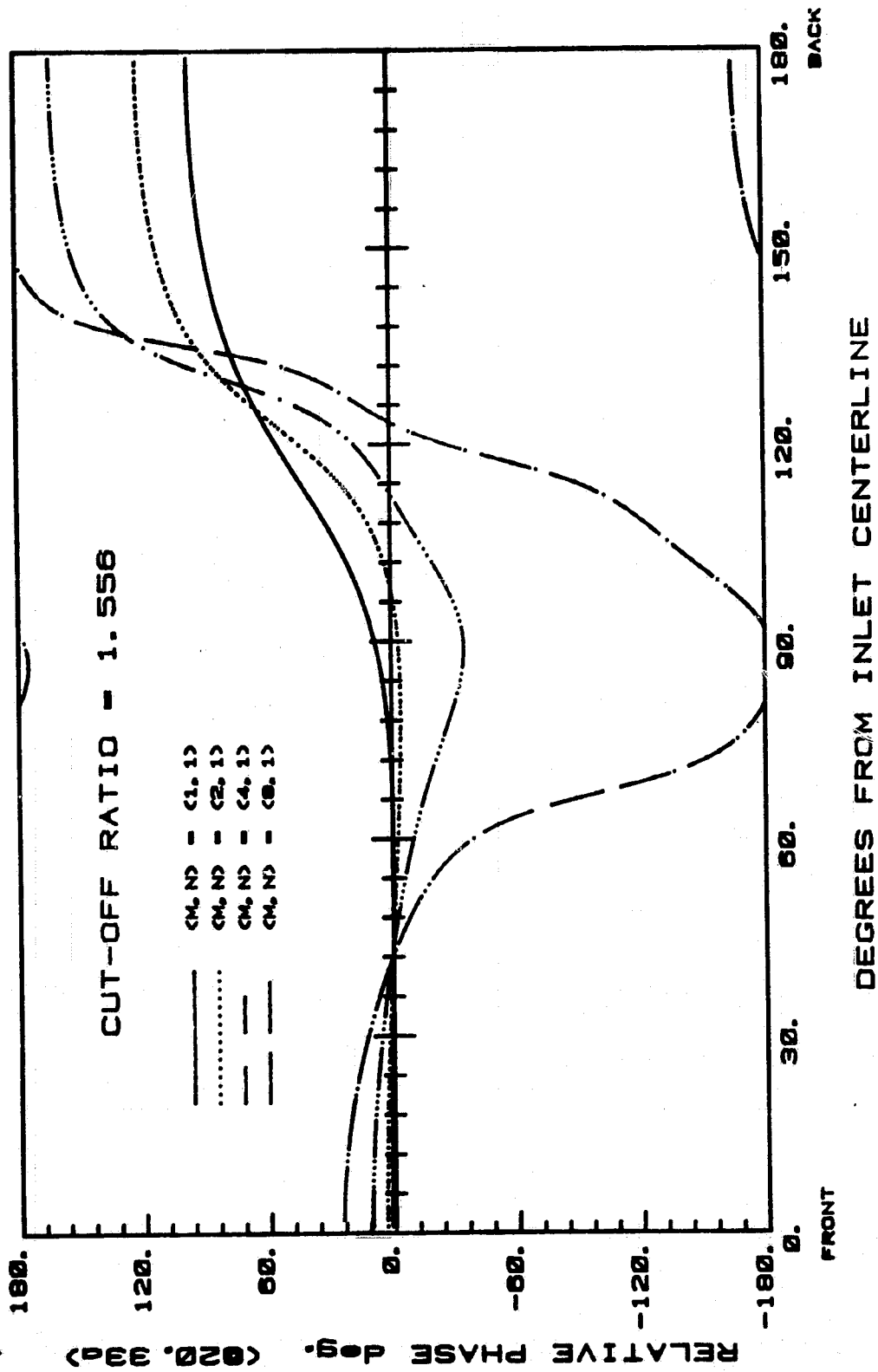
ORIGINAL PAGE IS
OF POOR QUALITY



THIN LIPPED ELLIPTICAL INLET

Fig. 37b

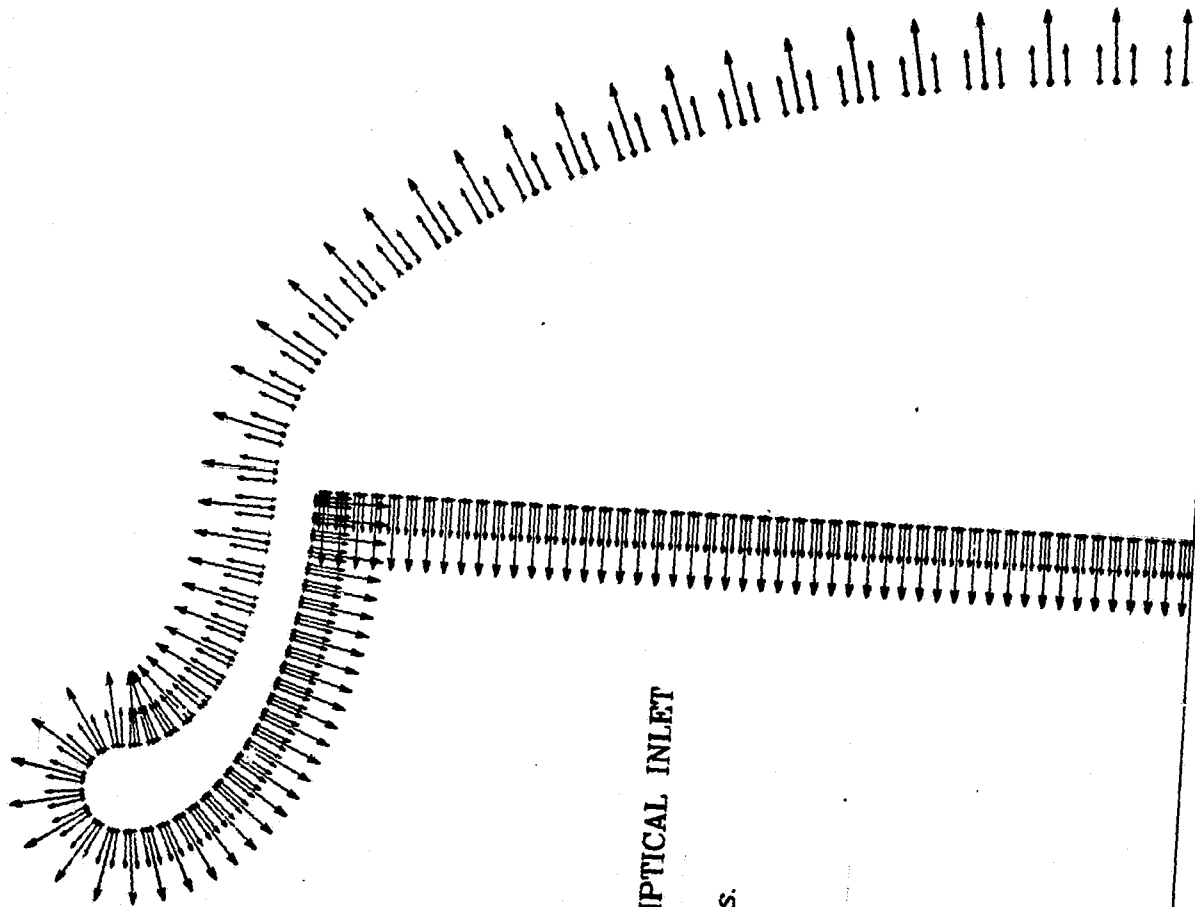
ORIGINAL PAGE IS
OF POOR QUALITY



THIN LIPPED ELLIPTICAL INLET

Fig. 37c

ORIGINAL PAGE IS
OF POOR QUALITY

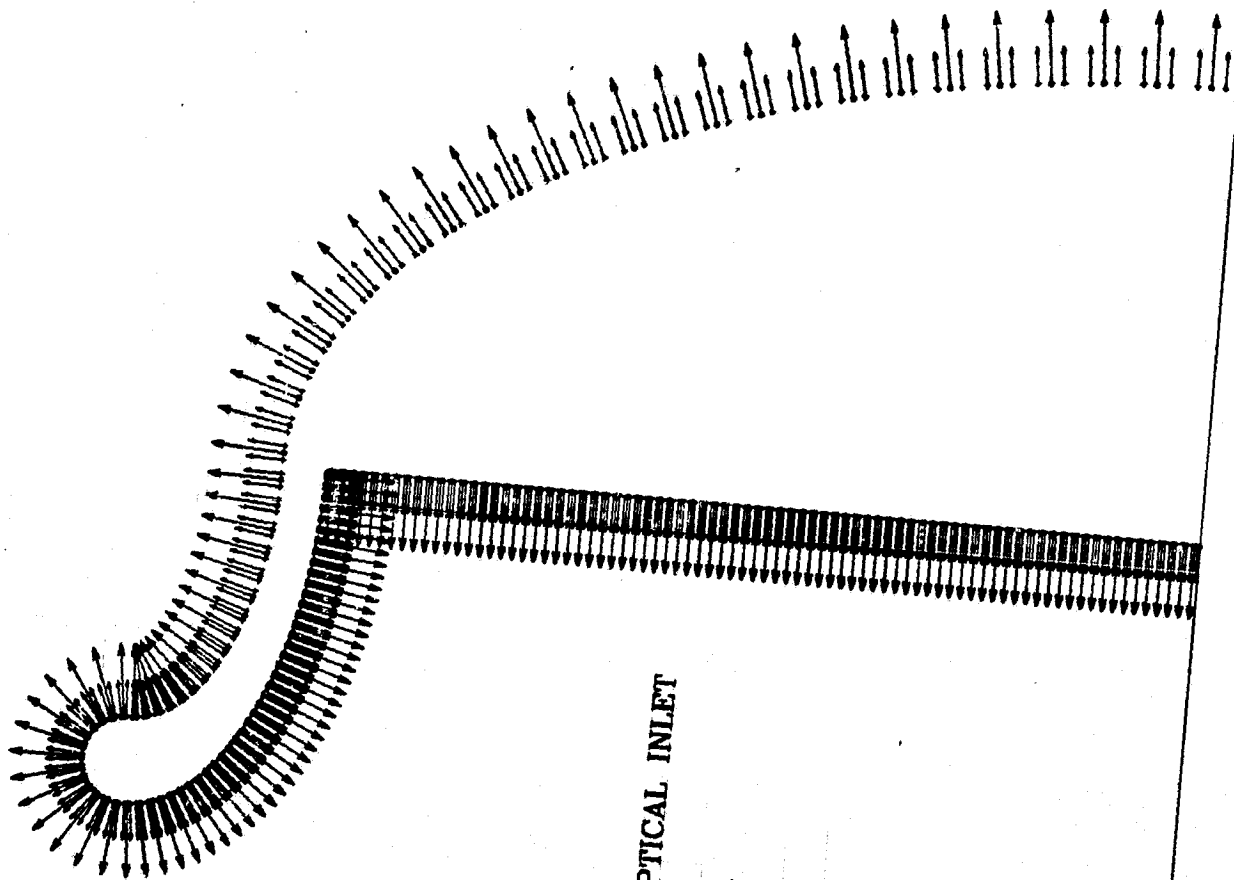


THICK LIPPED ELLIPTICAL INLET

116 pts.

Fig. 38

ORIGINAL PAGE IS
OF POOR QUALITY



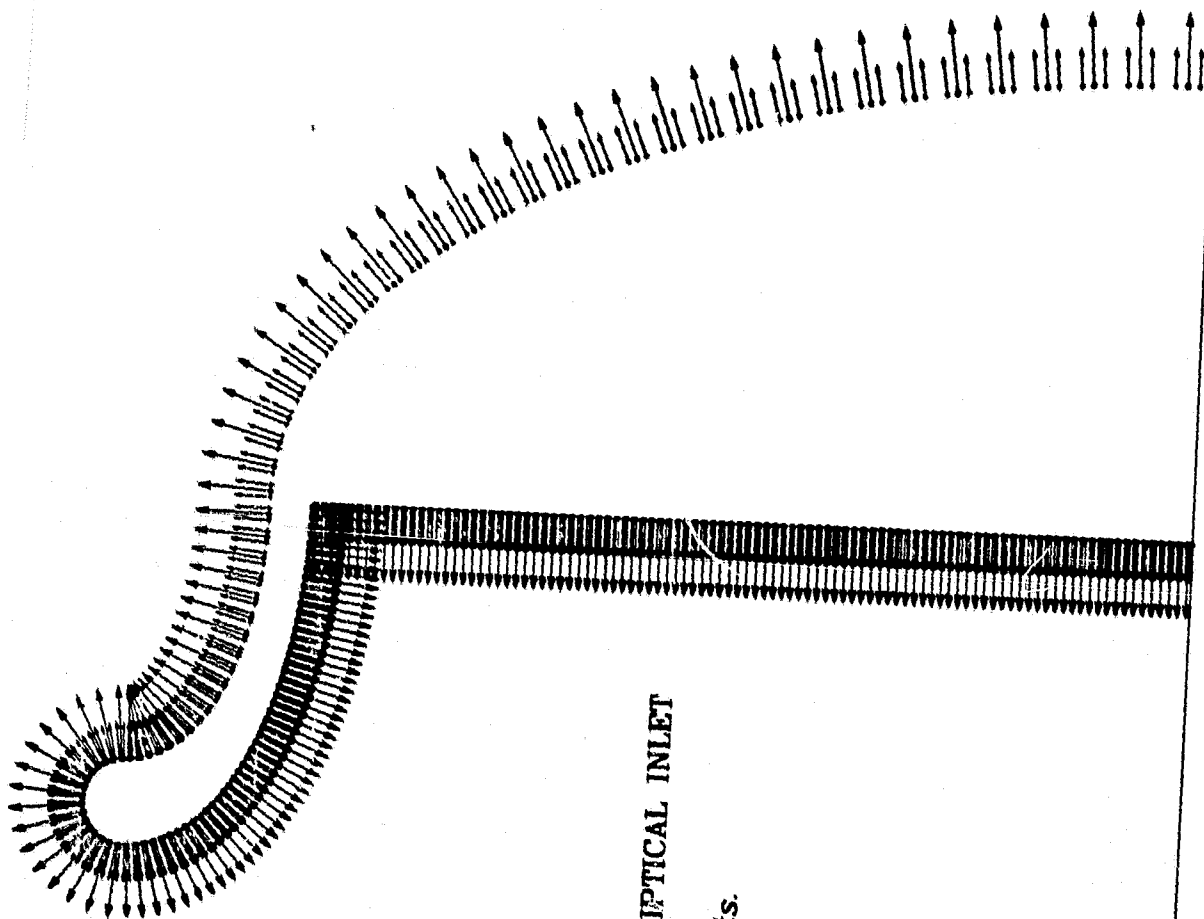
THICK LIPPED ELLIPTICAL INLET

176 pts.

C-3

Fig. 39

ORIGINAL PAGE IS
OF POOR QUALITY



THICK LIPPED ELLIPTICAL INLET

216 pts.

Fig. 40

THICK LIPPED ELLIPTICAL INLET

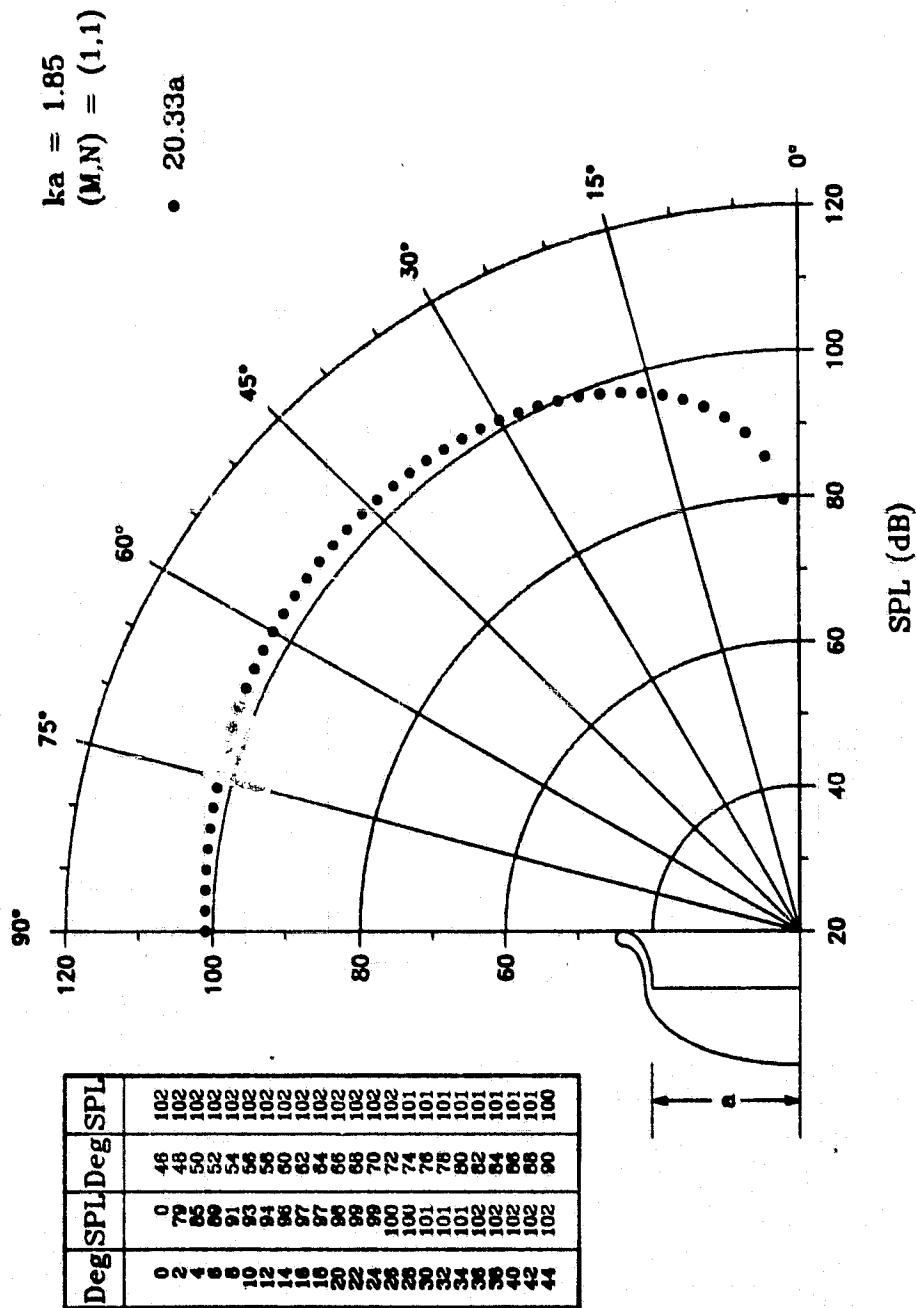


Fig. 41a

THICK LIPPED ELLIPTICAL INLET

$ka \approx 1.87$
 $(M,N) = (1,1)$

• 20.33a

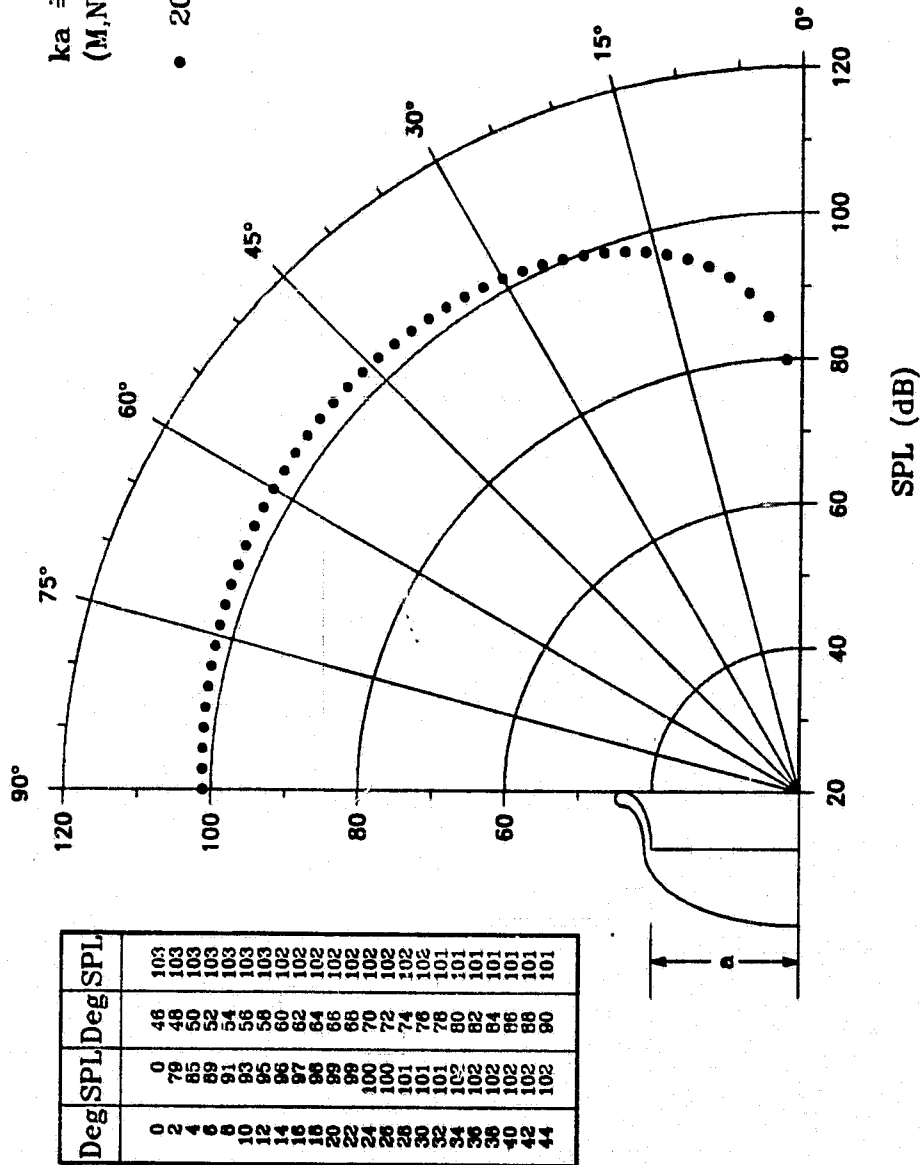


Fig. 41b

THICK LIPPED ELLIPTICAL INLET

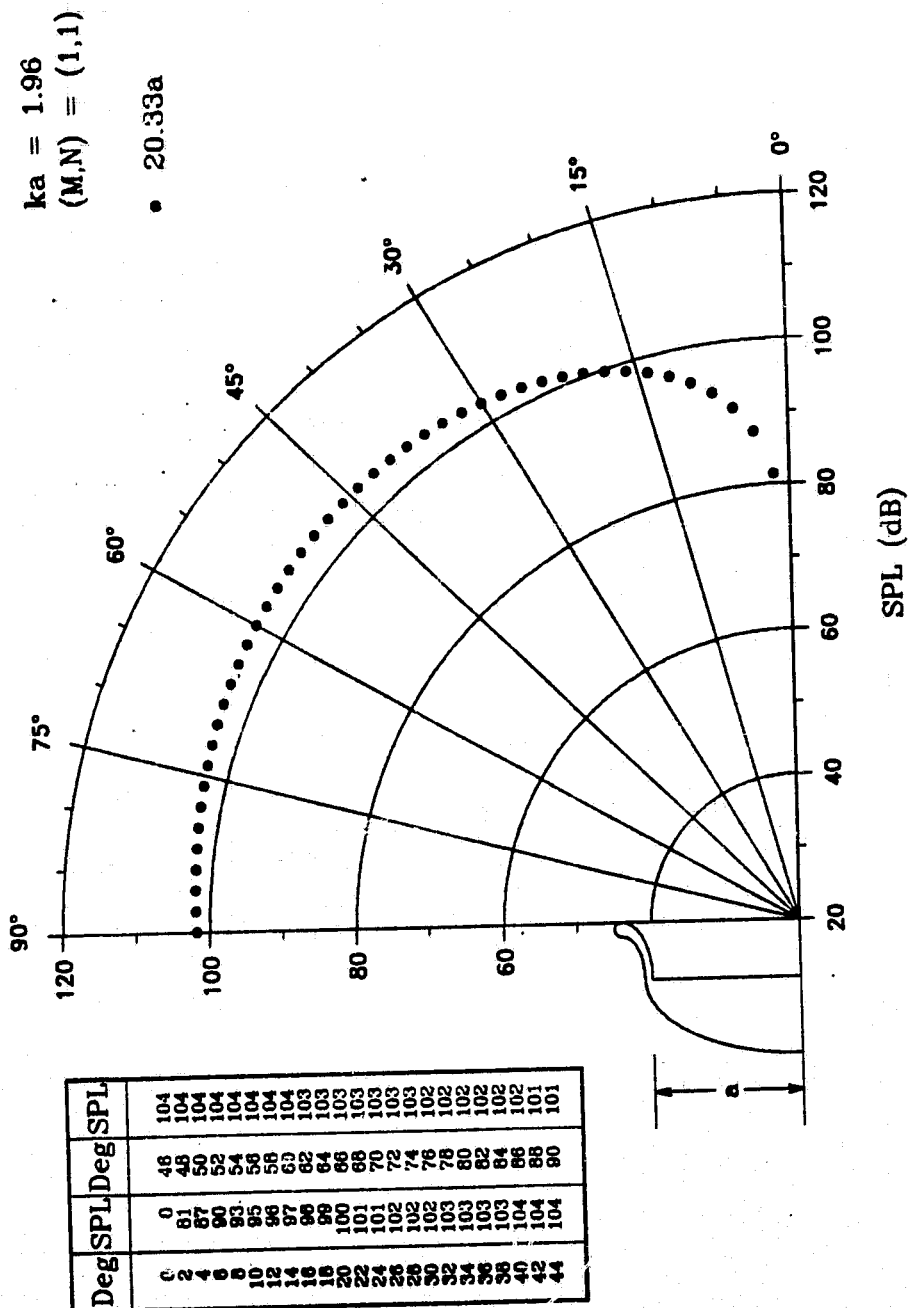


Fig. 41c

ORIGINAL PAGE IS
OF POOR QUALITY

THICK LIPPED ELLIPTICAL INLET

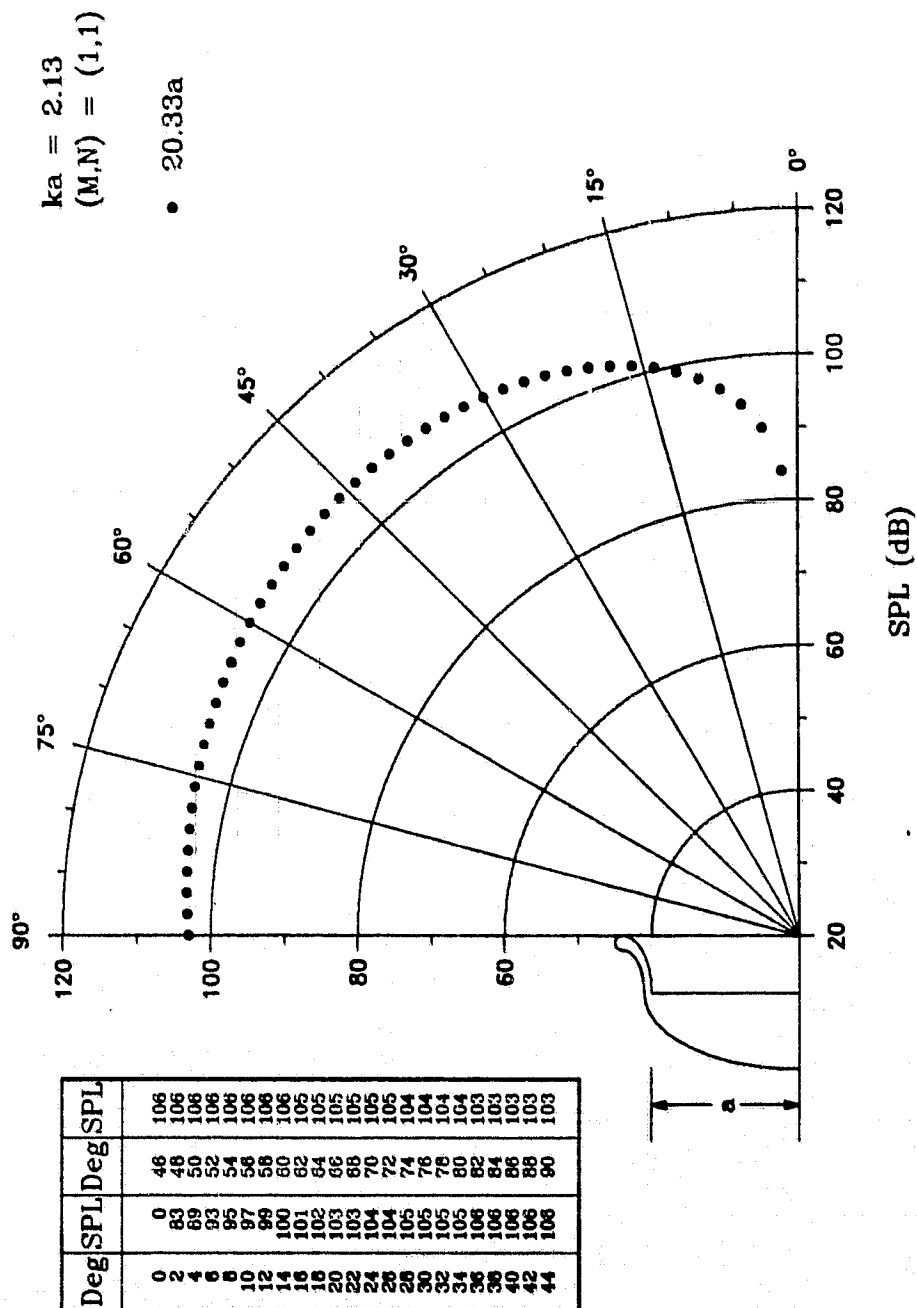


Fig. 41d

ORIGINAL PAGE IS
OF POOR QUALITY

THICK LIPPED ELLIPTICAL INLET

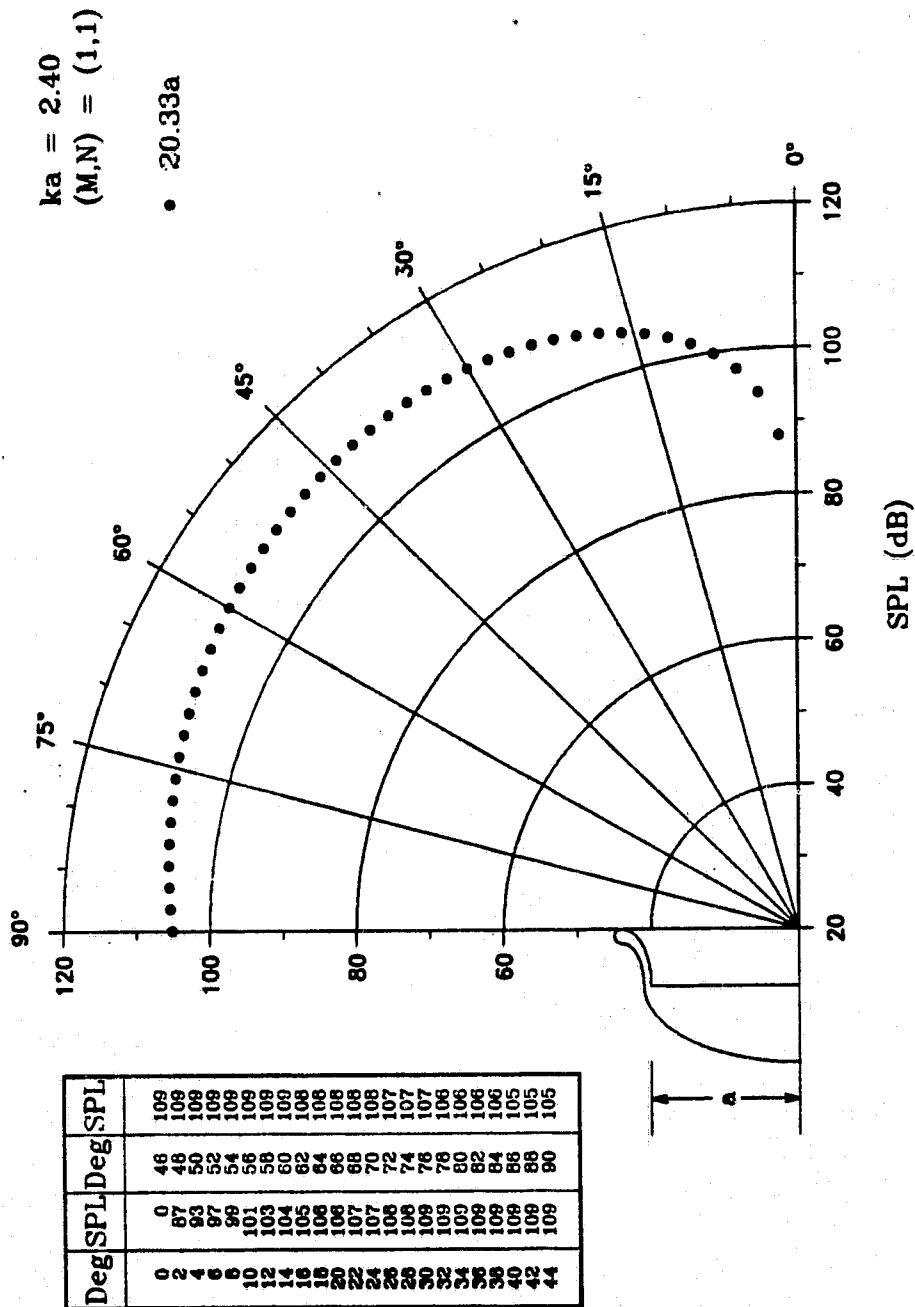


Fig. 41e

THICK LIPPED ELLIPTICAL INLET

ORIGINAL PAGE IS
OF POOR QUALITY

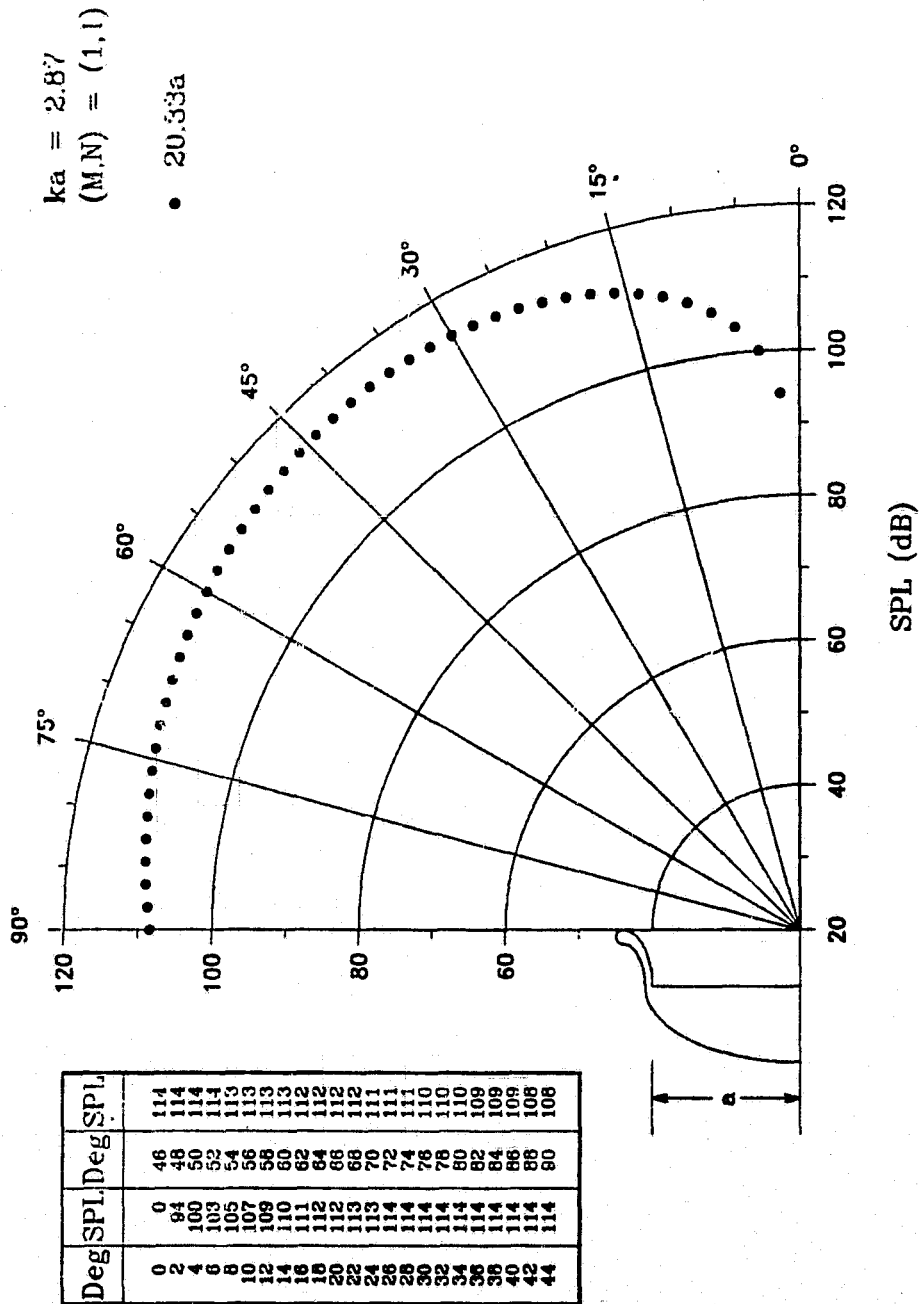


Fig. 41f

THICK LIPPED ELLIPTICAL INLET

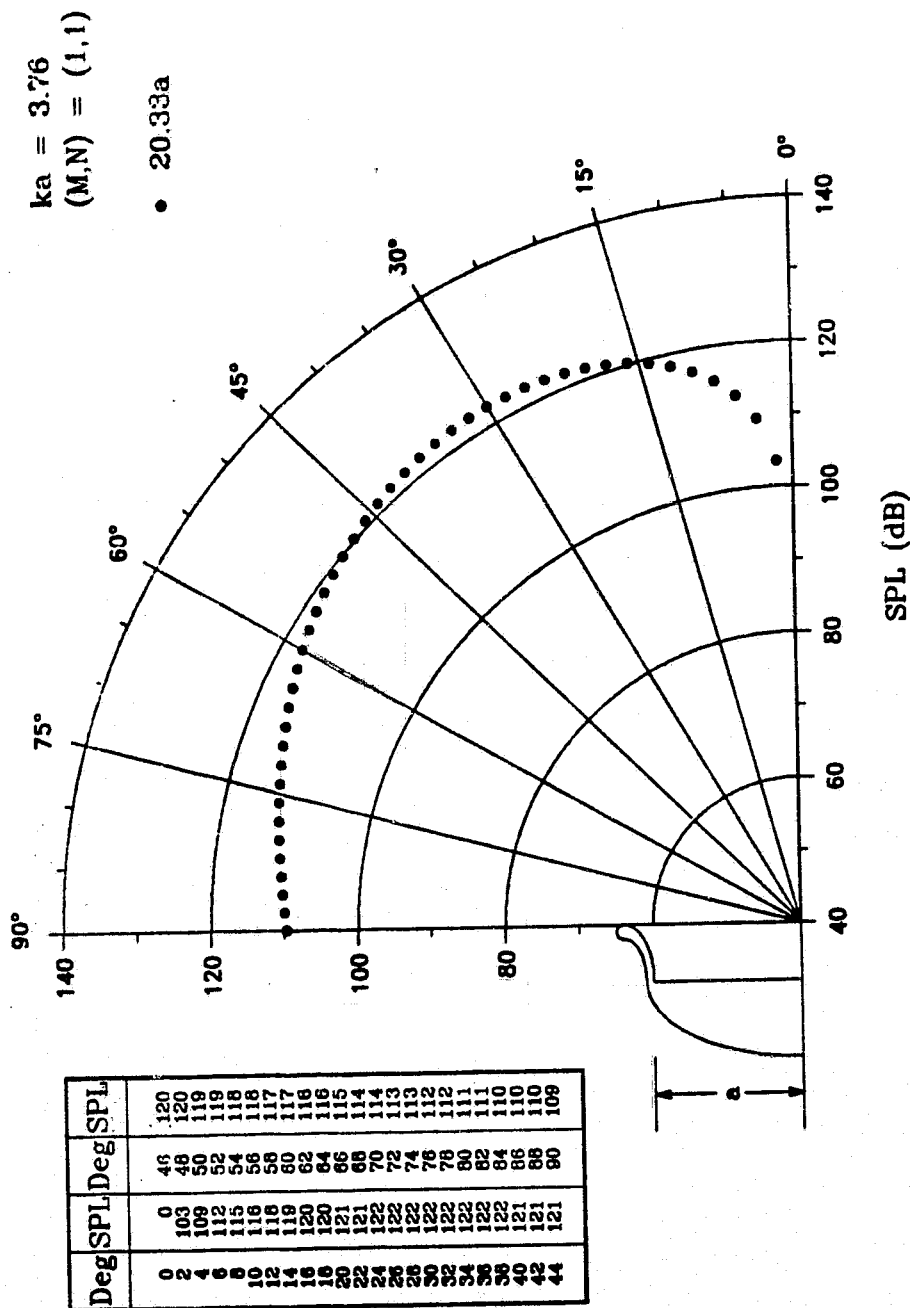


Fig. 418

ORIGINAL PAGE IS
OF POOR QUALITY

THICK LIPPED ELLIPTICAL INLET

$ka = 4.60$
 $(M,N) = (1,1)$

• 20.33a

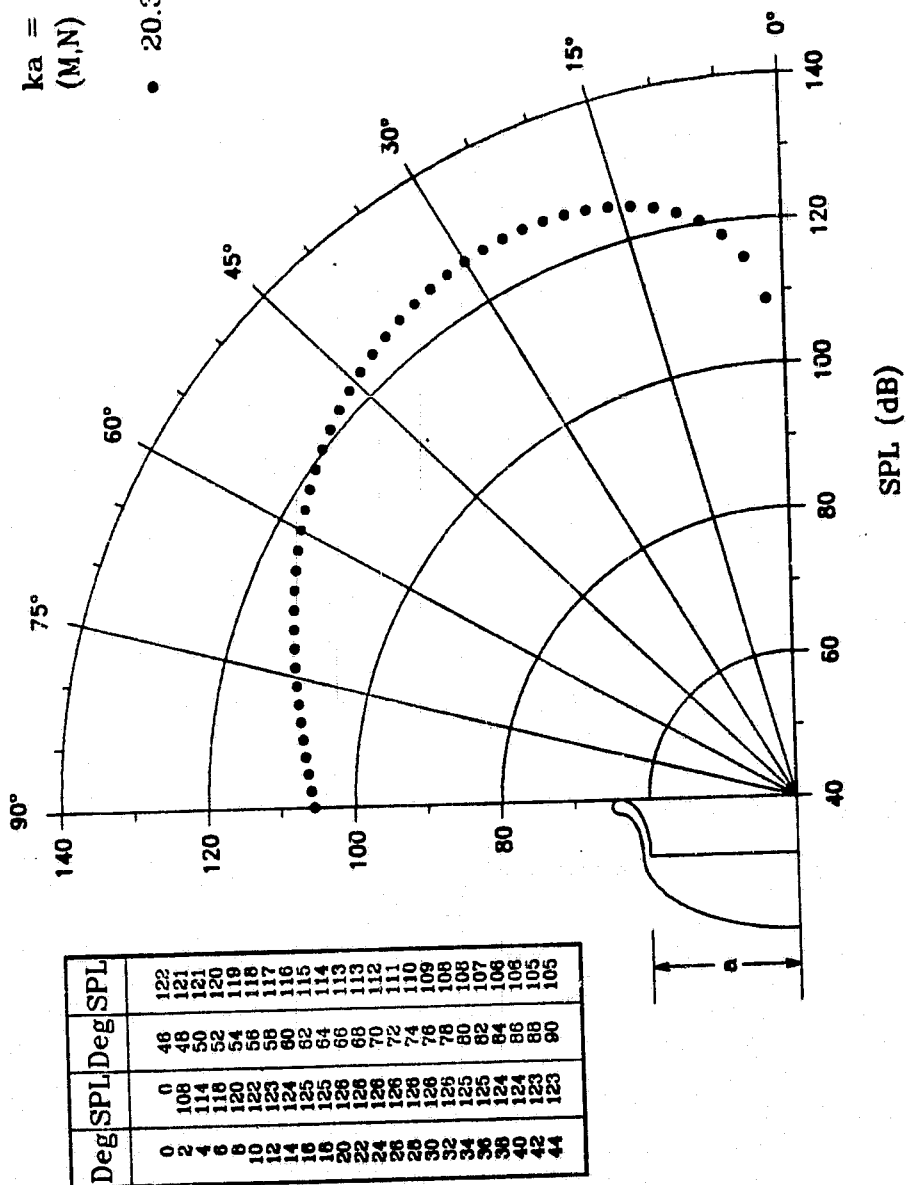


Fig. 41h

ORIGINAL PAGE IS
 OF POOR QUALITY

THICK LIPPED ELLIPTICAL INLET

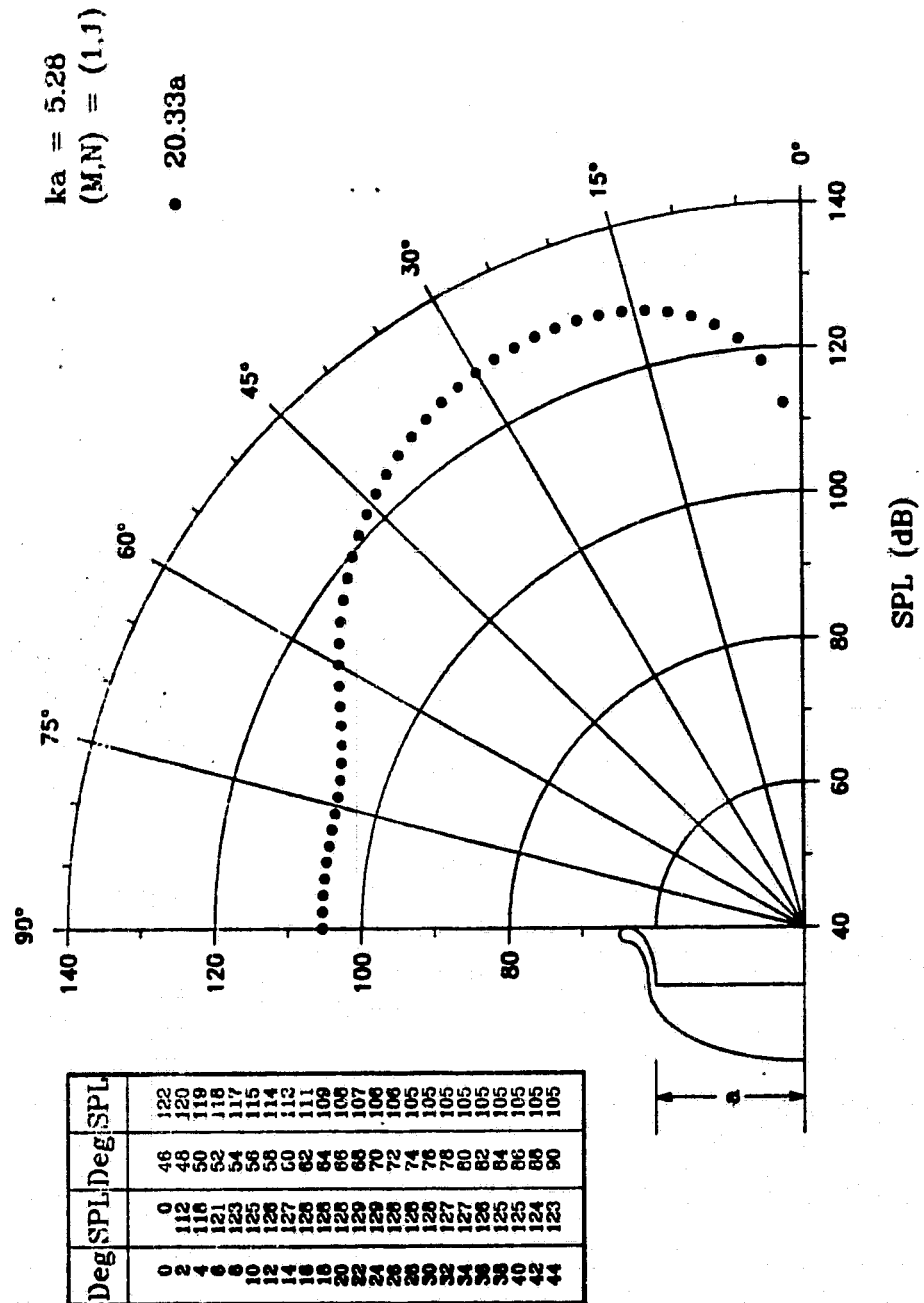


Fig. 41i

THICK LIPPED ELLIPTICAL INLET

ORIGINAL PAGE IS
OF POOR QUALITY

$ka = 3.07$
 $(M,N) = (2,1)$

• 20.33a

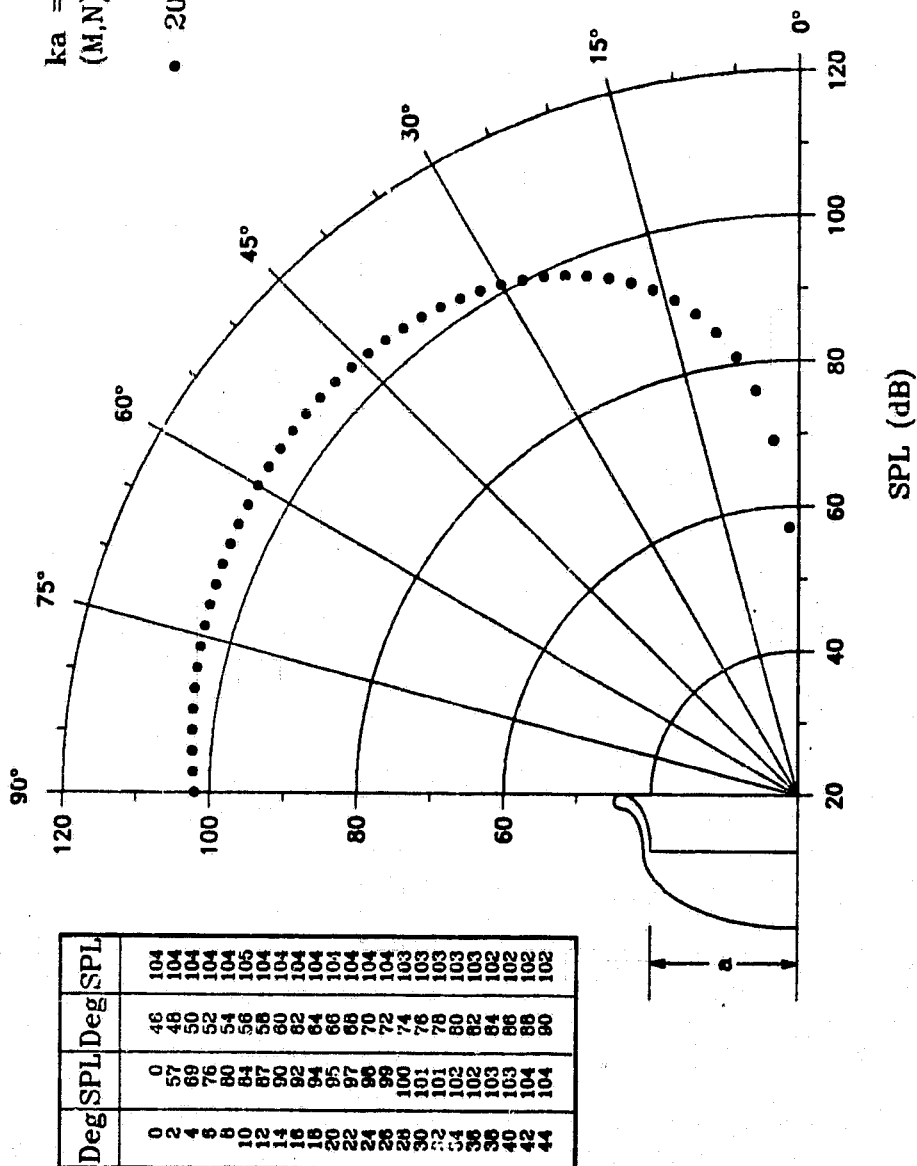


Fig. 42a

THICK LIPPED ELLIPTICAL INLET

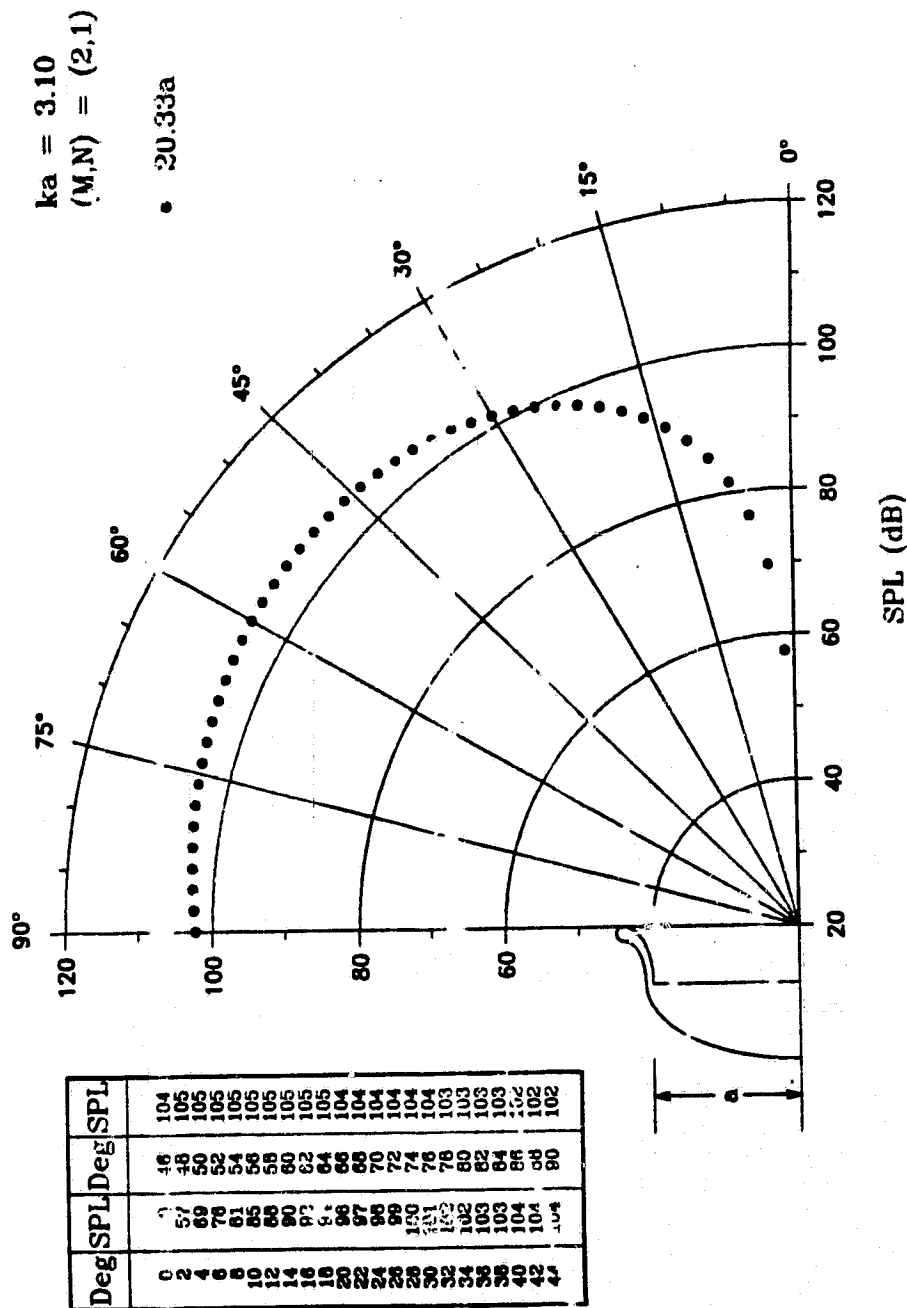


Fig. 42b

ORIGINAL PAGE IS
OF POOR QUALITY

THICK LIPPED ELLIPTICAL INLET

ORIGINAL PAGE IS
OF POOR QUALITY

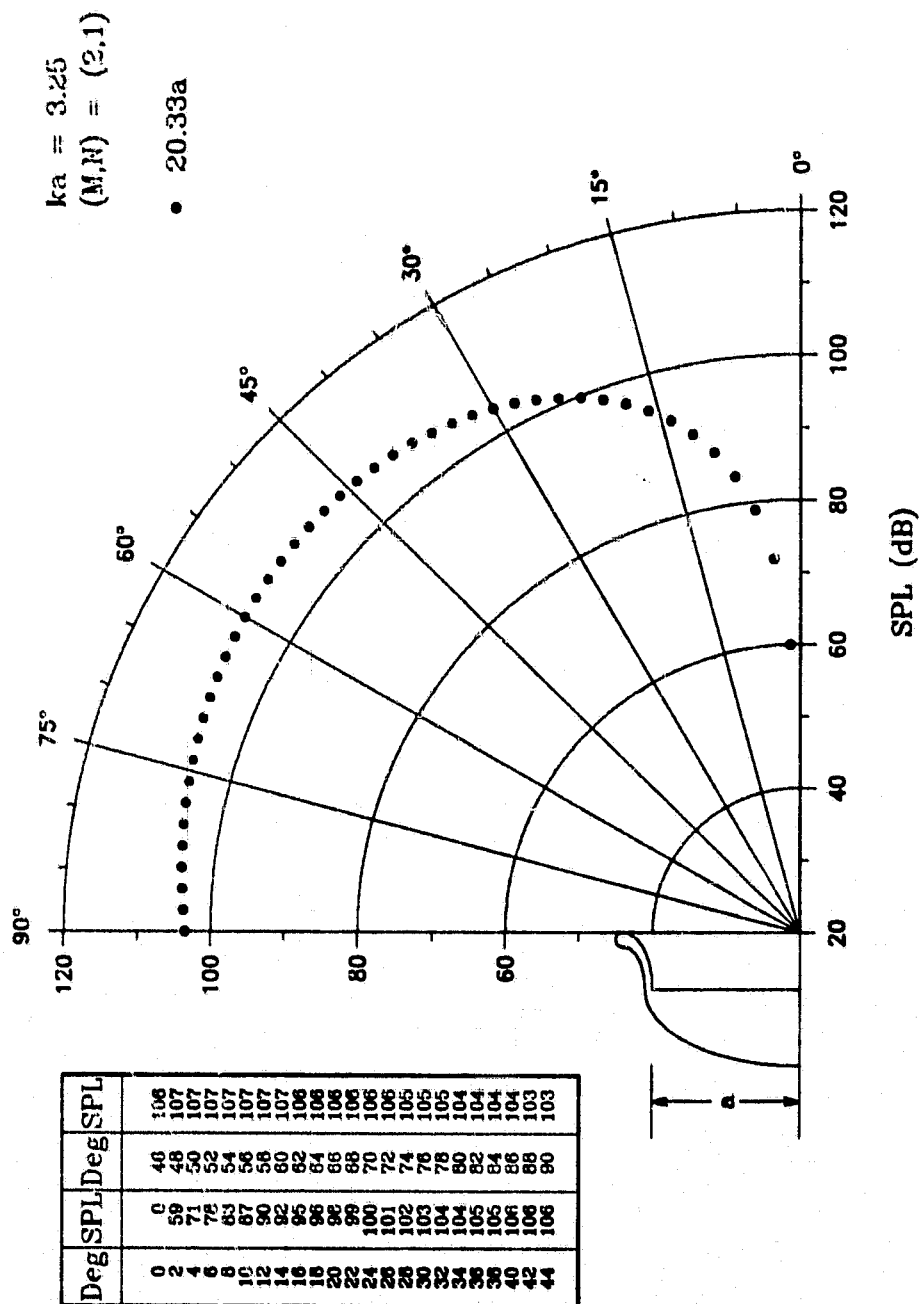


Fig. 42c

THICK LIPPED ELLIPTICAL INLET

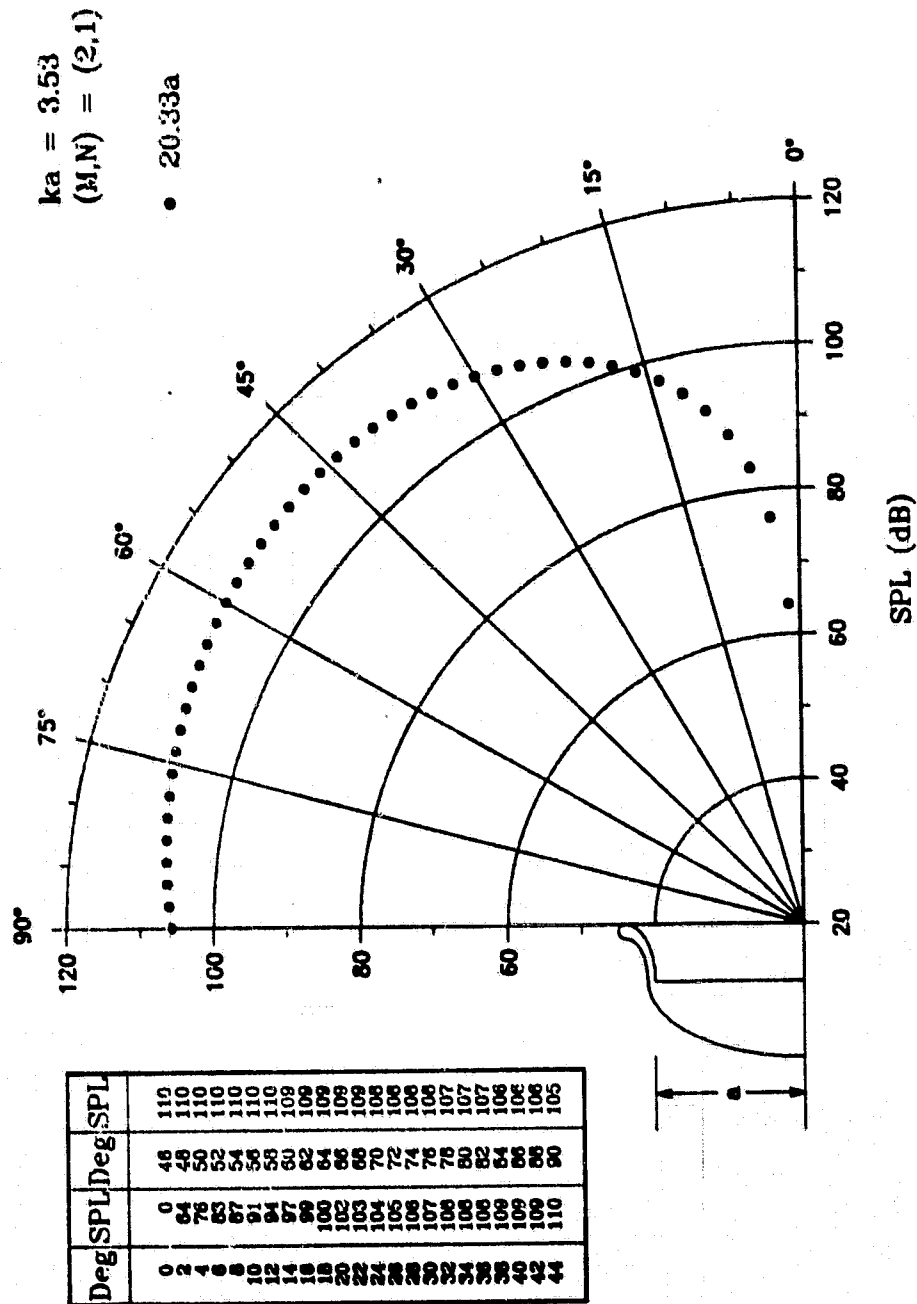


Fig. 42d

ORIGINAL PAGE 13
OF POOR QUALITY

THICK LIPPED ELLIPTICAL INLET

ORIGINAL PAGE 13
OF POOR QUALITY

$ka = 3.99$
(M.N) = (2,1)

• 20.33a

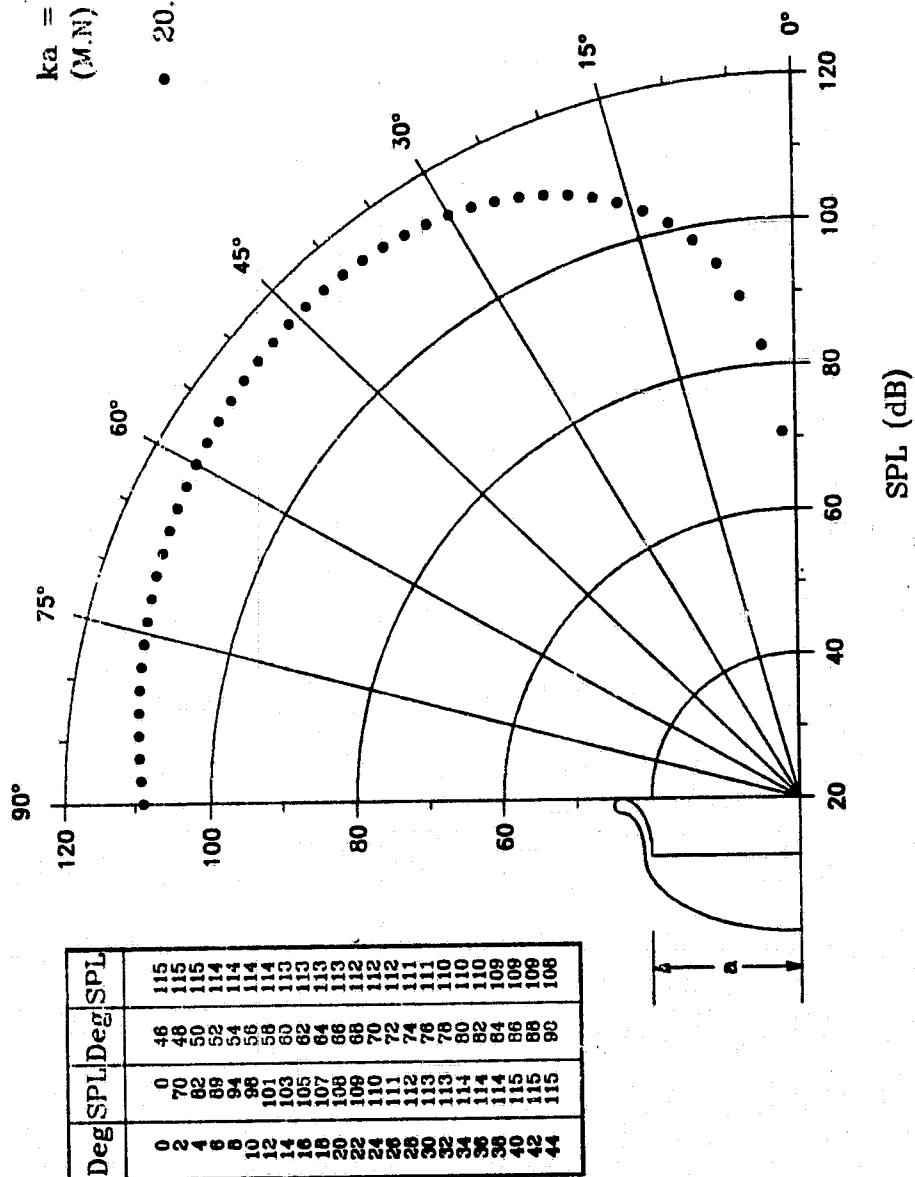


Fig. 42e

THICK LIPPED ELLIPTICAL INLET

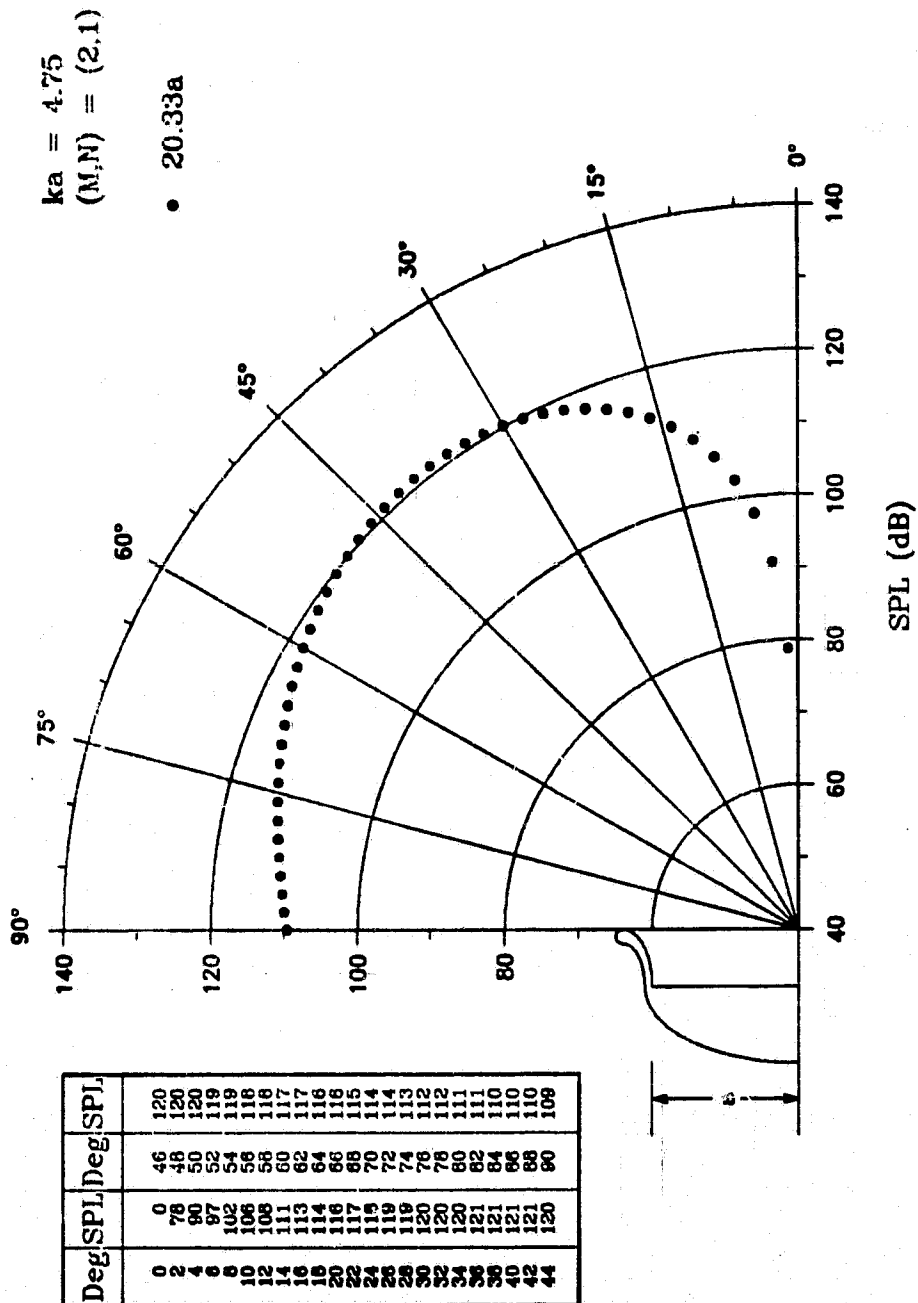


Fig. 42f

THICK LIPPED ELLIPTICAL INLET

ORIGINAL PAGE IS
OF POOR QUALITY

$ka = 5.31$
 $(M,N) = (2,1)$

• 20.33a

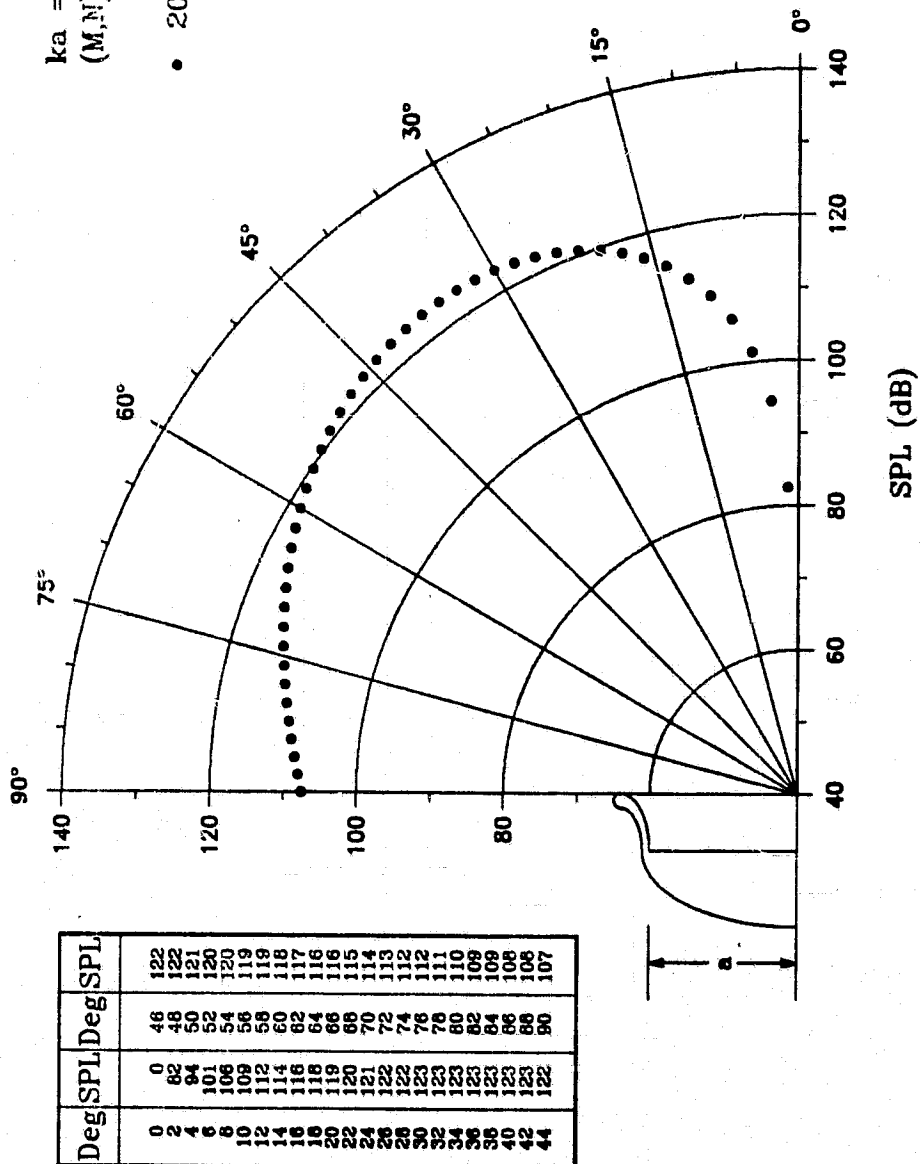
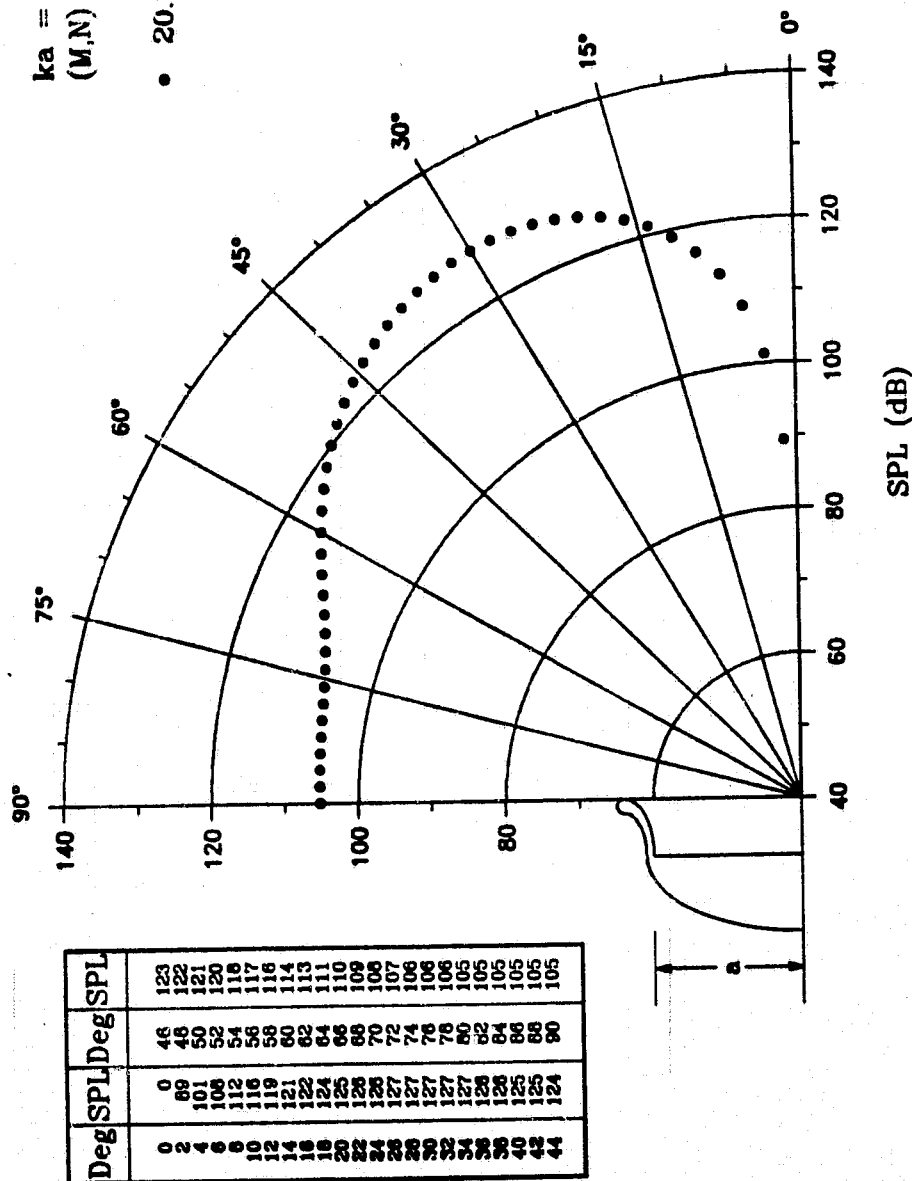


Fig. 42g

THICK LIPPED ELLIPTICAL INLET

$ka = 6.57$
 $(M,N) = (2,1)$

• 20.33a



ORIGINAL PAGE IS
 OF POOR QUALITY

Fig. 42h

THICK LIPPED ELLIPTICAL INLET

$ka = 5.35$
(M,N) = (4,1)

• 20.33a

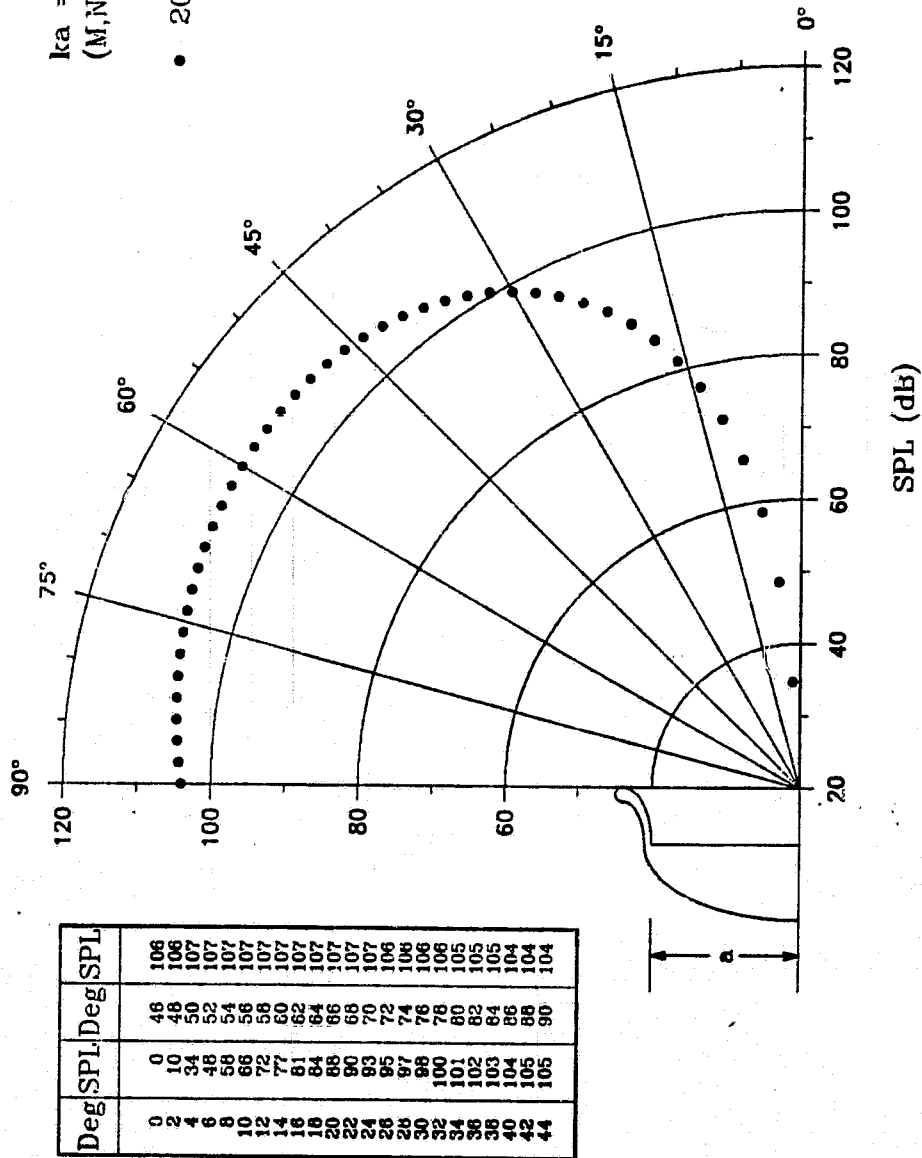


Fig. 43a

ORIGINAL PAGE IS
OF POOR QUALITY

THICK LIPPED ELLIPTICAL INLET

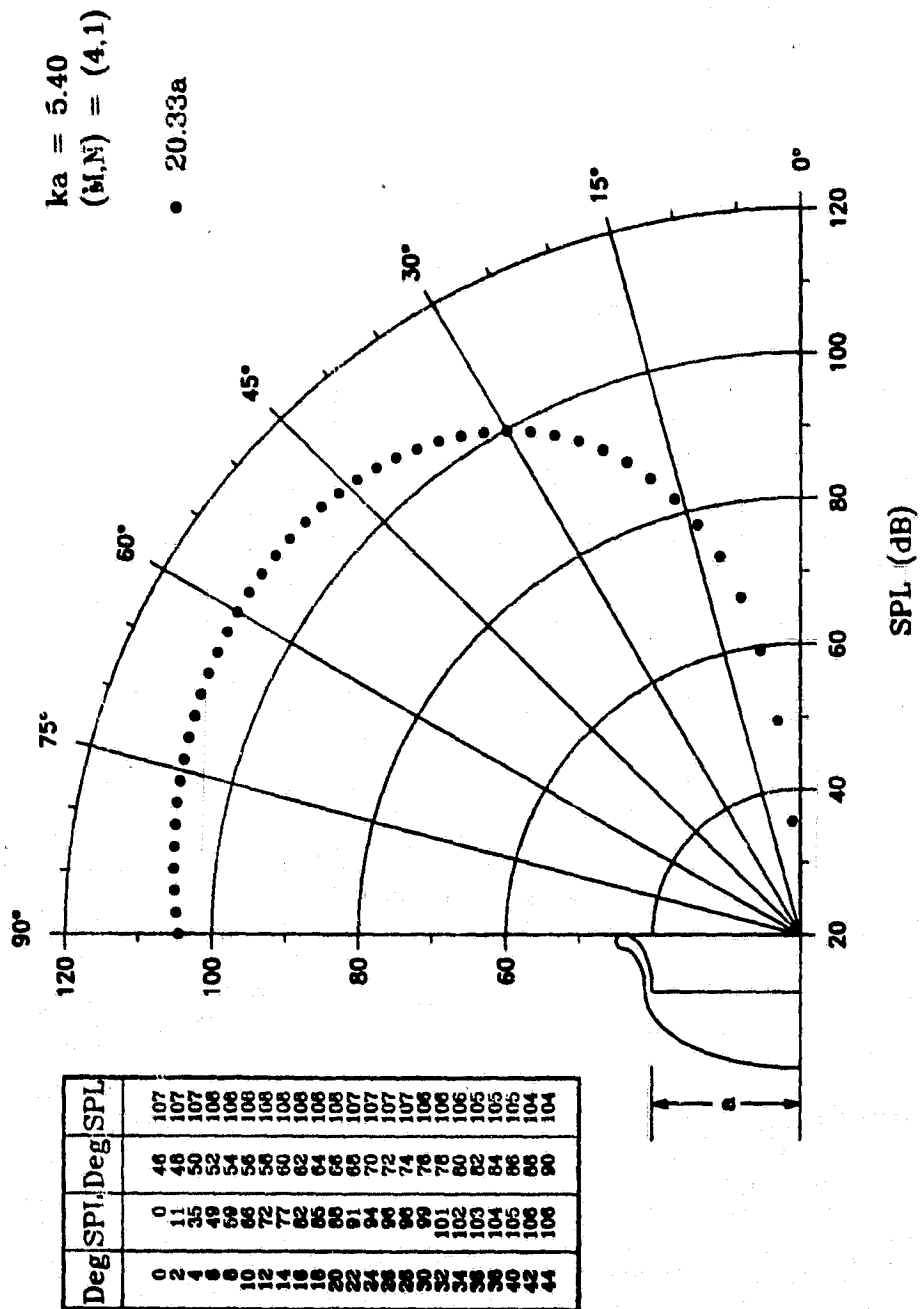


Fig. 43b

THICK LIPPED ELLIPTICAL INLET

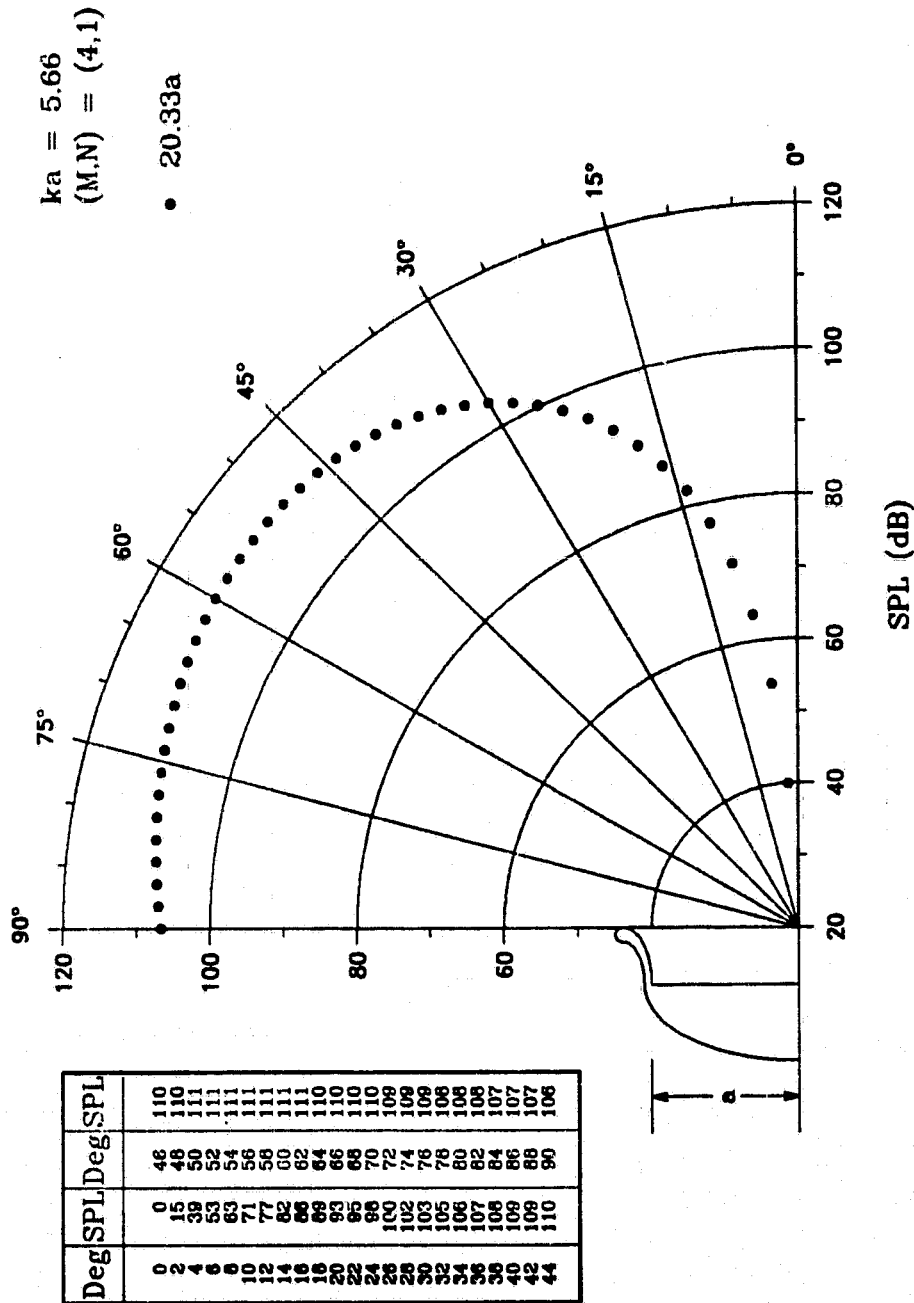


Fig. 43c

ORIGINAL PAGE IS
OF POOR QUALITY

THICK LIPPED ELLIPTICAL INLET

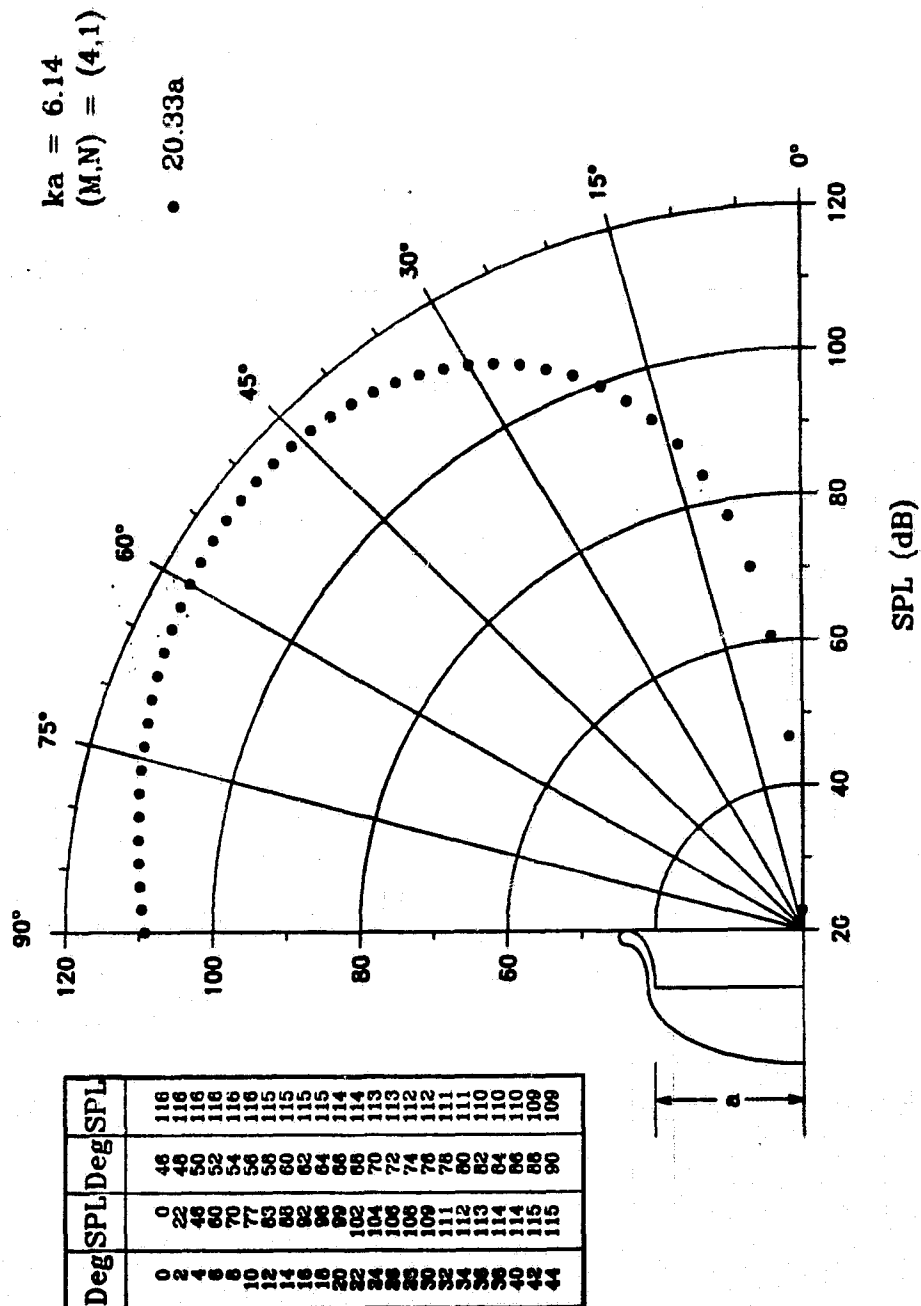


Fig. 43d

THICK LIPPED ELLIPTICAL INLET

ORIGINAL PAGE IS
OF POOR QUALITY

$ka = 6.94$
 $(M,N) = (4,1)$

• 20.33a

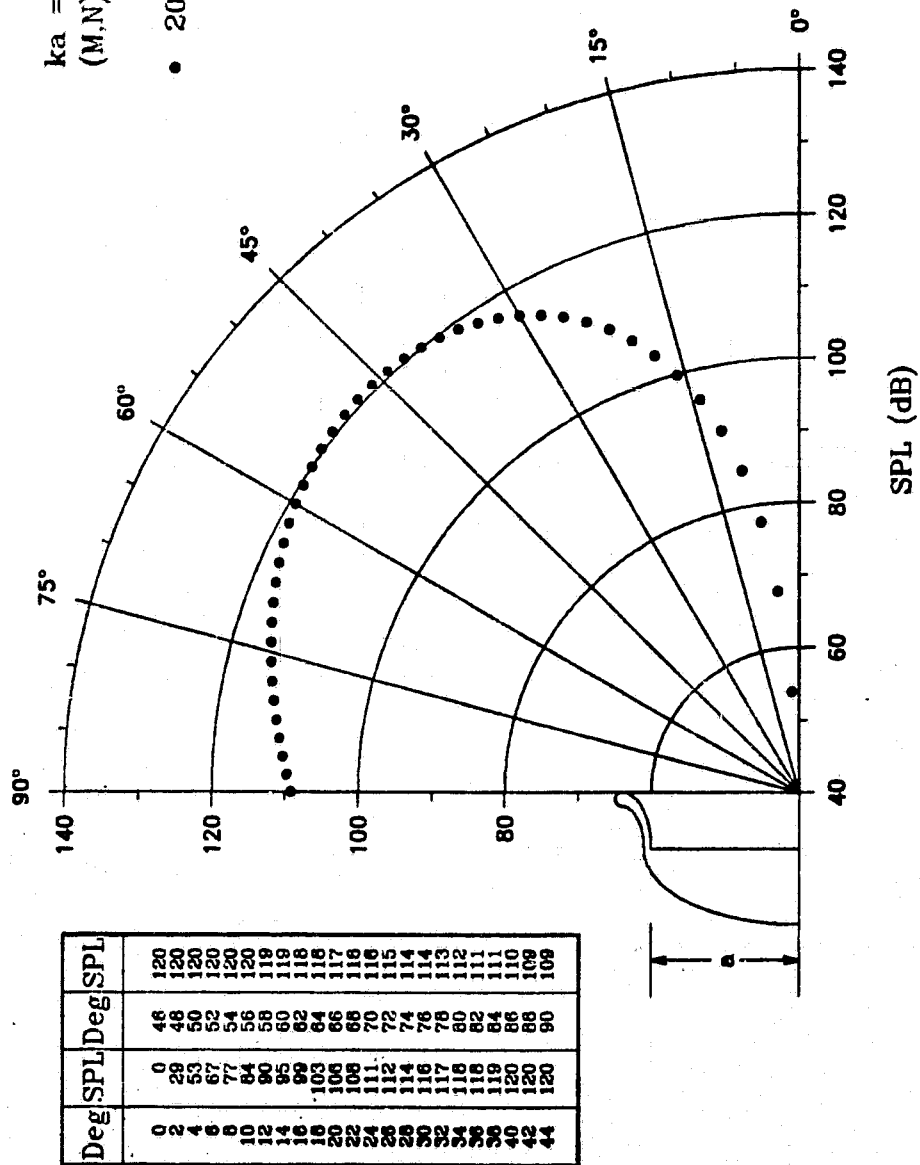


Fig. 43e

THICK LIPPED ELLIPTICAL INLET

$ka = 8.28$
 $(M,N) = (4,1)$

• 20.33a

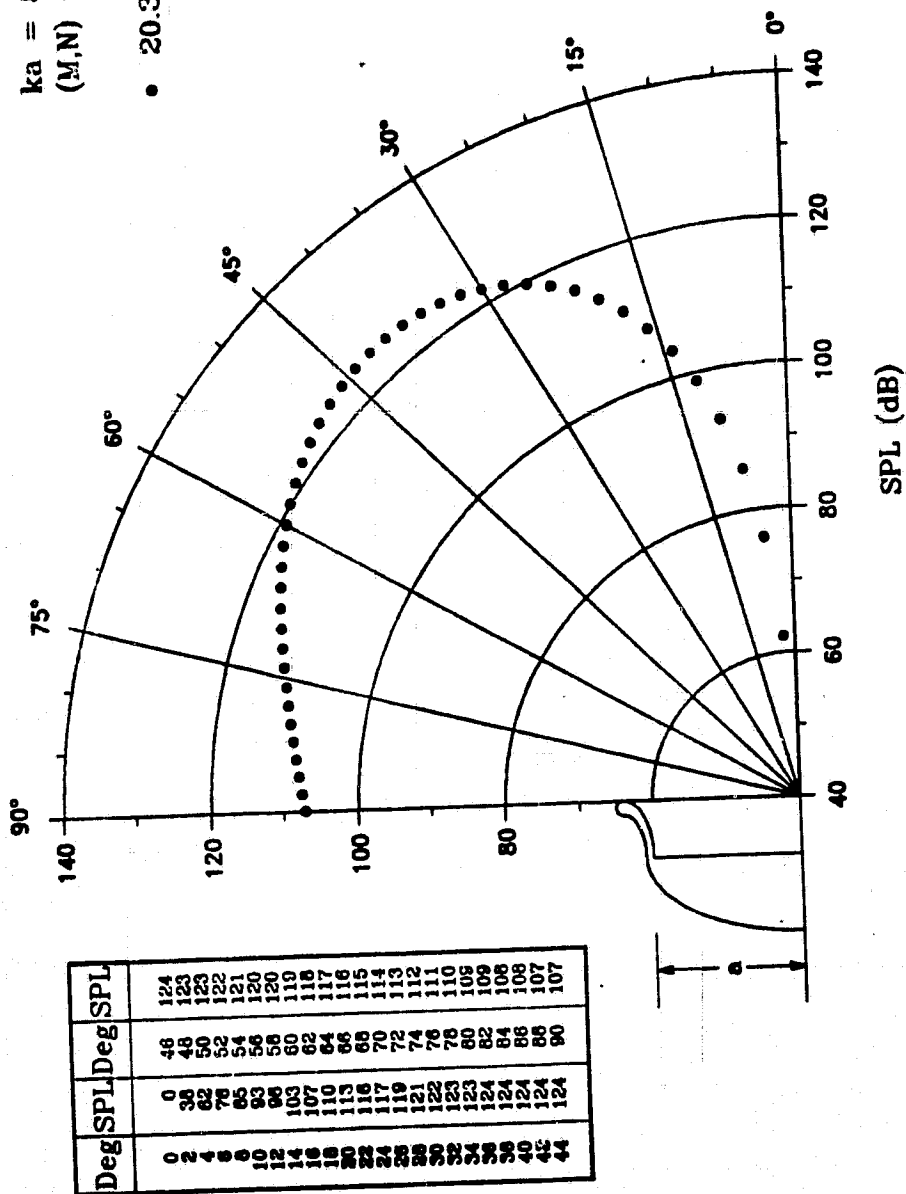


Fig. 43f

ORIGINAL PAGE IS
OF POOR QUALITY

THICK LIPPED ELLIPTICAL INLET

ORIGINAL PAGE IS
OF POOR QUALITY

$ka = 9.70$
 $(M,N) = (8,1)$

• 20.33a

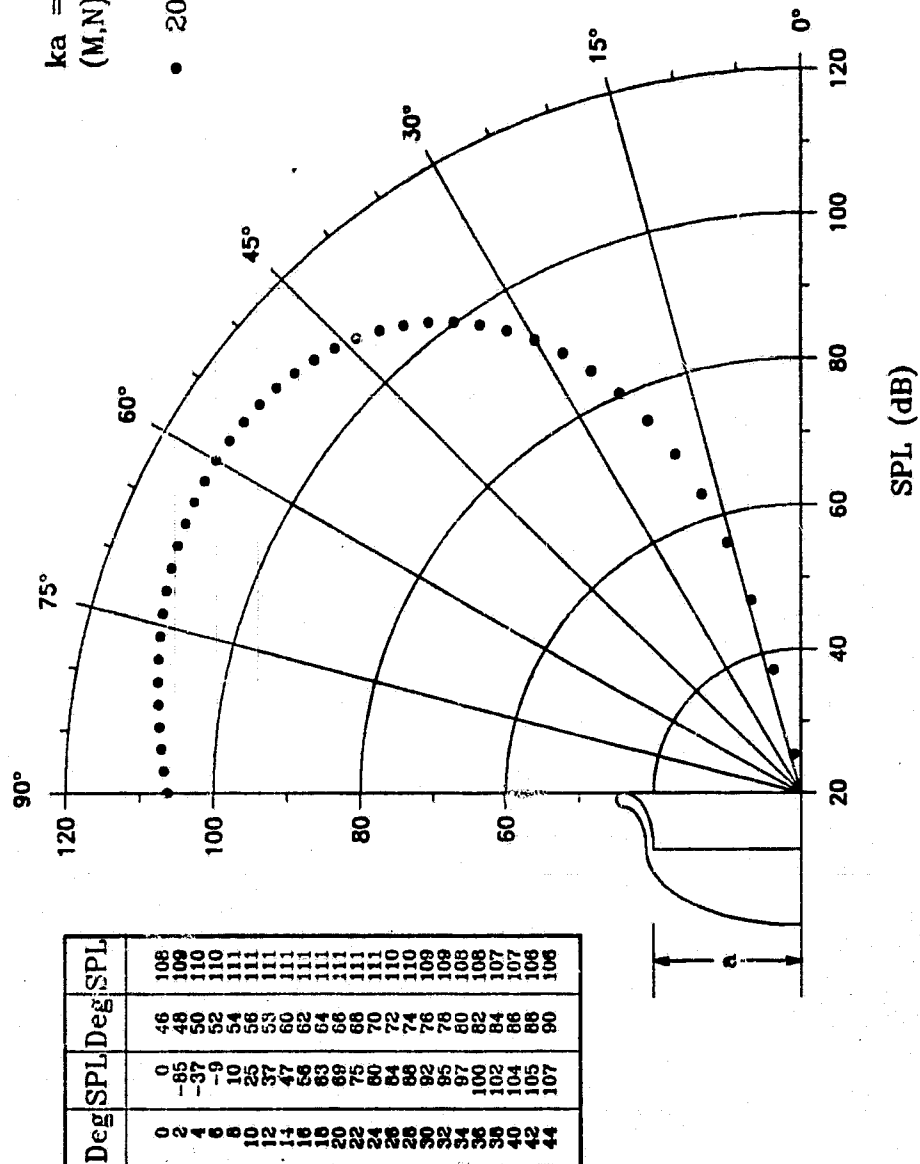


Fig. 44a

THICK LIPPED ELLIPTICAL INLET

ORIGINAL PAGE 13
OF POOR QUALITY

$ka = 9.79$
 $(M,N) = (8,1)$

• 20.33a

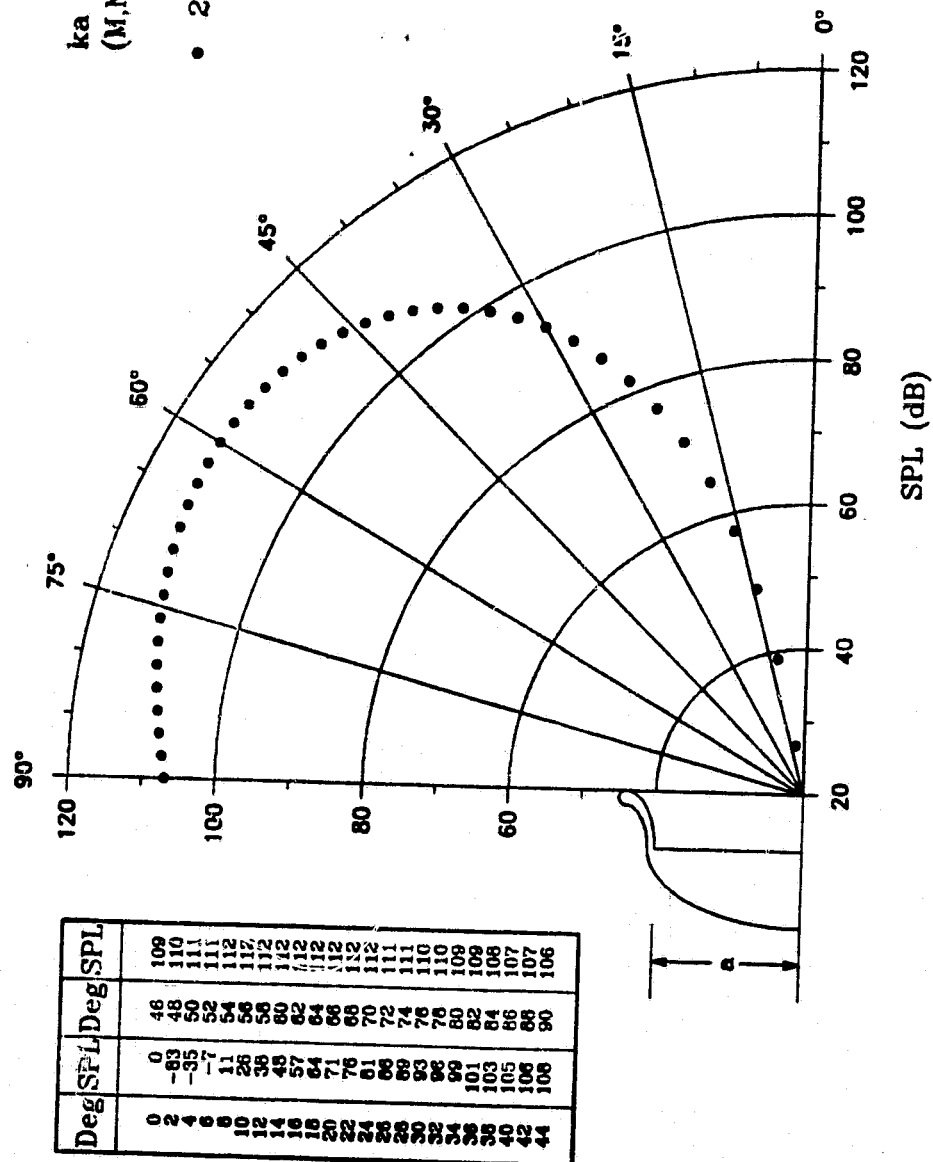


Fig. 44b

THICK LIPPED ELLIPTICAL INLET

$ka = 10.26$
 $(MN) = (8,1)$

• 20.33a

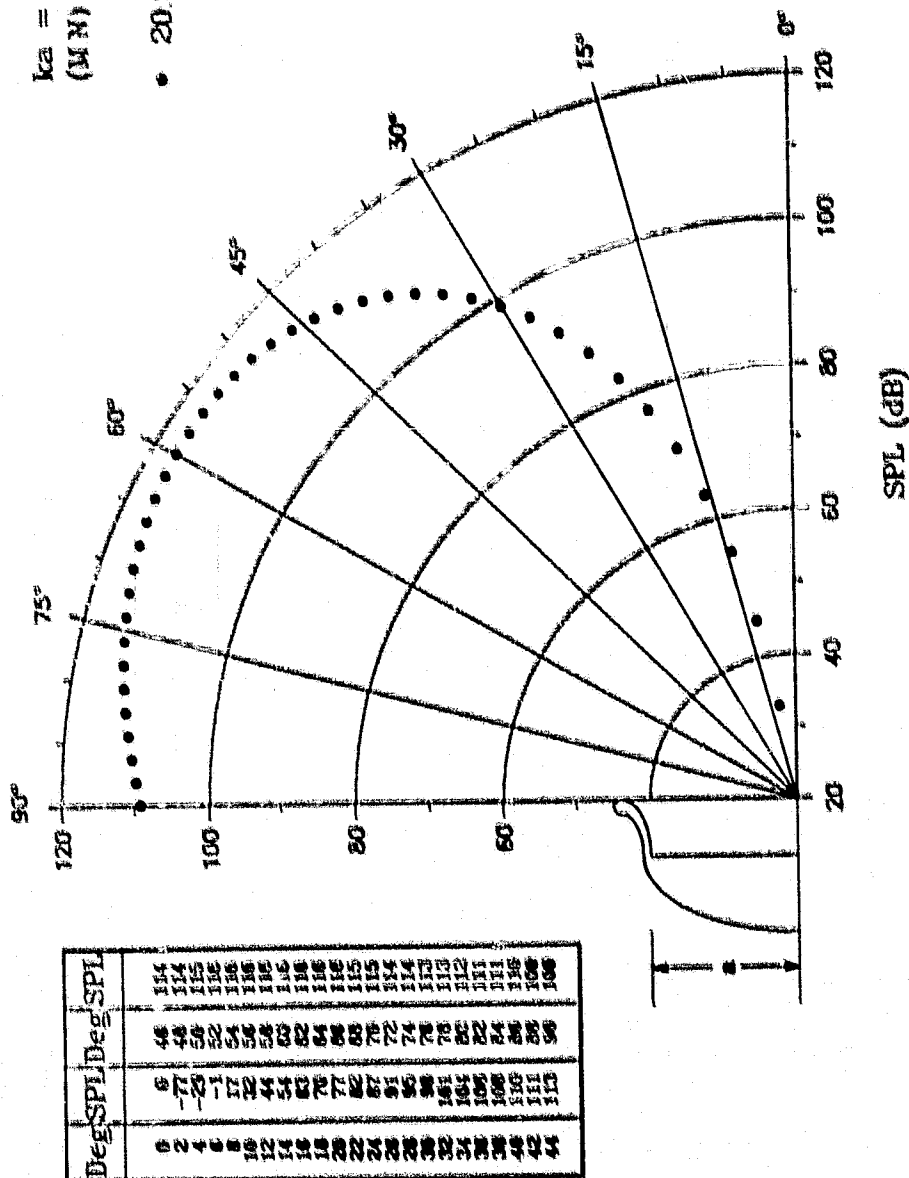


Fig. 44c

ORIGINAL PAGE IS
 OF POOR QUALITY

THICK LIPPED ELLIPTICAL INLET

$ka = 11.14$
 $(M,N) = (8,1)$

• 20.33a

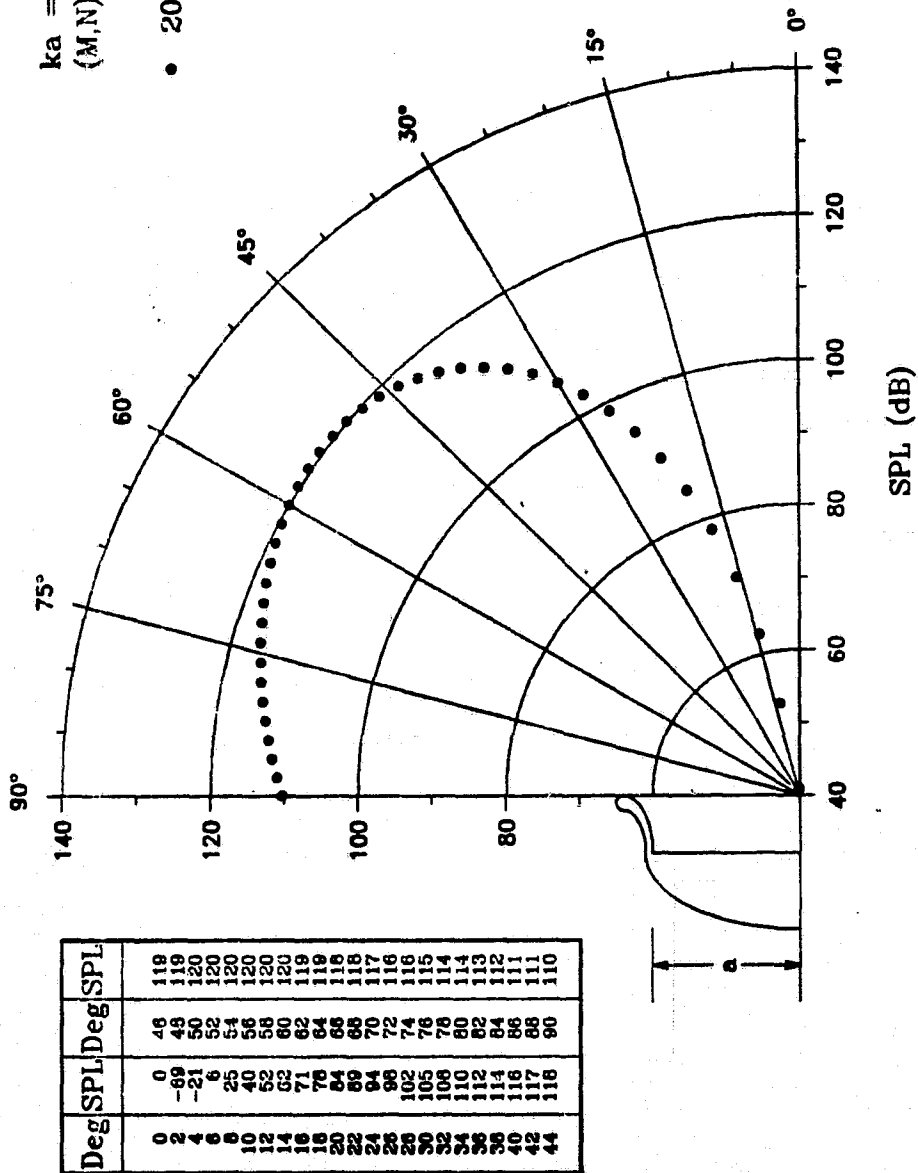


Fig. 44d

ORIGINAL PAGE IS
 OF POOR QUALITY

THICK LIPPED ELLIPTICAL INLET

$ka = 12.59$
 $(M,N) = (8,1)$

• 20.33a

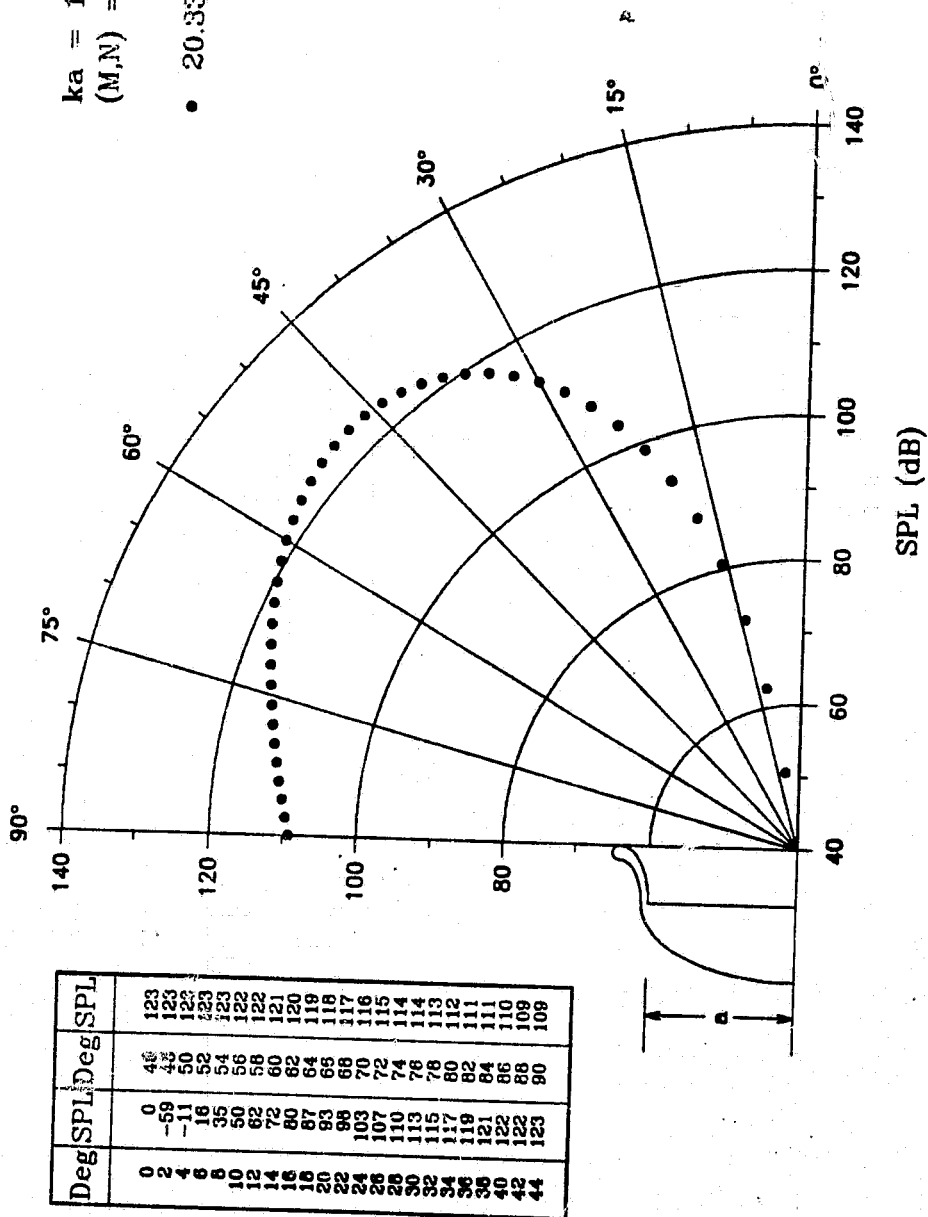


Fig. 44e

ORIGINAL PAGE IS
 OF POOR QUALITY

THICK LIPPED ELLIPTICAL INLET

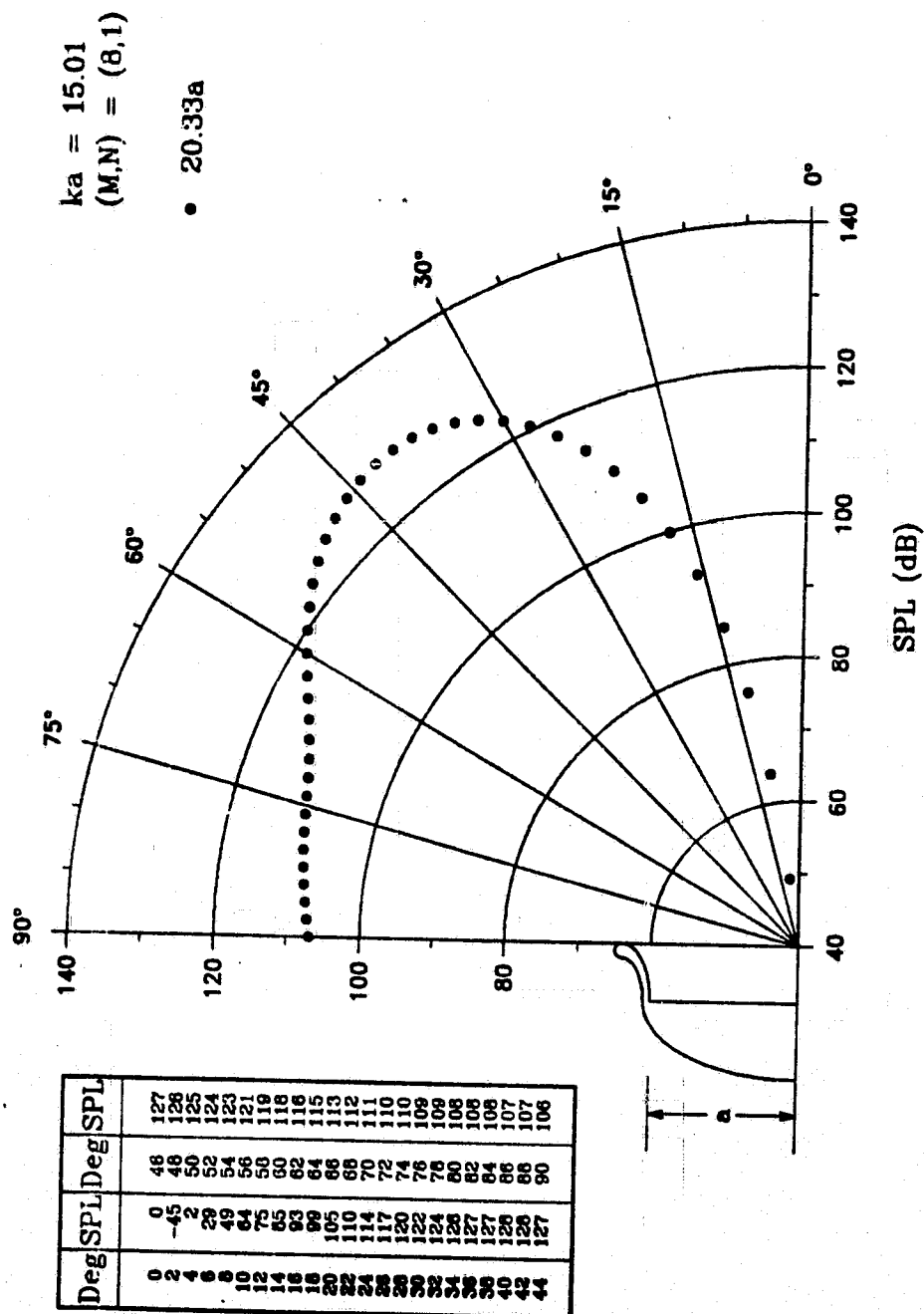


Fig. 44f

THICK LIPPED ELLIPTICAL INLET

ORIGINAL PAGE 13
OF POOR QUALITY

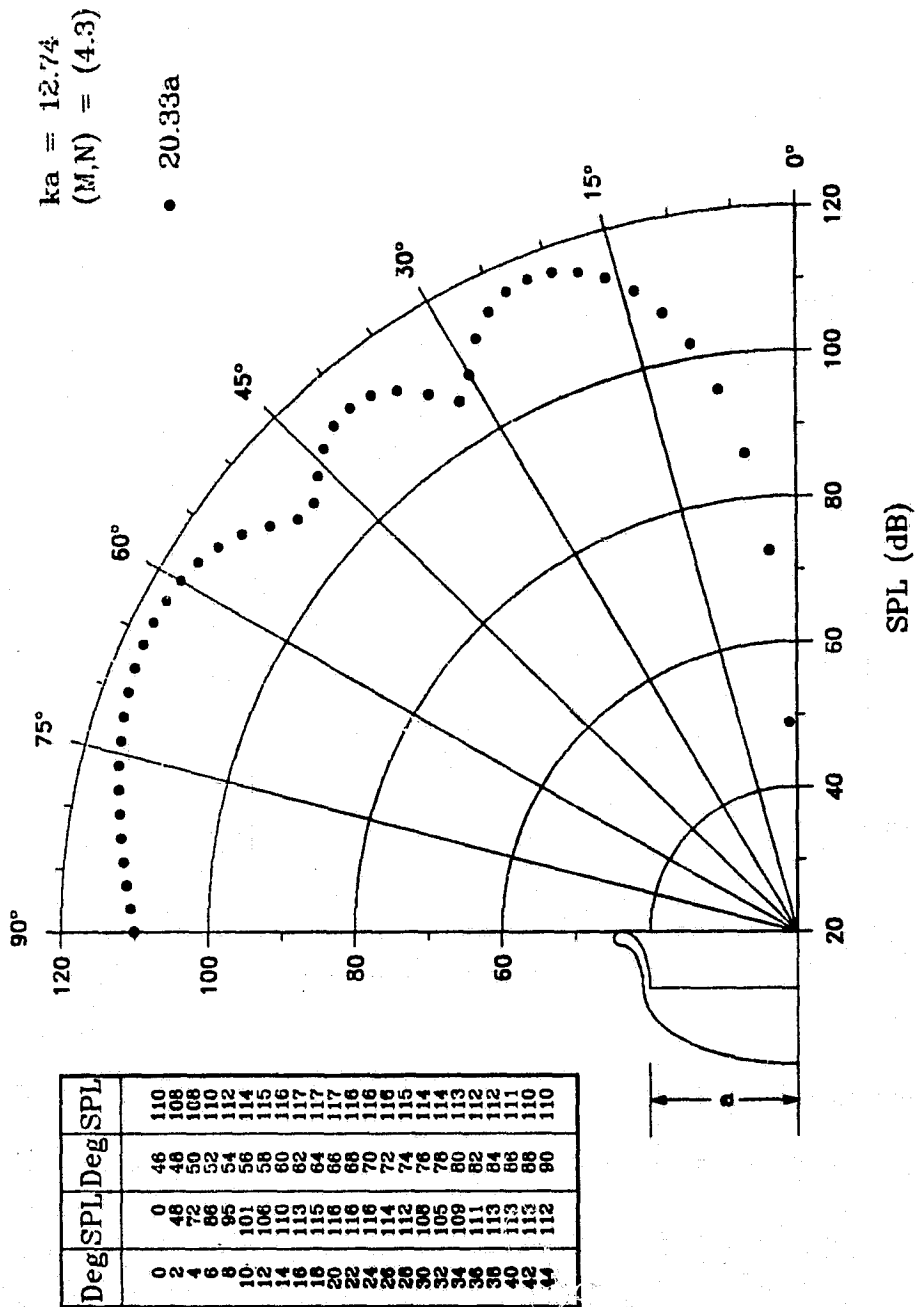


Fig. 45a

THICK LIPPED ELLIPTICAL INLET

$ka = 12.87$
 $(M,N) = (4,3)$
 $\bullet 20.33a$

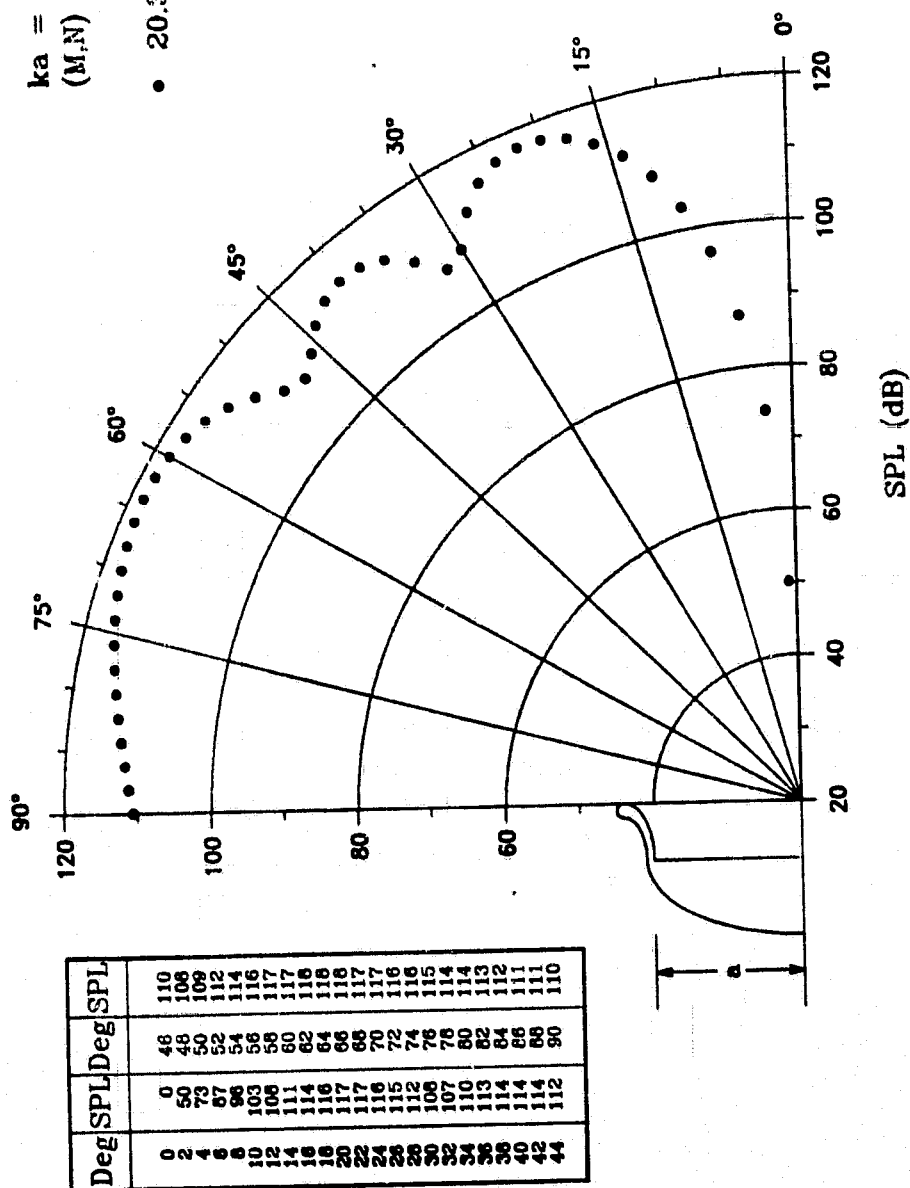


Fig. 45b

THICK LIPPED ELLIPTICAL INLET

$ka = 13.49$
 $(M,N) = (4,3)$

• 20.33a

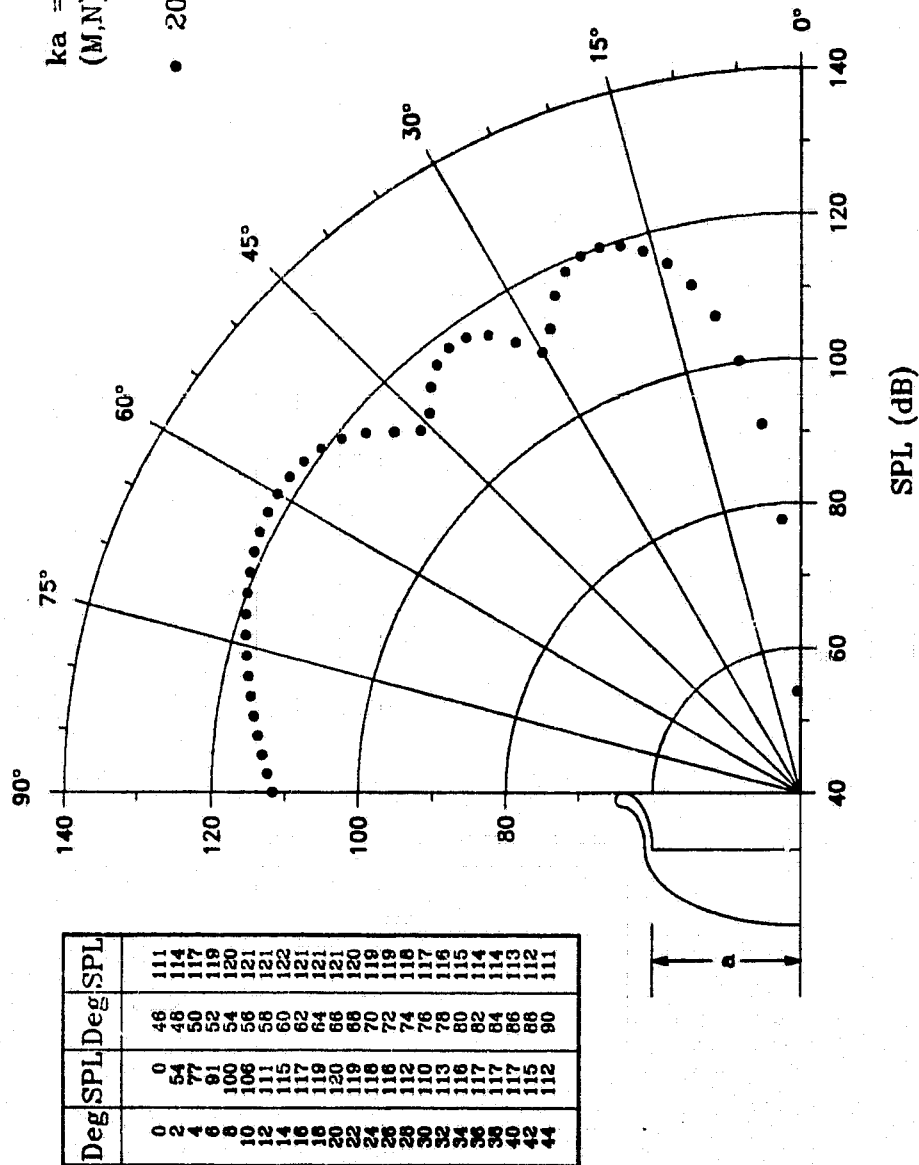


Fig. 45c

ORIGINAL PAGE IS
 OF POOR QUALITY

THICK LIPPED ELLIPTICAL INLET

ORIGINAL PAGE IS
OF POOR QUALITY

$ka = 14.65$
(M,N) = (4,3)

• 20.33a

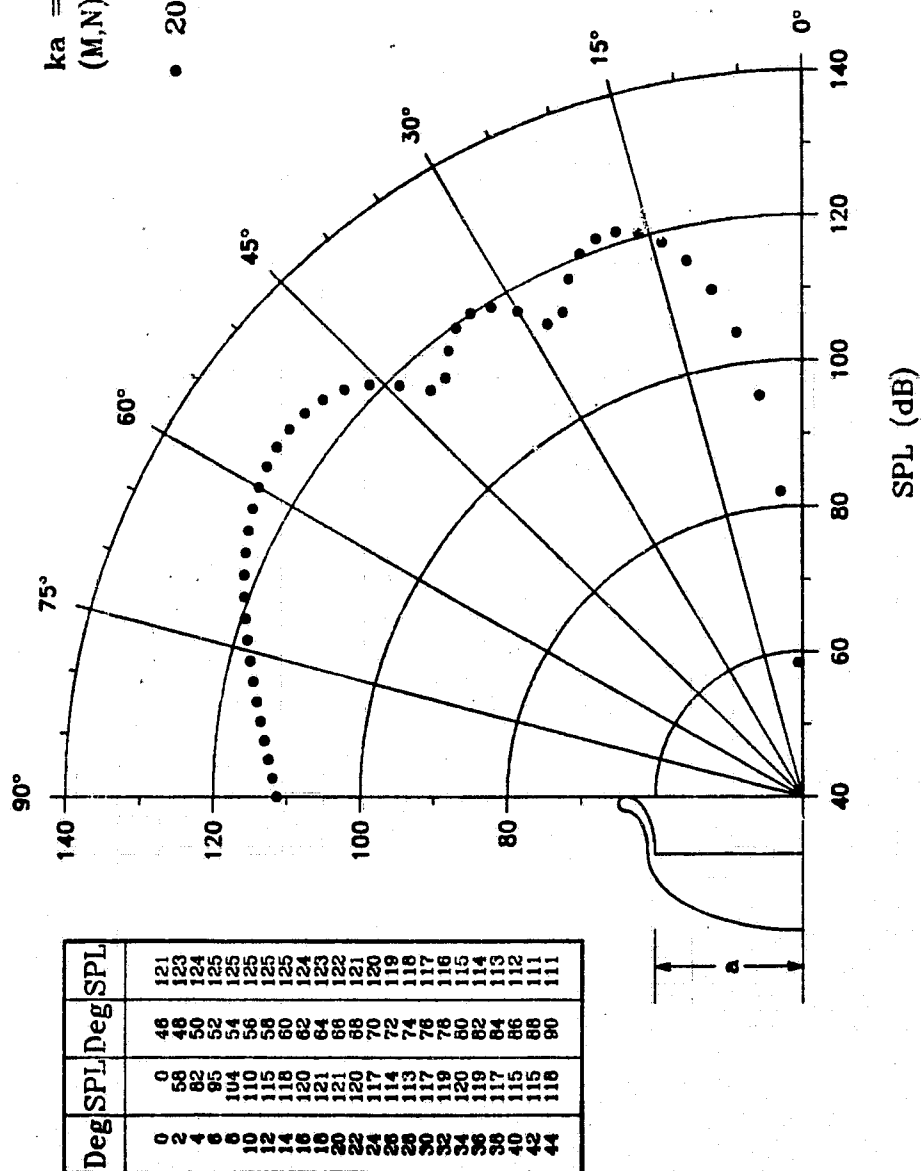


Fig. 45d

THICK LIPPED ELLIPTICAL INLET

ORIGINAL PAGE IS
OF POOR QUALITY

$ka = 16.55$
(M.N) = (4.3)

• 20.33a

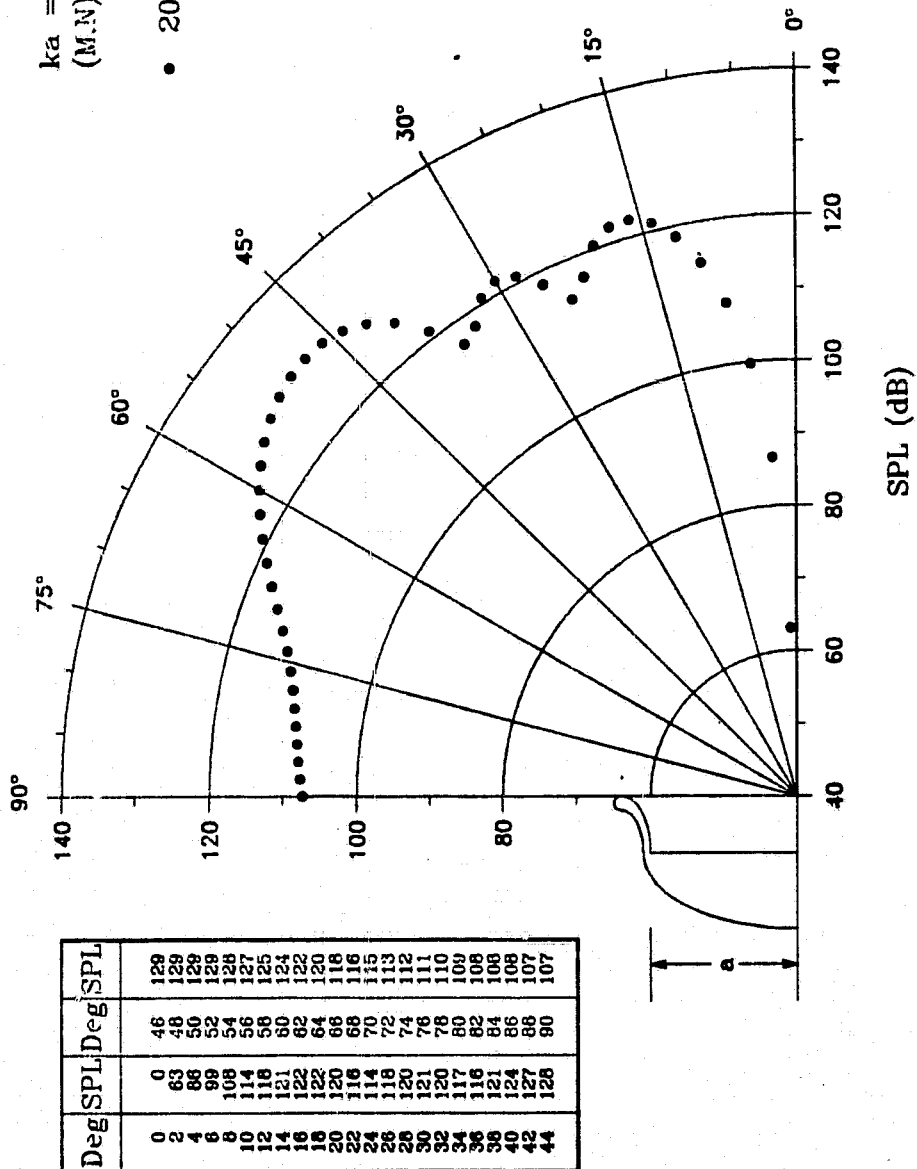


Fig. 45e

THICK LIPPED ELLIPTICAL INLET

Deg SPL	Deg SPL	Deg SPL
0	0	46
2	70	48
4	94	50
6	107	52
8	115	54
10	120	56
12	123	58
14	124	60
16	123	62
18	120	64
20	116	66
22	122	68
24	124	70
26	121	72
28	121	74
30	121	76
32	127	78
34	130	80
36	133	82
38	134	84
40	134	86
42	133	88
44	132	90

ka = 19.73
(M,N) = (4,3)

• 20.33a

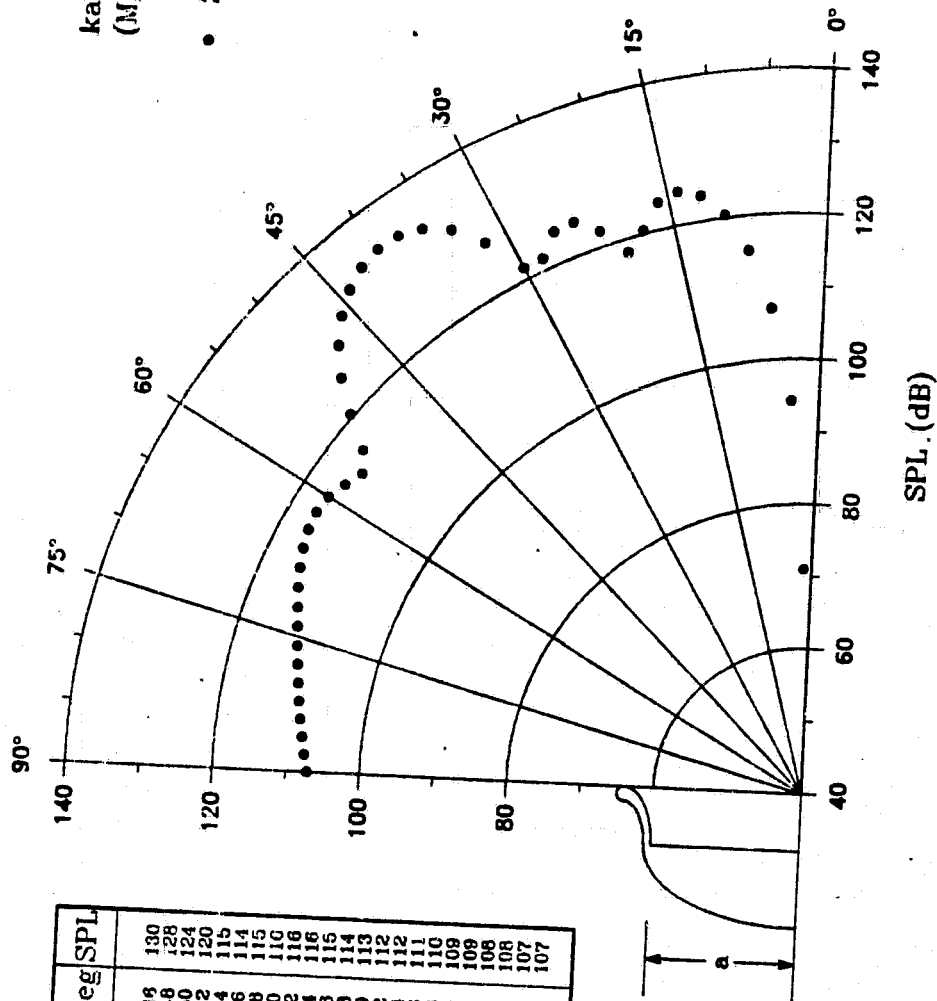


Fig. 45f

ORIGINAL PAGE IS
OF POOR QUALITY

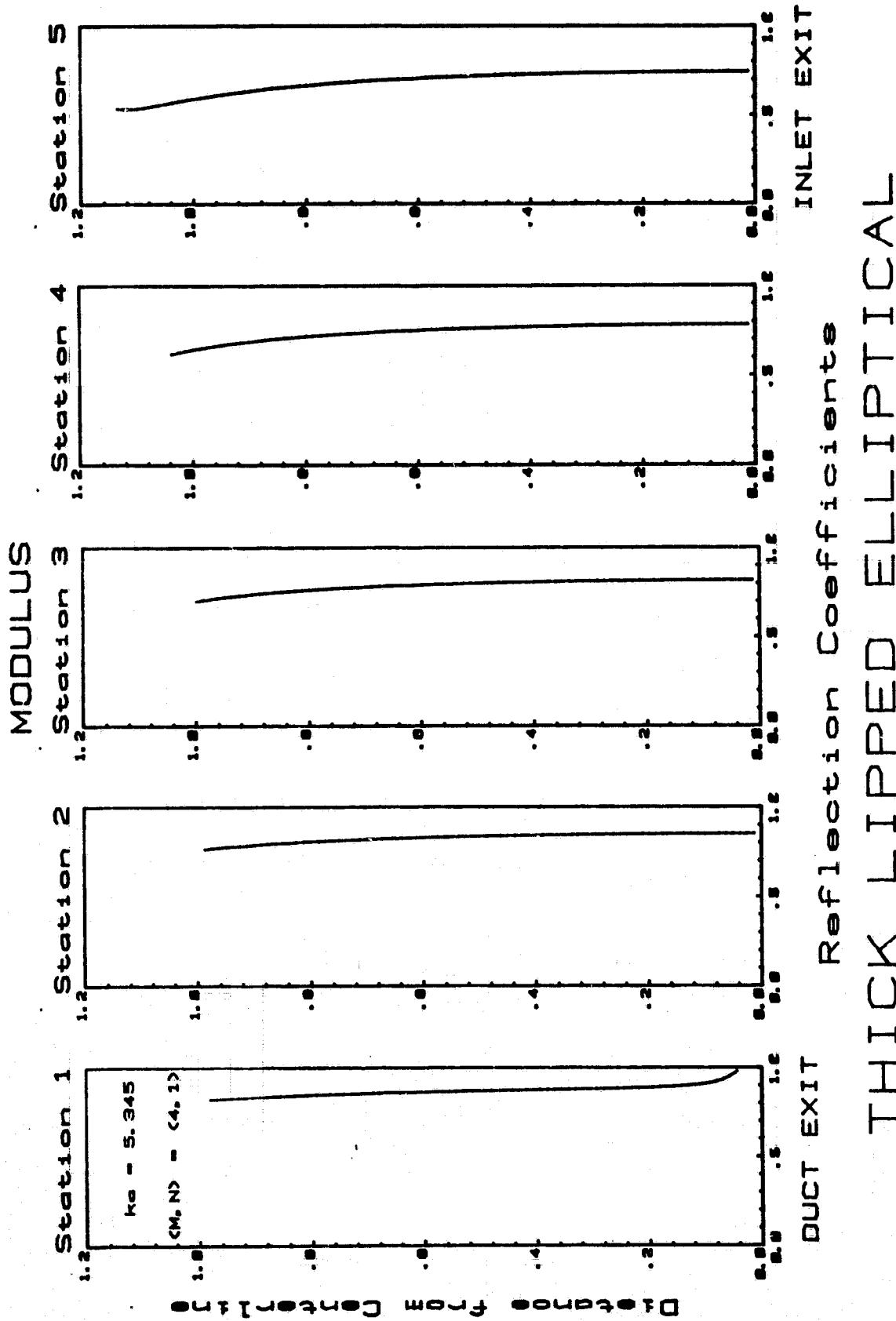


Fig. 46a

ORIGINAL PAGE IS
OF POOR QUALITY

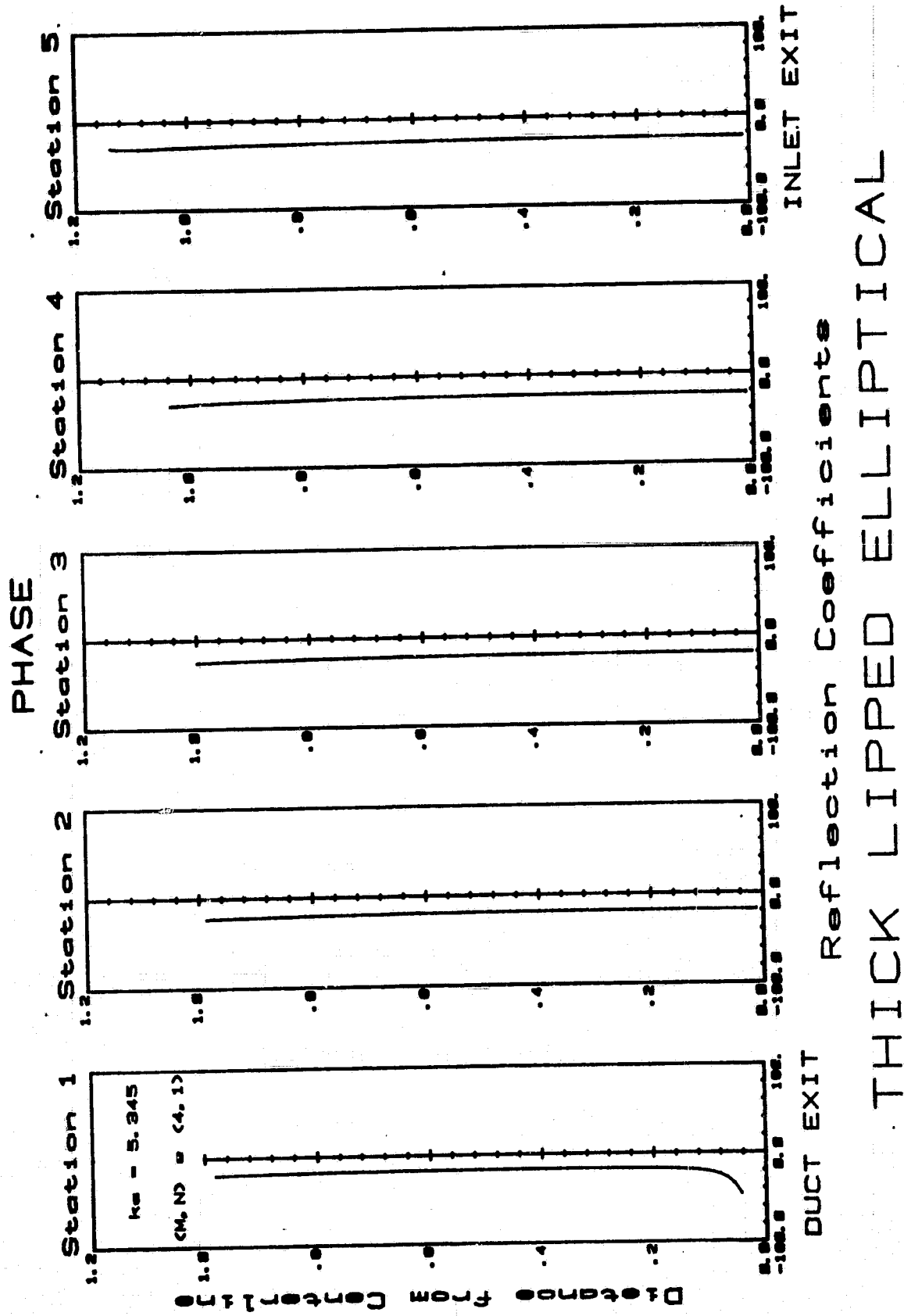
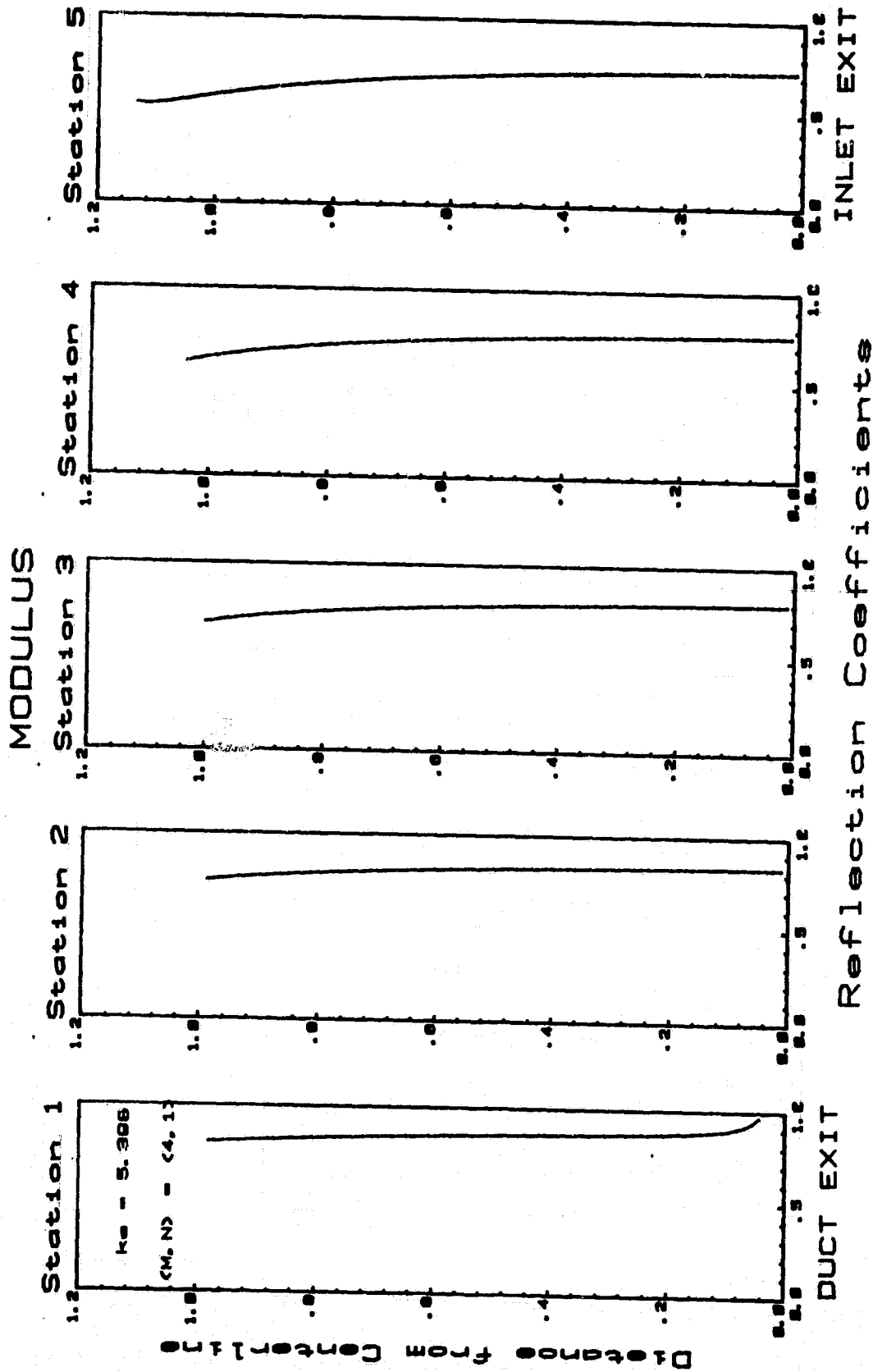


Fig. 46b



THICK LIPPED ELLIPTICAL

Fig. 46c

ORIGINAL PAGE 19
OF POOR QUALITY

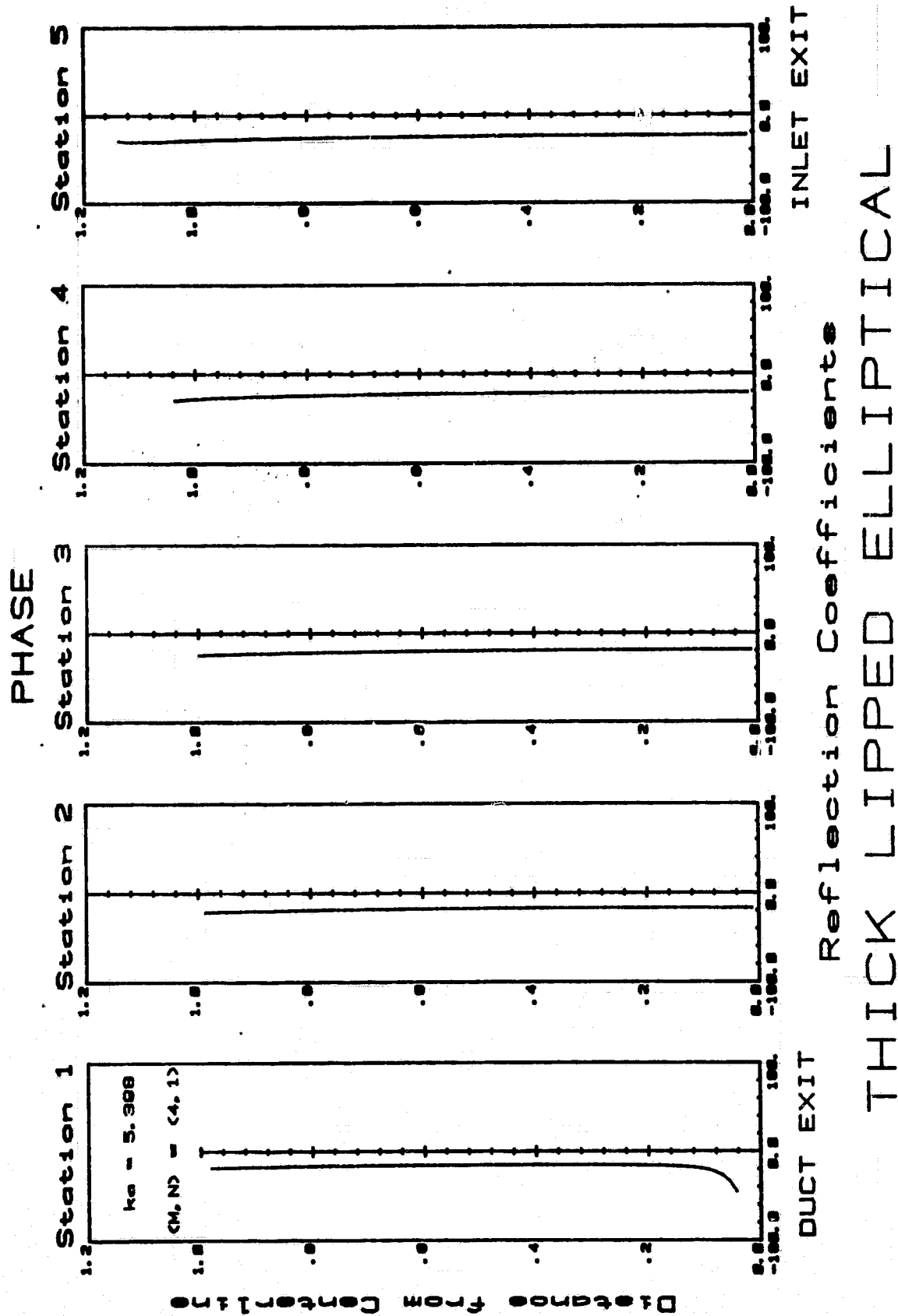


Fig. 46d

ORIGINAL PAGE IS
OF POOR QUALITY

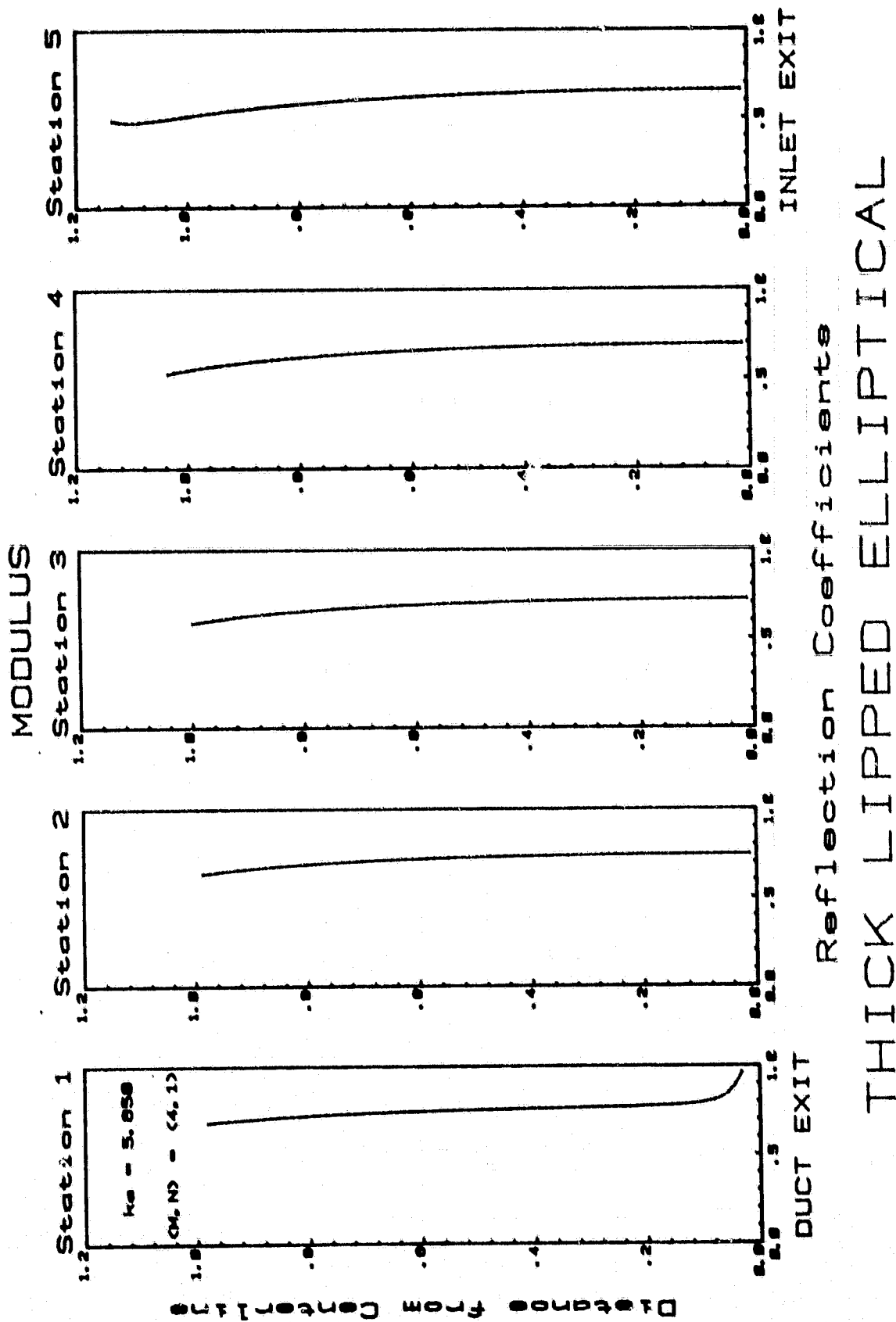


Fig. 46e

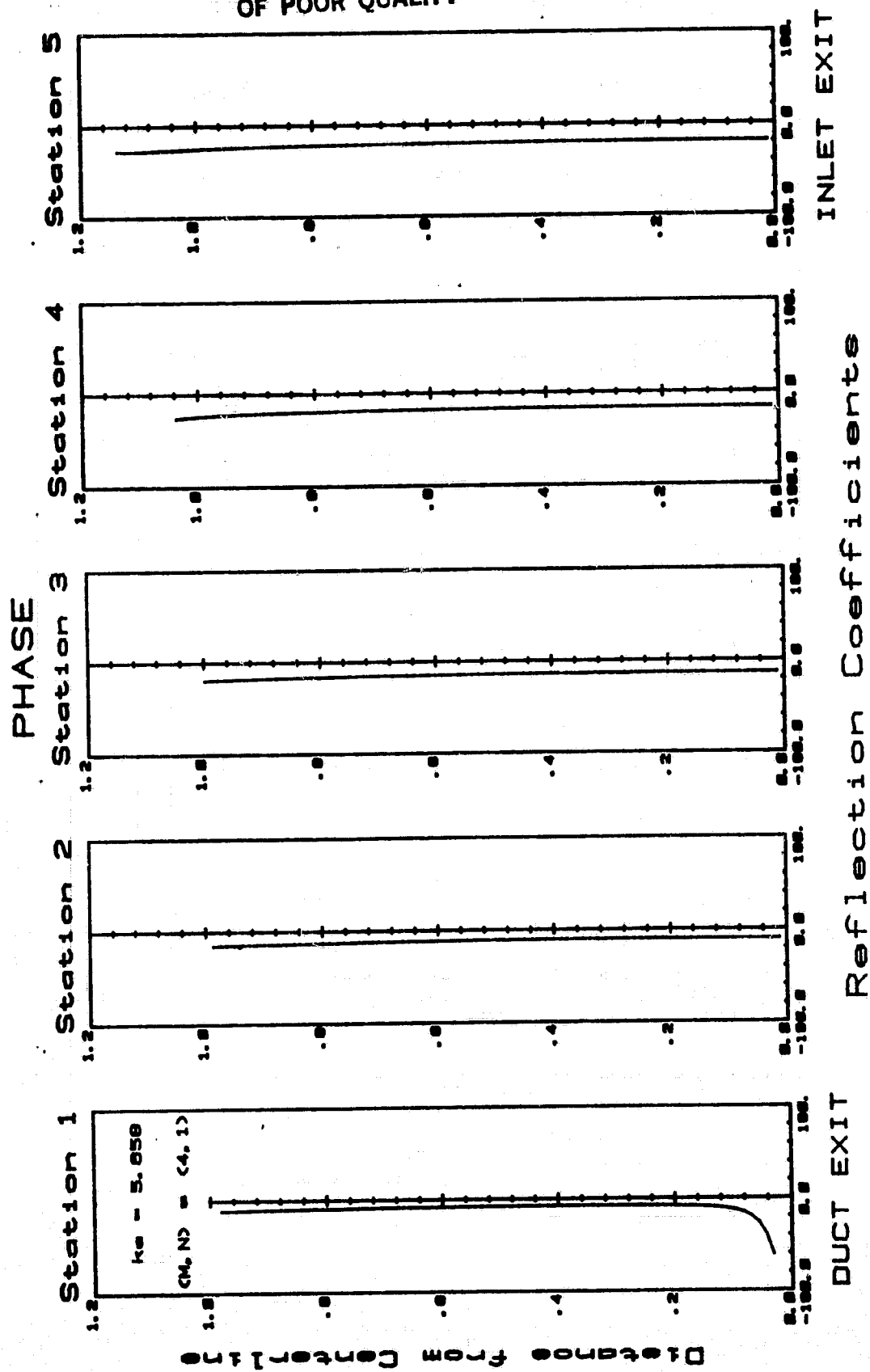


Fig. 46f

MODULUS

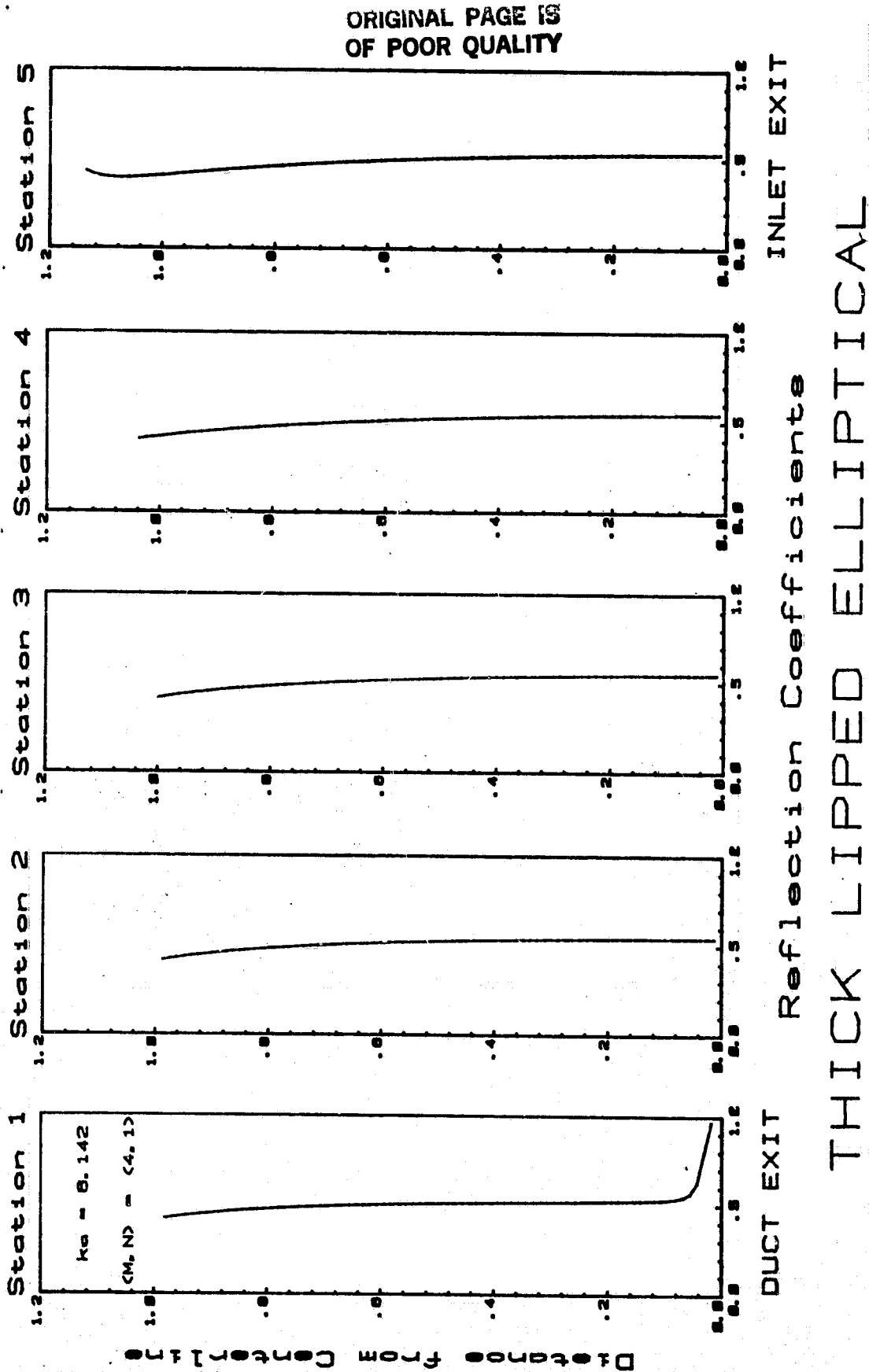


Fig. 46g

ORIGINAL PAGE IS
OF POOR QUALITY

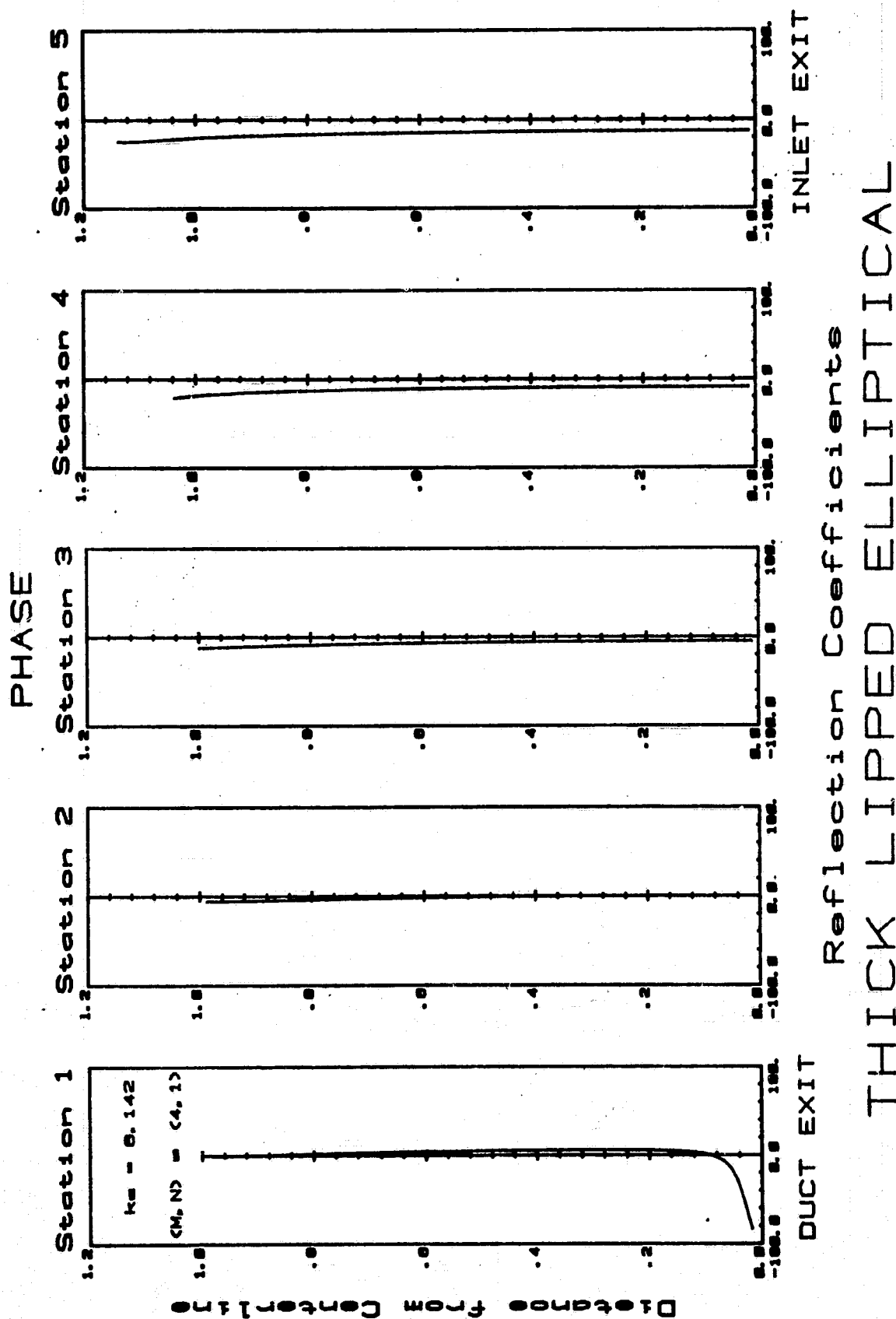


Fig. 46h

ORIGINAL PAGE IS
OF POOR QUALITY

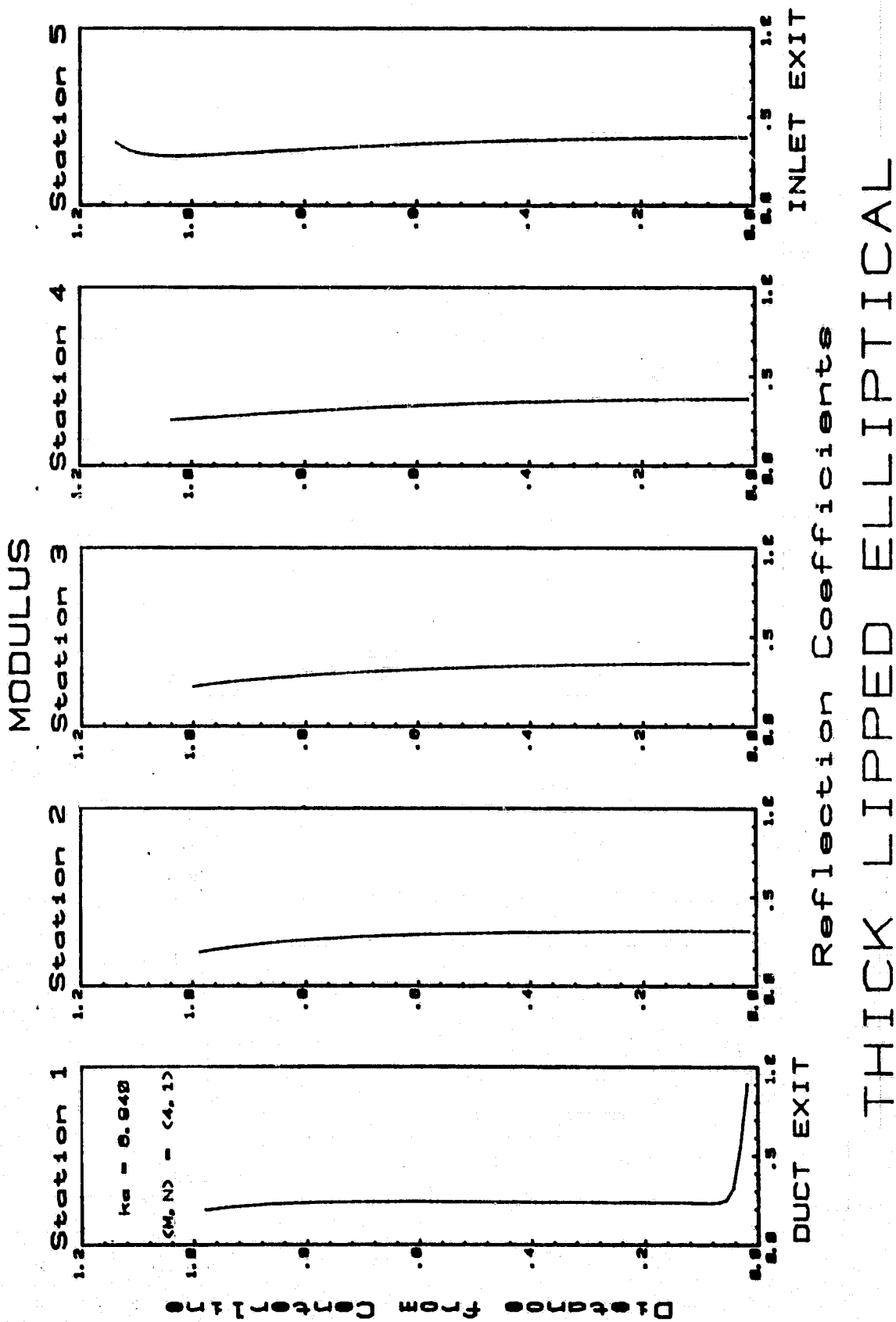
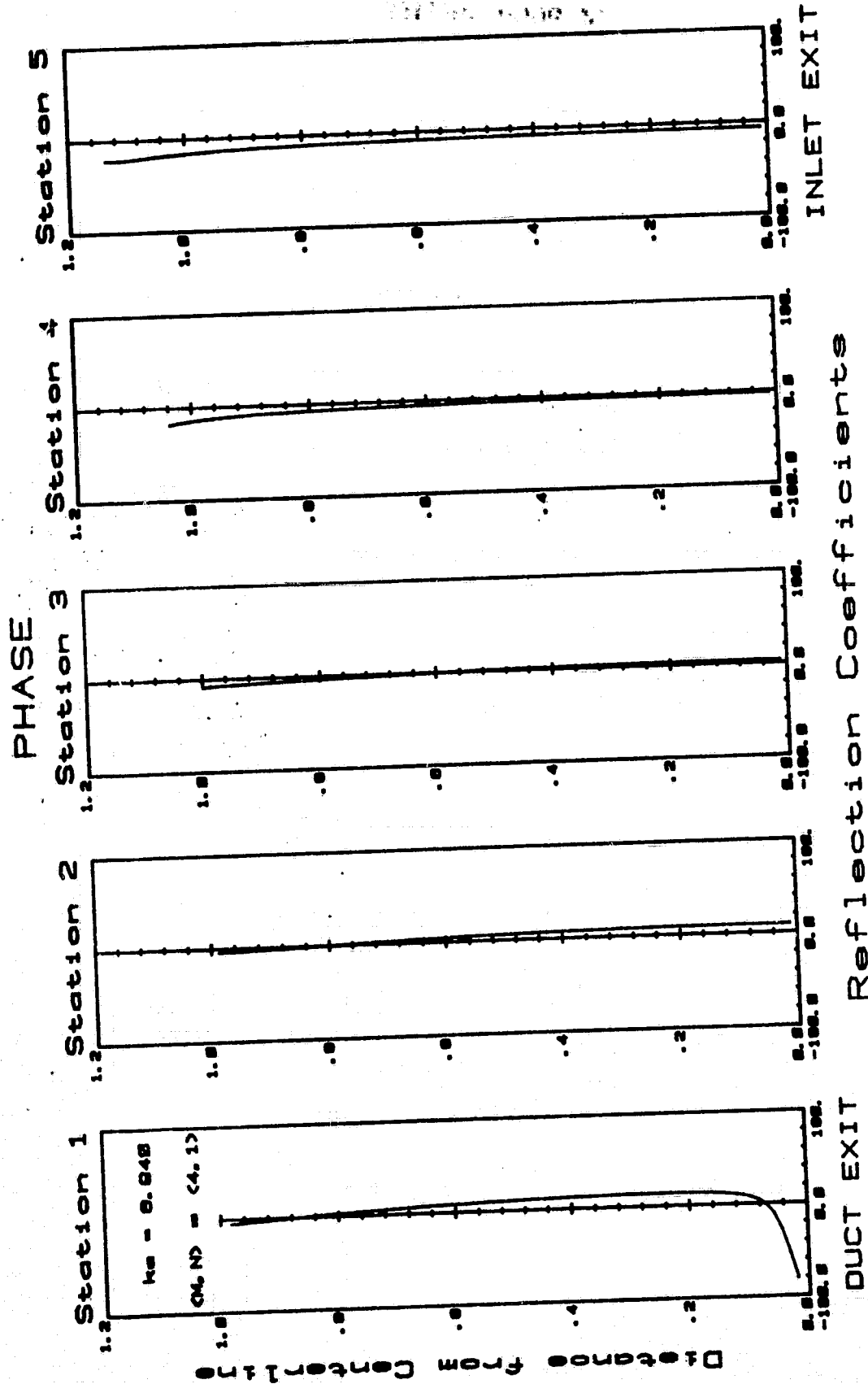


Fig. 46i

ORIGINAL PAGE IS
OF POOR QUALITY



THICK LIPPED ELLIPTICAL

Fig. 46j

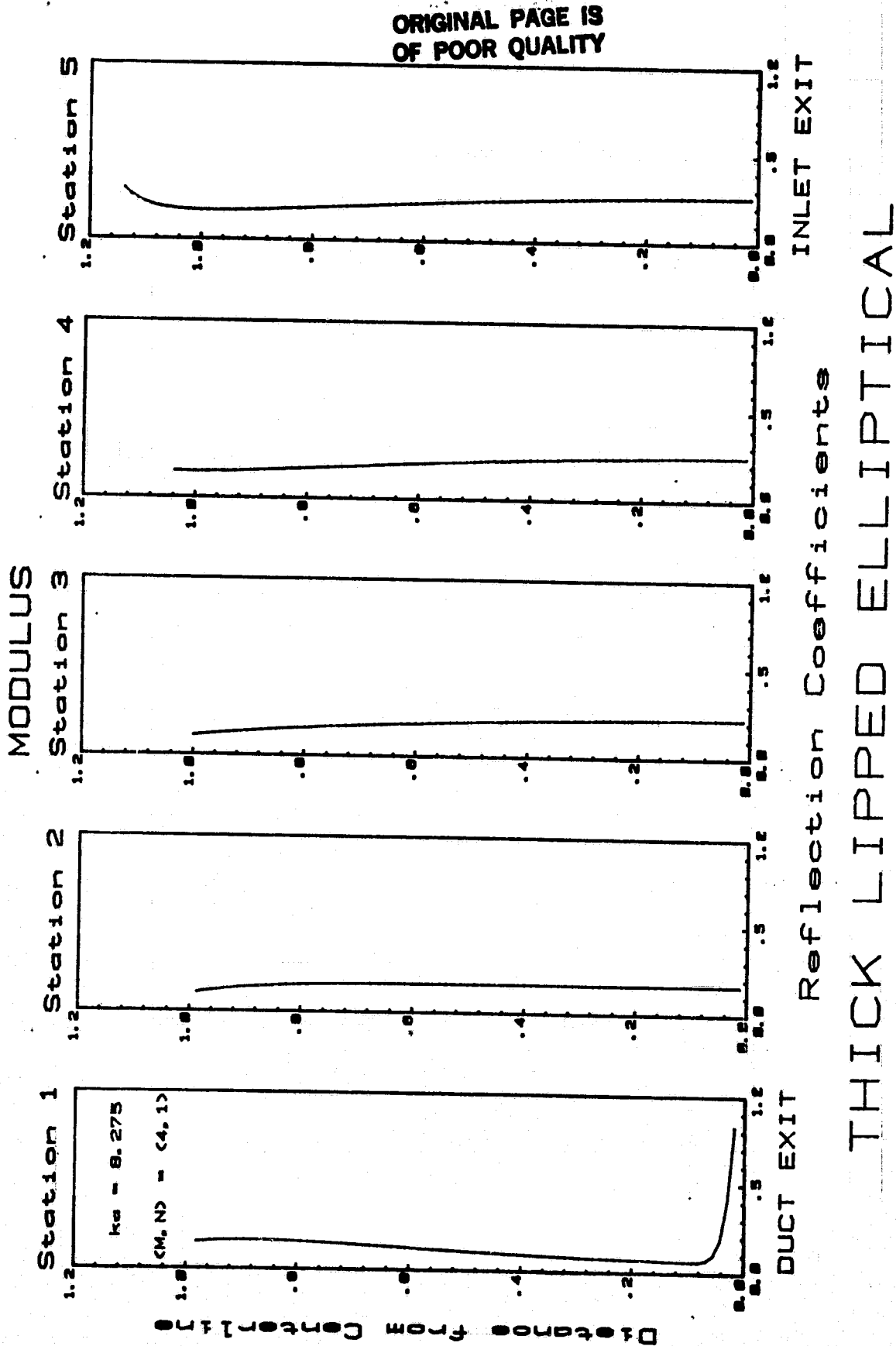
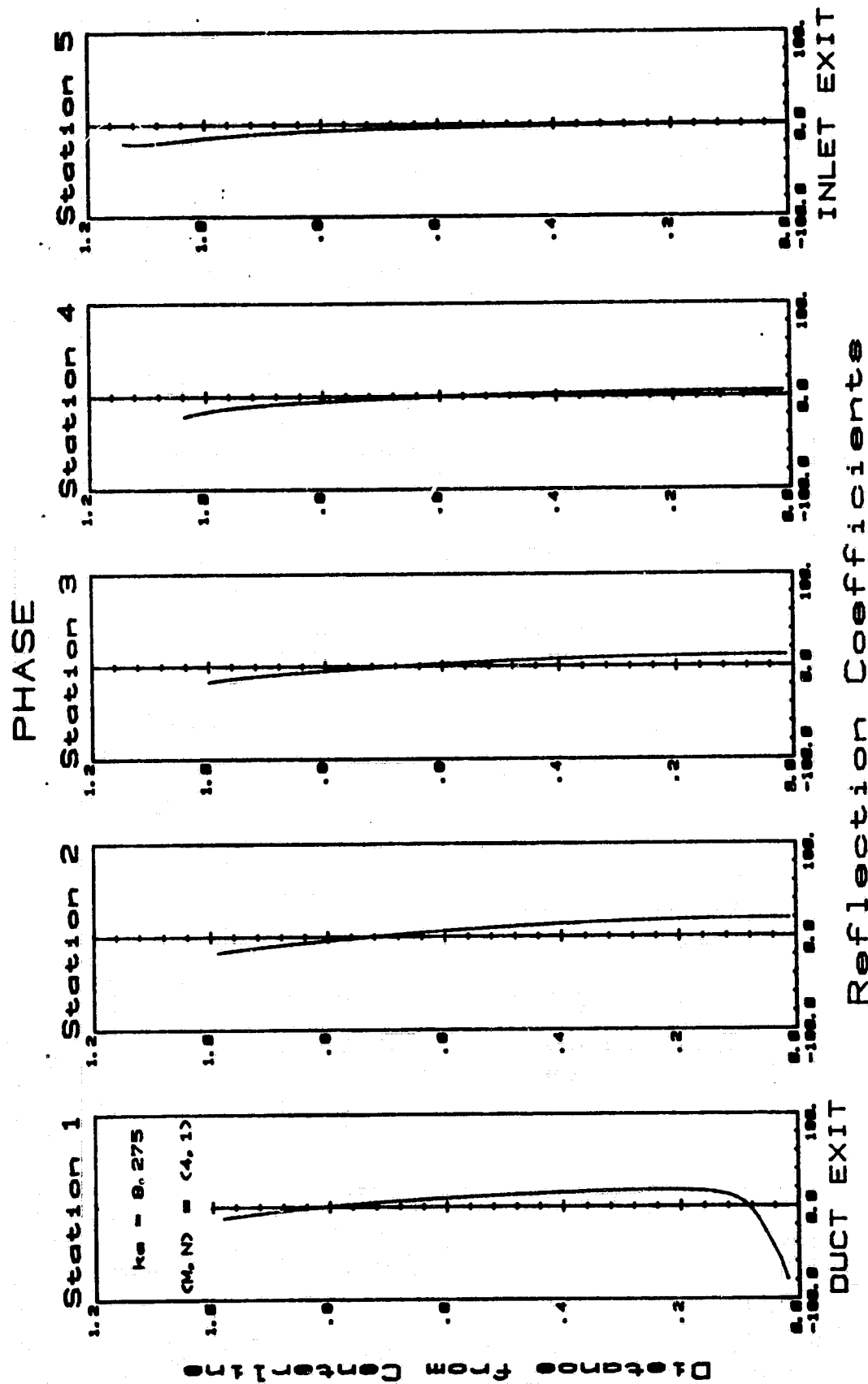


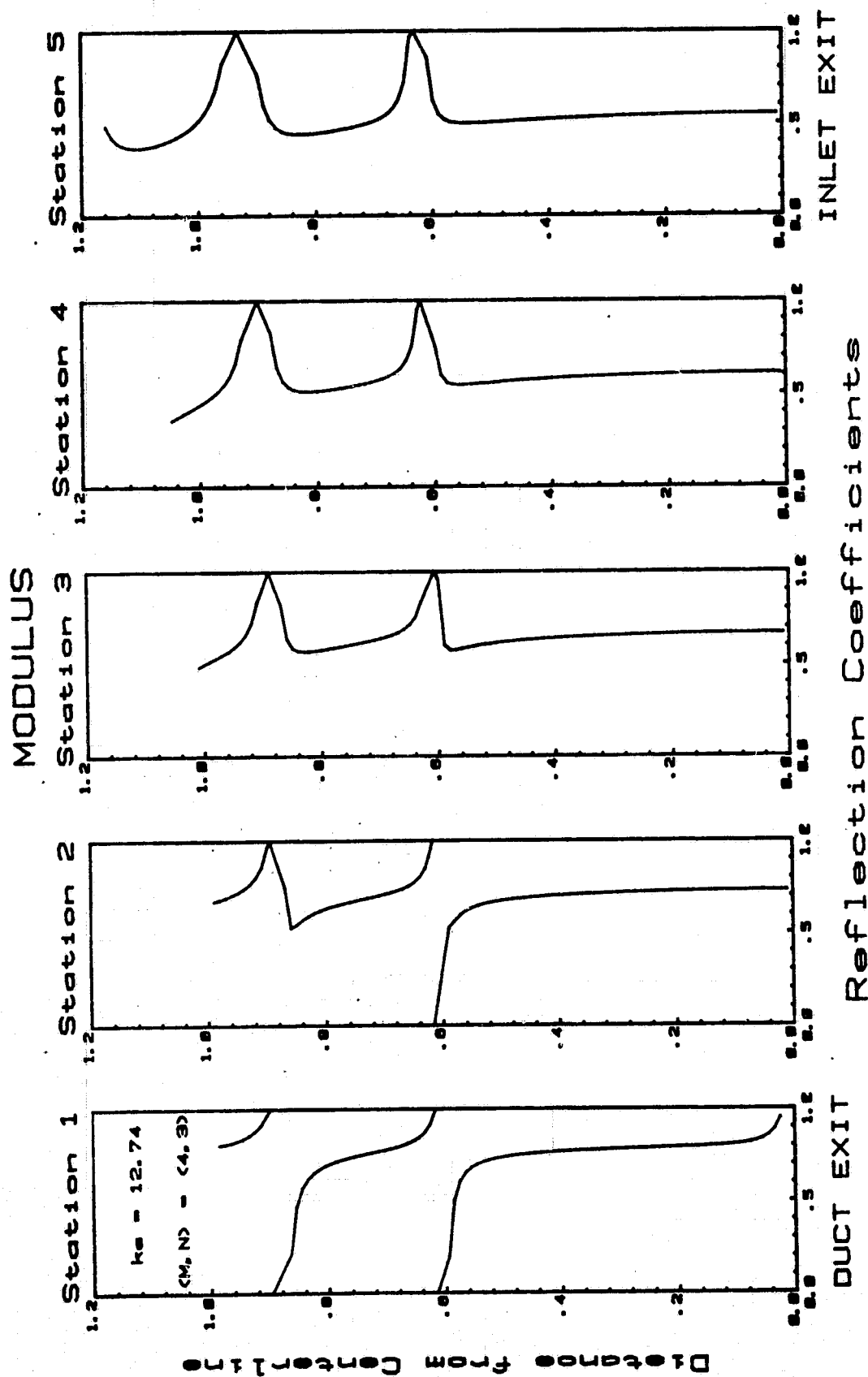
Fig. 46k



THICK LIPPED ELLIPTICAL

Fig. 461

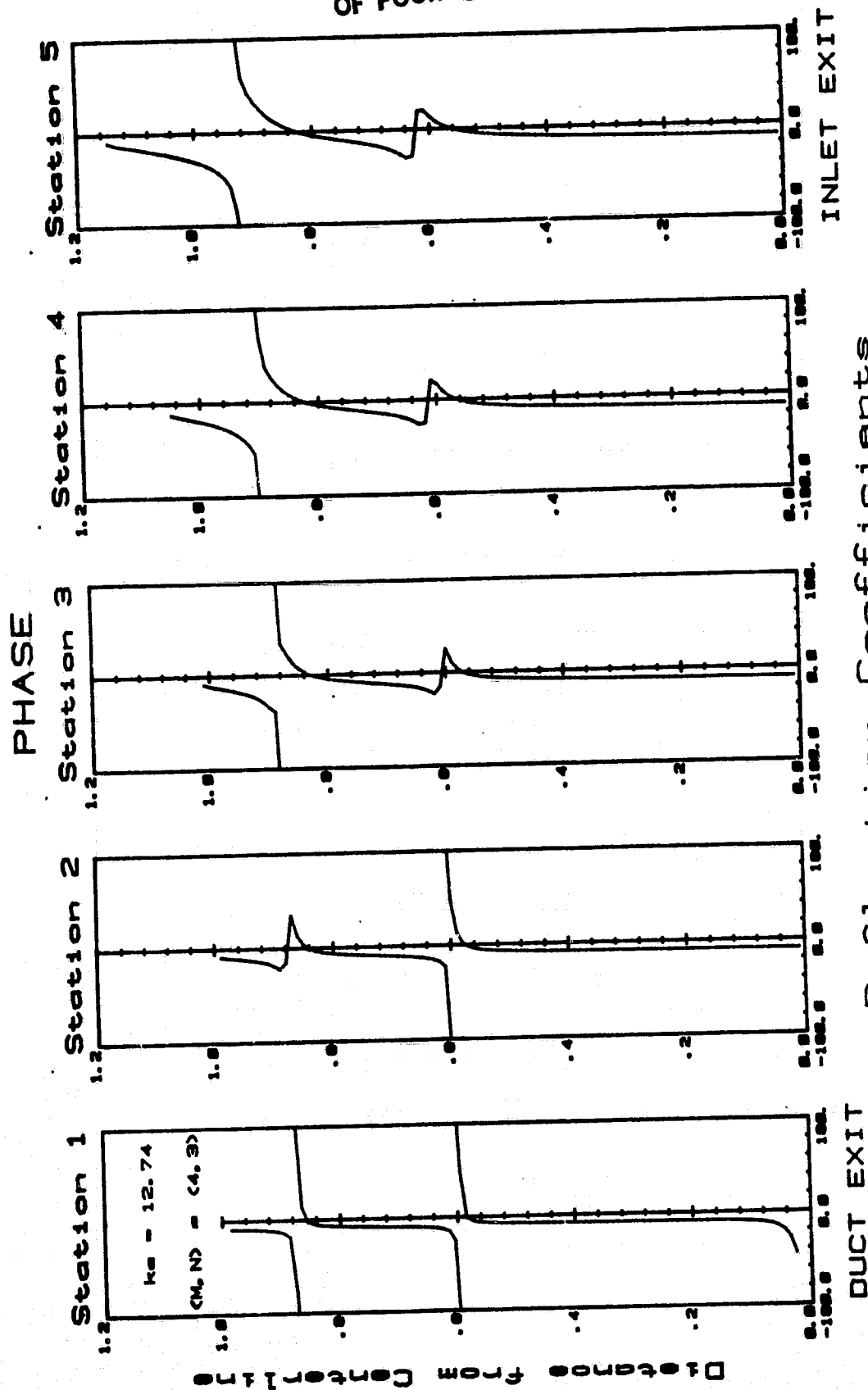
ORIGINAL PAGE IS
OF POOR QUALITY



THICK LIPPED ELLIPTICAL

Fig. 47a

ORIGINAL PAGE IS
OF POOR QUALITY



THICK LIPPED ELLIPTICAL

Fig. 47b

ORIGINAL PAGE IS
OF POOR QUALITY

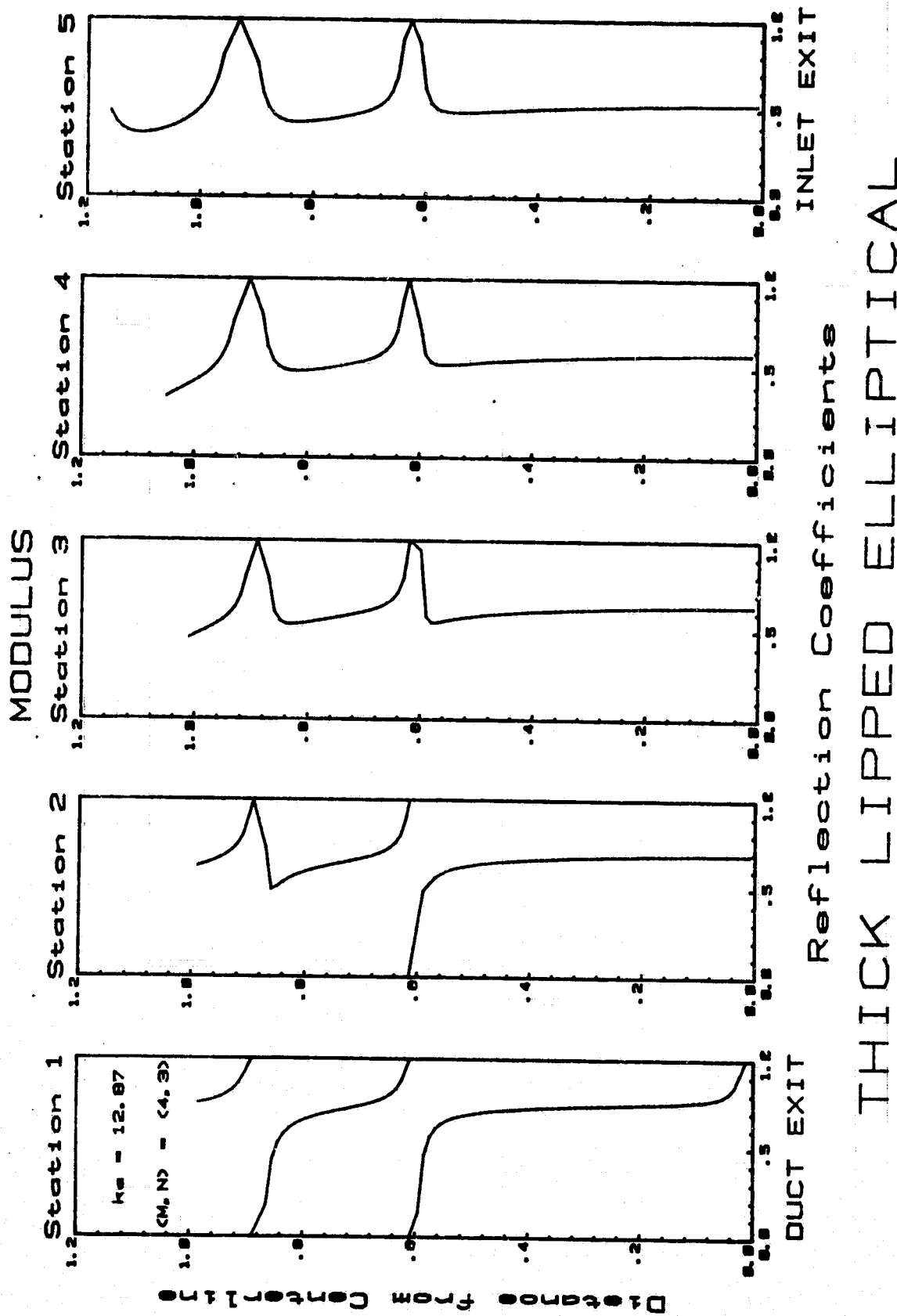


Fig. 47c

ORIGINAL PAGE IS
OF POOR QUALITY

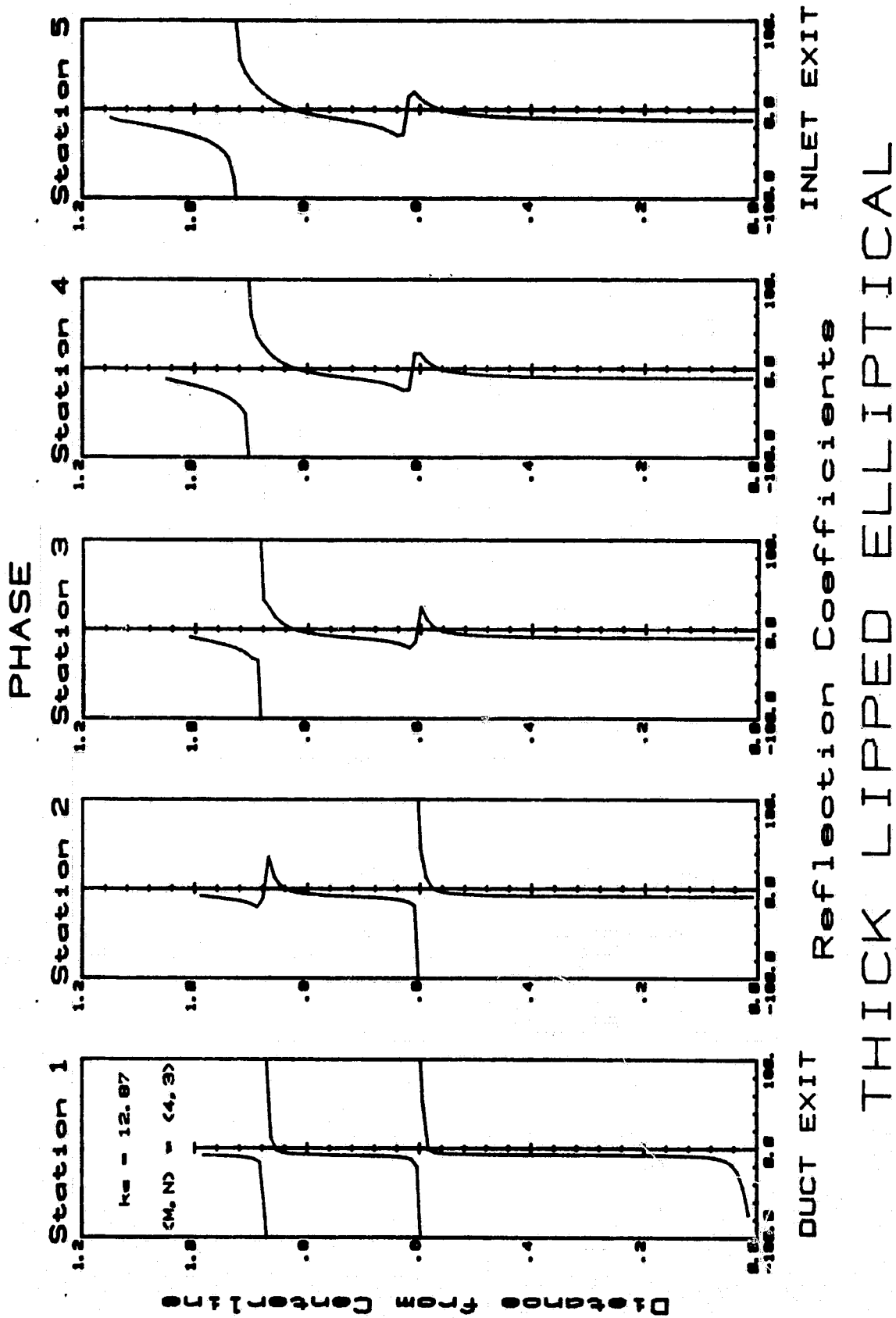
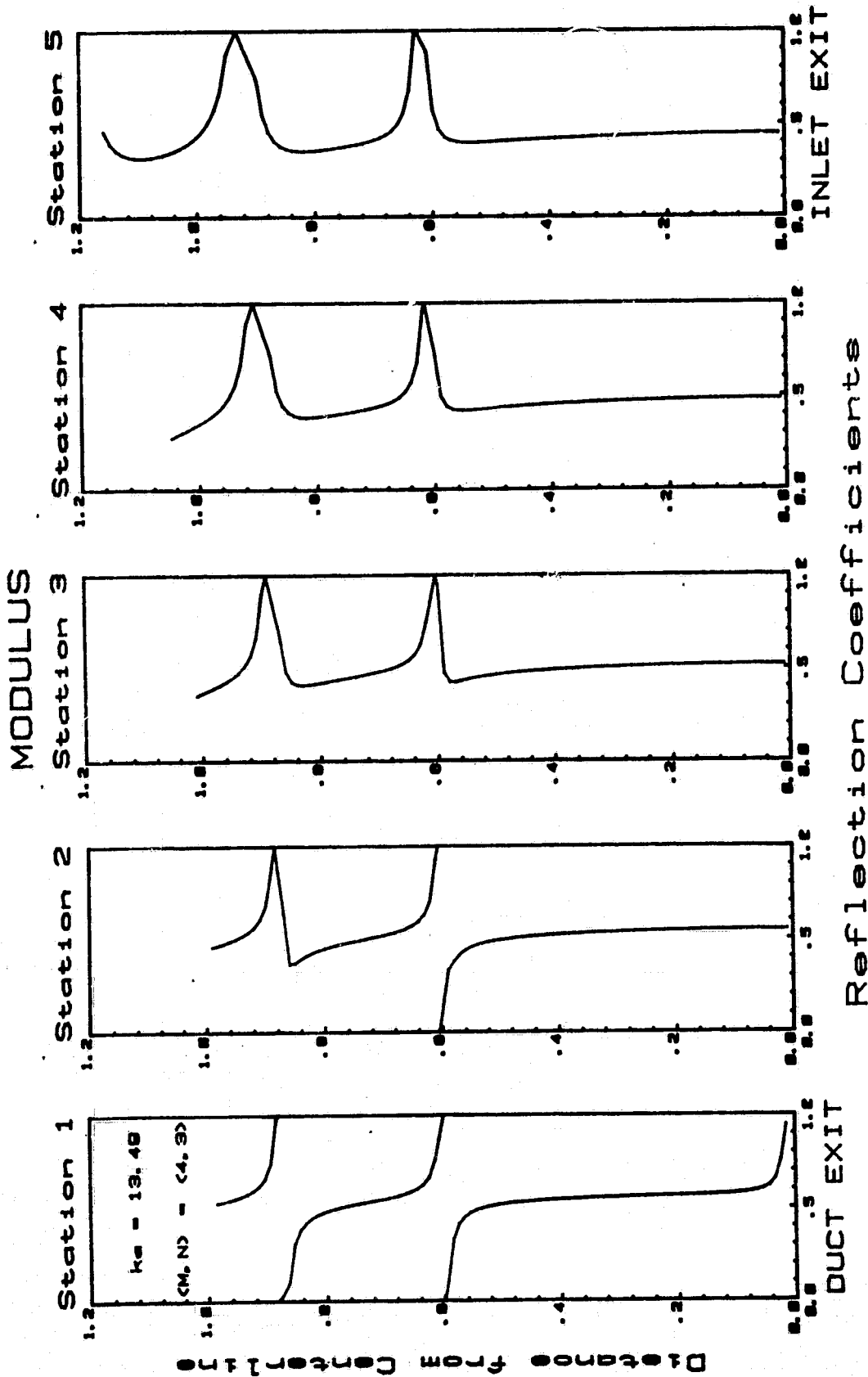


Fig. 47d

ORIGINAL PAGE IS
OF POOR QUALITY



THICK LIPPED ELLIPTICAL

Fig. 47e

ORIGINAL PAGE IS
OF POOR QUALITY

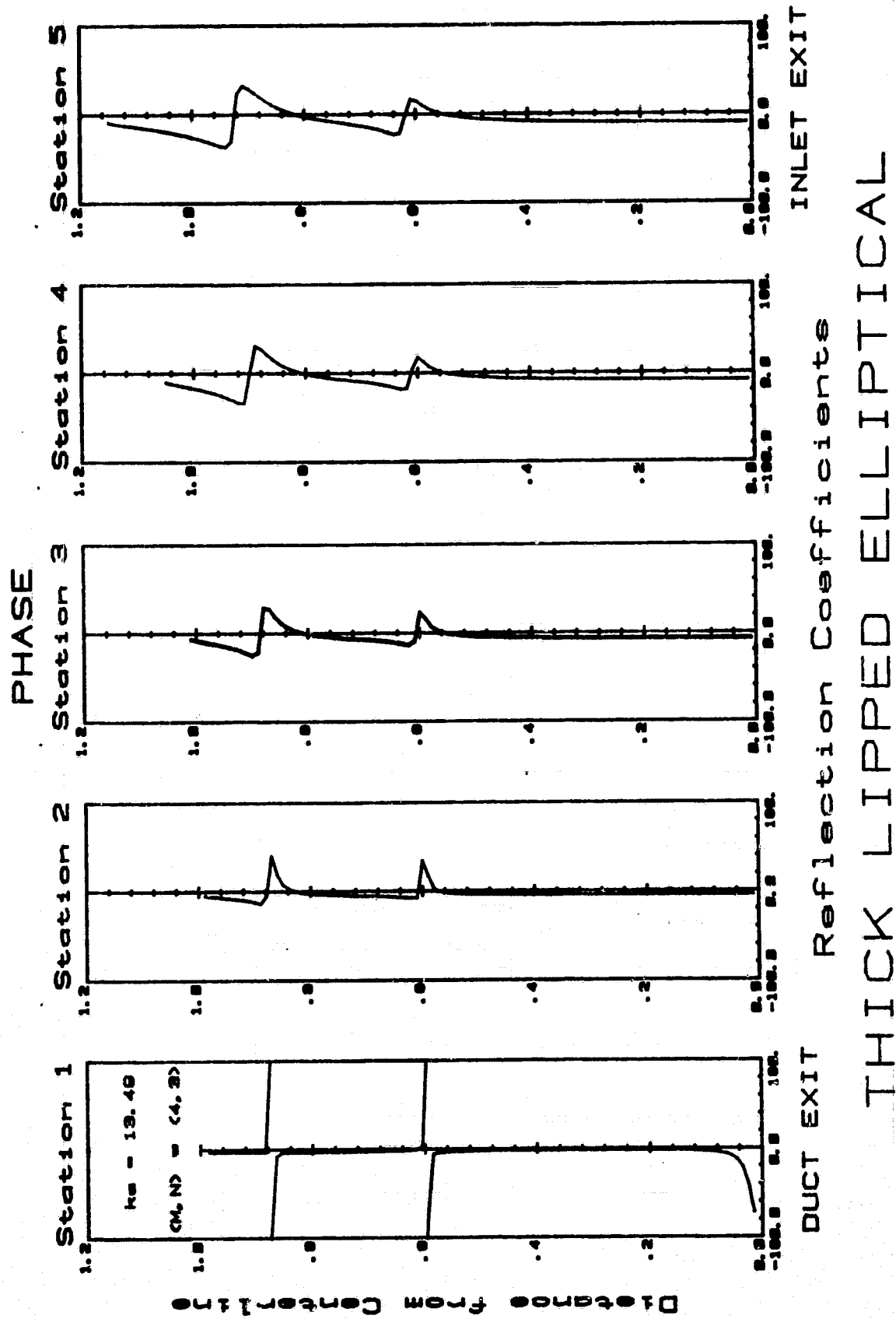


Fig. 47f

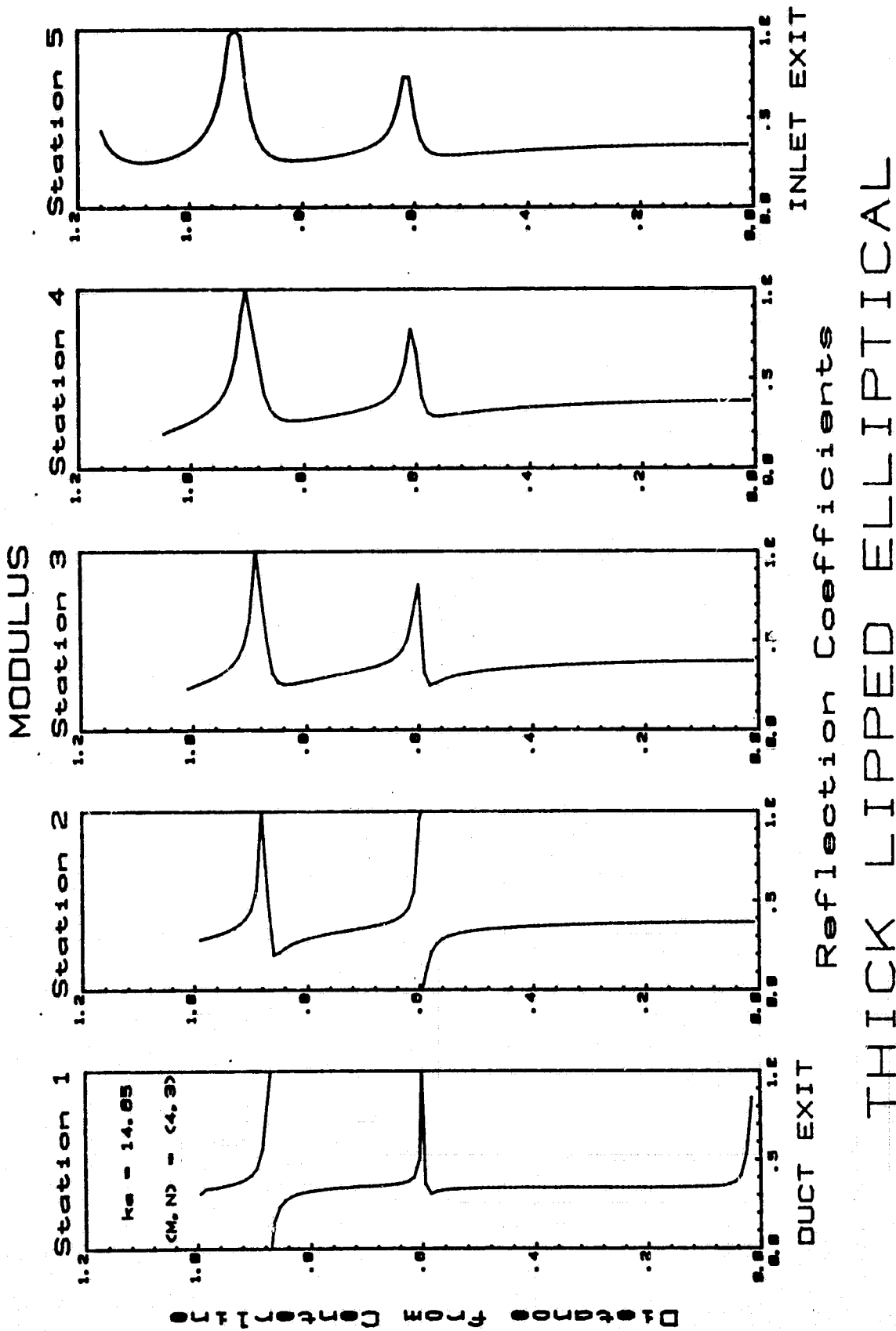


Fig. 47g

ORIGINAL PAGE 13.
OF POOR QUALITY

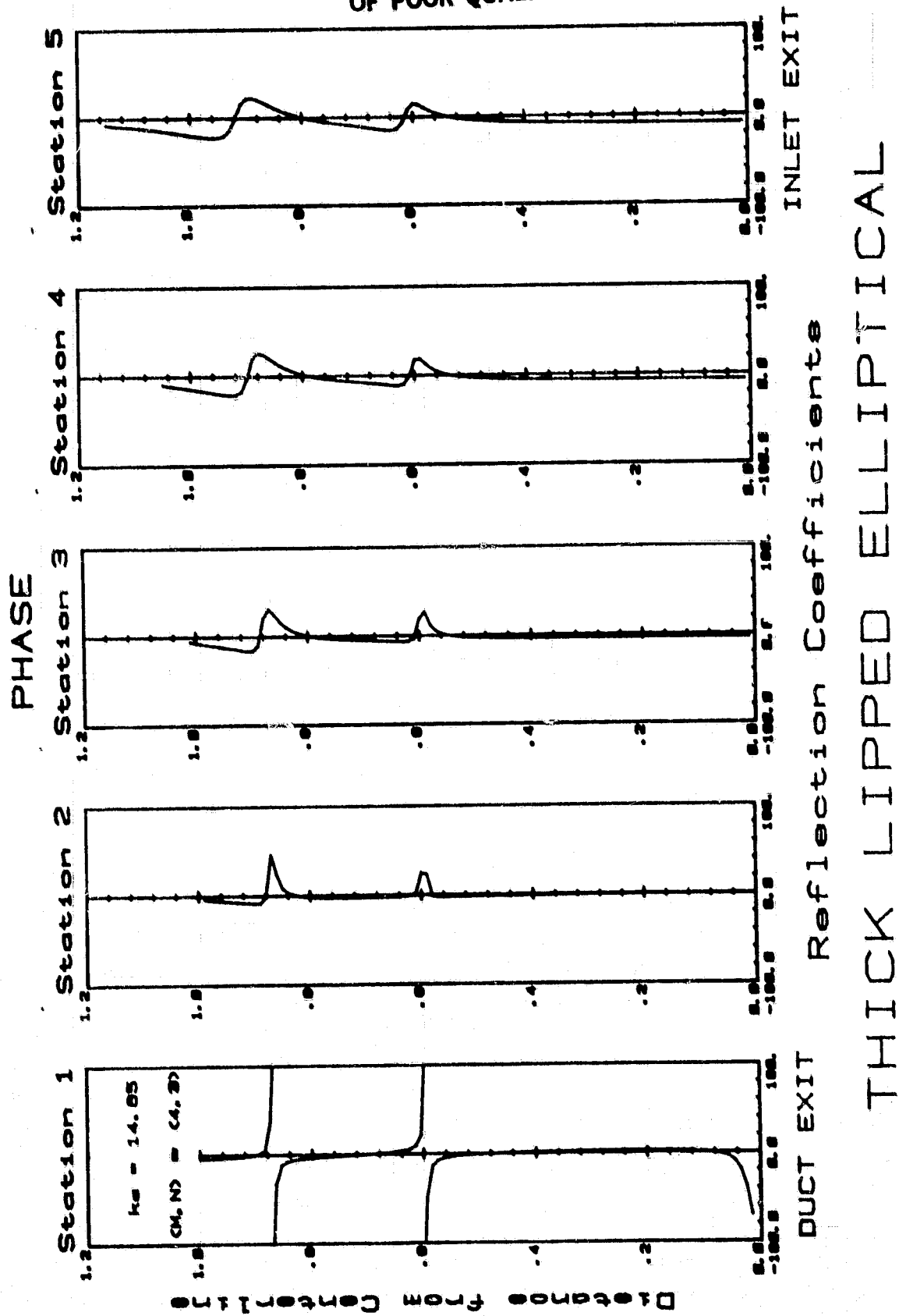


Fig. 47h

ORIGINAL PAGE IS
OF POOR QUALITY

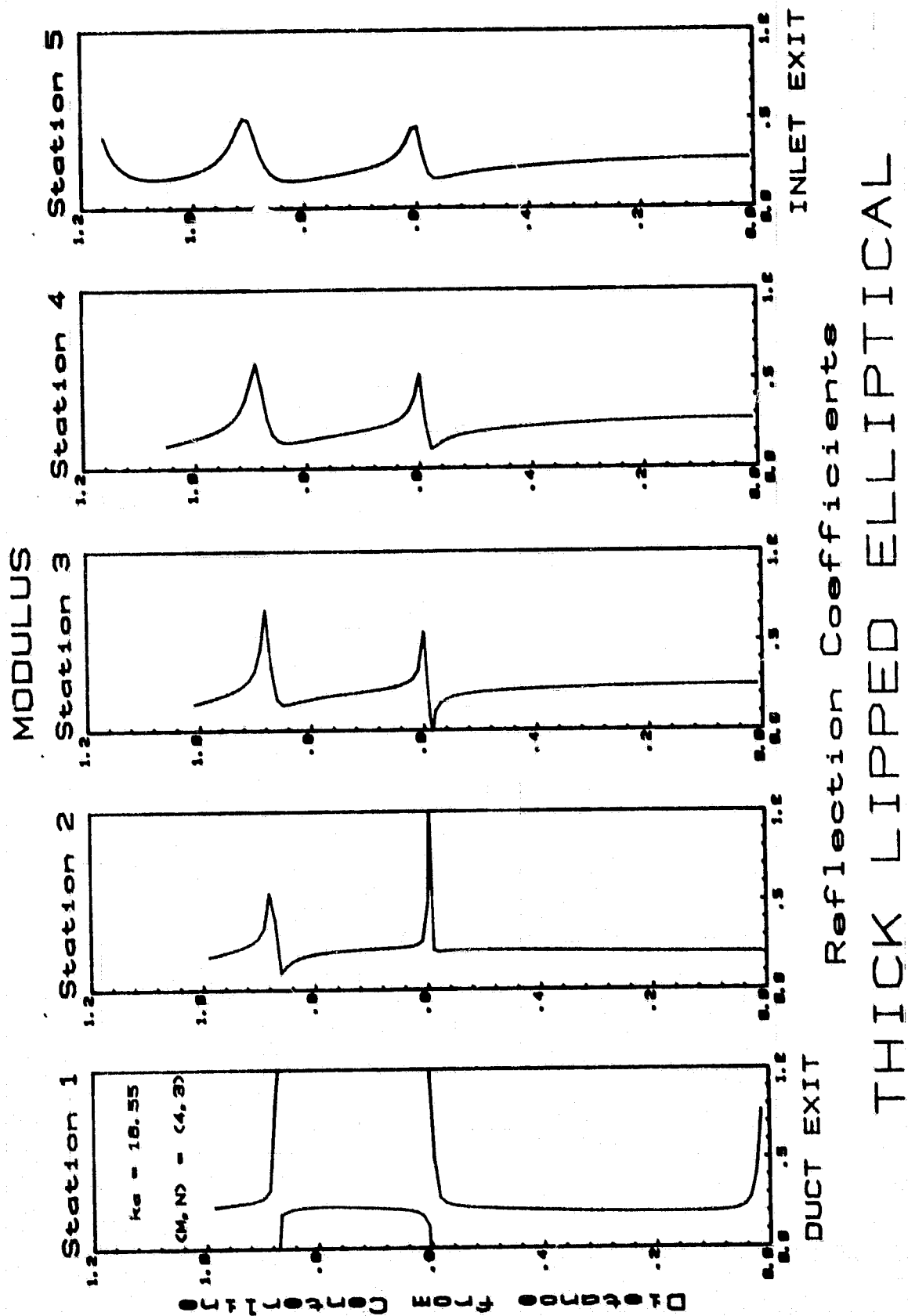


Fig. 471

ORIGINAL PAGE IS
OF POOR QUALITY

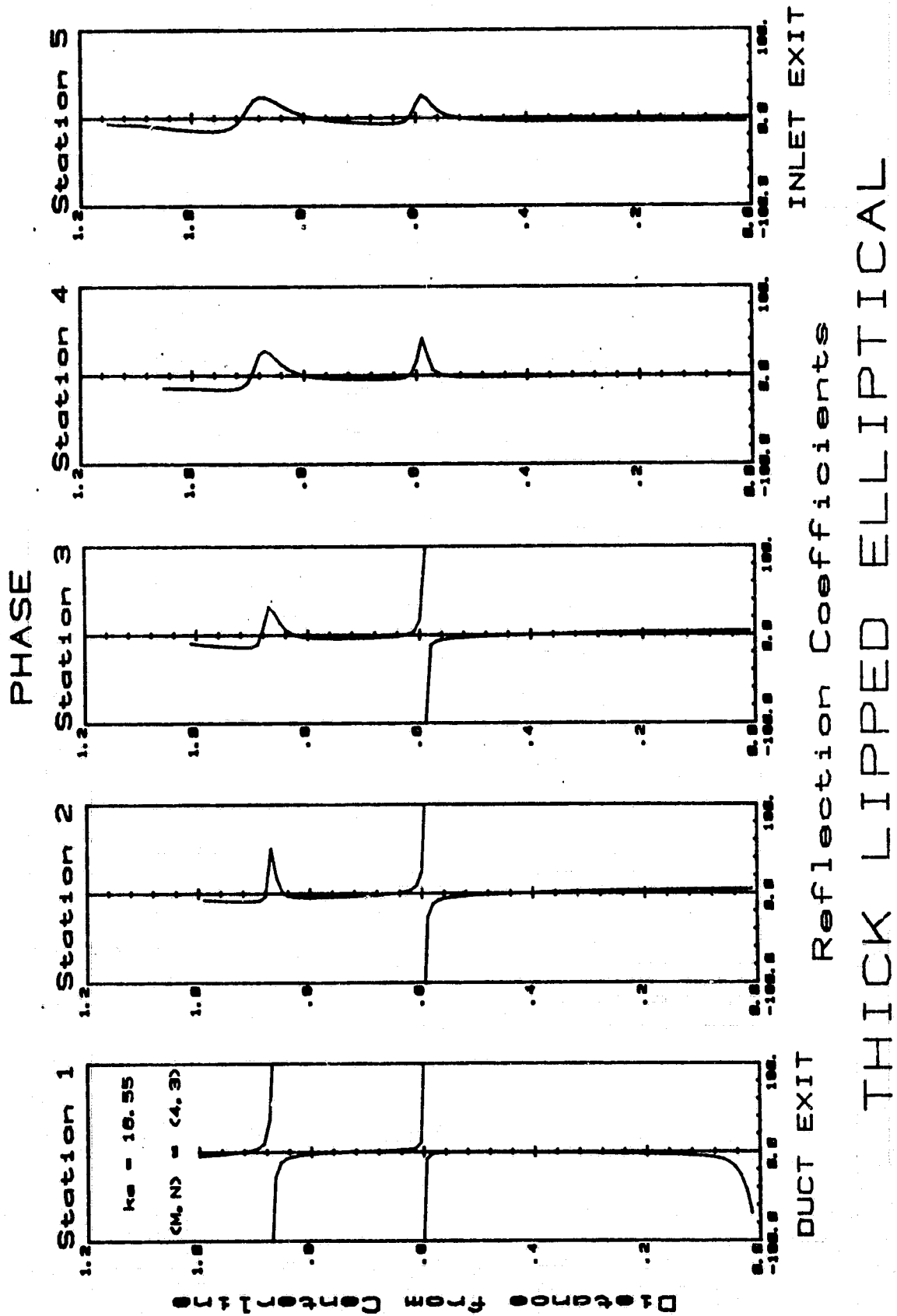


Fig. 47j

ORIGINAL PAGE IS
OF POOR QUALITY

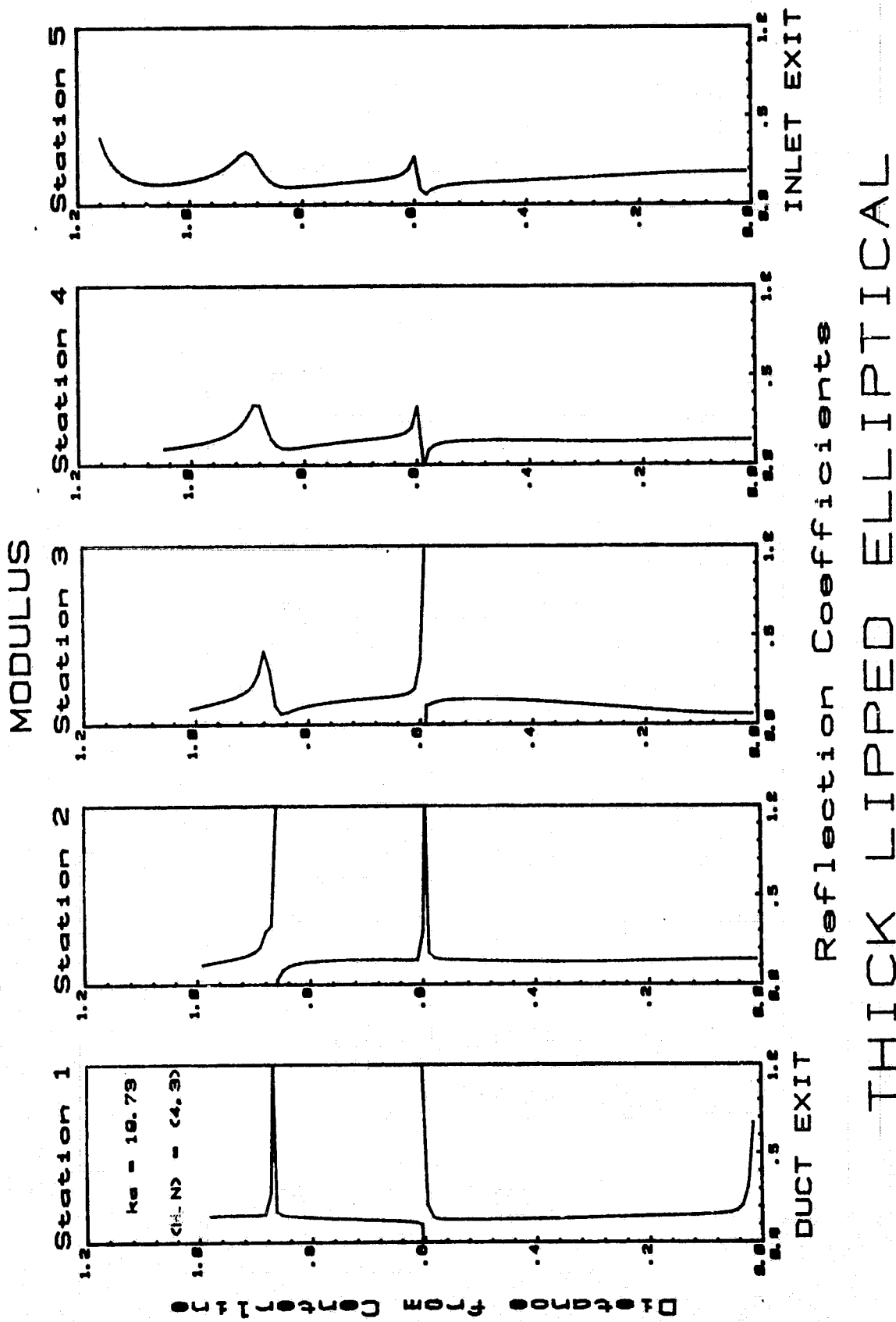


Fig. 47k

ORIGINAL PAGE IS
OF POOR QUALITY

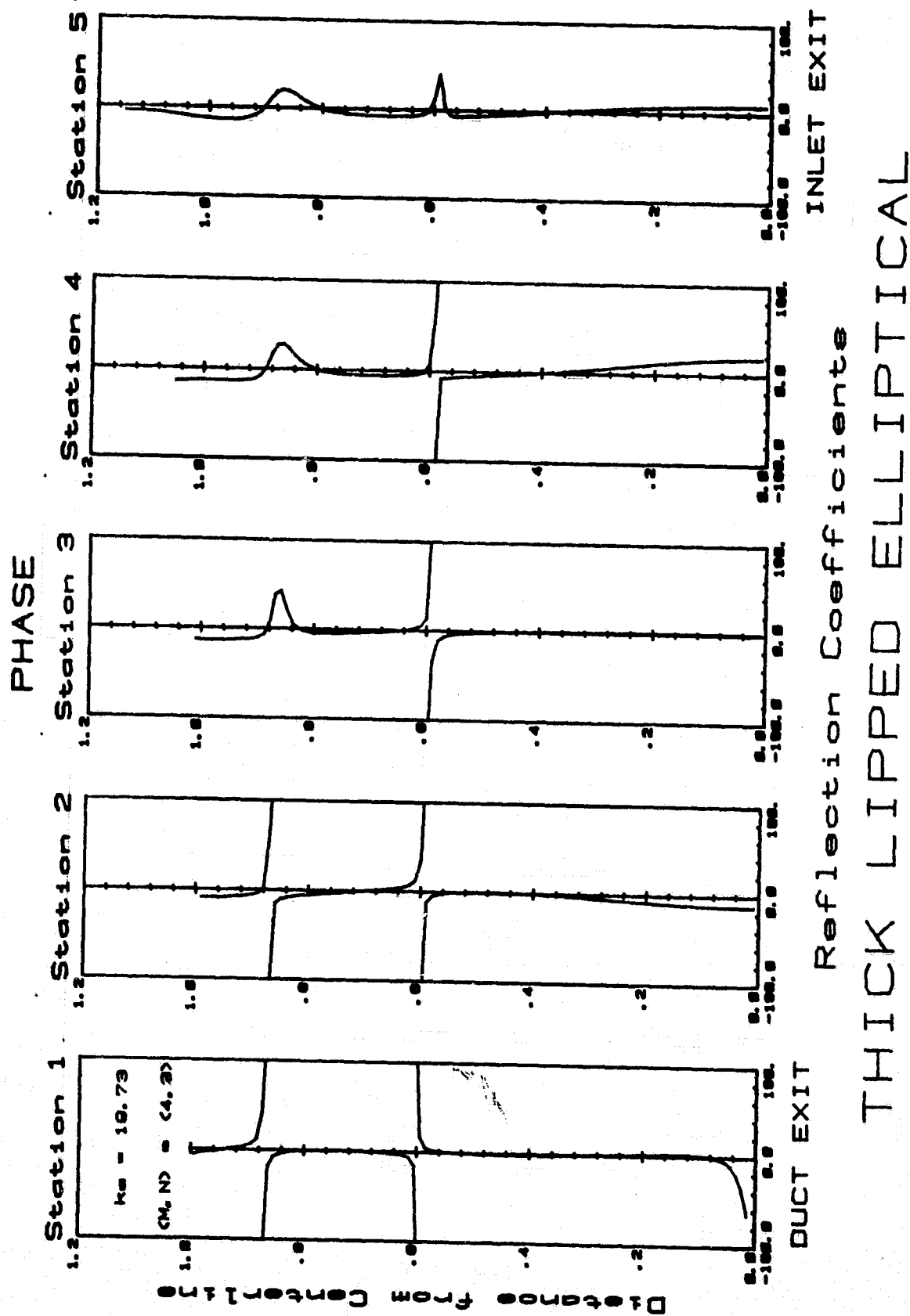


Fig. 471

ORIGINAL PAGE IS
OF POOR QUALITY

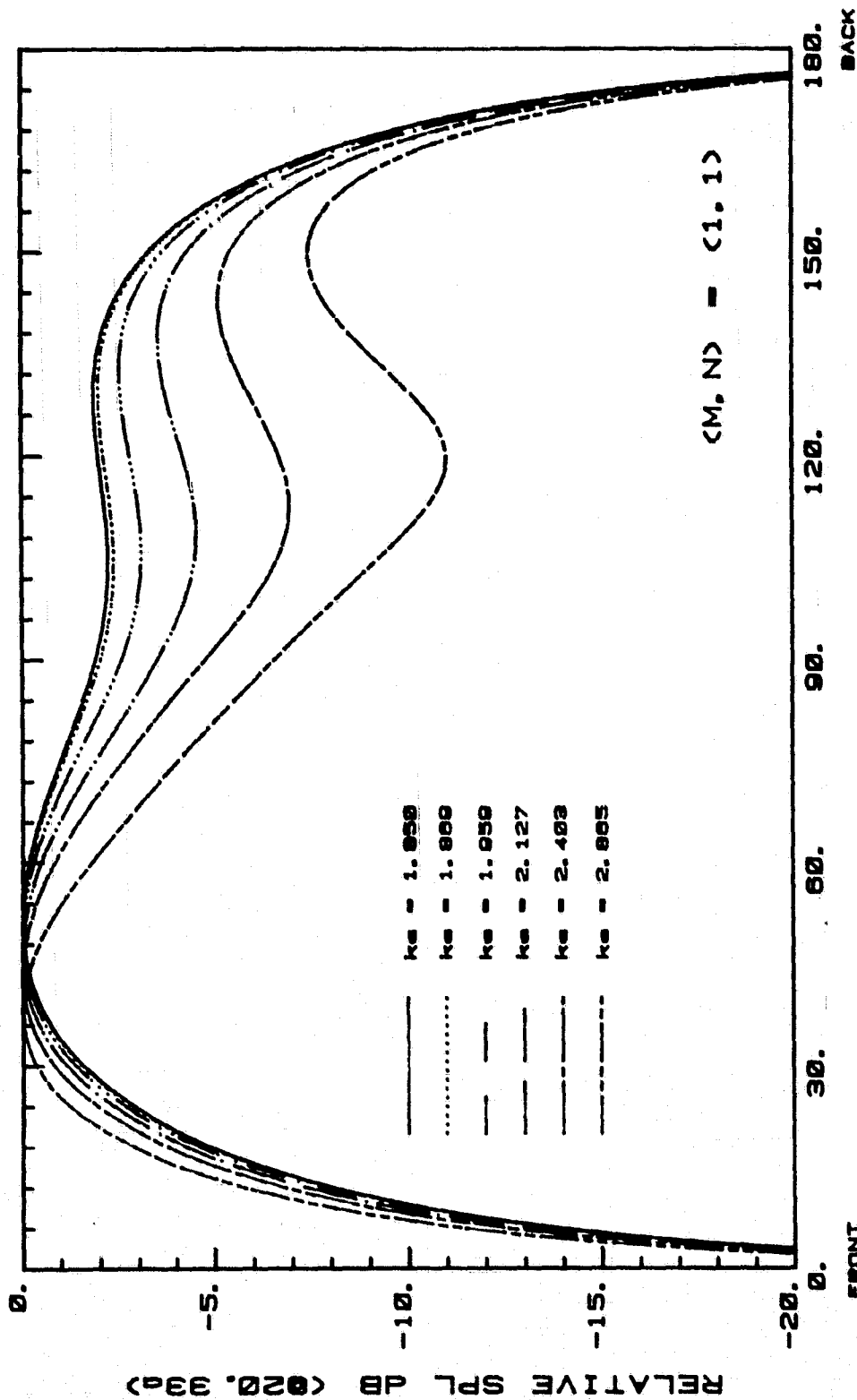
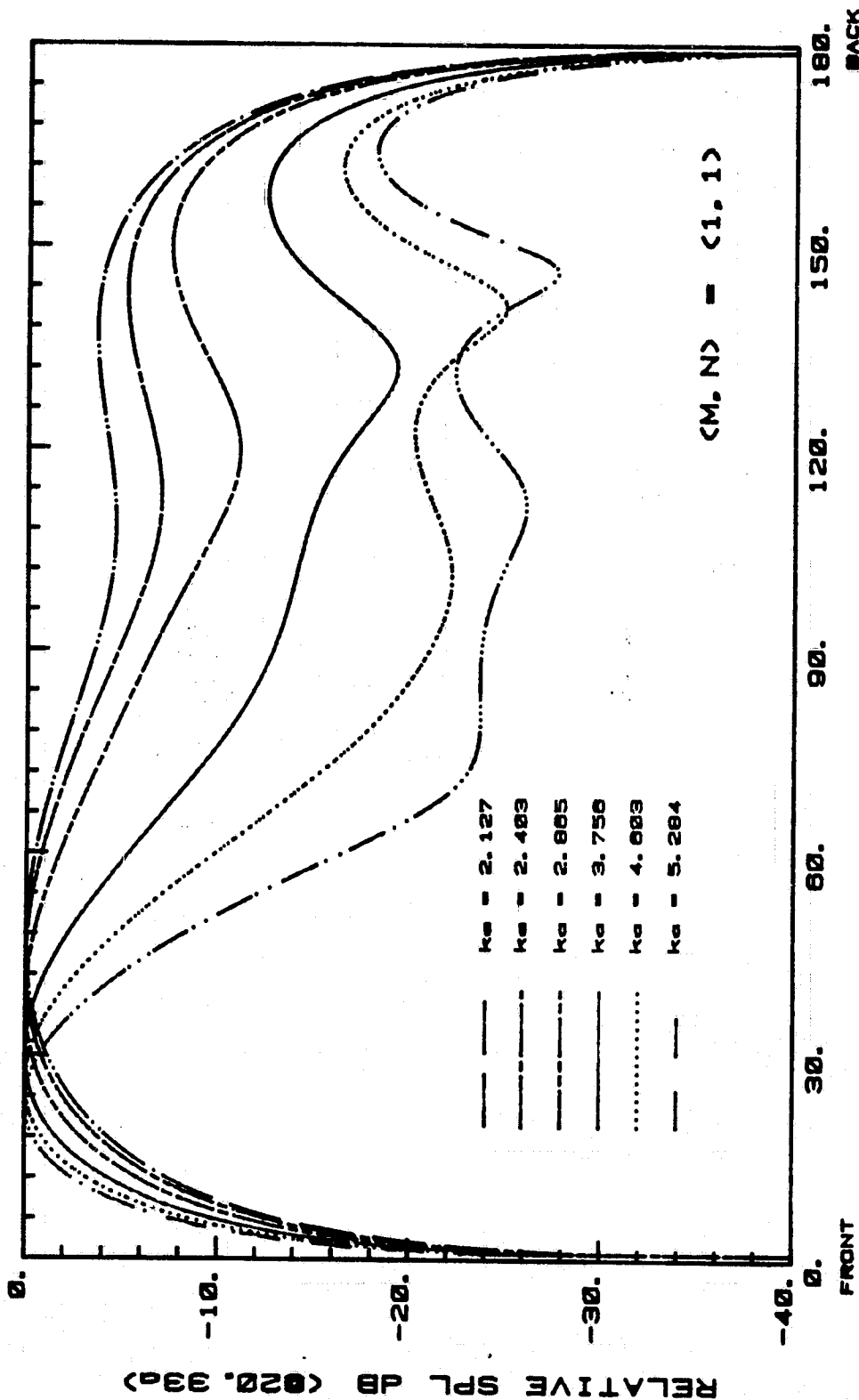


Fig. 48a

THICK LIPPED ELLIPTICAL INLET

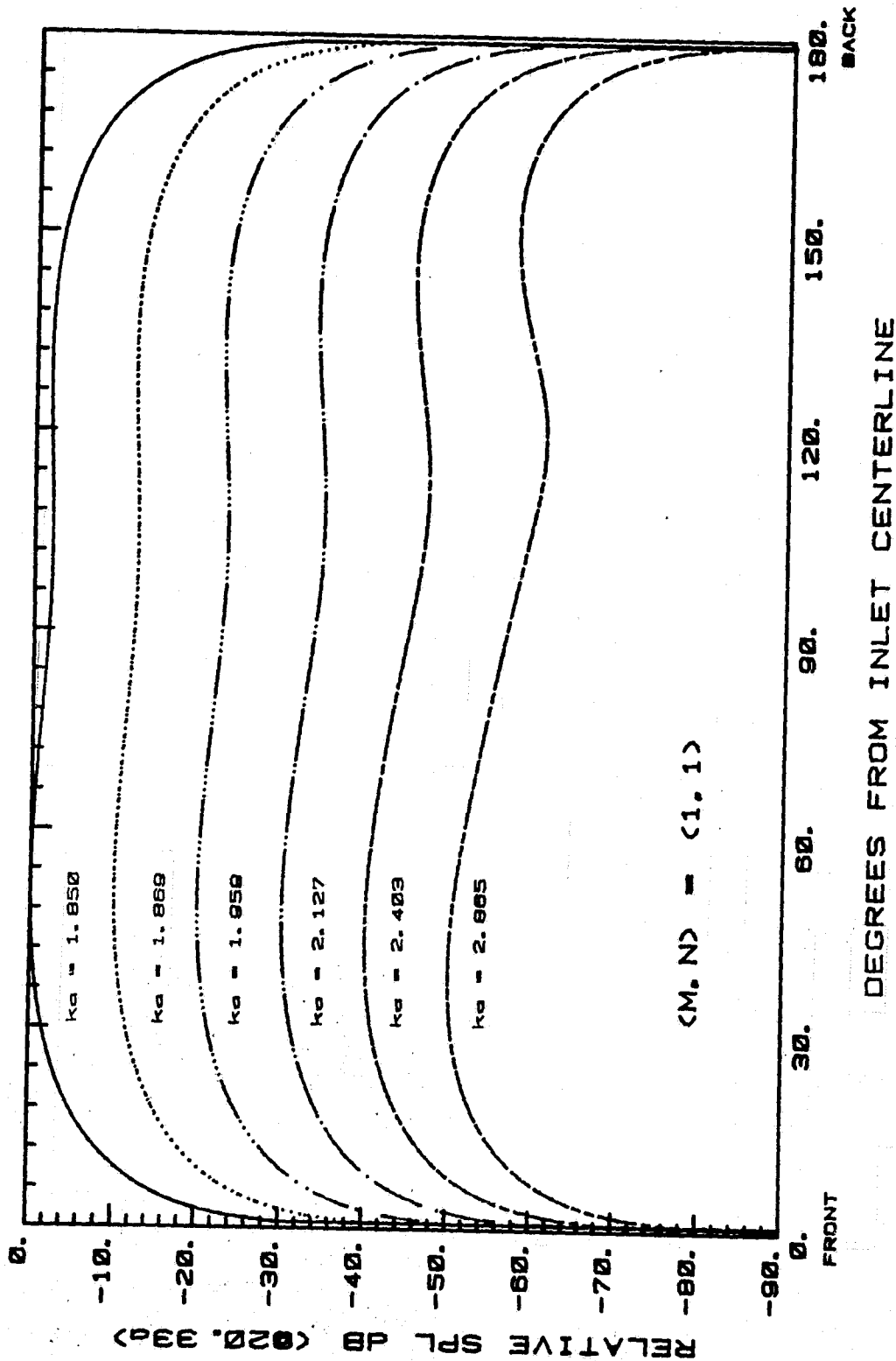
ORIGINAL PAGE IS
OF POOR QUALITY



THICK LIPPED ELLIPTICAL INLET

Fig. 48b

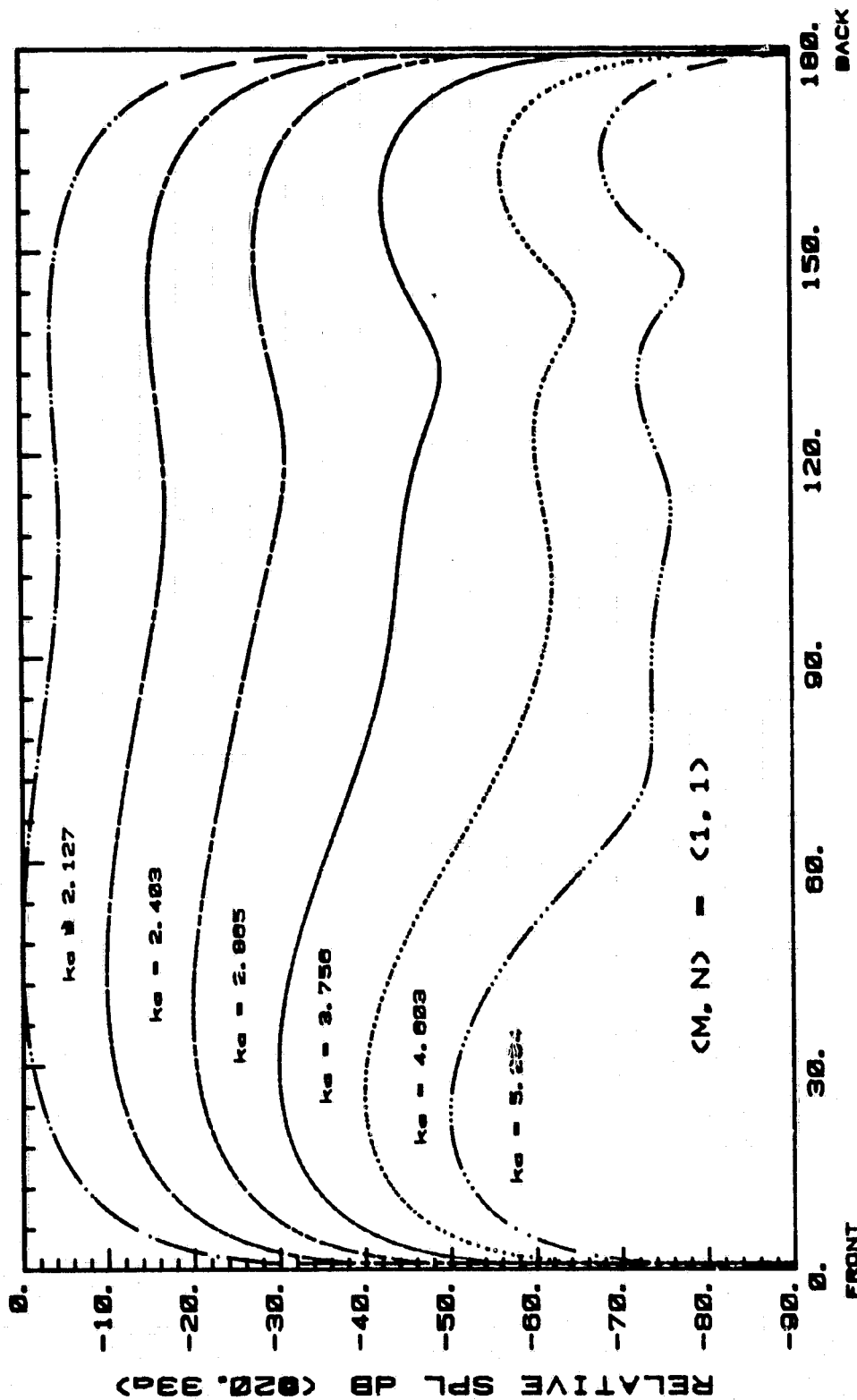
ORIGINAL PAGE IS
OF POOR QUALITY



THICK LIPPED ELLIPTICAL INLET

Fig. 48c

ORIGINAL PAGE IS
OF POOR QUALITY



DEGREES FROM INLET CENTERLINE

THICK LIPPED ELLIPTICAL INLET

Fig. 48d

ORIGINAL PAGE IS
OF POOR QUALITY

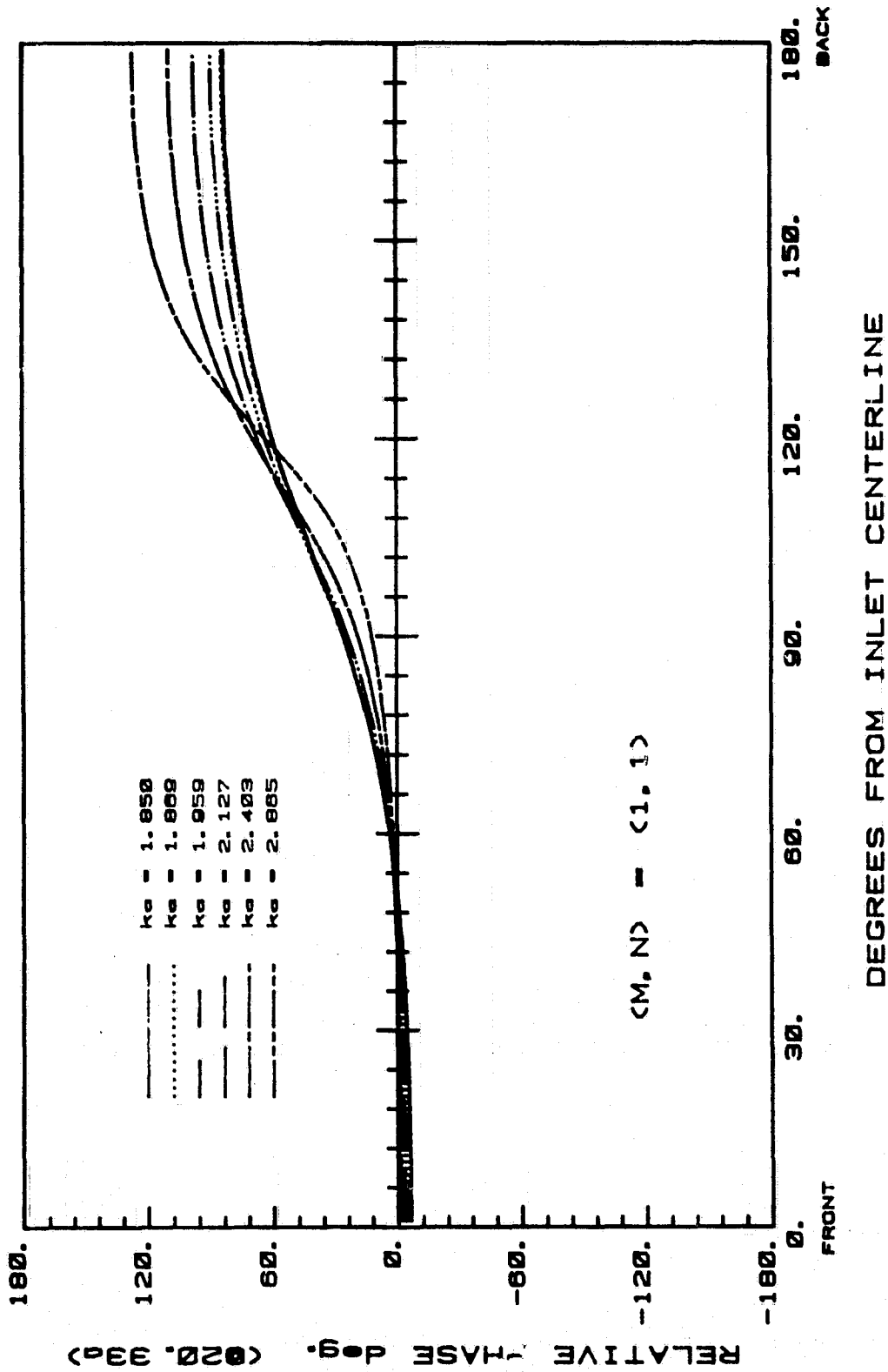
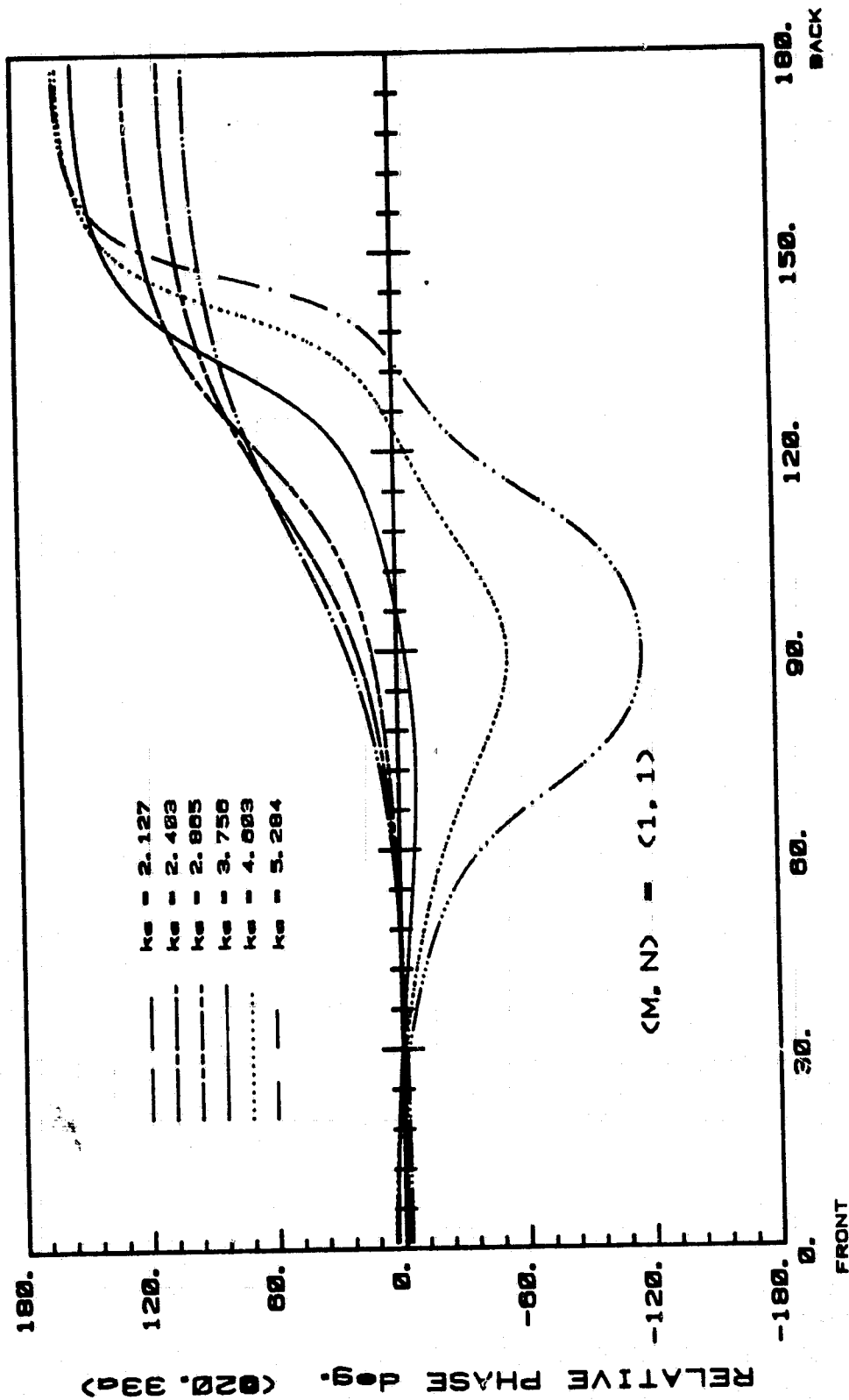


Fig. 48e

THICK LIPPED ELLIPTICAL INLET

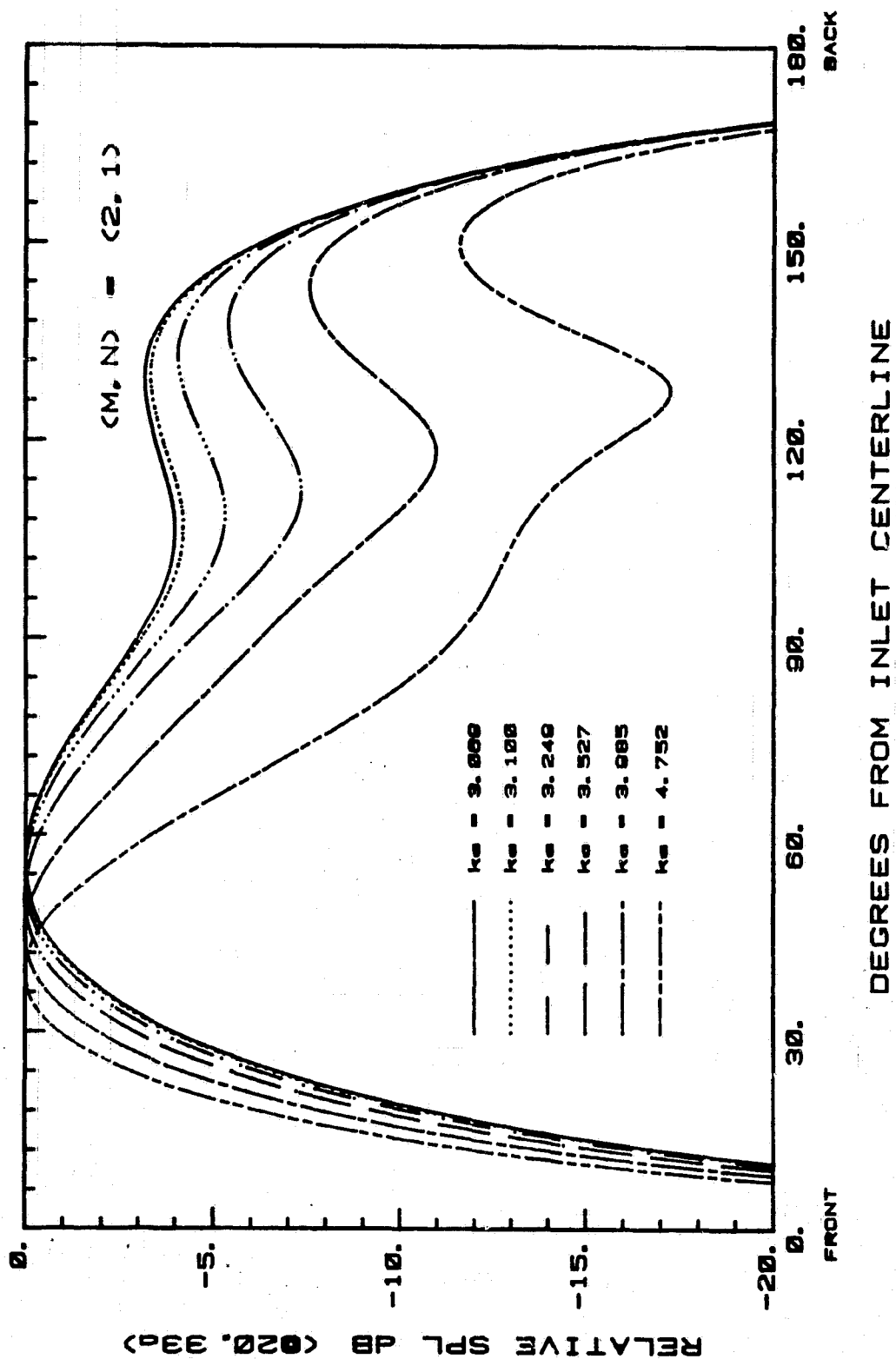
ORIGINAL PAGE IS
OF POOR QUALITY



THICK LIPPED ELLIPTICAL INLET

Fig. 48f

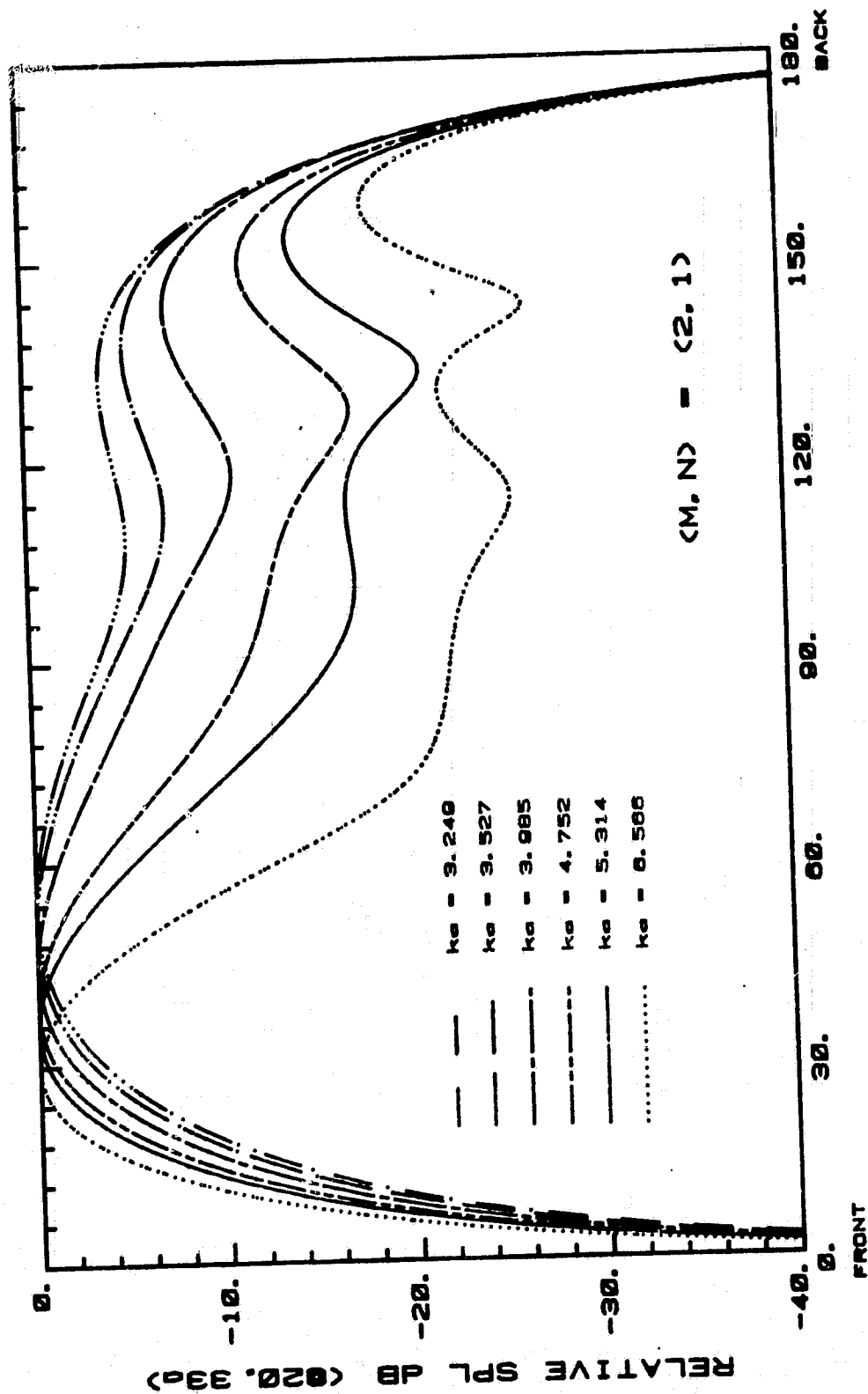
ORIGINAL PAGE IS
OF POOR QUALITY



THICK LIPPED ELLIPTICAL INLET

Fig. 49a

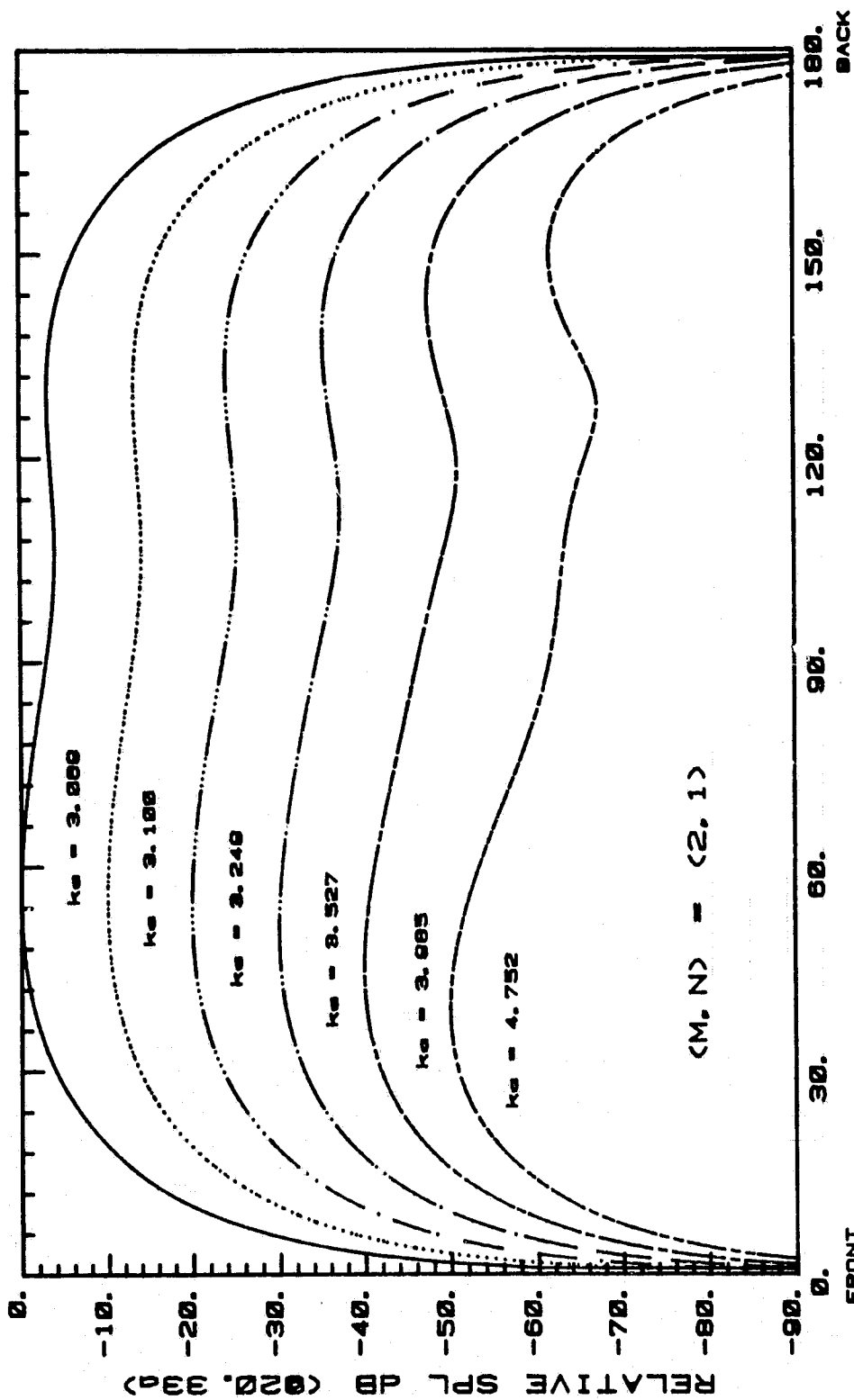
ORIGINAL PAGE IS
OF POOR QUALITY



THICK LIPPED ELLIPTICAL INLET

Fig. 49b

ORIGINAL PAGE IS
OF POOR QUALITY

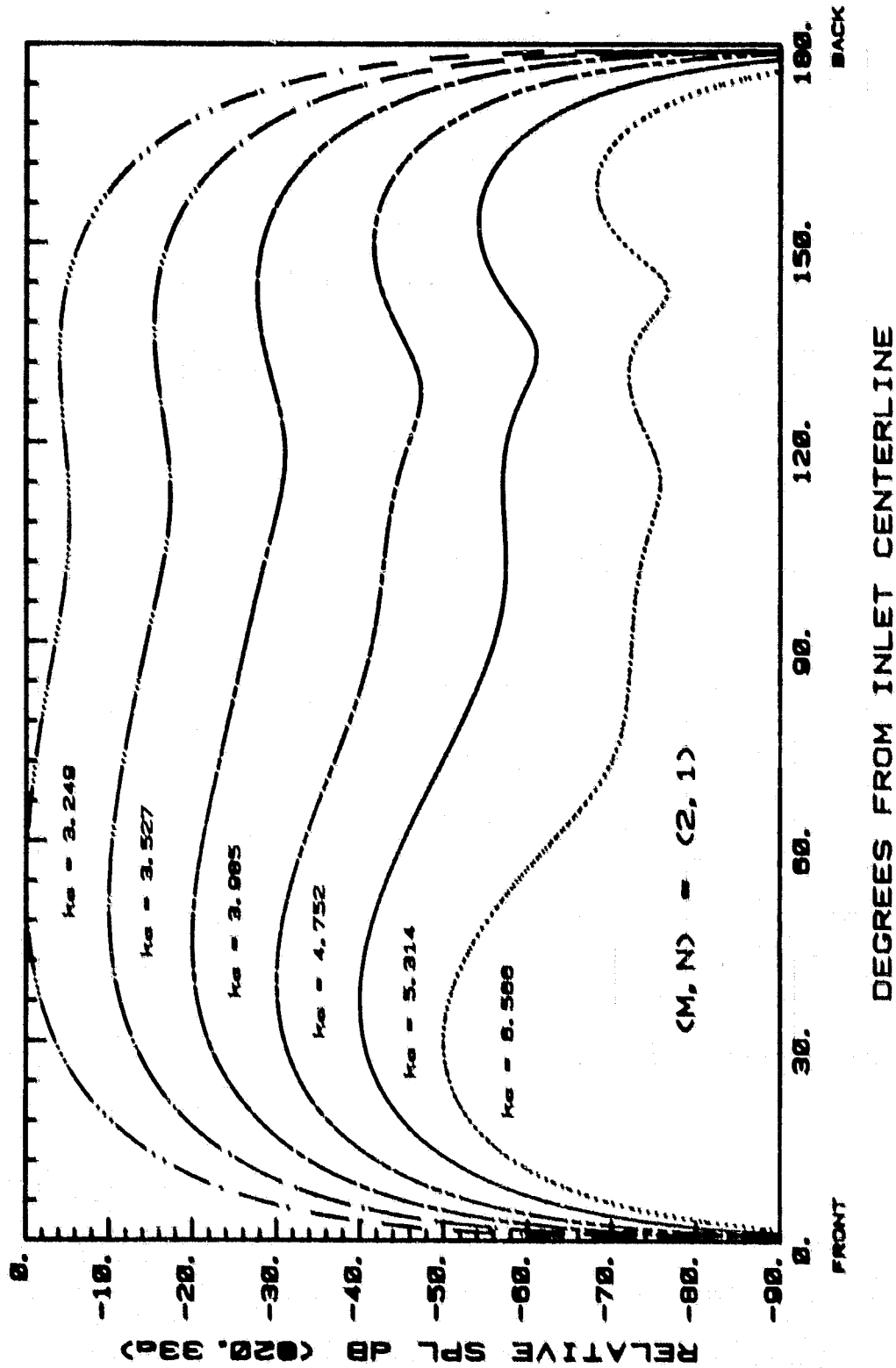


DEGREES FROM INLET CENTERLINE

THICK LIPPED ELLIPTICAL INLET

Fig. 49c

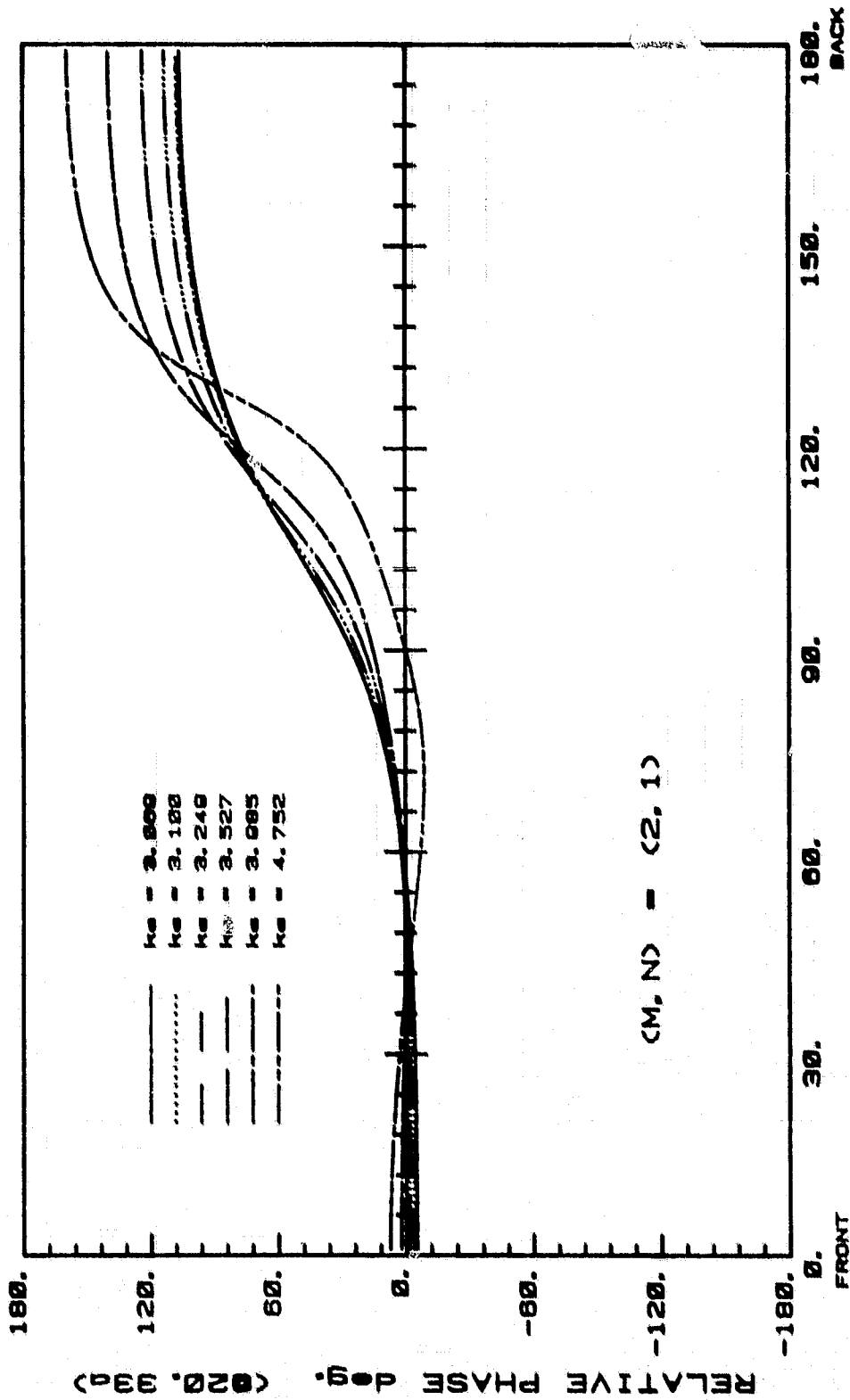
OF POOR QUALITY



THICK LIPPED ELLIPTICAL INLET

Fig. 49d

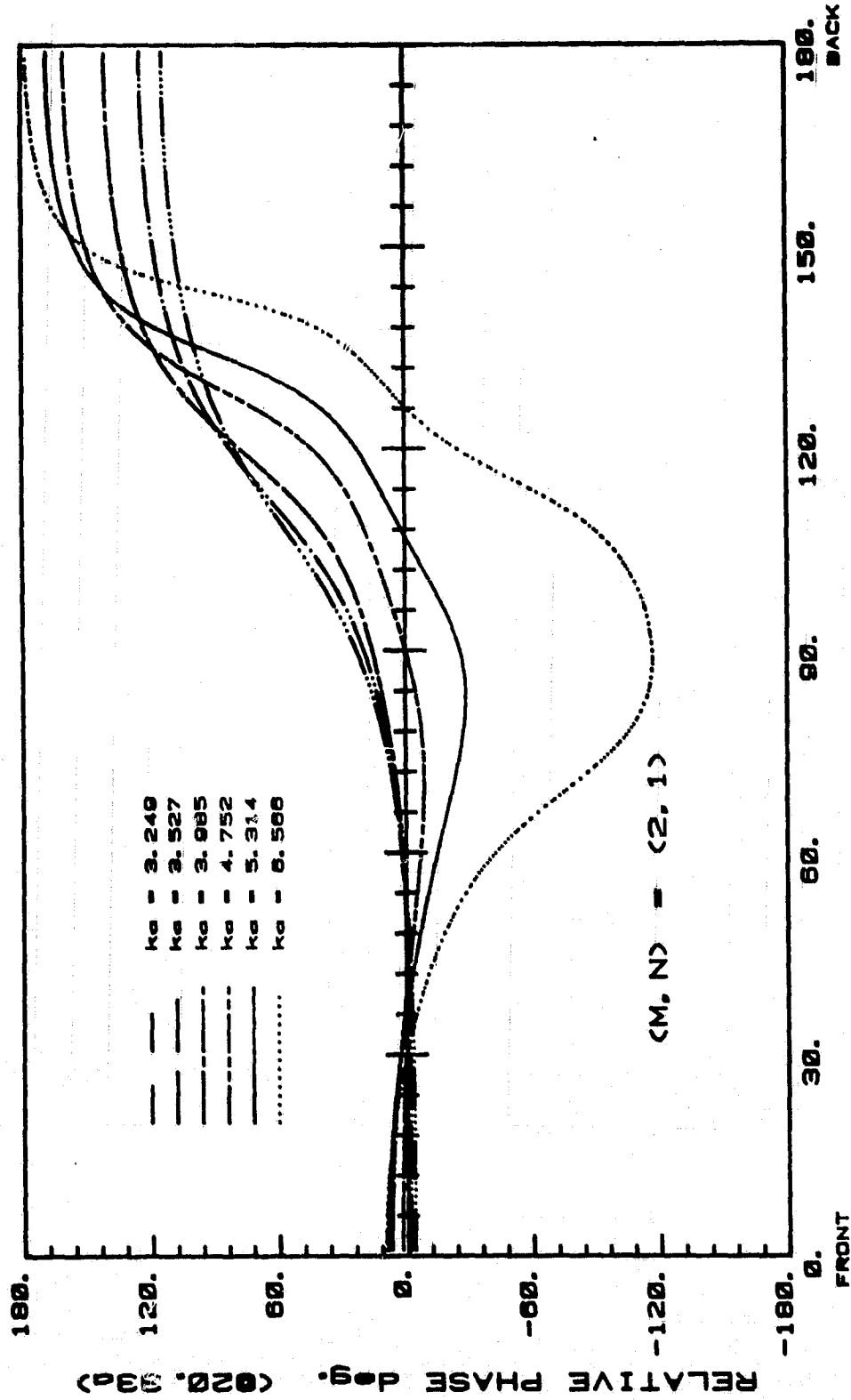
ORIGINAL PAGE IS
OF POOR QUALITY



DEGREES FROM INLET CENTERLINE

THICK LIPPED ELLIPTICAL INLET

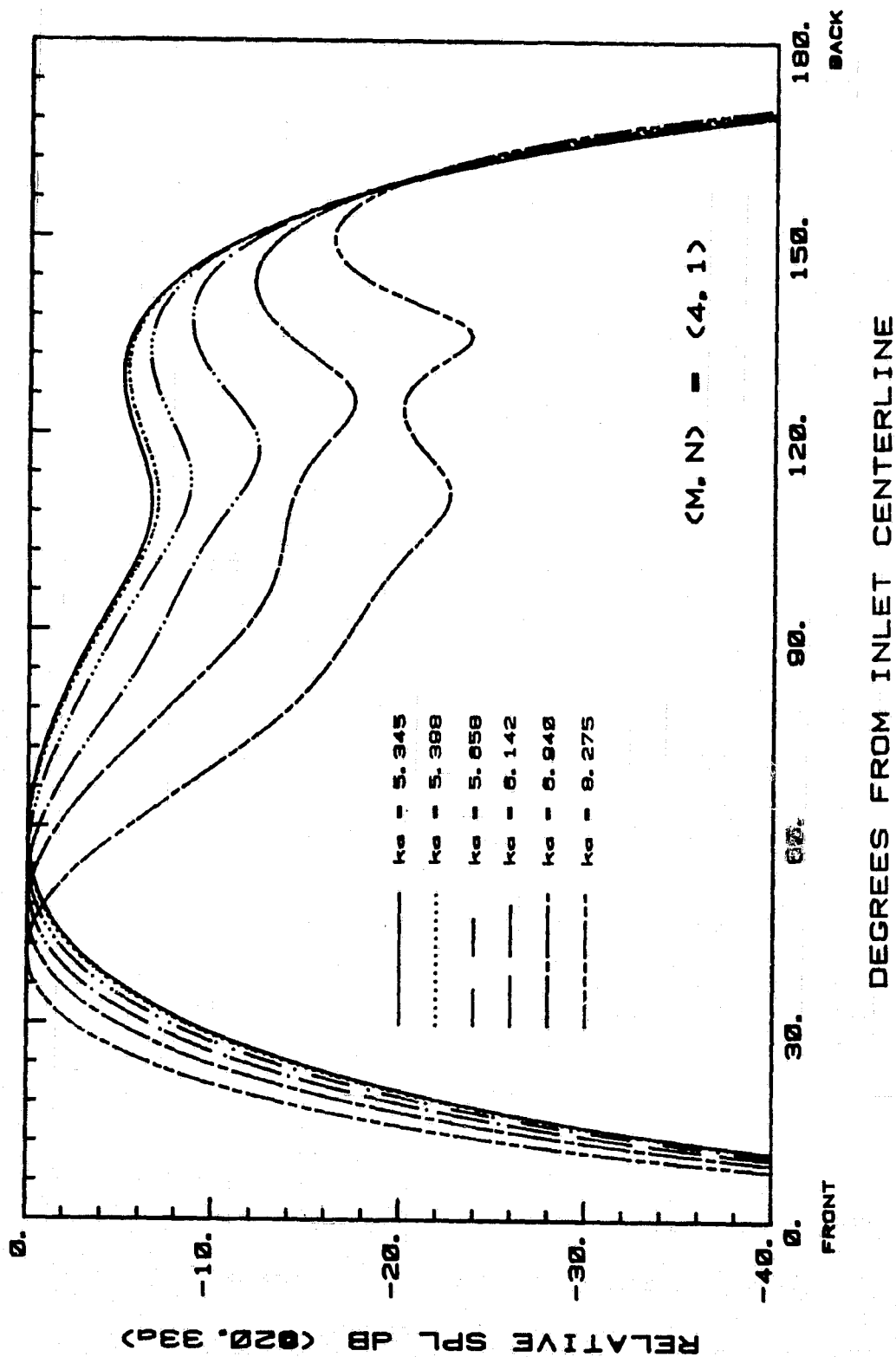
Fig. 49e



DEGREES FROM INLET CENTERLINE

THICK LIPPED ELLIPTICAL INLET

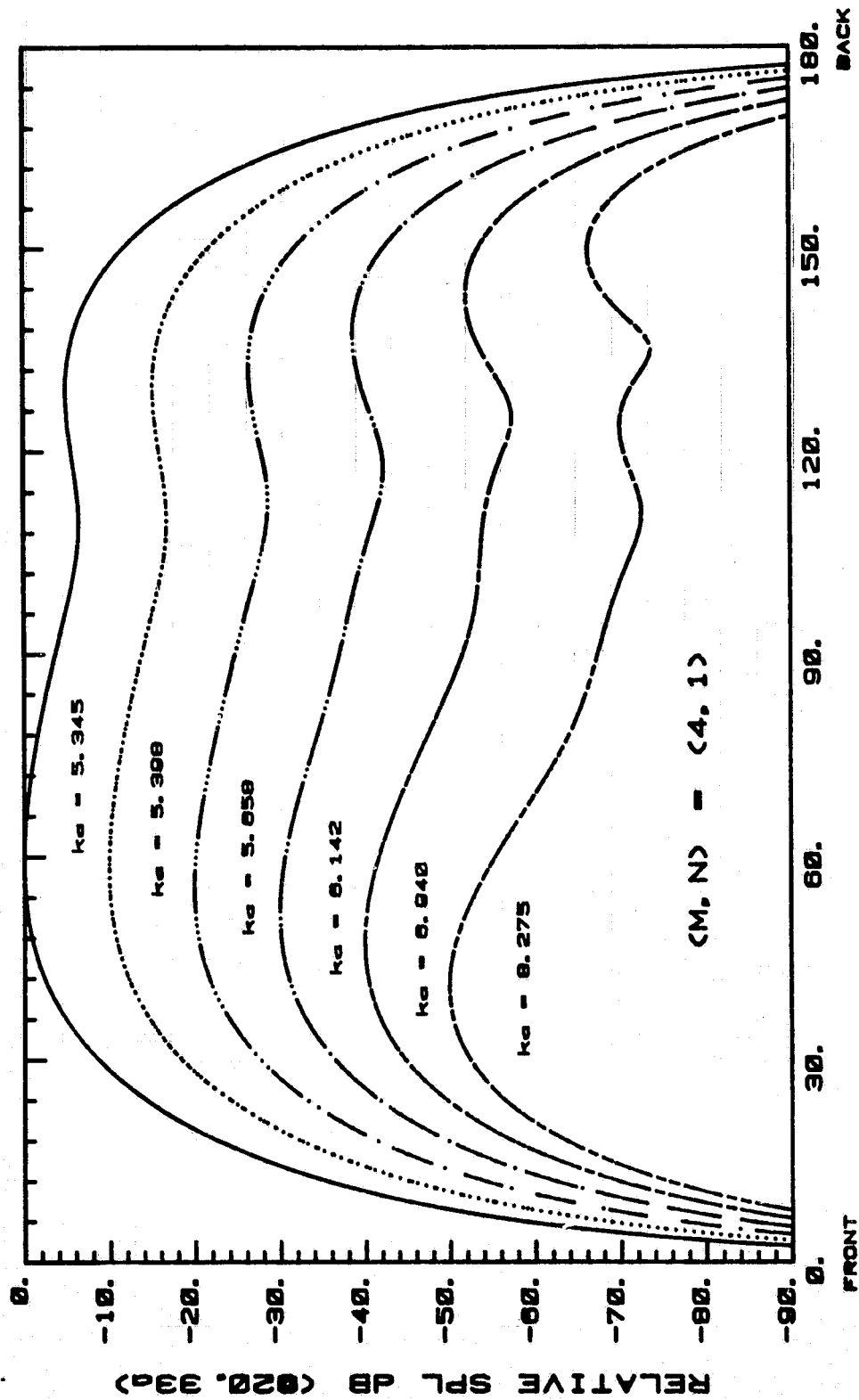
Fig. 49f



THICK LIPPED ELLIPTICAL INLET

Fig. 50a

ORIGINAL PAGE IS
OF POOR QUALITY



THICK LIPPED ELLIPTICAL INLET

Fig. 50b

ORIGINAL PAGE IS
OF POOR QUALITY

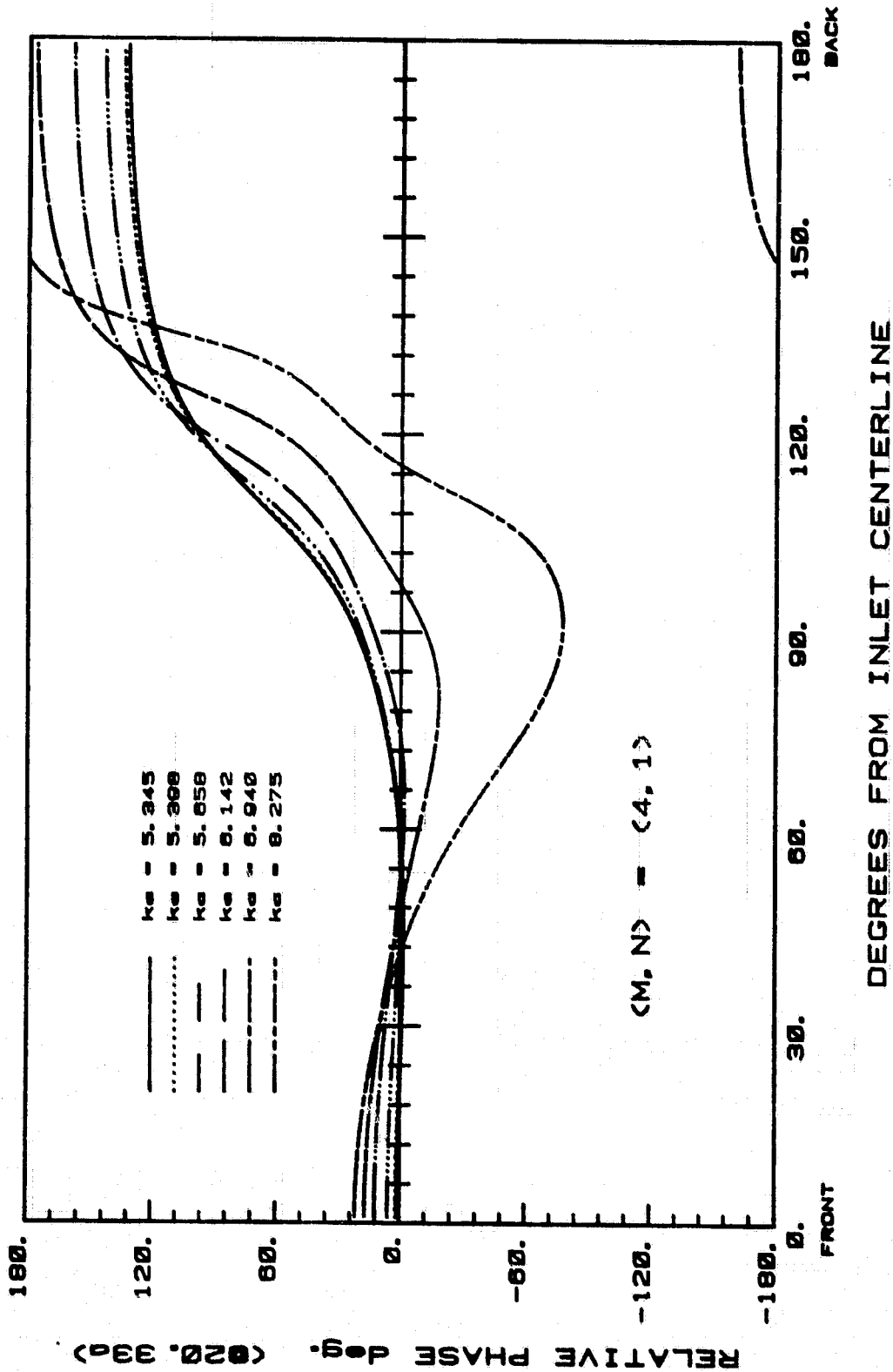
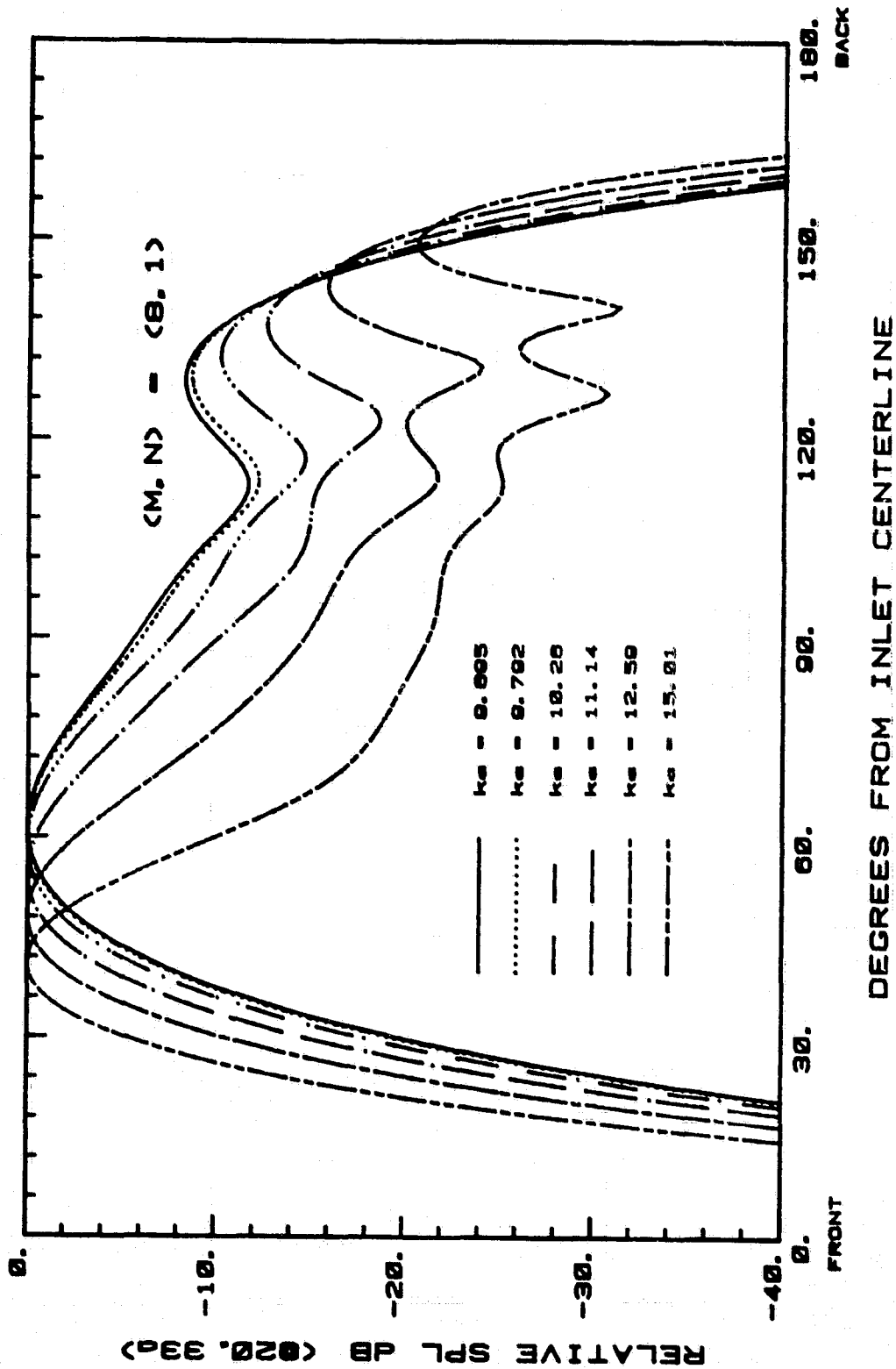


Fig. 50c

THICK LIPPED ELLIPTICAL INLET

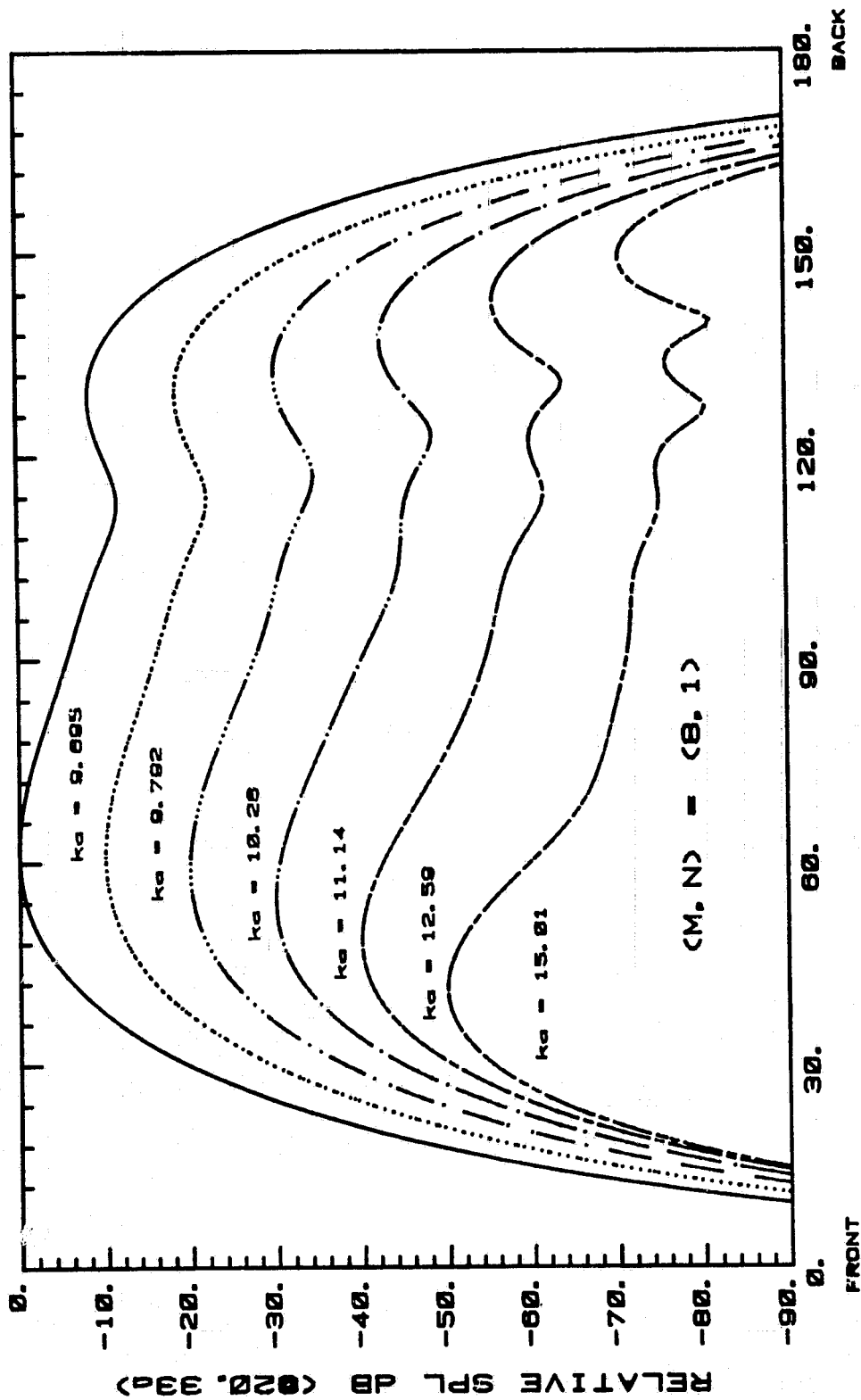
ORIGINAL PAGE IS
OF POOR QUALITY



THICK LIPPED ELLIPTICAL INLET

Fig. 51a

ORIGINAL PAGE IS
OF POOR QUALITY



DEGREES FROM INLET CENTERLINE

THICK LIPPED ELLIPTICAL INLET

Fig. 51b

ORIGINAL PAGE IS
OF POOR QUALITY

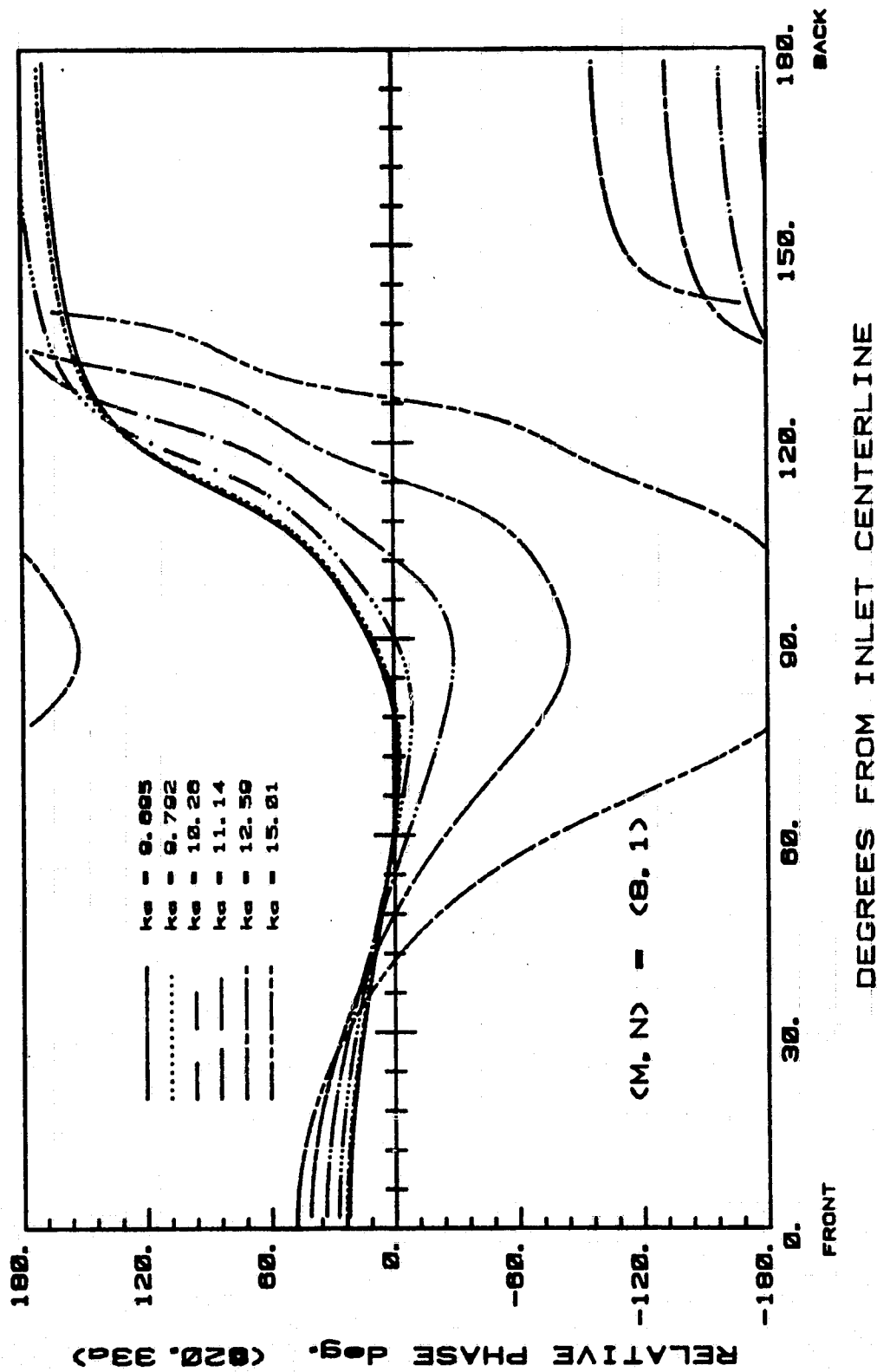
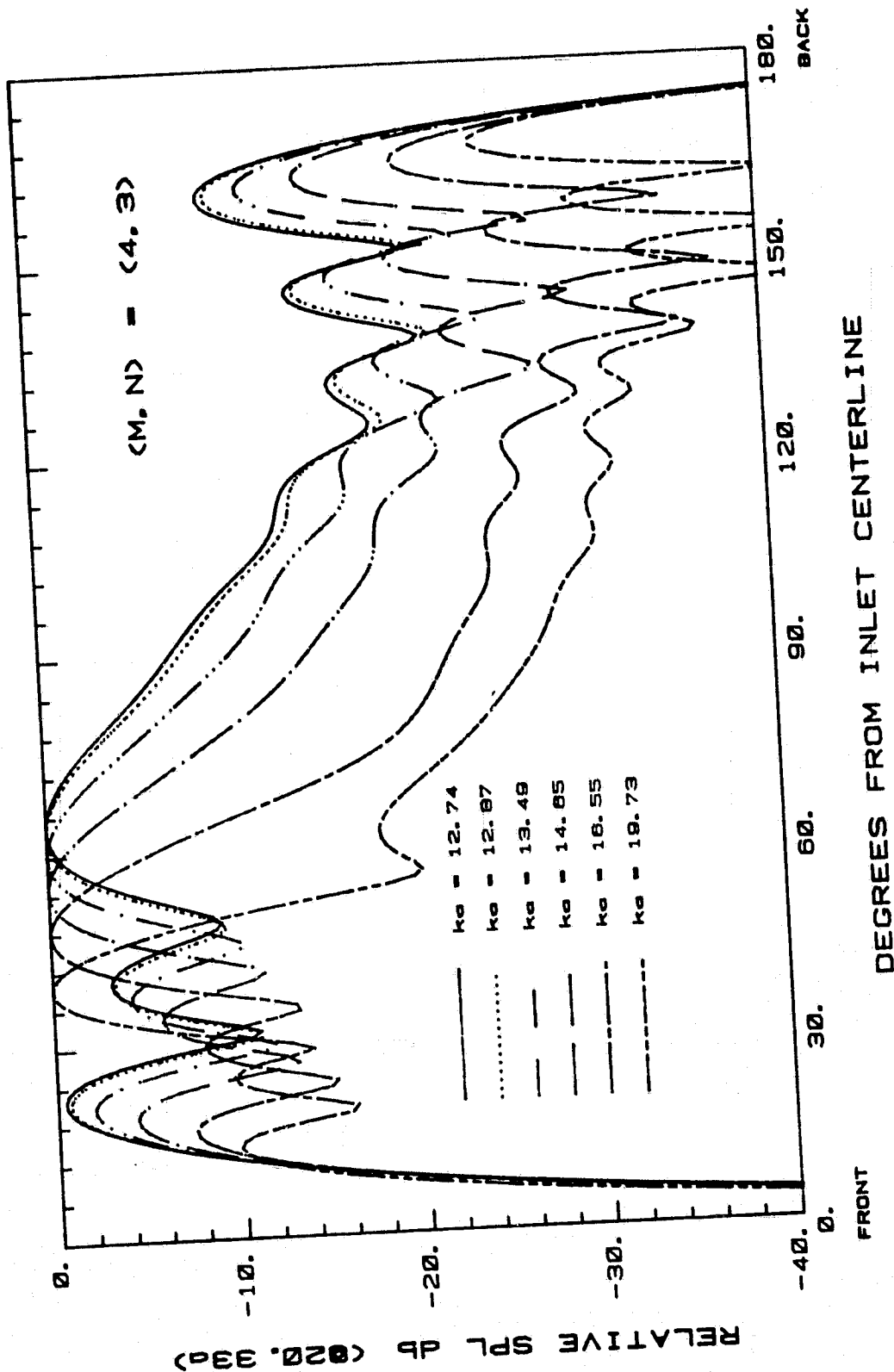


Fig. 51c

THICK LIPPED ELLIPTICAL INLET

ORIGINAL PAGE IS
OF POOR QUALITY



THICK LIPPED ELLIPTICAL INLET

Fig. 52a

ORIGINAL PAGE IS
OF POOR QUALITY

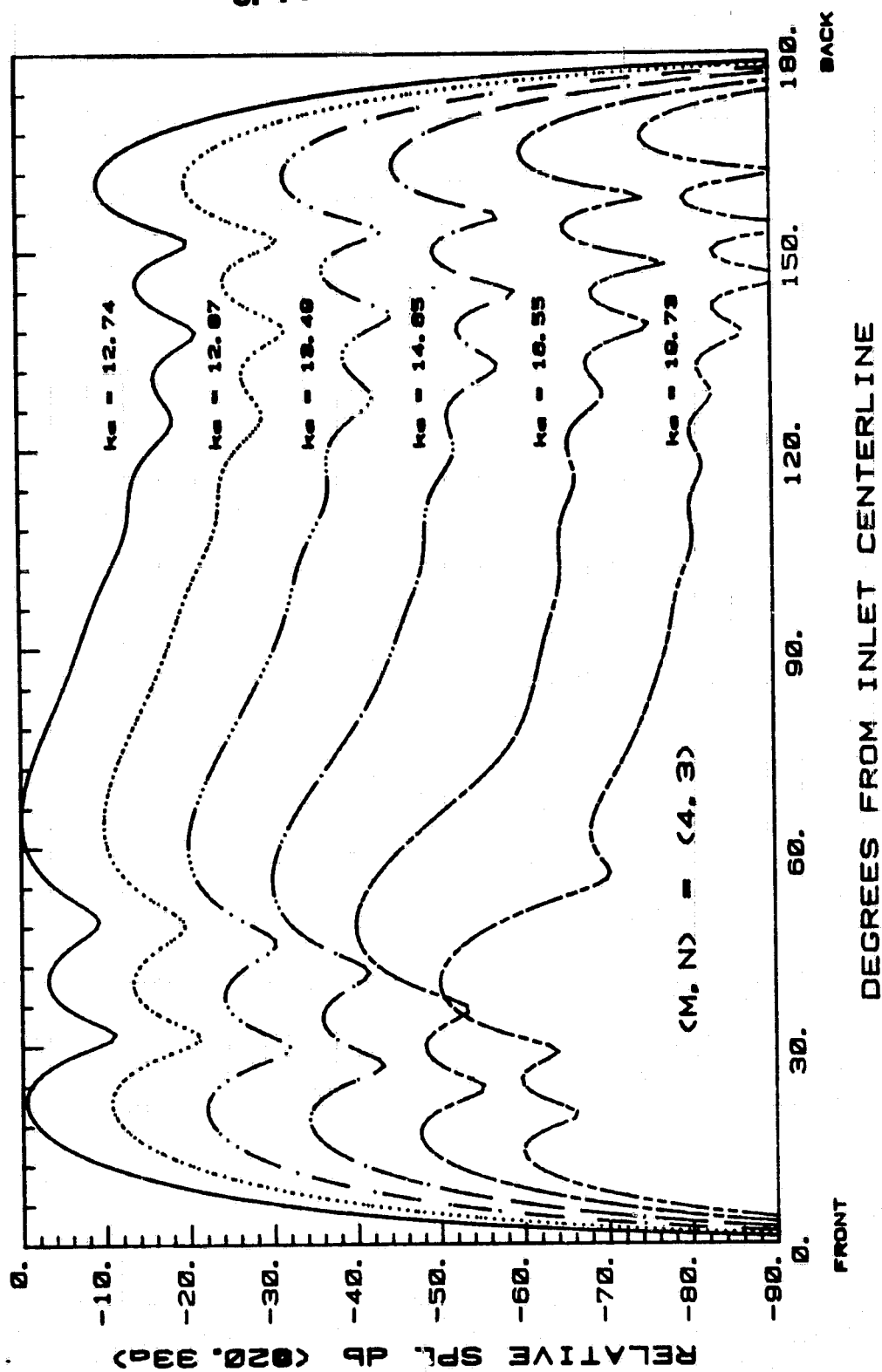
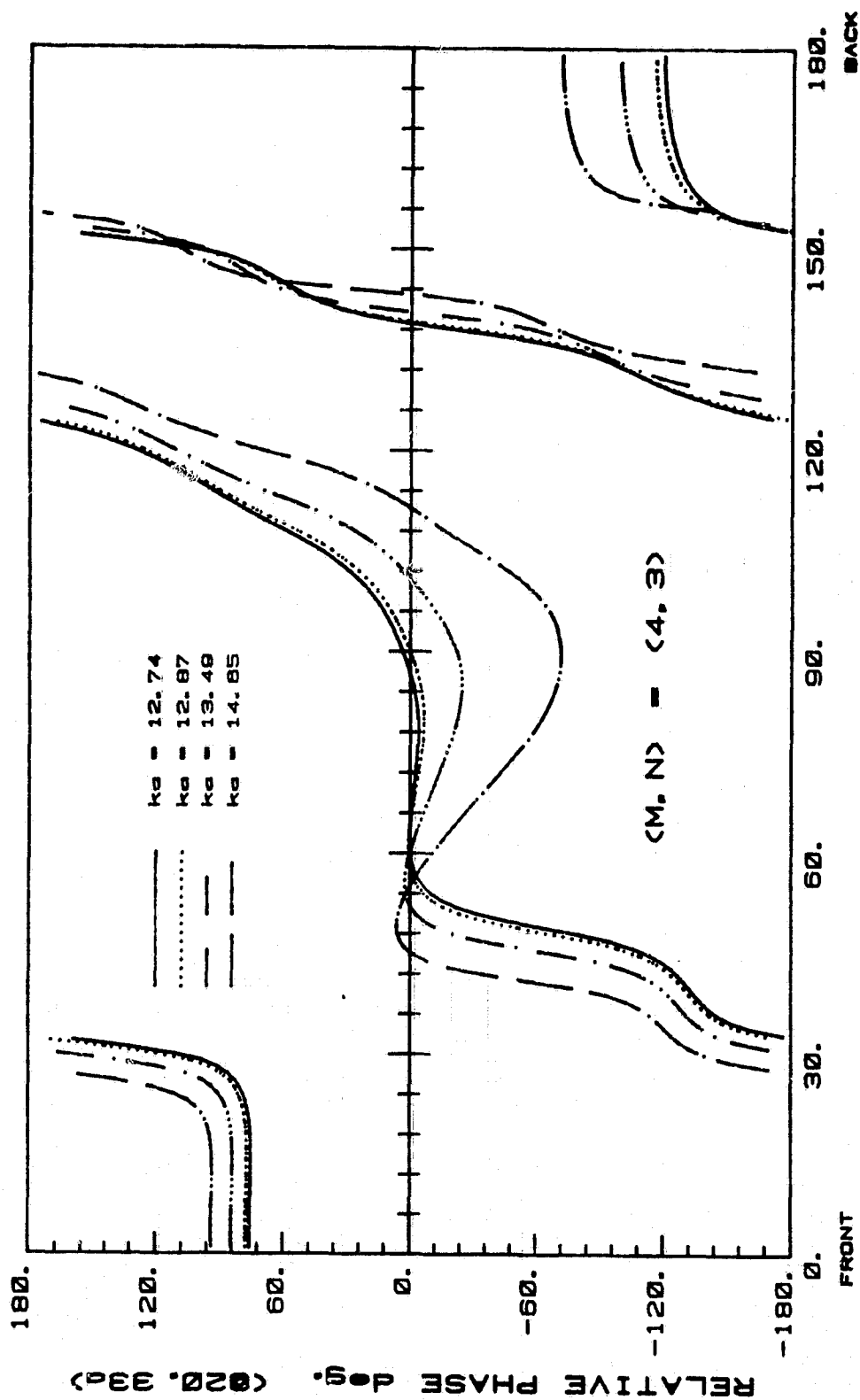


Fig. 52b

THICK LIPPED ELLIPTICAL INLET

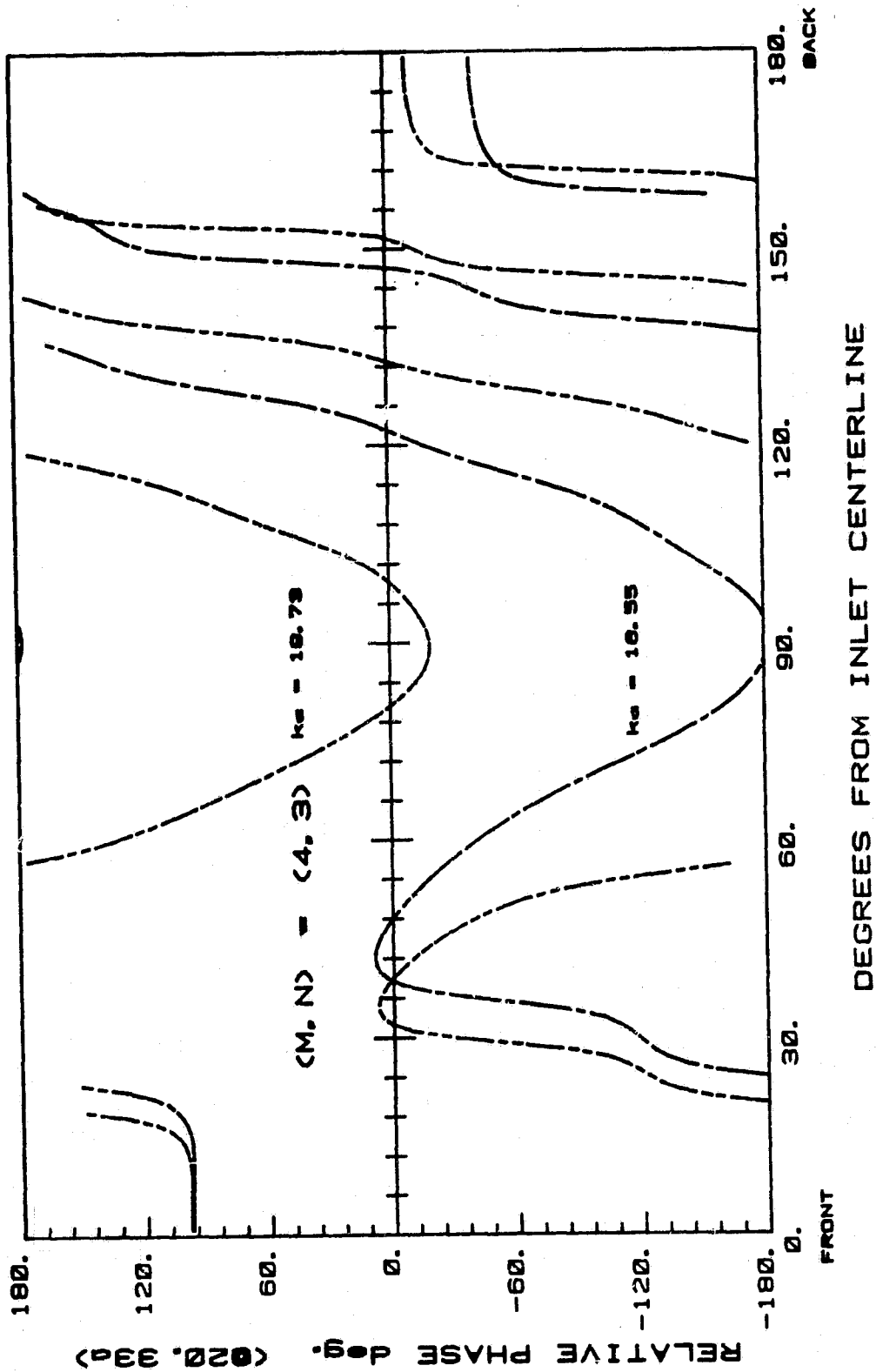


DEGREES FROM INLET CENTERLINE

THICK LIPPED ELLIPTICAL INLET

Fig. 52c

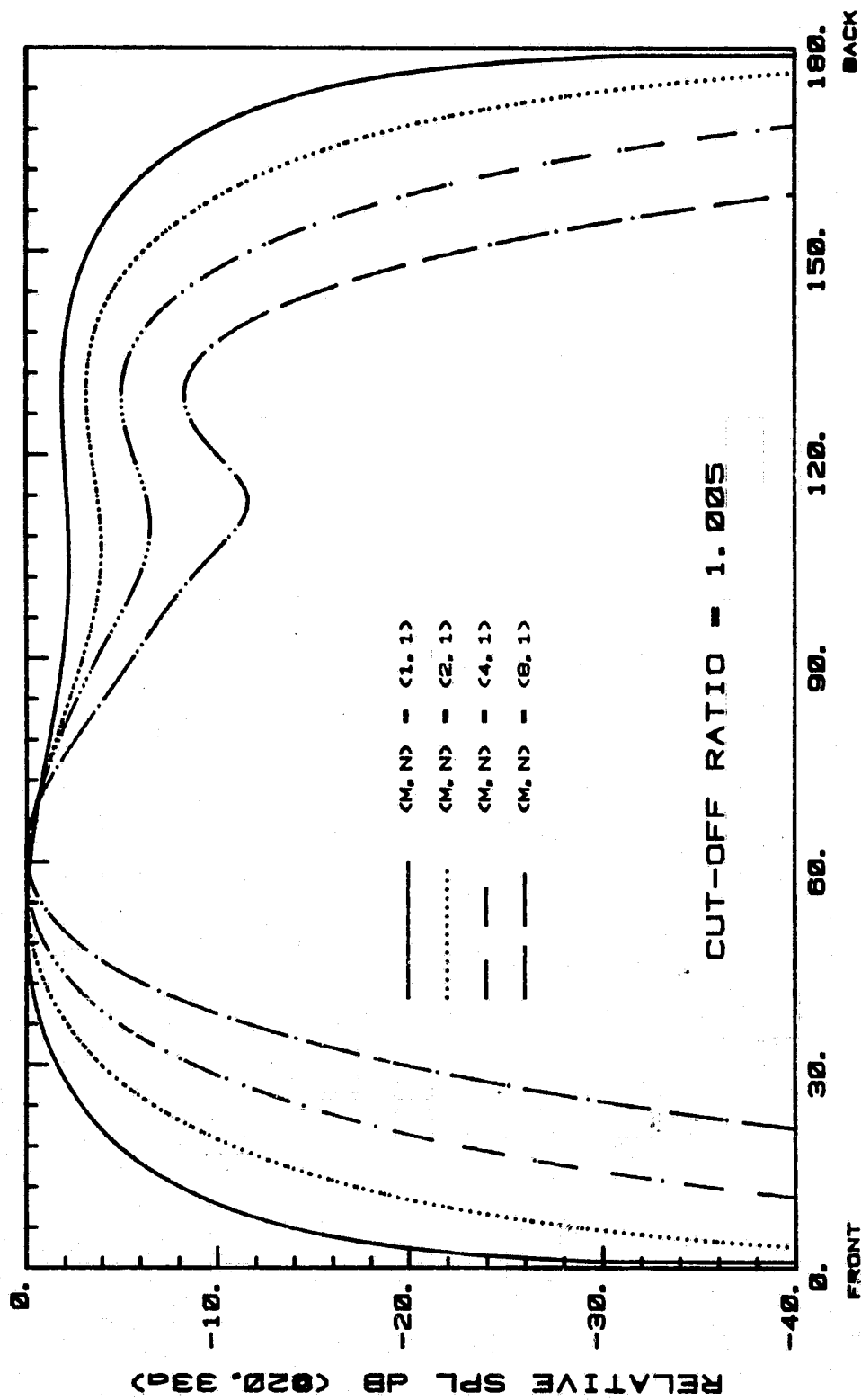
ORIGINAL PAGE IS
OF POOR QUALITY



THICK LIPPED ELLIPTICAL INLET

Fig. 52d

ORIGINAL PAGE IS
OF POOR QUALITY

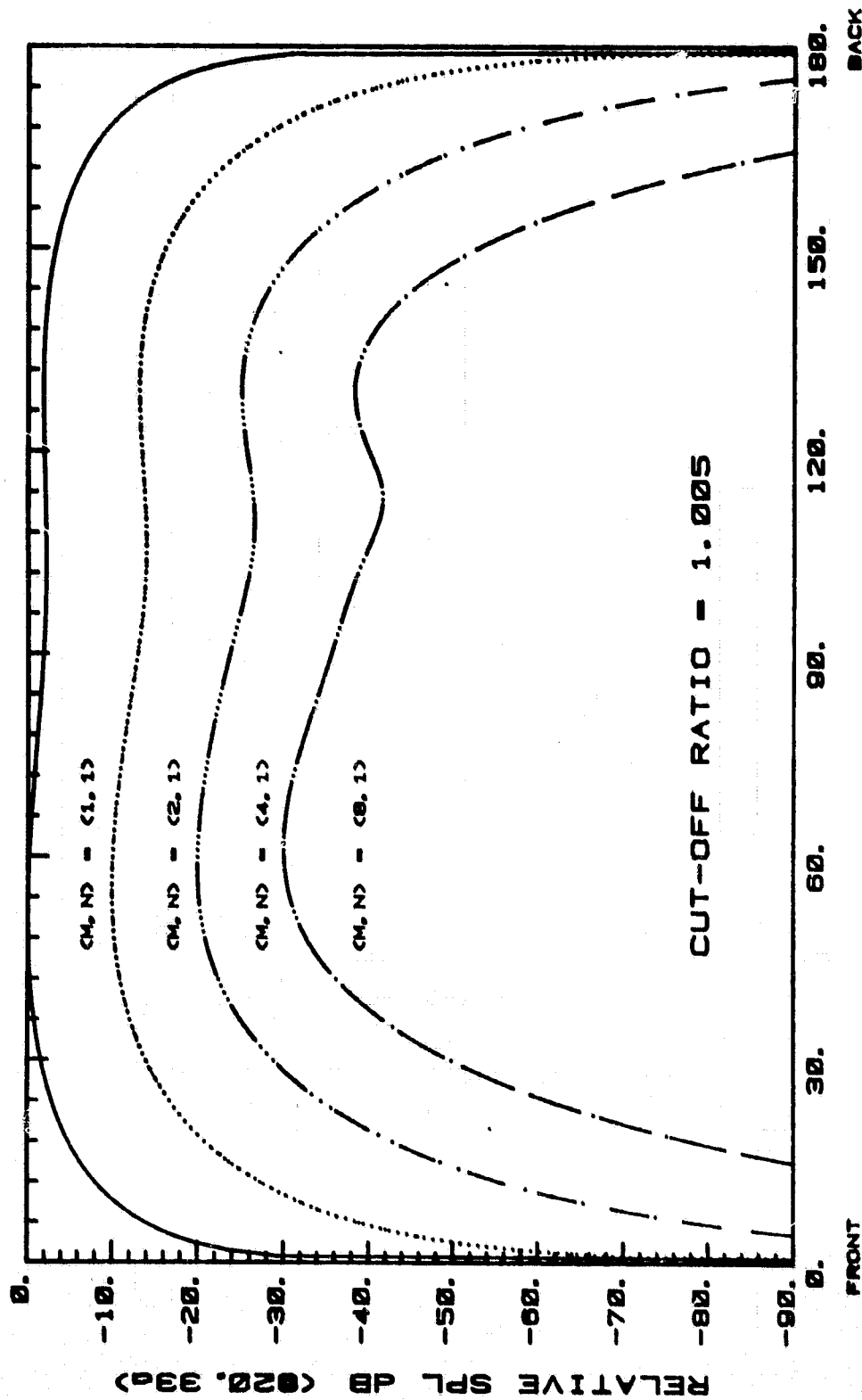


DEGREES FROM INLET CENTERLINE

THICK LIPPED ELLIPTICAL INLET

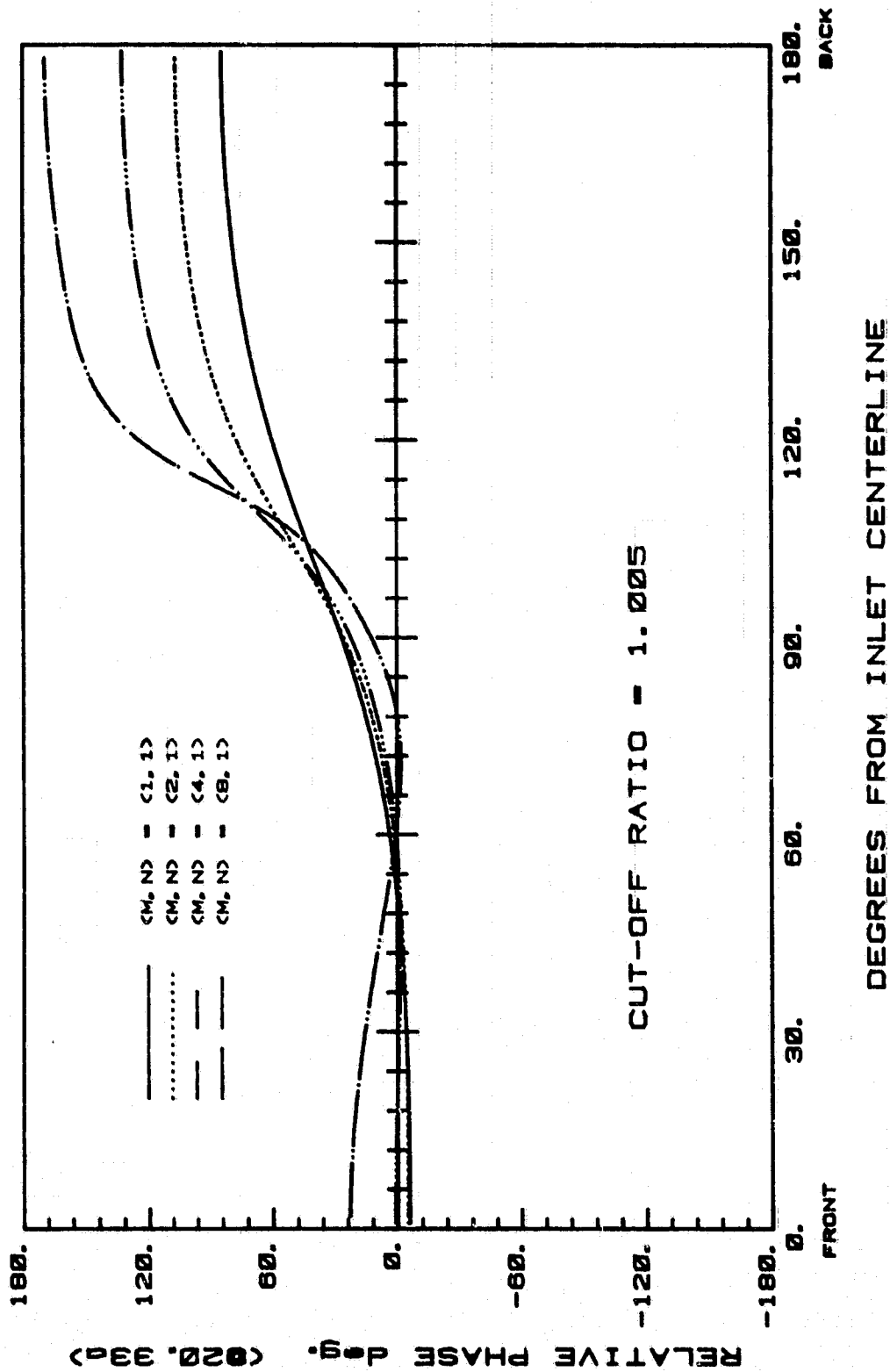
Fig. 53a

ORIGINAL PAGE IS
OF POOR QUALITY



THICK LIPPED ELLIPTICAL INLET

Fig. 53b



THICK LIPPED ELLIPTICAL INLET

Fig. 53c

ORIGINAL PAGE IS
OF POOR QUALITY

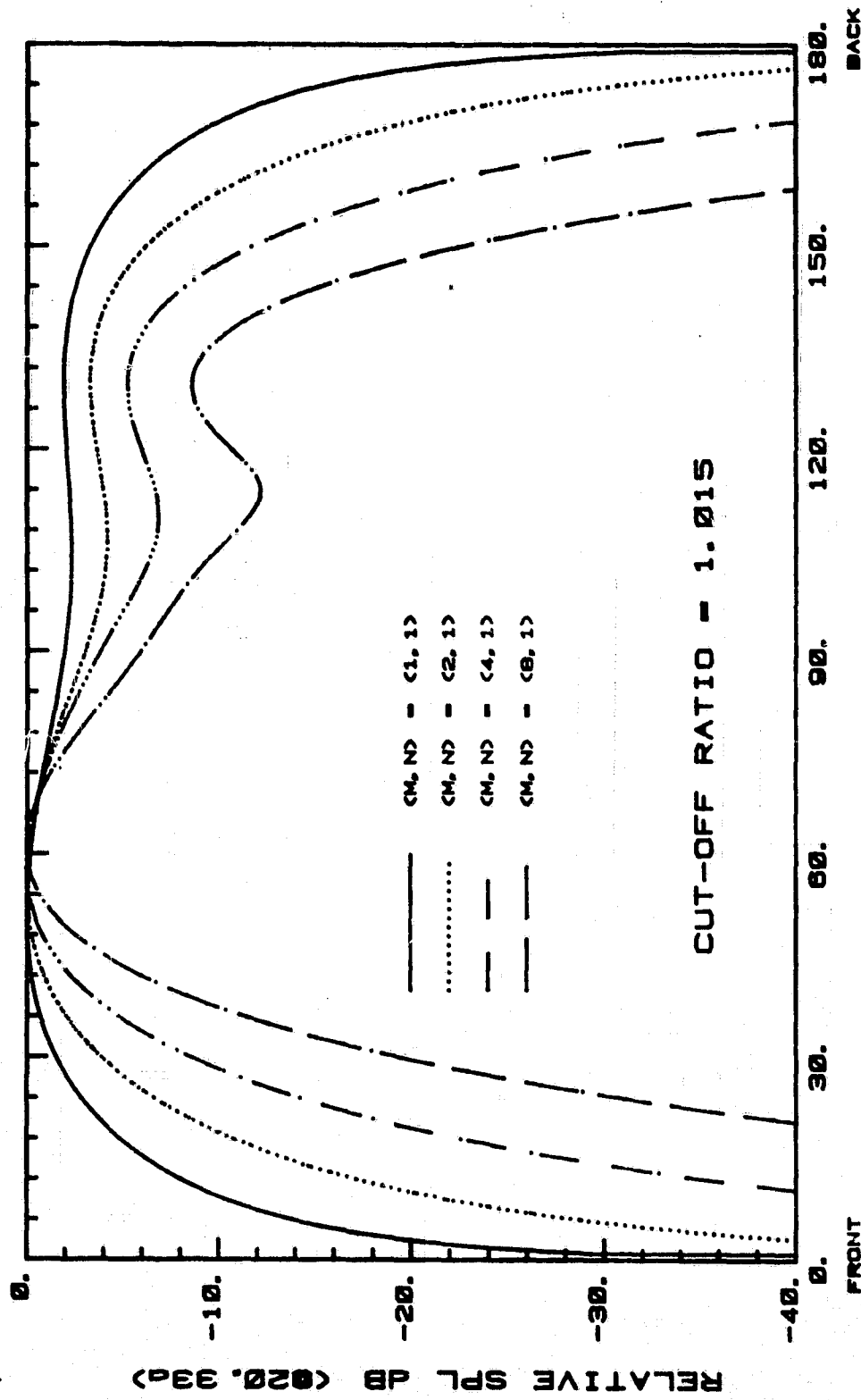
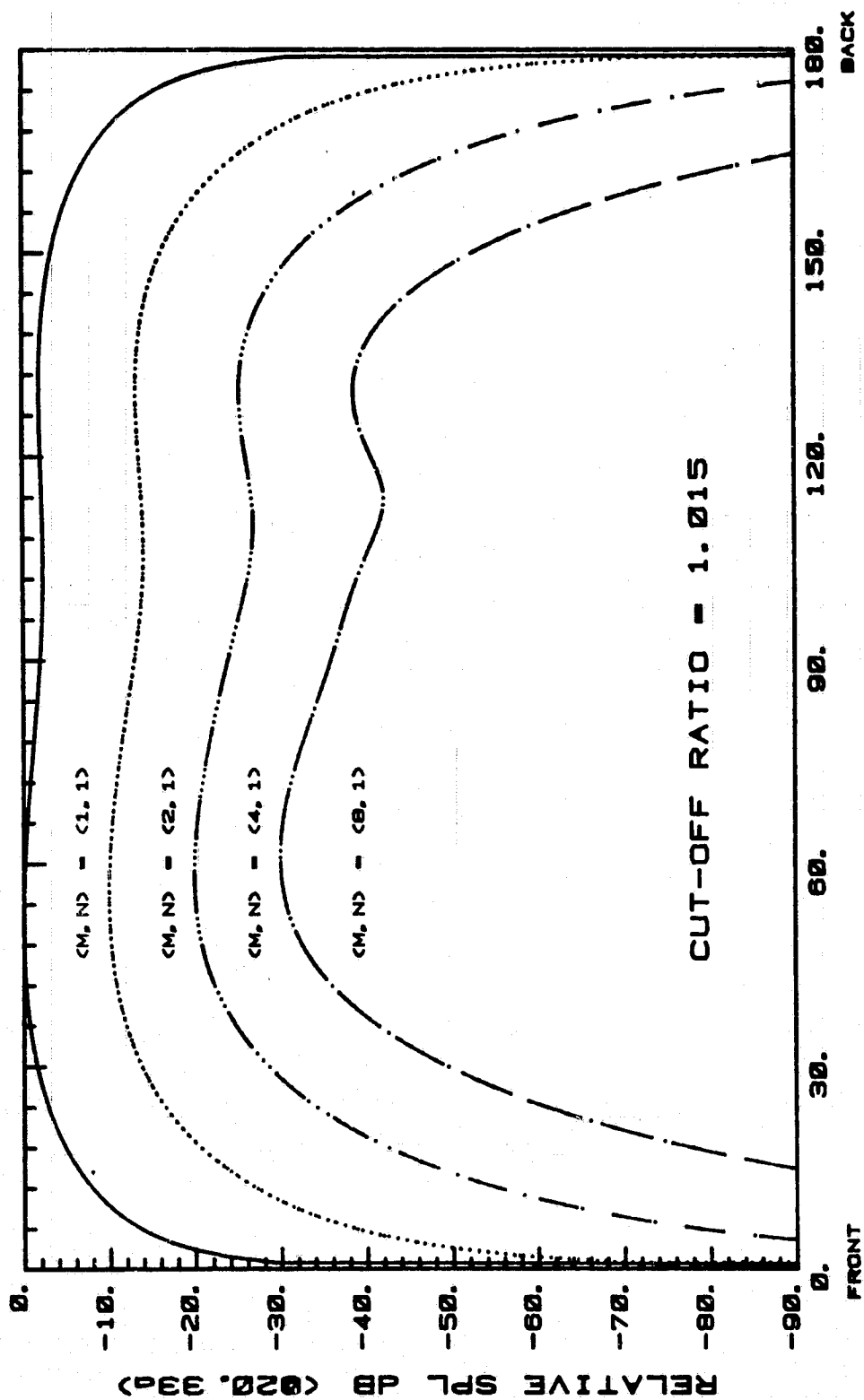


Fig. 54a

THICK LIPPED ELLIPTICAL INLET

ORIGINAL PAGE IS
OF POOR QUALITY



THICK LIPPED ELLIPTICAL INLET

Fig. 54b

ORIGINAL PAGE IS
OF POOR QUALITY

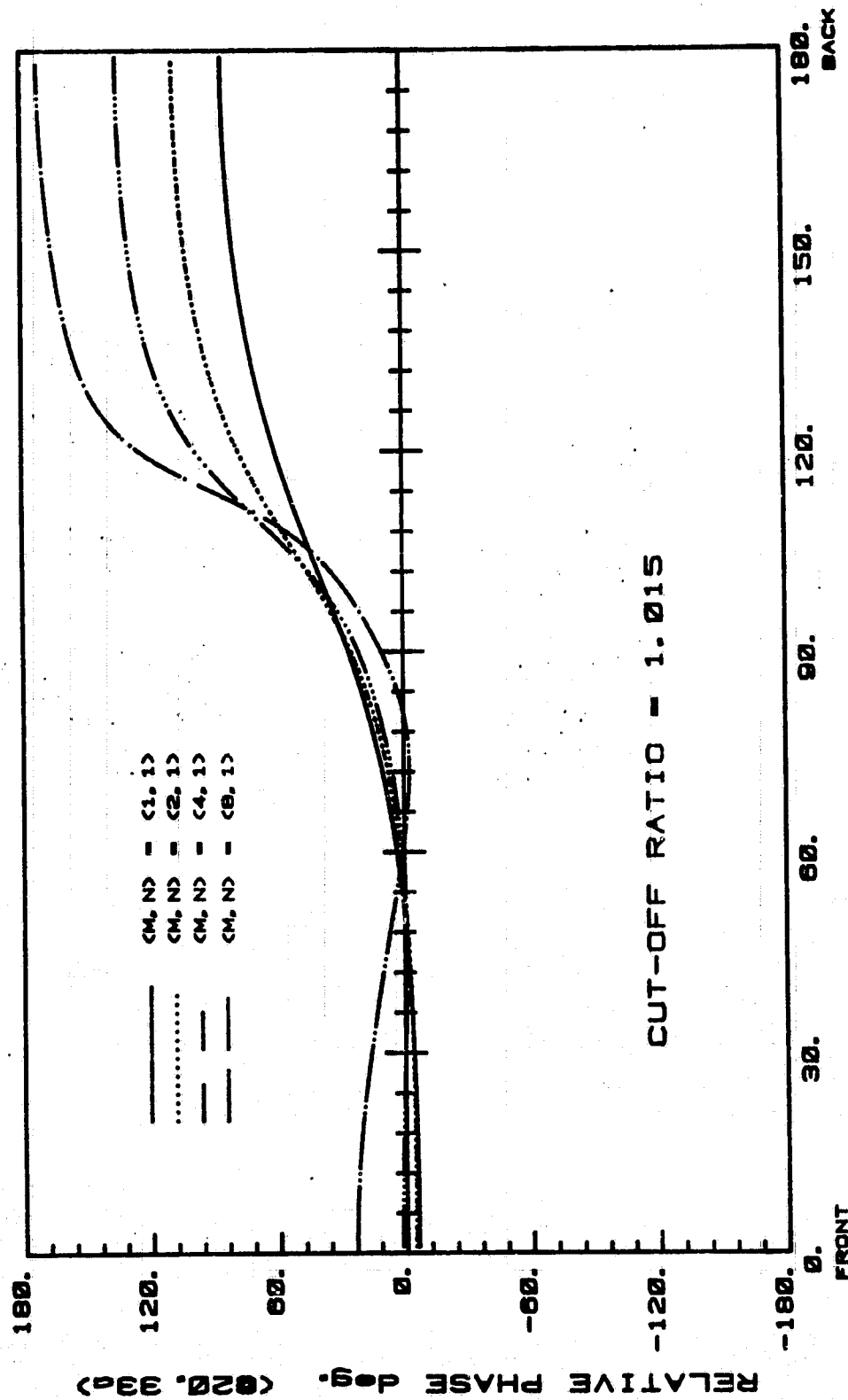


Fig. 54c

ORIGINAL PAGE IS
OF POOR QUALITY

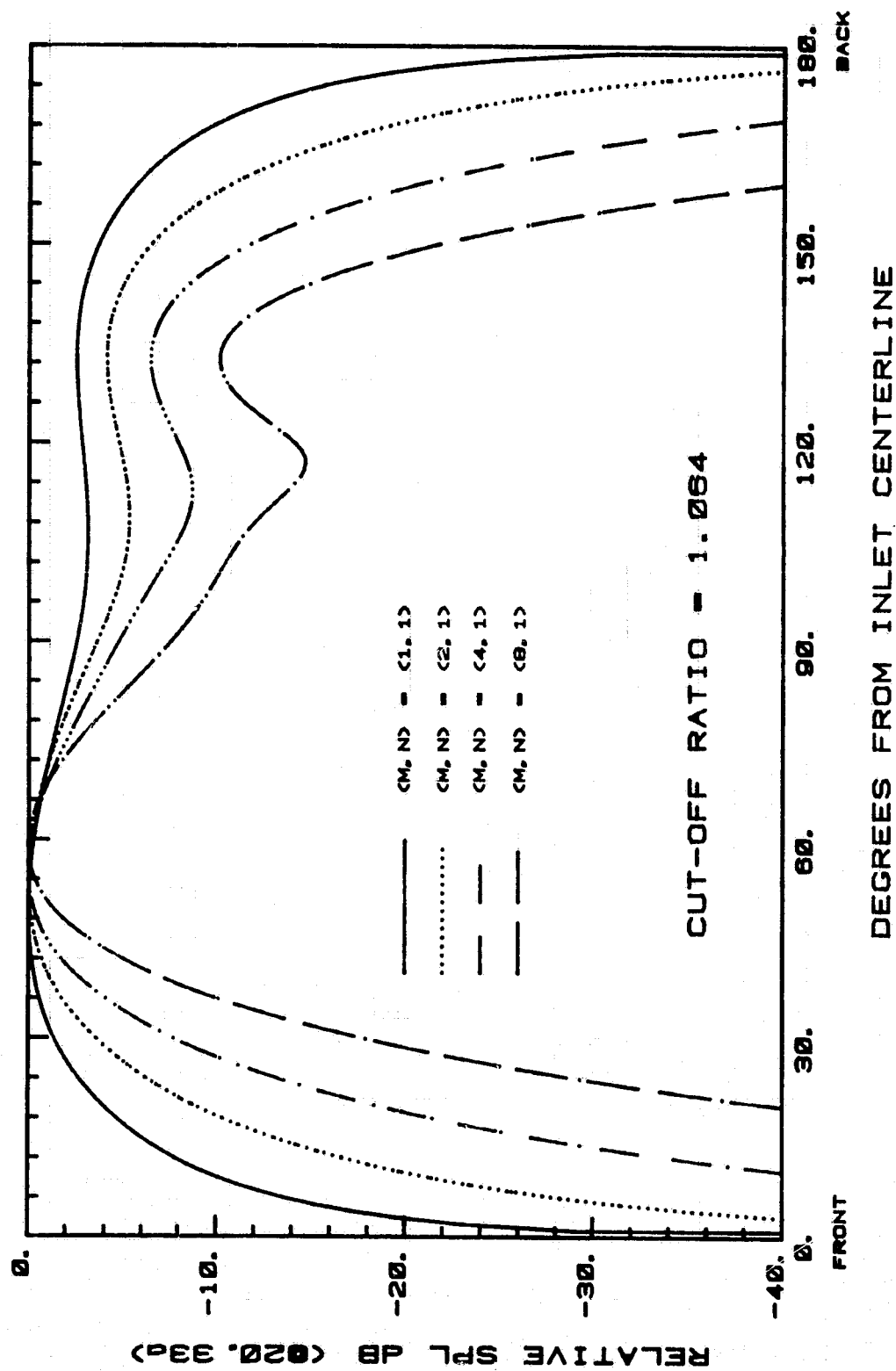
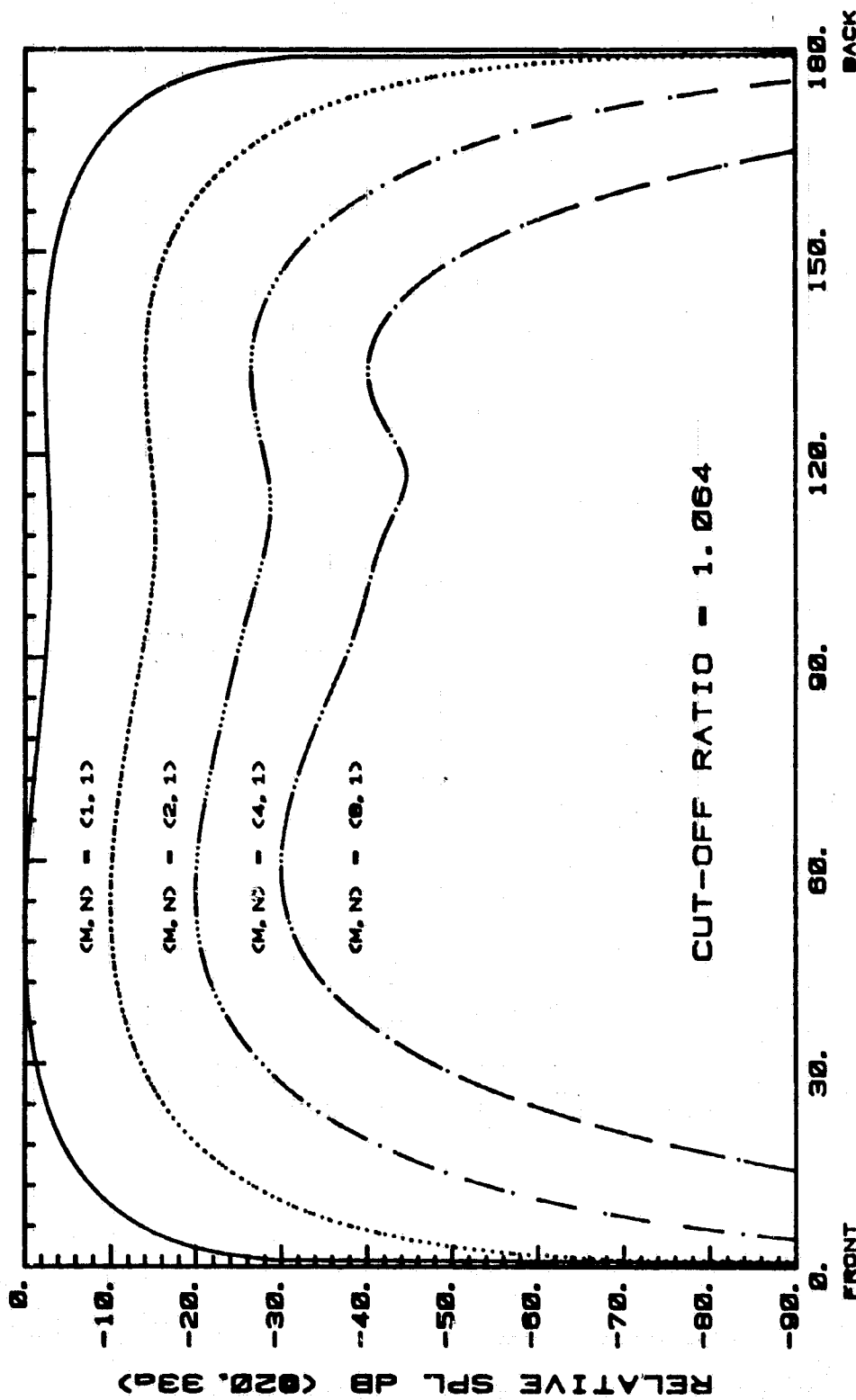


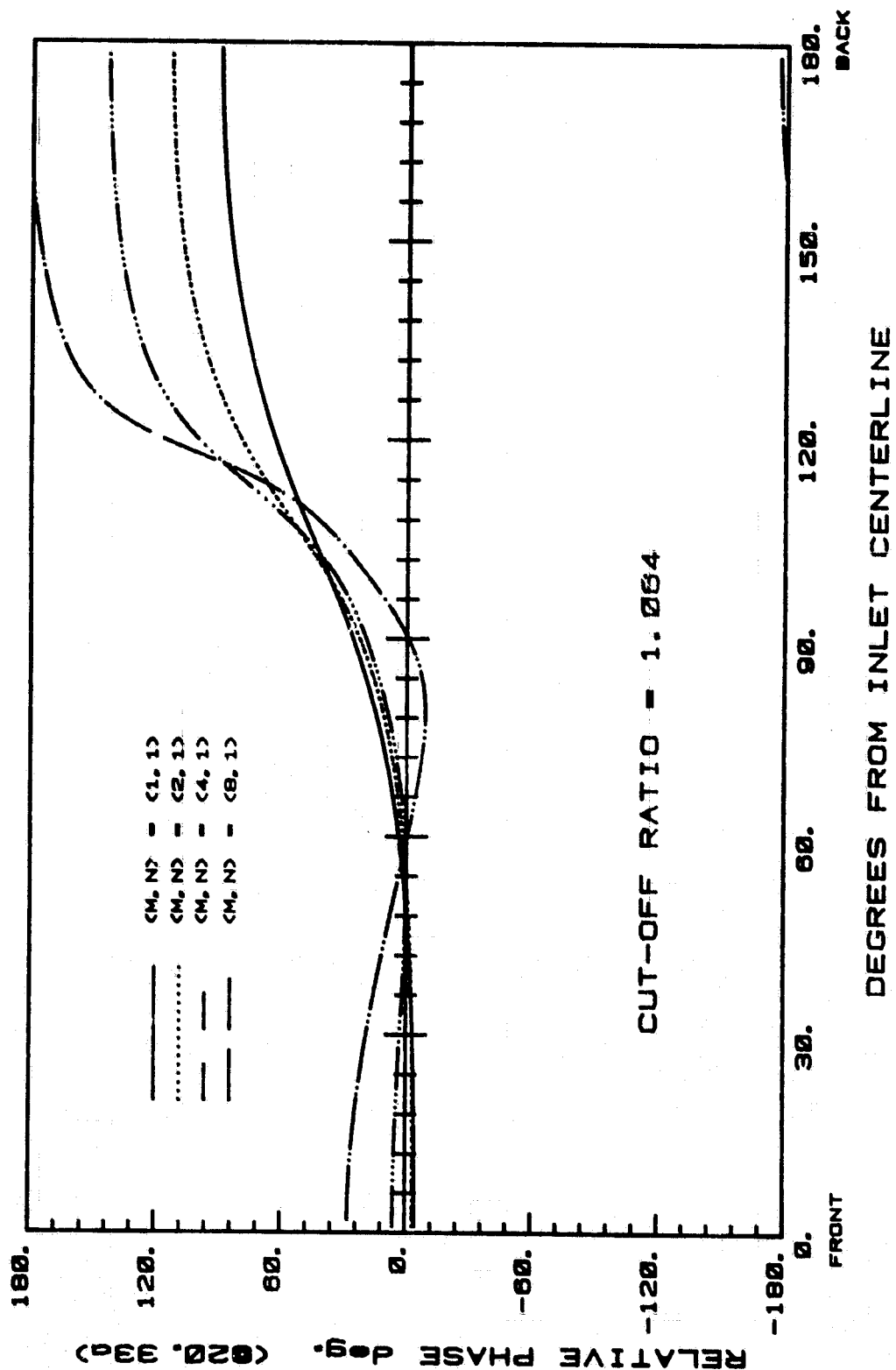
Fig. 55a



THICK LIPPED ELLIPTICAL INLET

Fig. 55b

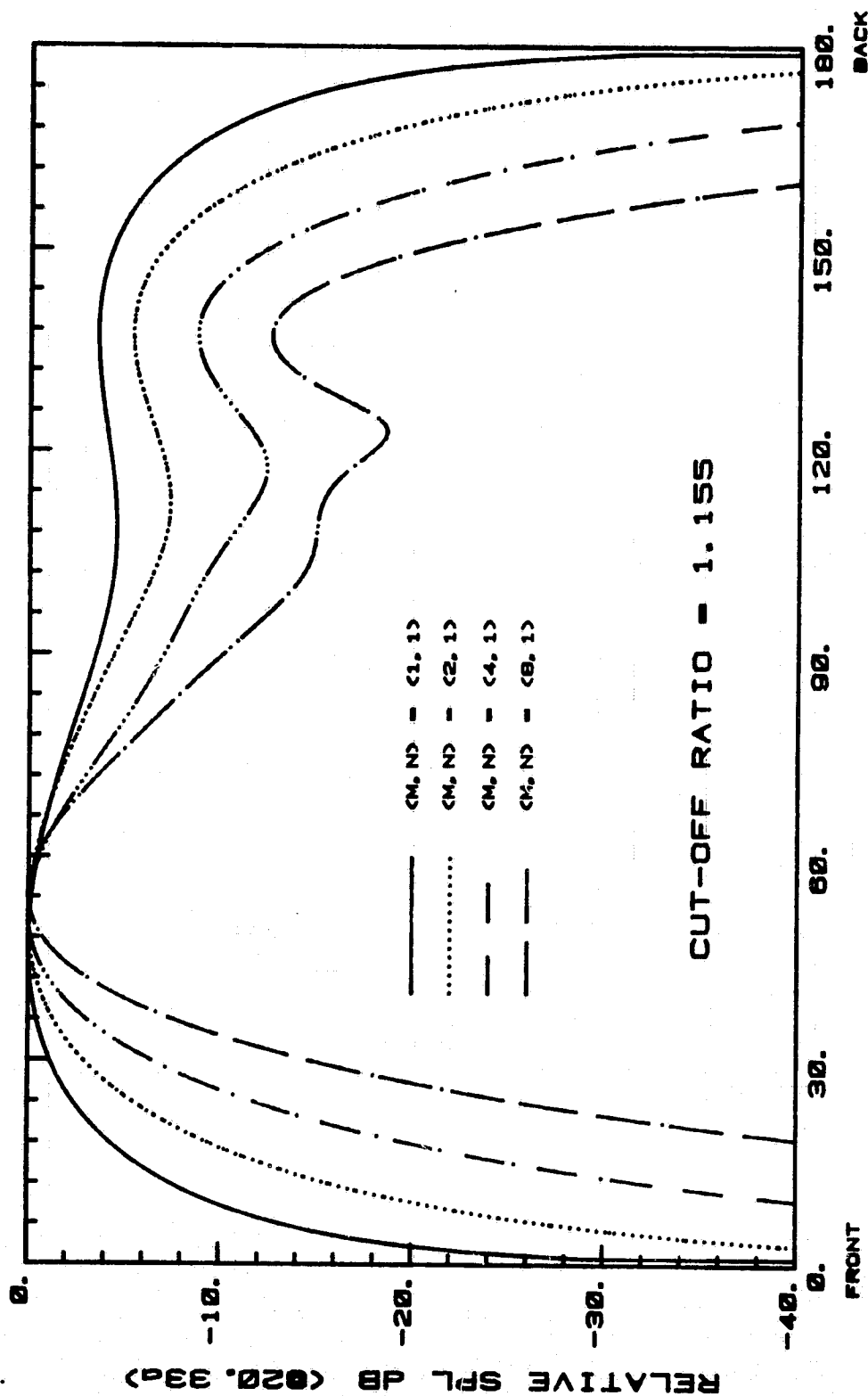
ORIGINAL PAGE IS
OF POOR QUALITY



THICK LIPPED ELLIPTICAL INLET

Fig. 55c

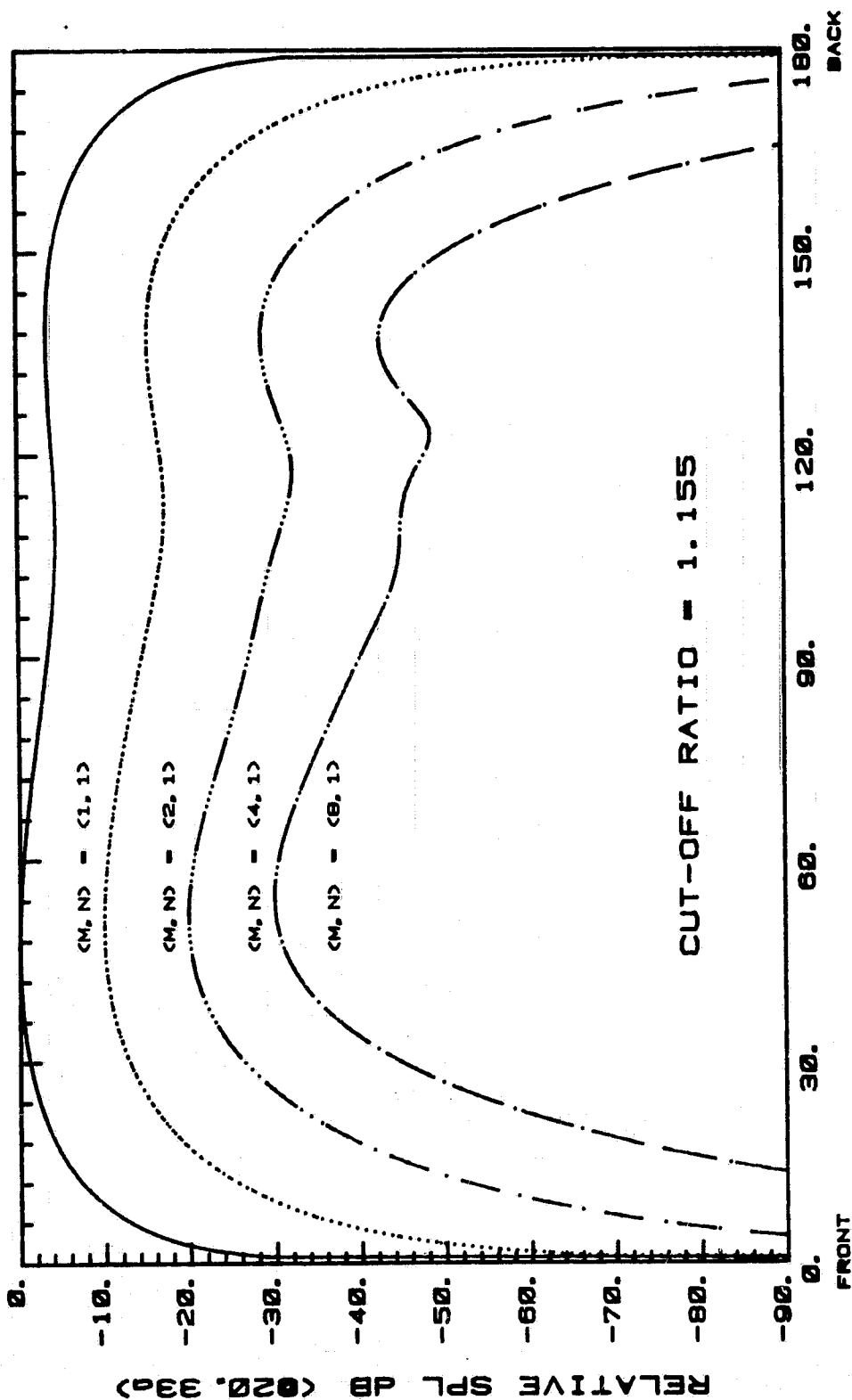
ORIGINAL PAGE IS
OF POOR QUALITY



THICK LIPPED ELLIPTICAL INLET

Fig. 56a

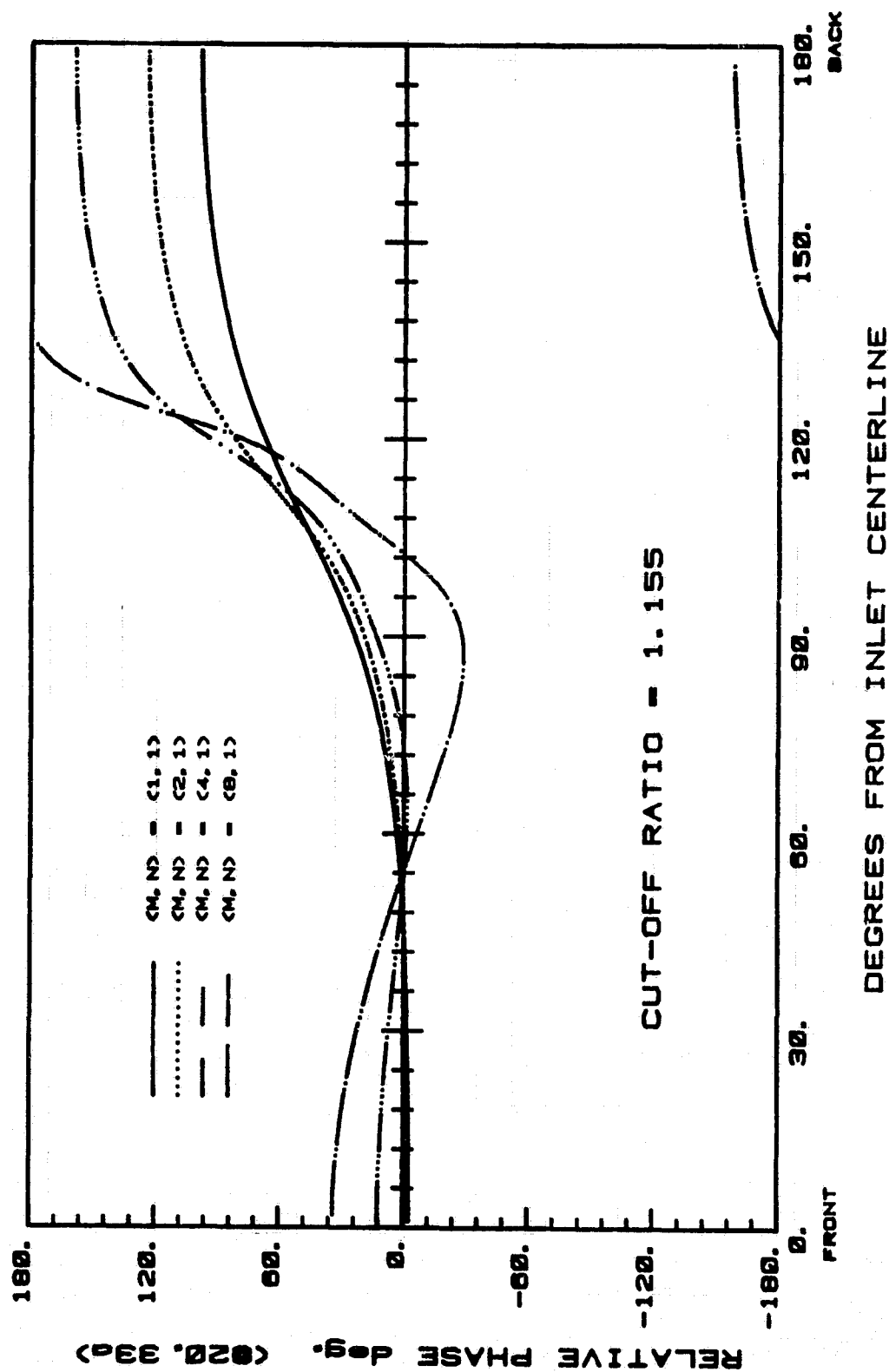
ORIGINAL PAGE IS
OF POOR QUALITY



DEGREES FROM INLET CENTERLINE

THICK LIPPED ELLIPTICAL INLET

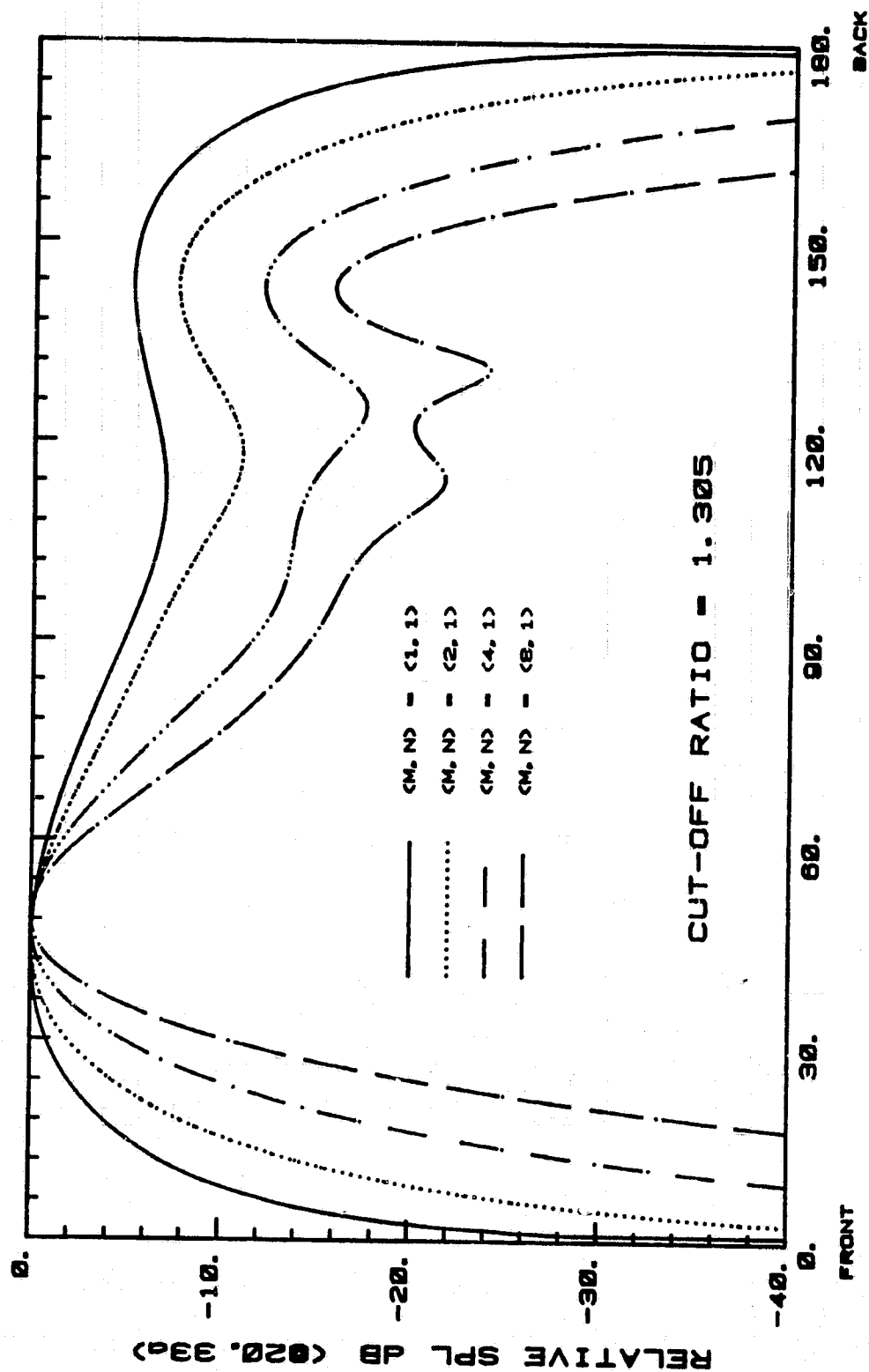
Fig. 56b



THICK LIPPED ELLIPTICAL INLET

Fig. 56c

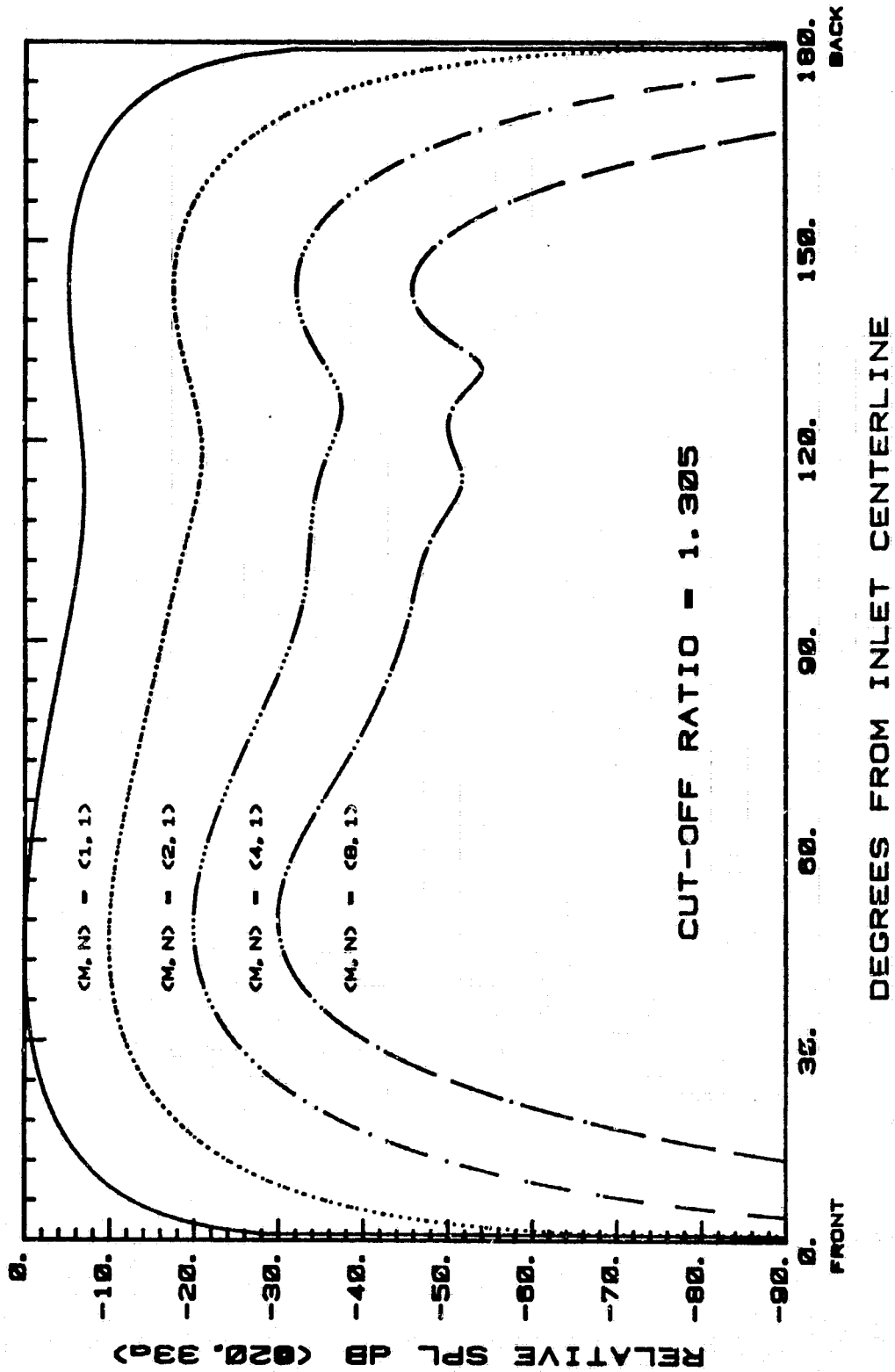
ORIGINAL PAGE 13
OF POOR QUALITY



THICK LIPPED ELLIPTICAL INLET

Fig. 57a

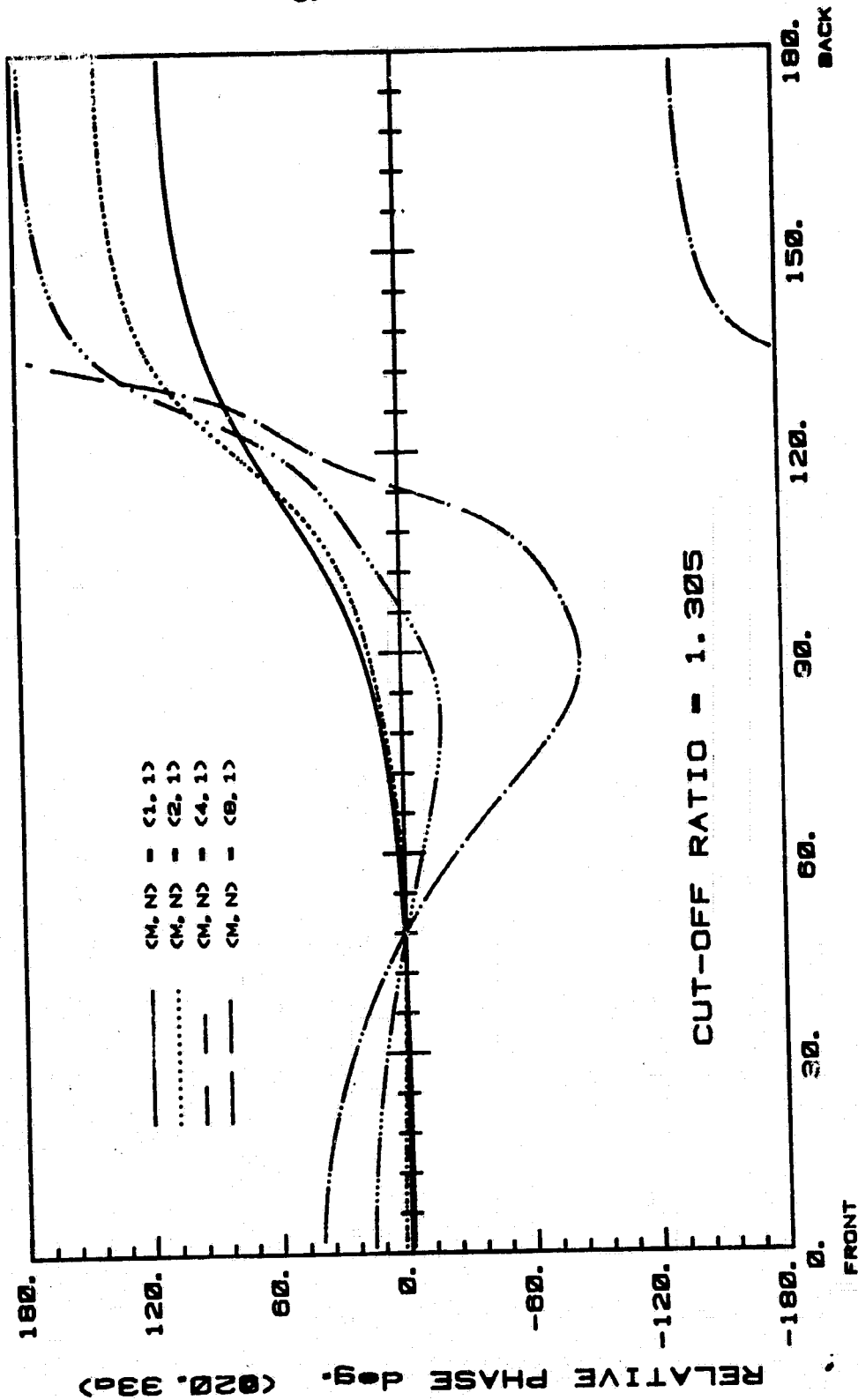
ORIGINAL PAGE IS
OF POOR QUALITY



THICK LIPPED ELLIPTICAL INLET

Fig. 57b

ORIGINAL PAGE 19
OF POOR QUALITY



THICK LIPPED ELLIPTICAL INLET

Fig. 57c

ORIGINAL PAGE IS
OF POOR QUALITY

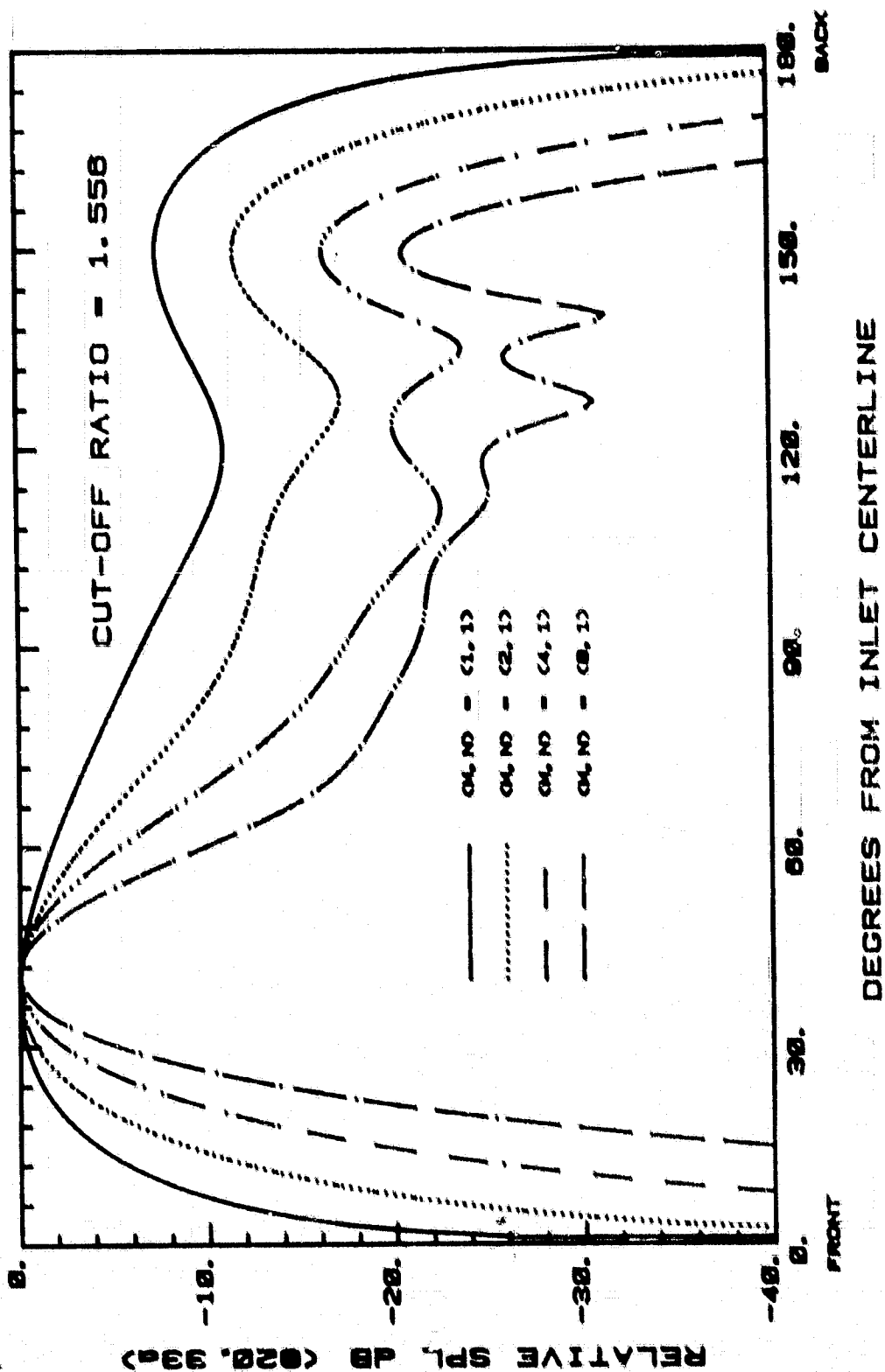
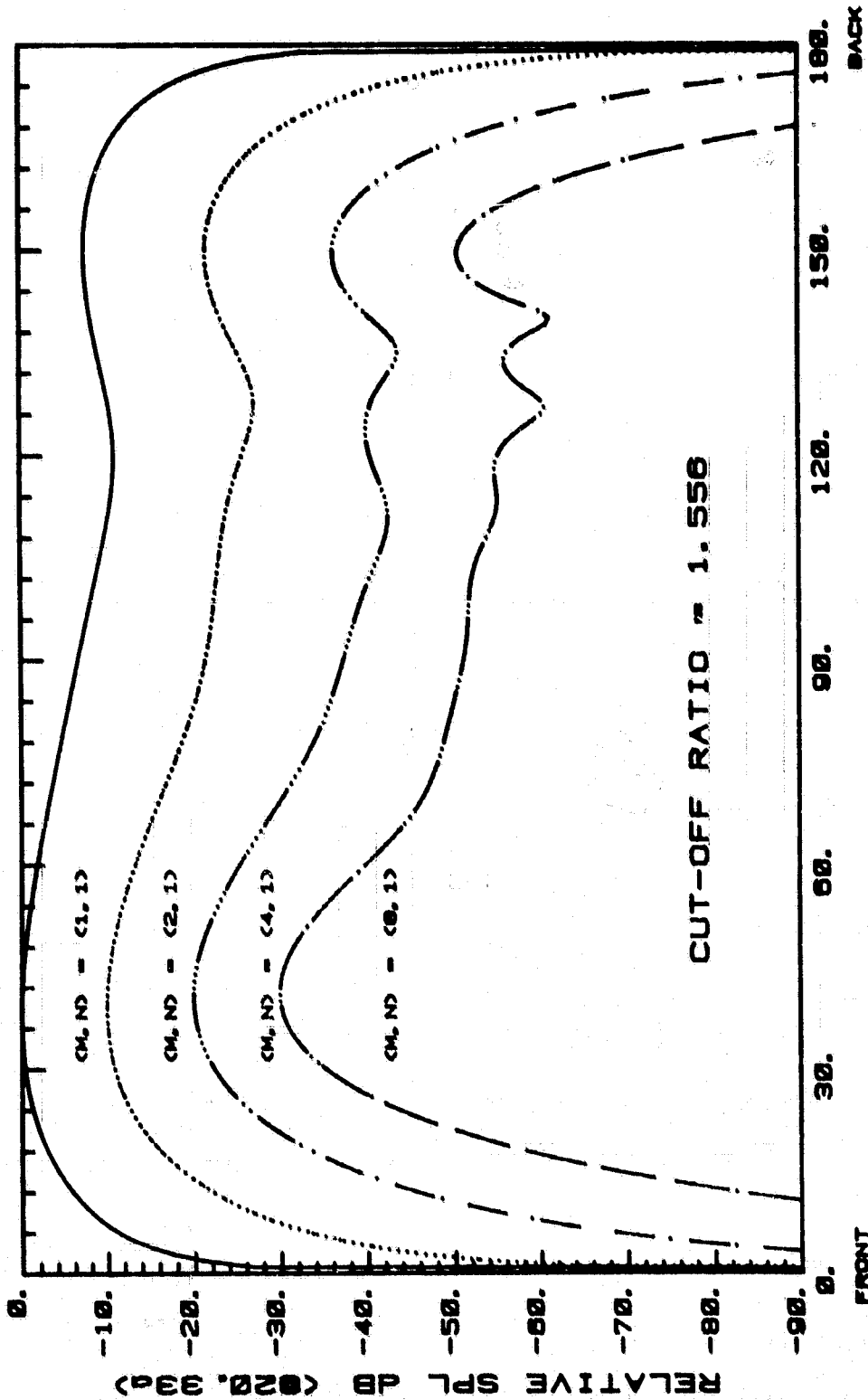


Fig. 58a

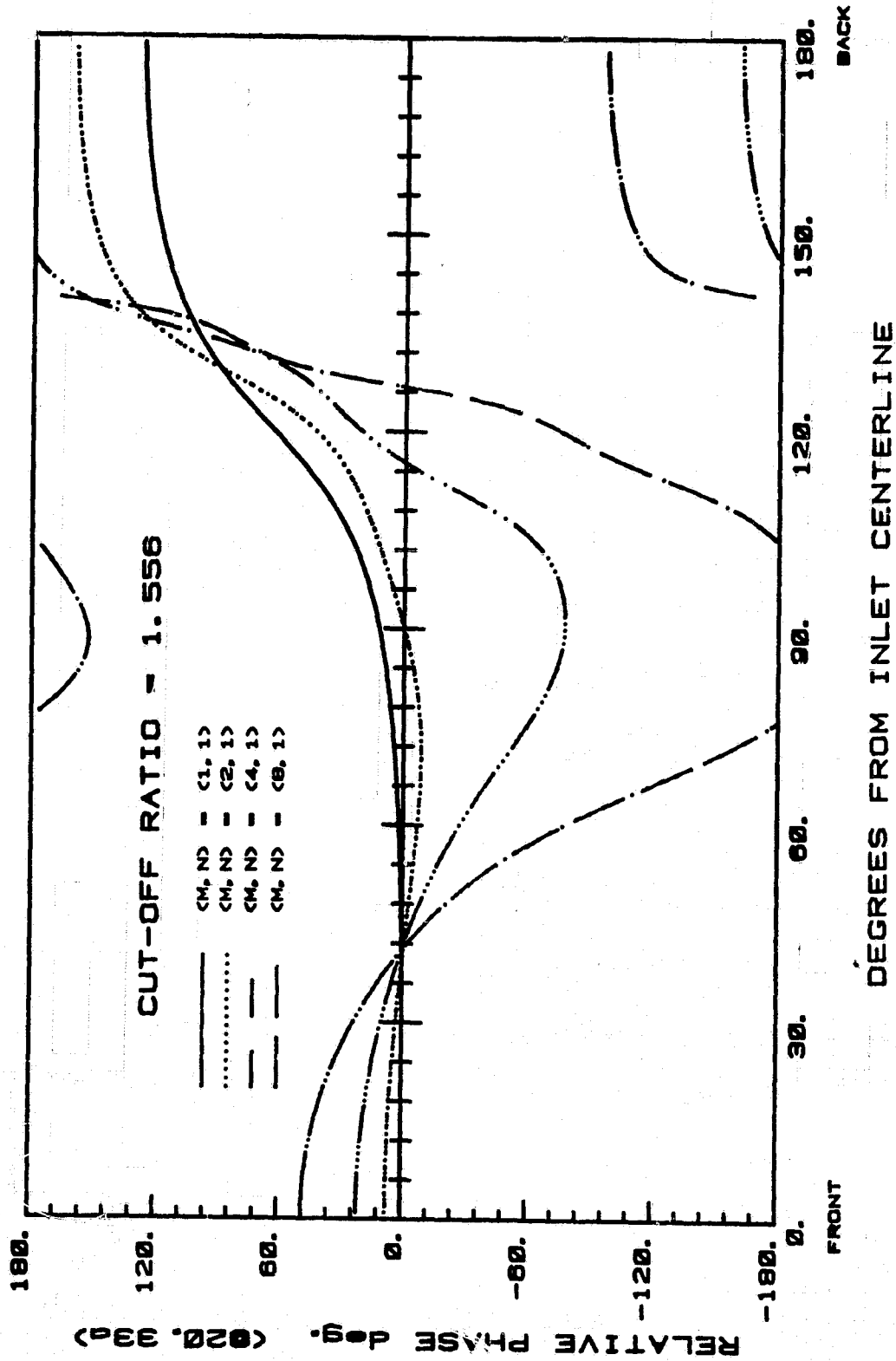
THICK LIPPED ELLIPTICAL INLET

ORIGINAL PAGE IS
OF POOR QUALITY



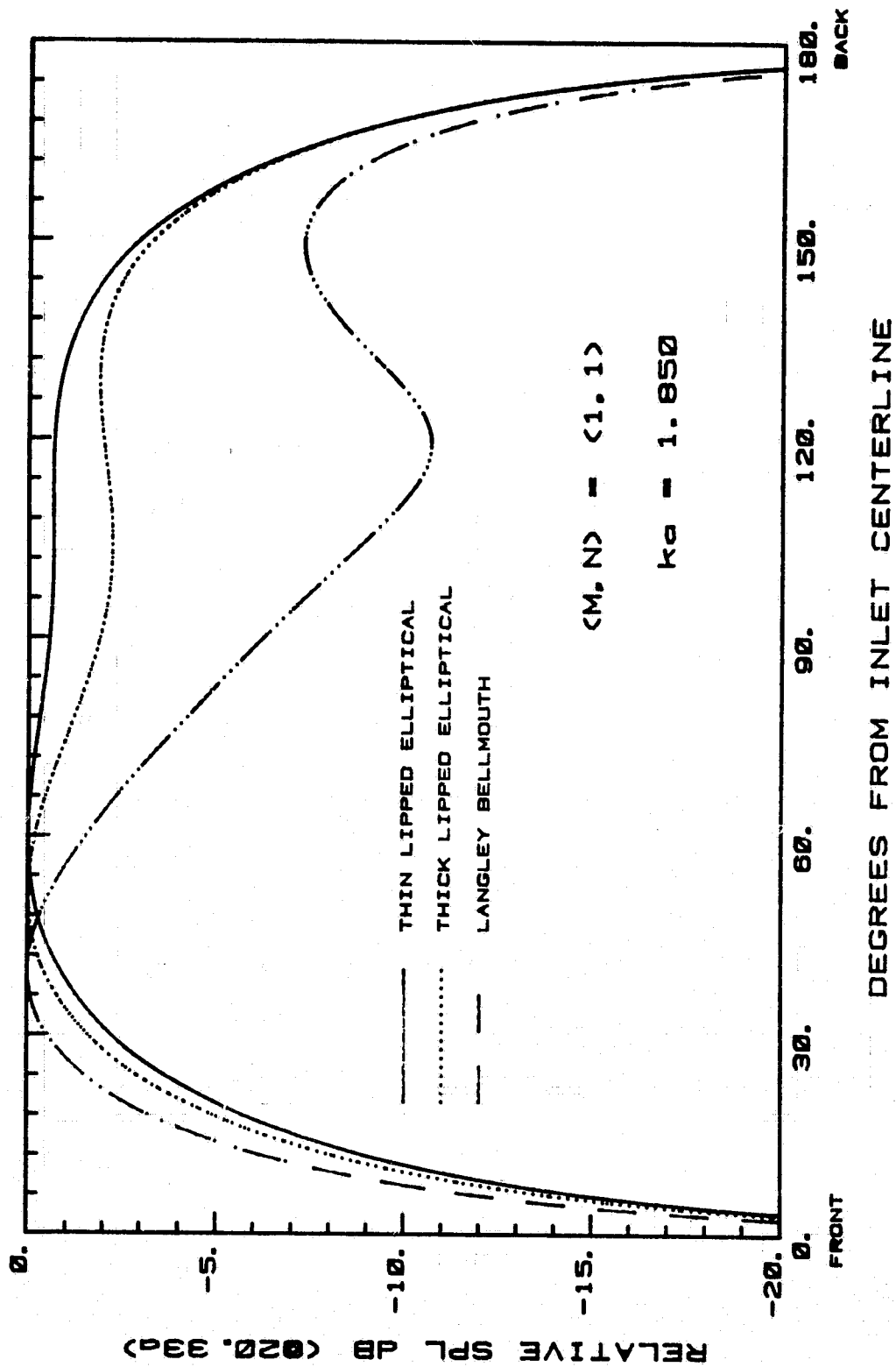
THICK LIPPED ELLIPTICAL INLET

Fig. 58b



THICK LIPPED ELLIPTICAL INLET

Fig. 58c



CUT-OFF RATIO = 1.005

Fig. 59a

ORIGINAL PAGE IS
OF POOR QUALITY

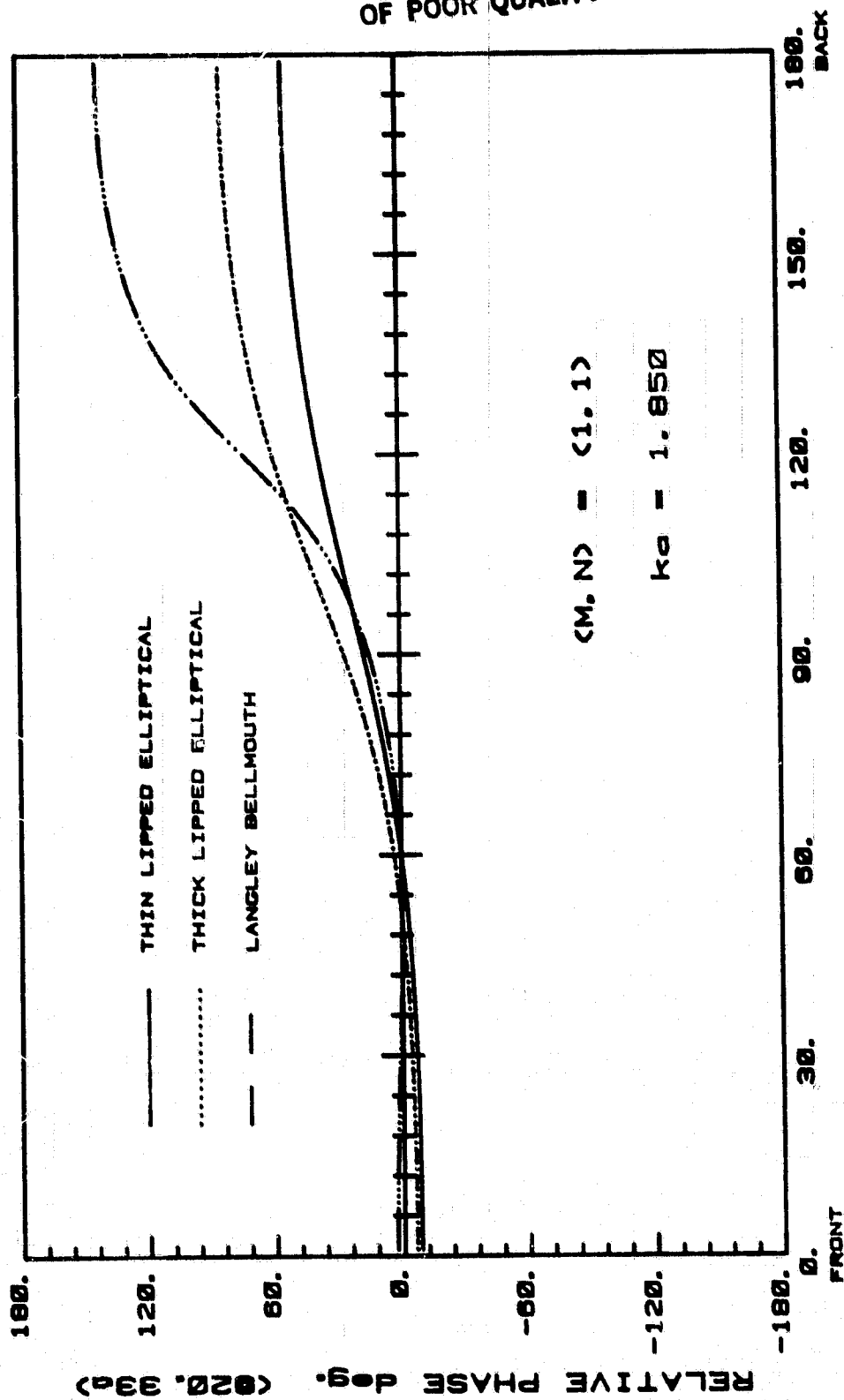
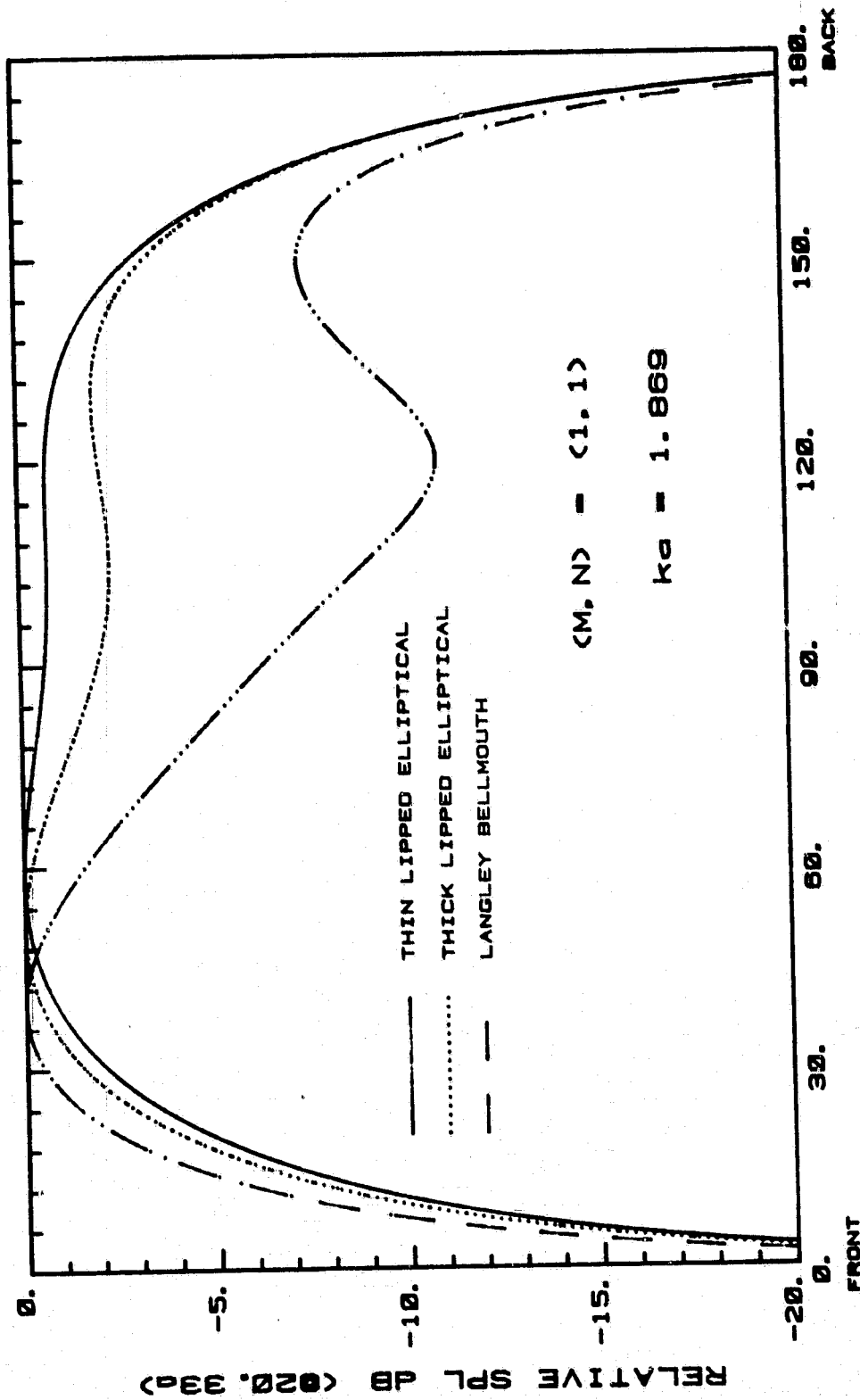


Fig. 59b

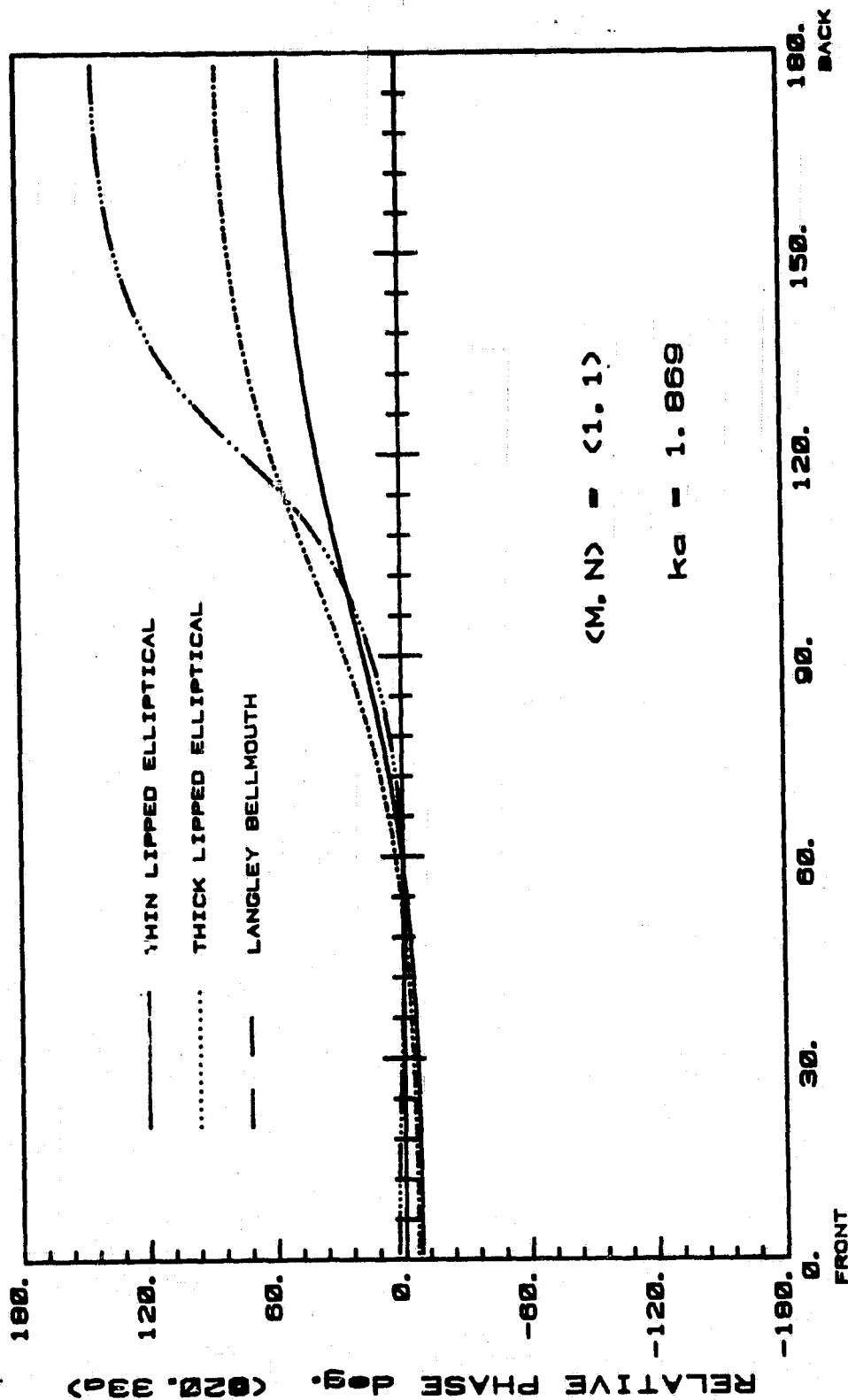
ORIGINAL PAGE IS
OF POOR QUALITY



CUT-OFF RATIO = 1.015

Fig. 59c

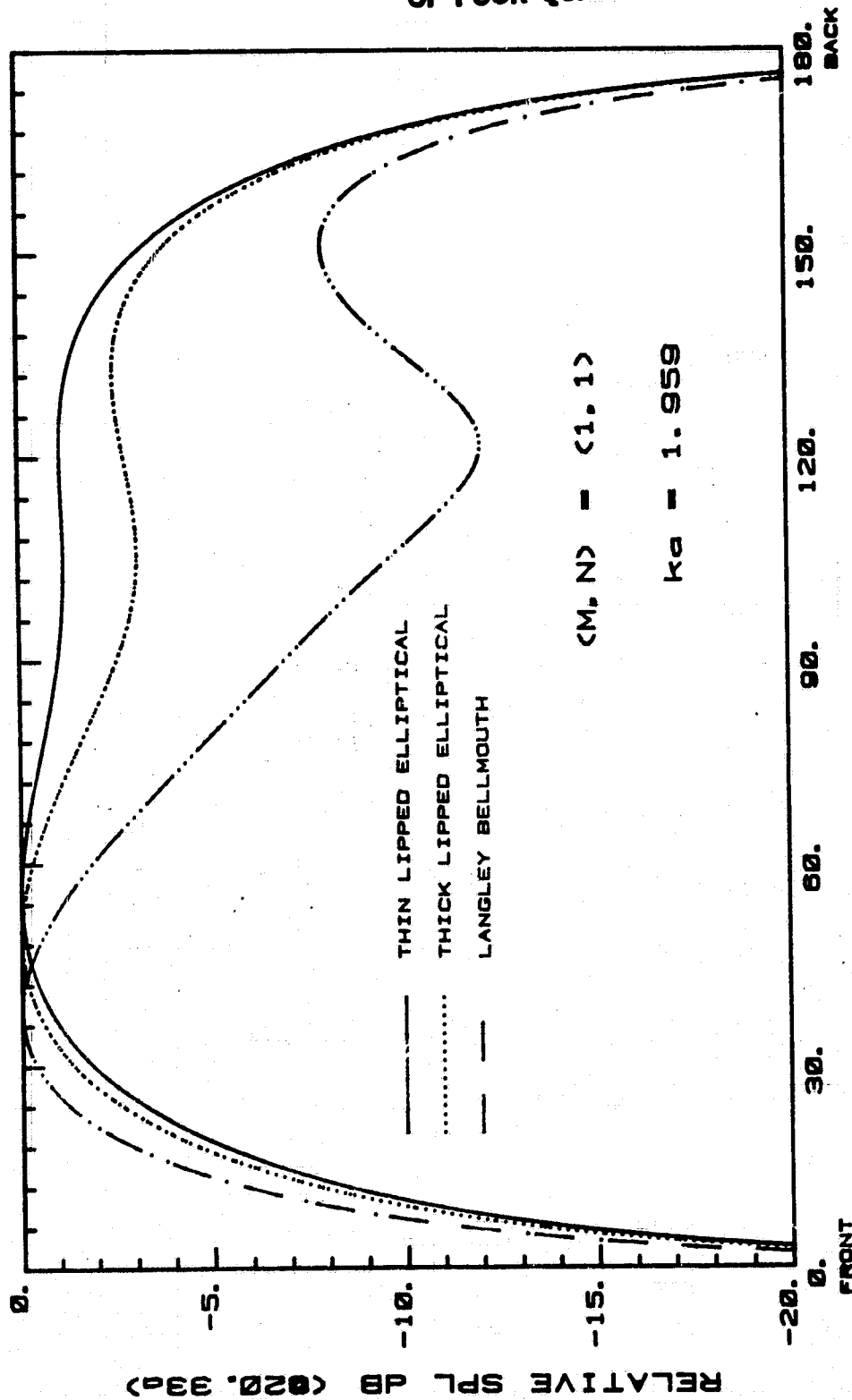
ORIGINAL PAGE IS
OF POOR QUALITY



CUT-OFF RATIO = 1.015

Fig. 59d

ORIGINAL PAGE IS
OF POOR QUALITY



CUT-OFF RATIO = 1.064

Fig. 59e

ORIGINAL PAGE IS
OF POOR QUALITY

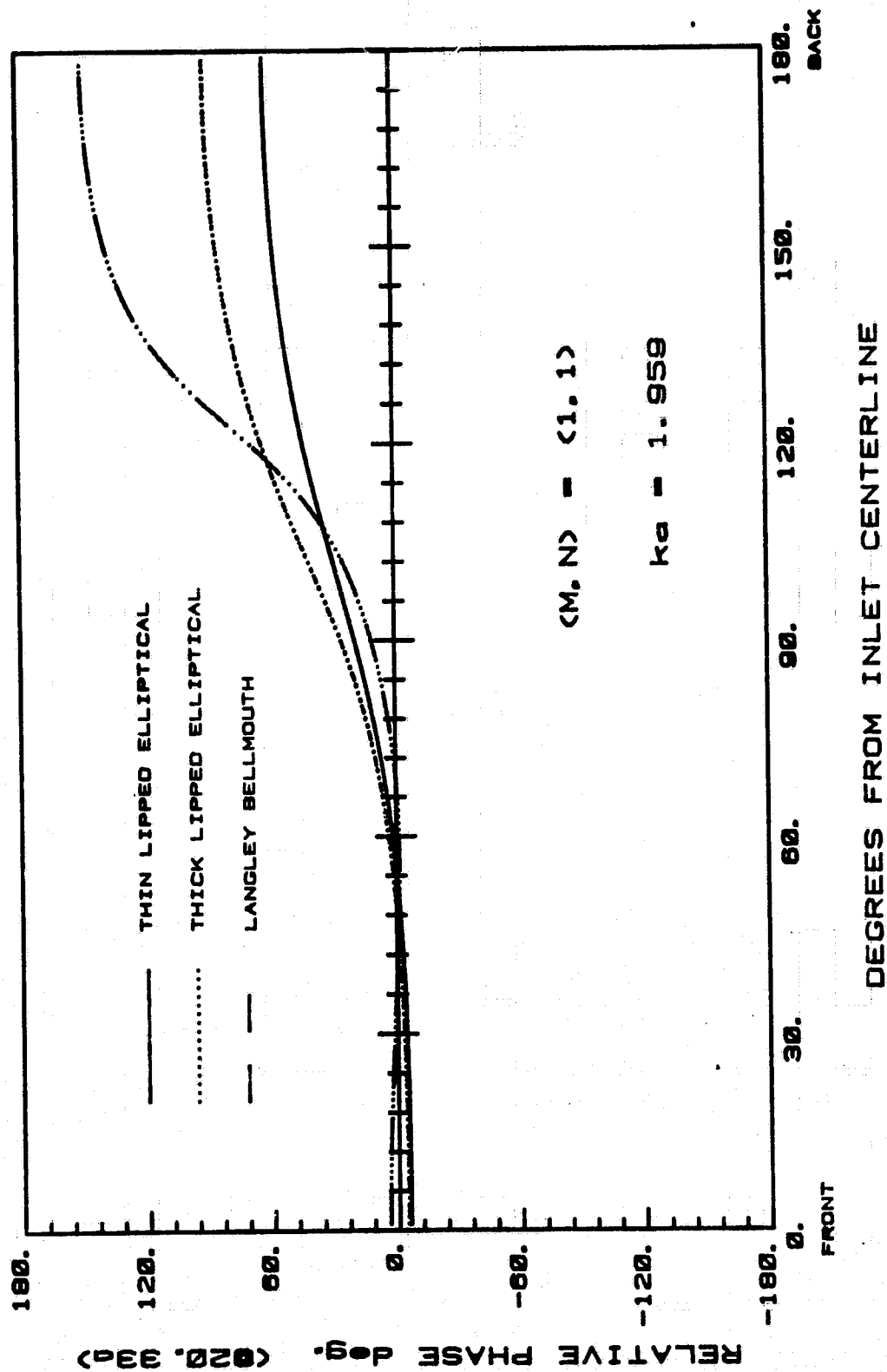
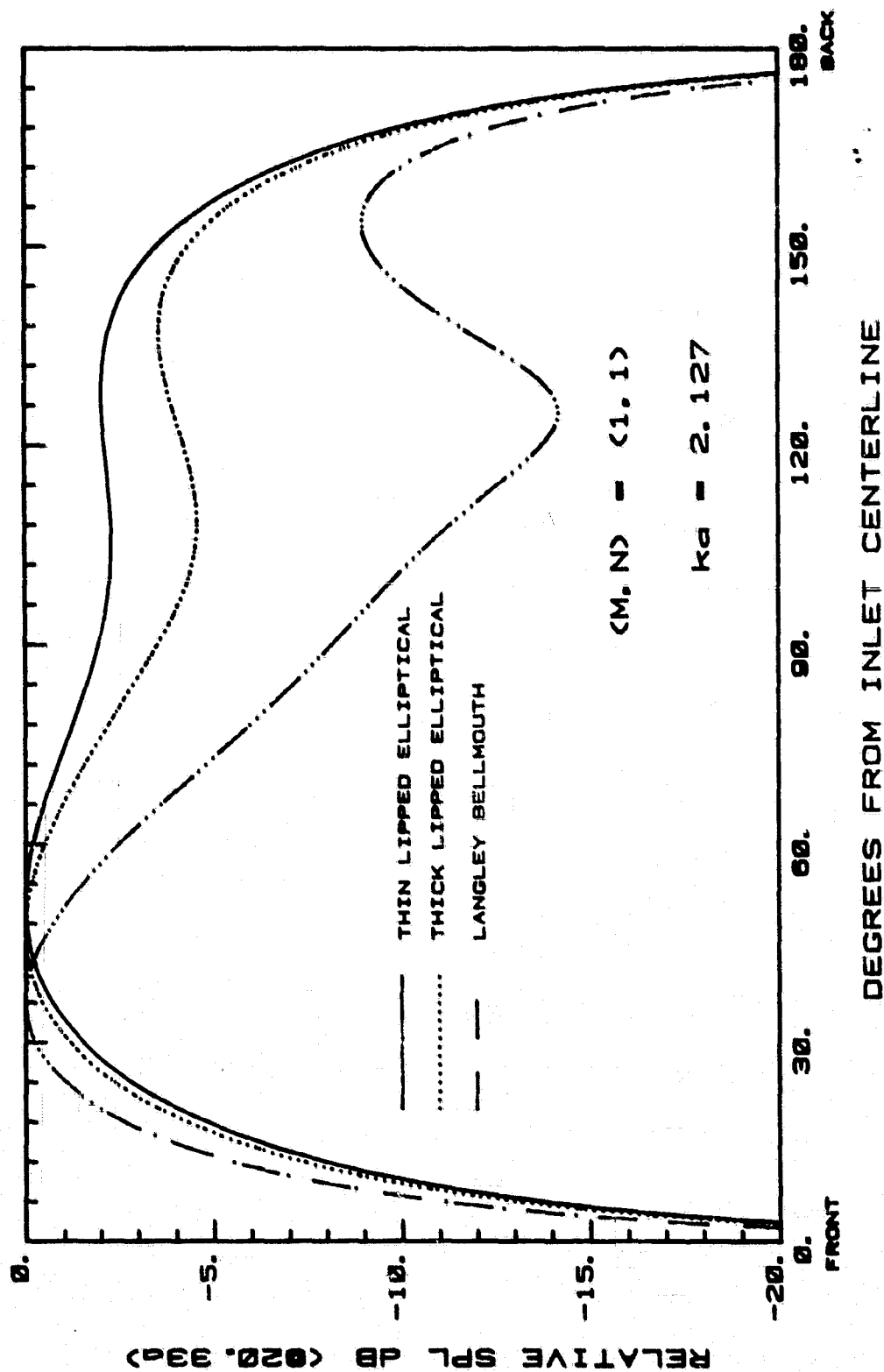


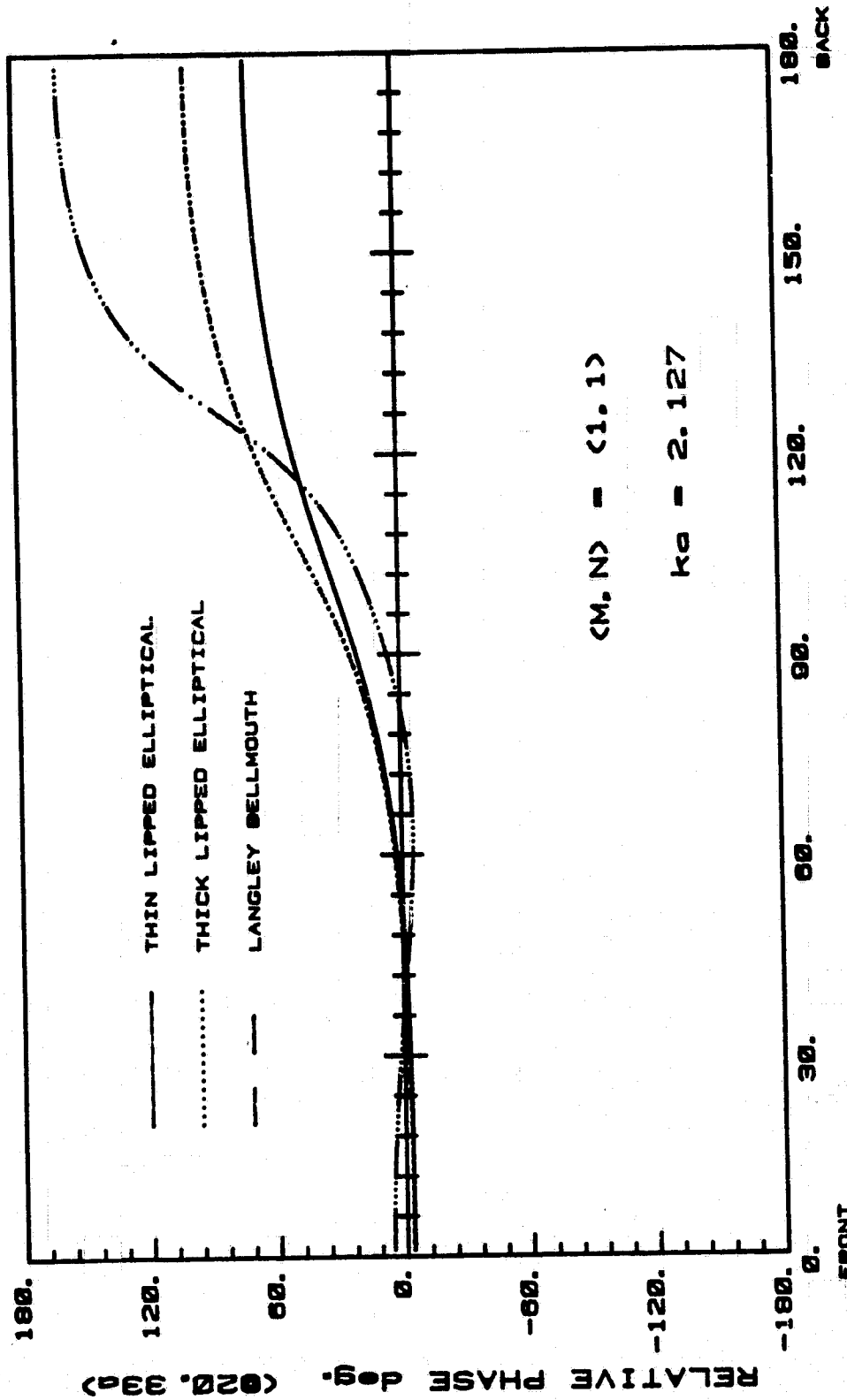
Fig. 59f

ORIGINAL PAGE 15
OF POOR QUALITY



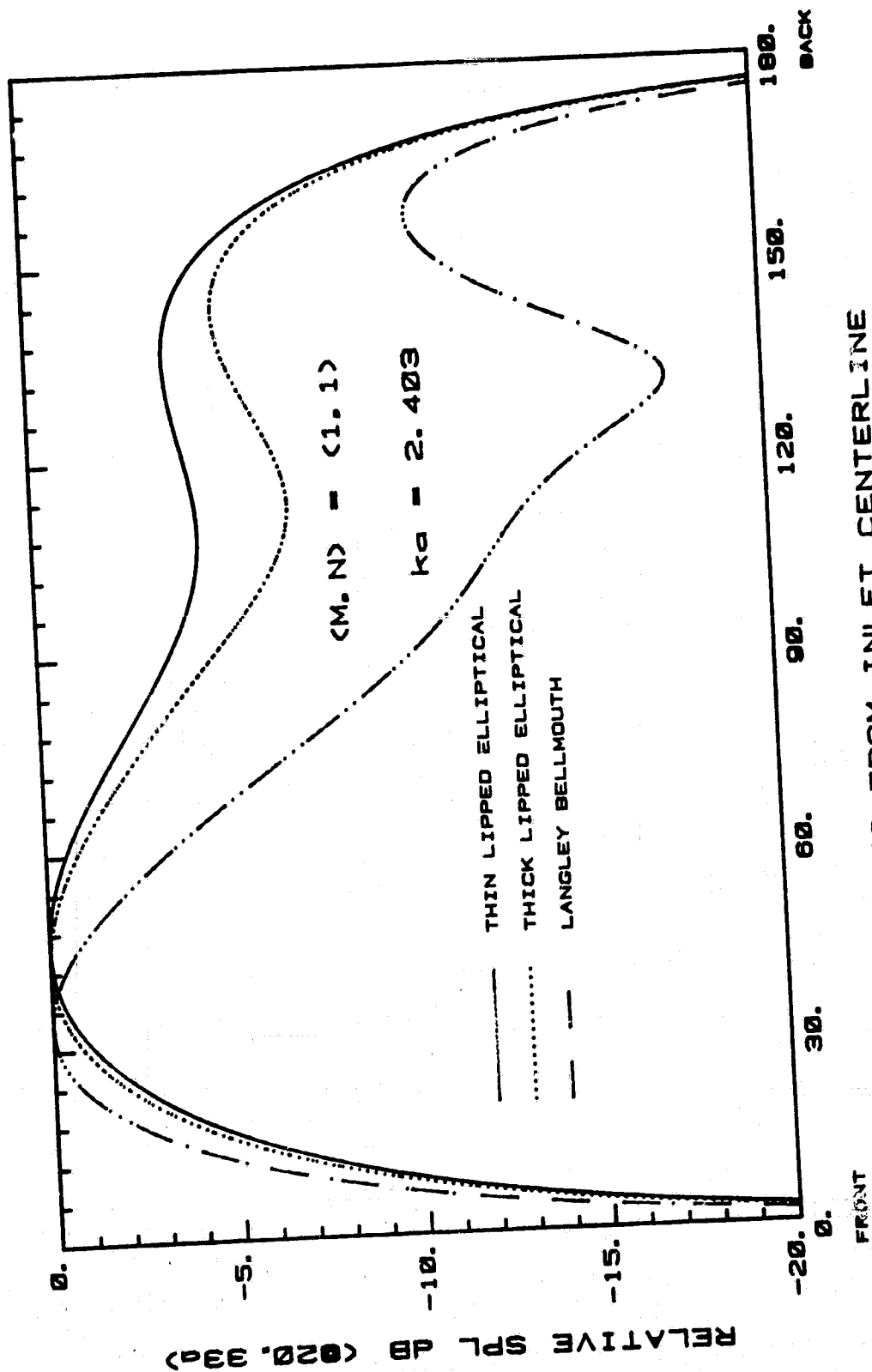
CUT-OFF RATIO = 1.155

Fig. 59g



CUT-OFF RATIO = 1.155

Fig. 59h

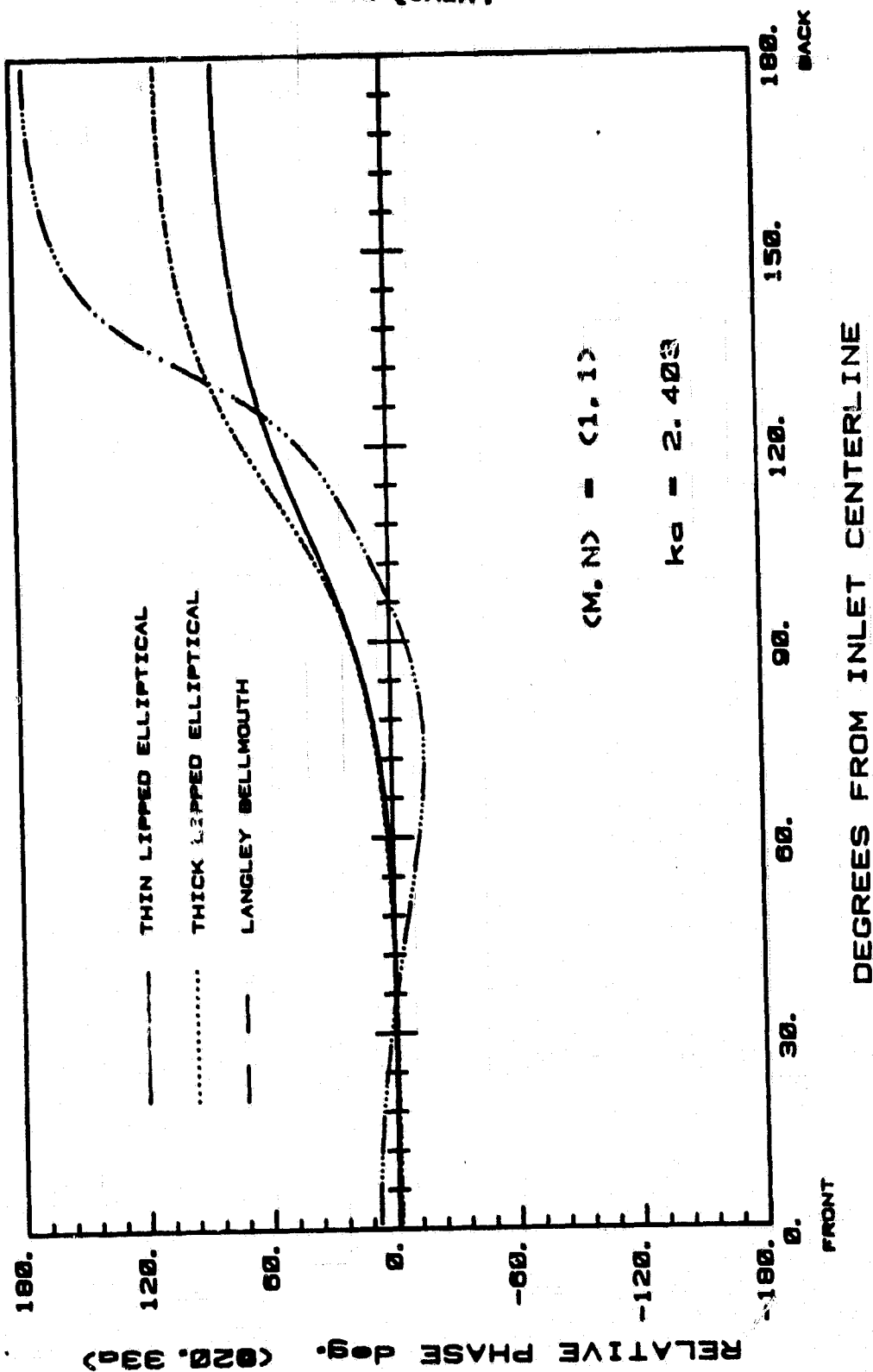


DEGREES FROM INLET CENTERLINE

CUT-OFF RATIO = 1.305

Fig. 591

ORIGINAL PAGE IS
OF POOR QUALITY



CUT-OFF RATIO = 1.305

Fig. 59j

ORIGINAL PAGE IS
OF POOR QUALITY

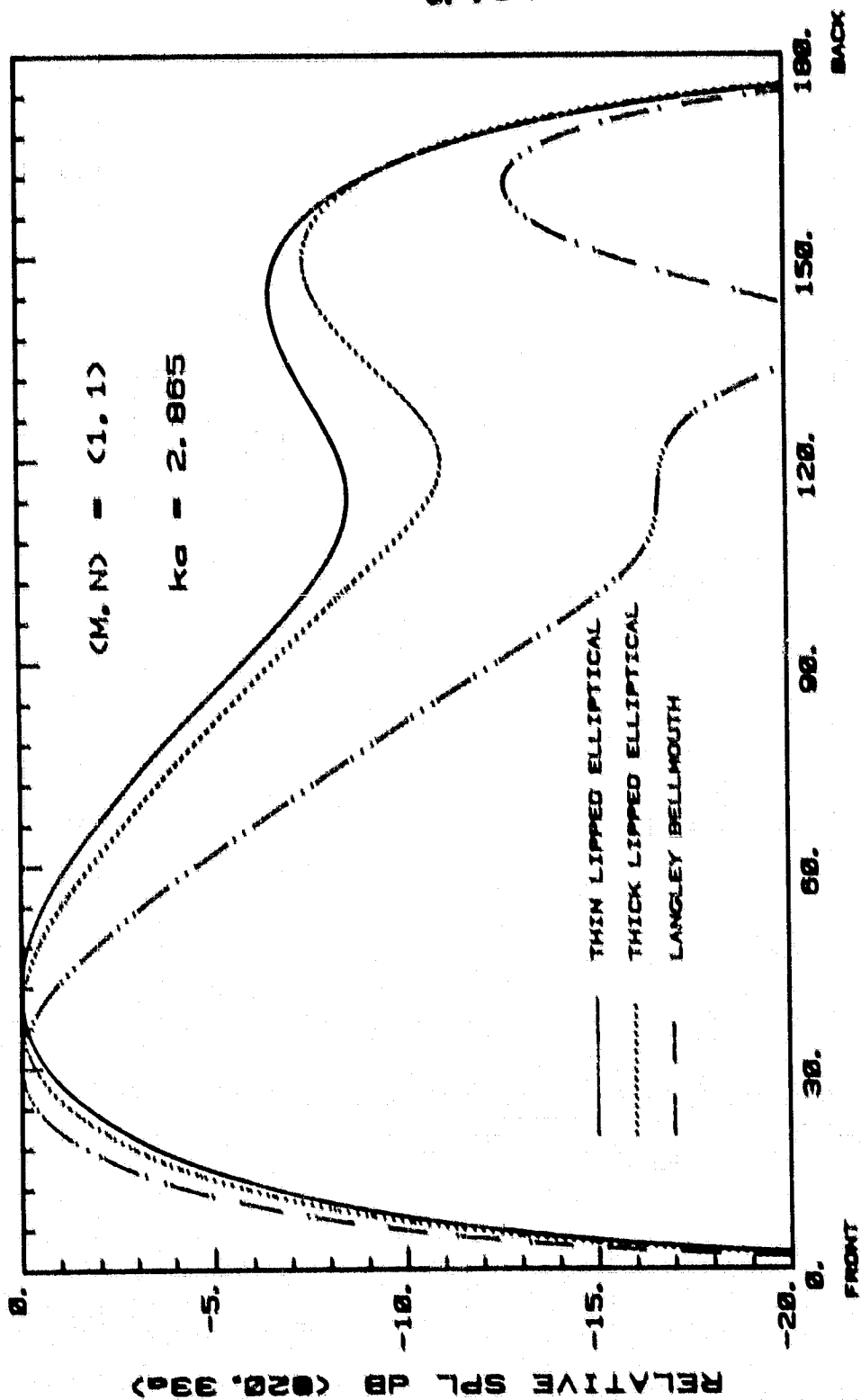
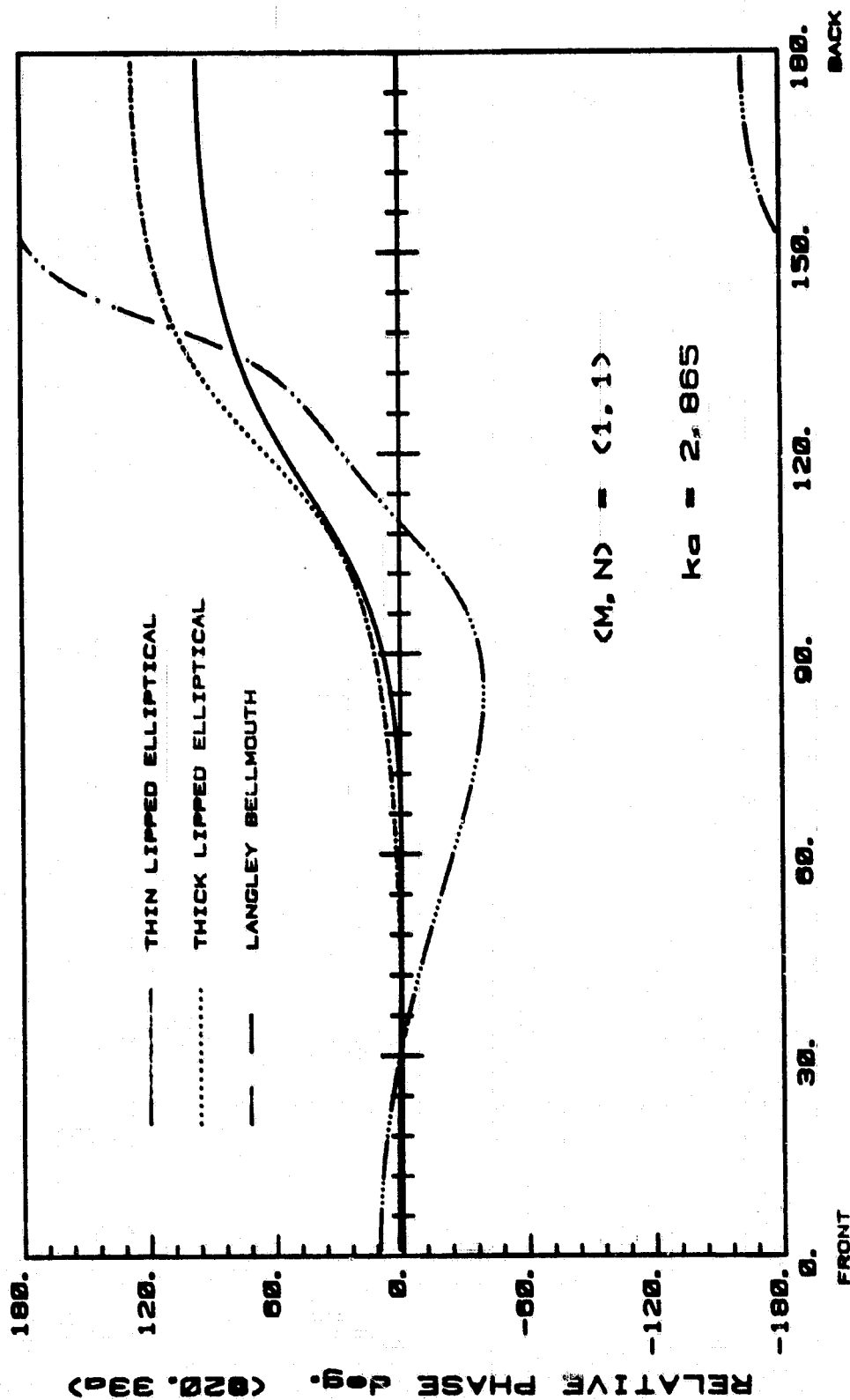


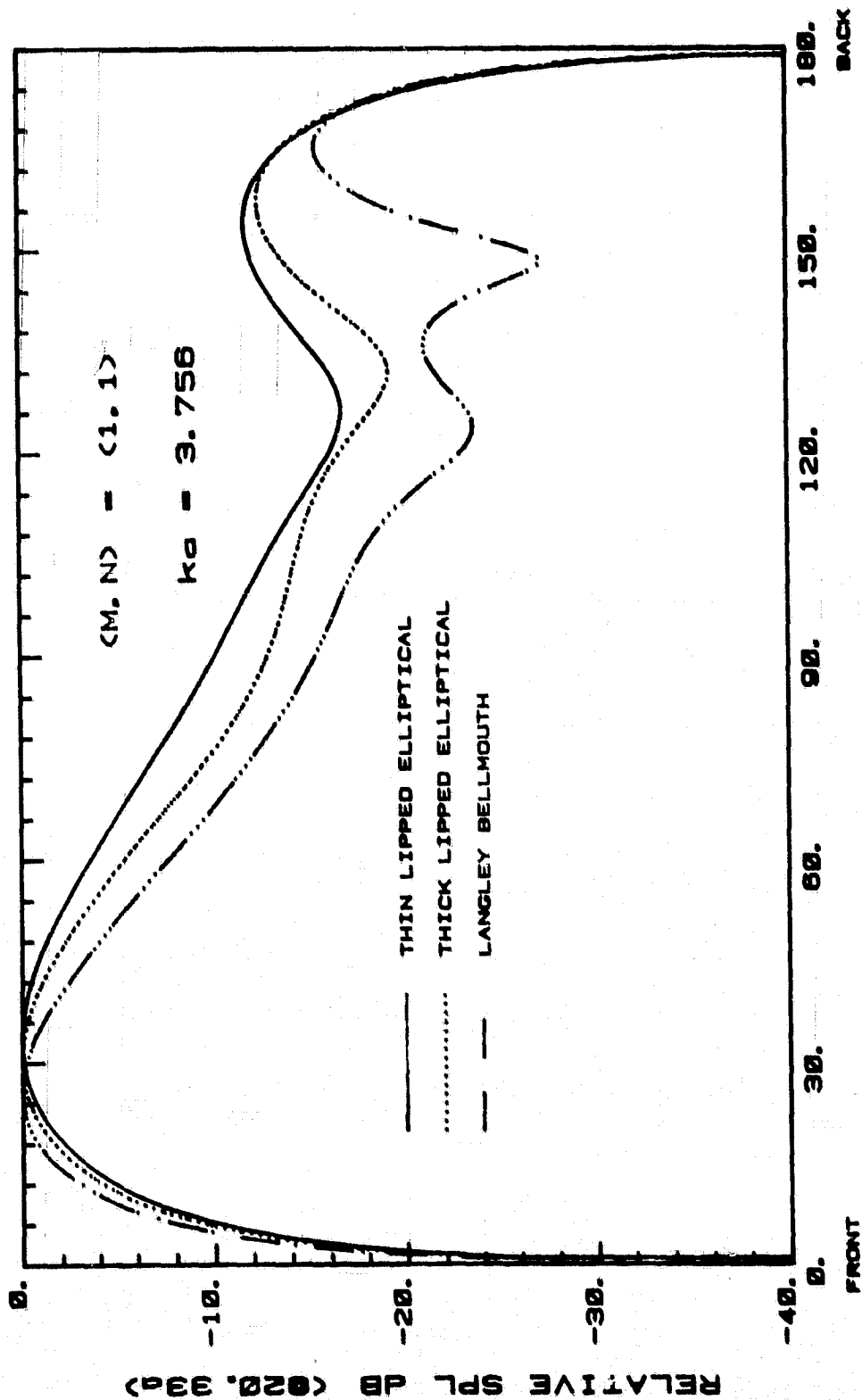
Fig. 59k



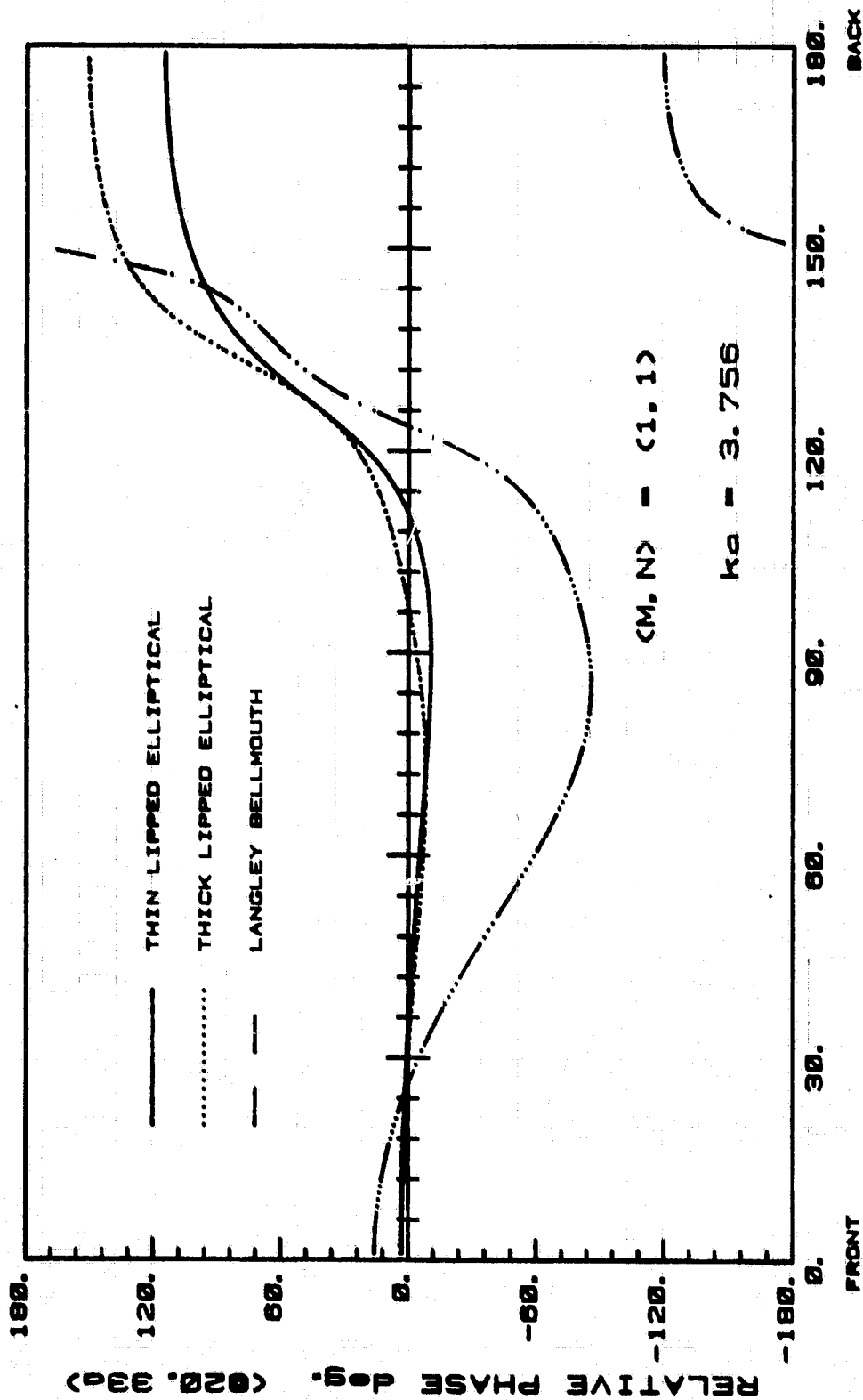
CUT-OFF RATIO = 1.556

Fig. 591

ORIGINAL PAGE IS
OF POOR QUALITY



ORIGINAL PAGE IS
OF POOR QUALITY



CUT-OFF RATIO = 2.04

Fig. 59n

ORIGINAL PAGE IS
OF POOR QUALITY

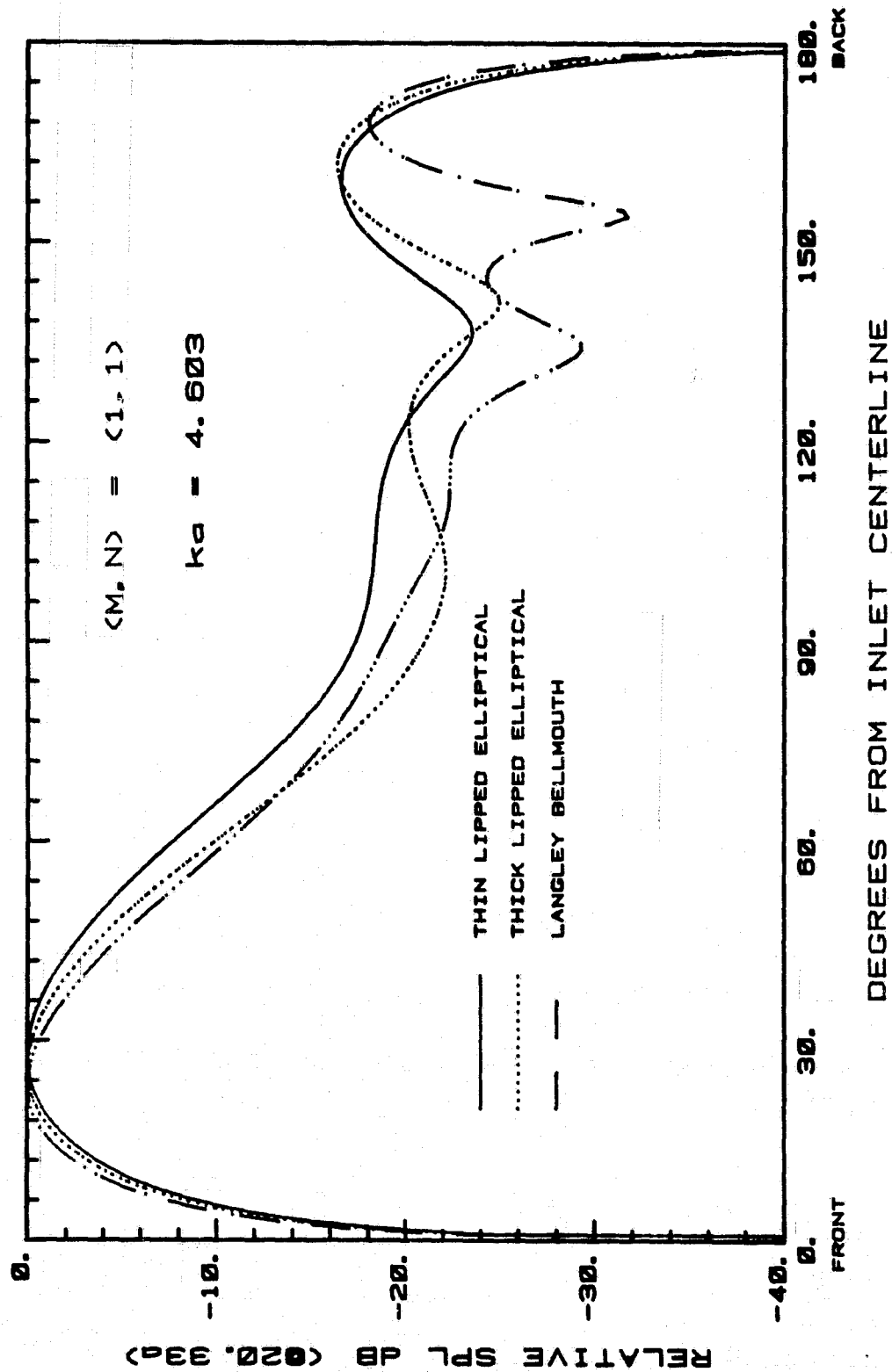
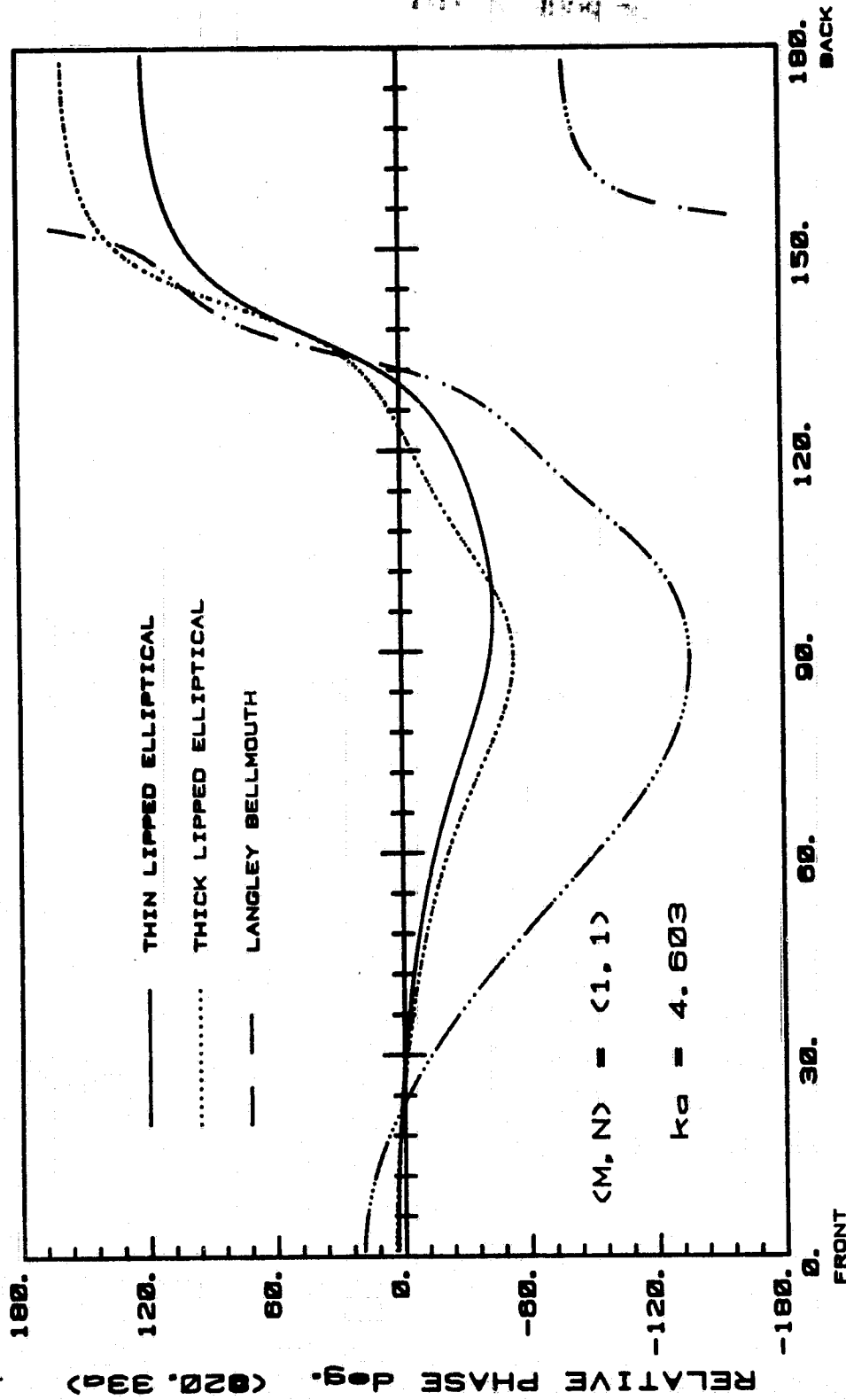


Fig. 590

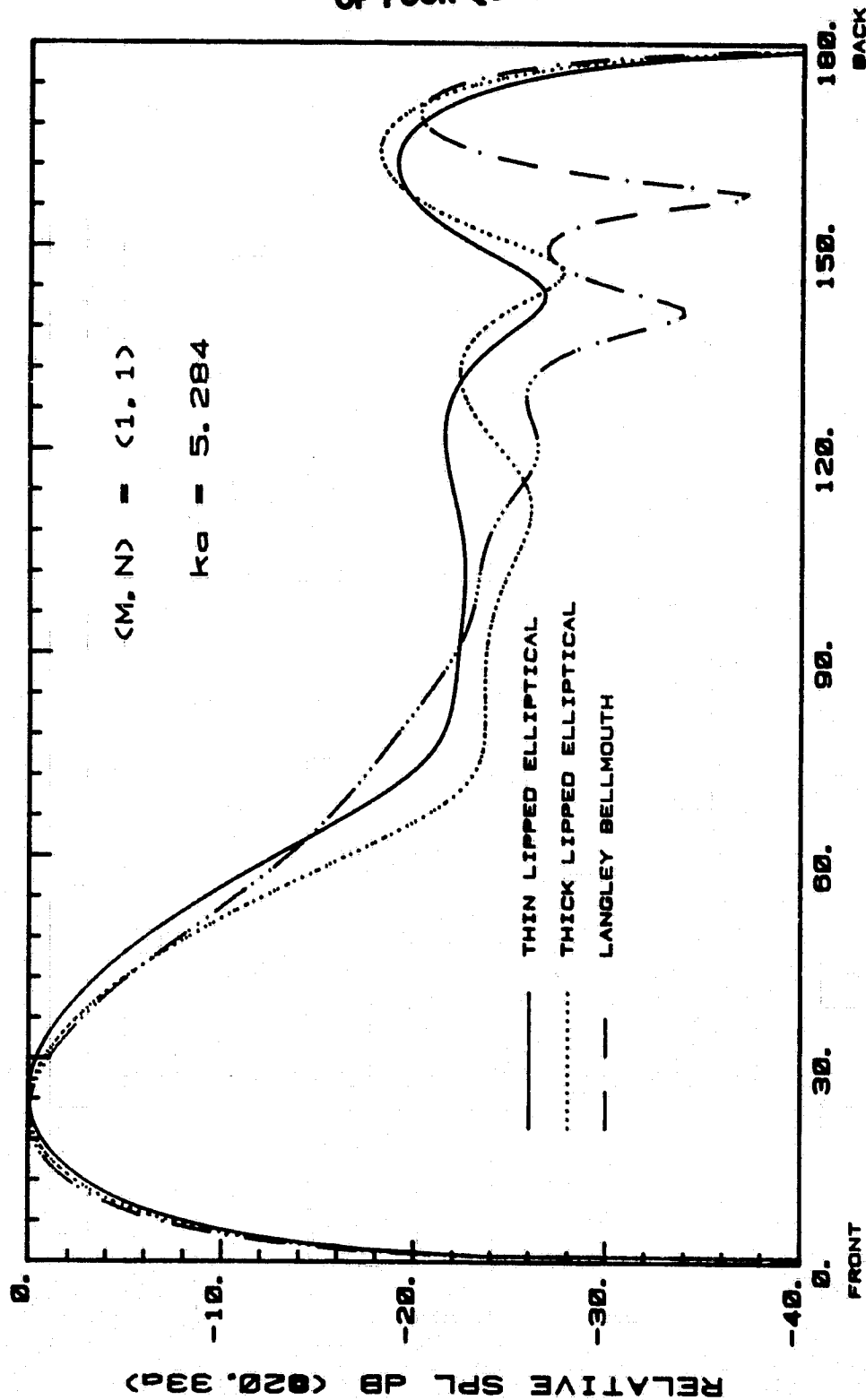
ORIGINAL PAGE IS
OF POOR QUALITY



CUT-OFF RATIO = 2.50

Fig. 59p

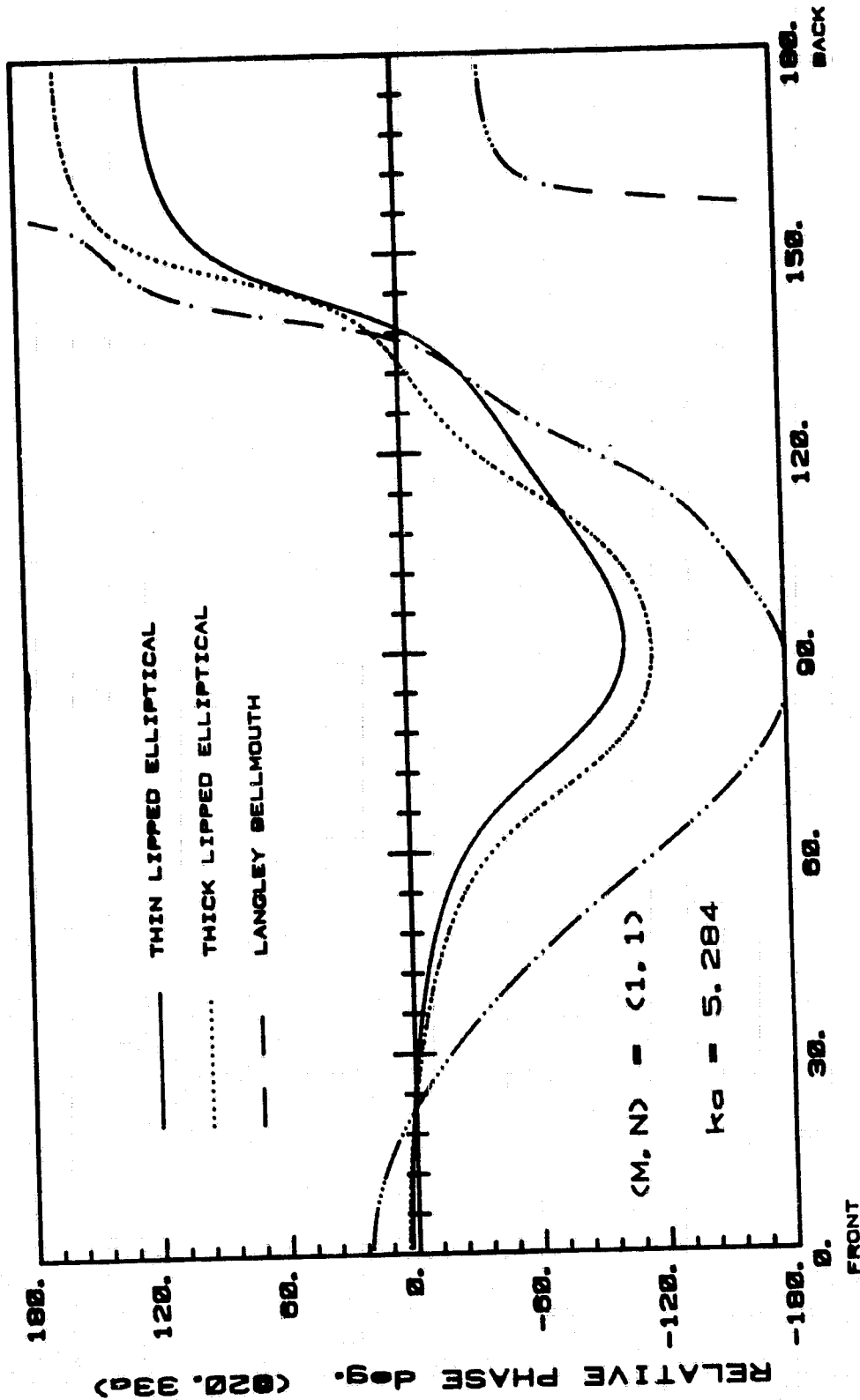
ORIGINAL PAGE IS
OF POOR QUALITY



CUT-OFF RATIO = 2.87

Fig. 59q

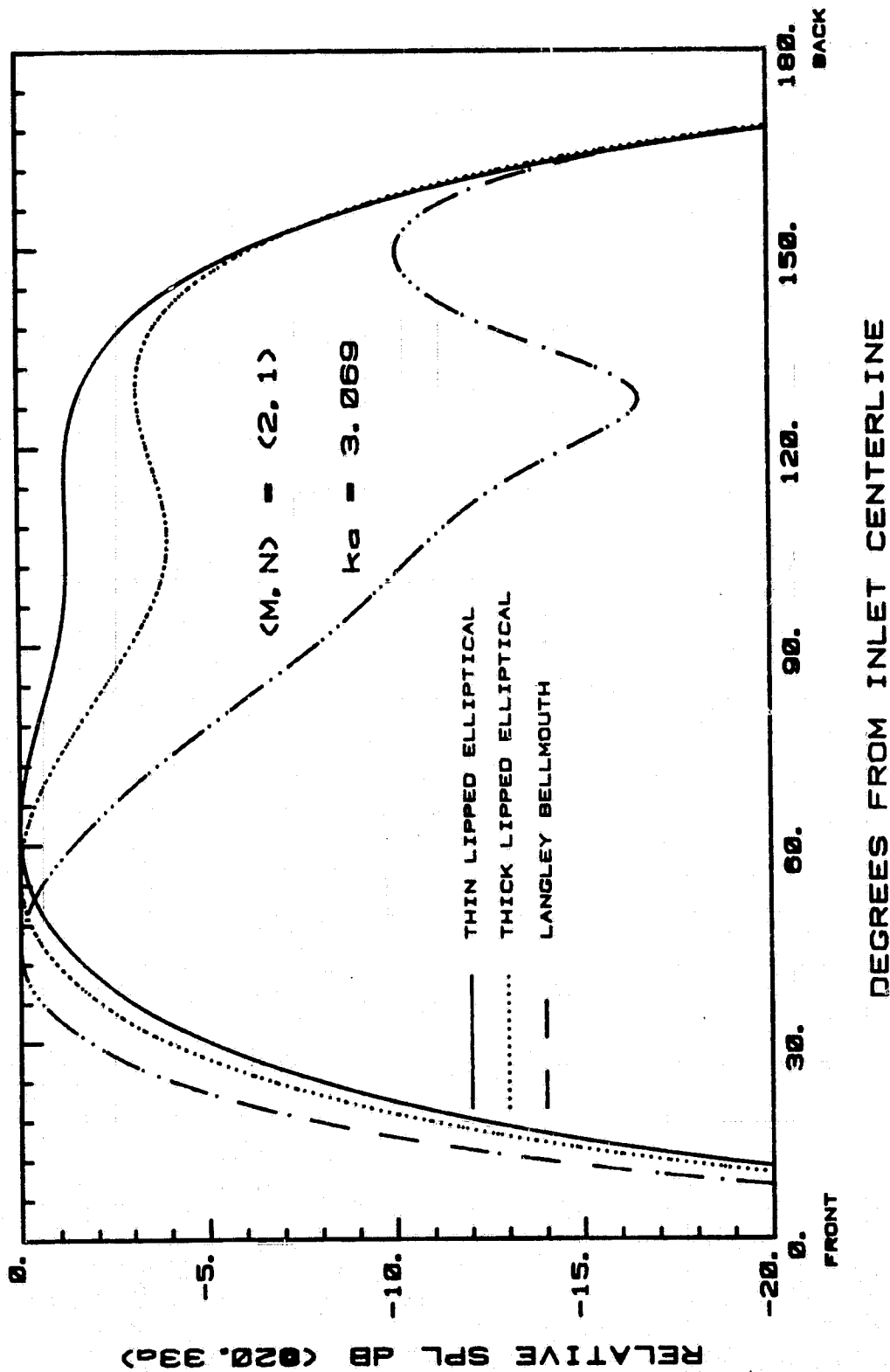
ORIGINAL PAGE IS
OF POOR QUALITY



CUT-OFF RATIO = 2.87

Fig. 59r

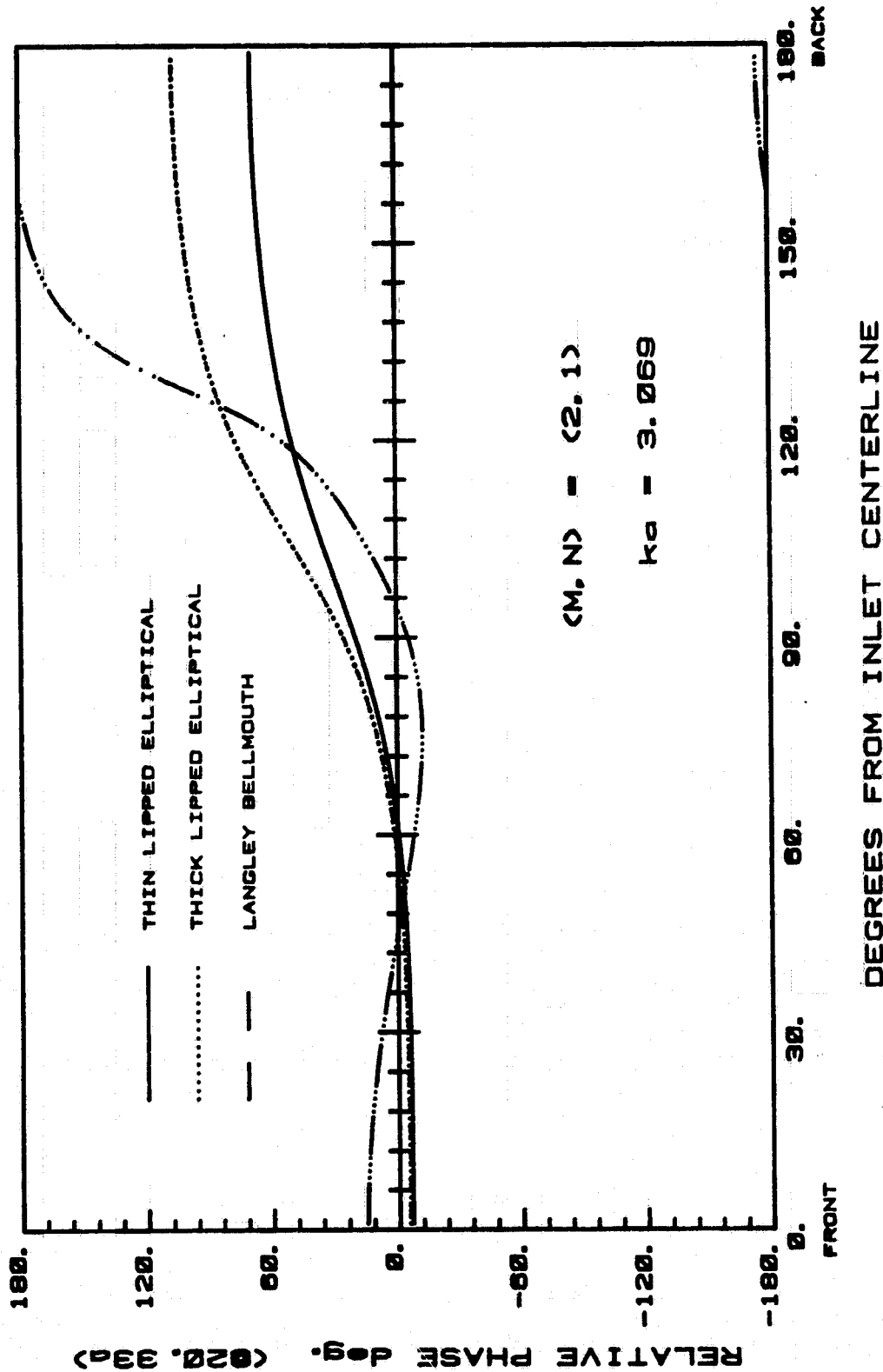
ORIGINAL PAGE IS
OF POOR QUALITY



CUT-OFF RATIO = 1.005

Fig. 60a

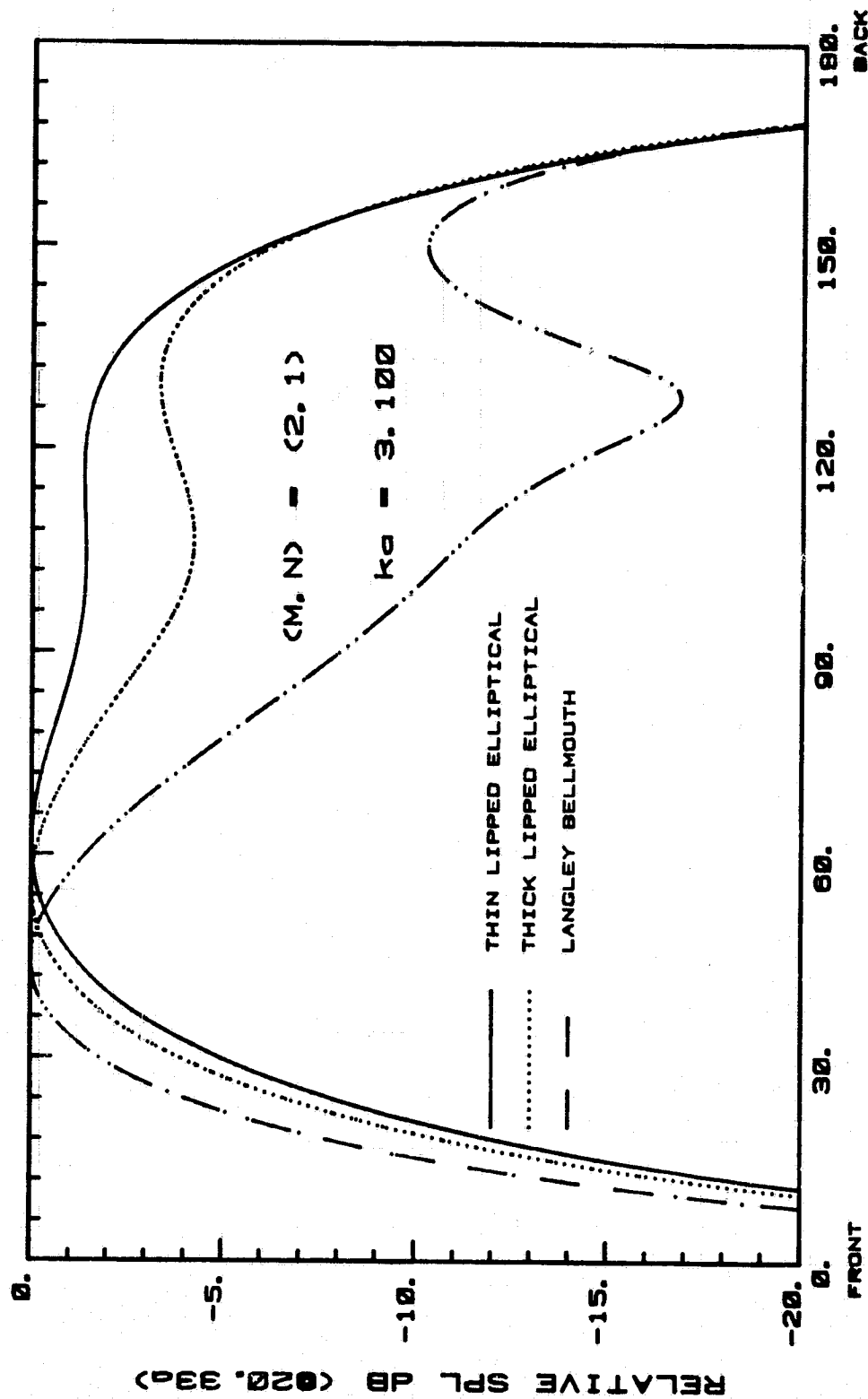
ORIGINAL PAGE IS
OF POOR QUALITY



CUT-OFF RATIO = 1.005

Fig. 60b

ORIGINAL PAGE IS
OF POOR QUALITY

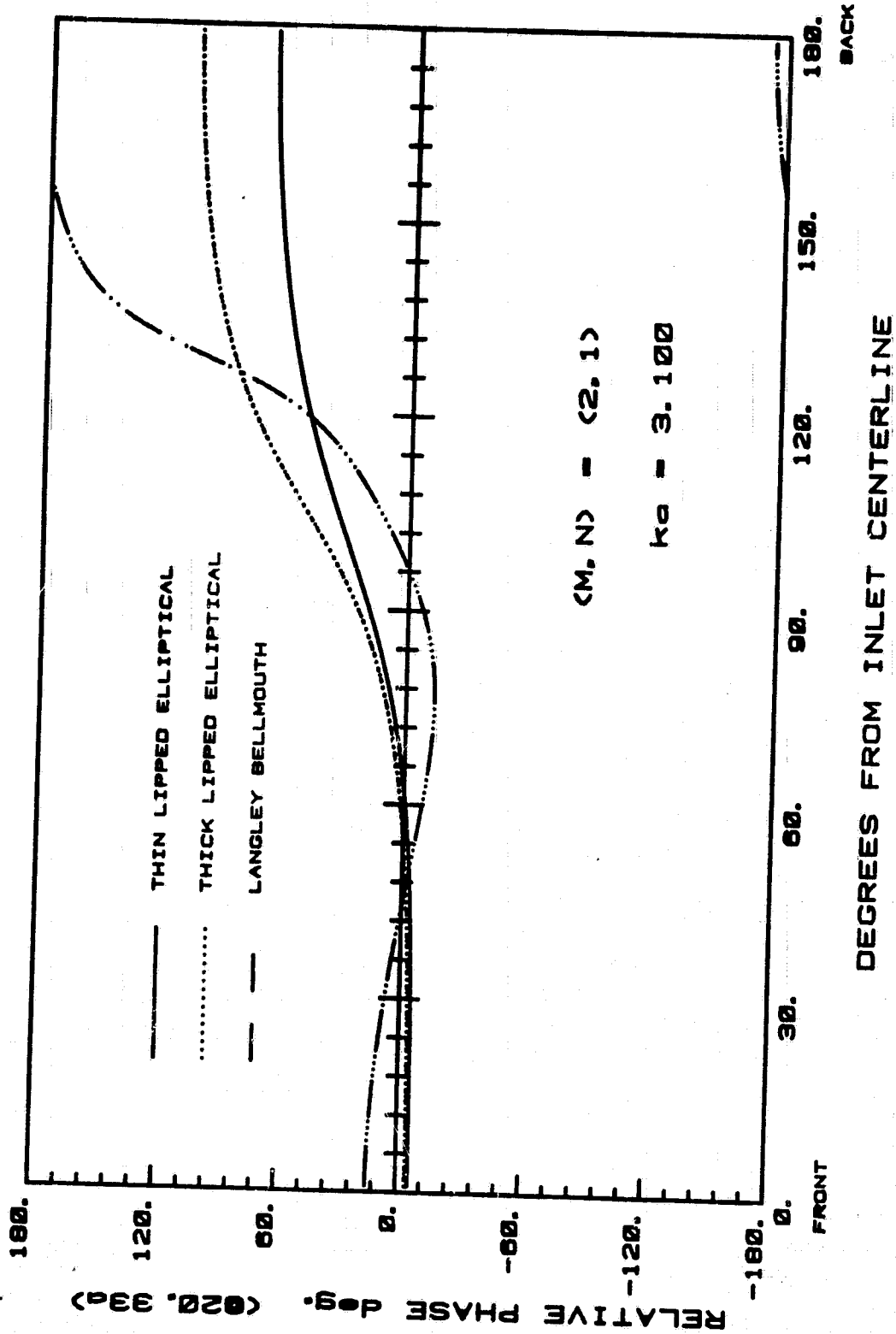


DEGREES FROM INLET CENTERLINE

CUT-OFF RATIO = 1.015

Fig. 60c

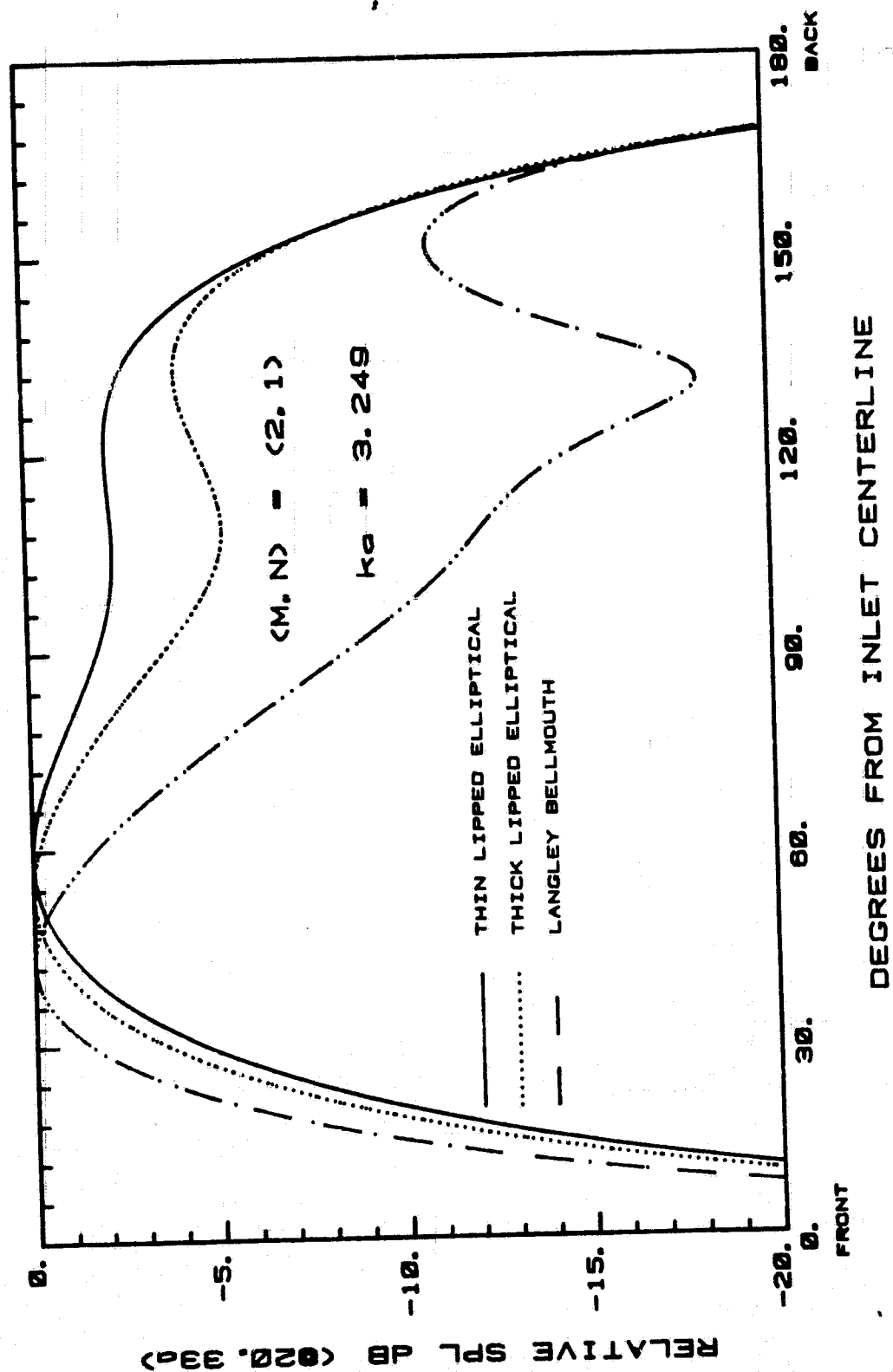
ORIGINAL PAGE IS
OF POOR QUALITY



CUT-OFF RATIO = 1.015

Fig. 60d

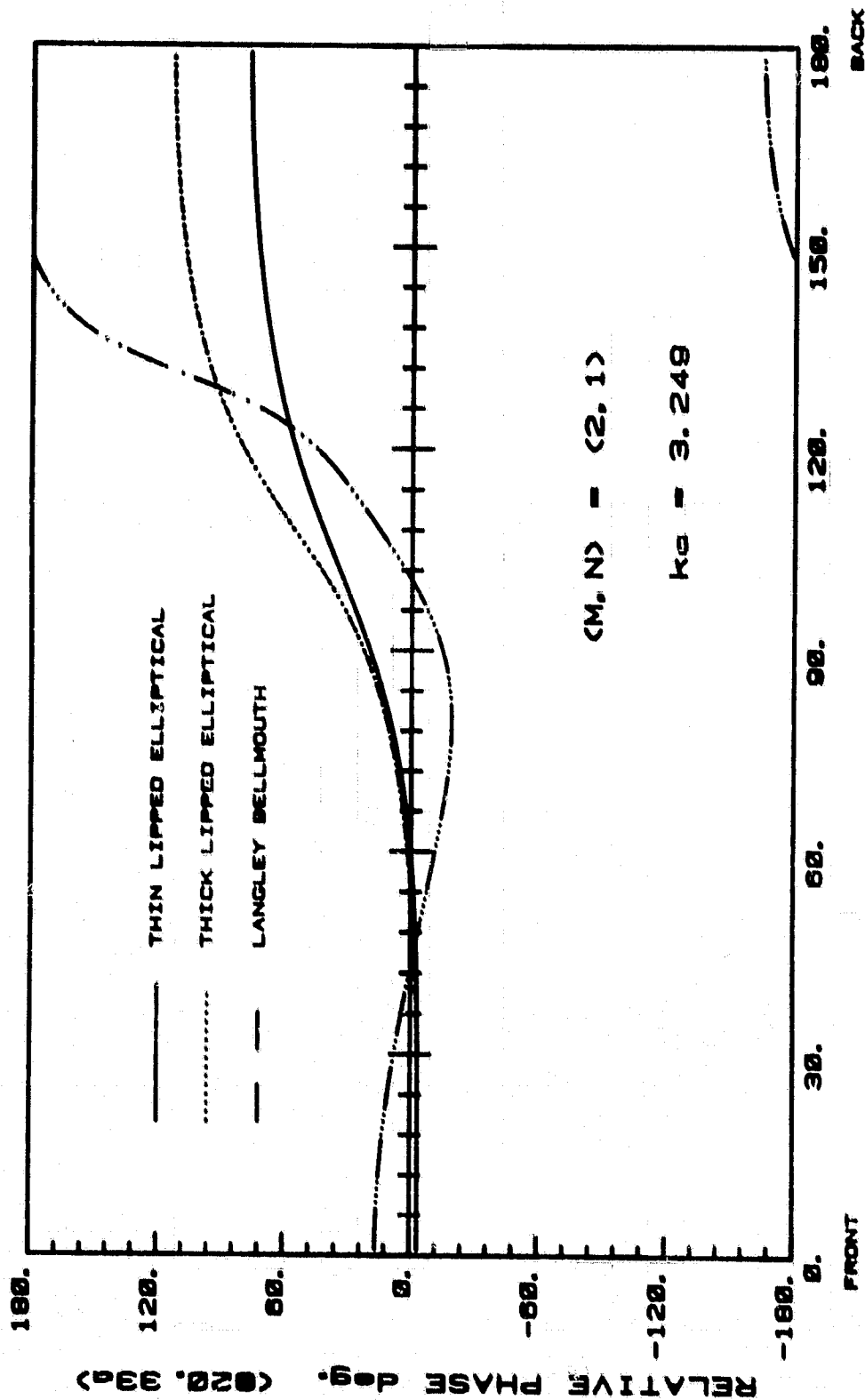
ORIGINAL PAGE IS
OF POOR QUALITY



CUT-OFF RATIO = 1.064

Fig. 60e

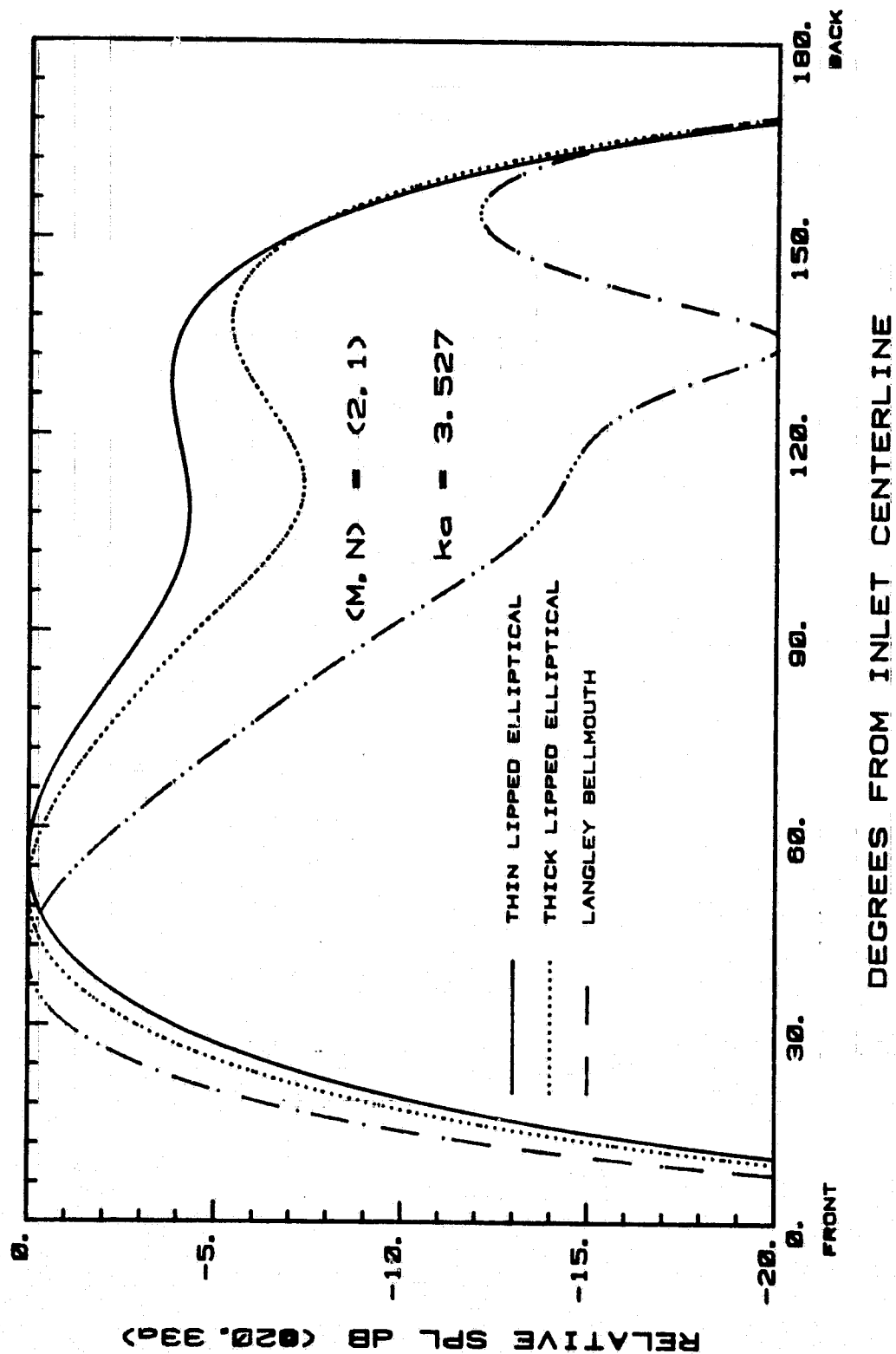
ORIGINAL PAGE IS
OF POOR QUALITY



CUT-OFF RATIO = 1.064

Fig. 60f

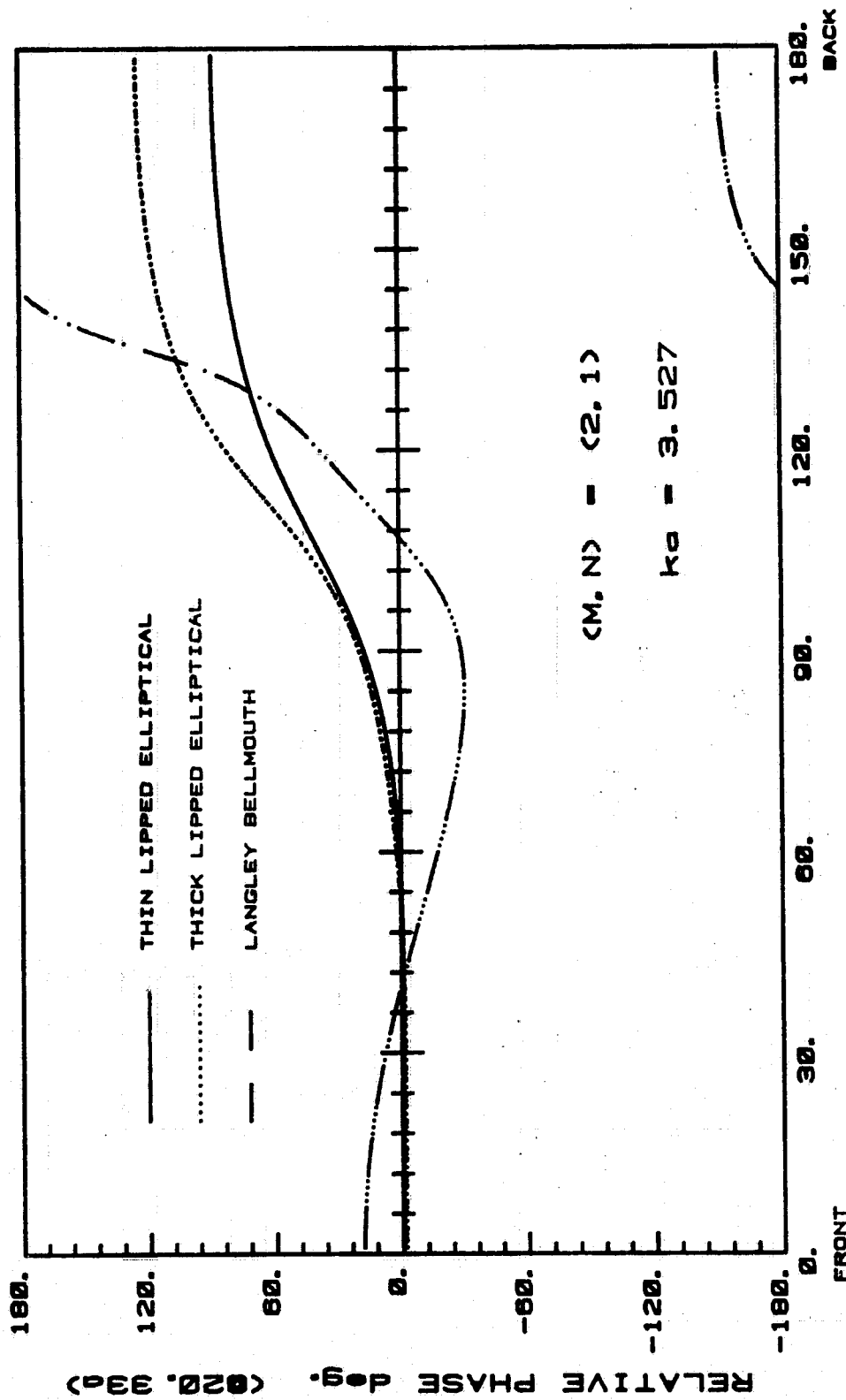
ORIGINAL PAGE IS
OF POOR QUALITY



CUT-OFF RATIO = 1.155

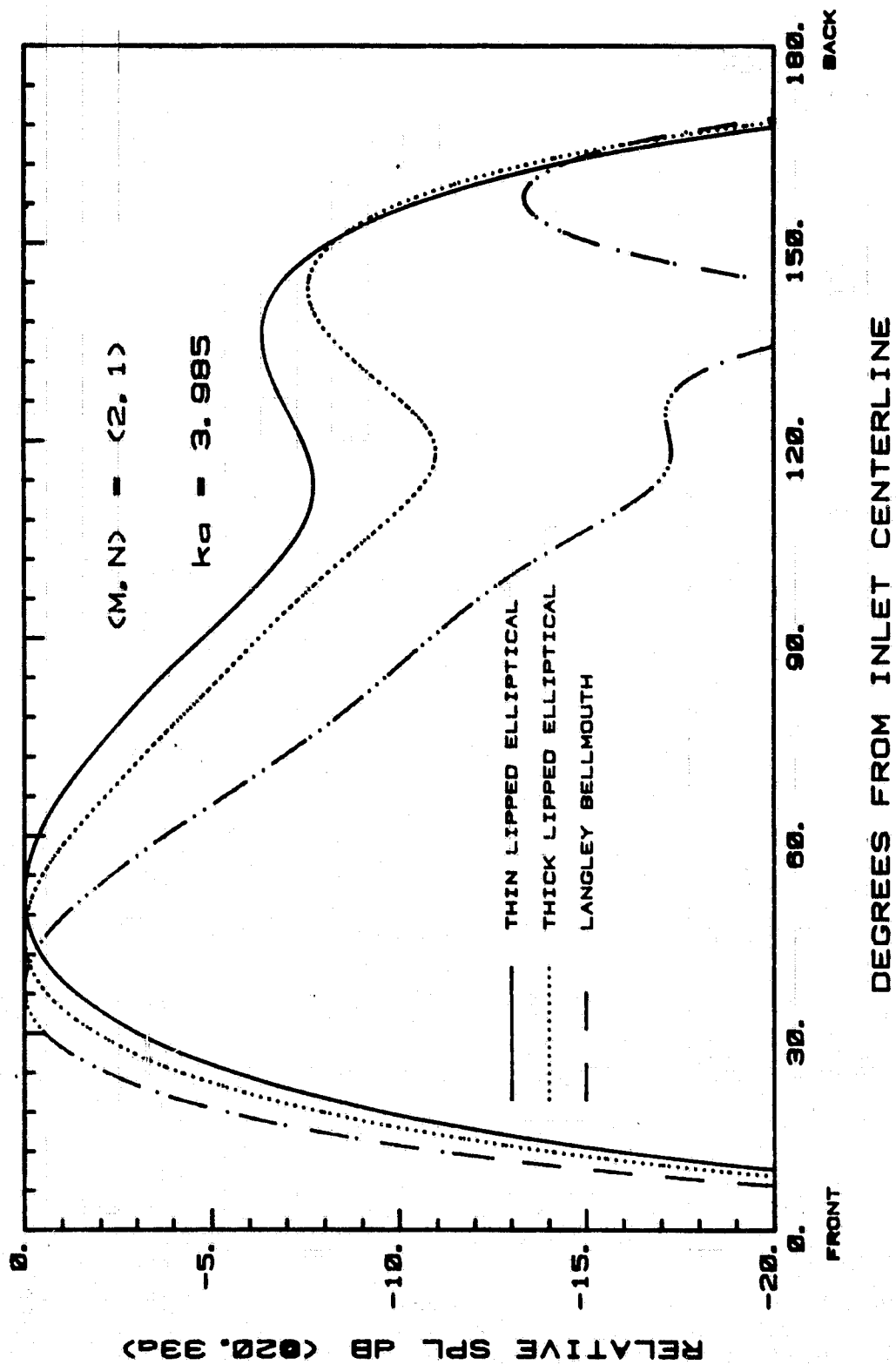
Fig. 60g

ORIGINAL PAGE IS
OF POOR QUALITY



CUT-OFF RATIO = 1.155

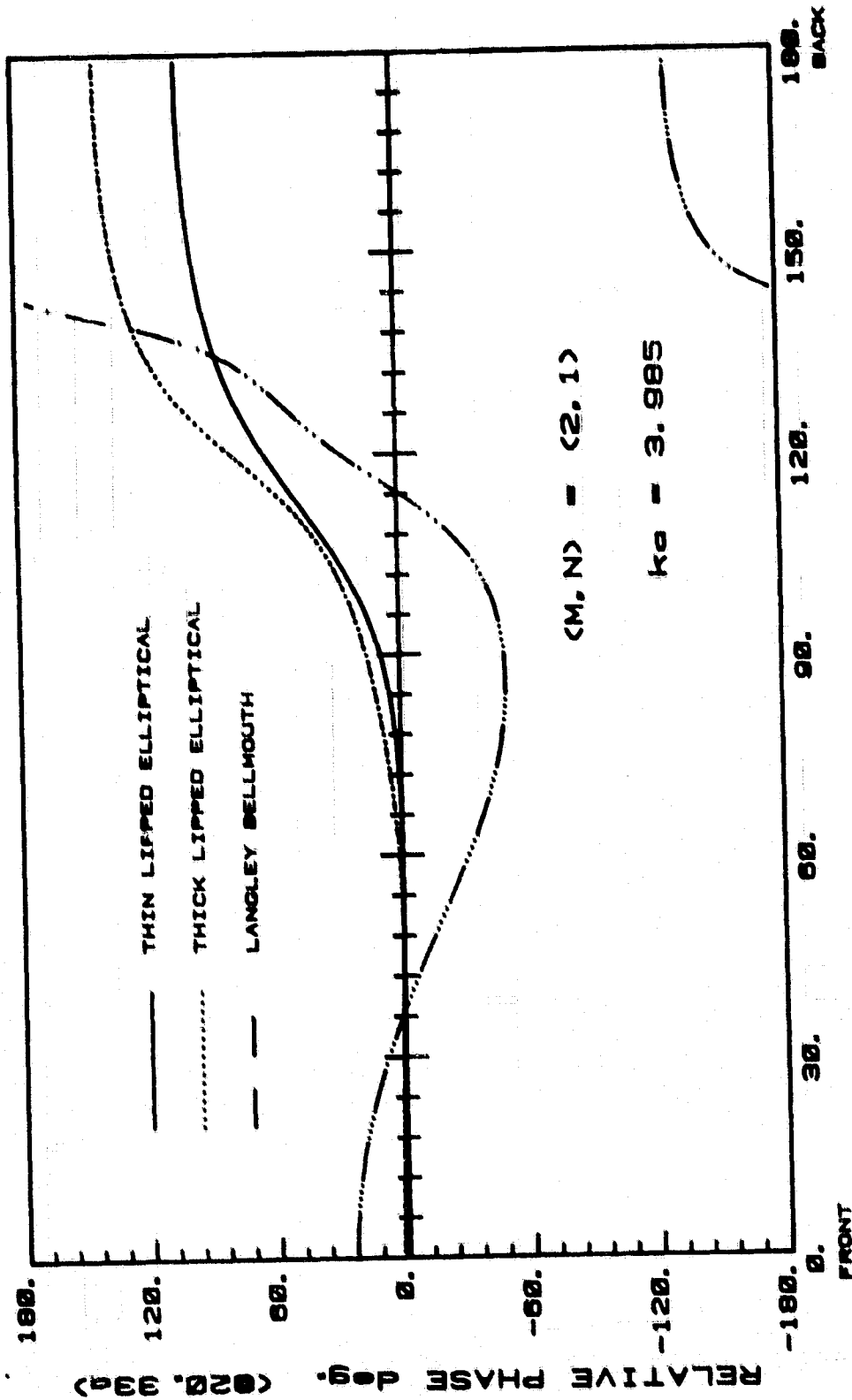
Fig. 60h



CUT-OFF RATIO = 1.305

Fig. 60i

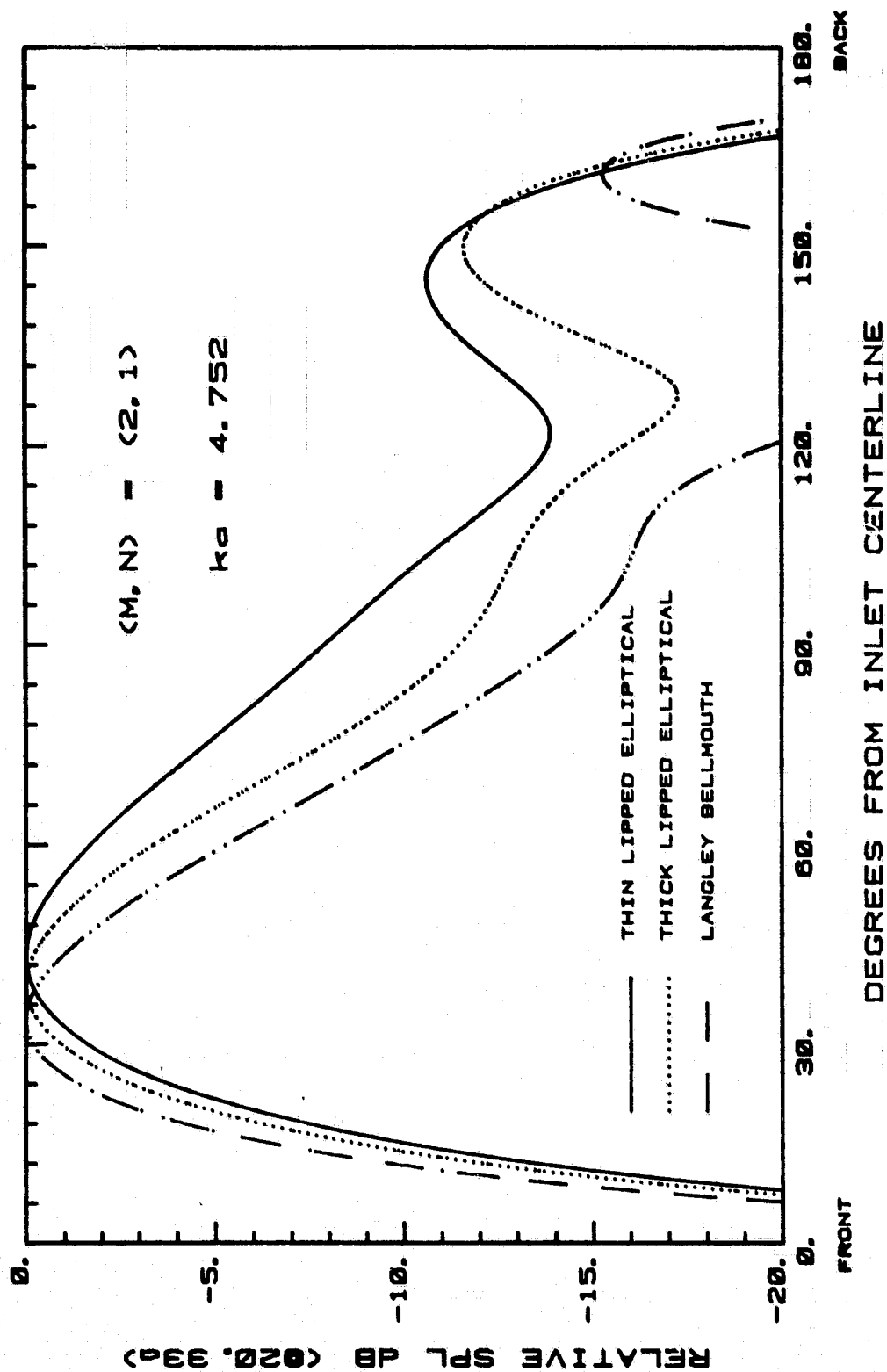
ORIGINAL PAGE IS
OF POOR QUALITY



CUT-OFF RATIO = 1.305

Fig. 60j

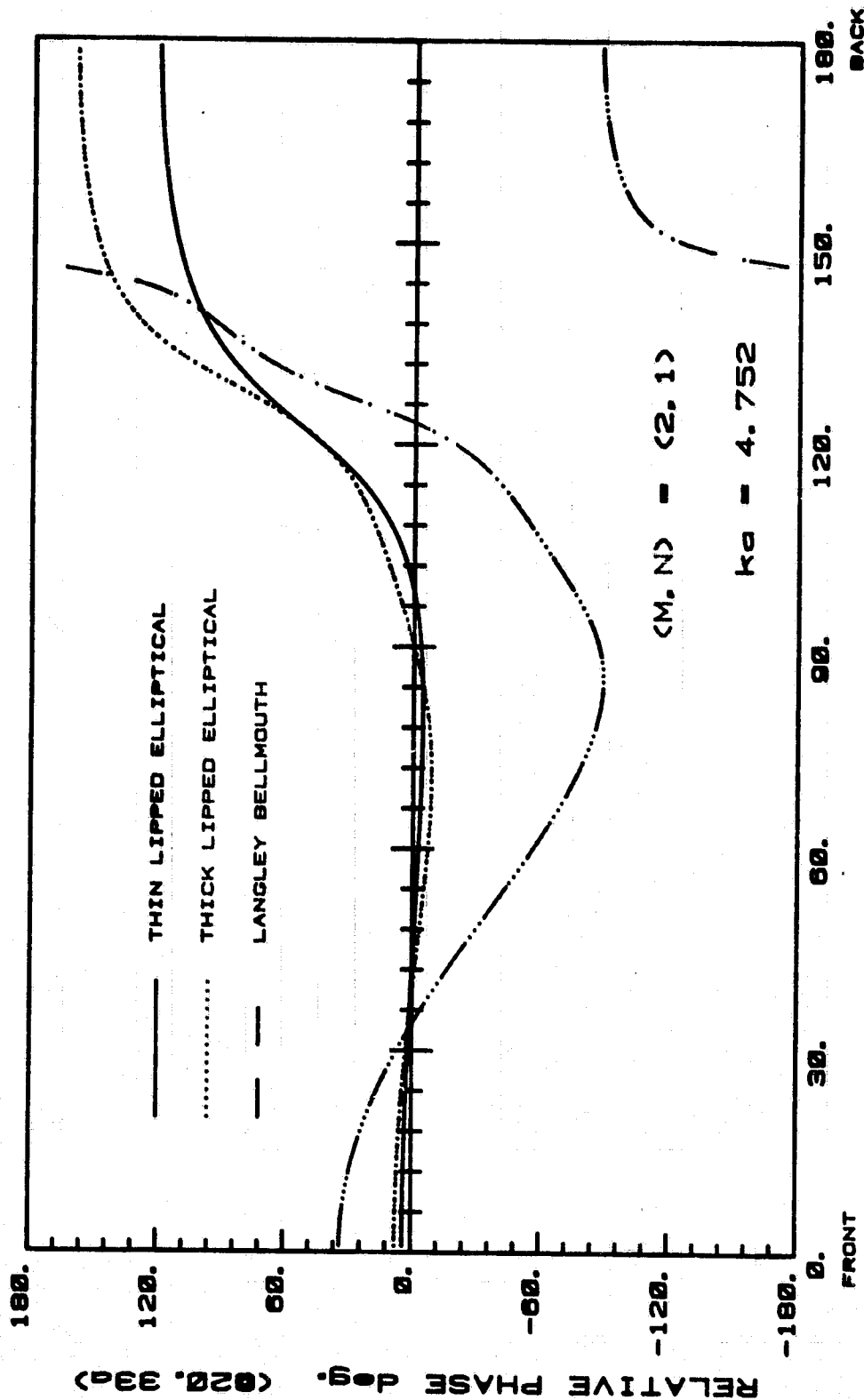
ORIGINAL PAGE IS
OF POOR QUALITY



CUT-OFF RATIO = 1.556

Fig. 60k

ORIGINAL PAGE IS
OF POOR QUALITY

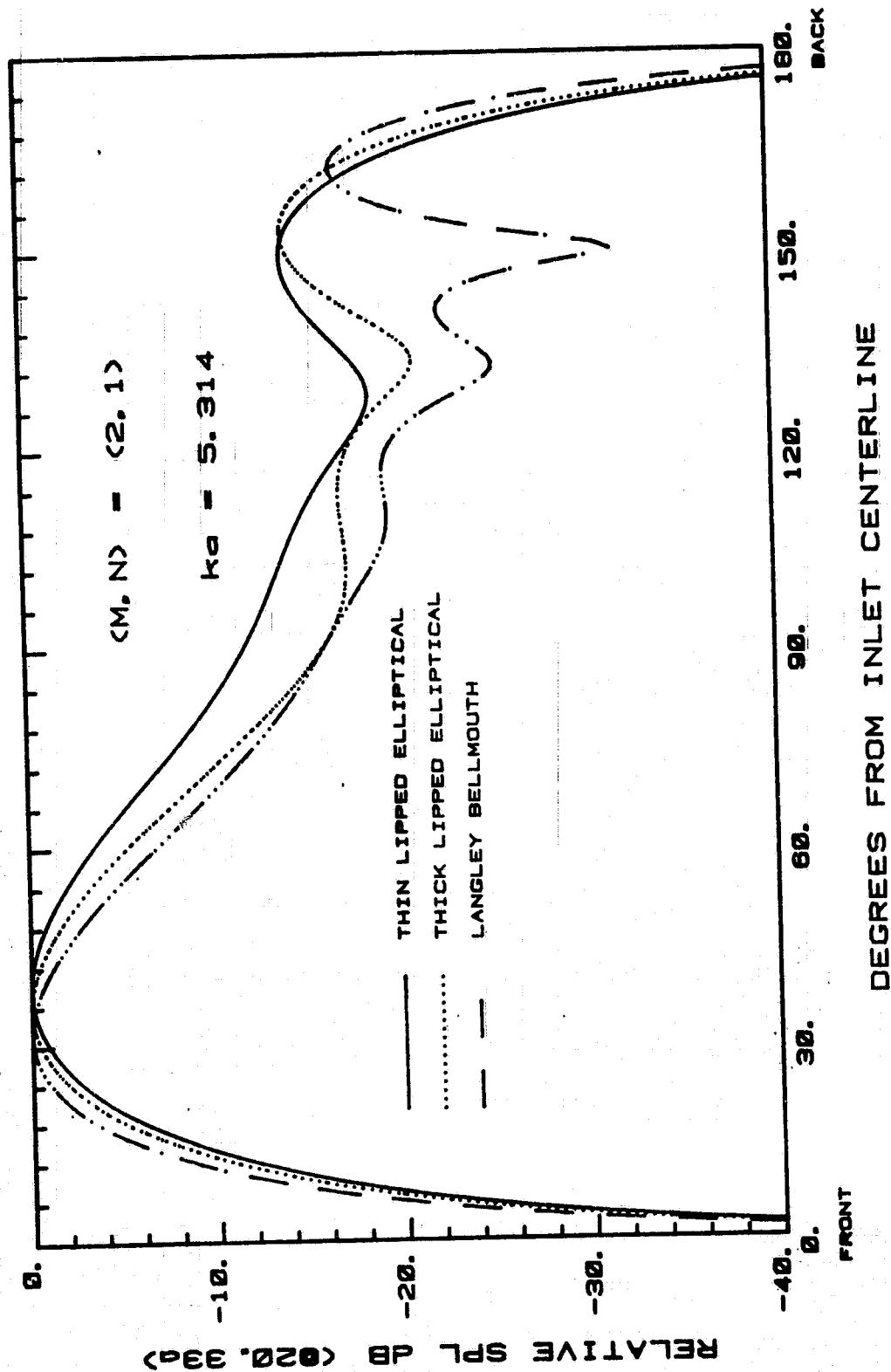


DEGREES FROM INLET CENTERLINE

CUT-OFF RATIO = 1.556

Fig. 601

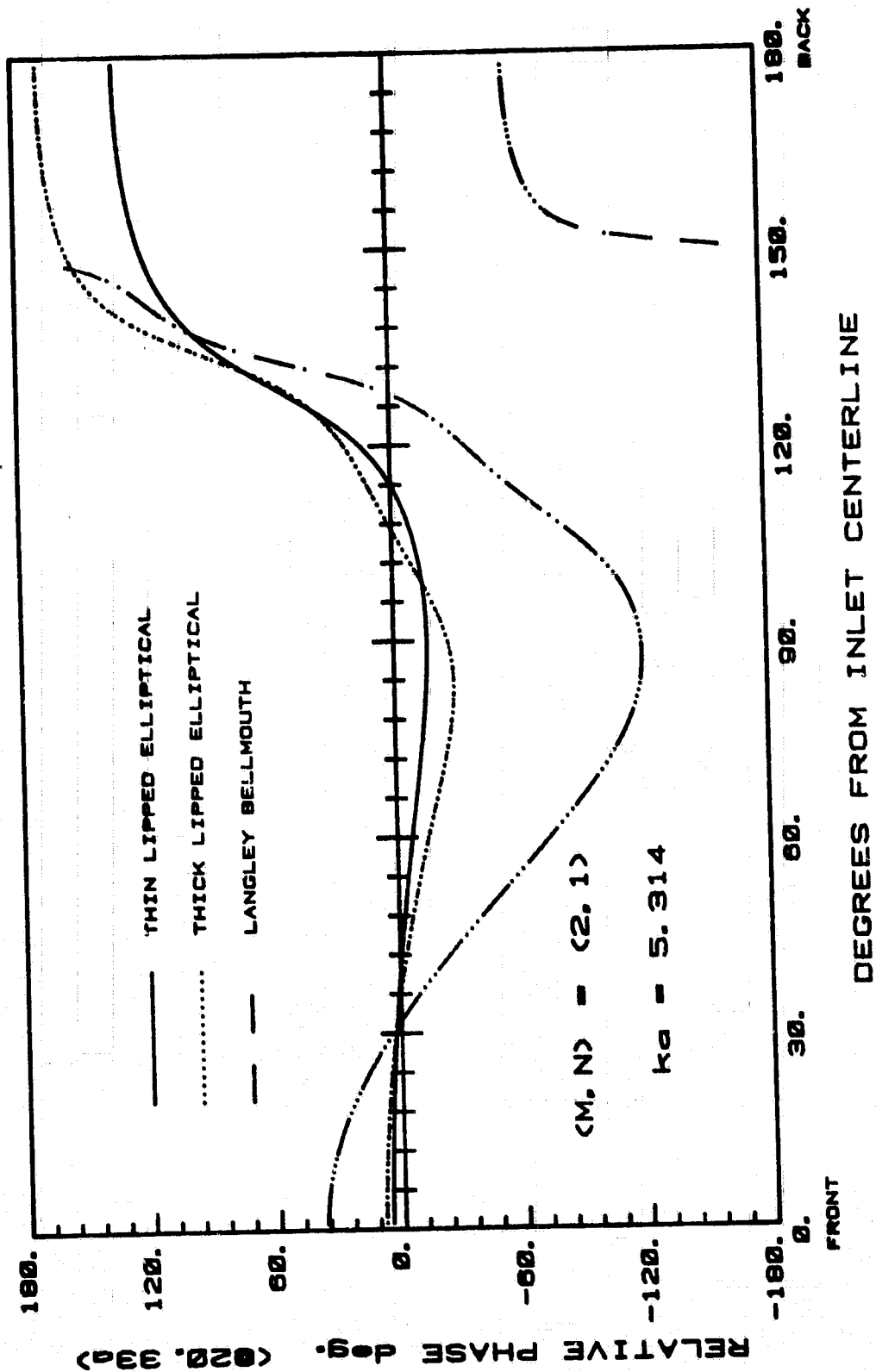
ORIGINAL PAGE IS
OF POOR QUALITY



CUT-OFF RATIO = 1.74

Fig. 60m

ORIGINAL PAGE IS
OF POOR QUALITY



CUT-OFF RATIO = 1.74

Fig. 60n

ORIGINAL PAGE IS
OF POOR QUALITY

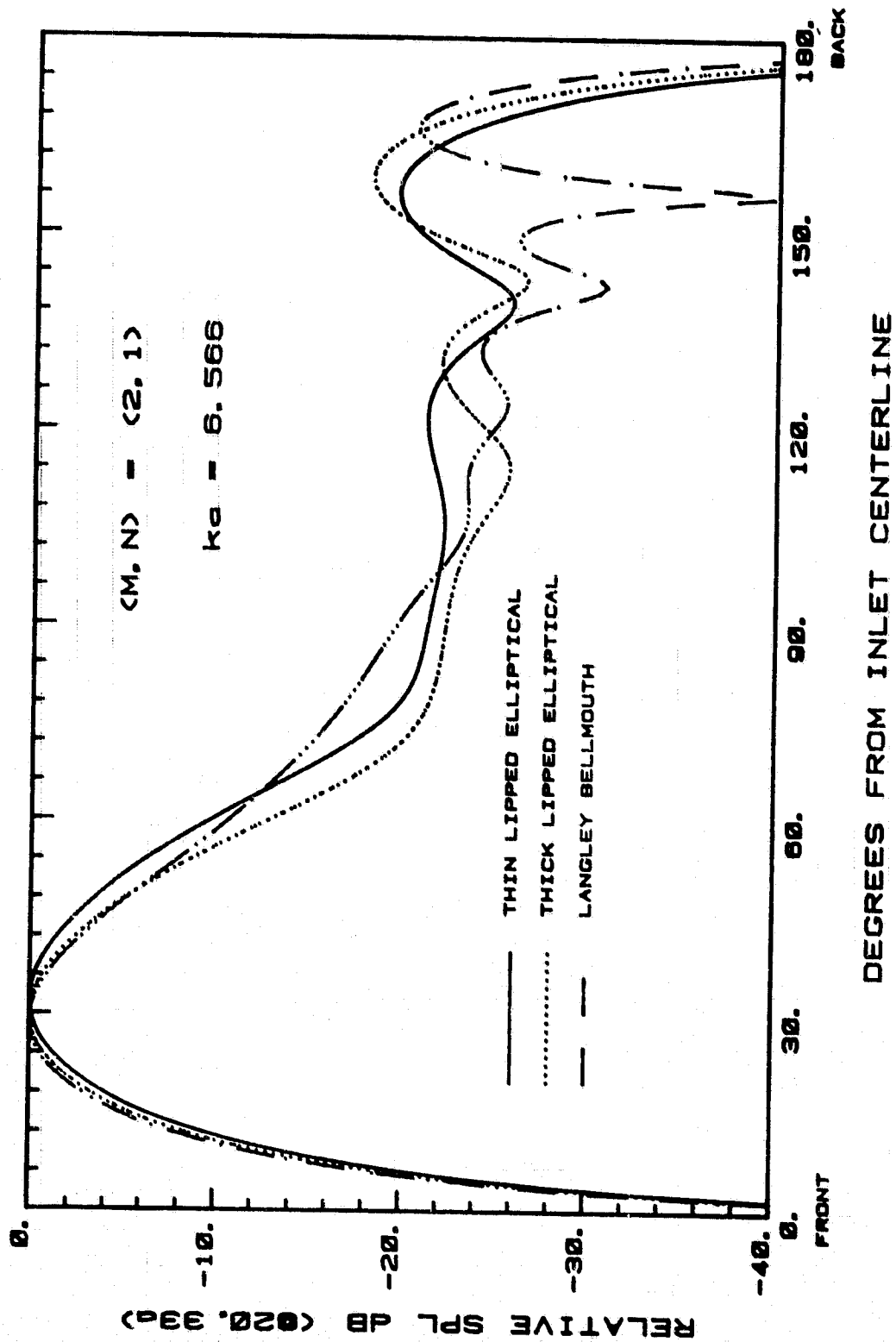
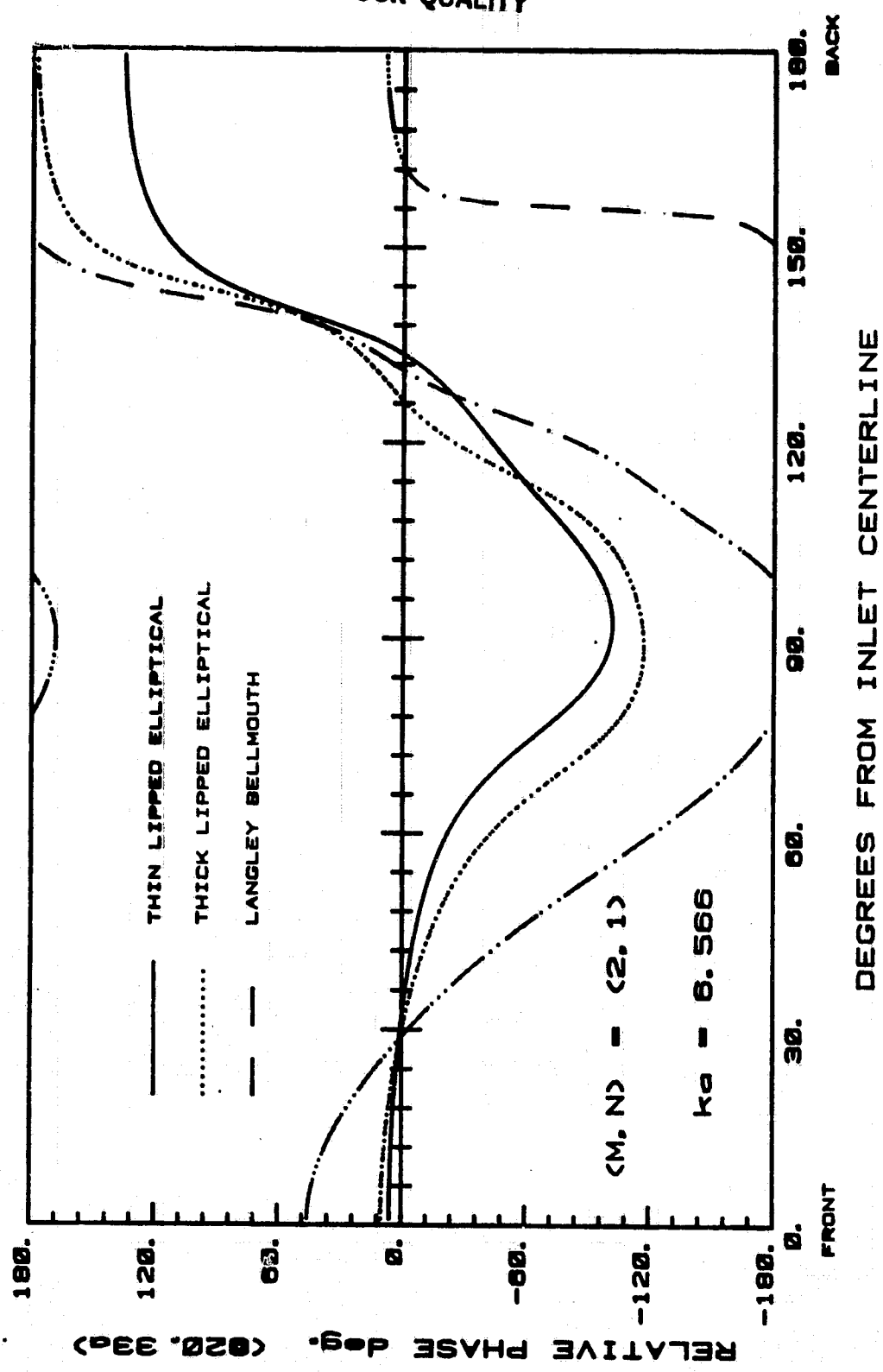


Fig. 60o

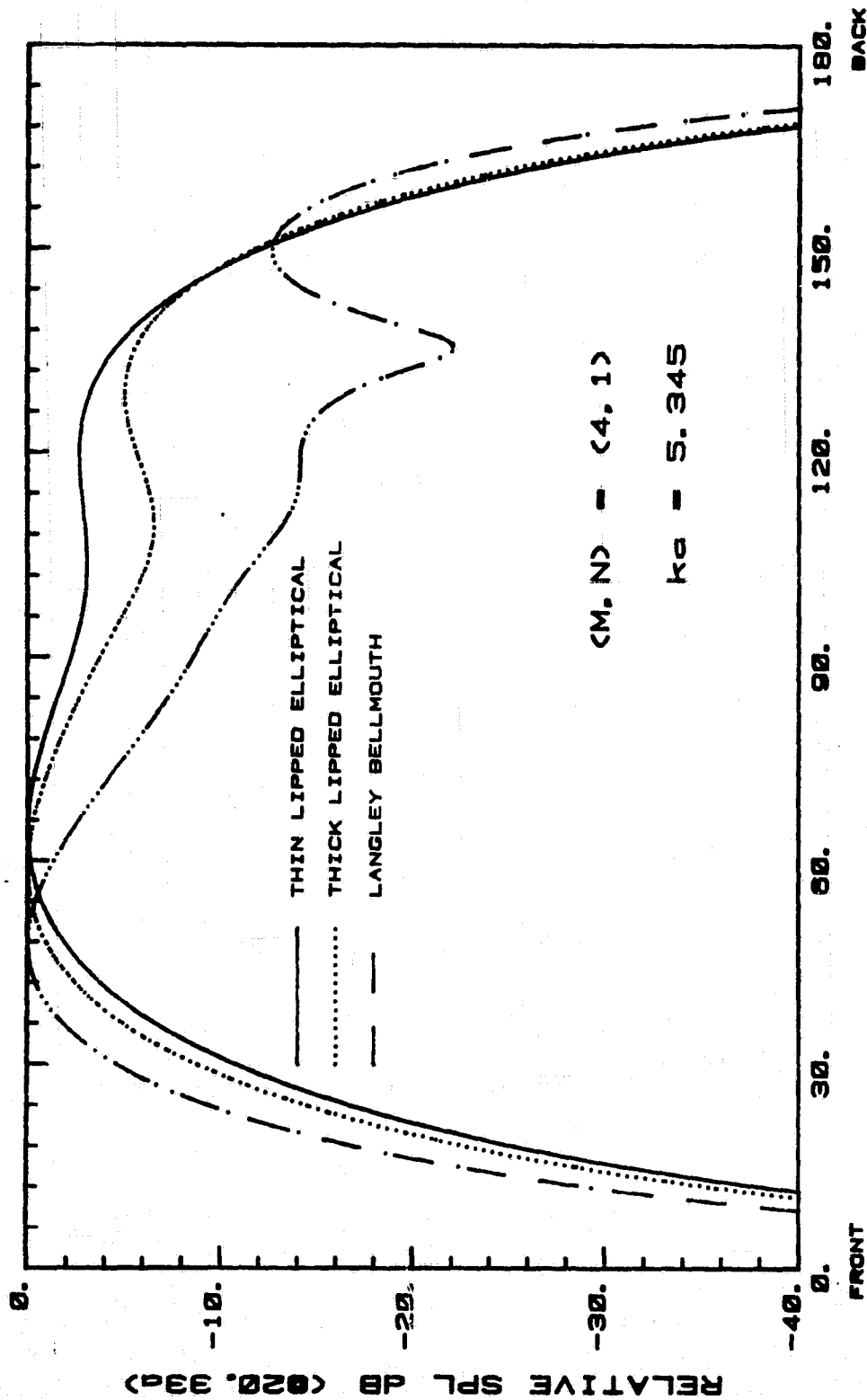
ORIGINAL PAGE 16
OF POOR QUALITY



CUT-OFF RATIO = 2.15

Fig. 60p

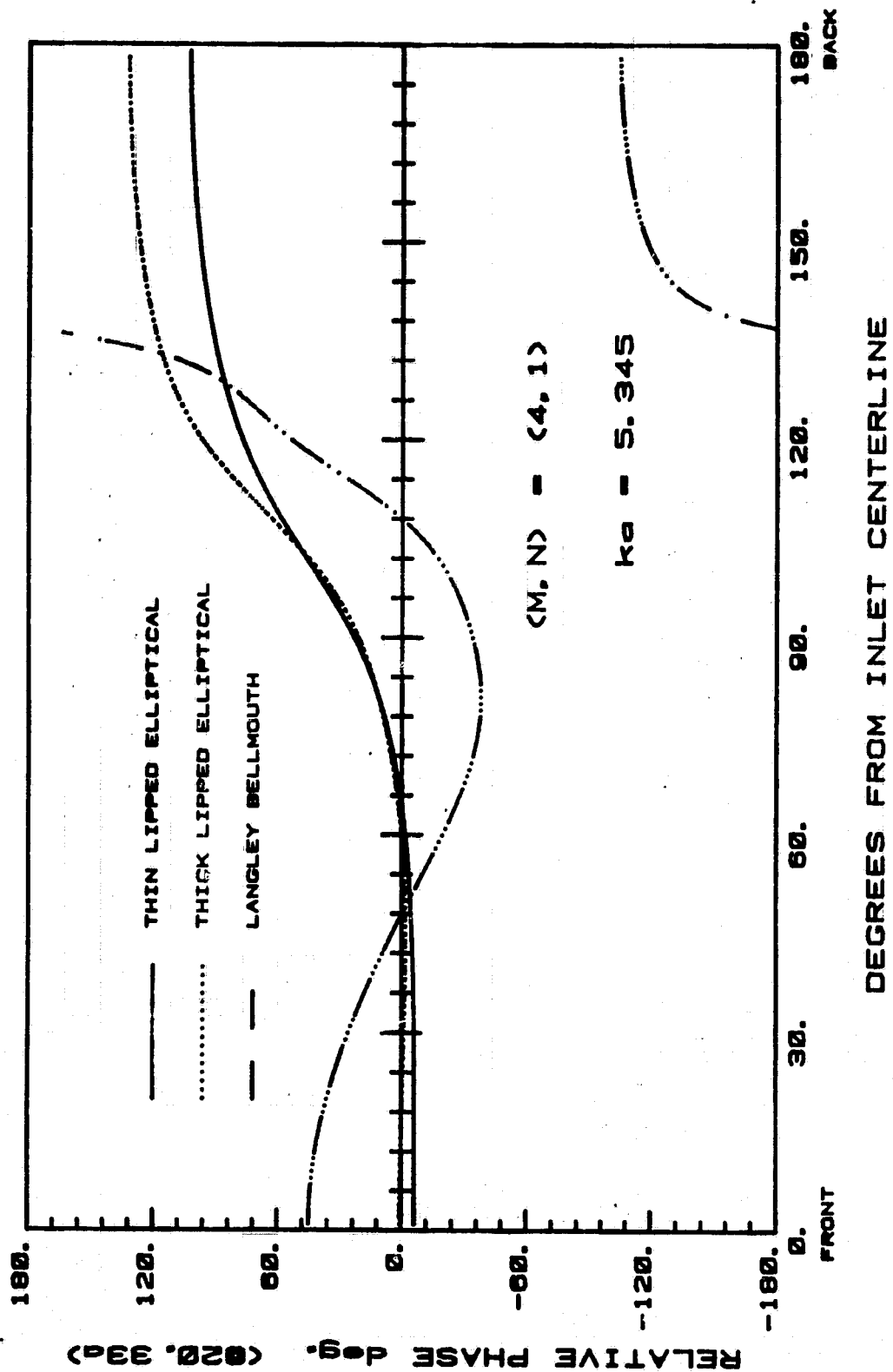
ORIGINAL PAGE 18
OF POOR QUALITY



CUT-OFF RATIO = 1.005

Fig. 61a

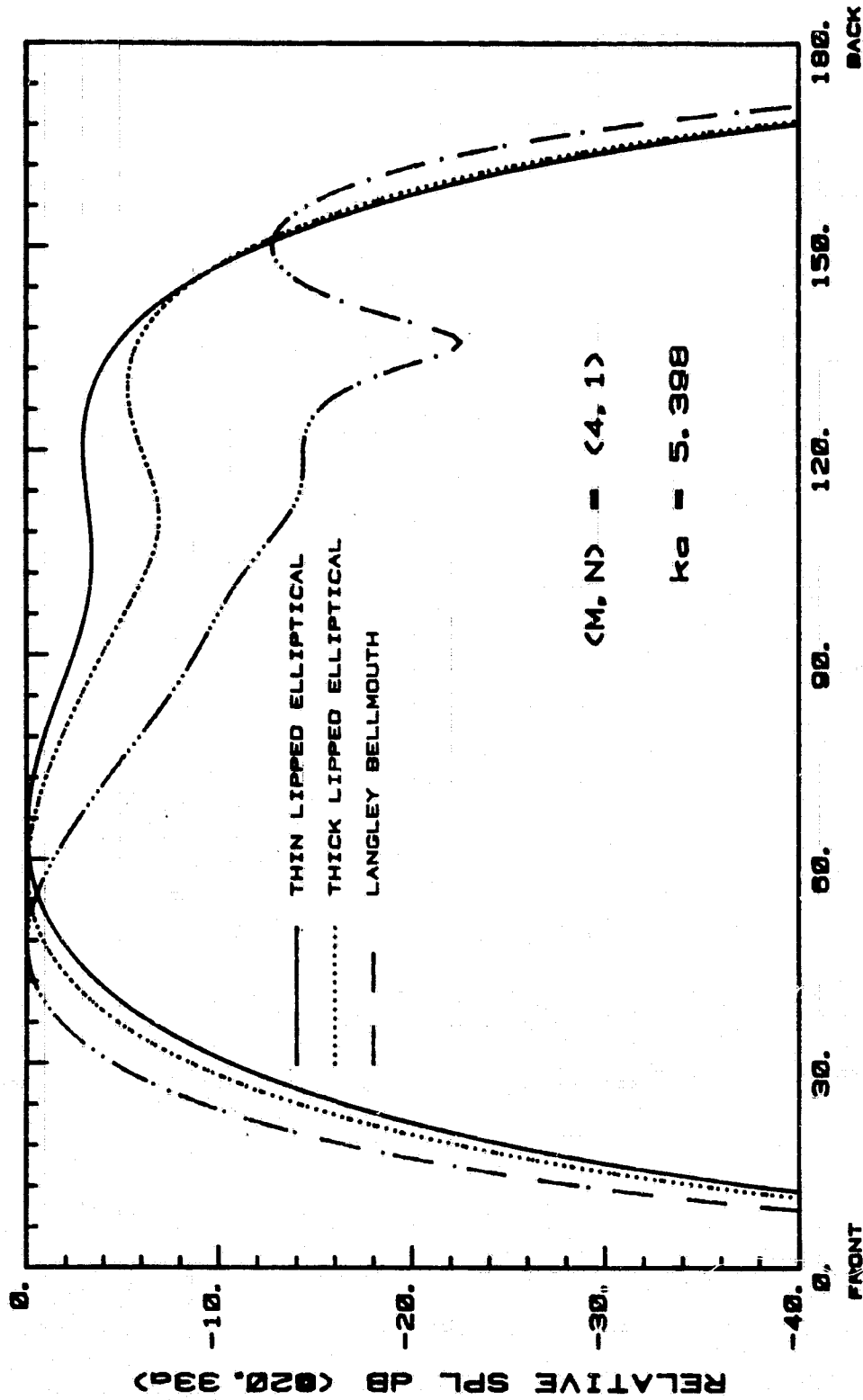
ORIGINAL PAGE IS
OF POOR QUALITY



CUT-OFF RATIO = 1.005

Fig. 61b

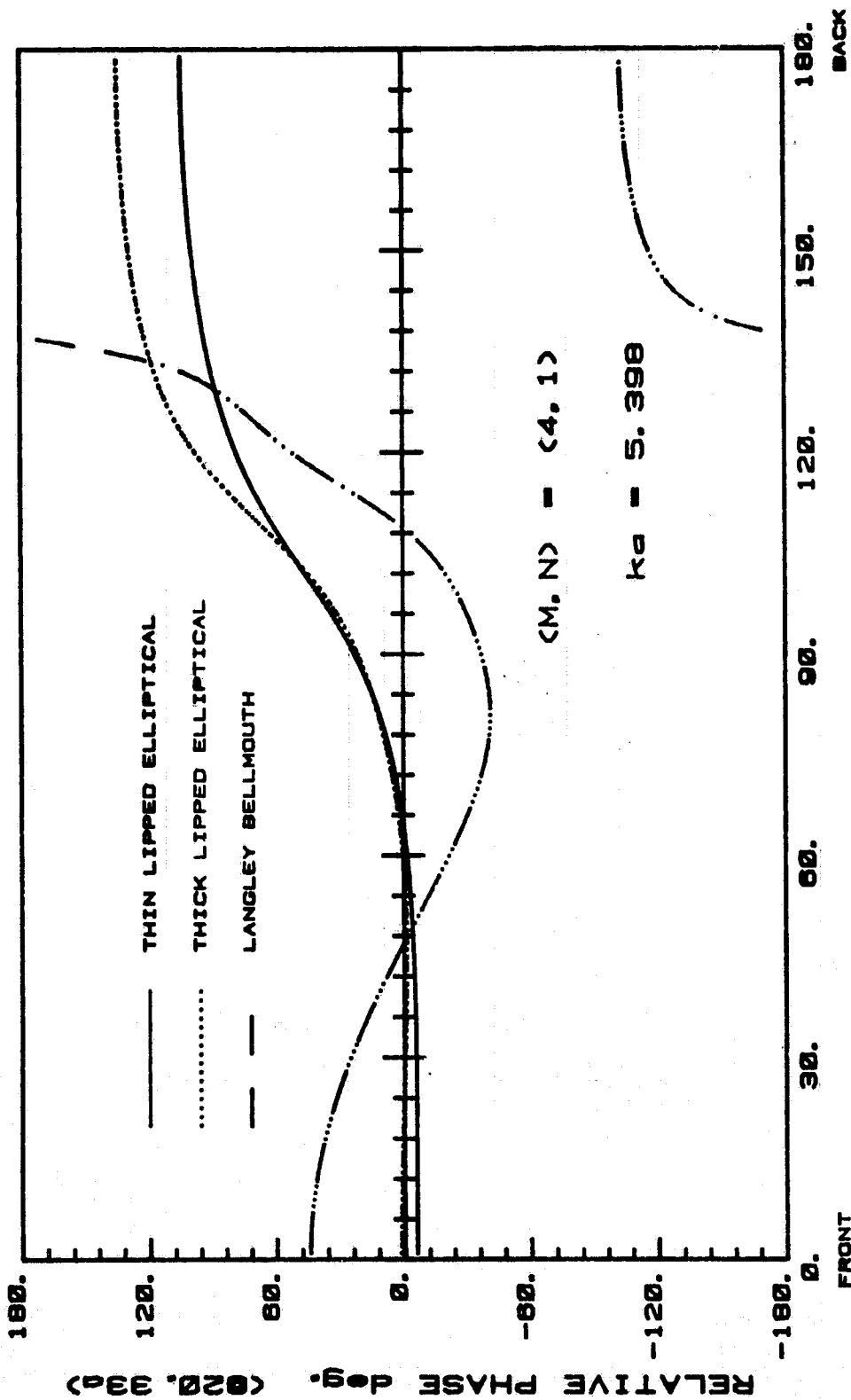
ORIGINAL PAGE IS
OF POOR QUALITY



DEGREES FROM INLET CENTERLINE

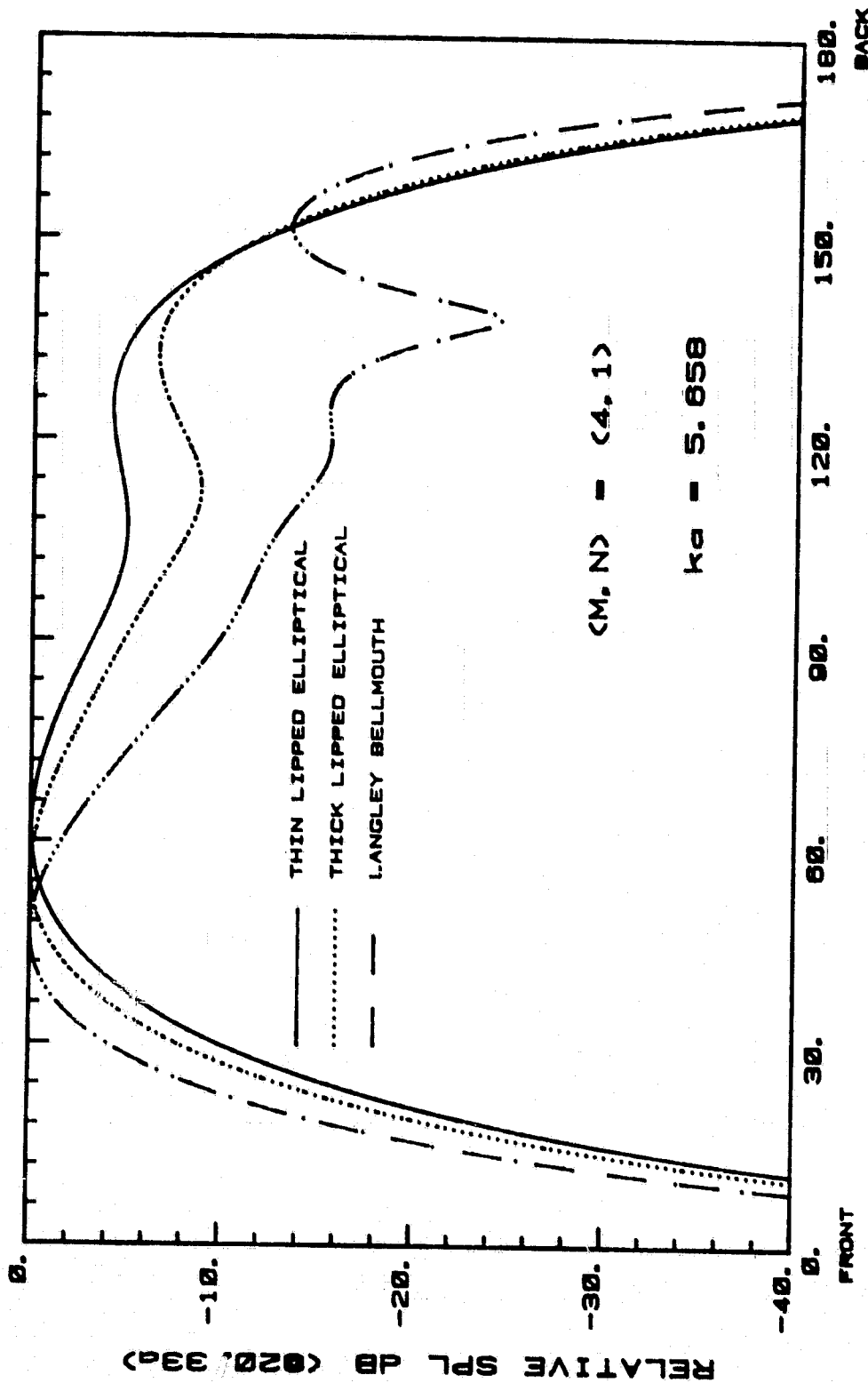
CUT-OFF RATIO = 1.015

Fig. 61c



CUT-OFF RATIO = 1.015

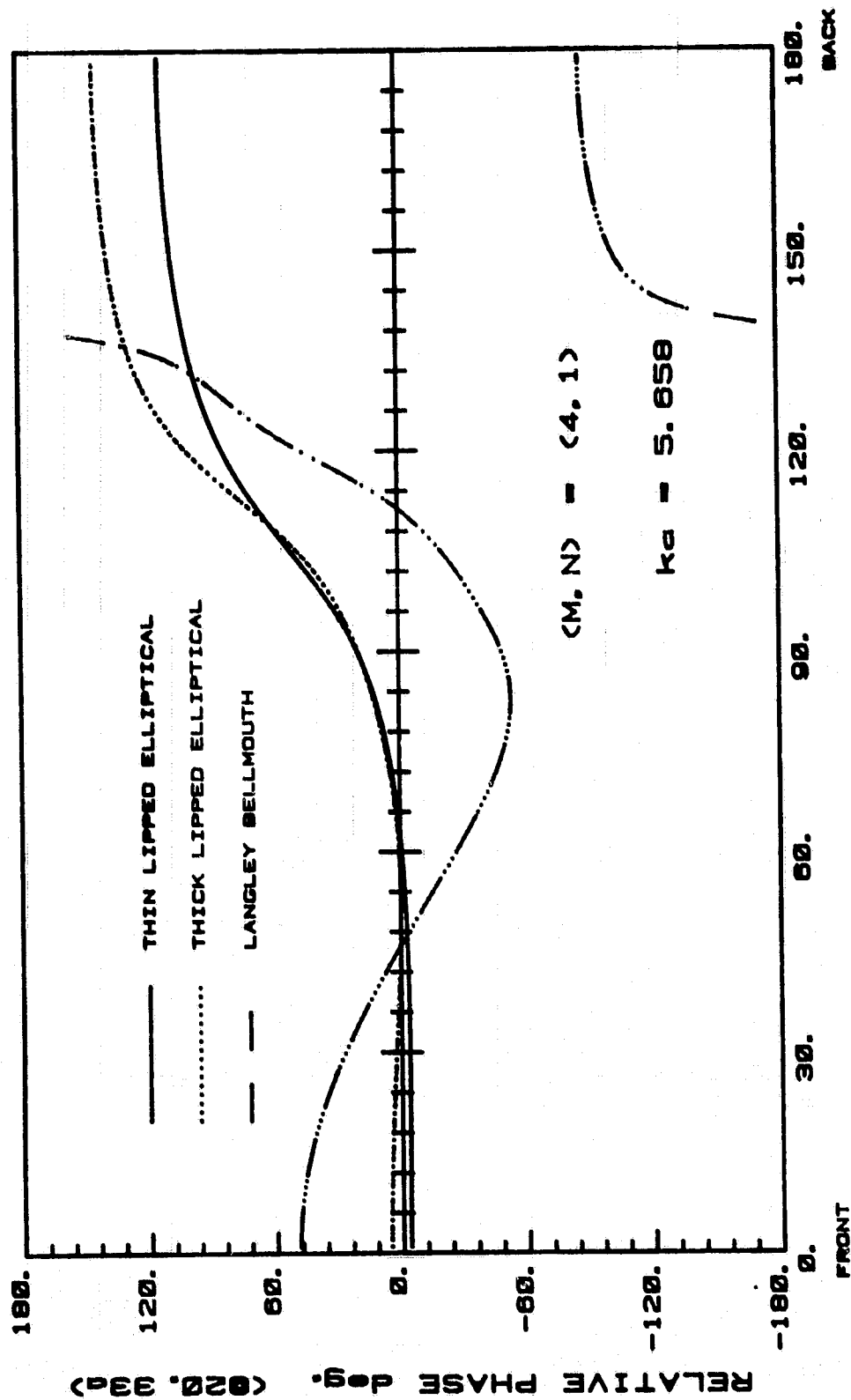
Fig. 61d



CUT-OFF RATIO = 1.064

Fig. 61e

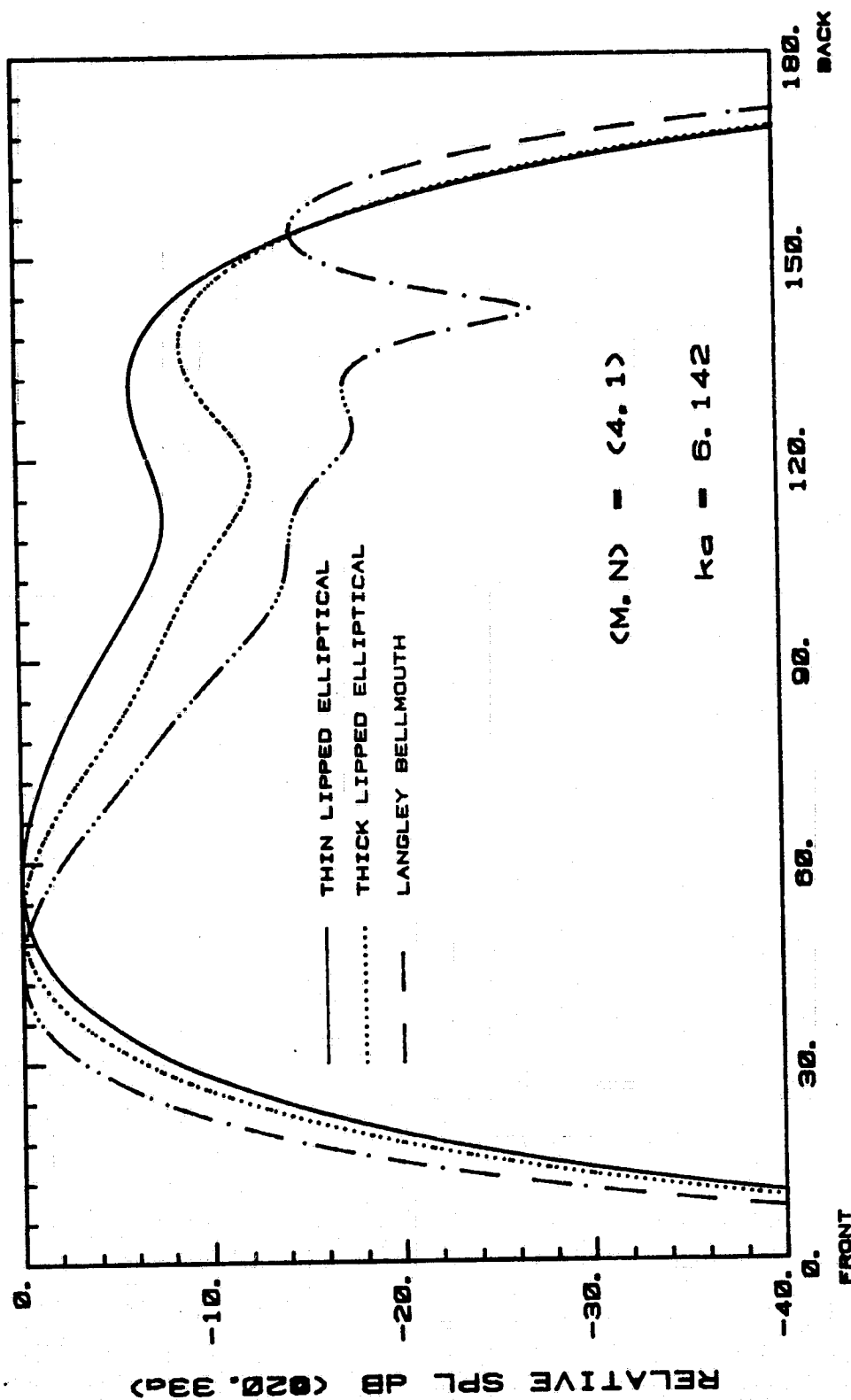
ORIGINAL PAGE IS
OF POOR QUALITY



CUT-OFF RATIO = 1.064

Fig. 61f

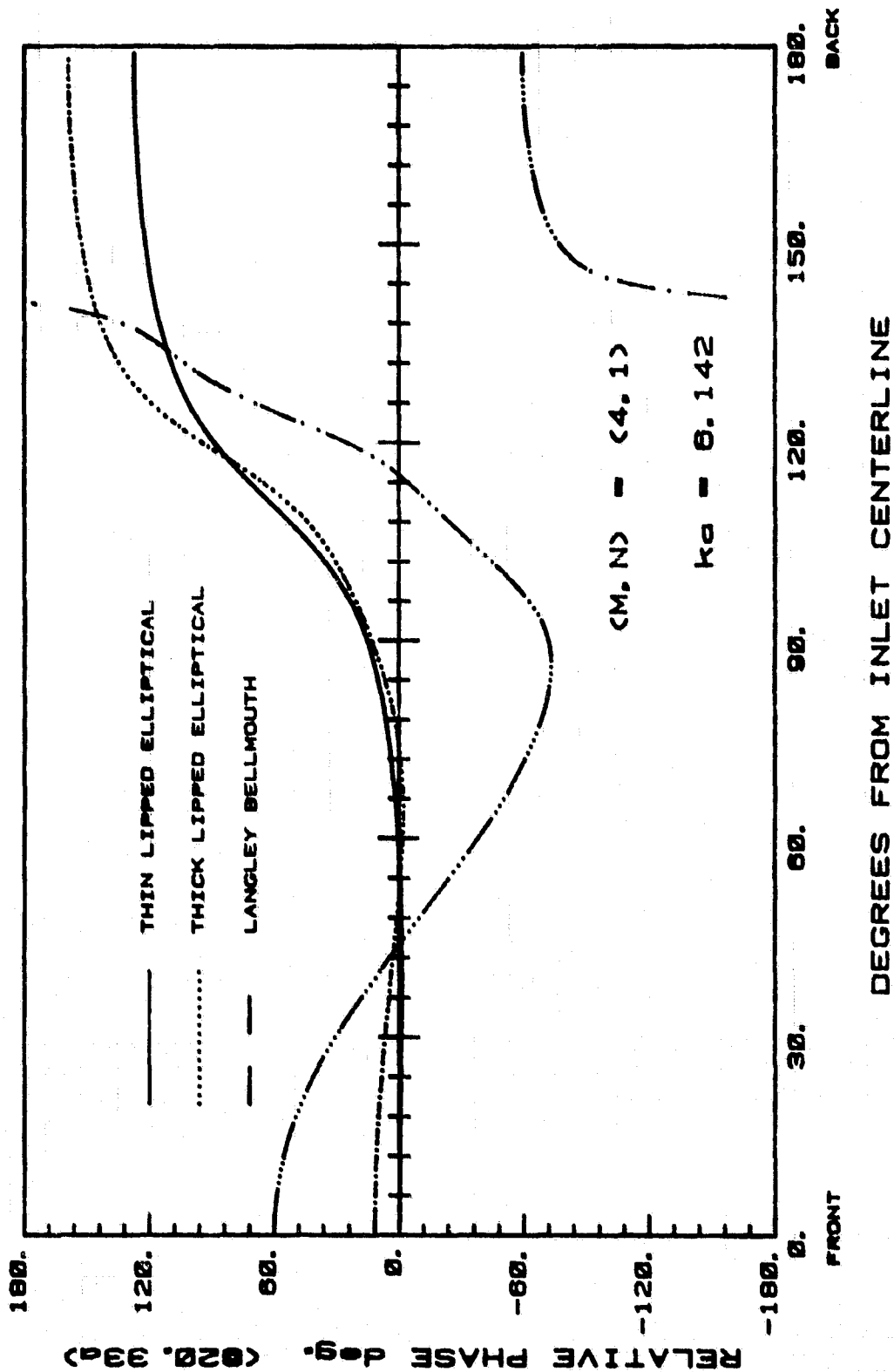
ORIGINAL PAGE IS
OF POOR QUALITY



CUT-OFF RATIO = 1.155

Fig. 618

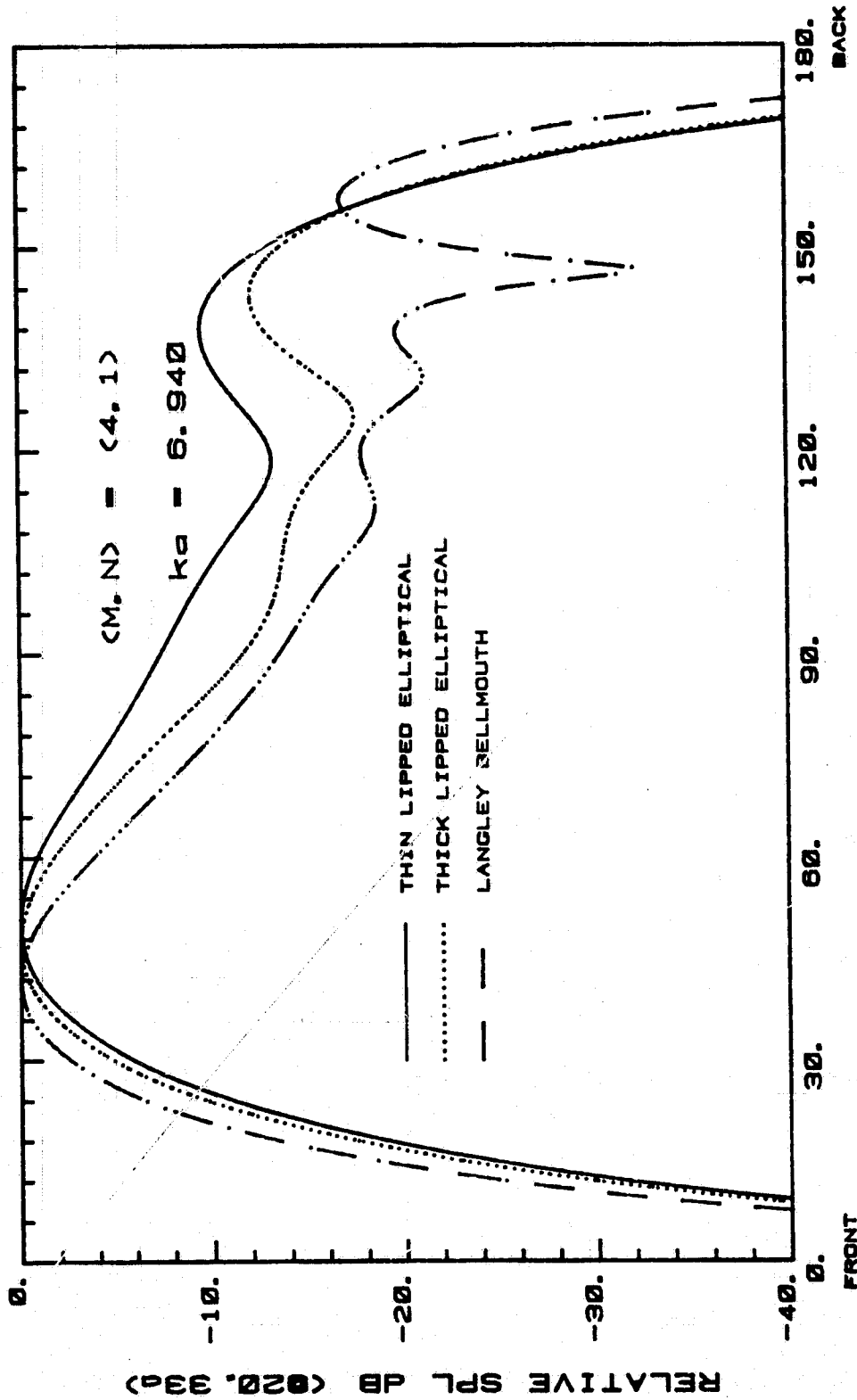
ORIGINAL PAGE IS
OF POOR QUALITY



CUT-OFF RATIO = 1.155

Fig. 61h

ORIGINAL PAGE IS
OF POOR QUALITY

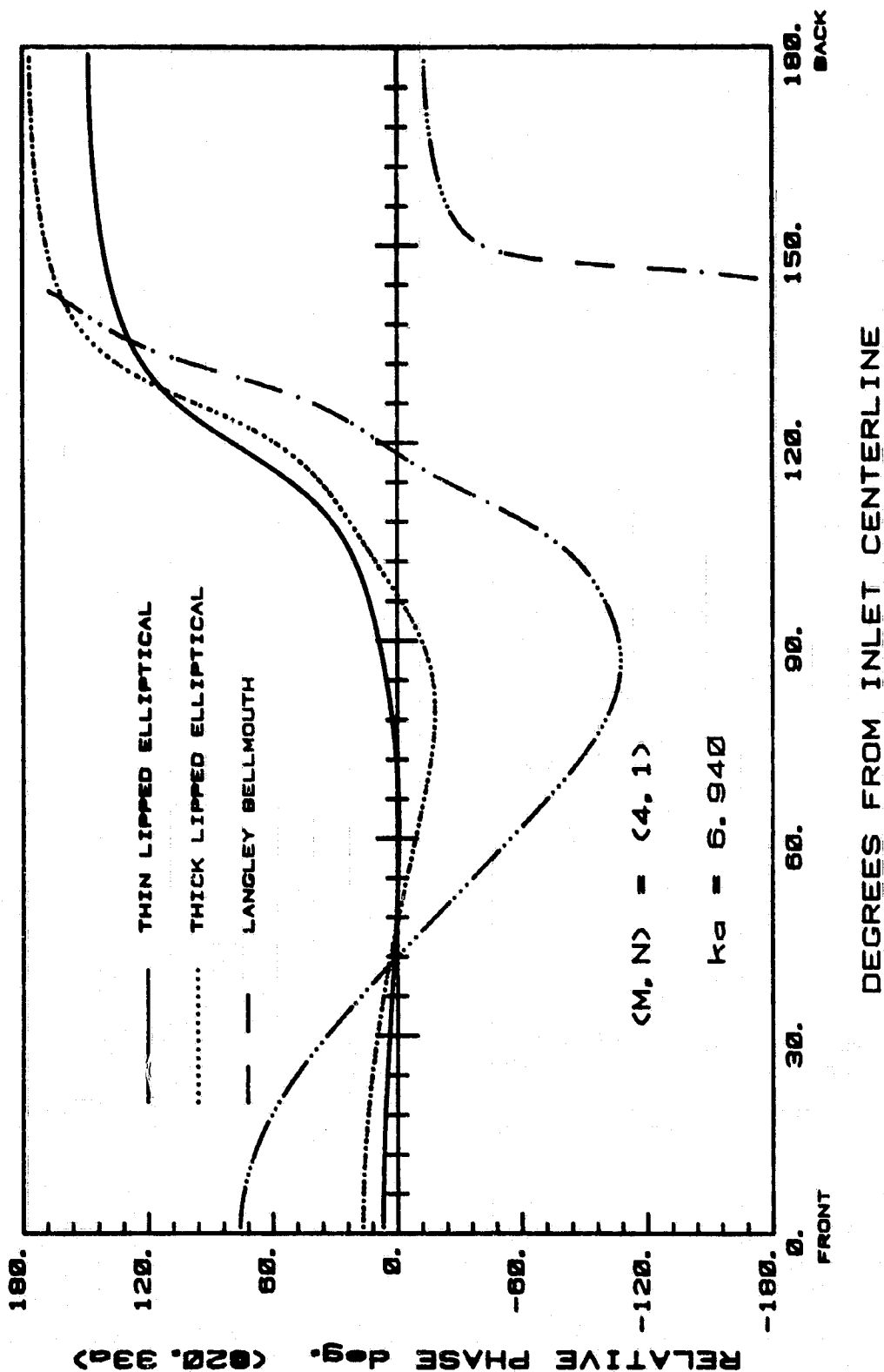


DEGREES FROM INLET CENTERLINE

CUT-OFF RATIO = 1.305

Fig. 61 i

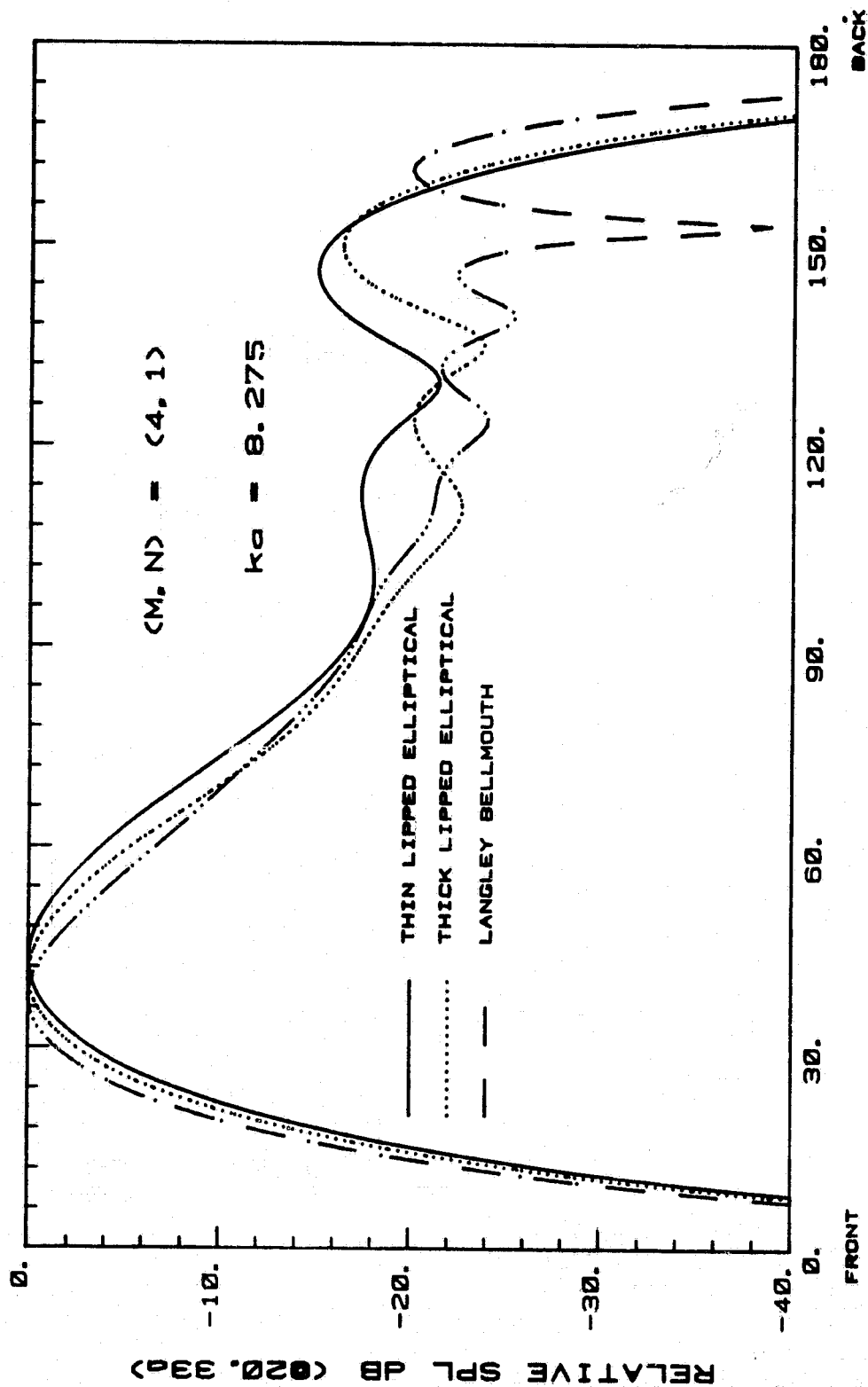
ORIGINAL PAGE IS
OF POOR QUALITY



CUT-OFF RATIO = 1.305

Fig. 61j

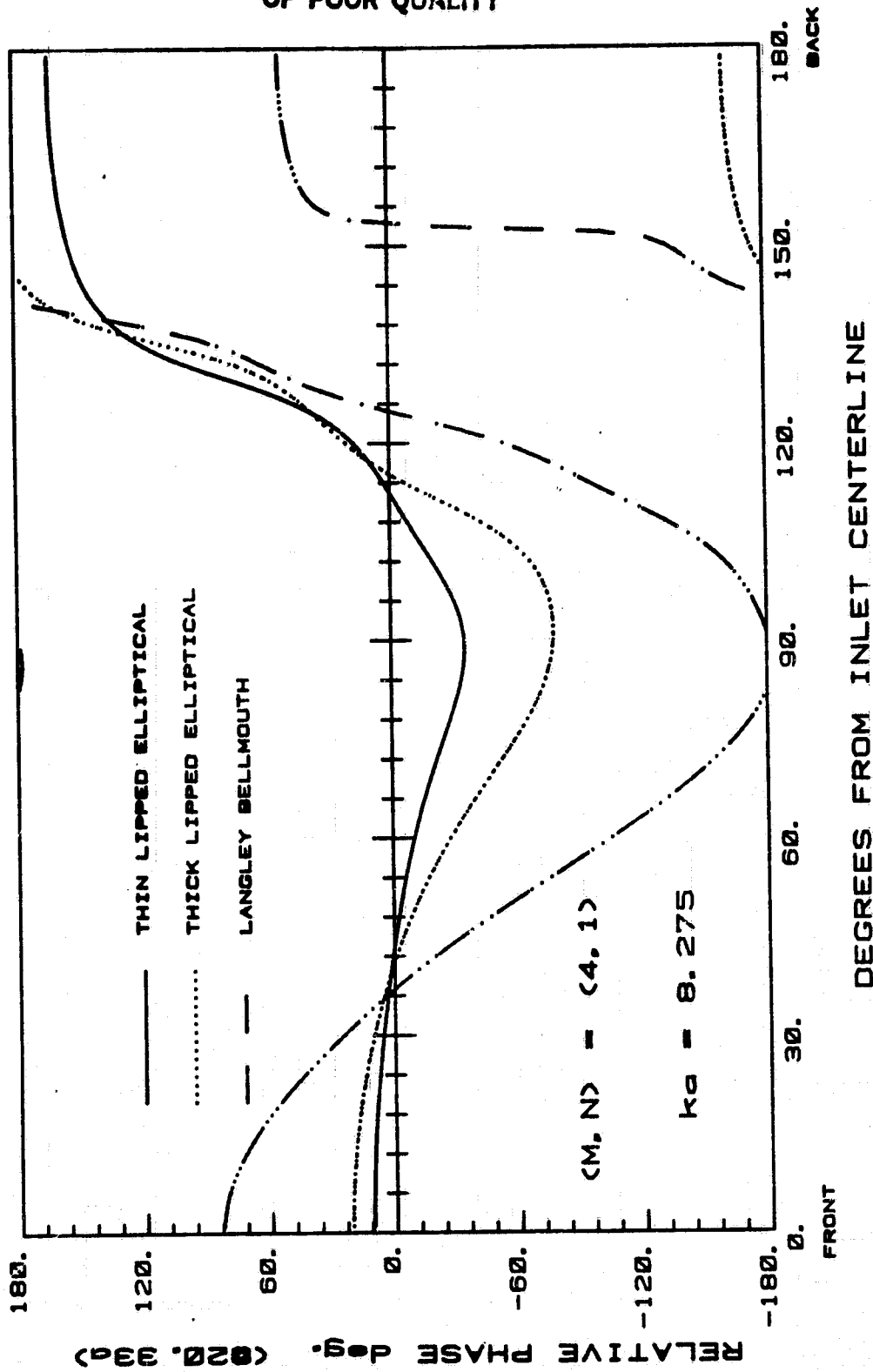
ORIGINAL PAGE IS
OF POOR QUALITY



CUT-OFF RATIO = 1.556

Fig. 61k

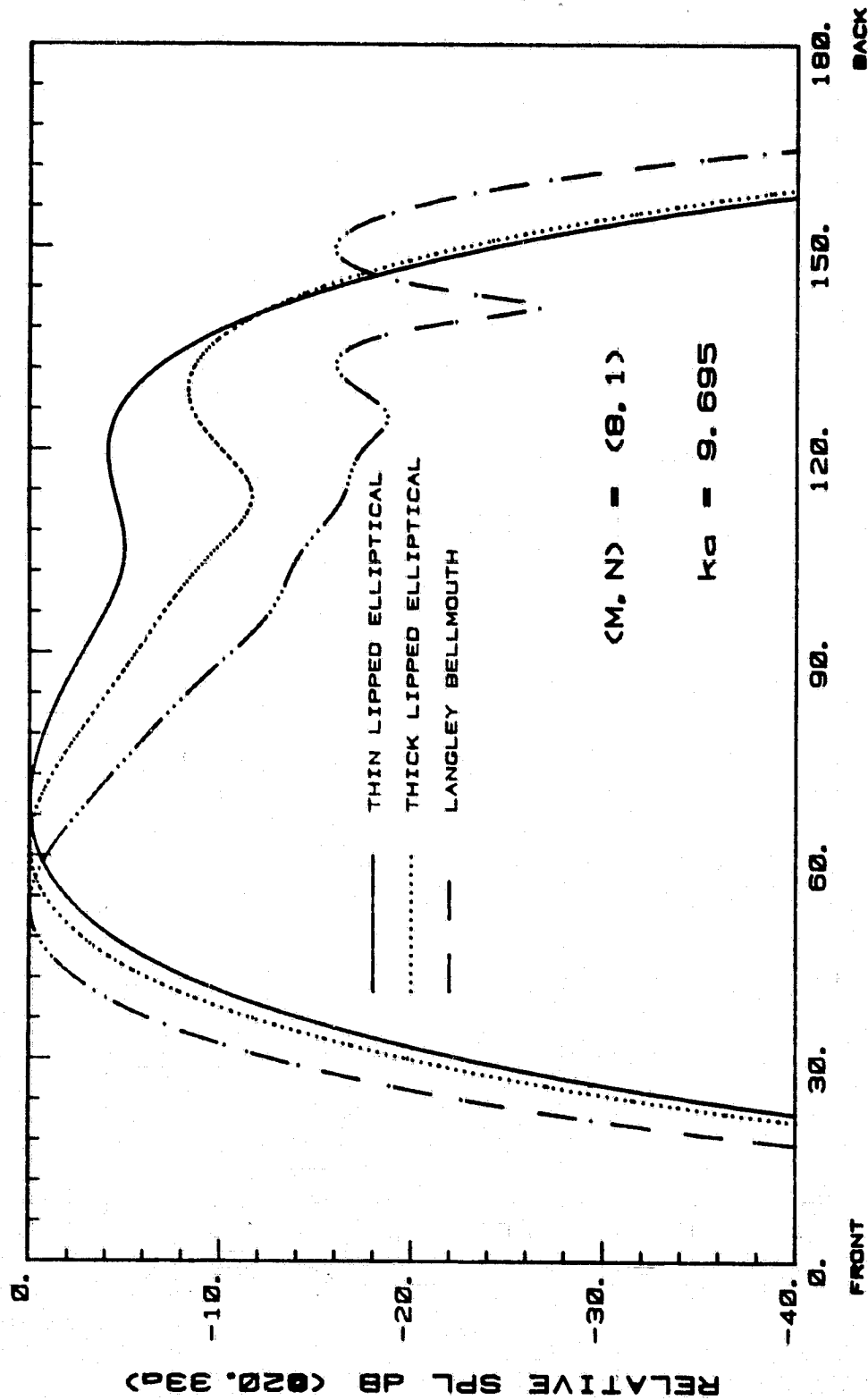
ORIGINAL PAGE IS
OF POOR QUALITY



CUT-OFF RATIO = 1.556

Fig. 611

ORIGINAL PAGE IS
OF POOR QUALITY

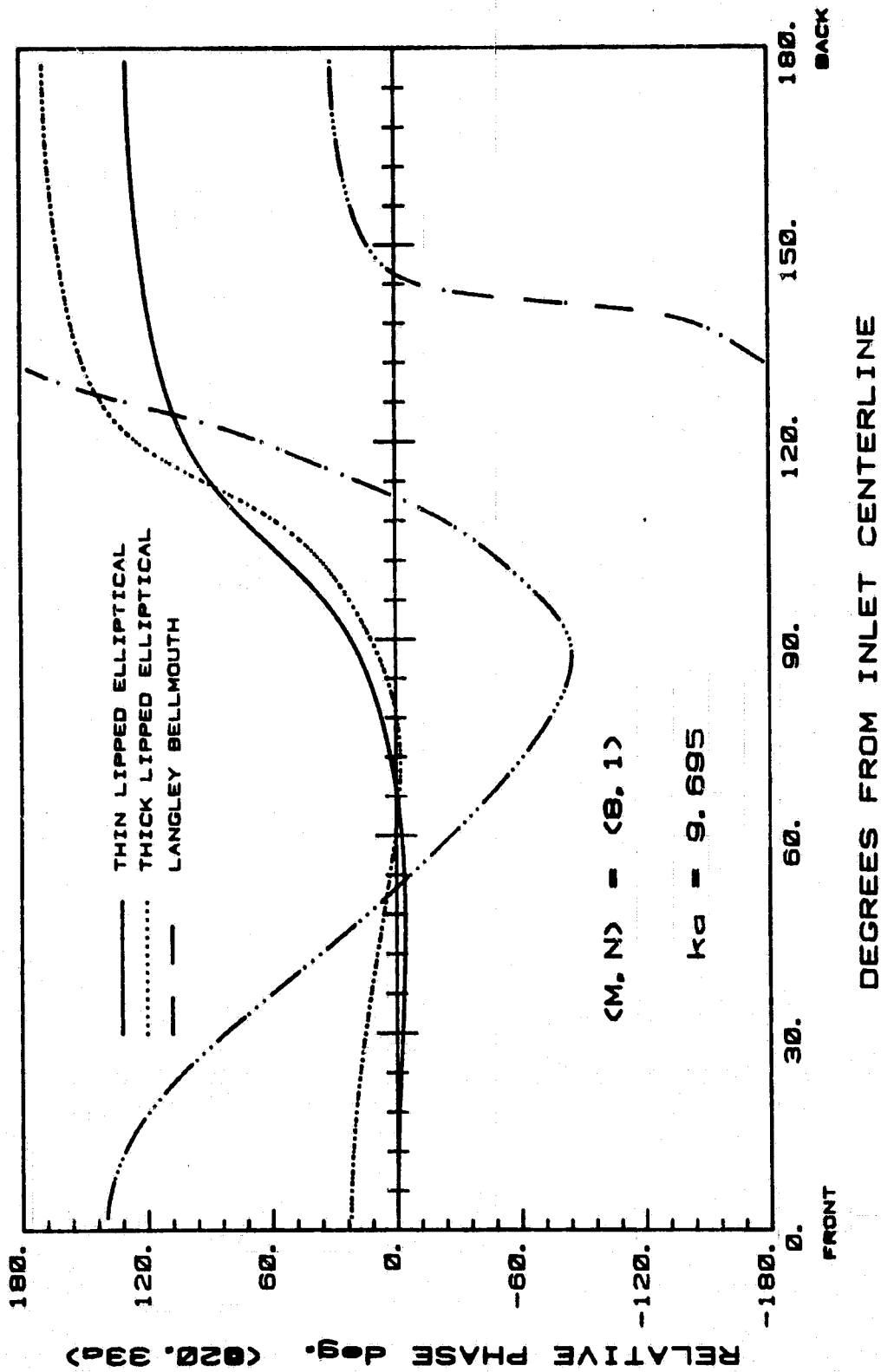


DEGREES FROM INLET CENTERLINE

CUT-OFF RATIO = 1.005

Fig. 62a

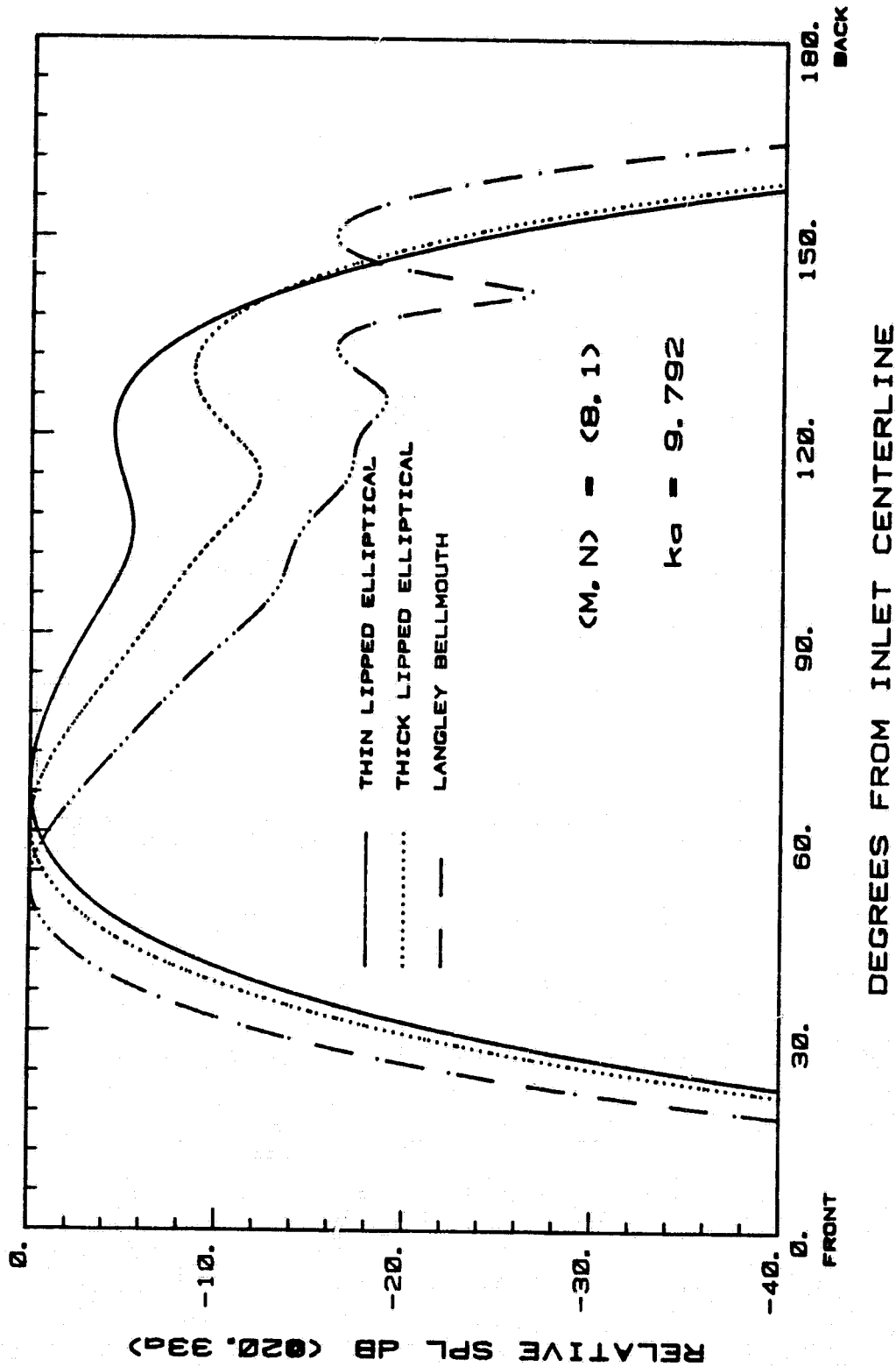
ORIGINAL PAGE IS
OF POOR QUALITY



CUT-OFF RATIO = 1.005

Fig. 62b

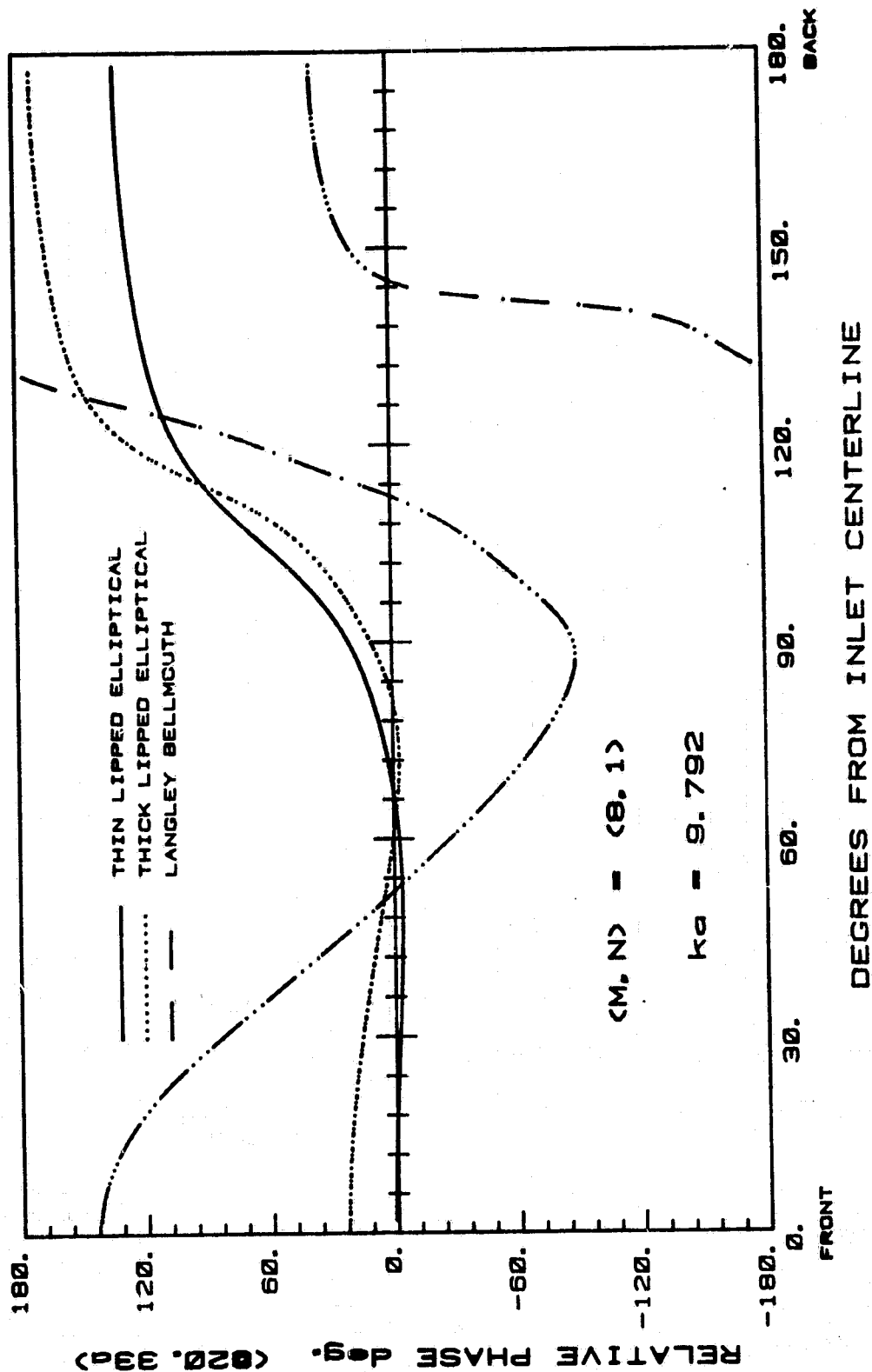
ORIGINAL PAGE 18
OF POOR QUALITY



CUT-OFF RATIO = 1.015

Fig. 62c

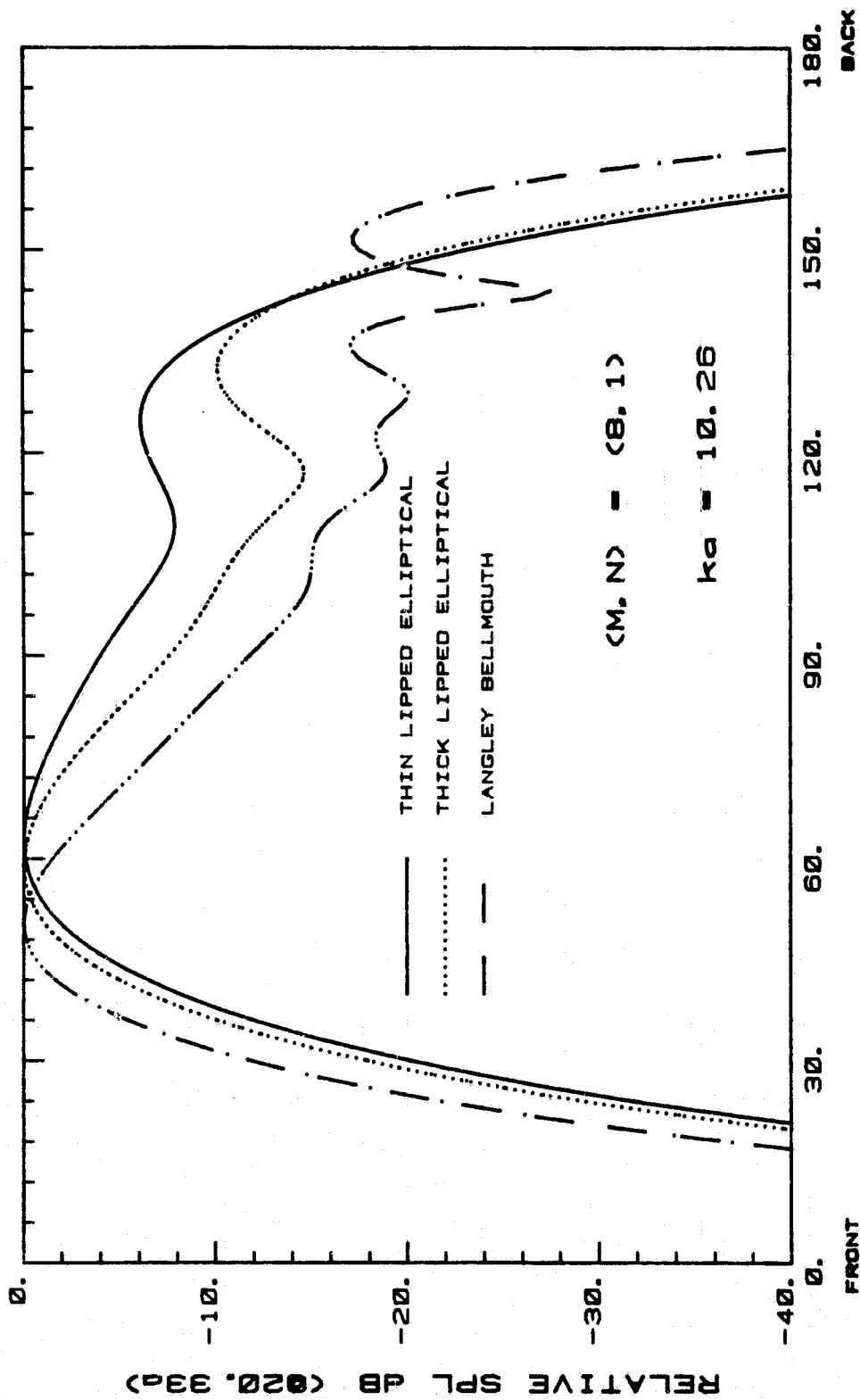
ORIGINAL PAGE IS
OF POOR QUALITY



CUT-OFF RATIO = 1.015

Fig. 62d

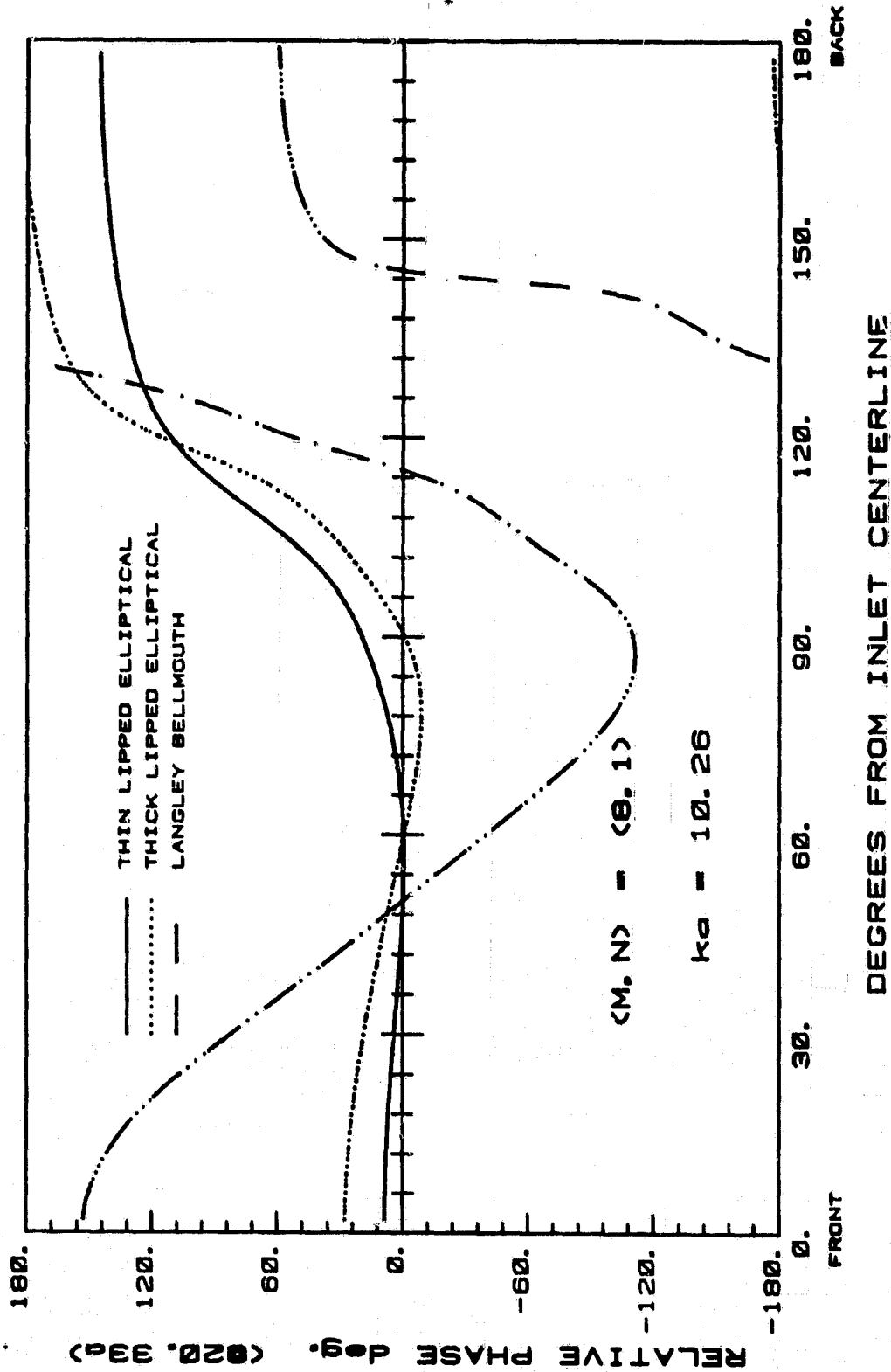
ORIGINAL PAGE IS
OF POOR QUALITY



CUT-OFF RATIO = 1.064

Fig. 62e

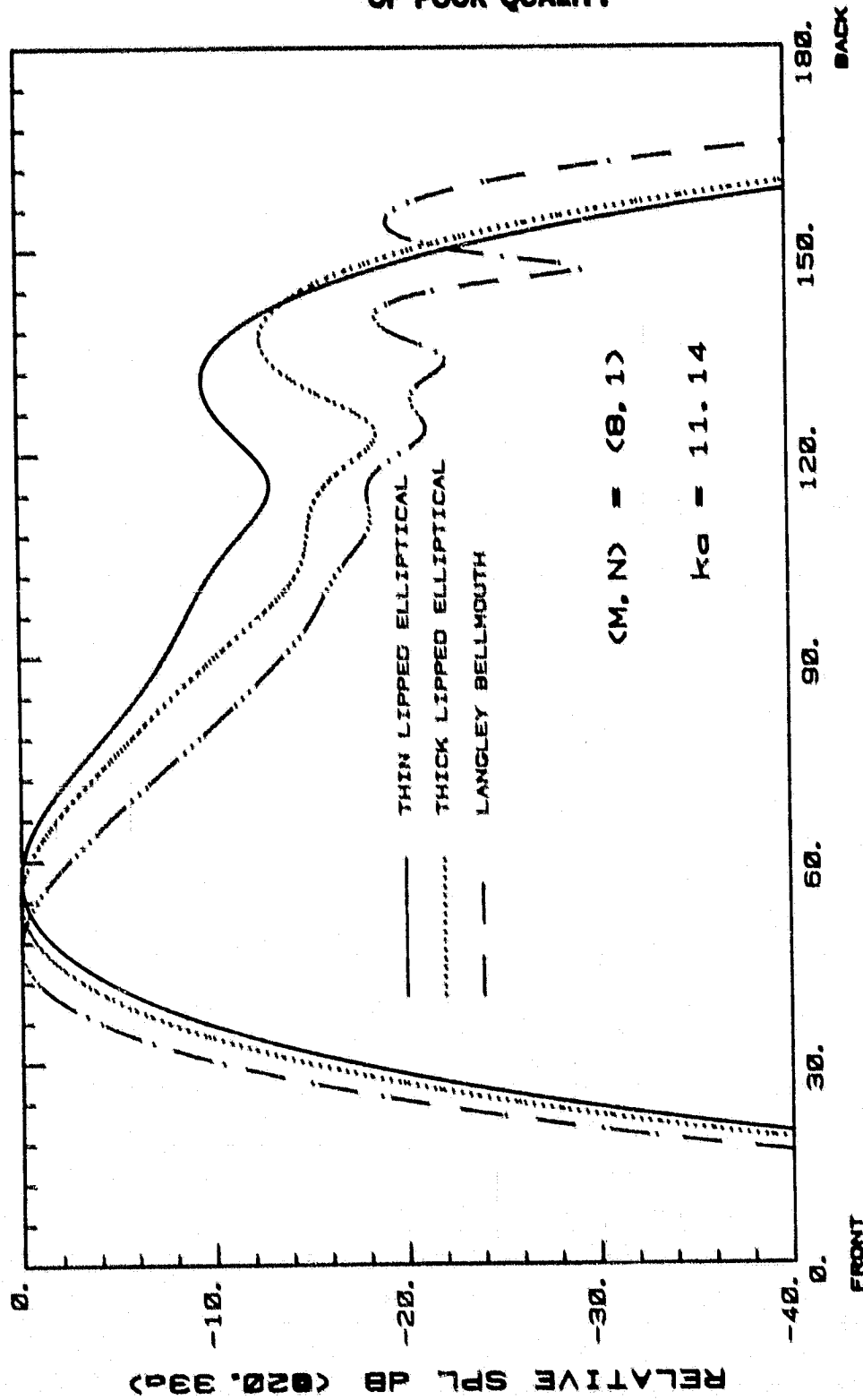
ORIGINAL PAGE 13
OF POOR QUALITY



CUT-OFF RATIO = 1.064

Fig. 62f

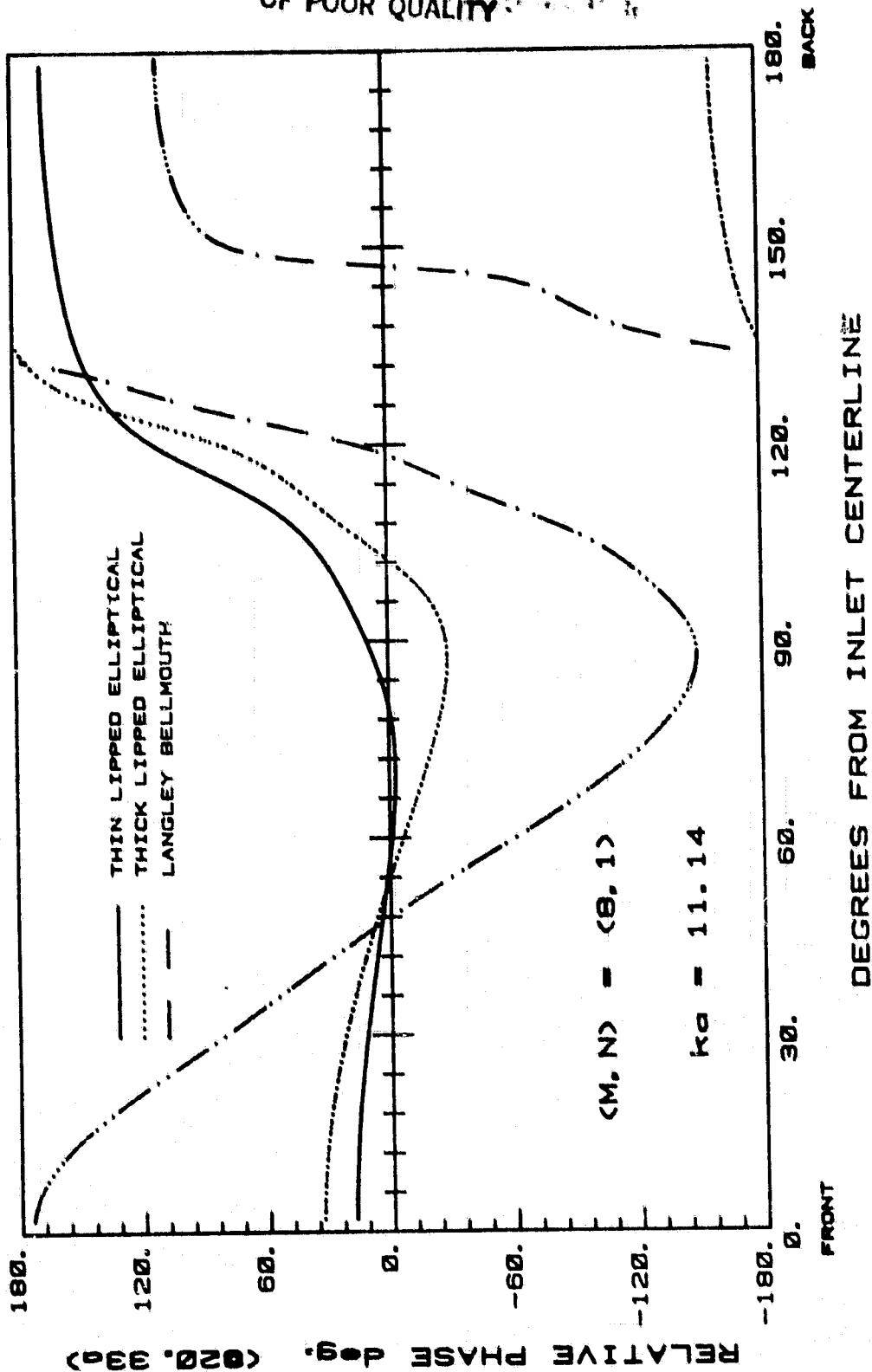
ORIGINAL PAGE IS
OF POOR QUALITY



CUT-OFF RATIO = 1.155

Fig. 62g

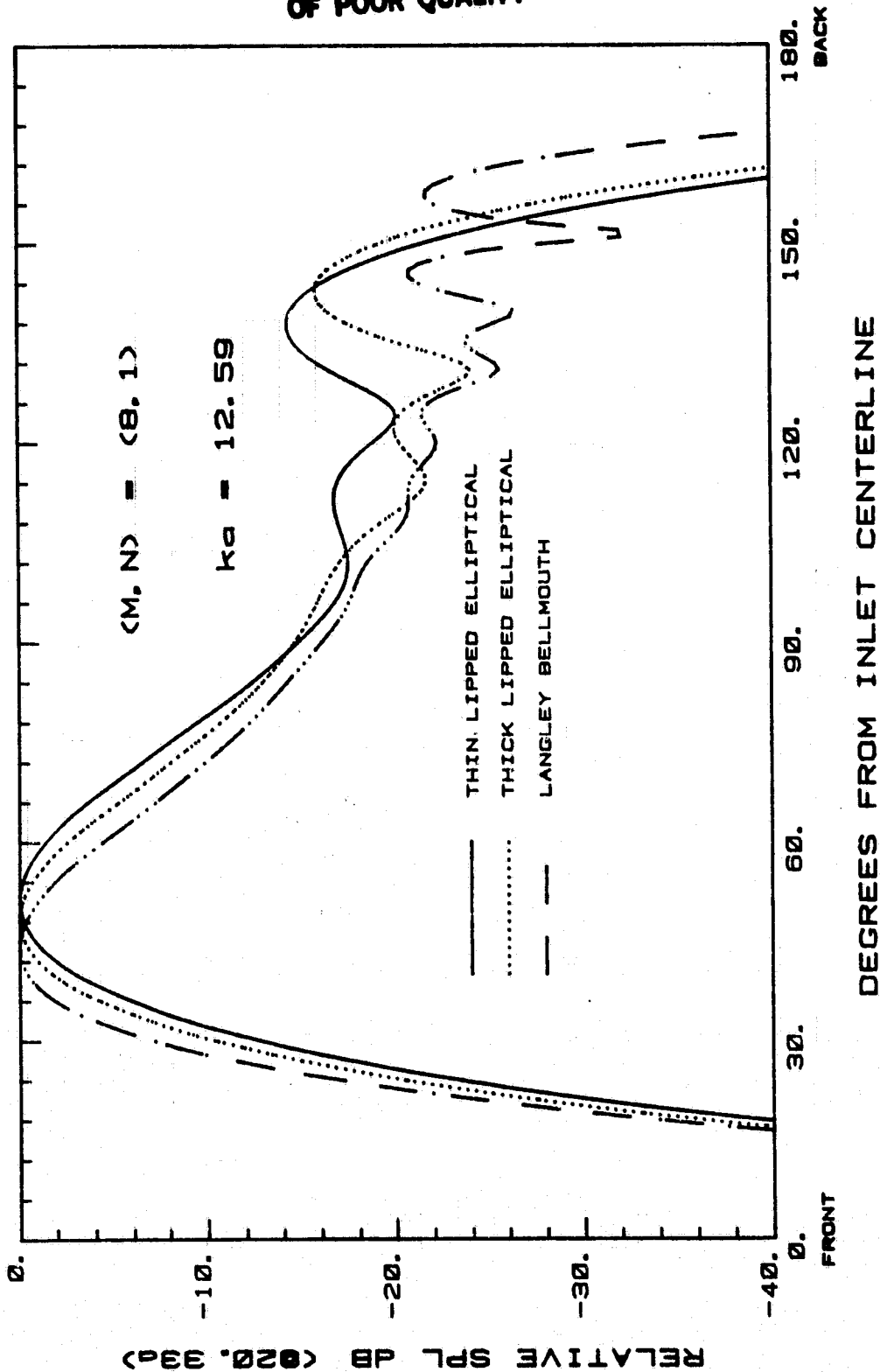
ORIGINAL PAGE IS
OF POOR QUALITY



CUT-OFF RATIO = 1.155

Fig. 62h

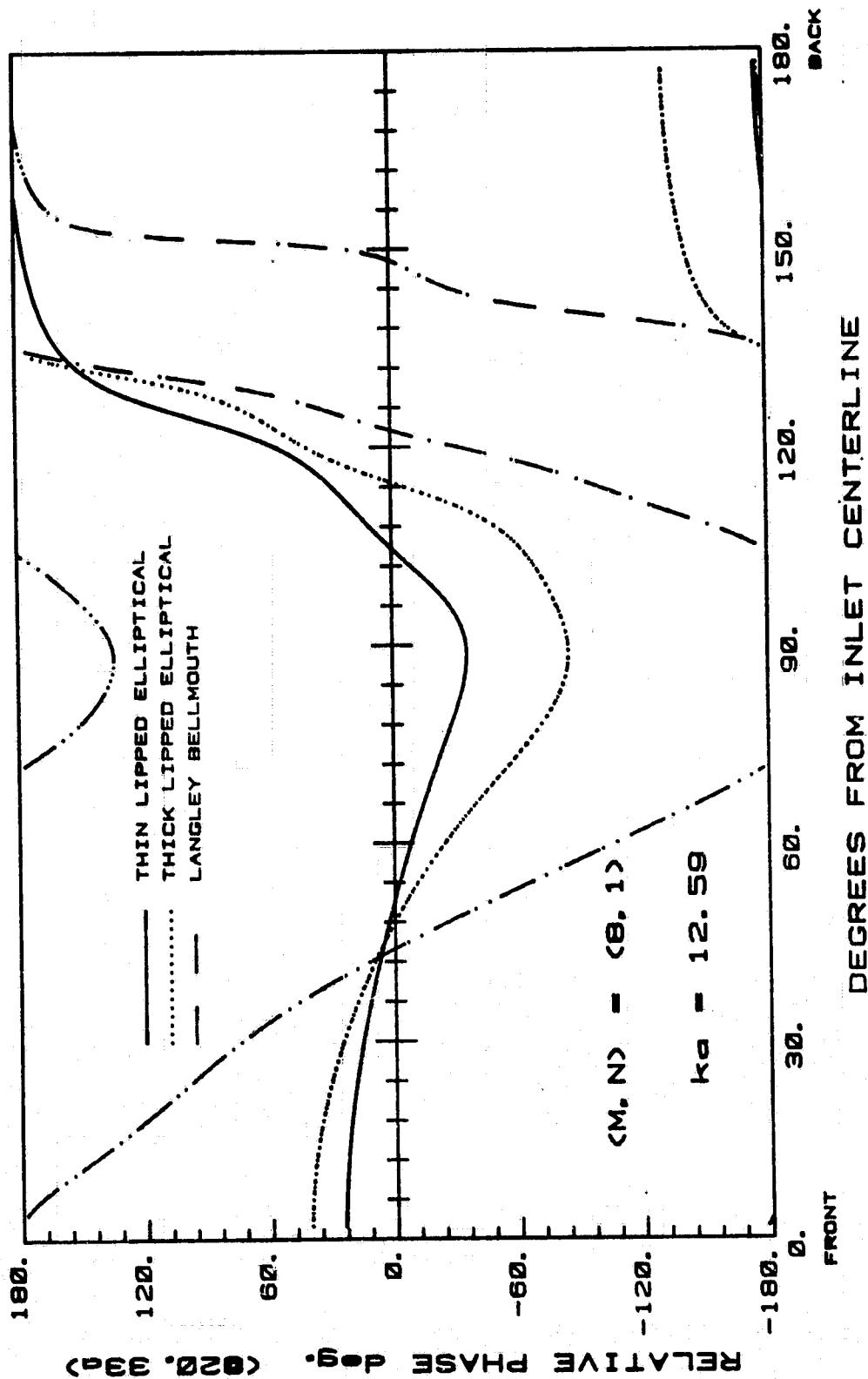
ORIGINAL PAGE IS
OF POOR QUALITY



CUT-OFF RATIO = 1.305

Fig. 62i

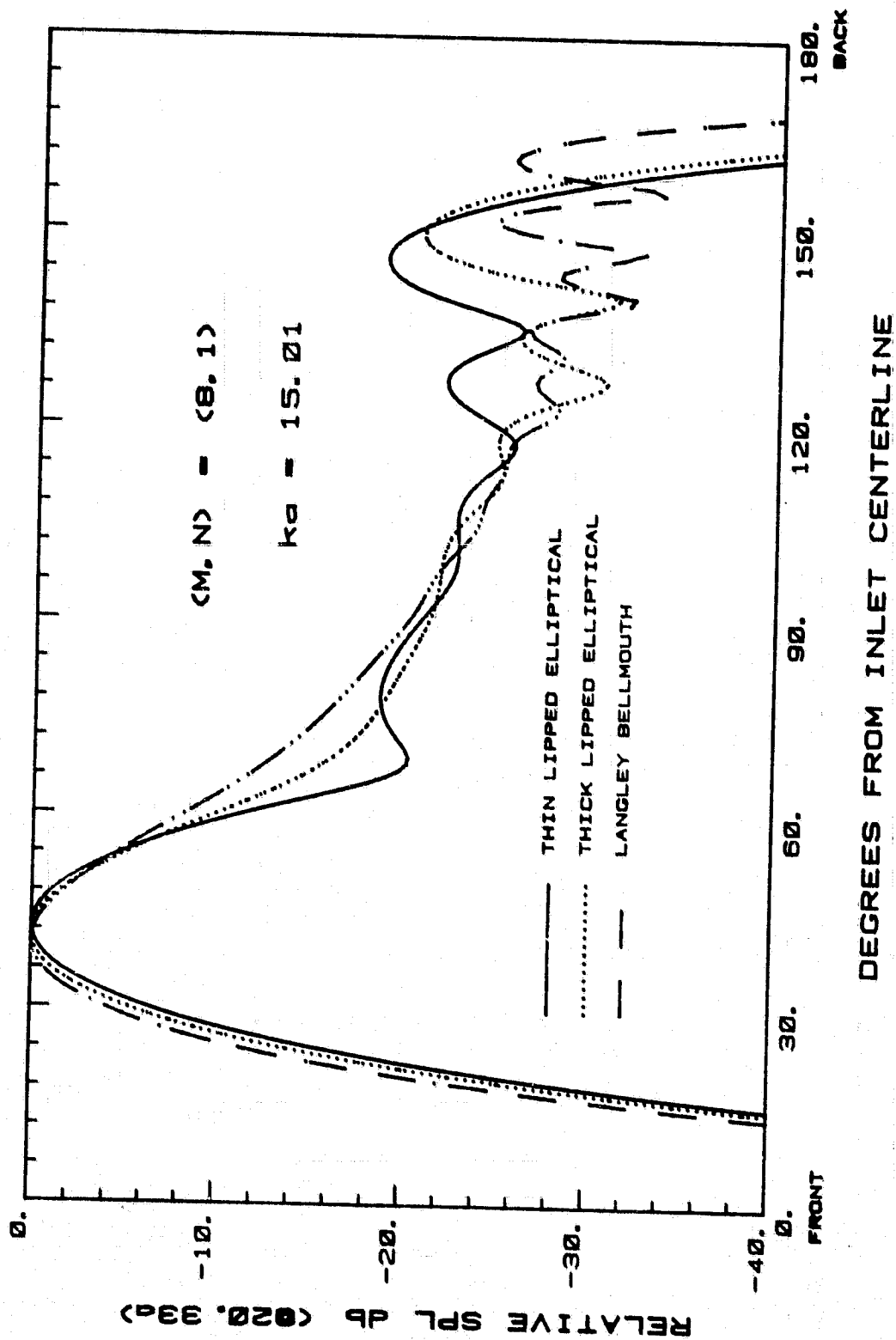
ORIGINAL PAGE 13
OF POOR QUALITY



CUT-OFF RATIO = 1.305

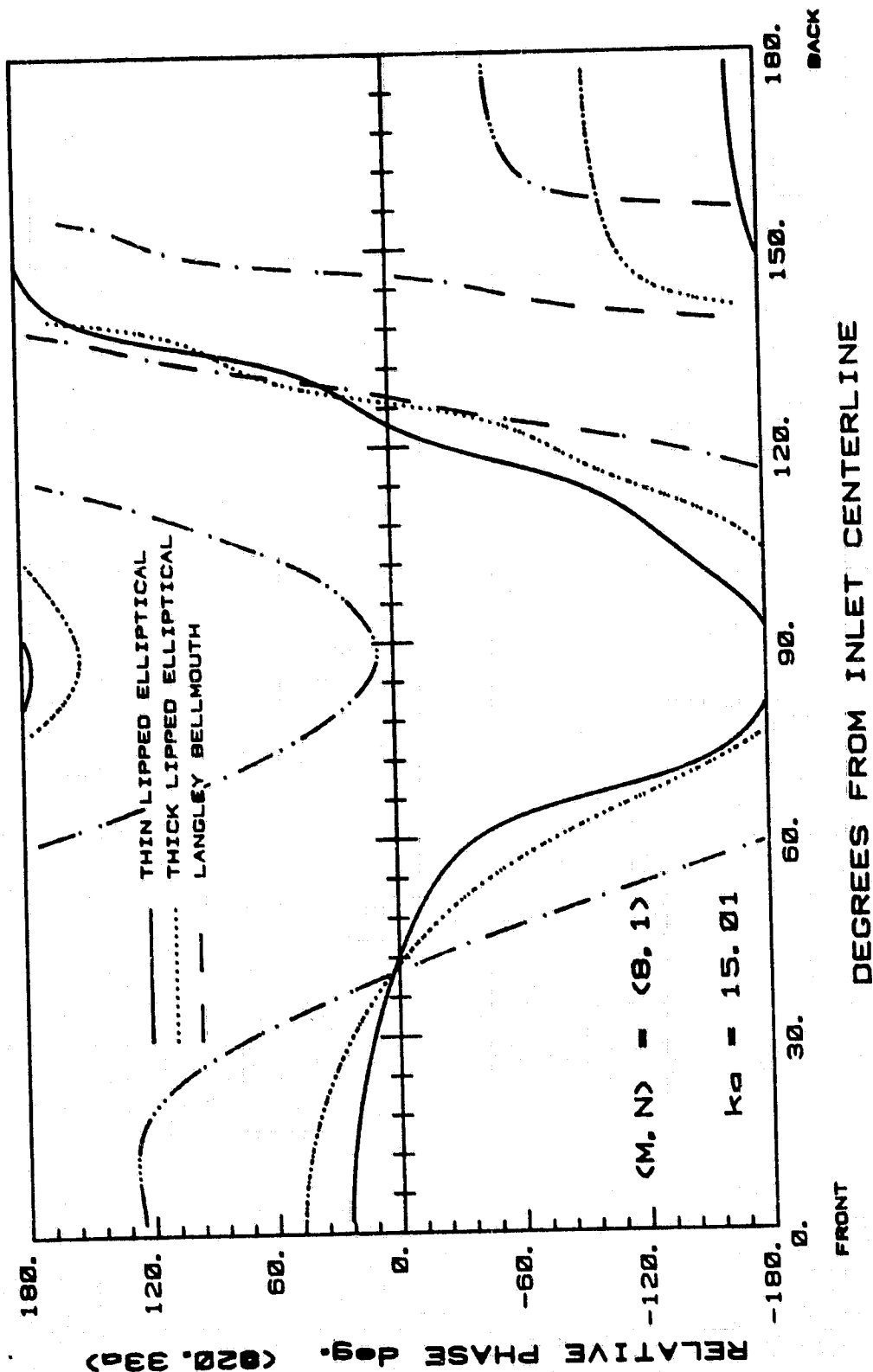
Fig. 62j

ORIGINAL PAGE IS
OF POOR QUALITY



CUT-OFF RATIO = 1.556

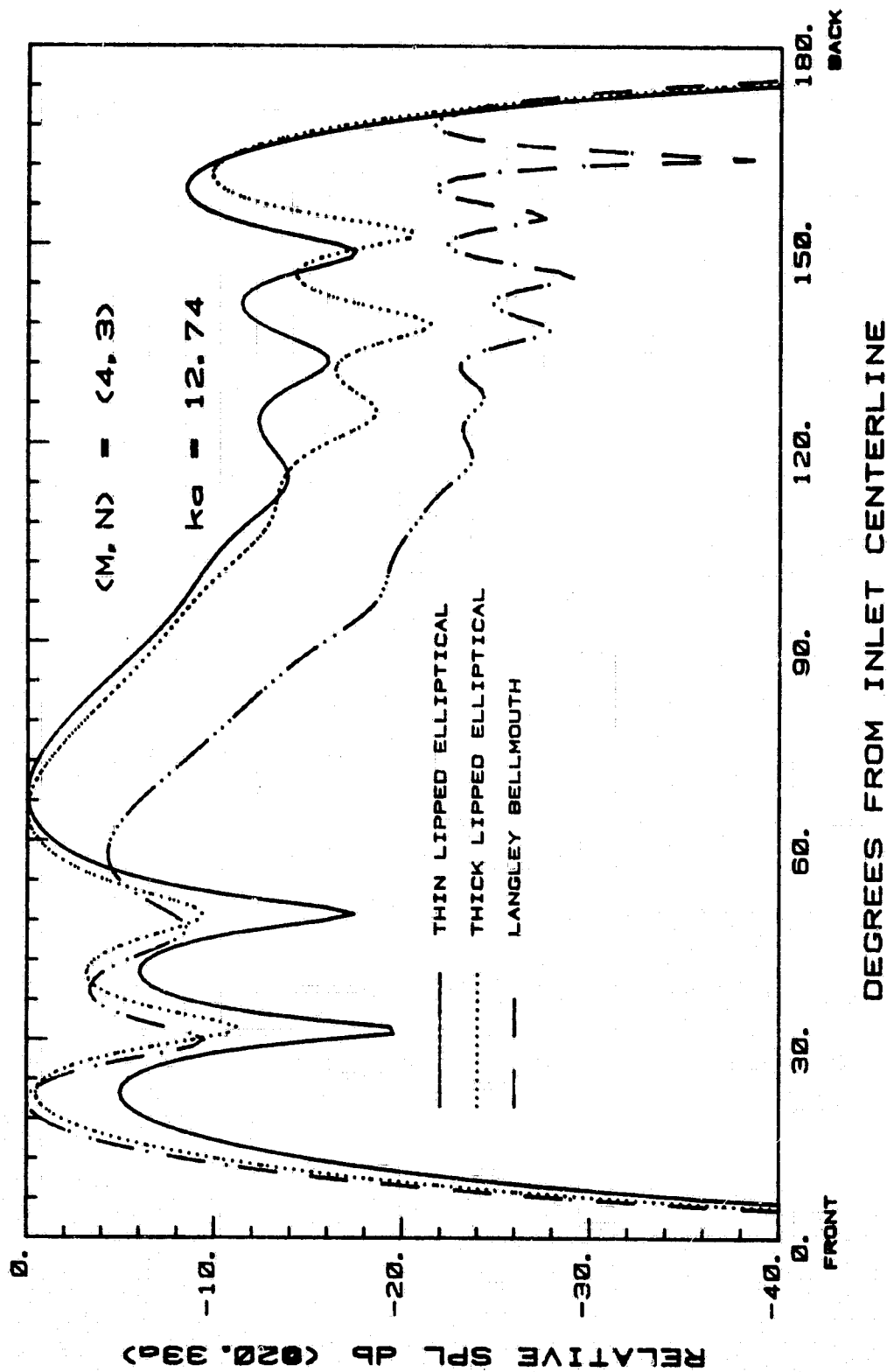
Fig. 62k



CUT-OFF RATIO = 1.556

Fig. 621

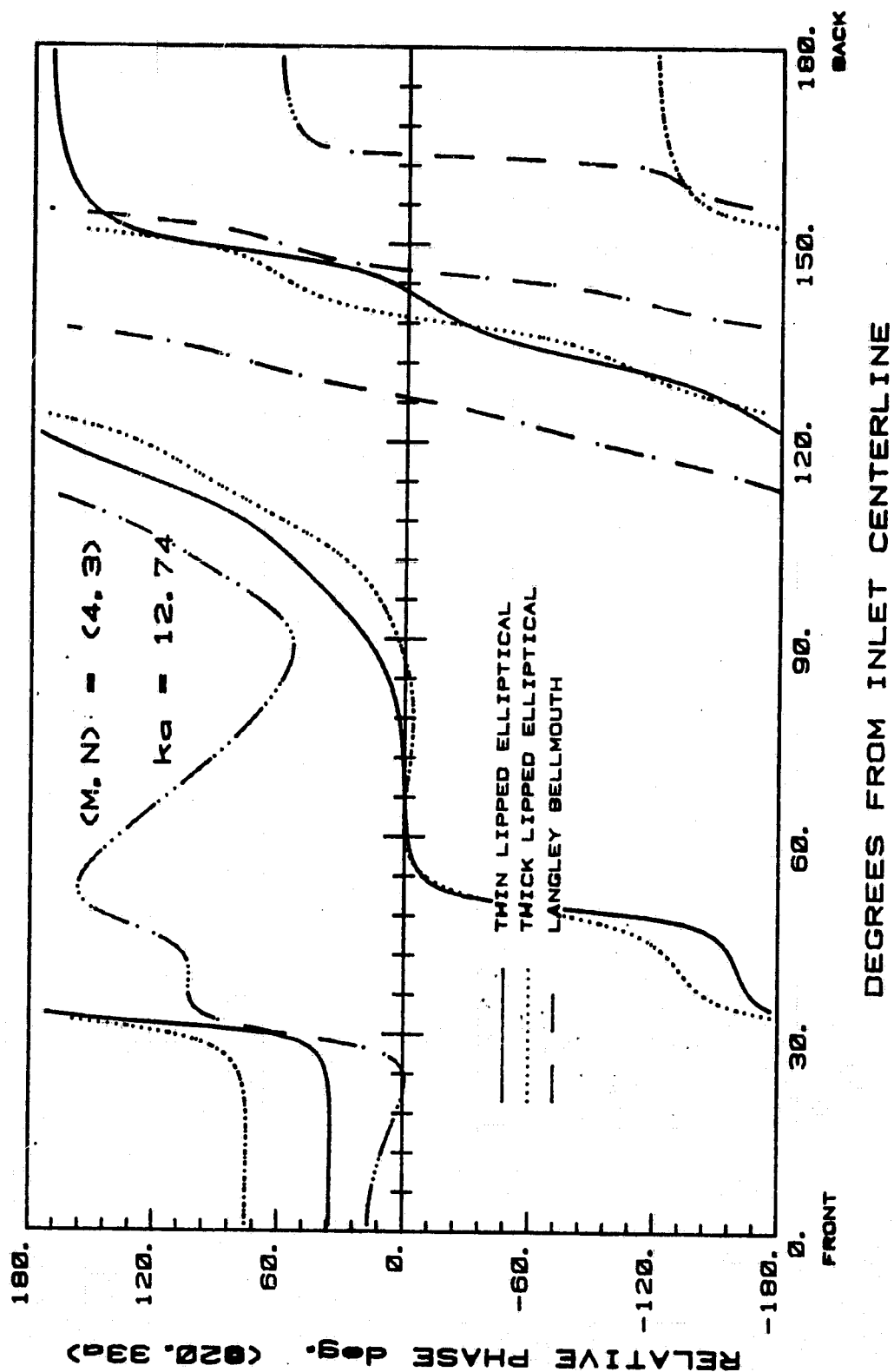
ORIGINAL PAGE 18
OF POOR QUALITY



CUT-OFF RATIO = 1.005

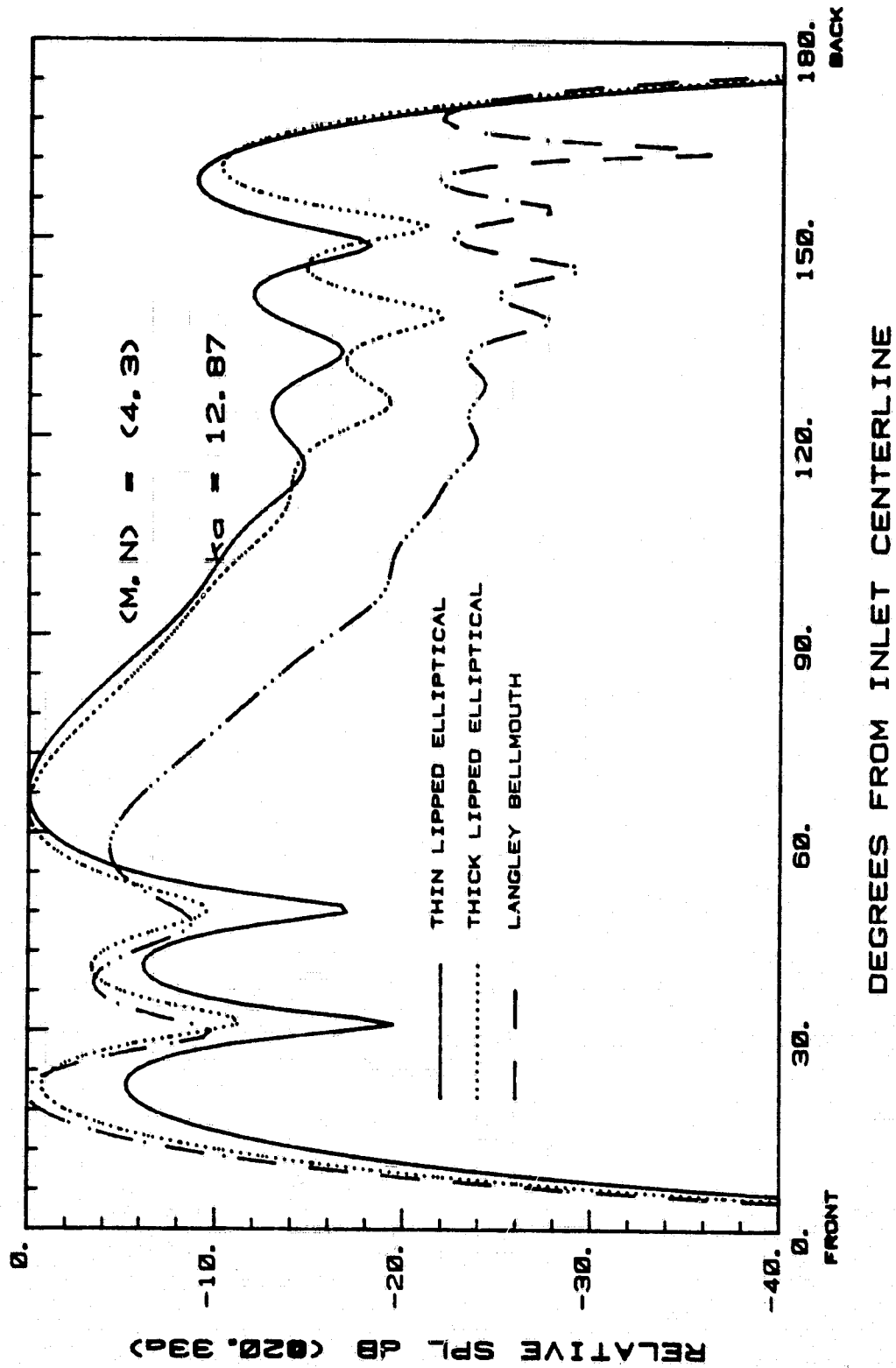
Fig. 63a

ORIGINAL PAGE IS
OF POOR QUALITY



CUT-OFF RATIO = 1.005

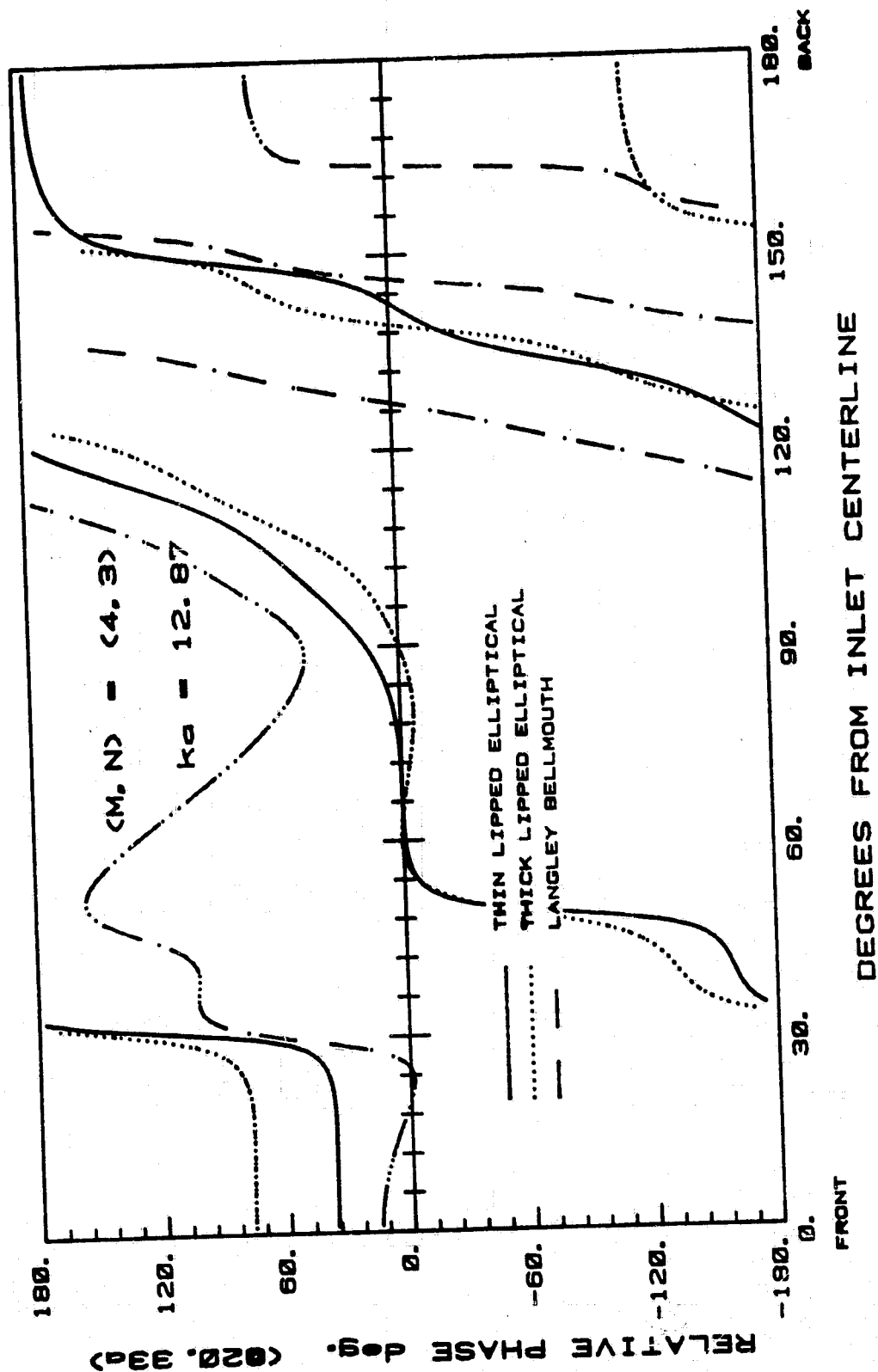
Fig. 63b



CUT-OFF RATIO = 1.015

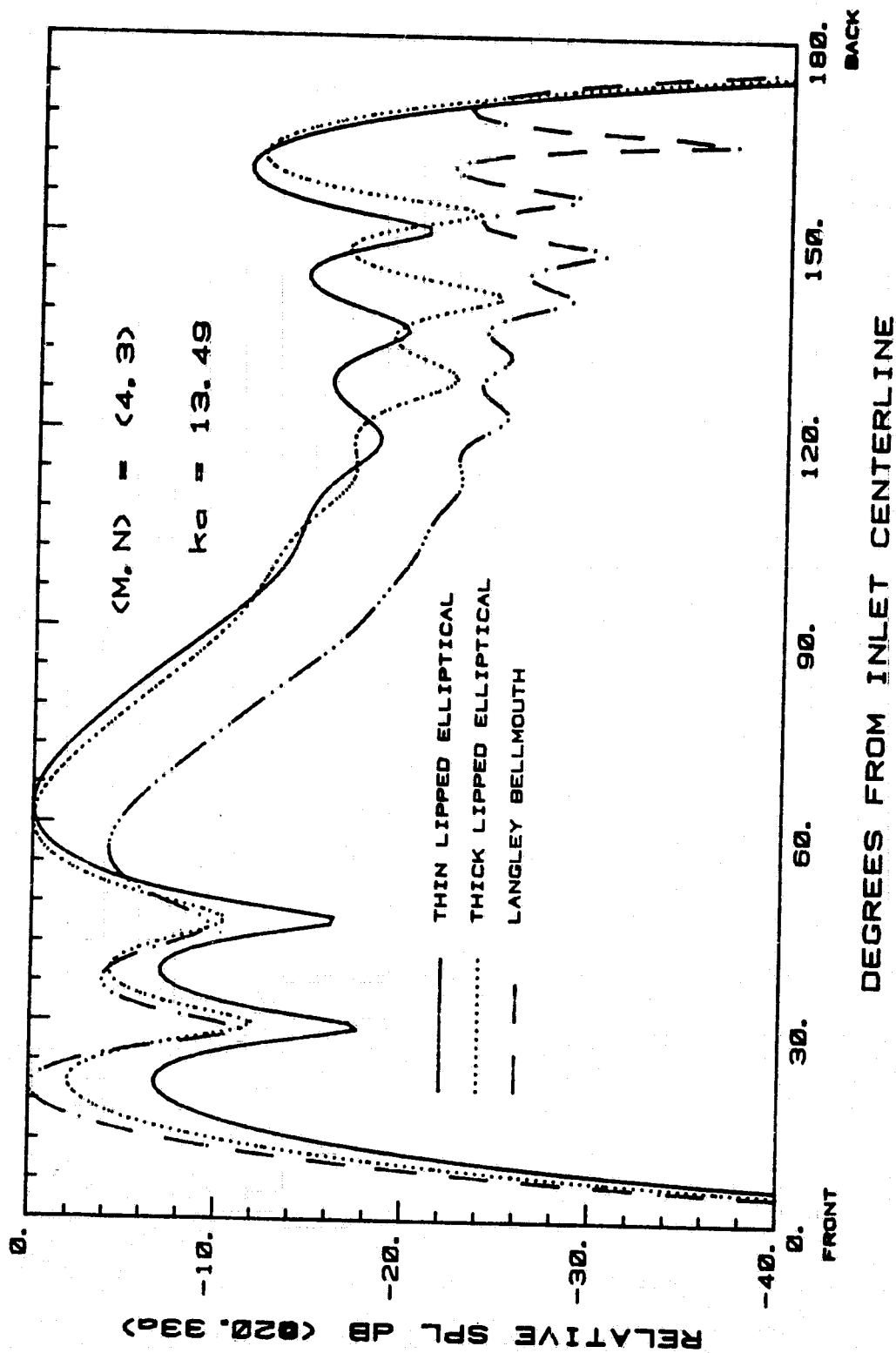
Fig. 63c

ORIGINAL PAGE 13
OF POOR QUALITY



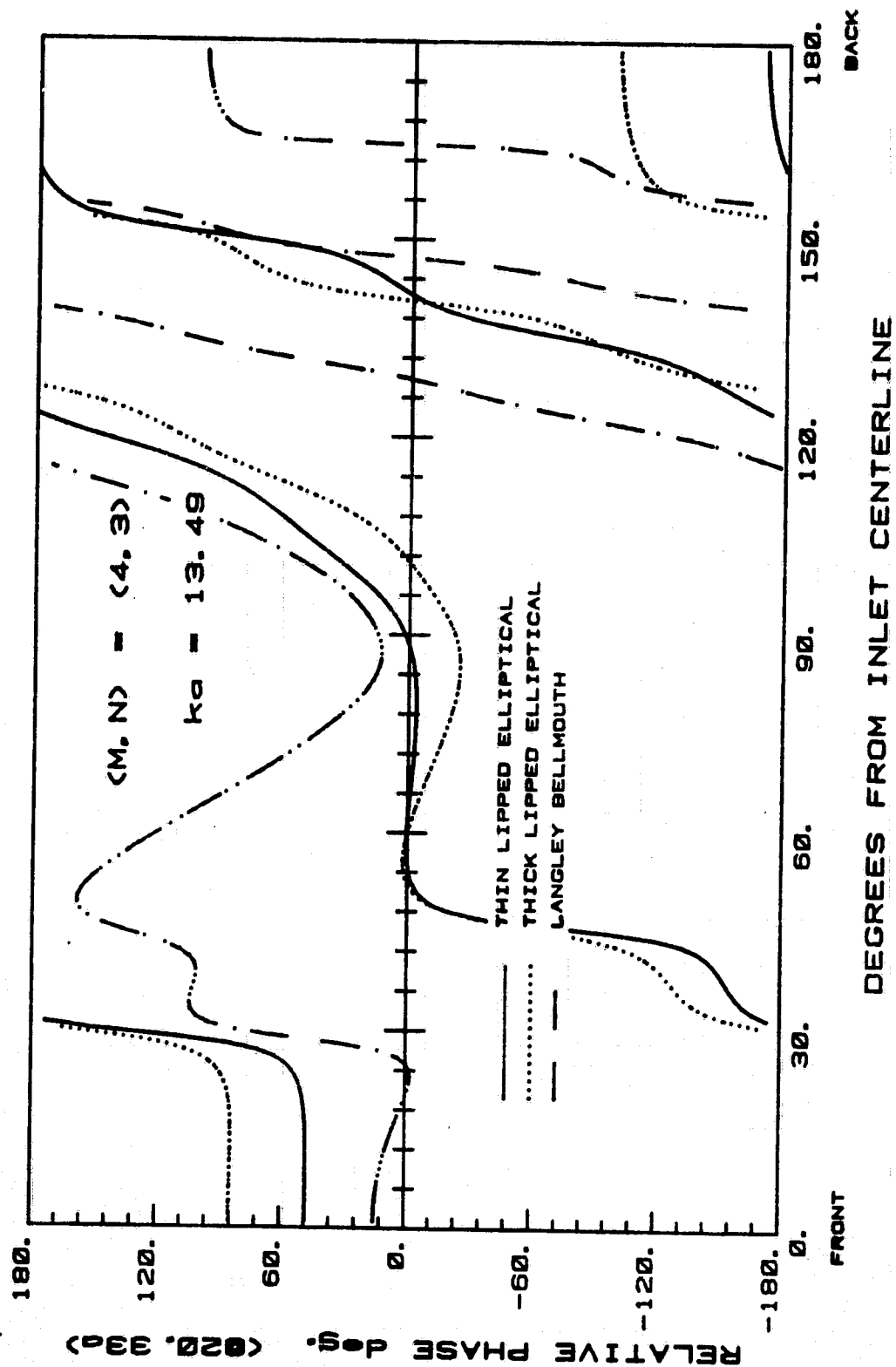
CUT-OFF RATIO = 1.015

Fig. 63d



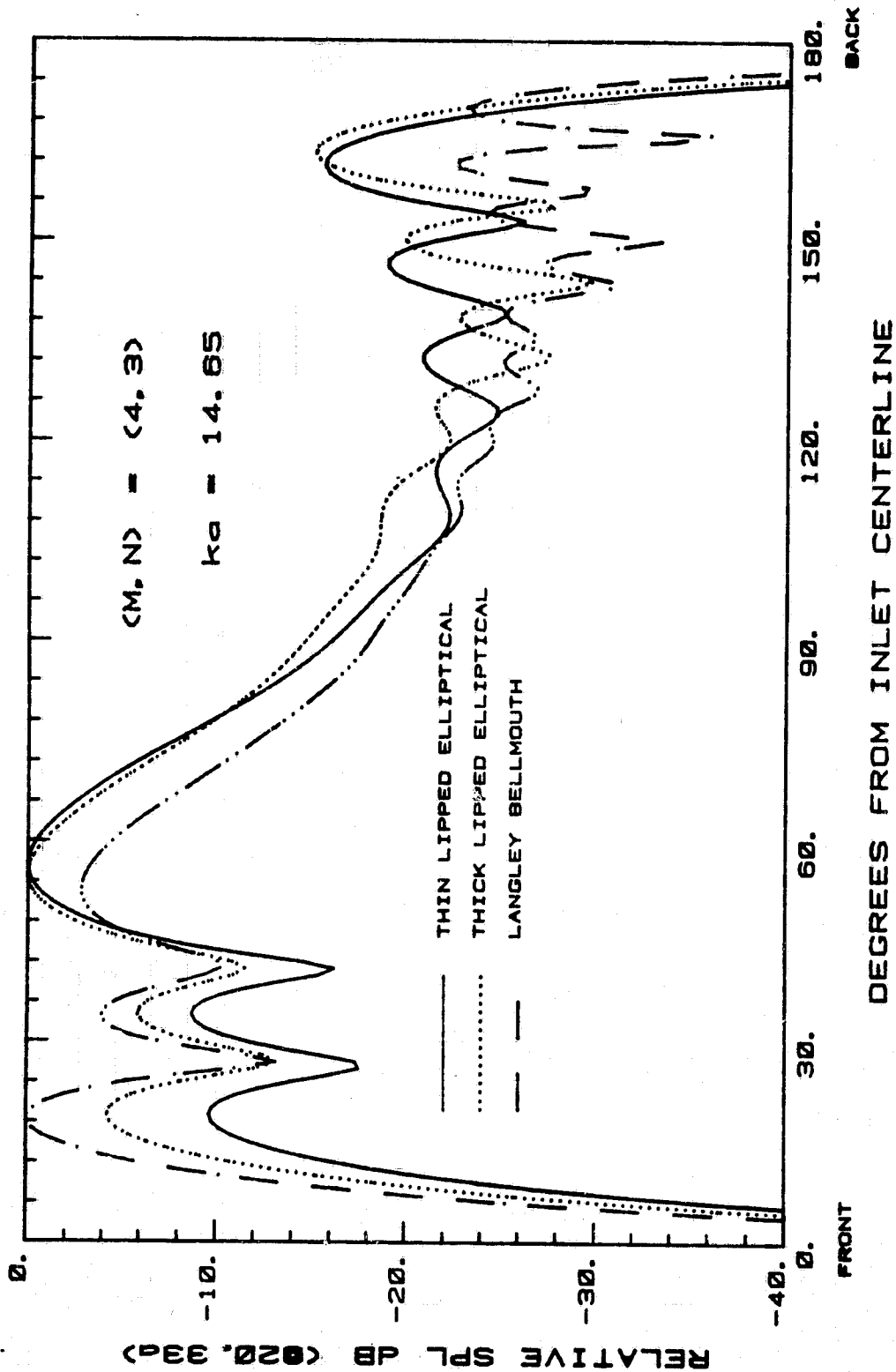
CUT-OFF RATIO = 1.064

Fig. 63e



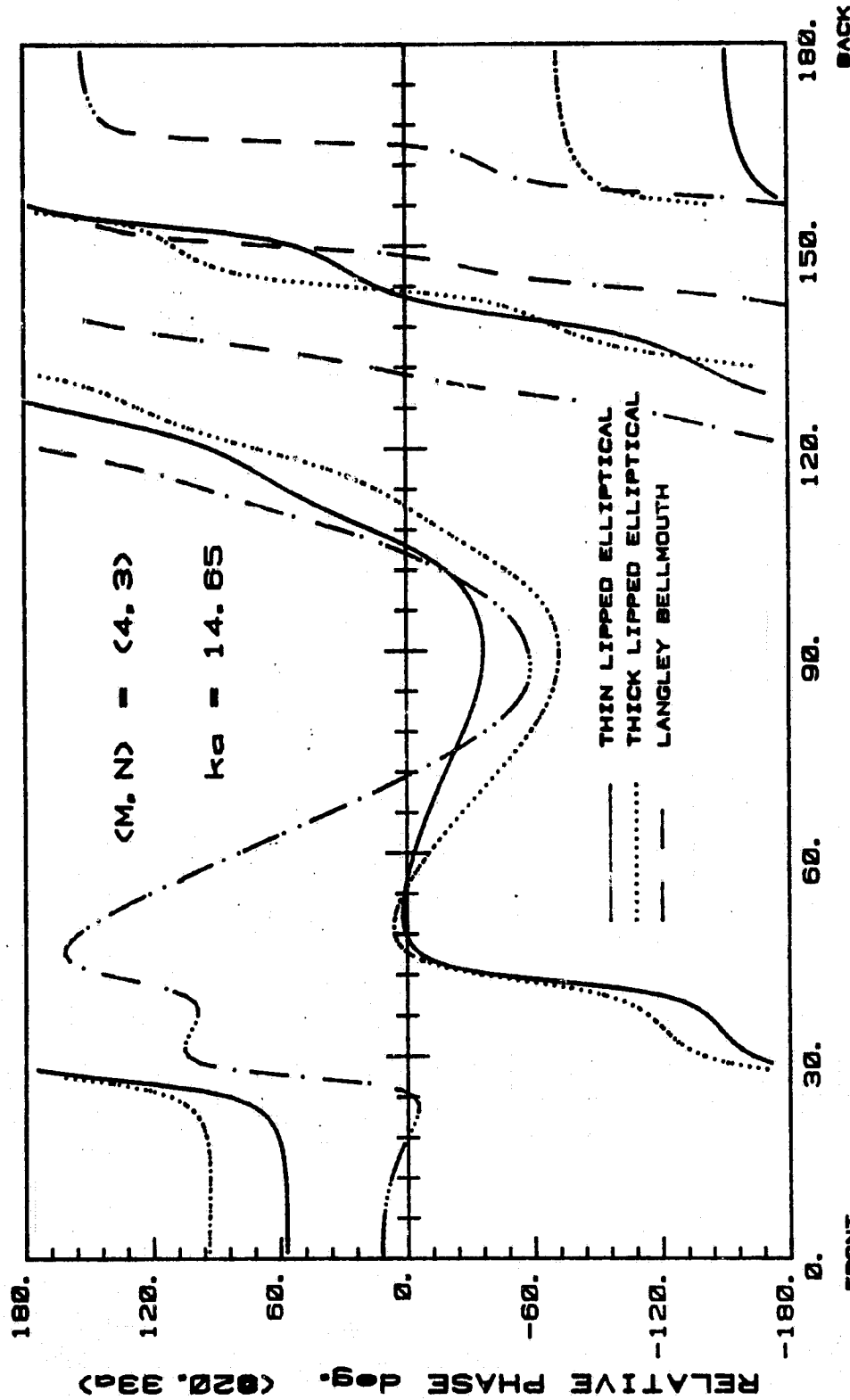
CUT-OFF RATIO = 1.064

Fig. 63f



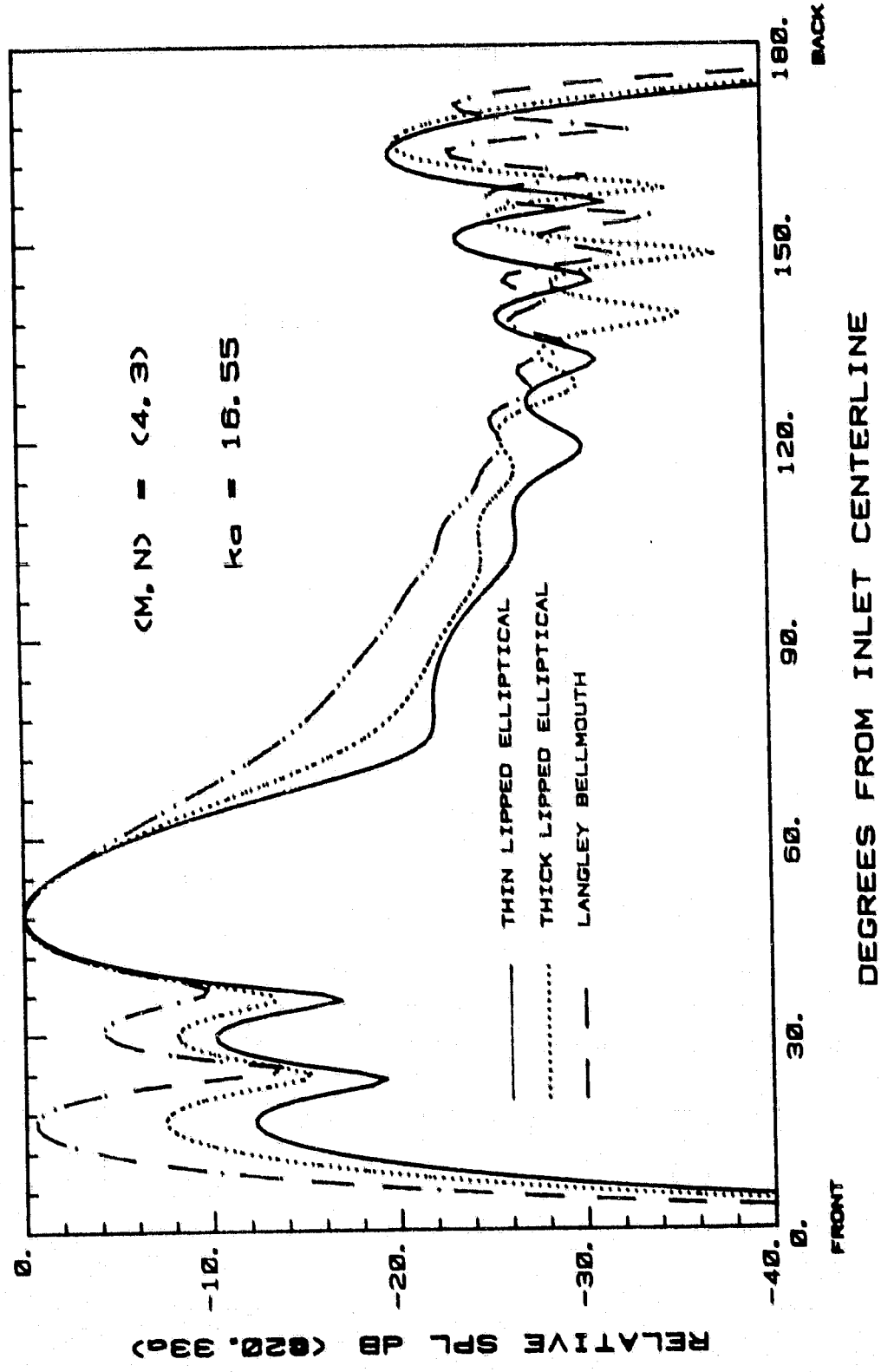
CUT-OFF RATIO = 1.155

Fig. 63g



CUT-OFF RATIO = 1.155

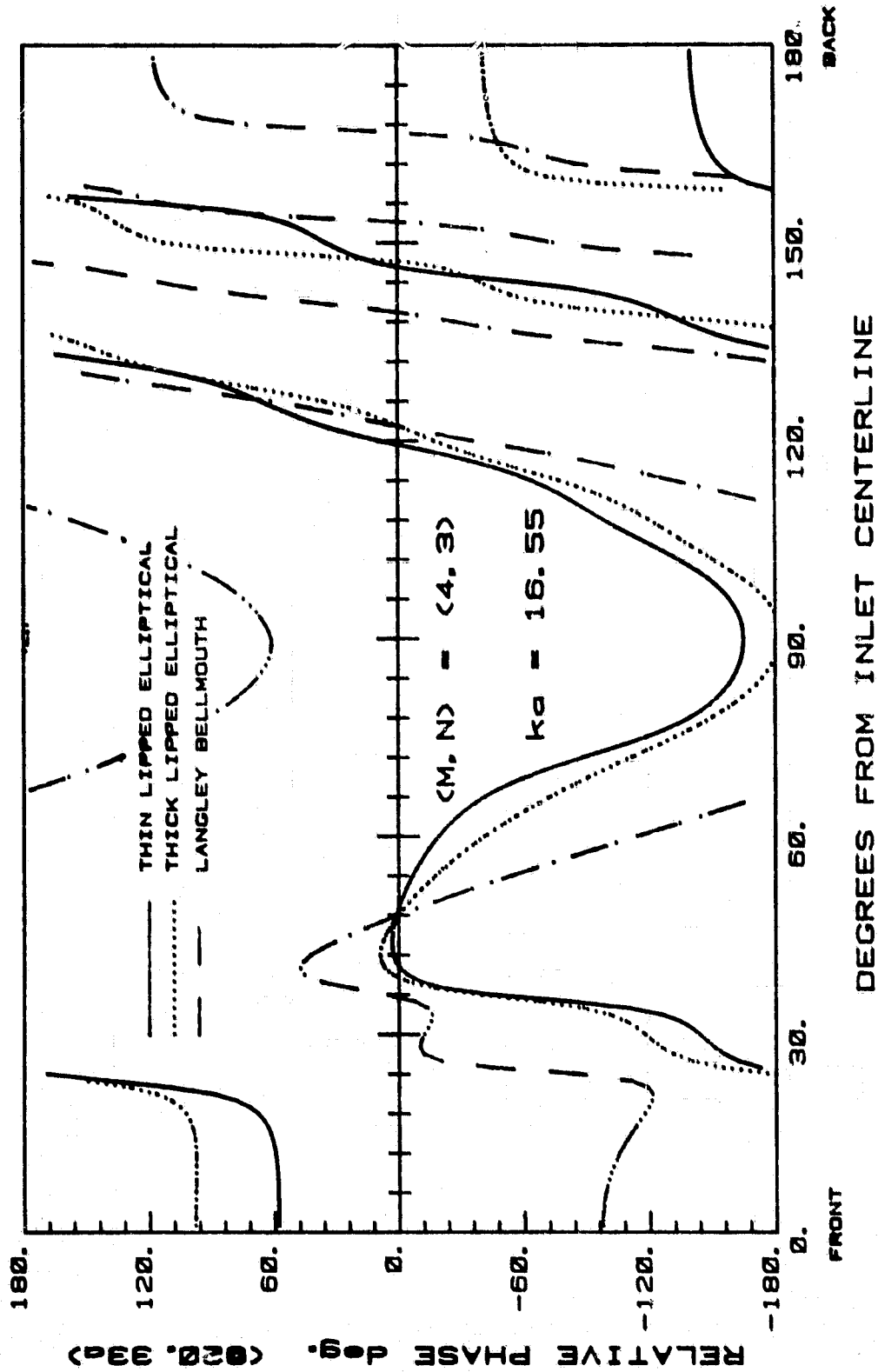
Fig. 63h



CUT-OFF RATIO = 1.305

Fig. 631

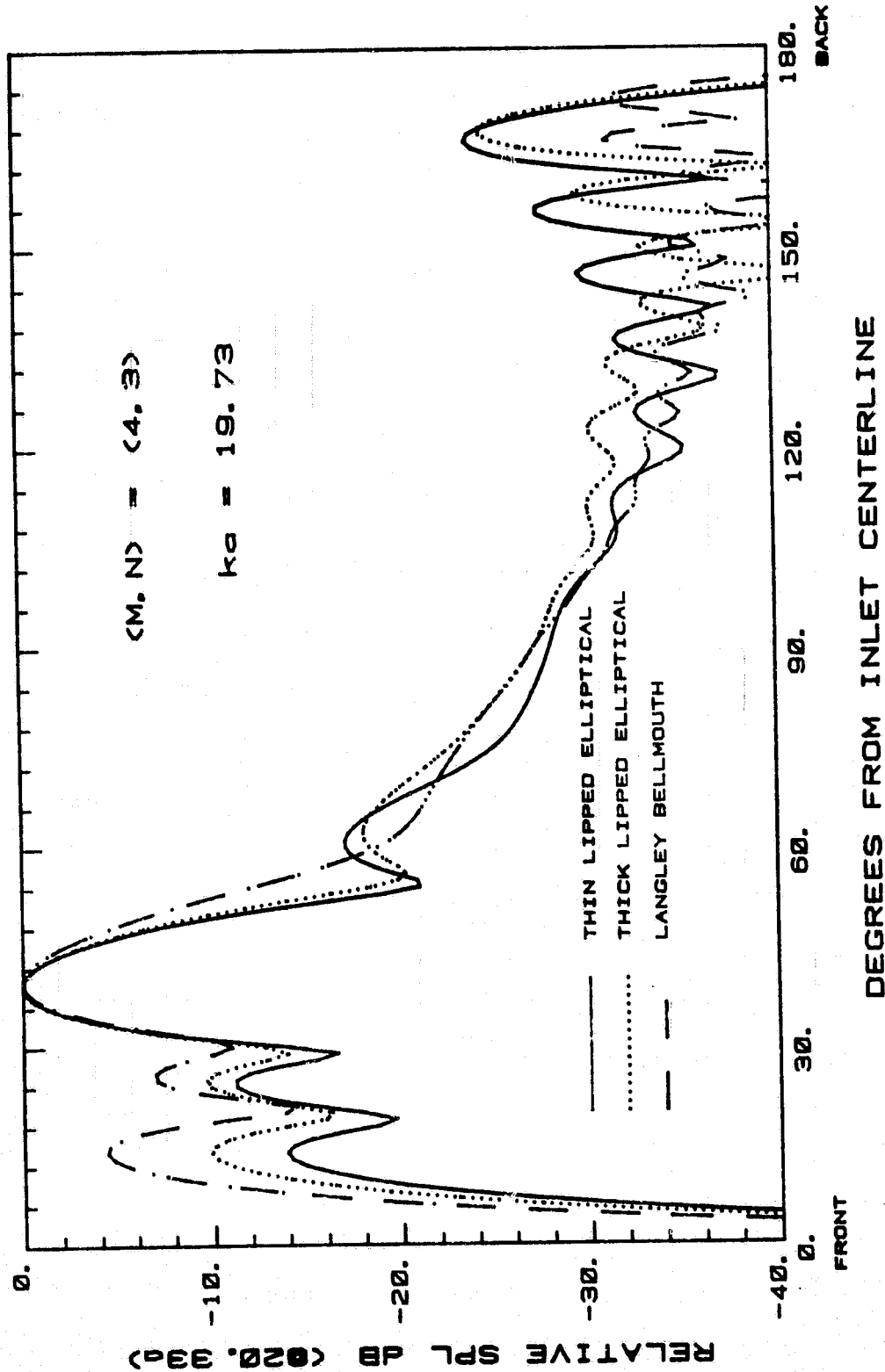
ORIGINAL PAGE IS
OF POOR QUALITY



CUT-OFF RATIO = 1.305

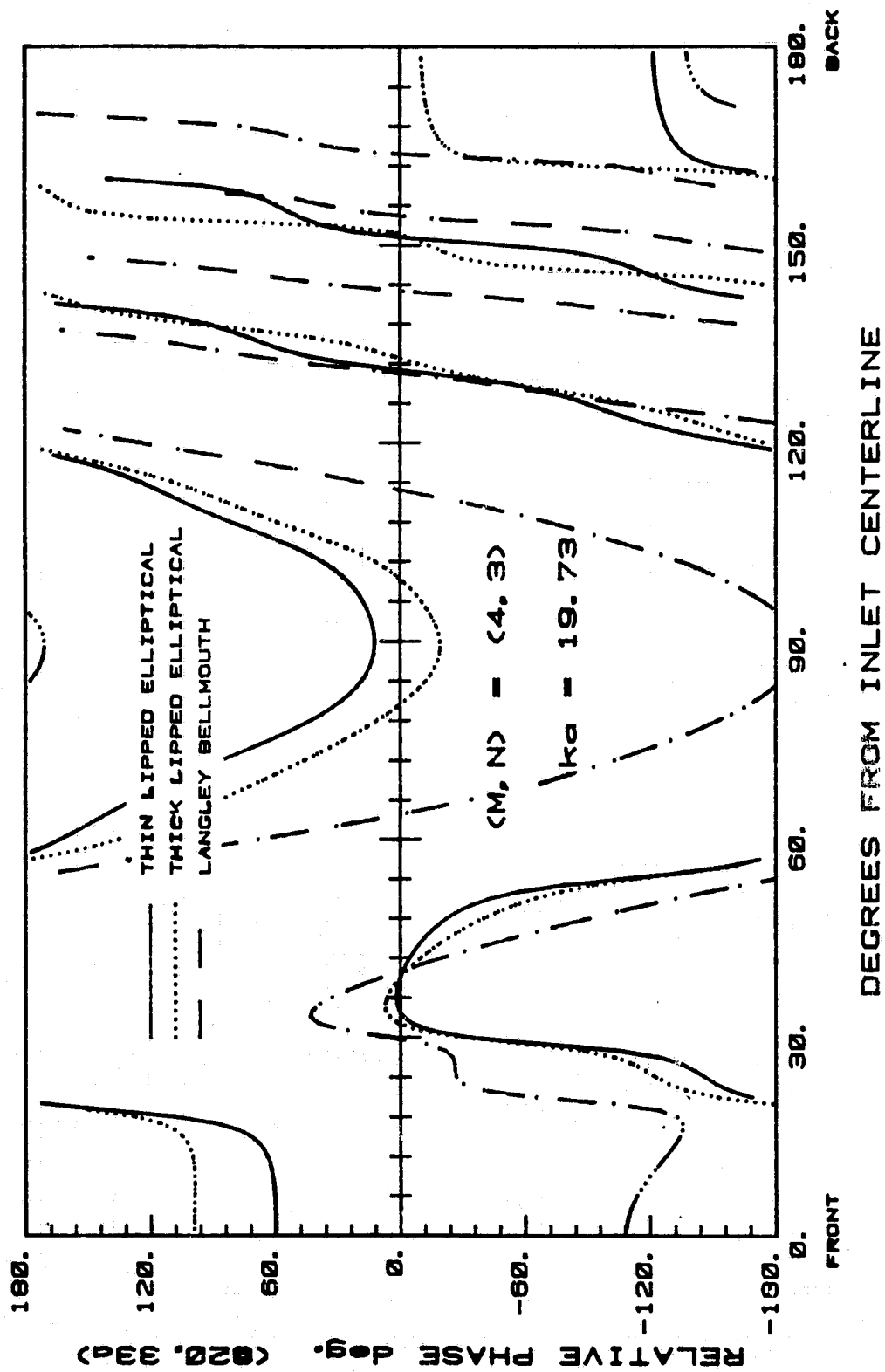
Fig. 63j

ORIGINAL PAGE IS
OF POOR QUALITY



CUT-OFF RATIO = 1.556

Fig. 63k



CUT-OFF RATIO = 1.556

Fig. 631